

PHYLOGENETIC SYSTEMATICS  
OF THE BOROPHAGINAE  
(CARNIVORA: CANIDAE)

XIAOMING WANG

*Research Associate, Division of Paleontology  
American Museum of Natural History  
and  
Department of Biology, Long Island University,  
C. W. Post Campus, 720 Northern Blvd.,  
Brookville, New York 11548-1300*

RICHARD H. TEDFORD

*Curator, Division of Paleontology  
American Museum of Natural History*

BERYL E. TAYLOR

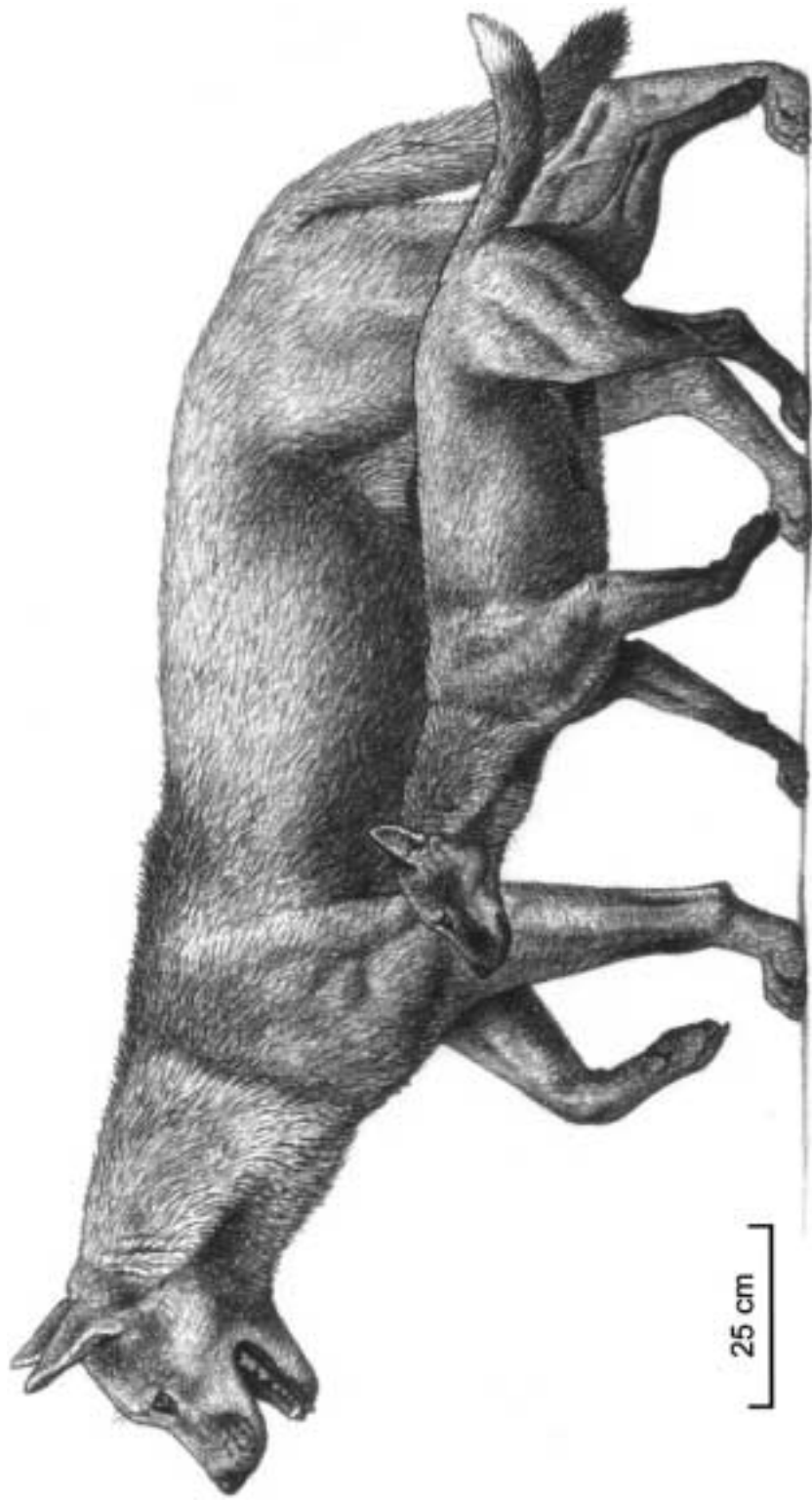
*Curator Emeritus, Division of Paleontology  
American Museum of Natural History*

BULLETIN OF THE AMERICAN MUSEUM OF NATURAL HISTORY

Number 243, 391 pages, 147 figures, 2 tables, 3 appendices

Issued November 17, 1999

Price: \$32.00 a copy



Reconstruction of *Epicyon saevus* (small individual, based on AMNH 8305) and *Epicyon haydeni* (large individual, composite figure, based on specimens from Jack Swayze Quarry). These two species co-occur extensively during the late Clarendonian and early Hemphillian of western North America. Illustration by Mauricio Antón.

## CONTENTS

Abstract .....	9
Introduction .....	10
Institutional Abbreviations .....	11
Acknowledgments .....	12
History of Study .....	13
Materials and Methods .....	18
Scope .....	18
Species Determination .....	18
Taxonomic Nomenclature .....	19
Format .....	19
Chronological Framework .....	20
Definitions .....	21
Systematic Paleontology .....	21
Subfamily Borophaginae Simpson, 1945 .....	23
<i>Archaeocyon</i> , new genus .....	23
<i>Archaeocyon pavidus</i> (Stock, 1933) .....	24
<i>Archaeocyon leptodus</i> (Schlaikjer, 1935) .....	28
<i>Archaeocyon falkenbachi</i> , new species .....	37
<i>Oxetocyon</i> Green, 1954 .....	38
<i>Oxetocyon cuspidatus</i> Green, 1954 .....	39
<i>Otarocyon</i> , new genus .....	40
<i>Otarocyon macdonaldi</i> , new species .....	42
<i>Otarocyon cooki</i> (Macdonald, 1963) .....	43
<i>Rhizocyon</i> , new genus .....	47
<i>Rhizocyon oregonensis</i> (Merriam, 1906) .....	47
Phlaocyonini, new tribe .....	49
<i>Cynarctoides</i> McGrew, 1938 .....	49
<i>Cynarctoides lemur</i> (Cope, 1879) .....	50
<i>Cynarctoides roii</i> (Macdonald, 1963) .....	54
<i>Cynarctoides harlowi</i> (Loomis, 1932) .....	56
<i>Cynarctoides luskensis</i> , new species .....	56
<i>Cynarctoides gawnae</i> , new species .....	57
<i>Cynarctoides acridens</i> (Barbour and Cook, 1914) .....	60
<i>Cynarctoides emryi</i> , new species .....	64
<i>Phlaocyon</i> Matthew, 1899 .....	66
<i>Phlaocyon minor</i> (Matthew, 1907) .....	66
<i>Phlaocyon latidens</i> (Cope, 1881) .....	68
<i>Phlaocyon annectens</i> (Peterson, 1907) .....	72
<i>Phlaocyon achoros</i> (Frailey, 1979) .....	74
<i>Phlaocyon multicuspus</i> (Romer and Sutton, 1927) .....	76
<i>Phlaocyon marslandensis</i> McGrew, 1941 .....	77
<i>Phlaocyon leucosteus</i> Matthew, 1899 .....	79
<i>Phlaocyon yatkolai</i> , new species .....	83
<i>Phlaocyon mariae</i> , new species .....	84
Borophagini, new tribe .....	85
<i>Cormocyon</i> Wang and Tedford, 1992 .....	85
<i>Cormocyon haydeni</i> , new species .....	86
<i>Cormocyon copei</i> Wang and Tedford, 1992 .....	88
<i>Desmocyon</i> , new genus .....	93
<i>Desmocyon thomsoni</i> (Matthew, 1907) .....	94
<i>Desmocyon matthewi</i> , new species .....	101

Subtribe Cynarctina McGrew, 1937 .....	106
<i>Paracynarctus</i> , new genus .....	106
<i>Paracynarctus kelloggi</i> (Merriam, 1911) .....	106
<i>Paracynarctus sinclairi</i> , new species .....	113
<i>Cynarctus</i> Matthew, 1902 .....	114
<i>Cynarctus galushai</i> , new species .....	116
<i>Cynarctus marylandica</i> (Berry, 1938) .....	118
<i>Cynarctus saxatilis</i> Matthew, 1902 .....	118
<i>Cynarctus voorhiesi</i> , new species .....	121
<i>Cynarctus crucidens</i> Barbour and Cook, 1914 .....	124
<i>Metatomarctus</i> , new genus .....	126
<i>Metatomarctus canavus</i> (Simpson, 1932) .....	127
<i>Metatomarctus</i> sp. A .....	131
<i>Metatomarctus</i> sp. B .....	131
<i>Euoplocyon</i> Matthew, 1924 .....	132
<i>Euoplocyon spissidens</i> (White, 1947) .....	133
<i>Euoplocyon brachygnathus</i> (Douglass, 1903) .....	135
<i>Psalidocyon</i> , new genus .....	137
<i>Psalidocyon marianae</i> , new species .....	137
<i>Microtomarctus</i> , new genus .....	140
<i>Microtomarctus conferta</i> (Matthew, 1918) .....	140
<i>Protomarctus</i> , new genus .....	149
<i>Protomarctus optatus</i> (Matthew, 1924) .....	149
<i>Tephrocyon</i> Merriam, 1906 .....	154
<i>Tephrocyon rurestris</i> (Condon, 1896) .....	154
Aelurodontina, new subtribe .....	156
<i>Tomarctus</i> Cope, 1873 .....	157
<i>Tomarctus hippophaga</i> (Matthew and Cook, 1909) .....	157
<i>Tomarctus brevirostris</i> Cope, 1873 .....	165
<i>Aelurodon</i> Leidy, 1858 .....	170
<i>Aelurodon asthenostylus</i> (Henshaw, 1942) .....	170
<i>Aelurodon mcgrewi</i> , new species .....	176
<i>Aelurodon stirtoni</i> (Webb, 1969) .....	179
<i>Aelurodon ferox</i> Leidy, 1858 .....	182
<i>Aelurodon taxoides</i> (Hatcher, 1893) .....	193
Borophagina, new subtribe .....	202
<i>Paratomarctus</i> , new genus .....	202
<i>Paratomarctus temerarius</i> (Leidy, 1858) .....	202
<i>Paratomarctus euthos</i> (McGrew, 1935) .....	212
<i>Carpocyon</i> Webb, 1969 .....	218
<i>Carpocyon compressus</i> (Cope, 1890) .....	219
<i>Carpocyon webbi</i> , new species .....	223
<i>Carpocyon robustus</i> (Green, 1948) .....	227
<i>Carpocyon limosus</i> Webb, 1969 .....	228
<i>Protepicyon</i> , new genus .....	229
<i>Protepicyon raki</i> , new species .....	229
<i>Epicyon</i> Leidy, 1858 .....	233
<i>Epicyon aelurodontoides</i> , new species .....	234
<i>Epicyon saevus</i> (Leidy, 1858) .....	236
<i>Epicyon haydeni</i> Leidy, 1858 .....	252
<i>Borophagus</i> Cope, 1892 .....	266
<i>Borophagus littoralis</i> VanderHoof, 1931 .....	267
<i>Borophagus pugnator</i> (Cook, 1922) .....	272

<i>Borophagus orc</i> (Webb, 1969) .....	278
<i>Borophagus parvus</i> , new species .....	280
<i>Borophagus secundus</i> (Matthew and Cook, 1909) .....	284
<i>Borophagus hilli</i> (Johnston, 1939) .....	296
<i>Borophagus dudleyi</i> (White, 1941) .....	299
<i>Borophagus diversidens</i> Cope, 1892 .....	301
Character Analysis .....	308
Skull .....	309
Mandible .....	314
Dentition .....	316
Phylogeny .....	324
Comments on Stratigraphy, Zoogeography, and Diversity .....	337
Stratigraphy .....	337
Zoogeography .....	340
Diversity .....	341
References .....	344
Appendix I. List of Taxa by Localities .....	356
Appendix II. Cranial Measurements of Borophaginae .....	364
Appendix III. Statistical Summaries of Dental Measurements of Borophaginae .....	378

## FIGURES

1. Phylogeny of Canidae, Procyonidae, and Ursidae by Matthew .....	13
2. Phylogeny of Cynoidea by Wang and Tedford .....	16
3. Phylogeny of Canidae by Tedford .....	17
4. Dental terminology .....	22
5. <i>Archaeocyon pavidus</i> (F:AM 63970, 63222) .....	26
6. <i>Archaeocyon pavidus</i> skeleton (F:AM 63970) .....	27
7. <i>Archaeocyon leptodus</i> (F:AM 63971; UNSM 25399, 4486) .....	30
8. <i>Archaeocyon leptodus</i> (UNSM 26097; FMNH P14797; F:AM 50221) .....	31
9. <i>Archaeocyon leptodus</i> (MCZ 2878, F:AM 49045, 49052, 49447, 49032, 49033) .....	32
10. <i>Archaeocyon leptodus</i> (F:AM 49060) .....	33
11. <i>Archaeocyon leptodus</i> skeleton (F:AM 49060) .....	34
12. Log-ratio diagram for cranial measurements of <i>Archaeocyon</i> , <i>Otarocyon</i> , and <i>Rhizocyon</i> .....	35
13. Log-ratio diagram for dental measurements of <i>Archaeocyon</i> , <i>Oxetocyon</i> , <i>Otarocyon</i> , and <i>Rhizocyon</i> .....	36
14. <i>Archaeocyon falkenbachi</i> (F:AM 49029) .....	38
15. <i>Oxetocyon cuspidatus</i> (SDSM 2980; UNSM 25381, 25698, 2665) .....	40
16. <i>Otarocyon cooki</i> (F:AM 49020) and <i>Otarocyon macdonaldi</i> (AMNH 38986) .....	44
17. <i>Otarocyon cooki</i> (SDSM 54308; F:AM 49043, 49042) .....	45
18. <i>Otarocyon cooki</i> basicranium (F:AM 49043) .....	46
19. <i>Rhizocyon oregonensis</i> (AMNH 6879) .....	48
20. <i>Cynarctoides roii</i> (SDSM 53321, 54132), <i>C. lemur</i> (AMNH 6888, 6889, 6892; CMNH 11334; YPM 903; SDSM 54307), and <i>C. harlowi</i> (ACM 31-34) .....	52
21. Log-ratio diagram for cranial measurements of four species of <i>Cynarctoides</i> .....	54
22. Log-ratio diagram for dental measurements of seven species of <i>Cynarctoides</i> .....	55
23. <i>Cynarctoides acridens</i> (F:AM 63140, 49109, 49112, 49126; AMNH 20502), <i>C. gawnae</i> (F:AM 49249), and <i>C. luskensis</i> (F:AM 49005, 49003) .....	58
24. <i>Cynarctoides acridens</i> (FMNH UC1547, UC1564; F:AM 49001, 99360; AMNH 82558) and <i>C. emryi</i> (UNSM 25455, 25456, 25615) .....	59
25. <i>Phlaocyon minor</i> (F:AM 49054, 49081, 50218; AMNH 12877) .....	68
26. <i>Phlaocyon latidens</i> (AMNH 6896, 6897) and <i>P. minor</i> (F:AM 49004) .....	69
27. Log-ratio diagram for cranial measurements of five species of <i>Phlaocyon</i> .....	70
28. Log-ratio diagram for dental measurements of five species of primitive <i>Phlaocyon</i> .....	71
29. <i>Phlaocyon annectens</i> (CMNH 11332, 1602; F:AM 49006) .....	73

30. <i>Phlaocyon achoros</i> (UF 18389, 18501, 16963, 171365, 18415, 16991) and <i>Phlaocyon multicuspis</i> (FMNH UC1482) .....	75
31. <i>Phlaocyon leucosteus</i> (YPM 12801), <i>P. marslandensis</i> (F:AM 93370; FMNH P26314), <i>P. yatkolai</i> (UNSM 62546), and <i>P. mariae</i> (F:AM 25466) .....	78
32. Log-ratio diagram for dental measurements of five species of advanced <i>Phlaocyon</i> .....	79
33. <i>Phlaocyon leucosteus</i> (AMNH 8768, cranial) .....	80
34. <i>Phlaocyon leucosteus</i> (UNSM 26524) .....	81
35. <i>Phlaocyon leucosteus</i> (AMNH 8768, postcranial) .....	82
36. <i>Cormocyon haydeni</i> (F:AM 49448, cranial) .....	87
37. <i>Cormocyon haydeni</i> (F:AM 49448, postcranial) .....	88
38. <i>Cormocyon haydeni</i> (F:AM 49058, 49064) .....	89
39. Log-ratio diagram for cranial measurements of <i>Rhizocyon</i> , <i>Cormocyon</i> , and <i>Desmocyon</i> .....	90
40. Log-ratio diagram for dental measurements of <i>Rhizocyon</i> , <i>Cormocyon</i> , and <i>Desmocyon</i> .....	91
41. <i>Cormocyon copei</i> (AMNH 6885) .....	92
42. <i>Desmocyon thomsoni</i> (AMNH 12874) .....	96
43. <i>Desmocyon thomsoni</i> (F:AM 49096B) .....	97
44. <i>Desmocyon thomsoni</i> (F:AM 49096[2]) .....	98
45. <i>Desmocyon matthewi</i> (F:AM 49177) .....	102
46. <i>Desmocyon matthewi</i> (F:AM 49176, 49181) and <i>Desmocyon thomsoni</i> (F:AM 62890) .....	103
47. Log-ratio diagram for cranial measurements of <i>Desmocyon</i> , <i>Cynarctus</i> , and <i>Euoplocyon</i> .....	104
48. Log-ratio diagram for dental measurements of <i>Desmocyon</i> , <i>Cynarctus</i> , <i>Metatomarctus</i> , and <i>Euoplocyon</i> .....	105
49. <i>Paracynarctus kelloggi</i> (ACM 11391; F:AM 27352, 50144; UCMP 11562) .....	108
50. <i>Paracynarctus kelloggi</i> (F:AM 61001) .....	109
51. <i>Paracynarctus kelloggi</i> (F:AM 27487, 50137, 61000 ) and <i>Paracynarctus sinclairi</i> (F:AM 61007) .....	110
52. Log-ratio diagram for cranial measurements of <i>Paracynarctus</i> and <i>Cynarctus</i> .....	111
53. Log-ratio diagram for dental measurements of <i>Paracynarctus</i> and <i>Cynarctus</i> .....	112
54. <i>Paracynarctus sinclairi</i> (F:AM 61009) .....	113
55. <i>Cynarctus galushai</i> (F:AM 27543, 27555, 27542) .....	117
56. ? <i>Cynarctus marylandica</i> (USNM 15561), <i>C. voorhiesi</i> (F:AM 105094, 49144), and <i>C. saxatilis</i> (AMNH 9453) .....	119
57. <i>Cynarctus saxatilis</i> (UCMP 29891; FMNH P25537) and <i>C. crucidens</i> (F:AM 49307; UNSM 25465) .....	122
58. <i>Cynarctus crucidens</i> (F:AM 49172, 49312, 49146) .....	123
59. <i>Metatomarctus canavus</i> (UF V-5260; F:AM 49197, 49199; UNSM 25662, 25658, 25609) ..	130
60. <i>Euoplocyon brachygnathus</i> (CMNH 752; AMNH 18261; F:AM 25489, 50120, 50123, 27314) and <i>E. spissidens</i> (MCZ 4246, 7310) .....	134
61. <i>Psalidocyon marianae</i> (F:AM 27397, 61296) .....	138
62. Log-ratio diagram for cranial measurements of <i>Desmocyon</i> , <i>Psalidocyon</i> , <i>Microtomarctus</i> , and <i>Protomarctus</i> .....	139
63. Log-ratio diagram for dental measurements of <i>Desmocyon</i> , <i>Psalidocyon</i> , <i>Microtomarctus</i> , and <i>Protomarctus</i> .....	140
64. <i>Microtomarctus conferta</i> (AMNH 17203; F:AM 61039) .....	142
65. <i>Microtomarctus conferta</i> (LACM-CIT 1229; F:AM 27548) .....	143
66. <i>Microtomarctus conferta</i> (F:AM 27398X, 27398) .....	144
67. <i>Protomarctus optatus</i> (AMNH 18916; F:AM 61272, 61278) .....	152
68. <i>Tephrocyon rurestris</i> (UO 23077) .....	155
69. <i>Tomarctus hippophaga</i> (F:AM 61146, 61174, 61174A; AMNH 13836) .....	162
70. <i>Tomarctus hippophaga</i> (F:AM 61156; AMNH 18244) .....	163
71. Log-ratio diagram for cranial measurements of <i>Tephrocyon</i> , <i>Tomarctus</i> , and <i>Aelurodon</i> .....	164
72. Log-ratio diagram for dental measurements of <i>Tephrocyon</i> , <i>Tomarctus</i> , and <i>Aelurodon</i> .....	165
73. <i>Tomarctus brevirostris</i> (F:AM 61158, 67319, 61130, 28302; AMNH 8302, 18246; TMM 2379) .....	168
74. <i>Aelurodon asthenostylus</i> (LACM-CIT 781) .....	171
75. <i>Aelurodon asthenostylus</i> (F:AM 27161, 27159) .....	172
76. <i>Aelurodon asthenostylus</i> (F:AM 27170A, 28356, 28351) .....	173
77. <i>Aelurodon stirtoni</i> (UCMP 33473) and <i>A. mcgrewi</i> (UCMP 63657; F:AM 22410) .....	178

78. <i>Aelurodon stirtoni</i> (UNSM 25789) .....	180
79. <i>Aelurodon stirtoni</i> (F:AM 25178, 27492) .....	181
80. <i>Aelurodon ferox</i> (UNSM 1093; F:AM 61742; USNM 523) .....	190
81. <i>Aelurodon ferox</i> (F:AM 61753) .....	191
82. <i>Aelurodon taxoides</i> (F:AM 67047; YPM-PU 10635) and <i>A. ferox</i> (F:AM 61771) .....	192
83. Scatter diagram of P4 length vs. P4 width for <i>Aelurodon ferox</i> and <i>A. taxoides</i> .....	193
84. Histogram of m1 length for <i>Aelurodon ferox</i> and <i>A. taxoides</i> .....	194
85. <i>Aelurodon taxoides</i> (F:AM 67006, 67008, 25111, 67039) .....	199
86. <i>Aelurodon taxoides</i> (F:AM 61781, 67395) .....	200
87. <i>Paratomarctus temerarius</i> (USNM 768; F:AM 61070, 67121, 67142) .....	208
88. <i>Paratomarctus euthos</i> (F:AM 61075) and <i>P. temerarius</i> (F:AM 27255; YPM-PU 10453) ..	209
89. Log-ratio diagram for cranial measurements of <i>Paratomarctus</i> and <i>Carpocyon</i> .....	210
90. Log-ratio diagram for dental measurements of <i>Paratomarctus</i> and <i>Carpocyon</i> .....	211
91. <i>Paratomarctus euthos</i> (UCMP 29282) .....	215
92. <i>Paratomarctus euthos</i> (F:AM 61089) .....	216
93. <i>Paratomarctus euthos</i> (F:AM 61101) .....	217
94. <i>Carpocyon compressus</i> (AMNH 8543; YPM 12788; UNSM 25883; F:AM 25120) .....	221
95. <i>Carpocyon compressus</i> (UNSM 2556-90) .....	222
96. <i>Carpocyon webbi</i> (F:AM 61328) .....	225
97. <i>Carpocyon webbi</i> (F:AM 61322, 27366B, 61335), <i>C. robustus</i> (UCMP 33569), and <i>C. limosus</i> (UF 12069; F:AM 61017) .....	226
98. <i>Protepicyon raki</i> (F:AM 27175, 61738, 61705) .....	231
99. Log-ratio diagram for cranial measurements of <i>Protepicyon</i> and <i>Epicyon</i> .....	232
100. Log-ratio diagram for dental measurements of <i>Protepicyon</i> and <i>Epicyon</i> .....	233
101. <i>Epicyon aelurodontoides</i> (F:AM 67025) .....	235
102. <i>Epicyon saevus</i> (F:AM 25102, 70621; USNM 126; AMNH 8305) .....	245
103. <i>Epicyon saevus</i> (AMNH 8305) .....	246
104. <i>Epicyon saevus</i> (UCMP 32328; F:AM 70767) .....	247
105. <i>Epicyon saevus</i> (F:AM 67331, 25140) .....	248
106. <i>Epicyon saevus</i> (F:AM 61382) .....	249
107. <i>Epicyon saevus</i> (F:AM 61420) .....	250
108. <i>Epicyon saevus</i> (F:AM 61387, 61432, 61574) and <i>E. haydeni</i> (USNM 127; F:AM 61453) ..	251
109. <i>Epicyon haydeni</i> (F:AM 61461, 61443) .....	260
110. <i>Epicyon haydeni</i> (AMNH 81004, 14147; F:AM 61501) .....	261
111. <i>Epicyon haydeni</i> (F:AM 61501A, 67628F, 67628G, 67617, 67618D, 67619A, 67620B, 67621A) .....	262
112. <i>Epicyon haydeni</i> (F:AM 67628D, 67627, 67628E, 67622A, 67623A, 67624, 67625A, 67626) ..	263
113. <i>Epicyon haydeni</i> (F:AM 61474, 61535) .....	264
114. Histogram of the length of m1 for <i>Epicyon saevus</i> and <i>E. haydeni</i> .....	265
115. <i>Borophagus littoralis</i> (UCMP 31503) .....	269
116. <i>Borophagus littoralis</i> (UCMP 34515) .....	270
117. <i>Borophagus littoralis</i> (UCMP 33477, 33476) .....	271
118. Log-ratio diagram for cranial measurements of <i>Borophagus</i> .....	272
119. Log-ratio diagram for dental measurements of <i>Borophagus</i> .....	273
120. <i>Borophagus pugnator</i> (DMNH 184 [3]) .....	275
121. <i>Borophagus pugnator</i> (F:AM 61662, 61671) .....	276
122. <i>Borophagus parvus</i> (F:AM 75857, 75877, 75881) and <i>B. orc</i> (UF 13180, 12313) .....	279
123. <i>Borophagus secundus</i> (F:AM 23350; AMNH 18126, 18130, 13831) .....	291
124. <i>Borophagus secundus</i> (F:AM 23350) .....	292
125. <i>Borophagus secundus</i> (AMNH 18919; F:AM 61640) .....	293
126. <i>Borophagus hilli</i> (TWM 1558; UCMP 43306; F:AM 67387A) .....	298
127. <i>Borophagus dudleyi</i> (MCZ 3688) .....	300
128. <i>Borophagus diversidens</i> (F:AM 67364; TMM 40287-10; MU 8034) .....	305
129. <i>Borophagus diversidens</i> (MU 8034) .....	306
130. <i>Borophagus diversidens</i> (IGM 162) .....	307
131. Illustration of characters, dorsal view of skulls .....	311
132. Illustration of characters, lateral view of skulls .....	312
133. Illustration of characters, lateral view of mandibles .....	315

134. Illustration of characters, occlusal view of upper teeth .....	317
135. Illustration of characters, occlusal view of P4 of <i>Aelurodon ferox</i> and <i>Epicyon saevus</i> .....	318
136. Illustration of characters, occlusal view of lower teeth .....	321
137. Illustration of characters, lingual view of m1–m2 .....	323
138. Alternative trees for four segments of phylogeny .....	326
139. Strict consensus tree .....	328
140. Proposed phylogeny of the Borophaginae .....	330
141. Stratigraphic distribution and postulated phyletic relationship of Borophaginae .....	339
142. Correlation of stratigraphy and phylogeny .....	340
143. Species diversity of Cenozoic canids .....	342
144. Log-ratio diagram for postcranial measurements of selected Borophaginae .....	343
145. Definition of cranial measurements, lateral and dorsal aspects of skull .....	365
146. Definition of cranial measurements, ventral aspect of skull .....	366
147. Definition of dental measurements .....	378

### TABLES

1. Previous classifications of borophagine canids .....	14
2. Character matrix of Borophaginae .....	325



## ABSTRACT

The subfamily Borophaginae (Canidae, Carnivora, Mammalia) was erected by G. G. Simpson in 1945 to include seven genera of large, bone-crushing "dogs" in the late Tertiary of the northern continents. As a monophyletic group of canids, the Borophaginae is now known to be much more diverse than was originally envisioned but is confined within the middle to late Tertiary of North America. Fossil records of the borophagines are well represented and members of this prolific clade are often the most common predators in the late Tertiary deposits.

Largely due to the Childs Frick Collection at the American Museum of Natural History, borophagines are represented by some of the best materials among fossil carnivorans in anatomical representation, sample size, and stratigraphic density. As a result of this explosive growth of new information, borophagine systematics is now in need of a complete rethinking at a level that could not have been attempted by previous studies.

A detailed study of borophagine phylogenetic systematics is presented here, publishing for the first time the entire Frick Collection. A total of 66 species of borophagines, including 18 new species, ranging from Orellan through Blancan ages, are presently recognized. A phylogenetic analysis of these species is performed using cladistic methods, with Hesperocyoninae, an archaic group of canids, as an outgroup. At its base, the Borophaginae has a sister relationship with the subfamily Caninae, which includes all living canids and their most recent fossil relatives. The Borophaginae–Caninae clade is in turn derived from the subfamily Hesperocyoninae.

Apart from some transitional forms, most of the Borophaginae can be organized in four major clades (all erected as new tribes or subtribes): Phlaocyoniini, Cynarctina, Aelurodontina, and Borophagina. The Borophaginae begins with a group of small fox-sized genera, such as *Archaeocyon*, *Oxetocyon*, *Otarocyon*, and *Rhizocyon*, in the Orellan through early Arikareean. Relationships among these genera are difficult to resolve due to their primitiveness. Slightly more derived, but still near the base of the Borophaginae, is the Phlaocyoniini, a hypocarnivorous clade of the Arikareean and Hemingfordian that includes *Cynarctoides* and *Phlaocyon*. These two genera represent divergent approaches toward hypocarnivory. Species of *Cynarctoides* trend toward selenodonty and remain small in size, whereas species of *Phlaocyon* specialize toward bunodont dentitions but of increasing size, with an unusual trend toward hypercarnivory by two terminal species in the clade.

Four transitional taxa (species of *Cormocyon* and *Desmocyon*) occupy intermediate positions between the Phlaocyoniini and Cynarctina, and represent a gradual size increase toward medium-size individuals. The subtribe Cynarctina, the second hypocarnivorous clade, includes *Paracynarctus* and *Cynarctus* in the Hemingfordian through Clarendonian, and represents a larger size group than the Phlaocyoniini, although there is a tendency toward size reduction among advanced species of *Cynarctus*. The cynarctines feature the most bunodont dentition known among canids.

The next series of transitional taxa (*Metatomarctus*, *Euoplocyon*, *Psalidocyon*, *Microtomarctus*, *Protomarctus*, and *Tephrocyon*) are of medium size and occupy a pectinated sequence that contains a rather diverse set of dental morphology. These include the most hypercarnivorous borophagine *Euoplocyon*, the peculiarly trenchant *Psalidocyon*, and the dwarf lineage *Microtomarctus*. The next clade, Aelurodontina, is the first major hypercarnivorous group and is represented by *Tomarctus* and *Aelurodon* in the Barstovian and Clarendonian. The aelurodontines evolve around a more consistent theme of increasingly more hypercarnivorous dentitions with strong premolars, forming a rather linear series from *Tomarctus* to various species of *Aelurodon*.

The terminal clade Borophagina, sister to the Aelurodontina, begins with the mostly mesocarnivorous *Paratomarctus* and *Carpocyon* in the late Barstovian through late Hemphillian. The terminal species of *Carpocyon*, *C. limosus*, shows some hypocarnivorous adaptations. *Protepicyon* in the Barstovian initiates the hypercarnivorous trend in the terminal clade. *Epicyon*, the largest known canid, is the dominant predator in the Clarendonian and Hemphillian. Finally, an enlarged concept of *Borophagus* consists of a series of pectinated species terminated by *B. diversidens* in the late Blancan. *Epicyon* and *Borophagus* are the most highly evolved in their capacity to crush bones.

Phylogenetic reconstruction was greatly aided by the high quality of fossil records and the large number of transitional forms. The latter ensures a morphological continuity that facilitates the identification of homoplasies that otherwise could easily be mistaken as synapomorphies. Confidence in the phylogeny is further enhanced by a high congruence between the cladistic rank and the stratigraphic sequence. The temporal and morphological continuity in many borophagine lineages also permits further postulation about their evolutionary processes, such as cladogenetic and anagenetic events.

Our considerably enlarged concept of the Borophaginae indicates a much broader trophic diversity than has previously been envisioned. In addition to the commonly recognized hyenalike forms, members of the Borophaginae acquired a

wider spectrum of morphologies that surpassed either the hesperocyonine or canine canids. The Borophaginae played broad ecological roles that are performed by at least three living carnivoran families, Canidae, Hyaenidae, and Procyonidae.

## INTRODUCTION

Members of the subfamily Borophaginae, an archaic group in the dog family Canidae, are common carnivorans in North America from the middle Oligocene through the Pliocene. Together with the extinct bear dogs (Amphicyonidae) and occasional immigrant bears and cats from the Eurasia, borophagines were the dominant predators during much of this time. These “hyenoid dogs” are most commonly known for their specialized predatory features, such as robust, bone-cracking dentitions and jaws that parallel those of some Old World hyenas. On the other hand, certain omnivorous borophagines are noted for their specializations toward bunodont dentitions, which led them to be regarded as possible precursors to the raccoon family Procyonidae. Between these extreme forms of trophic adaptations is a wide spectrum of cranial and dental patterns that seems to fill every conceivable intermediate morphology, a striking demonstration of morphological flexibility unequalled by modern families of Carnivora.

Despite the diverse ecological roles of the borophagines and the presence of abundant fossil remains, no detailed phylogenetic study has been attempted since G. G. Simpson first erected the subfamily in 1945 (see History of Study below). This is especially notable in light of the fact that fossil borophagines are often the most common carnivorans in many Neogene deposits of North America. Nonetheless, carnivorans, being on top of the food chain, represent a small portion of the biomass and their fossil remains are relatively scarce.

It is therefore fortunate that Tertiary carnivorans attracted the keen interest of the late Dr. Childs Frick, who, with his personal fortune, launched a massive collection program unequalled in the history of vertebrate paleontology. With the help of a dedicated staff, the Frick Laboratory brought together a mag-

nificent collection of Tertiary mammals, known as the Frick Collection (Galusha, 1975a). The impact of the Frick Collection can be felt in the vastly increased quality, quantity, and stratigraphic density of fossil records of many taxa. Significantly, the increased density permits the recognition of numerous intermediate taxa, which fill gaps in the previously known morphology and geological range, and represents a quantum leap in our ability to reconstruct their phylogeny.

In collaboration with his long-time assistant Beryl E. Taylor, Childs Frick intended to publish a comprehensive account of late Cenozoic carnivorans of North America, an ambitious project that remained incomplete at the time of his death in 1965. Since then, the Frick Collection at the American Museum of Natural History became available to the general scientific public. In the 1970s, two of the present authors, B. E. Taylor and R. H. Tedford, began a reanalysis of the systematics and phylogeny of two subfamilies of fossil canids, the Borophaginae and Caninae, under the then new cladistic paradigm. Under this new partnership, every taxon was examined anew and hypodigms were reassembled, and a preliminary phylogenetic analysis was produced without the benefit of computer programs. By the time of Taylor's retirement in 1980, the borophagine manuscript consisted of diagnoses and hypodigms of most taxa, measurements of approximately 80% of the specimens, and 89 plates of illustrations. In 1995, a renewed effort on the borophagine phylogeny became possible with the support from the National Science Foundation to Wang and Tedford. As Wang joined this latest collaboration, all specimens in the Taylor and Tedford manuscript were critically reexamined once again and additional material from more recent collections in several institutions was added to the hy-

podigm. Although the resulting phylogeny is in many ways consistent with the main framework of the Taylor and Tedford manuscript, significant differences exist in the number of taxa recognized, contents of hypodigms, and positions of some clades. In addition, descriptive sections for all taxa have been added. In the final stage of collaboration, the two senior authors did not attempt to persuade Taylor to share the views expressed in the present form, which differs substantially from his previous manuscript, and therefore they must bear responsibility for all of the errors in this monograph.

As the final product of a long search for a historical explanation of a complex group of carnivorans, this monograph represents the fruit of labors of three generations. The evolution of the ideas in each generation broadly reflects its own times in phylogenetic methodology and in the state of knowledge of particular taxa. The task of assembling all relevant information, morphologic and stratigraphic, on thousands of specimens proved to be daunting even with the energetic pursuit of the three generations. Although every effort was made to examine all relevant materials, we undoubtedly have missed some and probably misidentified others. While there surely are alternative hypotheses that we did not fully explore, especially in ways of constructing species, we are confident of the essential validity and internal consistency of our phylogeny given the current state of knowledge.

#### INSTITUTIONAL ABBREVIATIONS

ACM	Amherst College Museum (Pratt Museum), Amherst	FMNH	Field Museum of Natural History, Chicago
AMNH	Department of Vertebrate Paleontology, American Museum of Natural History, New York	HAFO	Hagerman Fossil Beds National Monument, Hagerman
ANSP	Academy of Natural Science of Philadelphia, Philadelphia	IGM	Instituto de Geologia Museo, Universidad Nacional Autonoma de Mexico, Mexico D.F.
BF	Private collection of Barbara Fite, Lutz, Florida	IMNH	Idaho Museum of Natural History, Pocatello
CMNH	Carnegie Museum of Natural History, Pittsburgh	JODA	John Day Fossil Beds National Monument, John Day
DMNH	Denver Museum of Natural History, Denver	KUVP	Division of Vertebrate Paleontology, Museum of Natural History, University of Kansas, Lawrence
F:AM	Frick Collection, Department of Vertebrate Paleontology, American Museum of Natural History, New York	LACM	Natural History Museum of Los Angeles County, Los Angeles
		LACM-CIT	California Institute of Technology, now in the collection of the LACM
		MCZ	Museum of Comparative Zoology, Harvard University, Cambridge
		MSU	Midwestern State University, Wichita Falls
		NMC	National Museum of Canada, Ottawa
		OMNH	Oklahoma Museum of Natural History, Norman (= OMP or OUSM, Stoval Museum of Science and History, University of Oklahoma)
		PPHM	Panhandle-Plains Historical Museum, Canyon
		SDSM	Museum of Geology, South Dakota School of Mines and Technology, Rapid City
		TMM	Texas Memorial Museum, University of Texas, Austin
		TMM-BEG	University of Texas Bureau of Economic Geology, now in the collection of the TMM
		TMM-TAMU	Texas A&M University, now in the collection of the TMM
		TRO	Timberlane Research Organization, Florida
		UA	University of Arizona, Tucson
		UCMP	Museum of Paleontology, University of California at Berkeley
		UCM	University of Colorado Museum, Boulder
		UCR	University of California at Riverside
		UF	University of Florida, Gainesville
		UF V-	Formerly Florida Geological Survey, Tallahassee, now part of the University of Florida collection
		UM	University of Michigan, Ann Arbor
		UMMP	University of Montana Museum of Paleontology, Missoula

UNM	University of New Mexico, Albuquerque
UNSM	Nebraska State Museum, University of Nebraska, Lincoln
UO	University of Oregon Condon Museum of Geology, Eugene
USGS D	United States Geological Survey, Denver register
USGS M	United States Geological Survey, Menlo Park register
USNM	United States National Museum of Natural History, Smithsonian Institution, Washington, D.C.
UW	University of Wyoming, Laramie
UWBM	University of Washington Burke Museum, Seattle
WTSU	West Texas A&M University, formerly WTM, West Texas State University Museum, Canyon
YPM	Yale Peabody Museum of Natural History, Yale University, New Haven
YPM-PU	Princeton University Natural History Museum, now in the collection of the YPM

#### ACKNOWLEDGMENTS

It is obvious that the most critical asset in a project such as this is the presence of the magnificent fossil carnivoran collections at the American Museum of Natural History. Our foremost gratitude thus goes to Dr. Childs Frick, whose lifelong passion for fossil carnivorans helped produce the legendary Frick Collection. Borophagines were part of a larger plan by Frick to revise the entire North American Carnivora, an ambitious project that was never published. While we are the direct beneficiaries of his collection, the ideas in this volume are solely our own.

It is equally apparent that the Frick Collection would not be possible without the dedicated staff of the Frick Laboratory. The professionalism exhibited by these people in their exhaustive sampling and field documentation greatly enriches our knowledge of these canids. Among the most exceptional are Morris S. Skinner and Ted Galusha, assisted by Marie Skinner and Marian Galusha, whose collections and stratigraphic studies laid down the foundation of faunal successions.

We are deeply indebted to Raymond J. Gooris, who accomplished the monumental

task of illustrating nearly all of the specimens and who painstakingly compiled much of the bibliography (except as noted otherwise, all specimen illustrations are drawn by Gooris). Sincere thanks are also due to the Frick Laboratory registrar George Krochak, to preparators Otto Simonis and Ernest Heying, and more recently to Edward Pederson for their skillful preparations of important specimens and casts of materials from many other institutions, to Alejandra Lora for her patience in typing the initial draft of this manuscript, to Lorrain Meeker for her excellent photographic plates used in this paper, and to Robert L. Evander for database input and cross-checking. We also thank Henry Galiano, Barbara Fite, and Jim Ranson for donations or loans of their private casts and specimens.

For their permission to study the collections in their care and their assistance in arranging loans and casts (and their patience with overdue loans) and in supplying locality data or measurements, we express our gratitude to the following individuals: Lawrence G. Barnes, Samuel A. McLeod, and David P. Whistler, Natural History Museum of Los Angeles County; Phil Bjork and James E. Martin, South Dakota School of Mines and Technology; C. S. Churcher, University of Toronto; Richard Cifelli, University of Oklahoma; Margery Coombs, University of Massachusetts; Walter W. Dalquest, Midwestern University; Mary R. Dawson, Carnegie Museum of Natural History; Robert J. Emry, United States National Museum of Natural History; John Flynn, William Turnbull, and William Simpson, Field Museum of Natural History; Lawrence J. Flynn and Charles R. Schaff, Harvard University; C. David Frailey, Johnson County Community College; Theodore J. Fremd, John Day Fossil Beds National Monument; Frederic G. Hayes, Marc S. Frank, Bruce J. MacFadden, and S. David Webb, University of Florida; Robert M. Hunt, Jr., Michael R. Voorhies, Richard G. Corner, and Bruce E. Bailey, University of Nebraska; John H. Hutchison and Pat Holroyd, University of California at Berkeley; Everett H. Lindsay, University of Arizona; Spencer G. Lucas, New Mexico Museum of Natural History and Science; Larry D. Martin and Desui Miao, University of Kansas; H. Gregory McDonald, Hager-

man Fossil Beds National Monument; Guy G. Musser, Department of Mammalogy, American Museum of Natural History; William N. Orr, University of Oregon; John M. Rensberger, University of Washington; Mary Ann Turner and John Ostrom, Yale University; and John A. Wilson and Ernest L. Lundelius, Jr., University of Texas at Austin.

We owe a deep debt of gratitude to our reviewers, Jon A. Baskin and Annalisa Berta, for their kindness to take up such a daunting task with good humor. We also greatly appreciate the moral support and encourage-

ment by Berta during her tenure as program director of the NSF. We are especially grateful to Jon Baskin for sharing his insights on the evolution of *Aelurodon* and *Epicyon* and for his sensible comments that greatly improved the substance and presentation of this paper.

Finally, we gratefully acknowledge financial supports from the National Science Foundation (DEB-9420004, to Wang and Tedford; DEB-9707555, to Tedford and Wang), and a Frick Postdoctoral Fellowship to Wang. Additional financial assistance was provided by the Frick Endowment Fund.

## HISTORY OF STUDY

In 1858, Joseph Leidy described two partial lower jaws and an isolated upper fourth premolar (carnassial) collected from deposits exposed along the Niobrara River in north-central Nebraska by F. V. Hayden, pioneer geo-

logical explorer of the west. Leidy named two genera based on this material, *Aelurodon* and *Epicyon*, thus beginning a series of discoveries of the "hyenoid dogs" in the Tertiary of North America. In the ensuing decades

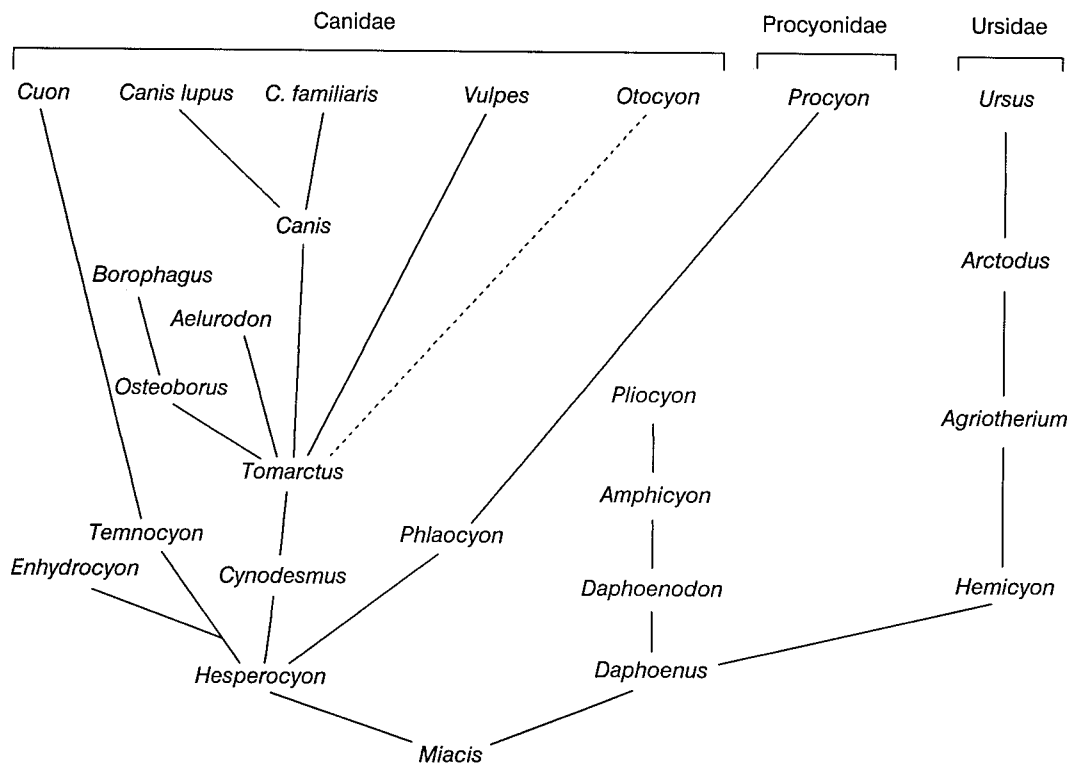


Fig. 1. Phylogeny of Canidae, Procyonidae, and Ursidae by W. D. Matthew, redrawn from Matthew (1930). Some taxa are substituted with current usages (e.g., *Tomarctus* for *Tephrocyon*, *Borophagus* for *Hyaenognathus*).

TABLE 1

**Previous Classifications (or Phylogenies Modified into Classifications) of Borophagine Canids**

- 
1. Cope (1883: 247)  
 Family Canidae  
 Basal lineage  
*Megalotis* (= *Otocyon*)  
*Amphicyon*  
*Galecyon* (= *Cormocyon* sensu Cope)  
*Galecyon*–*Hyaenocyon* lineage  
*Tennocyon* (including *Mesocyon*)  
*Enhydrocyon*  
*Hyaenocyon* (= *Enhydrocyon*)  
*Galecyon*–*Aelurodon* lineage  
*Canis*  
*Aelurodon*  
*Oligobunus* and others
2. Scott (1895: 75)  
 Cynoids  
*Miacis*–*Cynodictis* lineage  
*Cynodictis* (= *Hesperocyon*)  
*Miacis*–*Canids* lineage  
*Daphoenus*  
*Tennocyon*  
*Cynodesmus*  
*Aelurodon*  
*Canis*
3. Wortman and Matthew (1899: 139, taken from phylogeny)  
 Family Canidae  
*Uintacyon*–*Cuon* lineage  
*Daphoenus*  
*Enhydrocyon*  
*Hyaenocyon*  
*Tennocyon*  
*Cuon*  
*Procynodictis*–*Canis* lineage  
*Cynodictis* (= *Hesperocyon*) *lippincottianus*  
*Cynodesmus*  
*Hypotemnodon* = *Mesocyon*  
*Canis*  
*Vulpavus*–*Nothocyon* lineage  
*Cynodictis* (= *Hesperocyon*) *gregarius*  
*Nothocyon* (= *Cormocyon*)
4. Matthew (1930: 132, taken from phylogeny in fig. 1, canid part only)  
 Family Canidae  
*Miacis*–*Cuon* lineage (trenchant talonid)  
*Tennocyon*  
*Enhydrocyon*  
*Cuon*  
*Miacis*–*Canis* lineage (basined talonid)  
*Cynodictis*  
*Cynodesmus* (= *Tomarctus thomsoni*)  
*Tephrocyon* (= *Tomarctus*)  
*Vulpes*  
*Canis*  
*Aelurodon*  
*Osteoborus*  
*Borophagus*
5. Loomis (1936: 50, taken from phylogeny in fig. 6)  
 Canids with trenchant talonid  
*Daphoenus*–*Amphicyon* group (amphicyonids)  
*Tennocyon* group  
*Tennocyon*  
*Cuon*  
*Icticyon* (= *Speothos*)  
*Lycaon*  
*Mesocyon* group  
*Mesocyon*  
*Enhydrocyon* group  
*Brachyrhynchocyon*  
*Enhydrocyon*  
 Canids with basined talonid  
*Nothocyon* group  
*Cynodictis* (= *Hesperocyon*)  
*Nothocyon* (= *Cormocyon*)  
*Cynodesmus* (sensu stricto for *Tomarctus thomsoni*)  
*Tomarctus*  
*Canis*  
*Tephrocyon* group  
*Tephrocyon*  
*Aelurodon* group  
*Aelurodon*  
*Borophagus*  
*Hyaenognathus*  
*Pliocyon*  
*Allocyon* group (ursids)  
*Allocyon*  
*Hemicyon*
6. VanderHoof and Gregory (1940: 144)  
 Hyaenoid dogs  
*Cynodesmus*  
*Tomarctus* (including *Tephrocyon*)  
*Aelurodon*  
*Osteoborus*  
*Borophagus* (including *Hyaenognathus* and *Porthocyon*)
7. Simpson (1945: 108–111, in part)  
 Superfamily Canoidea  
 Family Canidae  
 Subfamily Caninae  
*Cynodictis*  
*Pseudocynodictis* (= *Hesperocyon*)  
*Nothocyon* (= *Cormocyon*)  
*Cynodesmus*  
*Mesocyon*  
*Tomarctus*  
*Leptocyon*  
 Subfamily Simocyoninae  
*Brachyrhynchocyon*  
*Enhydrocyon*  
*Philotrox*  
*Euoplocyon*
-

TABLE 1—(Continued)

Subfamily Borophaginae	Subfamily Caninae
<i>Aelurodon</i>	<i>Leptocyon</i>
<i>Borocyon</i> (= <i>Daphoenodon</i> )	<i>Vulpes</i>
<i>Borophagus</i>	<i>Nyctereutes</i>
<i>Gobicyon</i>	<i>Canis</i>
<i>Hadrocyon</i>	<i>Lycaon</i>
<i>Osteoborus</i>	
<i>Pliocyon</i>	10. Munthe (1989: fig. 1)
<i>Pliogulo</i>	Subfamily Borophaginae
8. Macdonald (1963: 201, taken from phylogeny in fig. 23)	<i>Tomarctus</i> sensu lato
Trenchant talonid group	<i>Euoplocyon</i>
<i>Hesperocyon</i>	<i>Cynarctus</i>
<i>Mesocyon</i>	<i>Carpocyon</i>
<i>Enhydrocyon</i>	<i>Aelurodon</i>
<i>Sunkahetanka</i>	<i>Strobodon</i>
Basined talonid group	<i>Epicyon</i>
<i>Nothocyon</i>	<i>Osteoborus</i>
<i>Cynodesmus</i>	<i>Borophagus</i>
<i>Neocynodesmus</i>	
<i>Tomarctus</i>	11. McKenna and Bell (1997: 244–245)
Other Borophaginae unspecified	Infraorder Cynoidea
9. Tedford (1978)	Family Canidae
Family Canidae	Subfamily Borophaginae
Subfamily Hesperocyoninae	<i>Oxetocyon</i>
<i>Hesperocyon</i>	<i>Cormocyon</i>
<i>Mesocyon</i>	<i>Euoplocyon</i>
<i>Enhydrocyon</i>	<i>Phlaocyon</i>
Subfamily Borophaginae	<i>Tomarctus</i>
<i>Nothocyon</i> (= <i>Cormocyon</i> )	<i>Aletocyon</i>
<i>Tomarctus</i>	<i>Bassarriscops</i>
<i>Cynarctus</i>	<i>Cynarctoides</i>
<i>Prohyaena</i> (= <i>Aelurodon</i> )	<i>Strobodon</i>
<i>Aelurodon</i> (= <i>Epicyon</i> )	<i>Aelurodon</i>
<i>Osteoborus</i>	<i>Carpocyon</i>
<i>Borophagus</i>	<i>Epicyon</i>
	<i>Cynarctus</i>
	<i>Osteoborus</i>
	<i>Borophagus</i>

around the turn of the twentieth century, generic names such as *Tomarctus* (Cope, 1873), *Tephrocyon* (Merriam, 1906), and *Borophagus* (Cope, 1892) became well established in the literature. Taxonomic studies during this early period were mainly revisions of individual genera, e.g., *Tomarctus* (including *Tephrocyon*) by Matthew (1924), *Borophagus* (including *Hyaenognathus*) by Matthew and Stirton (1930), *Osteoborus* by Stirton and VanderHoof (1933), and *Aelurodon* by VanderHoof and Gregory (1940). Although these forms were frequently compared with one another or linked together in phylogenies (Matthew, 1924, 1930; VanderHoof and Gregory, 1940; McGrew, 1935; fig. 1), there was no explicit proposal to include them in a higher taxon, other than with informal references such as “hyenoid dogs.”

In his influential classification of mammals, Simpson (1945: 111) listed seven extinct genera under a newly erected subfamily Borophaginae: *Borocyon*, *Aelurodon*, *Gobicyon*, *Pliocyon*, *Osteoborus*, *Pliogulo*, and *Borophagus*, with an additional genus, *Hadrocyon*, as Borophaginae incertae sedis. Simpson (1945: 224) informally defined his new subfamily as including “large, later Tertiary canids with heavy jaws, rather distantly convergent toward the hyenas and so sometimes called ‘hyenoid dogs.’” Although Simpson considered that borophagines might be polyphyletic “in detailed origin,” citing the study by VanderHoof and Gregory (1940) as evidence, he nonetheless concluded that the included genera “must have had a common origin very little, if at all, before the rise of the morphological family” (Simpson, 1945: 224).

Of his original list of seven genera, four are now commonly regarded to be amphicyonids: *Borocyon*, *Gobicyon*, *Hadrocyon*, and *Pliocyon*. The remaining three genera, *Aelurodon*, *Osteoborus*, and *Borophagus* (including *Pliogulo*), were generally considered a natural group, in so far as higher level relationships of Canidae are concerned. More recent taxonomic studies of borophagines were mostly limited to these few highly hypercarnivorous forms plus a few mesocarnivorous forms such as *Tomarctus* (Williams, 1967; Dalquest, 1968; Webb, 1969b; Richey, 1979). A summary of previous classifications is presented in table 1.

Earlier studies of canid phylogeny generally follow a theme of bipartite division based on talonid structure of the lower carnassial, i.e., those with a basined, bicuspid talonid vs. those with a trenchant, unicuspid talonid, as championed by Matthew (1924, 1930) and followed until rather recently (e.g., Macdonald, 1963). A strict adherence to this dichotomy had led Matthew (1924, 1930) to divide the entire Canidae (plus some noncanids) into these two main categories, and to envision a highly heterogeneous group with trenchant talonids that includes such distantly related taxa as *Temnocyon* (an Arikareean amphicyonid), *Enhydrocyon* (an Arikareean hesperocyonine), and *Cuon* (Asiatic dhole, a living canine).

The concept of the Borophaginae was generally confined to a few highly specialized, bone-eating, hyenoid dogs until a brief review by Tedford (1978), who proposed a phylogenetic framework of selected genera of fossil and living canids. Two of his critical points are relevant in the present project. First, a tripartite division of the Canidae was proposed, which included the existing subfamilies Borophaginae and Caninae, and a new, more primitive, subfamily Hesperocyoninae. Such a division of canids has since been more or less adopted by contemporary vertebrate systematists (Berta, 1988; Martin, 1989; Munthe, 1989, 1998; Wang, 1990, 1994; Van Valkenburgh, 1991). The central concept of this phylogeny envisions three successive, partially overlapping radiations of canids replacing each other during the Tertiary (fig. 2). The earliest radiation is represented by the hesperocyonines, which first

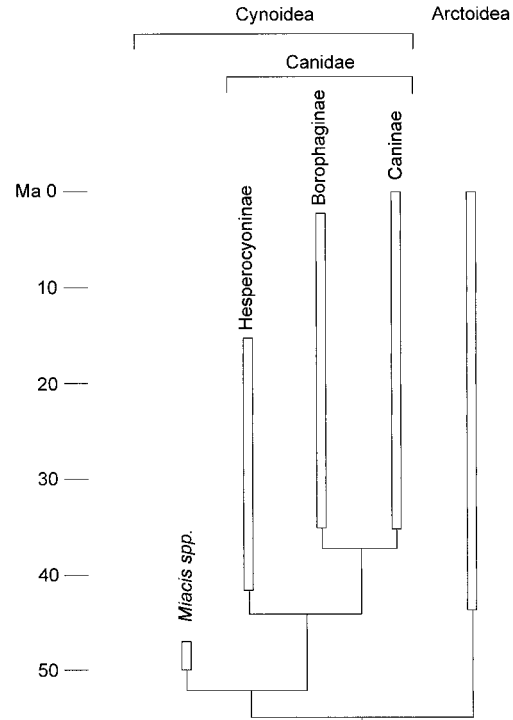


Fig. 2. Phyletic relationship of the major divisions of the Canidae and their temporal ranges. Relationships with other Caniformia are as developed in Wang and Tedford (1994: fig. 9).

appeared in the late Eocene (Duchesneau, about 40 Ma) of North America, flourished during the Arikareean–Hemingfordian, and became extinct in the early Barstovian (Wang, 1994). During the Orellan, two lineages arose from *Hesperocyon*. One is represented by small fox-sized, *Cormocyon*-like animals that eventually gave rise to the borophagines. The other lineage is represented by *Leptocyon*, which became the precursor of the canines (including all living canids). The borophagines diversified before the canines, attained their maximal species richness during the Clarendonian, and became extinct by the start of the Pleistocene. The canines, on the other hand, maintained an inconspicuous presence during much of this time and did not achieve their present diversity until they had successfully dispersed into the Old World and South America in the Plio-Pleistocene.



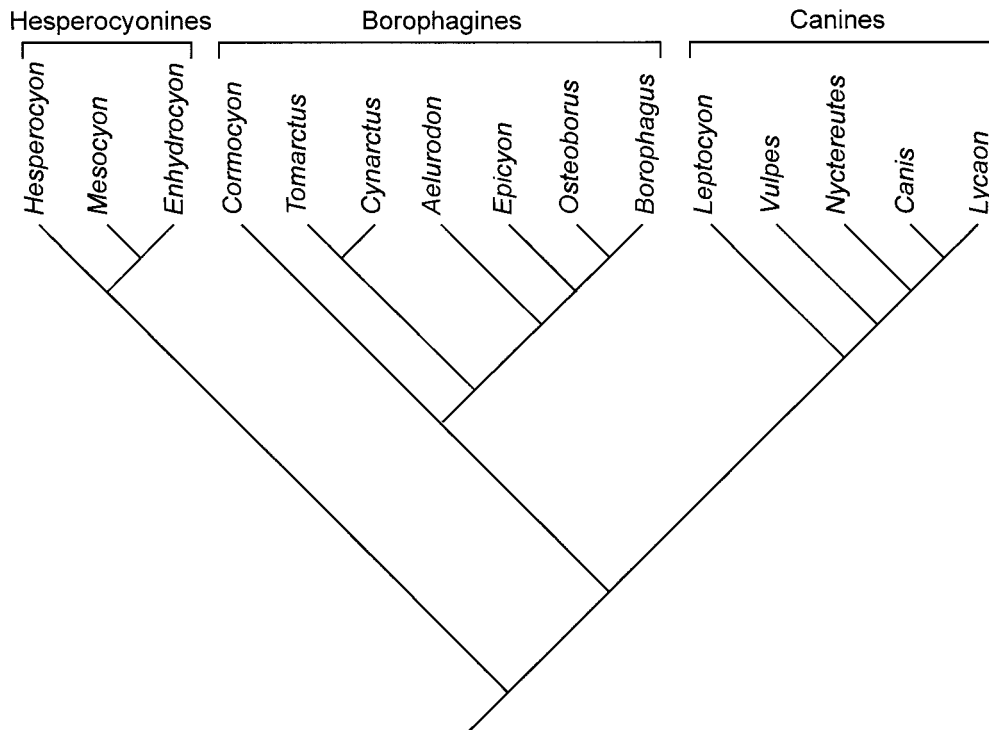


Fig. 3. Phylogeny of Canidae proposed by R. H. Tedford (redrawn from Tedford, 1978). Some taxa are substituted with current usages (e.g., *Cormocyon* for *Nothocyon*, *Aelurodon* for *Prohyaena*, *Epicyon* for *Aelurodon*).

Second, Tedford (1978: fig. 3) broadened the original concept of the Borophaginae (Simpson, 1945) to include such stem taxa as *Cormocyon* (formerly *Nothocyon*, see Wang and Tedford, 1992) and *Tomarctus* (formerly including *Cynodesmus*), as well as hypocarnivorous taxa such as *Phlaocyon* and *Cynarctus*. The small, generalized borophagines *Tomarctus* and *Cormocyon* had previously been regarded as directly ancestral to both the living canines as well as the derived borophagines (Matthew, 1924, 1930). The hypocarnivorous *Phlaocyon* and *Cynarctus*, on the other hand, were formerly thought to be related to the procyonids (the raccoon family), again on the basis of dental similarities only (Wortman and Matthew, 1899; Matthew, 1930; McGrew, 1937, 1941; Simpson, 1945), but were later conclusively demonstrated to be canids by Hough (1948) and Dahr (1949). A recent update by McKenna and Bell (1997: 244) on the Simpson's 1945 classification of Borophaginae has signifi-

cantly expanded the original list of genera and is largely consistent with that proposed in this paper.

Munthe (1979, 1989) studied the functional morphology of borophagine postcranial skeletons. Her systematic framework is broadly consistent with that presented here, although her selected taxa are limited to a few forms that have adequate postcranial materials (see table 1). Munthe found a diverse array of postcranial adaptations among borophagines, in contrast to the stereotypical view that these hyenoid dogs were noncursorial, bone-crushing scavengers. Besides the obvious reason of better or more complete postcranial materials available, this is partly due to her modern view of borophagine systematics (see also Munthe, 1998), i.e., some of the included meso- and hypocarnivorous taxa were simply not considered borophagines in the past. The spectrum of cursorial capabilities and trophic adaptations is surely further enlarged in light of a much larger

content of the Borophaginae identified in this study (Munthe began her analysis with "*Thomomys thomsoni*" as the most primitive

borophagine and did not attempt to study such basal forms as *Archaeocyon*, *Cormocyon*, *Phlaocyon*, *Cynarctoides*, etc.).

## MATERIALS AND METHODS

### SCOPE

Because their specimens are usually the most common carnivorans in the middle to late Tertiary of North America, borophagines are present in nearly every institution housing a collection of Tertiary mammals. Although a completely exhaustive study is not practical, every effort was made to ensure a comprehensive review of all significant collections and all published materials, through loans, casts, or personal visits by at least one of us. Despite the fact that material comes from nearly 40 present or former institutions (see list under Institutional Abbreviations), the Frick Collection at the American Museum of Natural History comprises the largest single collection of borophagines and constitutes our primary database.

### SPECIES DETERMINATION

Morphological criteria are the only available means for discrimination of fossil species. Most species can be distinguished by a combination of qualitative and quantitative characters and morphometrics. Discontinuity in the morphospace is still a convenient criterion in species discrimination, whose usefulness has been demonstrated in recent studies of living sympatric canids (Dayan et al., 1989, 1992). In these studies, the lower carnassial length of coexisting species of desert canids in the Middle East was found to differ by approximately 18%, which was postulated to reflect character displacement in niche partitioning. Such a living analog can be successfully applied in fossil canids (e.g., Wang, 1994).

Studies of morphological variation in living canids also offer quantitative guides for the present study (e.g., Lawrence and Bossert, 1967, 1975; Kolenosky and Standfield, 1975; Clutton-Brock et al., 1976; Nowak, 1979). Species delineations, however, are rarely completely precise when variations through geologic range and among different

geographic regions are intermingled in large samples. Quantitative variations typically include one or more components, such as ontogenetic, sexual, geographic, and geologic variation. The latter often entails a moderate amount of size increase over the life-span of a species. Our evaluations of morphological variation in borophagines indicate that coefficients of variance in lower carnassial lengths generally fall within a range of 4 to 7, comparable to those in the hesperocyonines and living canids. Larger values would thus signal the possibility of a mixed sample, although allowance is sometimes made for cases in widespread taxa with long durations that have undergone noticeable size change. Furthermore, divisions of chronospecies along an anagenetic lineage (morphological change without cladogenetic event) contain a certain degree of arbitrariness when the fossil record is more or less continuous. Geological hiatuses sometimes serve as convenient breaks but may later be shown to be artifacts of poor records when transitional samples are obtained.

Except in rare cases when fossil material can be positively sexed through association of a baculum (e.g., some skeletons of *Desmocyon thomsoni* and *Carpocyon compressus*), sexual identity in most instances can only be inferred from a few dental and osteological features, most of which are quite subtle and thus do not offer unambiguous identification. Sexual dimorphism of canids is relatively subtle and appears strongly constrained by the phylogeny, in contrast to the markedly more dimorphic arctoids (Gittleman and Van Valkenburgh, 1997). Dimorphisms in cranial and dental measurements of living canids range from 3 to 6% in *Vulpes* (Churcher, 1960; Gingerich and Winkler, 1979; Dayan et al., 1989, 1992; Gittleman and Van Valkenburgh, 1997; personal obs.), 3 to 8% in *Canis* (Jolicoeur, 1975; Gittleman and Van Valkenburgh, 1997), and nearly 0% in *Urocyon* (Gittleman and Van Valken-

burgh, 1997; personal obs.); such differences are often well within the adult size variation of the population as a whole. Qualitatively, males of living canids tend to have slightly stronger canines, broader and deeper muzzles, more robust jaws, stronger postorbital processes and sagittal crest, and possibly broadly concave caudal edge of pubis (Munthe, 1989; Gittleman and Van Valkenburgh, 1997; personal obs.). Such morphological tendencies are useful as a general guide for allowance of intraspecific variation.

#### TAXONOMIC NOMENCLATURE

Ideally, higher level nomenclatures (genus and above) should be consistent with phylogenetic relationships. Traditional usage of some generic names, e.g., *Tomarctus* and *Cormocyon* (formerly *Nothocyon*), often reflects an evolutionary grade rather than strict genealogical relationships. For the most part, we use generic names for monophyletic clades only, although it is not practical to completely eliminate paraphyletic taxa. In fact, some species, as defined in this study, represent segments of a single lineage, and as such, recognition of more than one species along a continuous spectrum of morphological change is necessarily arbitrary and paraphyletic. Thus we do not designate a genus for every pectinated species unless it represents a distinct lineage (usually supported by autapomorphies) from adjacent species.

Above the generic level, we use the ranks of tribe or subtribe for several well-defined clades (e.g., Phlaocyonini, Cynarctina, Aelurodontina, and Borophagina) that represent specializations toward hypo- or hypercarnivory. These names are also convenient for discussions about relationships or functional morphology. However, we do not attempt to assign every taxon to a tribe or subtribe, leaving segments of pectinated clades without a higher level designation, except that they are within the subfamily Borophaginae.

Throughout the text we frequently use the conventional terms "primitive" or "derived" to describe certain taxa. These terms are convenient in discussions about relationships between phylogenetic positions and morphological features. It should be obvious that the relative primitiveness or derivedness

of a taxon is defined within the context of our phylogeny.

#### FORMAT

Owing to the large number of species and specimens involved in this study, as well as our emphasis on phylogenetic relationships, we adopt an abbreviated format for economical presentation of morphological information. Instead of the traditional bone-by-bone and tooth-by-tooth descriptions, we figure all historically important specimens (types) as well as anatomically well-preserved ones. In most instances, we illustrate multiple specimens for each species so that they complement each other in anatomical details and permit a sense of variations. The illustrations are done in a consistent manner to enable the reader to make certain morphological comparisons directly. The subtler proportional differences are more easily demonstrated in the log-ratio diagrams (sensu Simpson, 1941) that we compile for all species described in this paper. These proportional relationships can also be examined in tables of cranial and dental measurements presented in appendices II and III. In the tables for dental measurements, we list measurements for the holotype as well as all primary statistics to show quantitative variations. In the tables for cranial measurements, on the other hand, we present the original data, since measurable skulls are far more rare than are dental specimens. Together, the illustrations, ratio diagrams, and tables of measurements comprise the primary database for morphological information on all taxa. To supplement this system, we sometimes make brief comparisons among related species on relevant features that are not easily gathered from the above sources, or we note qualitative variations in a section labeled "Description and Comparison" under each species. Finally, a "Discussion" section is used to briefly comment on the phylogenetic implications and/or other important information about the taxon. Likewise, historical developments of each taxon are not presented in great detail. Instead, we strive to provide a comprehensive synonym list for past references of all taxa whenever an author's concept of the taxon is unambiguous (i.e., not just taxonomic lists). Readers

can thus look for such information from the synonym lists. We hope that this system is a viable alternative to detailed verbal descriptions and that it forms an adequate basis from which the reader can verify the data matrix in the phylogenetic analysis.

We attempt to make the diagnoses close reflections of our phylogenetic framework. However, the purpose of our diagnoses is to contrast and delineate closely related taxa and is not meant to be a mirror image of the characters mapped on the phylogenetic tree. Thus, while we point out the polarities of the diagnostic features whenever possible, these features tend to be more descriptive than are the characters coded in the matrix or mapped on the phylogenetic tree, and a character complex, sometimes coded as one character, may be split into several diagnostic features. In addition, the diagnosis is more directed toward contrasts of anatomies from actual materials rather than the assumed character transformations for missing data as demanded by the phylogenetic algorithm.

#### CHRONOLOGICAL FRAMEWORK

The time scale used in this work to calibrate the geologic ranges of borophagine (fig. 141) is derived from data in Tedford et al. (1987) as modified by new knowledge of the position of epoch boundaries and the placement of the boundaries of the North American Land Mammal ages (NALMa).

A significant reinterpretation of the position of the Eocene–Oligocene boundary places it now at about 34 Ma at the Chadronian–Orellan NALMa boundary (Prothero and Swisher, 1992). The revision of the geomagnetic polarity timescale (Cande and Kent, 1995) yields an Oligocene–Miocene boundary at 24 Ma (rounded from 23.8 Ma), a Miocene–Pliocene boundary of 5 Ma (rounded from 5.4 Ma), and a Pliocene–Pleistocene boundary of 1.8 Ma.

Continuing calibration of the NALMa using newly gathered correlations with the geomagnetic polarity timescale of Cande and Kent (1992, 1995) now allows placement of the Chadronian–Orellan boundary (Prothero and Swisher, 1992) nearly identical to the Eocene–Oligocene boundary at 34 Ma, the Orellan–Whitneyan boundary (Prothero and

Swisher, 1992, Tedford et al., 1996) at 32 Ma (rounded from 32.2 Ma), the Whitneyan–Arikareean boundary (Tedford et al., 1996) at 30 Ma (30.1 Ma), the Arikareean–Hemingfordian boundary (MacFadden and Hunt, in press) at 19 Ma, the Hemingfordian–Barstovian boundary at 16 Ma (15.9 Ma), the Barstovian–Clarendonian boundary (data discussed in Whistler and Burbank, 1992) about 12 Ma, the Clarendonian–Hemphillian boundary (see Whistler and Burbank, 1992) about 9 Ma, the Hemphillian–Blancan boundary (Repenning, 1987) at 5 Ma (approximately at the top of the Terra subchron within the Gilbert chron), and the Blancan–Irvingtonian boundary (Repenning, 1987) at 2 Ma (base of the Olduvai subchron, 1.95 Ma, within the Matuyama chron).

Subdivision of the NALMa follows the definition and characterization proposed by Tedford et al. (1987). Although the content of these subdivisions remains valid, calibration of their boundaries needs revision following reassessment of the ages of the NALMa boundaries. Work on the Whitneyan–Arikareean transition (Tedford et al., 1996) provided an approximate data on the faunal turnover marking the beginning of the medial Arikareean at 28 Ma. A 4-m.y.-long episode follows that lacks biochronologic typification but ends approximately at the beginning of the Miocene (late Arikareean) at 24 Ma. The Hemingfordian is divided into two parts. The first by immigration events and the second by the explosive cladogenesis of equine horses at approximately 17.5 Ma. Likewise, the Barstovian is divided into two parts with the rise of the medial Miocene Great Plains chronofauna at about 14.8 Ma. The Clarendonian is divided at about 10 Ma by the immigration of shovel-tusk mastodonts. A two-fold division of the Hemphillian recognizes the increase in immigrants during the later part of the age beginning around 7 Ma. We have chosen to divide the Blancan at approximately 4 Ma at the boundary between Blancan II and III of Repenning (1987), placed in the late Gilbert above the Cochiti subchron recording the first appearance of muskrats in mid-latitude North America.

The geochrons of the taxa shown in the phylogenetic chart (fig. 141) were established using the above criteria and other spe-

cific chronological data related to their occurrence (stratigraphic association with radioisotopically dated rocks or relevant magnetostratigraphy). In some cases the precise position in time of the site or fauna containing borophagines is established by biological correlation with other sites with better chronological data. In cases where the taxon is a member of a fauna characteristic of a whole stratigraphic unit, the chronological limit of that unit is used as the temporal span of the taxon. These conventions will lead to some over-estimation of the geologic ranges for some taxa, which should be born in mind when assessing the average species longevity for the borophagines.

### DEFINITIONS

Unless otherwise stated, anatomical terminology, particularly the soft anatomy, follows that of Evans and Christensen (1979). The notation for dental formula is as follows: I1 I2 I3 C1 P1 P2 P3 P4 M1 M2 for upper teeth and i1 i2 i3 c1 p1 p2 p3 p4 m1 m2 m3 for lower teeth. Dental nomenclature follows Van Valen (1966). Frequently used terms are defined in figure 4. Most of these represent conventional usage that needs no further explanation. We use the term hypocone in the upper molars, whether it is a discrete, conate cusp arising from the lingual cingulum as in certain hypocarnivorous lineages, or is sim-

ply an enlargement of the internal (lingual) cingulum as is the primitive condition for all canids. Such usage is different from that in the hesperocyonine volume (Wang, 1994), in which the term internal cingulum is used to indicate its homology with the structure in the miacoid carnivorans.

The terms hyper- and hypocarnivory, convenient concepts for describing dental adaptation in carnivorans, were proposed by Crusafont-Pairó and Truyols-Santonja (1956) on the basis of two angles on the upper and lower carnassial teeth. Our own use of these terms, however, is somewhat broader in meaning, not limited to the tooth angles of their original definition, and refers to the dental tendencies that emphasize shearing vs. grinding functions. By hypercarnivory we mean any dental tendency toward increased efficiency in shearing, which in canids commonly involves elongated shearing blade of carnassial teeth, reduction or loss of m1 metaconid, shortened and simplified m1 talonid, reduction of M2 and m2–m3. In contrast, hypocarnivorous tendencies include shortening of shearing blade, as well as enlargement and increasing complexity of grinding part of the dentition (m1 talonid and m2–m3). We also employ the coordinate term mesocarnivory to indicate a dentition lacking these specializations. Mesocarnivorous canids approach the primitive condition in dental structure.

### SYSTEMATIC PALEONTOLOGY

CLASS MAMMALIA LINNAEUS, 1785  
 ORDER CARNIVORA BOWDICH, 1821  
 SUBORDER CANIFORMIA KRETZOI, 1943  
 INFRAORDER CYNOIDEA FLOWER, 1869  
 FAMILY CANIDAE FISCHER DE WALDHEIM, 1817

INCLUDED SUBFAMILIES: Hesperocyoninae Martin, 1989; Borophaginae Simpson, 1945; and Caninae Fischer de Waldheim, 1817.

DIAGNOSIS: The following synapomorphies uniting the canid clade are present in *Prohesperocyon* and *Hesperocyon*, the most basal members of the Canidae, although some of the characters are further modified in later and more derived taxa: presence of a low septum derived from the entotympanic bordering the suture of the ectotympanic with

the caudal entotympanic; presence of a small and shallow suprimeatal fossa; presence of an inflated entotympanic bulla; medial expansion of the petrosal in full contact with the basioccipital and basisphenoid; ossification of the tegmen tympani; extrabullar position of the internal carotid artery and loss of the stapedia artery; presence of posterior accessory cusps on the upper and lower third premolars; reduction of the M1 parastyle; and loss of the M3.

DISCUSSION: Phylogenetic analyses of basal cynoids and their higher taxonomic grouping follow recent studies by us (Wang, 1994; Wang and Tedford, 1994, 1996). Thus defined, our concept of the Canidae, especially

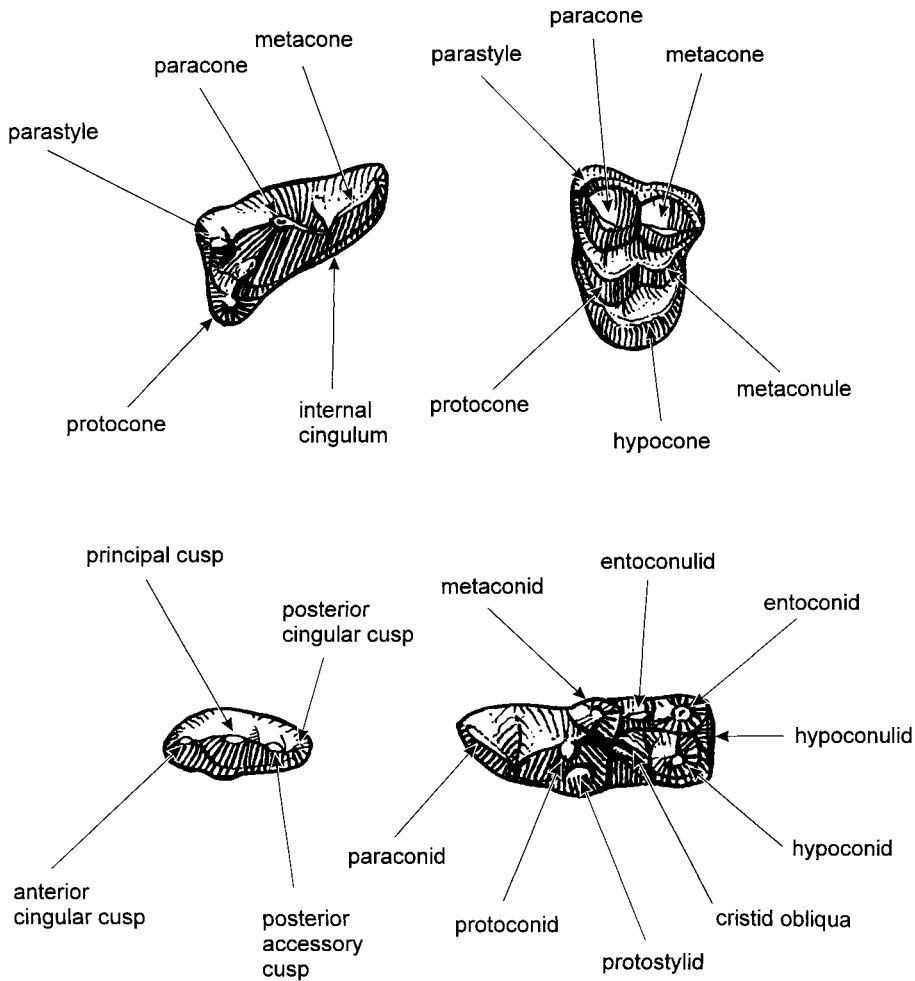


Fig. 4. Dental terminology for P4–M1 (upper part) and p4–m1 (lower part) in the present study.

as concerned with the extinct taxa, differs markedly from traditional treatments such as in Matthew (1924, 1930), Simpson (1945), and Piveteau (1961). Much of the difference can be attributed to a recent renewal of interest in the basicranial characters as a useful tool to unravel the fundamental relationships of caniform carnivores (see references cited in Wang and Tedford, 1994). The above canid basicranial characters remain quite stable throughout the history of Canidae, with the exception of a highly modified middle ear in *Otarocyon*, a new genus described below. We exclude amphicyonids from the Canidae because of their arctoid basicranium (Hough, 1948; Ginsburg, 1966; Hunt, 1977).

At the subfamily level, we follow a tripartite division of the Canidae proposed by one of us (Tedford, 1978) and substantiated later (Wang and Tedford, 1996). Such a scheme has gained some recent acceptance (e.g., Martin, 1989), and forms the basic framework of canid phylogeny in this study. According to this phylogenetic framework, all living canids and closely related fossil taxa (such as *Leptocyon* Matthew, 1918 and *Eucyon* Tedford and Qiu, 1996) belong to the Subfamily Caninae, whose living members were recently analyzed by Tedford et al. (1995) and whose fossil members are being monographed by Tedford, Taylor, and Wang (MS). Among early diverging lineages, a

North American radiation of early canids from late Eocene to middle Miocene comprises the Subfamily Hesperocyoninae, which was extensively treated by Wang (1994). Standing between the above two subfamilies (both in terms of phylogeny and in ecological replacement) is the Borophaginae, the subject of this study. See further comments about the interrelationship of the three subfamilies of the Canidae in the Discussion section under the subfamily Borophaginae.

#### SUBFAMILY BOROPHAGINAE SIMPSON, 1945

INCLUDED GENERA: *Archaeocyon*, new genus; *Oxetocyon* Green, 1954; *Otarocyon*, new genus; *Rhizocyon*, new genus; *Cynarctoides* McGrew, 1938a; *Phlaocyon* Matthew, 1899; *Cormocyon* Wang and Tedford, 1992; *Desmocyon*, new genus; *Paracynarctus*, new genus; *Cynarctus* Matthew, 1902; *Metatomarctus*, new genus; *Euoplocyon* Matthew, 1924; *Psalidocyon*, new genus; *Microtomarctus*, new genus; *Protomarctus*, new genus; *Tephrocyon* Merriam, 1906; *Tomarctus* Cope, 1873; *Aelurodon* Leidy, 1858; *Paratomarctus*, new genus; *Carpocyon* Webb, 1969b; *Protepicyon*, new genus; *Epicyon* Leidy, 1858; and *Borophagus* Cope, 1892.

DISTRIBUTION: Orellan through Blancan of North America and Hemphillian of Central America.

DIAGNOSIS: Borophagines and canines are distinguished from the hesperocyonines in further reduction of M1 parastyle, anteriorly extended lingual cingulum of M1, basined talonid of the m1, and tall m2 metaconid relative to protoconid. Compared to the canines, borophagines lack certain synapomorphies possessed by that subfamily: slender, elongated mandible, narrow and long premolars separated by diastemata, reduced or absent posterior accessory cusps on premolars, reduced P4 protocone, elongated trigonid of m1, and elongated m2, although most of these characters have been independently acquired by some derived borophagines. Except for the basal species, many borophagines progressively acquired additional synapomorphies that readily distinguish them from both hesperocyonine and canine canids: upper incisors with lateral cusps, more robust

premolars with strong accessory cusps, presence of a distinct parastyle on P4, quadrate M1 with enlarged metaconule, and strong posterior process of the premaxillary that eventually meets the frontal.

DISCUSSION: Although we exclude *Borocyon*, *Gobicyon*, and *Pliocyon* from Simpson's Borophaginae, we substantially expand his concept to include a much larger array of taxa. With the possible exception (see Phylogeny section) of the three most basal genera (*Archaeocyon*, *Oxetocyon*, and *Otarocyon*) our cladistic analysis suggests it is a monophyletic clade and a sister group of the Subfamily Caninae.

The tendency toward a basined, bicuspid talonid on the m1 appears to be a key innovation that initiates the borophagine and canine clades. The elevation of the entoconid (from a primitively low ridge in *Hesperocyon*) to a cusp that, together with the hypoconid, encloses the talonid basin is the first step toward an increased grinding function for the dentition. The basined talonid may have been the most critical structure that enabled the early borophagines to avoid competition with the medium- to large-size hesperocyonines that dominate the hypercarnivorous niches—they were able to explore hypocarnivorous niches almost immediately after they diverged from *Hesperocyon*. Such a dental morphology forms the basis of repeated evolution of hypocarnivorous dentitions not only in borophagines (such as *Cynarctoides*, *Phlaocyon*, *Cynarctus*, and *Carpocyon*), but also in certain living canines (such as *Urocyon* and *Nyctereutes*). The basined, bicuspid talonid is thus a key innovation similar to the development of hypodentitions in the upper dentitions of many orders of eutherian mammals (Hunter and Jernvall, 1995). On the other hand, this basic talonid structure in the borophagines is noticeably modified toward more trenchant talonids in certain highly advanced taxa, such as *Euoplocyon*, *Aelurodon*, and *Borophagus*. These exceptions are clearly phylogenetic reversals as a result of the repeated evolution of hypercarnivorous tendencies.

#### *Archaeocyon*, new genus

TYPE SPECIES: *Pseudocynodictis pavidus* Stock, 1933.

ETYMOLOGY: Greek: *archaeo*, beginning; *cyon*, dog.

INCLUDED SPECIES: *A. pavidus* (Stock, 1933); *A. leptodus* (Schlaikjer, 1935); and *A. falkenbachi*, new species.

DISTRIBUTION: Whitneyan of Nebraska, South Dakota, and Wyoming; late Whitney or early Arikareean of California; early Arikareean of Nebraska, Wyoming, Montana, South Dakota, North Dakota, and Oregon; and medial Arikareean of Wyoming.

DIAGNOSIS: As a basal taxon in the Caninae–Borophaginae clade, *Archaeocyon* possesses all the synapomorphies that unite these two subfamilies and differentiate them from the hesperocyonines: M1 parastyle weak, M1 lingual cingulum anteriorly extended to surround protocone, basined talonid of m1, and m2 metaconid slightly higher than protoconid. In contrast to the Caninae clade (*Leptocyon* through living canids), *Archaeocyon* lacks derived characters for that clade: a slender horizontal ramus, narrow and elongated premolars that are set apart by diastemata, premolar posterior accessory cusps reduced or absent, reduced P4 protocone, more open trigonid of m1, and elongated m2. *Archaeocyon* remains primitive relative to most borophagines (*Rhizocyon* and higher sister taxa) in its unenlarged auditory bulla, posteriorly oriented paroccipital process that does not articulate with the bulla (except in some of the latest individuals of *A. pavidus*), posteriorly restricted M1 hypocone, and M2 lingual cingulum not connected to metacornule.

DISCUSSION: Phylogenetically, *Archaeocyon* is similar to *Hesperocyon* in its basal position to more than one clade. *Hesperocyon* is a paraphyletic genus that includes species which gave rise to the common ancestor of the Caninae–Borophaginae clade as well as to members of the Hesperocyoninae (Wang, 1994). Likewise, *Archaeocyon* is basal to both the Borophaginae and Caninae. Lacking a derived character of its own, *Archaeocyon* is a paraphyletic genus that does not exhibit a clear morphological tendency toward either the Caninae or Borophaginae. Considering that the dental morphology of basal borophagines tends to be more conservative (i.e., more similar to *Hesperocyon*) than their counterparts in the canines (*Lep-*

*tocyon*), we place *Archaeocyon* in the Borophaginae along with *Oxetocyon* and *Otarocyon*, which occupy a similarly ambiguous position in the cladogram. The earliest occurrence of *Leptocyon* is in the Orellan (Wang and Tedford, 1996); records of *Archaeocyon* postdate the Orellan. It is thus unlikely that *Archaeocyon* had given rise to the Caninae. Instead, the genus is morphologically and stratigraphically in the right position to be the most basal member of the Borophaginae.

Of the few derived dental characters of *Archaeocyon* (more basined talonid, expanded lingual cingulum on M1, etc.), all are pointed toward an initial tendency of hypocarnivory relative to the condition in *Hesperocyon*. Such a tendency enabled the early borophagines to exploit hypocarnivorous niches bypassed by the far more hypercarnivorous hesperocyonines.

Lacking any clearly defined morphological trends, the species of *Archaeocyon* do not easily lend themselves to cladistic analysis. This kind of difficulty is not uncommon in small, basal caniforms that are conservative in just about every aspect of their morphology and show little inclination toward hyper- or hypocarnivory (see Phylogeny section for further discussion).

*Archaeocyon pavidus* (Stock, 1933)

Figures 5, 6

*Pseudocynodictis* (?) *pavidus* Stock, 1933: 31, pl. 1, figs. 1–5.

“*Hesperocyon*” *pavidus* (Stock): Wang, 1994: 34 (in part), fig. 11A–C.

*Cormocyon pavidus* (Stock): Wang and Tedford, 1996: 446 (in part), fig. 7.

HOLOTYPE: LACM-CIT 466, crushed anterior half of skull and mandible with left P2–M1, right P3–M2, left and right p2–m2, and alveoli for p1 and m3 (Wang, 1994: fig. 11A, B), Kew Quarry Local Fauna (LACM-CIT loc. 126), Las Posas Hills, Sespe Formation (late Whitneyan or early Arikareean), Ventura County, California.

REFERRED SPECIMENS: From type locality: LACM 1338, partial ramus with p4–m1; and LACM 5276, partial ramus with p3–m1.

Whitneyan of northwestern Nebraska: F: AM 50338, partial left maxillary with I1–I3,



P2–M2, and associated partial mandible with left and right c1–m3, 1 mi northeast of Crow Butte, Dawes County, 30 ft above a gray, ashy layer in Whitney Member of Brule Formation; F:AM 63970 (Wang and Tedford, 1996: fig. 7), crushed skull with I3–P1, P2 broken–P4, M1–M2 both broken, both partial rami with c1–m3 (p1 alveolus) (figs. 5A–E, 6), articulated partial skeleton including atlas and incomplete vertebral column, humerus, radius, ulna, and distal end of femur through metatarsals I–V, east side of Roundhouse Rock, 5 mi southwest of Bridgeport, Morrill County, 20 ft below contact of the Whitney and Horn members of the Brule Formation; F:AM 63976, right ramus fragment with m2–m3, Plunkett-Parson Locality, 8 mi north of Harrison, Sioux County, below lower Whitney ash in a paleo-valley fill that cuts through the Orellan clays; F:AM 63990, partial left ramus with p4 broken–m2 and m3 alveolus, northeast of Crow Butte, 30 ft above green layer, Dawes County; UNSM 26142 (AMNH cast 96708), partial right ramus with p3 broken–m3, White River Group, probably Whitney Member of Brule Formation, Scotts Bluff County.

Whitneyan of southwestern South Dakota: F:AM 50342, fragment of left ramus with m1–m2, 6 mi southeast of Oelrichs, Fall River County, 20 ft above first gray nodule zone in Poleslide Member of Brule Formation; F:AM 63360, right ramus fragment with m1, 0.25 mi west of Cedar Pass, Jackson County, in basal Poleslide Member, Brule Formation; and LACM 9602 (AMNH cast 129651), right ramal fragment with m1–m2, LACM loc. 1973, Godsell Ranch.

Southeast corner of Sheep Mountain, uppermost part of Poleslide Member, Brule Formation, 3 ft below base of Rockyford Ash (late Whitneyan), Shannon County, South Dakota: F:AM 63220, partial crushed skull with C1–M2 (M1 broken) and both partial rami with p1–m2 and m3 alveolus.

Southeast corner of Sheep Mountain in lower part of Sharps Formation (early Arikareean), Shannon County, South Dakota: F:AM 63221, articulated partial skull and mandible with worn C1–M2, mandible with c1 (broken)–m3, articulated partial scapula through partial ulna, partial femur, and limb fragments, 15 ft above base of Rockyford

Ash; and F:AM 63222, skull with I2 (broken)–M2 (fig. 5F–I), left ramus with c1–m3 (fig. 5J, K), humerus, distal end femur, partial scapula, and articulated cervical vertebrae, 18 ft above the base of the Rockyford Ash.

Picture Gorge 30, Blue Basin level 1, UCMP loc. V4849-1, Turtle Cove Member, John Day Formation, Oregon: UCMP 76652, maxillary and mandible fragments with left C1, P1–P2 alveoli, P3–M2, right P3–M2, left m1, and right p2–m2.

DISTRIBUTION: Whitneyan of Nebraska and South Dakota, early Arikareean of South Dakota and Oregon, and late Whitneyan or early Arikareean of California.

EMENDED DIAGNOSIS: *Archaeocyon pavidus* lacks derived borophagine characters other than those uniting the Borophaginae and Caninae clades. Being possibly the most primitive member of the genus, *A. pavidus* possesses all the synapomorphies of *Archaeocyon* as contrasted to the primitive conditions in the hesperocyonines: reduced M1 parastyle, anteriorly extended lingual cingulum on M1, incipient development of basined talonid on m1, and tall m2 metaconid. *A. pavidus* has an autapomorphy that distinguishes it from other species of the genus: presence of a lateral groove on the lower canine. Additionally, it is distinguished from *A. leptodus* in its smaller size and shorter m1, and from *A. falkenbachi* in its unshortened rostrum. *A. pavidus* differs from *Rhizocyon oregonensis* in having a smaller size, narrower upper molars, and M2 lingual cingulum not connected to metaconule.

DESCRIPTION AND COMPARISON: A detailed description of dental morphology of this species can be found in Wang (1994: fig. 11A, B). A significant addition of new material to the present study is four complete or partial skulls and skeletons from the latest Whitneyan to earliest Arikareean of Nebraska and South Dakota (figs. 5, 6). As expected from its phylogenetic position, *Archaeocyon pavidus* differs little from a small *Hesperocyon*. It retains an uninflated auditory bulla, a small suprimateal fossa, a posteriorly oriented paroccipital process, and relatively small braincase, all of which are primitive characters present in basal canids such as *Prohesperocyon* and *Hesperocyon*. A slightly enlarged bulla and ventrally oriented paroccipital pro-

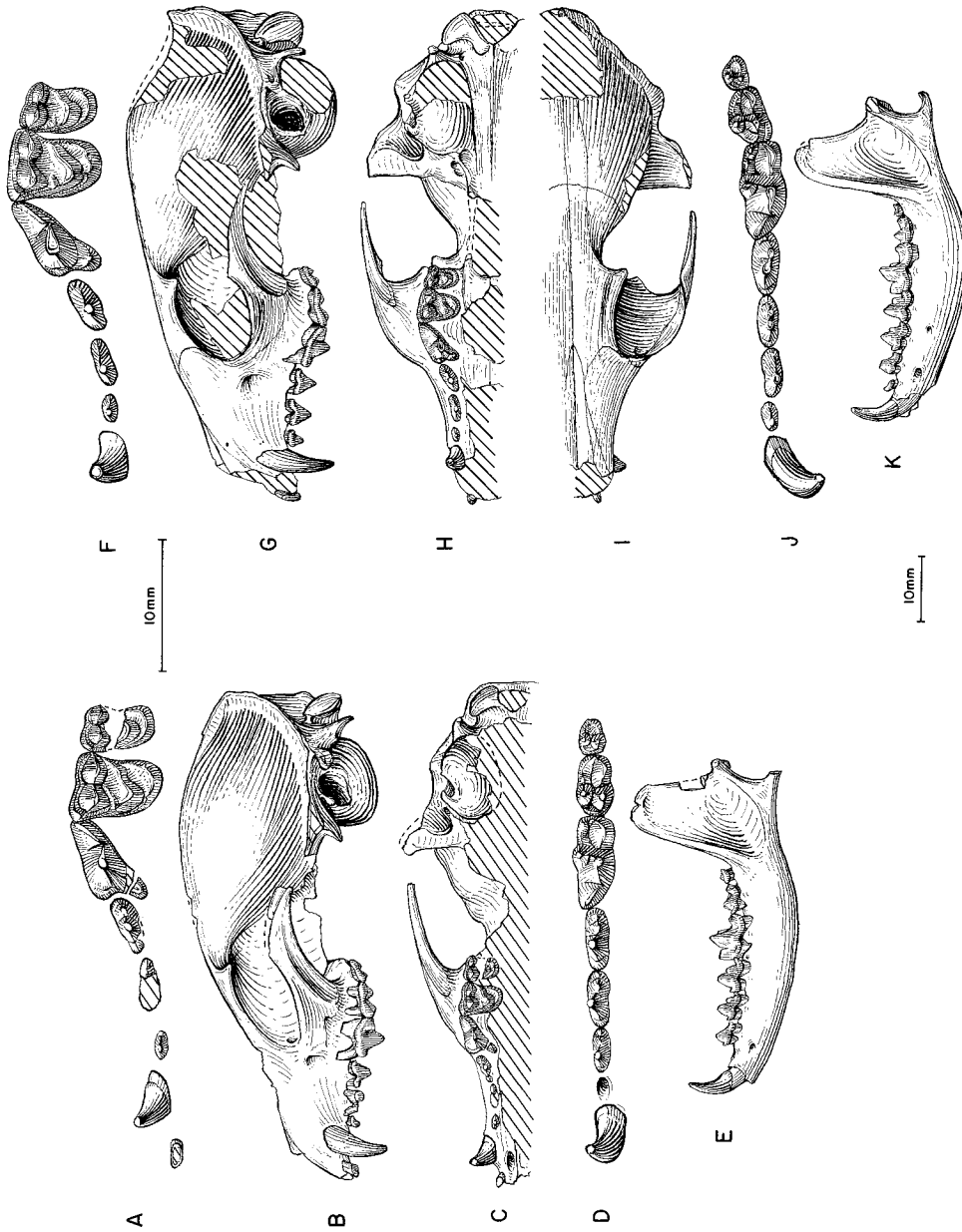


Fig. 5. *Archaeocyon pavidus*. A, Upper teeth, B, lateral and C, ventral views of skull, D, lower teeth, and E, ramus of F:AM 63970 (II, Pl. I, lingual parts of M1-M2, c1, and paroccipital process reversed from right side), east side of Roundhouse Rock, Whitney Member, Brule Formation (Whitneyan), Morrill County, Nebraska. F, Upper teeth, G, lateral, H, ventral, and I, dorsal views of skull, J, lower teeth, and K, ramus of F:AM 63222, Sheep Mountain, lower part of Sharps Formation (early Arikareean), Shannon County, South Dakota. The longer (upper) scale is for A, D, F, and J, and the shorter (lower) scale is for the rest.



Fig. 6. Partial articulated skeleton of *Archaeocyon pavidus*, F:AM 63970 (skull reversed from that of the left side), east side of Roundhouse Rock, Whitney Member, Brule Formation (Whitneyan), Morrill County, Nebraska. Photograph by Lorraine Meeker.

cess in individuals from the latest Whitneyan through earliest Arikareean of South Dakota indicate their slightly more derived morphology relative to individuals of older geologic age. The paroccipital process in the South Dakota specimens, although fully bent toward the ventral side, is still only partially fused with the bulla, i.e., there is a free tip at the distal end (fig. 5G).

*Archaeocyon pavidus* is smaller than *Hesperocyon gregarius*. Additionally, it has acquired some subtle dental features that signal its advance toward the Caninae–Borophaginae clade. *A. pavidus* is less hypercarnivorous than *Hesperocyon*, as is reflected in its slight increase in grinding dentition such as broadening of the M1 by reduction of the parastyle and anterior expansion of the lingual cingulum to surround the protocone, lowering of the m1 trigonid, lowering of the hypoconid and elevation of the entoconid on m1 to form a more basined talonid, and elevation of metaconid on m2 so that it is higher than the protoconid. Many of above features are in an initial stage of development

and subject to variation that may be reminiscent of conditions in *Hesperocyon*. For example, although the M1 of F:AM 50338 has a reduced parastyle, it still has the lingual cingulum restricted to the posterolingual corner.

The postcranial skeleton of *Archaeocyon pavidus* is also much like that of *Hesperocyon*. The humerus is somewhat bowed and has an entepicondylar foramen. The olecranon of ulna lacks a prominent medial process. The digits are closely appressed for both metacarpals and metatarsals. Such a limb structure suggests an initial adaptation toward a scansorial life that probably has not quite achieved the full digitigrade posture (Wang, 1993).

DISCUSSION: Aside from the few subtle dental features that ally it with the borophagine–canine clade, *Archaeocyon pavidus* is rather *Hesperocyon*-like in size and proportions. *A. pavidus* was recognized by Wang (1994) as possibly a very primitive borophagine, but was tentatively referred to “*Hesperocyon*” to indicate its primitive sim-

ilarity to *H. gregarius*. Wang and Tedford (1996) adopted the interim name *Cormocyon pavidus* to express its basal borophagine position. In both papers, a small sample of fragmentary jaws from the Cedar Creek Member (Orellan) of White River Formation of Colorado in the KUVF collection [referred to as "*Pseudocynodictis* sp. (small form)" by Galbreath, 1953: 76] was included in the hypodigm of *C. pavidus*. Our present analysis of this sample, however, indicates that Wang's earlier reference, mainly based on size considerations, lacks the morphological basis established in this study. Most importantly, the talonid structure of the Colorado sample is basically that of a *Hesperocyon*. Such morphology is inconsistent with our phylogenetic hypothesis of early borophagines, which predicts that if a sister relationship between the Borophaginae and Caninae is correct, the basined talonid should have evolved during Orellan, since it occurs in the earliest *Leptocyon*. The small form in the Orellan of Colorado may represent a distinct species of *Hesperocyon* after all, although the fragmentary materials are not suitable for establishment of a new species.

Presence of *Archaeocyon pavidus* in the John Day Formation of Oregon is suggested by one individual, UCMP 76652, from the basal part of the Turtle Cove Member. Other than its slightly larger size, UCMP 76652 compares well with its counterparts in the Great Plains.

*Archaeocyon leptodus* (Schlaikjer, 1935)

Figures 7–11

*Nothocyon leptodus* Schlaikjer, 1935: 131, fig. 6.

*Hesperocyon leptodus* (Schlaikjer): Macdonald, 1963: 203; 1970: 54.

*Nothocyon geismarianus* (Cope, 1877): Macdonald, 1970: 55 (in part).

HOLOTYPE: MCZ 2878 (AMNH cast 129680), left partial ramus with c1–p2 alveoli, p3 root, p4–m2, and m3 root (fig. 9A, B). Schlaikjer (1935: 131) reported that the type was from "Lower Harrison Formation, approximately 15 ft above the Brule-lower Harrison contact," 4.5 mi southeast of Fort Laramie, Goshen County, Wyoming. As pointed out by McKenna (1966: 6), these "Lower Harrison" sediments of Schlaikjer

belong to the lower Arikaree Group of other authors (early Arikareean).

REFERRED SPECIMENS: Schomp Ranch, north of Mitchell, lower ash of the Whitney Member of the Brule Formation (Whitneyan), Sioux County, Nebraska: F:AM 63971, crushed partial skull with I3–M2 (P1 alveolus) (fig. 7A–D), mandible with i1–i3 alveoli and p1–m3 (fig. 7E, F), articulated partial skeleton including most of the vertebral column, partial scapula through manus with most of phalanges, partial femur, partial tibia and fibula, and pes with most of the phalanges.

Whitney Member of Brule Formation (Whitneyan), Morrill County, Nebraska: UNSM 25699, right partial ramus with p3 alveolus–m1, UNSM loc. Mo-107 or Mo-108.

Horn Member of the Brule Formation (early Arikareean), Morrill County, Nebraska: Redington Gap area (UNSM loc. Mo-108): F:AM 99287, left ramus with i1–p3 alveoli, p4–m2, and m3 alveolus, 92 ft above the base of upper Whitney ash and 5 ft below the contact with the Gering Formation; UNSM 4486, left ramus with incisor and c1 alveoli, p1–m1, and m2 broken (fig. 7K, L), 13 ft above the base of the Horn Member; UNSM 4487, right partial maxillary with P4–M1 and M2 alveolus, west of Reddington Gap, from 30 to 40 ft above the base of the Horn Member; UNSM 25126, right partial ramus with c1–p1 alveoli, p2–p3 broken, p4, m1 broken, m2, and m3 alveolus, north of Reddington Gap, from 30 to 40 ft above the base of the Horn Member; UNSM 25398, left ramus with i3, c1–p1 alveoli, p2–m1, and m2 root, 1.25 mi west of Reddington Gap, 50 ft above base of the Horn Member; and UNSM 25399 (AMNH cast 96705), skull with I1–I2, I3 alveolus, and C1–M2 (fig. 7G–J), 100 yd west of road, from 10 ft above base of the Horn Member. One mi east of Birdcage Gap (UNSM loc. Mo-105): UNSM 25707, skull with I1–M2 and mandible with i2 broken–m3. Round House Rock (UNSM loc. Mo-104): FMNH P14797, skull with I1 alveolus–M2 and both rami with i1 broken–m3 (fig. 8C–G); and UNSM 25394, right partial ramus with m1–m2 and m3 alveolus, astragalus, and fragments, 15 ft above marl,

upper part of the Horn Member; and UNSM 25709, palate with C1–M2 (M1 broken).

Horn Member of Brule Formation (early Arikareean), Banner County, Nebraska: Three mi northeast of Wrights Gap: UNSM 26097, anterior part of skull I1–I2, I3 alveolus, C1, and P1 alveolus–M2 (fig. 8A, B). North side of point between Shobar and Logan Canyons: UNSM 25708, partial skull with I1–C1 and P1 alveolus–M2, right and left rami with i2–c1 and p1 alveolus–m3, distal end of humerus, and partial radius and ulna. Bayard Quarry (UNSM loc. Bn-102): UNSM 25710, right partial ramus with p3–p4 alveoli, m1 broken, and m2–m3 alveoli.

Three Tubs locality, north side of 66 Mountain, Whitney Member, Brule Formation (Whitneyan), Goshen County, Wyoming: F:AM 50298, articulated skull with I3–M2 and mandible with c1–m3 and articulated partial skeleton with cervical vertebrae, partial scapula, both humeri, and incomplete radii and ulnae, from 10 ft above the lower ash in the middle Whitney; F:AM 50299, right incomplete side of skull with C1–M2 (P1 alveolus) articulated with right ramus with i3–m3 and distal ends of both tibiae, distal fibula, and both articulated incomplete pes, 3 ft above the base of the lower ash in the middle Whitney; and F:AM 50300, right incomplete side of skull with I3–C1 alveoli, P1, P2 broken, and P4–M1, and right partial ramus with p1–m3 (m1 and m2 broken), 8 ft above the base of the lower ash in the middle Whitney.

Wounded Knee Area, middle and upper parts of the Sharps Formation (early Arikareean), Shannon County, South Dakota: LACM 5900, left partial ramus with p3 broken–m2, LACM loc. 1829; LACM 9200, right partial ramus with p2, alveolus p3–p4, and m1 broken–m2, LACM loc. 1861; LACM 9283 (AMNH cast 129647), right partial ramus with p2 alveolus–m1, LACM loc. 1966; LACM 9297, left partial ramus with p4 (broken)–m1, LACM loc. 1980; LACM 9360, left maxillary fragment with P3–M1, LACM loc. 1819; LACM 9371 (AMNH cast 129650), left maxillary fragment with P4–M1, LACM loc. 1955; LACM 9389, right ramal fragment with m1 and m2 alveolus, LACM loc. 1982; LACM 9408, left ramal fragment with m1, LACM loc. 1959;

LACM 9426, right ramal fragment with m1 and m2 broken alveolus, LACM loc. 1984; LACM 9446, right partial ramus with p4 broken–m2 (m3 alveolus), LACM loc. 1959; LACM 9518, right partial ramus with p2–m3, LACM loc. 1984; LACM 21661, right partial ramus with m1–m2, LACM loc. 1959; LACM 28982, left partial ramus with m1–m2 and m3 alveolus, LACM loc. 1956; SDSM 53323, crushed fragment of skull with P1–P3 alveoli and P4, SDSM loc. V5353; SDSM 53331, left maxillary fragment with M1, SDSM loc. V541; SDSM 54261, left ramal fragment with p4 (root)–m1, SDSM loc. V5357; SDSM 54272, left partial ramus with p3–p4 alveoli and m1–m2, SDSM loc. V5361; SDSM 54280, right partial ramus with p2 (alveolus) and p3–m2 (p4 broken), SDSM loc. V5359; SDSM 54292, skull with C1 alveolus, P1–P2 roots, and P3–M2, SDSM loc. V541; SDSM 54338, skull with I1 and I3, C1 alveolus, and P1–M2, SDSM loc. V541; SDSM 55101, right partial ramus with p2 (alveolus) p3, p4 root, and m1–m2, SDSM loc. V5351; and SDSM 56110, partial ramus with m1–m2 (both broken) and m3 alveolus, SDSM loc. V541.

East side of Cedar Pass, clay lens in capping channel, base of upper part of the Sharps Formation (early Arikareean), Jackson County, South Dakota: F:AM 49447, skull with I1–P3 alveoli and roots, P4–M1, and M2 alveolus (fig. 9J, K).

White Butte (Chalky Buttes), lower Arikaree Group (early Arikareean), Slope County, North Dakota: AMNH 8084, right partial ramus with p4–m1.

Little Muddy Creek, lower Arikaree Group (early Arikareean), Niobrara County, Wyoming: F:AM 49028, left partial ramus with m1 broken–m2 and m3 alveolus; F:AM 49044, partial skull with C1–P1 and M2 broken, both partial jaws with p2, p3–m1 (all broken or alveoli), and m2; F:AM 49045, skull with I1–M2 and both rami with c1–m3 (fig. 9C–H); F:AM 49047, right partial maxillary with P4–M2; F:AM 49048, left partial ramus with p1 alveolus and p2–m2 all broken; F:AM 49049, right partial ramus with m1–m2 and m3 root; F:AM 49051, left partial ramus with c1 broken, p1–p3 alveoli, p4–m1, and m2 root; F:AM 49052, left par-

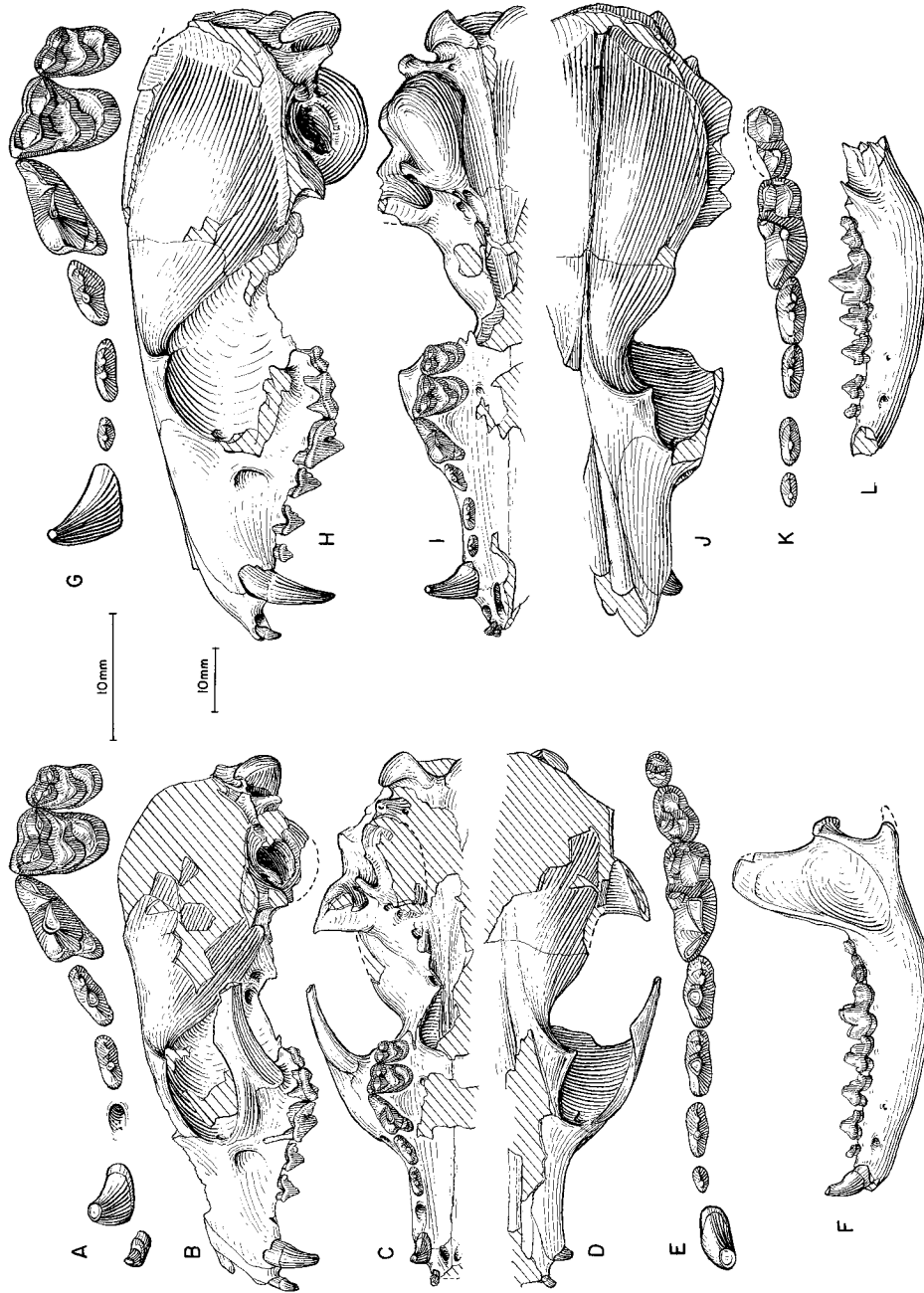


Fig. 7. *Archaeocyon leptodus*. A, Upper teeth, B, lateral, C, ventral, and D, dorsal views of skull, E, lower teeth, and F, ramus, F:AM 63971, Schomp Ranch, Whitney Member, Brule Formation (Whitneyan), Sioux County, Nebraska. G, Upper teeth, H, lateral, I, ventral, and J, dorsal views of skull (auditory bulla reversed from right side), UNSM 25399, Redington Gap, Horn Member, Brule Formation (early Arikarean), Morrill County, Nebraska. K, Lower teeth and L, ramus, UNSM 4486, Redington Gap, Horn Member of Brule Formation (early Arikarean), Morrill County, Nebraska. The longer (upper) scale is for A, E, G, and L, and the shorter (lower) scale is for the rest.

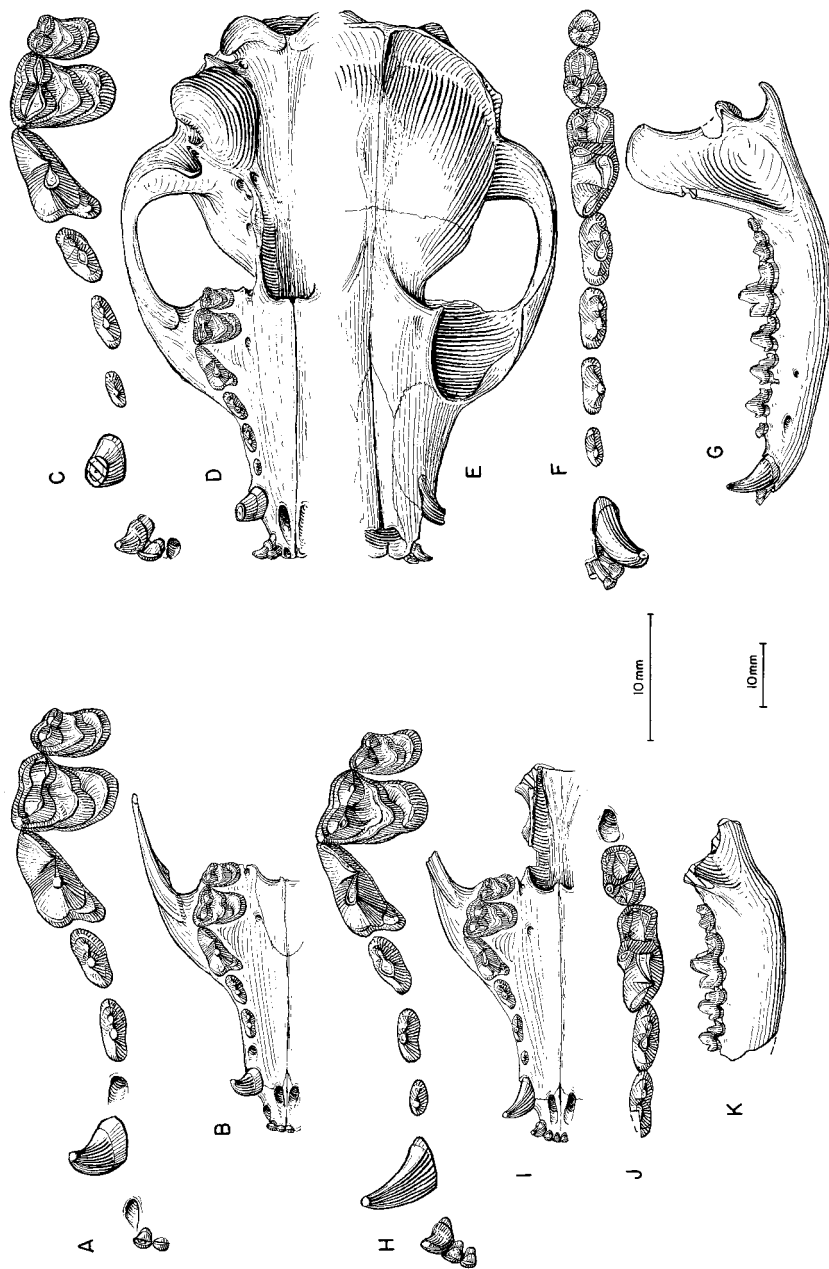


Fig. 8. *Archaeocyon leptodus*. A, Upper teeth and B, palate (P3 reversed from right side), UNSM 26097, 3 mi northeast of Wrights Gap, Horn Member, Brule Formation (early Arikareean), Banner County, Nebraska. C, Upper teeth, D, ventral, and E, dorsal views of skull, F, lower teeth (c1 reversed from right side), and G, ramus (reversed from right side), FMNH P14797, Round House Rock, Horn Member, Brule Formation (early Arikareean), Morrill County, Nebraska. H, Upper teeth, I, palate, J, lower teeth, and K, ramus (reversed from right side), F:AM 50221, south side of Bear Mountain, lower Arikaree Group (early Arikareean), Goshen County, Wyoming. The longer (upper) scale is for A, C, F, H, and J, and the shorter (lower) scale is for the rest.

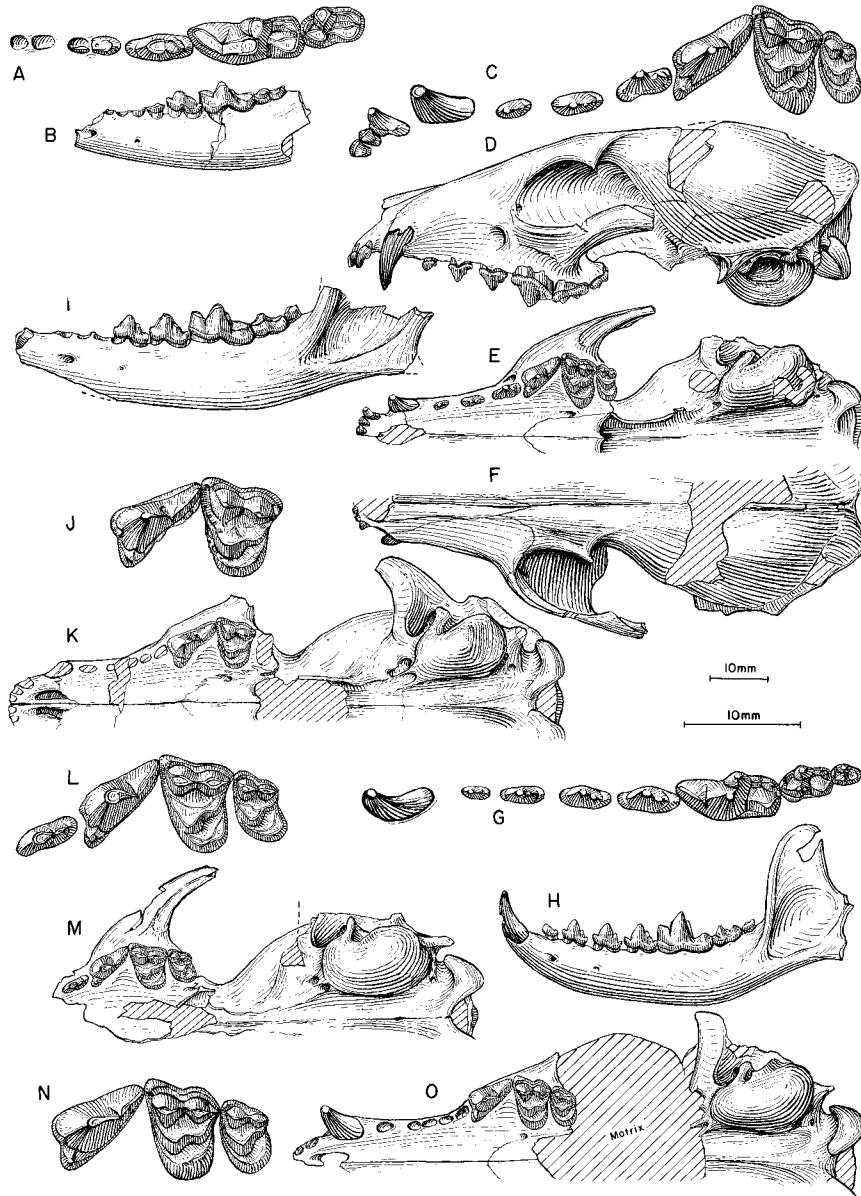


Fig. 9. *Archaeocyon leptodus*. **A**, Lower teeth and **B**, ramus, MCZ 2878, holotype, lower Arikaree Group (early Arikareean), Goshen County, Wyoming. **C**, Upper teeth, **D**, lateral, **E**, ventral, and **F**, dorsal views of skull, **G**, lower teeth, and **H**, ramus (all reversed from right side), F:AM 49045, Little Muddy Creek, lower Arikaree Group (early Arikareean), Niobrara County, Wyoming. **I**, Ramus, F:AM 49052, Little Muddy Creek. **J**, P4–M1, and **K**, ventral view of skull, F:AM 49447, east side of Cedar Pass, Sharps Formation (early Arikareean), Jackson County, South Dakota. **L**, Upper teeth and **M**, ventral view of skull (reversed from right side), F:AM 49032, Muddy Creek, lower Arikaree Group (medial Arikareean), Niobrara County, Wyoming. **N**, Upper teeth and **O**, ventral view of skull (reversed from right side), F:AM 49033, Muddy Creek. The longer (lower) scale is for **A**, **C**, **G**, **J**, **L**, and **N**, and the shorter (upper) scale is for the rest.



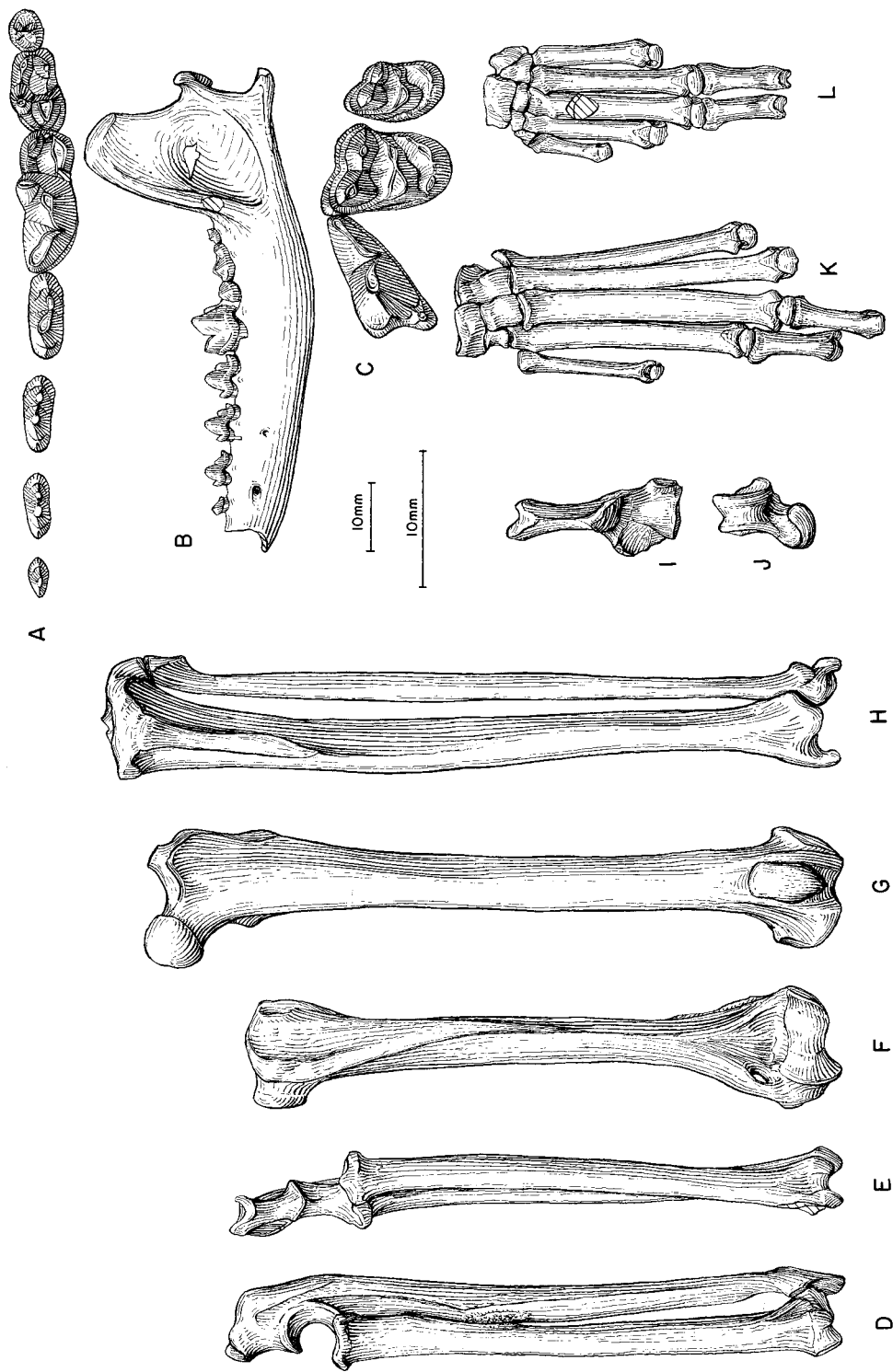


Fig. 10. *Archaeocyon leptodus*. A, Lower teeth, B, ramus, C, upper teeth, D, lateral and E, anterior views of radius and ulna, F, humerus, G, femur, H, tibia and fibula, I, calcaneum, J, astragalus, K, partial foot, and L, partial hand, F:AM 49060, Muddy Creek, lower Arikaree Group (medial Arikareean), Niobrara County, Wyoming (I–L reversed from right side). The longer (lower) scale is for A and C, and the shorter (upper) scale is for the rest.

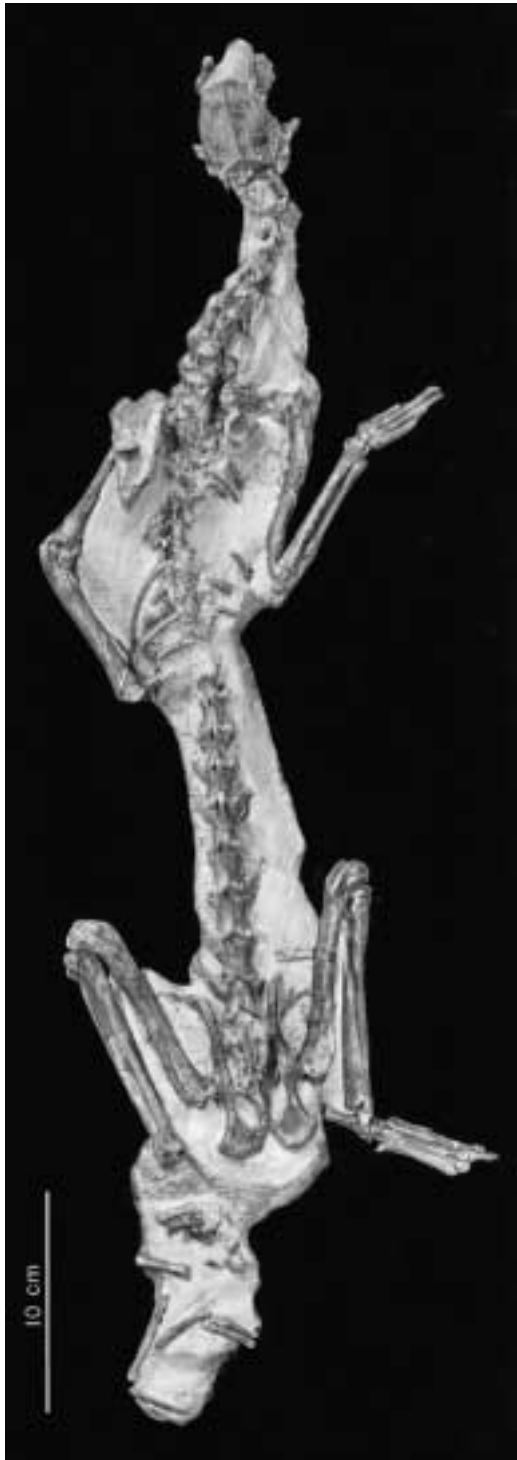


Fig. 11. Partial articulated skeleton of *Archaocyon leptodus*, F:AM 49060, Muddy Creek, lower Arikaree Group (medial Arika-

tial ramus with c1 broken, p1–p2 alveoli, and p3–m3 (fig. 9I); and F:AM 49053, left partial ramus with p3–m1 all broken and m2.

Willow Creek, lower Arikaree Group (early Arikareean), Niobrara County, Wyoming: F:AM 49076, right ramal fragment with p4 broken–m1.

Muddy Creek Area, lower Arikaree Group (medial Arikareean), Niobrara and Platte counties, Wyoming: F:AM 49021, left partial ramus with p3–p4 and m1–m2 both broken; F:AM 49026, right maxillary fragment with M1–M2 and right ramal fragment with m2; F:AM 49030, partial skull with P2 broken–M2, right and left partial rami with p3–m3, both humeri, radius, partial ulna, and carpals with the proximal ends of metacarpals II–IV; F:AM 49031, incomplete edentulous skull, humerus, tibia, and calcaneum; F:AM 49032, partial skull with right P3–M2 (fig. 9L, M); F:AM 49033, partial skull with I2–I3 alveoli, C1, P1–P3 alveoli, and P4–M2 (fig. 9N, O); F:AM 49035, right partial ramus with p1–p4 alveoli and roots and m1–m2; F:AM 49036, left partial maxillary with P4 broken–M2, left partial ramus with p2 alveolus–m3, right ramal fragments, detached broken bullae, and fragments; F:AM 49037, left partial ramus with p1–p3 alveoli and p4 broken–m2; F:AM 49038, right partial maxillary with P3–M2; F:AM 49039, right partial maxillary with P4–M2 (M1 broken); F:AM 49040, left partial ramus with c1–p1 broken and p2–m1; F:AM 49040A, left partial maxillary with P3 broken–M2; F:AM 49050, right and left partial rami with p4 broken–m3; F:AM 49060, partial skull with P3 broken–M2 (fig. 10C), partial mandible with c1 broken–m3 (fig. 10A, B), and partial postcranial skeleton (fig. 11) including articulated vertebrae, scapula, humerus (fig. 10F), radius and ulna (fig. 10D, E), nearly complete manus including metacarpals I–V and two first phalanges (fig. 10L), pelvis, femora (fig. 10G), tibiae and fibulae (fig. 10H), calcaneum (fig. 10I), astragalus (fig. 10J), tarsals, and metatarsals I–V and two first phalanges (fig. 10K); F:AM 50224, right partial ramus with c1 broken

←

reean), Niobrara County, Wyoming. Photograph by Lorrain Meeker.

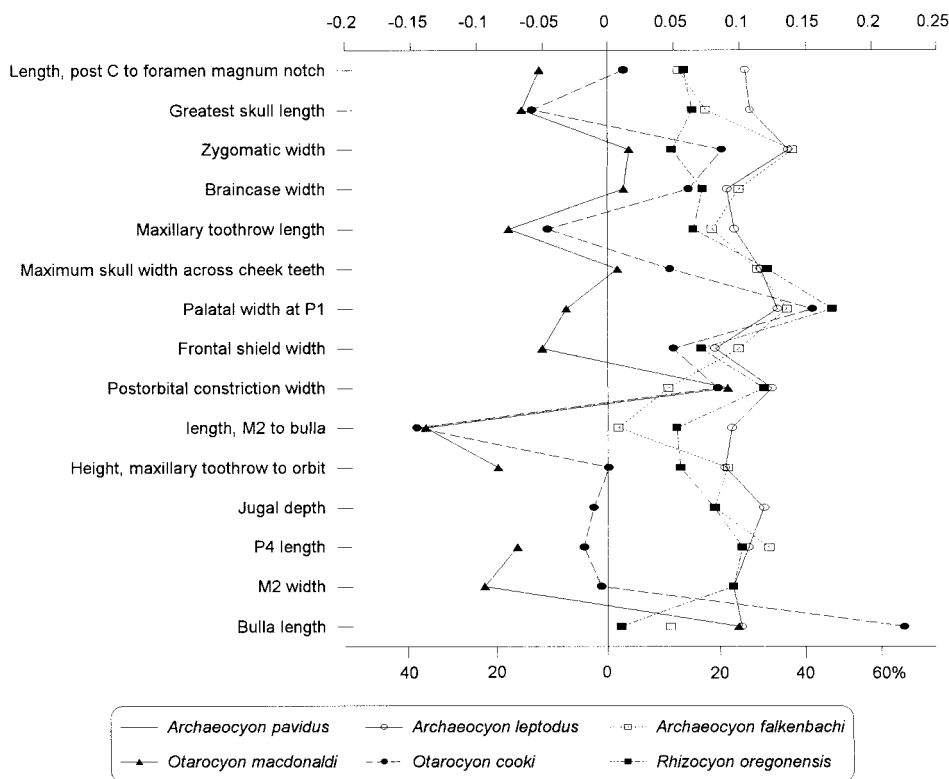


Fig. 12. Log-ratio diagram for cranial measurements of *Archaeocyon*, *Otarocyon*, and *Rhizocyon* using *A. pavidus* as a standard for comparison (straight line at zero). See text for explanations and appendix II for measurements and their definitions.

and p1 alveolus–m2; and F:AM 50226, right partial ramus with m1 broken.

South side of Bear Mountain, lower Arikaree Group (early Arikareean), Goshen County, Wyoming: F:AM 50221, anterior half of skull with I1–M2 and right partial ramus with p3–m2 and m3 alveolus (fig. 8H–K).

Horse Creek area, lower Arikaree Group (early Arikareean), Goshen County, Wyoming: F:AM 49069, right and left partial rami with p2–m2; F:AM 49072, left partial ramus with p2 alveolus, p3–m1 all broken, m2, and m3 alveolus; F:AM 50222, left partial ramus with i1–c1 broken, p1 alveolus, p2 broken–p4, and m1 broken–m2; and F:AM 99286, partial palate with P3 broken–M2 and associated partial cranium.

Canyon Ferry Area, Toston Formation (early Arikareean), Lewis and Clark County, Montana: USNM 19097, right partial ramus

with i1–p2 alveoli, p2–m1 all broken, m2, and m3 alveolus; and USNM 20144, right partial ramus with p1 alveolus–m2.

DISTRIBUTION: Whitneyan of Nebraska and Wyoming; early Arikareean of Nebraska, Wyoming, Montana, South Dakota, and North Dakota; and medial Arikareean of Wyoming.

EMENDED DIAGNOSIS: *Archaeocyon leptodus* differs from *A. pavidus* in its larger size and elongated lower first molar with an open trigonid. The rostrum in *A. leptodus* is not shortened, as contrasted with that of *A. falckenbachi*. *A. leptodus* is distinct from the phlaocyonine clade by its possession of the following primitive characters: posteriorly oriented paroccipital process that is not fused with the bulla, weak metaconule of M1, lack of a connection between metaconule and lingual cingulum of M2, and lack of a protostylid on m1.

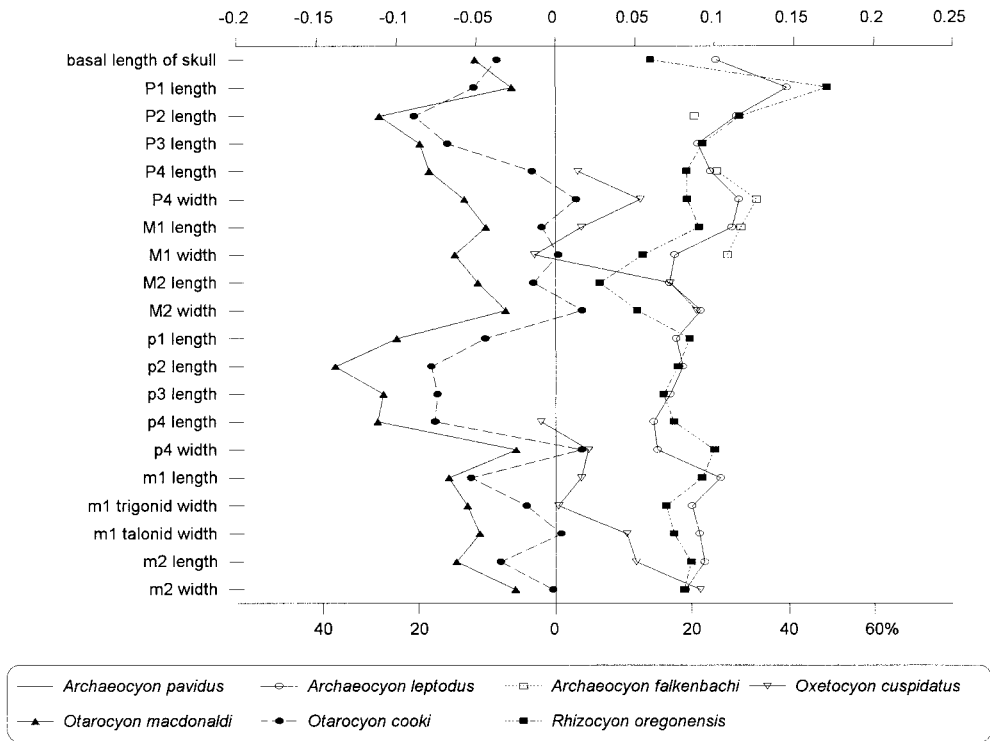


Fig. 13. Log-ratio diagram for dental measurements of *Archaeocyon*, *Oxetocyon*, *Otarocyon*, and *Rhizocyon* using *A. pavidus* as a standard for comparison (straight line at zero). See text for explanations and appendix III for summary statistics of measurements and their definitions.

**DESCRIPTION AND COMPARISON:** The present reference of a large number of specimens from the Whitneyan and early Arikarean of the northern Great Plains transforms *Archaeocyon leptodus* from that of an obscure species to one that has the best representation among early borophagines both in terms of its anatomy and in the continuity of its fossil record. Nearly complete skulls demonstrate the generalized morphology of this basal borophagine. The skull is primitive in its unshortened snout, a single temporal crest, a wide masseteric scar on the jugal, and lack of fusion between the paroccipital process and the auditory bulla. In overall cranial proportions, *A. leptodus* is very similar to *Rhizocyon* and *Cormocyon* (fig. 12). The UNSM sample from the Horn Member of Brule Formation tends to have a more ventrally oriented paroccipital process, whereas individuals from the Muddy Creek locality of the lower Arikaree Group have a less ventrally oriented process (two specimens, F:AM

49032 and 49060, still have fully posteriorly directed process). Even in individuals that have a mainly ventrally oriented paroccipital process, however, the base of the process is mostly free of contact with the posterior aspect of the bulla. There is a slight tendency in *A. leptodus* to enlarge its bulla relative to the primitive condition in *A. pavidus*.

Teeth of *Archaeocyon leptodus* are overall 24% larger than those of *A. pavidus*, 21% larger than those of *Rhizocyon oregonensis*, and 24% smaller than those of *Cormocyon copei* (average percentage of all measurements). Besides its intermediate size, *A. leptodus* is also intermediate in its possession of an open trigonid on m1 as opposed to the more closed trigonid in *A. pavidus* and *R. oregonensis*, but it lacks a distinct metaconule on M1 and a connection between the metaconule and lingual cingulum of M2 seen in *Cormocyon*.

The most prominent feature on the holotype of *A. leptodus* is its elongated, open tri-

gonid of m1. Its paraconid is more longitudinally oriented in contrast to the primitively more oblique orientation in other *Archaeocyon*. Related to this long trigonid, the p4 also becomes slender. In this latter feature, the holotype is the most extreme among referred specimens (see discussion below). Within the hypodigm, there is a gradual lengthening of the trigonid through time. Our sample from the Whitney and Horn Members of the Brule Formation shows little change in this feature, whereas those from the lower Arikaree Group of Wyoming tend to have a more open trigonid.

DISCUSSION: We recognize *Archaeocyon leptodus* from the Whitneyan through medial Arikareean of the northern Great Plains as distinct from *Rhizocyon oregonensis* of similar age from the John Day Basin. Earlier (from Whitney and Horn Members of Brule Formation) individuals of *A. leptodus* are not easily distinguished in the dentitions, both in quantitative and qualitative traits, from individuals of *R. oregonensis*. The main distinction between these lies in a few subtle characters in *A. leptodus*: more posteriorly oriented paroccipital process, slightly larger bulla, M1 hypocone more posteriorly positioned, M2 lacking a connection between metaconule and internal cingulum, and a more elongated m1. We thus recognize two similar, but morphologically distinguishable, species on either side of the continental divide, similar in this regard to the *Cormocyon copei* and *C. haydeni* species pair.

The elongated trigonid and slender premolars, especially prominent in the holotype of *Archaeocyon leptodus*, are more typically seen in the canine clade, as in the contemporaneous *Leptocyon*. However, the ramus of *A. leptodus* is relatively robust and its premolars are not widely spaced, unlike those in *Leptocyon*, which has a much more gracile horizontal ramus and long diastemata between premolars. Elsewhere, we (Wang and Tedford, 1996) have identified a *Leptocyon* specimen from the Orella Member of the Brule Formation as the earliest record of the subfamily Caninae. This fragmentary lower jaw, UNSM 25354, has the simplified premolars typical of *Leptocyon* but still has a relatively unelongated m1. If our recognition of this Orellan specimen as the most primi-

tive Caninae is correct, the elongation of the m1 must have happened after the simplification of the premolars. This would imply that the elongation of the m1 in *A. leptodus*, which lacks simplified premolars, was probably independently acquired, as it surely had happened at least once in *Cormocyon haydeni* and in more derived borophagines (see further discussion under Phylogenetic Analysis).

#### *Archaeocyon falkenbachi*, new species

Figure 14

HOLOTYPE: F:AM 49029, partial skull with C1–P1 alveoli and P2–M1 (P3 alveolus) (fig. 14) from the Muddy Creek Area, 1.5 mi west of bridge, 65 ft below the white layer, lower Arikaree Group (medial Arikareean), Niobrara County, Wyoming.

ETYMOLOGY: Named for the late Charles H. Falkenbach, who led the Frick Laboratory parties collecting extensively in Wyoming.

REFERRED SPECIMEN: Holotype only.

DISTRIBUTION: Medial Arikareean of Wyoming.

DIAGNOSIS: *Archaeocyon falkenbachi* differs from all other species of *Archaeocyon* in its inflated, more bulbous bulla with little anterolateral compression that characterize other species; short temporal fossa; wide zygoma; closely spaced premolars; reduced P2 posterior accessory cusp; and M1 very wide for its length.

DESCRIPTION AND COMPARISON: The single skull of the holotype constitutes the only specimen of this rare species. The shortening of its skull affects several proportional relationships of its cranium. Compared to most species of *Archaeocyon*, *Rhizocyon*, and *Cormocyon*, it has a shortened temporal fossa and a broadened zygomatic arch (fig. 12). The paroccipital process is posteriorly oriented in contrast to the ventrally oriented processes in *Cormocyon*. The bulla is shorter and less anteriorly narrowed than in *A. leptodus*. The opening for the external auditory meatus is more rounded, due to the development of a short meatal tube, than in most individuals of *A. leptodus*. Other than these differences, *A. falkenbachi* is very close to the general stage of evolution of *A. leptodus*.

Dental morphology of *Archaeocyon fal-*

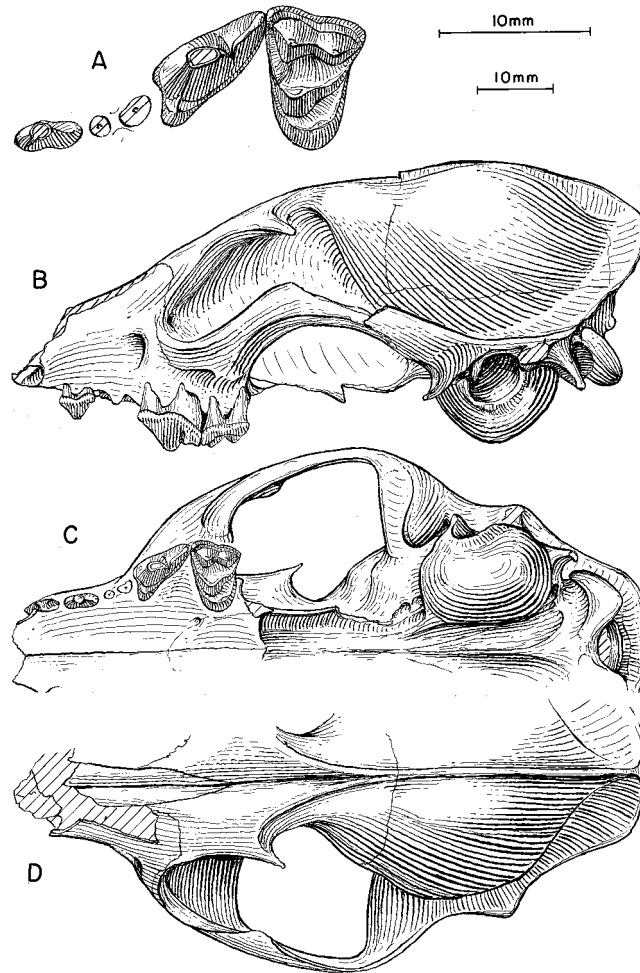


Fig. 14. *Archaeocyon falkenbachi*. A, upper teeth, B, Lateral, C, ventral and D, dorsal views of skull, and F:AM 49029, holotype, Muddy Creek, lower Arikaree Group (medial Arikareean), Niobrara County, Wyoming. The longer (upper) scale is for A, and the shorter (lower) scale is for the rest.

*kenbachi* is also very close to that of *A. leptodus*. The only differences between the two species are a simplified P2 (lacking a posterior accessory cusp) and a mediolaterally wider M1 in *A. falkenbachi*.

DISCUSSION: Slight wear on the tips of the upper molars and the presence of a low but distinct sagittal crest indicate that F:AM 49029 is an adult. It is unlikely that its unique cranial proportions cited above (features related to brachycephally) are due to young age. *Archaeocyon falkenbachi* thus represents a lineage divergent from *A. leptodus*, which does not appear to lead to other lineages.

#### *Oxetocyon* Green, 1954

TYPE SPECIES: *Oxetocyon cuspidatus* Green, 1954.

INCLUDED SPECIES: Type species only.

DISTRIBUTION: Whitneyan of South Dakota and Nebraska, and early Arikareean of Nebraska.

EMENDED DIAGNOSIS: In contrast to *Archaeocyon*, *Oxetocyon* shares with *Otarocyon* such derived characters as taller P4 parastyle, conate talonid cusps on m1, m1 entoconid separated from the metaconid by a notch, and m2 metaconid larger than protoconid. In addition, *Oxetocyon* has several au-

tapomorphies related to its unusual mode of hypocarnivory: enlarged and quadrate upper molars, strong anterolingual cingulum on M1, distinct cleft on the lingual cingulum that isolates the large conate hypocone on the M1, and a distinct metaconule on M1. *Oxetocyon* is primitive relative to *Rhizocyon* and more derived borophagines in its lack of a connection between metaconule and posterior lingual cingulum on M2, and absence of a protostyloid on m1.

*Oxetocyon cuspidatus* Green, 1954

Figure 15

*Oxetocyon cuspidatus* Green, 1954: 218, fig. 1. Galbreath, 1956: 375. Tanner, 1973: 66, fig. 1. Wang and Tedford, 1996: 446, fig. 8. Munthe, 1998: 134.

**HOLOTYPE:** SDSM 2980 (AMNH cast 80132), left maxillary fragment with M1 and broken alveoli of P4 and M2 (fig. 15A), from 7 mi east of Rockyford, Protoceras Channels, Poleslide Member of Brule Formation (Whitneyan), Shannon County, South Dakota.

**REFERRED SPECIMENS:** Whitney Member of Brule Formation (Whitneyan), Morrill and Sioux counties, Nebraska: UNSM 2665, partial skull with C1 broken alveolus, P1–P3 alveoli, and P4–M2 (Tanner, 1973: fig. 1A–C; fig. 15F–H) from UNSM loc. Mo-104, base of Roundhouse Rock, 8.5 ft below the base of the Upper Ash; UNSM 25081, left ramal fragment with p3–m1 all broken, UNSM loc. Sx-28; UNSM 25381, left maxillary fragment with P3 alveolus–M2 (fig. 15B, C) and fragment of dorsal roof cranium, UNSM loc. Mo-0, 7 mi southeast of Broadwater, 10 ft above railroad grade; and UNSM 25698 (AMNH cast 96707), right partial ramus with p3 alveolus–m3 (fig. 15D, E), UNSM loc. Mo-107 or Mo-108.

Gering Formation (early Arikareean), Morrill County, Nebraska: UNSM 11695 (AMNH cast 104655), right partial ramus with p4–m1 and alveoli of c1–p3.

**DISTRIBUTION:** Whitneyan of South Dakota and Nebraska, and early Arikareean of Nebraska.

**EMENDED DIAGNOSIS:** As for monotypic genus.

**DESCRIPTION AND COMPARISON:** Although Tanner's (1973) referred partial skull (UNSM

2665) substantially increased knowledge of *Oxetocyon cuspidatus*, which was established on a single M1, much remains to be learned about this rare species. Tanner's description of UNSM 2665 is still the main source of information on the cranial morphology of *Oxetocyon*. To this we can only add a fragment of skull roof associated with upper teeth (UNSM 25381), which only preserves the posterior segment of the sagittal crest (single crested) and partial nuchal crest. UNSM 25381 (fig. 15B, C) is a somewhat larger individual with primitive dental features compared to the holotype and UNSM 2665: it has a smaller protocone of P4, a less pronounced notch on the labial cingulum of M1, a less deep cleft anterior to the hypocone on the lingual cingulum of M1 and absence of such a cleft on M2, lack of a discrete hypocone on M1, metaconule less enlarged on M1–M2, and overall less transverse division of the M1. While certainly introducing additional dental variations, our inclusion of UNSM 25381 helps to bridge the large morphological gap between the holotype of *O. cuspidatus* and other basal borophagines such as *Archaeocyon*.

The present referral of two ramal fragments is largely based on their conate cusps of the lower molars and on the generally good occlusion between the upper and lower teeth. The rounded shape of the cusps of m1 talonid and m2 are in sharp contrast to the crestlike cusps of the contemporaneous *Hesperocyon* and to a lesser extent those of *Otarocyon*, but is consistent with the cusp shape of the upper teeth of *O. cuspidatus*. Furthermore, the high m2 entoconid occludes well with the basin between the enlarged lingual cingulum and protocone of the M2. Besides these salient features, the referred lower jaws and teeth are quite similar to those of *Archaeocyon* species.

Our reference of these jaws to *O. cuspidatus* has some interesting phylogenetic implications. While the upper teeth of *Oxetocyon* bear certain similarities to those of *Cynarctoides* and *Phlaocyon*, such as the quadrate appearance of M1 and the presence of a M1 hypocone (however, *Cynarctoides* and *Phlaocyon* do not have the transverse cleavage across the M1 so characteristic of *Oxetocyon*), the referred lower teeth lack the cor-

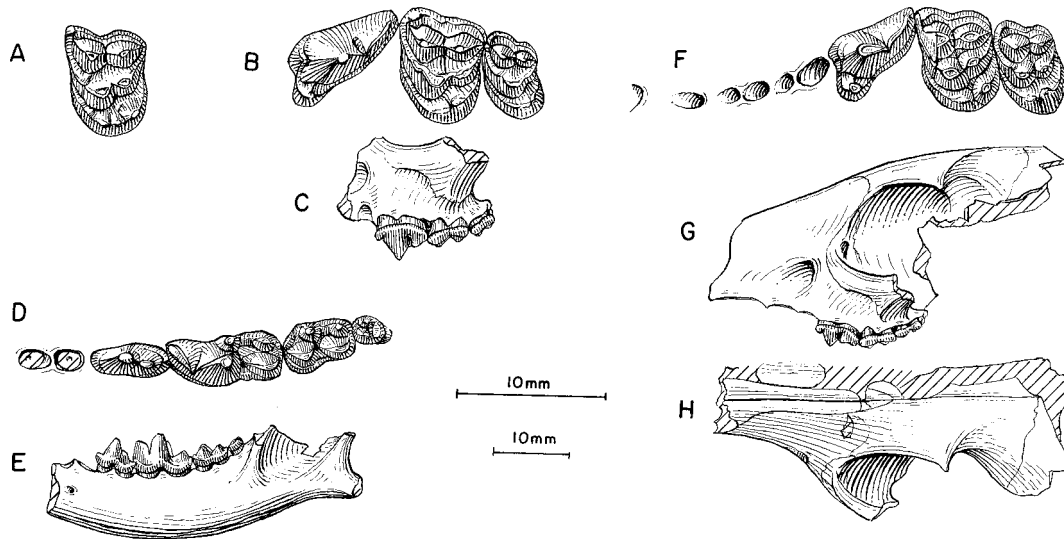


Fig. 15. *Oxetocyon cuspidatus*. **A**, M1, SDSM 2980, holotype, 7 mi east of Rockyford, Poleslide Member of Brule Formation (Whitneyan), Shannon County, South Dakota. **B**, Upper teeth and **C**, lateral view of maxillary, UNSM 25381, 7 mi southeast of Broadwater, Whitney Member, Brule Formation (Whitneyan), Morrill County, Nebraska. **D**, Lower teeth and **E**, ramus (reversed from right side), UNSM 25698, Whitney Member, Brule Formation (Whitneyan), Morrill County, Nebraska. **F**, Upper teeth, and **G**, lateral and **H**, dorsal views of partial skull, UNSM 2665, Roundhouse Rock, Whitney Member, Brule Formation (Whitneyan), Sioux County, Nebraska. The longer (upper) scale is for A, B, D, and F, and the shorter (lower) scale is for the rest.

responding specializations of the Phlaocyoniini, such as the presence of a protostylid on m1–m2. *Oxetocyon* thus possesses a mixture of features that suggests an evolutionary pathway independent from the phlaocyoniine clade.

**DISCUSSION:** *Oxetocyon* represents one of the first of many trends toward hypocarnivory within the subfamily Borophaginae. During the Whitneyan, it is also the most hypocarnivorous canid, with its own peculiar way of enlarging and squaring up the upper molars and dividing them into roughly symmetrical parts along a transverse cleavage in the middle of the crown. The absence of a connection between the metacone and lingual cingulum on M2 and the lack of a protostylid on m1 indicate only a basal relationship with regard to the phlaocyoniine clade, despite the common possession of a similarly developed hypocone on M1.

*Oxetocyon* and *Otarocyon* share a few derived features, such as conate cusps on lower molars, lingually opened talonid basin on m1, and high m2 metaconid. Although our

cladistic analysis indicates a sister relationship of the two genera because of these characters, it is conceivable that the hypocarnivorous characters may have been independently acquired since the dissimilarity between the upper molars of these genera is so great. Such speculation may be confirmed with knowledge of the basicranium of *Oxetocyon*. Meanwhile, we maintain two distinct genera in the recognition that they represent two distinct clades, even though they may be sister taxa.

#### *Otarocyon*, new genus

**TYPE SPECIES:** *Cynodesmus cooki* Macdonald, 1963.

**ETYMOLOGY:** Greek: *otaros*, large eared; *cyon*, dog.

**INCLUDED SPECIES:** *Otarocyon macdonaldi*, new species; and *Otarocyon cooki* (Macdonald, 1963).

**DISTRIBUTION:** Orellan of South Dakota and Montana, early Arikarean of South Da-



kota, and early to medial Arikareean of Wyoming.

**DIAGNOSIS:** Species of the highly derived *Otarocyon* are united by many synapomorphies: hypertrophied auditory bulla, antero-posteriorly flattened paroccipital process that is ventrally oriented, large suprameatal fossa, shortened rostrum, broadened braincase, short temporal fossa, paired temporal crests, single-cusped, short, and tall crowned premolars, enlarged P4 protocone, elevated lingual cingulum of M1, conical entoconid of m1 separated anteriorly from metaconid by a deep notch (lingually opened talonid basin), m2 metaconid much larger and higher than protoconid. *Otarocyon* is primitive compared to *Rhizocyon* and more derived borophagines in its transversely elongated upper molars and lack of a connecting ridge between the lingual cingulum and metaconule of M2.

**DISCUSSION:** The abrupt appearance of the morphologically highly derived *Otarocyon* in the Orellan without any apparent predecessor presents a problem for phylogenetic interpretation. Although *Otarocyon* shares with *Archaeocyon* derived characters of the canine-borophagine clade (reduced M1 parastyle, anteriorly extended M1 lingual cingulum, more basined talonid of m1, and high m2 entoconid), the ways that these morphologies are achieved, however, seem to suggest independent development of these characters. For example, the highly conate m1 entoconid is interrupted anteriorly by a deep notch separating the entoconid from the metaconid, and is in sharp contrast to a ridgelike entoconid, which reaches anteriorly to the base of the metaconid and fully encloses a talonid basin in all primitive hesperocyonines, canines, and borophagines. This peculiarity of the bicuspid talonid is not seen elsewhere in the borophagines. In absence of more transitional forms, however, we must assume for the purpose of parsimony that these derived characters in *Otarocyon* are synapomorphies shared with other borophagines, rather than being homoplasies.

For all its unique morphology, *Otarocyon* has a living canine analog, fennec fox (*Vulpes (Fennecus) zerda*), from desert regions of northern Africa and the Arabian Peninsula. In addition to being among the smallest foxes, the fennecs share with *Otarocyon* a

striking list of derived similarities: expanded braincase, short nasal process of frontal, parasagittal temporal crests, enlarged bulla and narrowed interbullar space, loss of low septum inside bulla, paroccipital process fully cupping bulla, simplified premolars, and enlarged m2 metaconid. The list is long enough to raise the intriguing possibility of the origin of ancestral fennecs from *Otarocyon*. The implicit long hiatus in the fossil record (approximately 25 m.y.) notwithstanding, such a proposition, however, would have to overcome a longer list of derived characters in fennecs that indicates their position within the Vulpini (Tedford et al., 1995: characters 4–18), although some of these characters are not unique to vulpines or cannot be observed in available materials of *Otarocyon*. For example, *Otarocyon* does not possess such canine characters as slender horizontal ramus, narrow premolars, elongated P4 and m1, m2 anterolabial cingulum, or loss of entepicondylar foramen of humerus. Furthermore, fennecs differs from *Otarocyon* in additional details that require explanation if they are postulated as sister-groups: presence of a frontal depression (seen in most vulpines), lack of a suprameatal fossa, presence of a short bony external auditory meatus, and an extension of the ectotympanic ring to form the dorsal passage of auditory meatus. It is therefore more parsimonious to view the similarities between *V. zerda* and *Otarocyon* as independently derived. Such conclusion is also consistent with studies of chromosomes, allozymes, and mitochondrial DNA of living canids (Wayne et al., 1987a, 1987b; Wayne and O'Brien, 1987; Wayne et al., ms), which place the fennec within the clade of living foxes but not in a more basal position as would be predicted by an *Otarocyon*–*Fennecus* sister relationship.

This remarkable convergence in two subfamilies of Canidae provides a valuable living analog (*Vulpes zerda*) of a fossil group (*Otarocyon*) for inference of its soft anatomy and ecology. For example, we can reasonably infer that *Otarocyon* must have had a very large external ear, as have the fennecs, and that the auditory apparatus was sensitive to low-frequency hearing (Lay, 1972; Webster and Webster, 1980). The implication that *Otarocyon* may have lived in an open envi-

ronment, as do the living fennecs, is inherently less testable with the fossil alone, but no less interesting. The peculiar middle ear morphology in *Otarocyon* was already present in Orellan (in *O. macdonaldi*) and seems to indicate at least patchy presence of open environments at the time, as also concluded by Retallack (1983) in a study of soils of Orellan age in South Dakota.

***Otarocyon macdonaldi*, new species**

Figure 16G–L

**HOLOTYPE:** AMNH 38986, skull with I1–M2 (C1 broken) and mandible with i1–m3 (fig. 16G–L) from Scenic Member of Brule Formation (Orellan), south of White River, near Scenic, Pennington County, South Dakota.

**ETYMOLOGY:** Named for J. Reid Macdonald for his singular contributions to the Cenozoic paleontology and stratigraphy of South Dakota.

**REFERRED SPECIMEN:** Cooper Gulch Locality No. 1, Toston Formation (?Orellan), Lewis and Clark County, Montana: UMMP 7933 (AMNH cast 127173), partial rostrum with left P4–M2 and right P2–M2, UMMP loc. MV8303.

**DISTRIBUTION:** Orellan of South Dakota and Montana.

**DIAGNOSIS:** *O. macdonaldi* is easily distinguishable from *Archaeocyon* and other primitive borophagines by several derived characters shared with *O. cooki*: brachycephalic skull, shortened nasal process of frontal, laterally expanded braincase, paired temporal crests, enlarged auditory bulla, large supra-meatal fossa, flattened paroccipital process hugging the bulla, short, simple, and high-crowned premolars, enlarged P4 protocone, high M1–M2 lingual cingulum, short trigonid, high hypoconid and entoconid, lingually opened talonid basin on m1, and high metaconids of m1–m2. *O. macdonaldi* is more primitive than *O. cooki* in its lesser development of some of the above characters: smaller size; longer and narrower muzzle; P1–P3 and p1–p3 anteroposteriorly longer with crown height lower relative to length; P4 protocone smaller; braincase less expanded relative to length of skull; parasagittal crests weaker and more widely separated; m1

with trigonid more elongate and shear less oblique, metaconid smaller and lower crowned, and entoconid less conical and lower crowned.

**DESCRIPTION AND COMPARISON:** As in *Otarocyon cooki*, *O. macdonaldi* is easily distinguished from the far more conservative *Archaeocyon* in the numerous synapomorphies shared between *O. cooki* and *O. macdonaldi* (see Diagnosis above). Distinctions between *O. cooki* and *O. macdonaldi*, however, are far more subtle. Besides its slightly smaller size (3% in basal length of skull, but 9% in average dental measurements; see appendices II, III), *O. macdonaldi* is mainly distinct from *O. cooki* in its slightly lesser degree of development of the advanced features: skull less brachycephalic, parasagittal crests less prominent, braincase less expanded, m1 trigonid less shortened, and lower molar cusps lower. Similarly, the teeth of *O. macdonaldi* are little different from those of *O. cooki* other than their smaller size.

The single referred specimen from Montana (UMMP 7933) displays certain subtle variations that are not present in the holotype: a weak lingual cingulum on P2, presence of an additional (third) root on the P3 and a distinct lingual cingulum supported by this extra root, presence of a narrow labial cingulum on the P4, better developed P4 parastyle, and better developed M1 metaconule.

**DISCUSSION:** In a thesis on the evolution of mammalian molars, Patterson (1956: 48) used AMNH 38986 to illustrate the field concept of dental development and its interactions with phylogenetic constraints (he did not give a formal taxonomic identification of this specimen and merely called it “an undescribed Oligocene dog”). To him, the increased size and height of P4 protocone and M1–M2 hypocones (lingual cingula) and similar enlargements of m1 entoconid and m1–m2 metaconids are all related to a genetic process of increasing size of the lingual portions of the cheekteeth. It is relevant to note that Patterson’s observation is even better illustrated in UMMP 7933, in which the lingual cingula of the entire upper toothrow, including that of the P2–P3, are well-developed.

Despite its much earlier appearance in the Orellan and being separated from its early

Arikareean sister-species *Otarocyon cooki* by at least 2 m.y., *O. macdonaldi* basically possesses all the morphological specializations present in *O. cooki*, although usually to a slightly lesser degree. In other words, once the major adaptive features were acquired, the *Otarocyon* lineage remained essentially unchanged except for slight size increase and slightly greater emphasis on the various features (e.g., greater expansion of braincase, stronger temporal crests, shorter premolars and m1 trigonid). These minor adjustments probably reflect an anagenetic series stretching from the Orellan to the early Arikareean.

*Otarocyon cooki* (Macdonald, 1963)

Figures 16A–F, 17, 18

*Cynodesmus cooki* Macdonald, 1963: 210, figs. 26, 27. 1970: 58.

**HOLOTYPE:** SDSM 54308, right partial ramus with p4–m2 (fig. 17A, B), from the Wounded Knee area, SDSM loc. V5359, upper part of the Sharps Formation (early Arikareean), Shannon County, South Dakota (Macdonald, 1963).

**REFERRED SPECIMENS:** From the type area: LACM 13975, right partial ramus with m1 broken, m2, and m3 alveolus, LACM loc. 1955; SDSM 55132, right partial ramus with p4 broken–m3, SDSM loc. V5410, upper part of the Sharps Formation (early Arikareean).

Little Muddy Creek, lower Arikaree Group (early Arikareean), Niobrara County, Wyoming: F:AM 49041, right partial ramus with c1 (broken), p1–p3 alveoli, and p4–m3; F:AM 49042, partial skull with I2–M2, right and left partial rami with i3–m3 (fig. 17H–J), articulated right humerus and radius and ulna (fig. 17K–M), left humerus and incomplete radius and ulna and first phalanx; F:AM 49043, posterior part of skull, left ramus with c1 (broken) and p1–m3 (fig. 17C–G), and distal part of tibia; F:AM 49046, left partial maxillary with P3 (broken)–M2; and F:AM 49055, right partial ramus with p3–m2 (m1 broken) and m3 (alveolus).

Muddy Creek, lower Arikaree Group (medial Arikareean), Niobrara County, Wyoming: F:AM 49020, skull with I1 (alveolus) and I2–M2, mandible with i2–m3 (fig. 16A–F), articulated left distal partial humerus, and

broken radius and ulna; F:AM 49022, left partial maxillary with P4–M2; F:AM 49023, partial skull with P1–P3 alveoli and P4 (broken)–M2; F:AM 49024, left partial ramus with p1–p2 (both broken) and p3–m1; F:AM 49025, right partial ramus with c1–m3; F:AM 49027, fragmentary skull with P4–M2, right partial ramus with c1–p1 both broken, p2–m2, and m3 alveolus, and postcranial fragments including articulated tarsals and metatarsals I–V, from 25 ft above the “Gering–Monroe Creek” contact; and F:AM 49034, left partial maxillary with P4–M1, from 25 ft below white layer.

North of Jeriah, lower Arikaree Group (?medial Arikareean), Niobrara County, Wyoming: F:AM 49071, right partial ramus with p3 (broken alveolus), p4 (broken), m1–m2, and m3 alveolus.

**DISTRIBUTION:** Early Arikareean of South Dakota, and early to medial Arikareean of Wyoming.

**EMENDED DIAGNOSIS:** As the terminal species in the *Otarocyon* clade, *O. cooki* has, relative to *O. macdonaldi*, more brachycephalic skull, more expanded braincase, and more prominent temporal crests.

**DESCRIPTION AND COMPARISON:** The present reference of more complete material than was available in the topotype series (Macdonald, 1963) reveals a remarkable animal with highly derived cranial morphology mixed with a relatively primitive, unspecialized dentition. This extraordinary combination of cranial and dental structures is unique in many ways and requires a more detailed description.

The brachycephally of *Otarocyon cooki* affects the skull shape in several ways. Besides having a relatively short and broad rostrum, the braincase is also considerably expanded laterally (fig. 12). The nasal process of the frontal between the maxillary and nasal is also shortened. The parallel temporal crests are strong.

The most prominent feature of the basicranium of *Otarocyon cooki* is its hypertrophied auditory bulla (fig. 16, 17). The external dimensions of the bulla far exceed in relative size of skull those of most carnivorans. The bulla is nearly twice as large as that of a similar-size *Hesperocyon* in linear dimensions and thus must be approximately eight

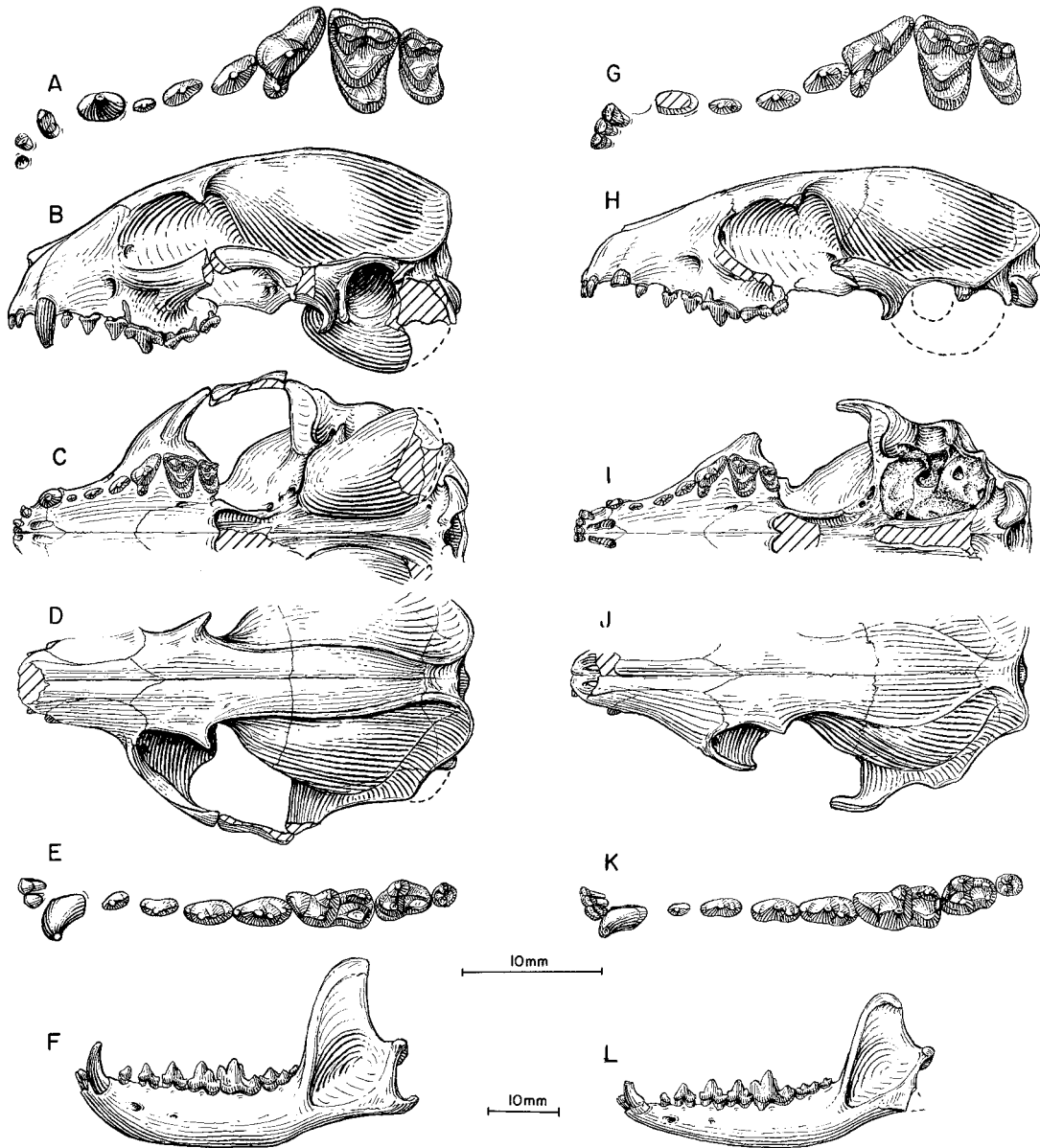


Fig. 16. **A**, Upper teeth, **B**, lateral, **C**, ventral and **D**, dorsal views of skull, **E**, lower teeth, and **F**, ramus, *Otarocyon cooki*, F:AM 49020 (P1, paroccipital process, p2, and p3 reversed from right side), Muddy Creek, lower Arikaree Group (medial Arikareean), Niobrara County, Wyoming. **G**, Upper teeth, **H**, lateral, **I**, ventral, and **J**, dorsal views of skull, **K**, lower teeth, and **L**, ramus, *Otarocyon macdonaldi*, AMNH 38986, holotype, south of White River near Scenic, Scenic Member, Brule Formation (Orellan), Pennington County, South Dakota. The longer (upper) scale is for A, E, G, and K, and the shorter (lower) scale is for the rest.

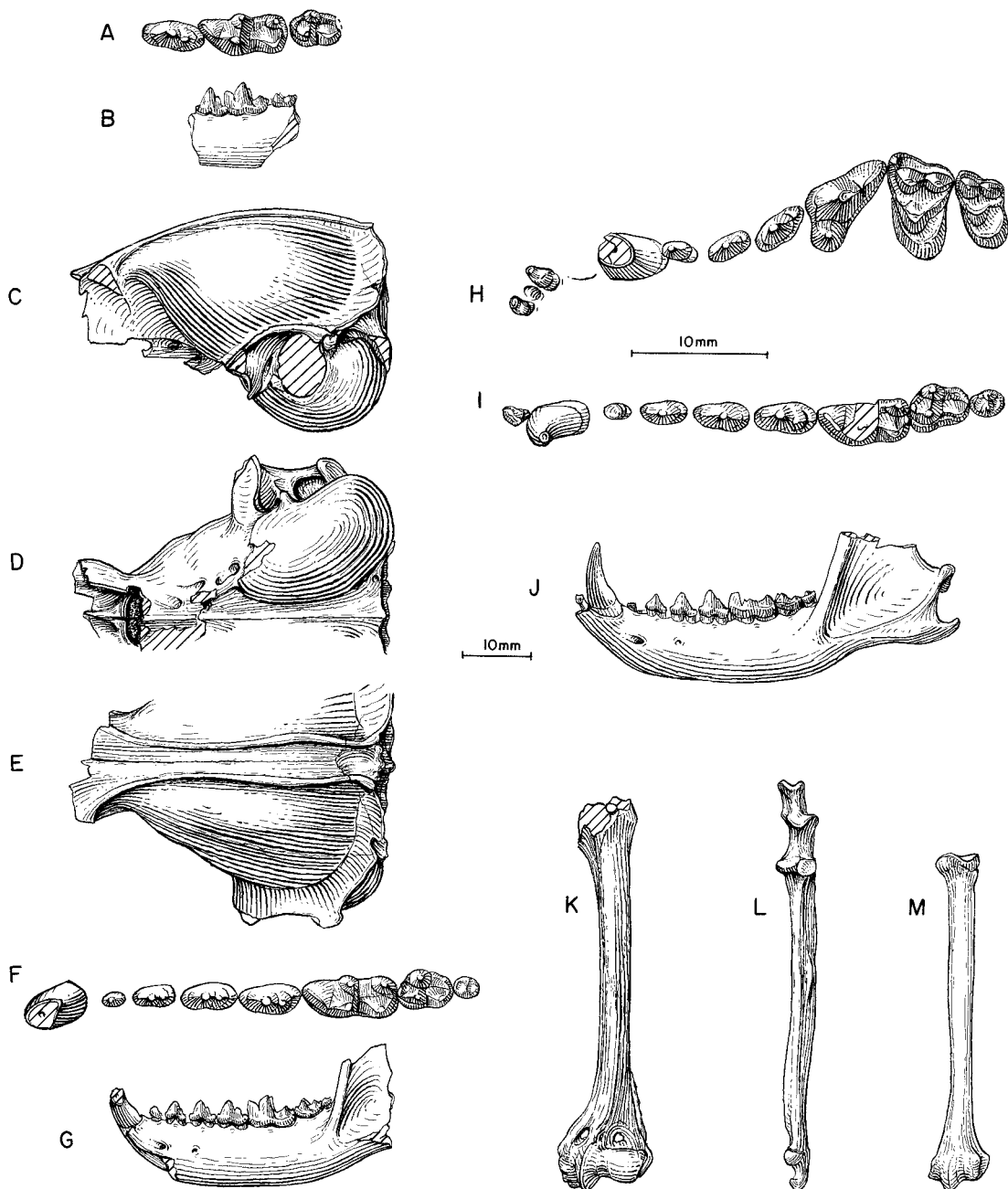


Fig. 17. *Otarocyon cooki*. **A**, Lower teeth and **B**, ramus (reversed from right side), SDSM 54308, holotype, Wounded Knee area, Sharps Formation (early Arikareean), Shannon County, South Dakota. **C**, Lateral, **D**, ventral, and **E**, dorsal views of partial skull (bulla from right side), **F**, lower teeth, and **G**, ramus, F:AM 49043, Little Muddy Creek, lower Arikaree Group (early Arikareean), Niobrara County, Wyoming. **H**, Upper teeth, **I**, lower teeth, **J**, ramus, **K**, humerus, **L**, ulna, and **M**, radius, F:AM 49042 (I1, I3, P4–M2, and all limb bones reversed from right side), Little Muddy Creek. The longer (upper) scale is for **A**, **F**, **H**, and **I**, and the shorter (lower) scale is for the rest.

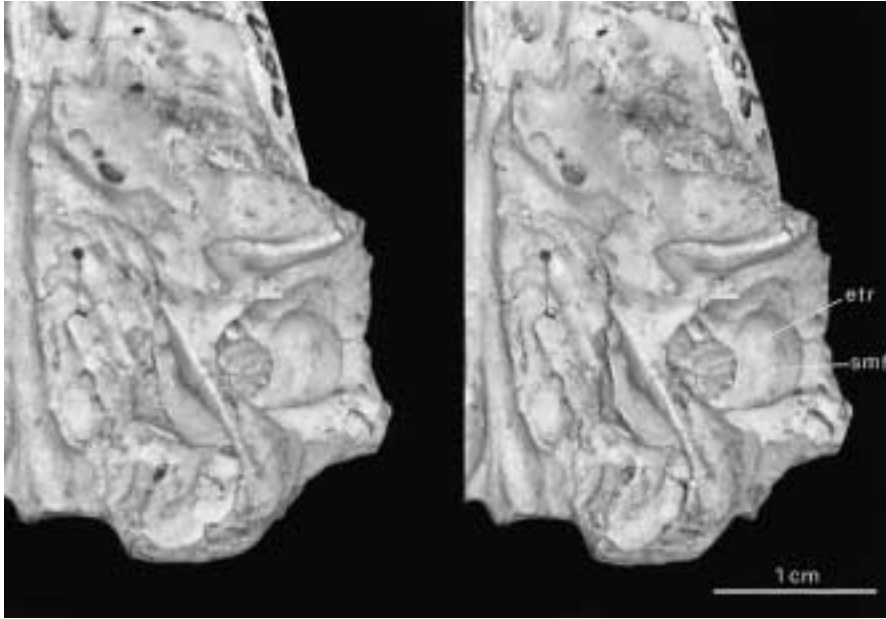


Fig. 18. Stereophotograph of basicranial region of *Otarocyon cooki*, F:AM 49043, Little Muddy Creek, lower Arikaree Group (early Arikareean), Niobrara County, Wyoming. Abbreviations: etr, epi-tympanic recess; smf, suprameatal fossa. Photograph by Lorrain Meeker.

times larger in volume. Exact proportions of the bullar components are difficult to ascertain due to fusion of the sutures, but expansion of the caudal entotympanic is presumably the primary cause of the bullar inflation, since this has been the case in living canids that expand their bullae (Hunt, 1974). There is no indication on the internal bullar surface of a low septum, a unique structure present in nearly all canids (Wang and Tedford, 1994). This absence of the septum is presumably a result of the extreme inflation of the thin-walled bulla, as also occurs in the living fennecs. The space between the two bullae is narrowed to about half the distance were the bullae not inflated. The opening of the external auditory meatus is also considerably enlarged. The paroccipital process is ventrally oriented, completely hugs the bulla, and has no free tip.

Another outstanding feature in the middle ear region of *O. cooki* is a large, deep, rounded suprameatal fossa (fig. 18), a condition thought to be diagnostic of the procyonids (Riggs, 1942, 1945; Segall, 1943; Hough, 1944, 1948). Although Schmidt-Kittler (1981) and Wolsan (1993) demonstrated a

more extensive presence and varying patterns of the suprameatal fossa in many lineages of musteloids, such a structure had not been reported in a canid except for a rudimentary stage of development in *Hesperocyon* (Wang and Tedford, 1994), which serves well as a morphological precursor for the structural elaboration in *Otarocyon*. The fossa in *Otarocyon* is dorsally excavated into the squamosal shelf of the external auditory meatus and is expanded posteriorly into the mastoid process, a condition found in the procyonids but not the mustelids (see Schmidt-Kittler, 1981 and Wolsan, 1993). Yet little else in the basicranium of *Otarocyon*, besides the suprameatal fossa, suggests any arctoid characters. The mastoid process, although excavated by the suprameatal fossa, is not enlarged, as is the case in many arctoids. There is an alisphenoid canal, which is lost in living procyonids and mustelids. *Otarocyon* thus becomes one more example of independent acquisition of a hypertrophied suprameatal fossa, and is the only canid known to have elaborated this structure to such an extent.

Dental morphology of *Otarocyon cooki*,

on the other hand, is for the most part that of a basal canid with certain autapomorphies. Associated with the brachycephalic skull, the cheekteeth also become shortened, resulting in short, simple, high-crowned premolars (fig. 13; appendix III). The trigonid of m1 is also shortened and the shearing blade is rather obliquely oriented. The cusps of the lower molars also become high-crowned, including metaconids of m1–m2, hypoconid and entoconid of m1, and entoconid of m2. In particular, a deep notch between the high entocoid and metaconid of m1 is a peculiar feature not seen in other borophagines.

DISCUSSION: *Otarocyon cooki* has remained in obscurity since its first description from the Wounded Knee area of South Dakota (Macdonald, 1963), partly because of the fragmentary topotype material. Although generally primitive, the lower teeth of the topotype material offer sufficiently diagnostic characters that our reference of more complete skulls and mandibles to this rare species is secure and reveals a surprising combination of cranial and dental characteristics.

In addition to the incomplete nature of the holotype, Macdonald's (1963) reference of this species to *Cynodesmus* further compounds the problem of its relationship among canids. Since its initial establishment by Scott (1893), the genus *Cynodesmus* (type species *C. thoooides*) has gradually included more borophagine species, particularly because of the early reference of *Desmocyon thomsoni* (see further comments under this taxon) to this genus. Macdonald's alliance of *cooki* with *Cynodesmus* further stretched the concept of this genus. *Cynodesmus* is now restricted to two species within the Hesperocyoninae (Wang, 1994) and has a very distant relationship to any borophagine.

### *Rhizocyon*, new genus

TYPE SPECIES: *Cynodictis* (?) *oregonensis* Merriam, 1906.

ETYMOLOGY: Greek: *rhiza*, root; *cyon*, dog.

INCLUDED SPECIES: Type species only.

DISTRIBUTION: Early Arikareean of Oregon.

DIAGNOSIS: *Rhizocyon* is derived relative to *Archaeocyon*, *Oxetocyon*, and *Otarocyon*

in having a wider frontal shield, more quadrate upper molars with anteriorly expanded lingual cingulum, and a connection between the lingual cingulum and metaconule on M2. It differs from members of the Phlaocyoni in its unenlarged bulla, posteriorly directed paroccipital process, small metaconule on M1, and lack of protostylids on lower molars. In contrast to *Cormocyon* and more derived borophagines, *Rhizocyon* lacks an elongated m1 trigonid.

### *Rhizocyon oregonensis* (Merriam, 1906)

Figure 19

*Canis gregarius* Cope, 1879a: 58.

*Canis lippincottianus* Cope, 1879a: 58.

*Galecyon gregarius* (Cope): Cope, 1883: 241 (in part); 1884: 916 (in part), pl. 68, figs. 5–8.

*Galecyon lippincottianus* (Cope): Cope, 1884: 920 (AMNH 6883 only).

*Cynodictis gregarius* (Cope): Wortman and Matthew, 1899: 130.

*Cynodictis* (?) *oregonensis* Merriam, 1906: 4, 5, 11, pl. 2, fig. 4. Merriam and Sinclair, 1907: 184. Thorpe, 1922a: 162–164.

*Cynodictis oregonensis* (Merriam): Matthew, 1909: 106.

*Nothocyon oregonensis* (Merriam): Hall and Martin, 1930: 283.

*Nothocyon lemur* (Cope, 1879b): Macdonald, 1970: 56–57 (in part).

*Cormocyon oregonensis* (Merriam): Fremd and Wang, 1995: 75.

LECTOTYPE: AMNH 6879, skull with I1–I2 both broken, I3–M2, and left ramus with c1 broken–m3 (Cope, 1884: 917, pl. LXVIII, figs. 5–8; fig. 19), John Day Basin, John Day Formation, ?early Arikareean of Oregon.

Merriam (1906) did not designate a holotype in his original description of *Cynodictis* (?) *oregonensis*, although he did indicate that UCMP 316, a partial left ramus with i3–c1 and p2–m2 (Merriam, 1906: pl. 2, fig. 4), was the “most important” among a series of jaw fragments in the UCMP collection. Museum labels associated with UCMP 316 have labeled it the holotype, even though no subsequent publication has selected it as such. Unfortunately, some of the most diagnostic elements of UCMP 316 have been lost. The entire p3, part of the principal cusp of p4, the entire m1, and partial m2 (originally incomplete) are missing from UCMP 316, and the published line drawing of a lateral view

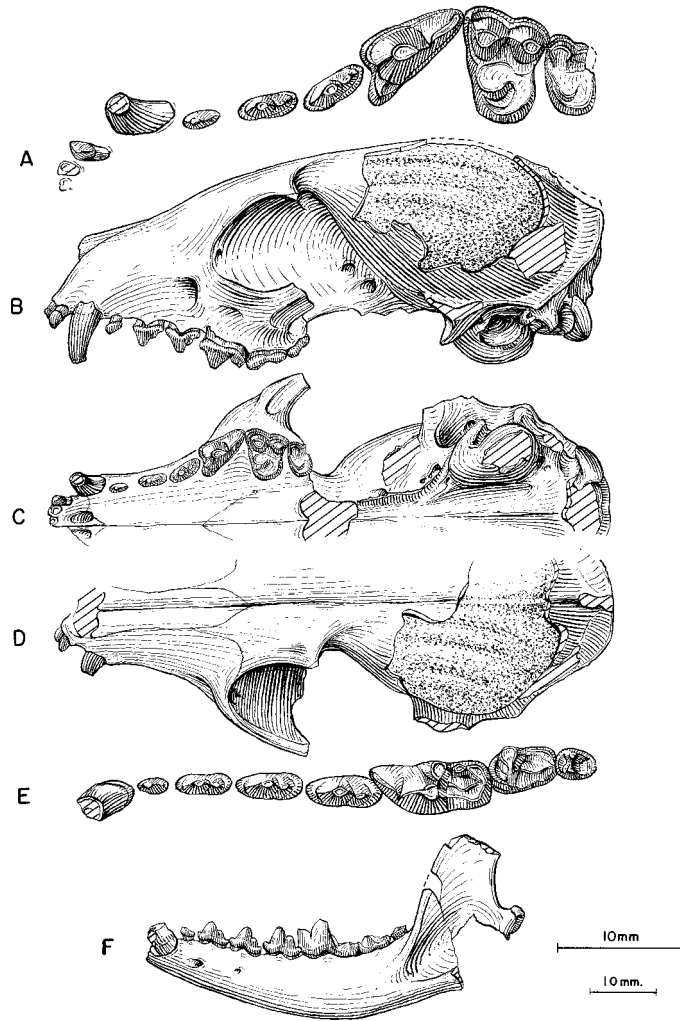


Fig. 19. *Rhizocyon oregonensis*. **A**, Upper teeth (P4–M2 reversed from right side), **B**, lateral, **C**, ventral, and **D**, dorsal views of skull, **E**, lower teeth, and **F**, ramus, AMNH 6879, lectotype, John Day Basin, John Day Formation (?early Arikareean), Oregon. The longer (upper) scale is for A and E, and the shorter (lower) scale is for the rest.

is the only information available on these structures. The remaining *i*3–*c*1, *p*2, and *p*4 are difficult to distinguish from similar-size John Day canids (e.g., *Phlaocyon latidens*). We choose AMNH 6879 as a lectotype, not only because of its far more complete and superior preservation, but also because the original diagnosis (Merriam, 1906: 11, fn. 3) included skull characteristics that could only have been observed on AMNH 6879, which thus must be part of the original syntype series.

REFERRED SPECIMENS: From Turtle Cove Member of John Day Formation (early Arikareean), Wheeler and Grant counties, Oregon (biostratigraphic positions of some JODA specimens in the Turtle Cove Member are placed within a letter system by Fremd et al., 1994 and Fremd and Wang, 1995): AMNH 6881, fragmentary palate with P3 broken, P3–M2, and right and left partial rami with *p*4–*m*3, from Camp Creek; AMNH 6883, right ramus fragment with worn *m*1–*m*2; AMNH 6914a, right ramus



fragment with p3–p4; JODA 398, left ramus fragment with p3–p4; JODA 688 (AMNH cast 129655), left maxillary fragment with M1–M2; JODA 735, left ramus fragment with m2; JODA 791 (AMNH cast 129654), right m1, Bed E; JODA 1624, right ramus fragment with p4–m2, Bed K; JODA 1639, left ramus fragment with p4–m2, Bed F; JODA 1654, rostral part of skull with nearly complete dentitions, Bed J; JODA 1847, right m1, Bed E; JODA 3041, right ramus fragment with m1–m2, Bed E2; JODA 3433, skull and mandible fragments with right P3–M1 and left p4–m1, Bed E; JODA TF10922, left ramus fragment with m1, Bed C; UCMP 316, partial left ramus with i3–c1 and p2–m2 (Merriam, 1906: pl. 2, fig. 4), from UCMP loc. 818, Blue Basin, Turtle Cove Member; UCMP 365, right ramus fragment with m1 and erupting p4 (Merriam, 1906: pl. 2, fig. 5); UCMP 79365, rostral part of skull with left and right P2–M2, UCMP loc. V-6322, Haystack 8-63, level 2; and YPM 12760, right ramus with p2–p3 and m1–m2 from Turtle Cove.

**DISTRIBUTION:** Early Arikarean of Oregon. Recent JODA collections suggest that *Rhizocyon oregonensis* is mostly restricted to the lower part (Beds B–J of Fremd and Wang, 1995) of the Turtle Cove Member in the John Day Formation, and this is in essential agreement with Merriam and Sinclair (1907: 188), who listed it as from the “Middle John Day.”

**EMENDED DIAGNOSIS:** Same as for monotypic genus.

**DESCRIPTION AND COMPARISON:** *Rhizocyon oregonensis* is 22% larger (average of all dental measurements, appendix III) and has a slightly more robust construction (fig. 12) than *Archaeocyon pavidus*. In addition, the anterior expansion of the braincase yields a wider postorbital constriction. Proportionally, *R. oregonensis* is most notable for having both a broad rostrum and short bulla as compared to other basal borophagines (palate width at P1 and bulla length in fig. 12). The basicranium is primitive in its small bulla with a V-shape notch on the auditory meatus, as well as posteriorly oriented paroccipital process lacking contact with the posterior part of the bulla. Breakage of the entotym-

panic bulla reveals a partial entotympanic septum at the ento- and ectotympanic suture.

The m1 entoconid is crestlike, and about the same height as the hypoconid. Metaconid of the m2 is higher than the protoconid. Although of larger size, the proportions of the teeth are similar to those in *A. pavidus*, with the exception of a longer P1 and slightly shorter M2 (fig. 13). The m1 trigonid in *Rhizocyon* is not as longitudinally oriented (i.e., more opened) as in *A. leptodus* or *Cormocyon* and more derived forms.

**DISCUSSION:** Earlier references of this Oregon species either directly to *Hesperocyon gregarius* (Cope, 1879a, 1883, 1884) or as a distinct species of *Hesperocyon* (*Cynodictis*) (Merriam, 1906; Matthew, 1909; Thorpe, 1922a) reinforced the idea of a relationship of *oregonensis* to the small canids in the White River, as was also suspected of *Archaeocyon pavidus*. Our cladistic analysis, however, suggests that *Rhizocyon* represents a basal borophagine with some of the initial synapomorphies of the borophagine clade.

#### **Phlaocyonini**, new tribe

Type Genus: *Phlaocyon* Matthew, 1899.

**INCLUDED GENERA:** *Cynarctoides* McGrew, 1938a; and *Phlaocyon* Matthew, 1899.

**DISTRIBUTION:** Early Arikarean through early Barstovian of North America.

**DIAGNOSIS:** Derived characters that distinguish early Phlaocyonini from *Archaeocyon* and *Rhizocyon* include a large M1 metacoenule and presence of a protostylid on m1. Phlaocyonines differ from *Cormocyon* in possessing a primitively short, closed m1 trigonid.

#### *Cynarctoides* McGrew, 1938

**TYPE SPECIES:** *Cynarctus acridens* Barbour and Cook, 1914.

**INCLUDED SPECIES:** *C. lemur* (Cope, 1879b); *C. roii* (Macdonald, 1963); *C. harlowi* (Loomis, 1932); *C. luskensis*, new species; *C. gawnae*, new species; *C. acridens* (Barbour and Cook, 1914); and *C. emryi*, new species.

**DISTRIBUTION:** ?Whitneyan of South Dakota; early Arikarean of Oregon, Nebraska, and South Dakota; medial or late Arikarean of South Dakota and Florida; late Arikarean

of Colorado, Nebraska, Wyoming, and New Mexico; early Hemingfordian of Nebraska, Idaho, Texas, and New Mexico; late Hemingfordian of Nebraska, Wyoming, and New Mexico; and early Barstovian of Nebraska, New Mexico, and California.

EMENDED DIAGNOSIS: Shared derived characters that distinguish all species of *Cynarctoides* include parasagittal crests and slender, shallow horizontal ramus. Advanced species of *Cynarctoides* (*C. luskensis* and more derived forms) further developed narrow rostrum, long jaws, narrow and long premolars, conical and high-crowned cusps in the lower molars, laterally shifted p4 accessory cusp, long M2 and m2, progressive larger hypocones in upper molars, higher metaconids in lower molars, and larger protostylids in lower molars, although the slender jaws and premolars are later reversed in *C. emryi*.

DISCUSSION: The type species *Cynarctoides acridens* was originally recognized as a species of *Cynarctus* (Barbour and Cook, 1914; Matthew, 1932; McGrew, 1937), mostly because of the fragmentary nature of the holotype (a ramal fragment with a single m1). The discovery of the upper teeth allowed direct comparisons of the relevant taxa and led to the establishment of the genus *Cynarctoides* by McGrew (1938a). However, McGrew regarded *Cynarctoides* as a primitive procyonid, as he did all other hypocarnivorous borophagines then known (e.g., *Phlaocyon* and *Cynarctus*). With only dental materials available to her, Hough (1948) challenged this arrangement and considered *Cynarctoides* a canid, a view that won firm support from Galbreath (1956) in his analysis of a basicranial fragment of *C. acridens* from Colorado. Past discussions about *Cynarctoides* systematics, however, were mostly based on a few specimens reported in the literature, and large morphological gaps left room for speculation.

Such a deficiency in the fossil record is partially bridged in this study—large numbers of specimens including skulls are now available from a wide range of geographic and geologic distributions. Additionally, three new species are described below, which, together with *C. acridens*, represent a nearly continuous series of intermediate stages of development toward a peculiar form of

hypocarnivory quite different from that of both *Phlaocyon* and *Cynarctus*. For example, the upper carnassial (P4) of *Cynarctoides* remains largely primitive without a hypocone and has never gone beyond the addition of a slightly widened lingual cingulum. Its M1–M2, however, usually have a discrete hypocone (except the basal species of *C. lemur* through *C. luskensis*), which is often surrounded lingually by a narrow cingulum, a peculiarity not seen in *Phlaocyon* and *Cynarctus*. The tendency to develop distinct crests (e.g., crista obliqua) in the lower molars is another reason for its unique appearance. Together, these features help to define a unique clade of borophagines and increase our confidence about the appearance of independently acquired hypocarnivorous characters, such as the presence of a discrete hypocone on M1–M2.

*Cynarctoides lemur* (Cope, 1879b)

Figure 20D–P

*Canis lemur* Cope, 1879b: 371.

*Galecyon lemur* (Cope): Cope, 1881b: 181; 1883: 241, fig. 7; 1884: 915, 931, pl. 70, figs. 6–8.

*Cynodictis lemur* (Cope): Scott, 1898: 400.

*Nothocyon lemur* (Cope): Wortman and Matthew, 1899: 127, 130. Matthew, 1899: 62; 1932: 3. Merriam, 1906: 13, pl. 2. Peterson, 1907: 53. Thorpe, 1922a: 165 (in part). Hall and Martin, 1930: 283. Hough, 1948: 100. Macdonald, 1963: 209; 1970: 56 (in part). Munthe, 1998: 138.

*Cynodictis* (?) *oregonensis* Merriam, 1906: 12, fig. 5 (in part).

*Bassariscops willistoni* (Peterson, 1924): Peterson, 1928: 97, fig. 7 (CMNH 11334 only).

*Bassariscops achoros* Frailey, 1979 (in part): 134, figs. 3B, 4C.

“*Cormocyon*” *lemur* (Cope): Fremd and Wang, 1995: 74.

HOLOTYPE: AMNH 6888, skull with I1–C1 alveoli and P1–M2 (P2 alveolus) (fig. 20D–F) from the John Day Basin, John Day Formation (early Arikarean), Wheeler or Grant counties, Oregon.

REFERRED SPECIMENS: From the type area (biostratigraphic positions of some JODA specimens in the Turtle Cove Member are placed within a letter system by Fremd and Wang, 1995): AMNH 6889, partial skull with P2–P3 alveoli and P4–M2 (fig. 20G–I);

AMNH 6890, fragmentary skull with P4 alveolus and M1 broken—M2; AMNH 6891, anterior part of skull with I3—P2 alveoli, P3—P4, and M1—M2 both broken; AMNH 6892, left partial ramus with p2—p3 alveoli and p4—m2 (fig. 20J, K), Camp Creek; AMNH 6893, right partial ramus with p4 broken, m1, and m2 alveolus; AMNH 6895, right ramal fragment with m2 broken; AMNH 6898, left isolated p4 and jaw fragment with m1; AMNH 6900, right ramal fragment with m1 broken—m2; AMNH 6914b, left ramal fragment with m2 and m3 alveolus; KUVF 600, partial skull with C1—M2 (Hall and Martin, 1930: figs. 1—3) and right ramus with p3—m2, from “Haystack Valley, below Turtle Cove”; JODA 355, edentulous right ramus fragment, unit E1; JODA 690, right P4; JODA 731, left M1; JODA 790, right ramus fragment with broken p4—m1, unit E1; JODA 825, rostral part of skull with left P3—M2 and right P4—M1, unit E2; JODA 1243, left ramus fragment with m1, unit E1; JODA 1352, partial skull, unit E2; JODA 1373, right ramus fragment with m1, unit E1; JODA 1390, right P4, unit E2; JODA 1401, left maxillary fragment with M1, unit C; JODA 1918, left M1, unit E1; JODA 2769, right ramus fragment with p3—p4, unit D; JODA 2856, left M1, unit C; JODA 2859, right P4, unit C; JODA 2918, right M1, unit E1; JODA 2971, right maxillary fragment with M1—M2, unit E2; JODA 2977, broken right P4, unit E2; JODA 2990, right ramus fragment with m1, unit E2; JODA 3049, p3, unit E3; JODA 3051 (AMNH cast 129656), rostral part of skull with left P4—M2 and right P4—M1, unit E1; JODA 3090, left ramus fragment with m1, unit E2; JODA 3380, left m1, unit D; JODA 3394, left ramus fragment with m1, unit E; JODA 3442, broken left M1; JODA TF8923, right M1; JODA TF3924PC, left ramus with p3—m1, unit E3; UCMP 352, left partial maxillary with P3 broken—M1 and M2 alveolus, Black Rock 3, loc. 839; UCMP 1104, left partial maxillary with P4—M2, Rudio Creek 1, UCMP loc. 869; UCMP 10208, partial skull with C1—M1 all broken, Logan Butte 1, UCMP loc. 898 (Merriam, 1906: pl. 2, fig. 2); UCMP 75217, left ramal fragment with m1, South Canyon Level 4, UCMP loc. V6600; uncataloged YPM specimen, field number 493, left partial maxillary with C1—

P3 alveoli, P4—M1, and M2 broken; uncataloged YPM specimen, field number 785, left ramal fragment with m1 broken—m2; uncataloged YPM specimen, field number 903, left maxillary fragment with M1—M2 (fig. 20L) and left ramal fragment with m1; uncataloged YPM specimen, field number 940, Box 11-118, right isolated M1 and right ramal fragment with m1 broken—m2, from Turtle Cove.

Cedar Pass, ?Poleslide Member of Brule Formation (?Whitneyan), South Dakota: UCMP loc. V7228; UCMP 4130, anterior part of skull with C1—M2 (P1 alveolus) and partial mandible with c1 broken—m3 (p2 and m2 all broken).

Sharps Formation (early Arikareean), Shannon County, South Dakota: F:AM 50356, left partial maxillary with P3—M2, lower part of Sharps Formation, 12 ft above the Rockyford Ash; LACM 9368, right partial maxillary with P4 broken—M1, LACM loc. 1955; SDSM 54307, right partial ramus with p4—m2 (fig. 20M, N), SDSM loc. V5359, south side of Sharps Cutoff road, upper part of Sharps Formation; and SDSM 55134, left ramal fragment with m1, SDSM loc. V5410, Godsell Ranch channel, base of upper part of Sharps Formation.

Browns Park Formation (?early Arikareean), Moffat County, Colorado: CMNH 11334 (AMNH cast 89666) (fig. 20O, P), left partial ramus with c1 and m1—m2, and alveoli of p1—p4 and m3, 1.5 mi southwest of Sunbeam (referred to *Bassariscops willistoni* Peterson, 1928: 96, fig. 7; this specimen is presumably lower in stratigraphic level than the better dated faunas found by Honey and Izett, 1988).

Buda Local Fauna (medial Arikareean), Alachua County, Florida: UF 171368, right p4; UF 16969, left M1; UF 160799, left ramal fragment with talonid of m1, m2, and m3 alveolus; UF 18403 (AMNH cast 105034; Frailey, 1979: figs. 3B, 4C), left maxillary fragment with M1—M2; UF 160796, right P4; and UF 160797, left P4.

DISTRIBUTION: ?Whitneyan of South Dakota, early Arikareean of Oregon and South Dakota, ?early Arikareean of Colorado, and medial Arikareean of Florida.

EMENDED DIAGNOSIS: In contrast to *Rhizocyon*, *Archaeocyon*, and other basal boro-

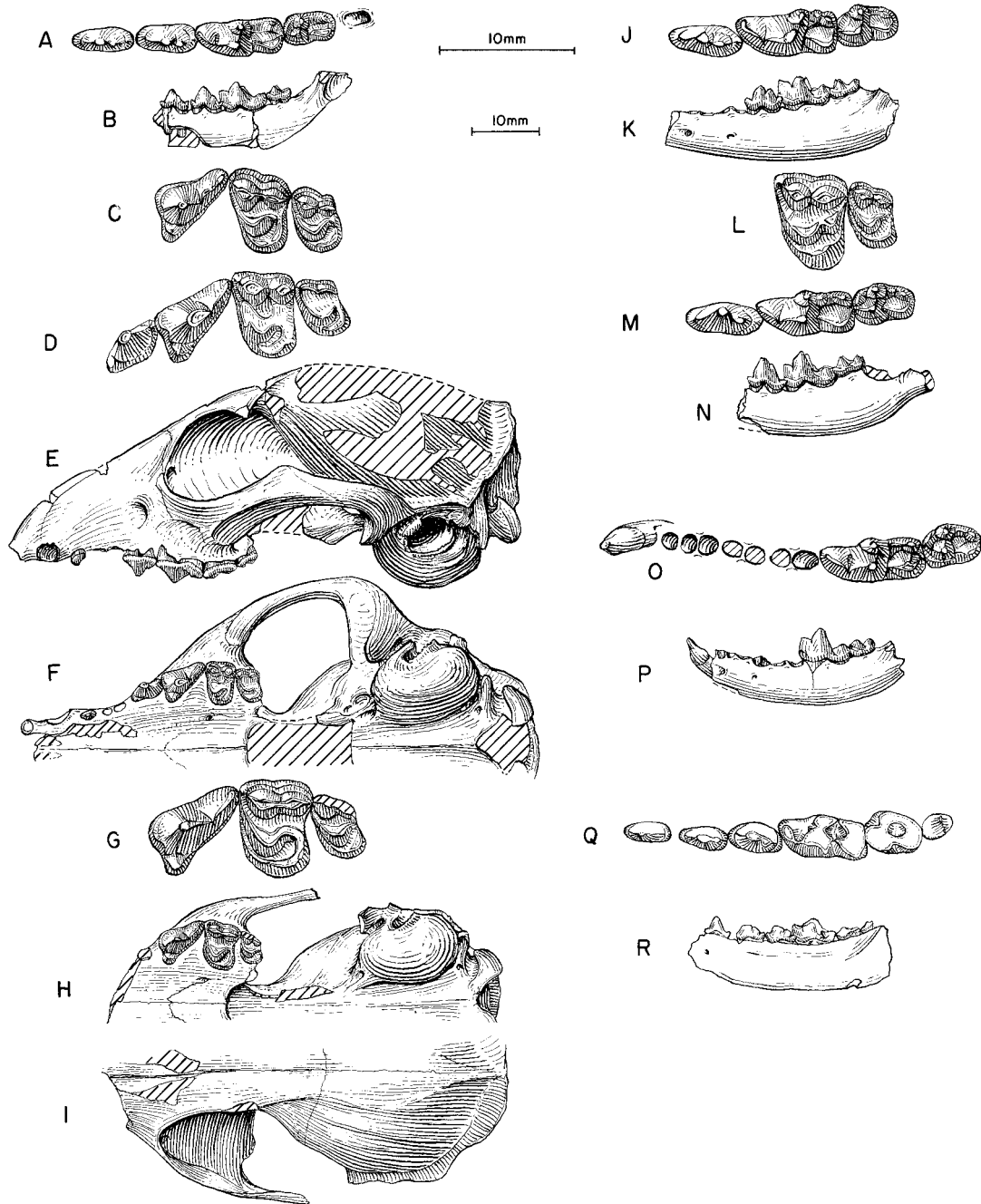


Fig. 20. **A**, Lower teeth and **B**, ramus (reversed from right side), *Cynarctoides roii*, SDSM 53321, holotype, Wounded Knee, Sharps Formation (early Arikareean), Shannon County, South Dakota. **C**, Upper teeth, *C. roii*, SDSM 54132, Wounded Knee, Sharps Formation. **D**, Upper teeth, and **E**, lateral and **F**, ventral views of skull, *C. lemur*, AMNH 6888, holotype, John Day Basin, John Day Formation (early Arikareean), Wheeler or Grant counties, Oregon. **G**, Upper teeth, and **H**, ventral and **I**, dorsal views of skull, *C. lemur*, AMNH 6889, John Day Formation. **J**, Lower teeth and **K**, ramus, *C. lemur*, AMNH 6892, Camp Creek, John Day Formation. **L**, M1–M2, *C. lemur*, YPM 903, John Day Formation.

phagines, derived characters of *Cynarctoides lemur* shared with other species of *Cynarctoides* and the *Phlaocyon* clades include a large M1 metaconule and the presence of a protostylid on m1–m2. *C. lemur* shows the initial tendency of the genus: slender ramus and separate temporal crests. *C. lemur* primitively lacks derived characters in more advanced species of the *Cynarctoides* clade: elongate premolars, conical talonid cusps of m1, and a protostylid on m2. It also primitively lacks other features that are synapomorphies of *Phlaocyon*: short and robust premolars, shortened P4 with enlarged lingual shelf, quadrate M1–M2, and wide m1 talonid.

**DESCRIPTION AND COMPARISON:** Descriptions of the general cranial and dental morphologies of *Cynarctoides lemur* have been available for some time (Cope, 1884; Merriam, 1906; Hall and Martin, 1930; Hough, 1948). In skull length, *C. lemur* is slightly larger than *Archaeocyon*. The most conspicuous feature often noted about *C. lemur* is its enlarged bulla, which is larger than that in *A. pavidus* and *Rhizocyon oregonensis*. Other relevant features in the present phylogenetic analysis are concerned with two subtle dental characters: (1) a more distinct metaconule on M1 begins to take shape in most specimens of *C. lemur*, and (2) a protostylid begins to appear on the m1 of *C. lemur*. The latter is a derived feature that signals the initiation of a hypocarnivorous clade, which quickly diverged into *Cynarctoides* and *Phlaocyon*. The skull roof of *C. lemur* has paired temporal crests instead of a single sagittal crest in the primitive condition. The double temporal crests do not seem to be related to ontogenetic age, as is common in small carnivores, because individuals with modest (AMNH 6889) and advanced (AMNH 6888 and 6891) wear on the permanent molars all exhibit this trait.

**DISCUSSION:** A protostylid on the m1 has been traditionally used to differentiate *Cynarctoides lemur* (considered absent) from the contemporaneous *Phlaocyon latidens* (e.g., Cope, 1884; Merriam, 1906; Macdonald, 1963). Both species have been closely linked in almost all past discussions. Our observations suggest that the protostylid is variably present in both species, although those in *P. latidens* tend to be better developed than in *C. lemur*. The protostylid therefore is a synapomorphy of a clade that includes *Cynarctoides* and *Phlaocyon*, and this cusp is further elaborated in the species of *Cynarctoides*.

Matthew (1932: 3) was the first to speculate that the origin of *Cynarctoides acridens* may be found in the John Day “*Nothocyon*” *lemur* or “*Nothocyon*” (= *Phlaocyon*) *latidens* (however, he did not think his new species, *Cynarctus mustelinus* [presently synonymized under *C. acridens*], was in the same group). In fact, he went so far as to suggest that the holotype of *C. acridens* be placed in the same genus (*Nothocyon*) as the two John Day species. Matthew’s suggestion is generally confirmed by our phylogenetic conclusions.

Collections made by JODA field teams in recent years restrict the stratigraphic distribution of *Cynarctoides lemur* to a narrow range within the Turtle Cove Member of the John Day Formation, as opposed to the more vague “John Day Basin” frequently used in the literature. The species is found in units A–F below the Picture Gorge Ignimbrite (Fremd and Wang, 1995), now estimated to be around 28.7 Ma (Woodburne and Swisher, 1995). Such a restricted range is consistent with the occurrence of representatives of this taxon in the Great Plains (Sharps Formation, South Dakota).

Fragmentary materials (including specimens referred to *Phlaocyon achoros*) from

←

**M**, Lower teeth and **N**, ramus (reversed from right side), *C. lemur*, SDSM 54307, Sharps Cutoff road, Wounded Knee, Sharps Formation. **O**, Lower teeth and **P**, ramus, *C. lemur*, CMNH 11334, Browns Park Formation (?early Arikareean), Moffat County, Colorado. **Q**, Lower teeth and **R**, ramus, *C. harlowi*, ACM 31-34, holotype, 3 mi southeast of Van Tassel, Upper Harrison beds, Niobrara County, Wyoming. The longer (upper) scale is for A, C, D, G, J, L, M, O, and Q, and the shorter (lower) scale is for the rest.

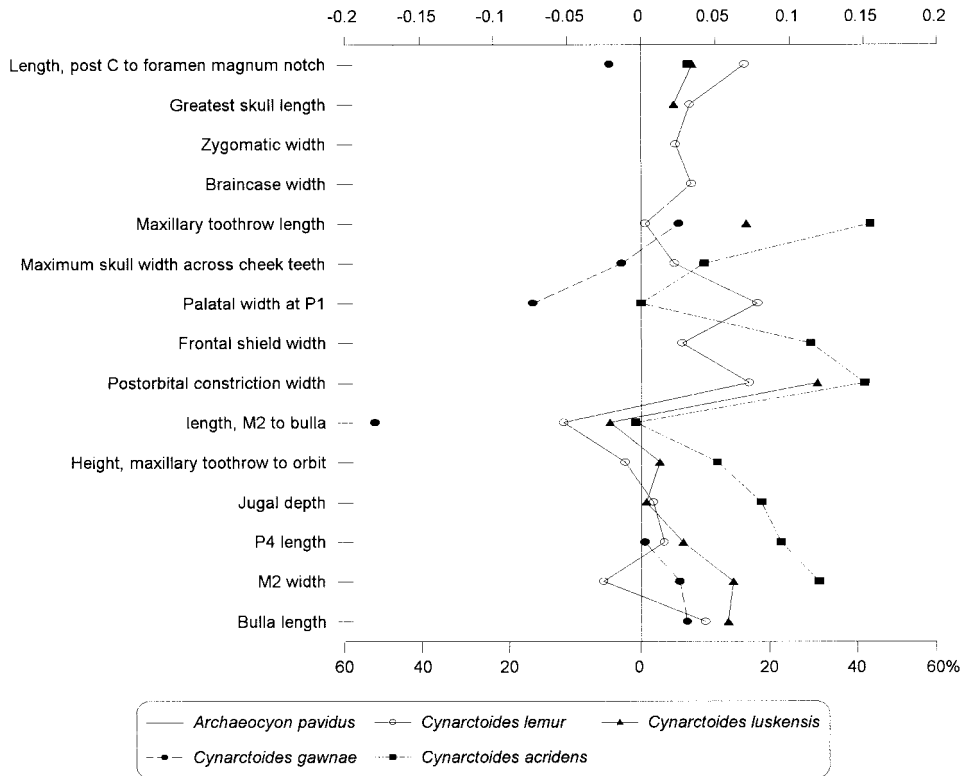


Fig. 21. Log-ratio diagram for cranial measurements of four species of *Cynarctoides* using *A. pavidus* as a standard for comparison (straight line at zero). See text for explanations and appendix II for measurements and their definitions.

the Buda Local Fauna, Florida, are provisionally referred to this species. It is of interest to note that JODA 3051, referred here to *Cynarctoides lemur*, exhibits certain initial features toward the development of *Phlaocyon achoros*, which is known only in the Buda Local Fauna (see discussion under that species).

*Cynarctoides roii* (Macdonald, 1963)

Figure 20A–C, O, P

?*Phlaocyon* Peterson, 1924: 303, fig. 2.

*Nothocyon roii* Macdonald, 1963: 206, figs. 24, 25. 1970: 54.

**HOLOTYPE:** SDSM 53321 (AMNH cast 129863), right partial ramus with p3–m2 and m3 alveolus (fig. 20A, B) from the Wounded Knee Area, SDSM loc. V5354, from near the top of the Sharps Formation (early Arikarean), Shannon County, South Dakota.

**REFERRED SPECIMENS:** From the Wounded

Knee Area, upper part of the Sharps Formation (early Arikarean), Shannon County, South Dakota: LACM 9196 (AMNH cast 129646), right partial ramus with p2–m1 (p4 broken), LACM loc. 1959; LACM 9284, right ramal fragment with m1 broken, LACM loc. 1966; LACM 9462, left detached m1, LACM loc. 1982; LACM 9507, left partial ramus with m1–m2 and m3 alveolus, LACM loc. 1984; SDSM 5581, right partial ramus with p4–m1, SDSM loc. V5350; SDSM 5583, right partial ramus with c1–p2 alveoli and p3–p4, SDSM loc. V5341; SDSM 53322, left partial ramus with p4 broken–m2 and m3 alveolus, SDSM loc. V5358; SDSM 54132, fragmentary skull with P4–M2 (Macdonald, 1963: fig. 25; fig. 20C), SDSM loc. V5354; SDSM 54252, left partial ramus with P4–M1, SDSM loc. V5354; SDSM 54273, left ramal fragment with m1, SDSM loc. V5360; UCMP 114775, left ramus fragment

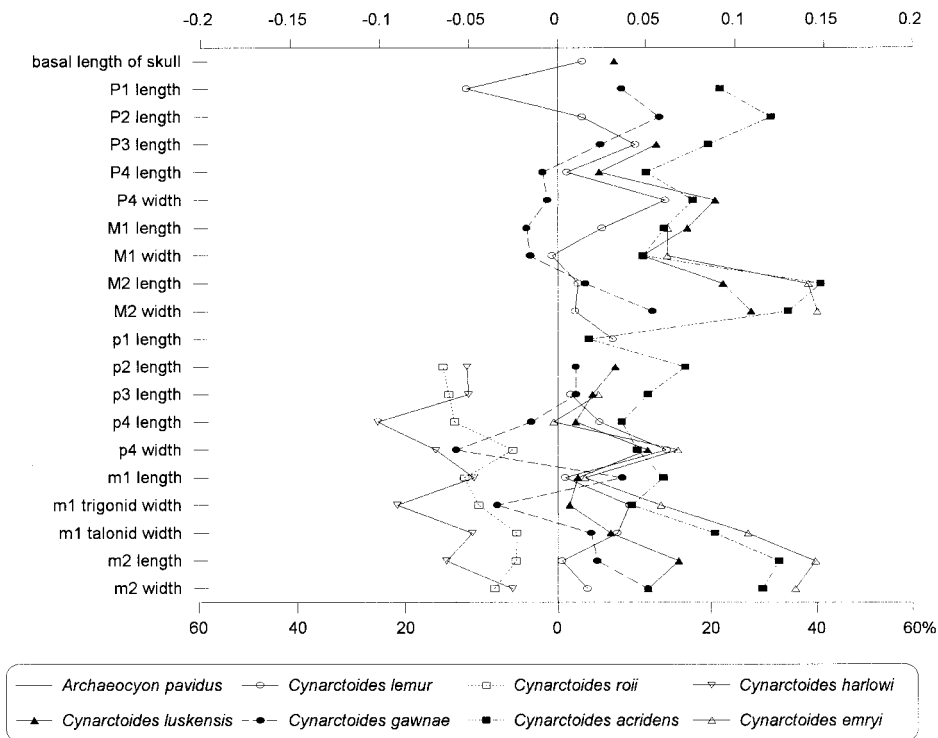


Fig. 22. Log-ratio diagram for dental measurements of seven species of *Cynarctoides* using *A. pavidus* as a standard for comparison (straight line at zero). See text for explanations and appendix III for summary statistics of measurements and their definitions.

with m1–m2, UCMP loc. V76043, Wolff Camp 2; and UCMP 121784, partial left ramus with p3 broken–m2 and m3 alveolus, UCMP loc. V75201 (= SDSM V5354).

One mi east of Nebraska/Wyoming line, Horse Creek Basin, lower Arikaree Group (early Arikareean), Banner County, Nebraska: F:AM 49070, left partial ramus with p3–m2, from 20 ft above White Layer.

DISTRIBUTION: Early Arikareean of South Dakota and Nebraska.

EMENDED DIAGNOSIS: *C. roii* differs from *C. lemur* in its smaller size, entoconid of m1 less prominent, protostylid on m2, and protoconid and metaconid of m2 close together. Compared to *C. harlowi*, *C. roii* is slightly larger and has longer premolars.

DESCRIPTION AND COMPARISON: *C. roii* is still poorly known and little can be added to the toptype series from the Wounded Knee Area, other than a questionable reference of a ramus from the early Arikareean of Ne-

braska and possibly one from younger rocks of the Browns Park Formation of Colorado. Macdonald's (1963) characterization of this species is thus still essentially valid, although his phylogenetic framework is quite different from ours. In general, *C. roii* is so primitive in its overall morphology that few characters can be identified to distinguish it from other basal borophagines.

In light of our phylogeny, *C. roii* is close to the base of the *Cynarctoides* clade. The only features that suggest it to be on this side of the clade (as opposed to the *Phlaocyon* side) are its slender ramus and development of a labial cingulum (precursor of a protostylid) lateral to the m2 protoconid. However, *C. roii* still lacks a protostylid on the m1, a character present in all other more derived phlaocyonines.

DISCUSSION: Much remains to be learned about this rare and tiny borophagine. Its small size and generally primitive morphol-

ogy call for comparisons with *C. lemur* and *C. harlowi*. Although the poorly preserved specimens of *C. roii* and *C. harlowi* do not lend themselves to a rigorous phylogenetic analysis, we may speculate that these two species, possibly including *C. lemur*, form a small clade of their own, within which continued size reduction seems to be the main trend.

*Cynarctoides harlowi* (Loomis, 1932)

Figure 20Q, R

*Pachycynodon harlowi* Loomis, 1932: 326, fig. 9.

HOLOTYPE: ACM 31-34 (AMNH cast 48830), right partial ramus with p2–m3 and alveoli of c1–p1 (fig. 20Q, R), from 3 mi southeast of Van Tassel, in the “Upper Harrison” beds (late Arikareean), Niobrara County, Wyoming.

DISTRIBUTION: Late Arikareean of Wyoming.

REFERRED SPECIMEN: Holotype only.

EMENDED DIAGNOSIS: *Cynarctoides harlowi* differs from *C. roii* in its smaller size and shorter premolars.

DESCRIPTION AND COMPARISON: The holotype of *C. harlowi* is still the only specimen known in the late Arikareean of Wyoming. It is the smallest borophagine and closest in size and morphology to *C. roii*. In fact, in all its dental measurements it is either near or slightly outside the lower end of corresponding measurements in *C. roii*. The only observable difference between these two species is shorter p2–p4 in *C. harlowi* (fig. 22).

DISCUSSION: The advanced stage of wear, especially on molars, and poor state of preservation of the holotype of *C. harlowi* make the determination of its taxonomic status difficult. Although ACM 31-34 matches reasonably well with some specimens of *C. roii*, its much younger age (late Arikareean) and proportional differences of the lower teeth suggest a distinct species. Macdonald (1963: 208) compared *C. harlowi* with *C. roii*, and commented that “*Nothocyon roii* is ideally an ancestor to *N. harlowi*, as there is very little modification of the lower molars during the intervening time, and the major difference is the reduction of the premolars in the younger species [*N. harlowi*].” In any case, wear on ACM 31-34 is so severe that to use

it as the holotype of a species is dubious at best. Until more and better-preserved materials are found, the status of *C. harlowi* cannot be clarified beyond the present recognition that it probably represents a small borophagine.

*Cynarctoides luskensis*, new species

Figure 23N–T

HOLOTYPE: F:AM 49005, partial skull with C1–P2 alveoli, P3–M2, and partial mandible with c1, p1–p3 alveoli, and p4–m3 (fig. 23N–R) from 18 mi southeast of Lusk, Upper Harrison Beds (late Arikareean), Goshen County, Wyoming.

ETYMOLOGY: In reference to the locality of the holotype near the town of Lusk in Goshen County, southeastern Wyoming.

REFERRED SPECIMENS: Upper Harrison Beds (late Arikareean), Wyoming: F:AM 49003, right partial ramus with p2–m2 and m3 alveolus (fig. 23S, T), 7 mi southeast of Chugwater, Platte County; and F:AM 50225, right partial maxillary with P3–M2, from Jay Em area, high brown sand, Goshen County.

DISTRIBUTION: Late Arikareean of Wyoming.

DIAGNOSIS: In contrast to *Cynarctoides lemur* and *C. roii*, *C. luskensis* has derived characters shared with all other more advanced species of *Cynarctoides*: long, slender horizontal ramus, P3 and p3 posterior cusplet weak or absent, long and narrow premolars, m1 talonid cusps high-crowned and conical, m1 entoconid exceeding height of the hypoconid, and presence of a protostylid on m2. *C. luskensis* lacks derived characters found in *C. gawnae* and more derived species: fully encircled ectotympanic ring forming the roof of the external auditory meatus, cleft on M1–M2 lingual cingulum and large conical hypocone, M2 paraconule, and strong m2 protostylid.

DESCRIPTION AND COMPARISON: The skull of the holotype, although laterally compressed, is the best preserved among all species of *Cynarctoides*. In contrast to other hypocarnivorous borophagines (such as *Otarocyon* and derived species of *Phlaocyon*, and, to a lesser extent, *Rhizocyon*), the rostrum of *Cynarctoides* is slightly elongated as first shown in *C. luskensis*. The temporal



crests, trailing behind the small postorbital processes, are poorly defined, although the crests seem to be separate, as is consistent with the similar pattern in taxa more primitive (*C. lemur*) and more derived (*C. gawnae* and *C. acridens*). The bulla is moderately inflated, although its form is modified due to the mediolateral compression. The mastoid process is not enlarged and there is no suprimeatal fossa. The ectotympanic does not extend dorsally to form a full ring. The paroccipital process is ventrally oriented and fully fused with the bulla, a derived state shared with *C. lemur* and the rest of the *Cynarctoides*–*Phlaocyon* clade. The masseteric scar (for origination of the superficial masseter muscle) on the anterior part of the jugal is wide, occupying approximately two-fifth of the total depth of the zygomatic arch. Beginning in *C. luskensis*, the mandible of *Cynarctoides* species becomes very slender (shallow) and long, to accommodate the elongated premolars. On the holotype, the anterior crest of the ascending ramus extends ventrally and anteriorly to form an elongated ridge below the lower molars (fig. 23R).

Dental morphology of *Cynarctoides luskensis* possesses an interesting mixture of primitive and derived characteristics. Besides the slender premolars, the upper teeth remain primitive and are close to the overall shape of those in *C. lemur*. The lingual cingulum in M1–M2 lacks a deep cleft that creates a conical hypocone in later species of *Cynarctoides* (beginning in *C. gawnae*), although the posterior end of the cingulum is slightly swollen (on the holotype, the left M1 has a vague indication of a cleft, whereas that on the right side is less conspicuous). The M2 metaconule is fully connected to the end of the lingual cingulum. The lower molars, on the other hand, are more derived, resembling advanced species of *Cynarctoides*. The m1 protostylid is still weakly developed. The m2 begins to develop a protostylid as well. Cusps on the m2 and on the talonid of m1 show signs of becoming conical and higher crowned, instead of the crestlike and low crowned as in *C. lemur* and basal *Phlaocyon* species (*P. minor* and *P. latidens*).

DISCUSSION: Presently identified as a transitional species of *Cynarctoides*, *C. luskensis* provides a crucial phylogenetic link between

the advanced species of *Cynarctoides* and the primitive *C. lemur*. Its slender ramus and premolars and its pattern of lower molars are unmistakably those of *Cynarctoides*, whereas its upper molars are little more advanced than those in *C. lemur*. An elevated entocoid on the lower molars thus precedes the emergence of an isolated hypocone on the upper molars, as is a general rule in other hypocarnivorous borophagines. The more cuspidate cheekteeth seem to indicate an emphasis toward puncturing, instead of shearing or grinding, reflecting an increasingly insectivorous diet.

### *Cynarctoides gawnae*, new species

Figure 23G–I

*Cynarctoides*, new species B Gawne, 1975: 2.

HOLOTYPE: F:AM 49249, partial skull with C1 alveolus–M2 and both partial rami with c1 broken and p1 alveolus–m3 (fig. 23G–I) from Jeep Quarry, upper part of Chamisa Mesa Member of the Zia Formation (early Hemingfordian), Arroyo Pueblo drainage, Sandoval County, New Mexico.

ETYMOLOGY: In honor of Dr. C. E. Gawne for her earlier recognition of this species in her dissertation on the Zia Sand faunas.

REFERRED SPECIMENS: Jeep Quarry and Jeep Quarry horizon, upper part of the Chamisa Mesa Member of the Zia Formation (early Hemingfordian), Arroyo Pueblo drainage, Sandoval County, New Mexico: F:AM 49233, left ramus fragment with c1–p1, left detached m1, and p2–m3 alveoli; F:AM 62775, right edentulous ramus fragment with p1–p4 alveoli.

Jemez Creek drainage, southwest corner of *Blickomylus* Hill, local green zone near base of hill, near middle of Chamisa Mesa Member, Zia Formation (early Hemingfordian), Arroyo Pueblo drainage, Sandoval County, New Mexico: F:AM 49213, left partial ramus with c1 broken, p1 alveolus, p2–p3 both broken, and p4–m2.

DISTRIBUTION: Early Hemingfordian of New Mexico.

DIAGNOSIS: Relative to the more primitive *Cynarctoides luskensis*, *C. gawnae* has acquired a fully encircled ectotympanic ring, a discrete hypocone on M1–M2, and an enlarged protostylid of m2. It is, on the

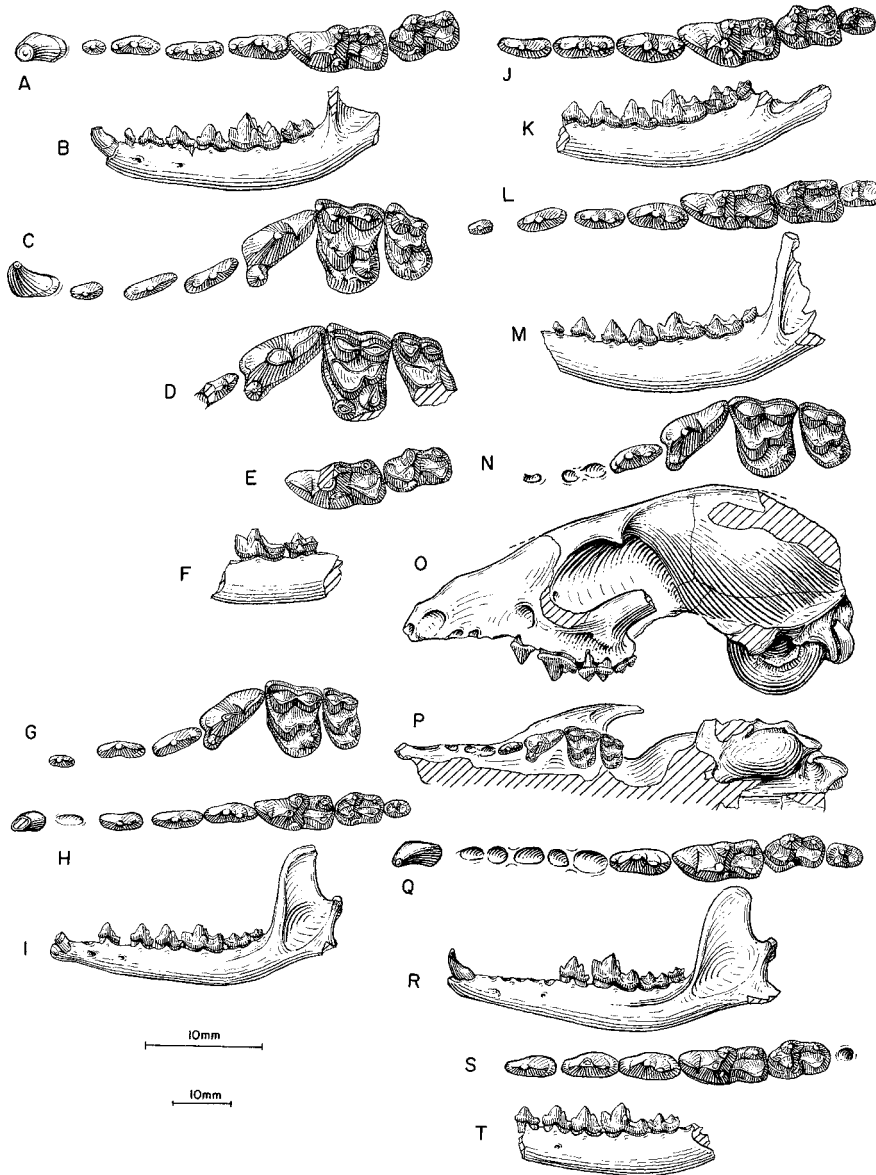


Fig. 23. **A**, Lower teeth, **B**, ramus, and **C**, upper teeth, *Cynarctoides acridens*, F:AM 63140, *Cynarctoides* Quarry, Chamisa Mesa Member, Zia Formation (early Hemingfordian), Sandoval County, New Mexico. **D**, Upper teeth, *C. acridens*, F:AM 49109, Ginn Quarry, temporally equivalent to Sheep Creek Formation (late Hemingfordian), Dawes County, Nebraska. **E**, Lower teeth and **F**, ramus (reversed from right side), *C. acridens*, AMNH 20502 (holotype of *C. mustelinus*), Stonehouse Draw, Sheep Creek Formation (late Hemingfordian), Sioux County, Nebraska. **G**, Upper teeth, **H**, lower teeth, and **I**, ramus (P1 and p2 reversed from right side), *C. gawnae*, F:AM 49249, holotype, Jeep Quarry, Chamisa Mesa Member, Zia Formation. **J**, Lower teeth and **K**, ramus (reversed from right side), *C. acridens*, F:AM 49112, Long Quarry, Sheep Creek Formation. **L**, Lower teeth and **M**, ramus (reversed from right side), *C. acridens*, F:AM 49126, Boulder Quarry, Olcott Formation (early Barstovian), Sioux County, Nebraska. **N**, Upper teeth (P3 reversed from right side), **O**, lateral and **P**, ventral views of skull, **Q**, lower teeth, and **R**, ramus, *C. luskensis*, F:AM 49005, holotype, 18 mi southeast of Lusk, Upper Harrison beds (late Arikareean), Goshen County, Wyoming. **S**, Lower teeth and **T**, ramus (reversed from right side), *C. luskensis*, F:AM 49003, 7 mi southeast of Chugwater, Upper Harrison beds (late Arikareean), Platte County, Wyoming. The longer (upper) scale is for A, C–E, G, H, J, L, N, Q, and S, and the shorter (lower) scale is for the rest.

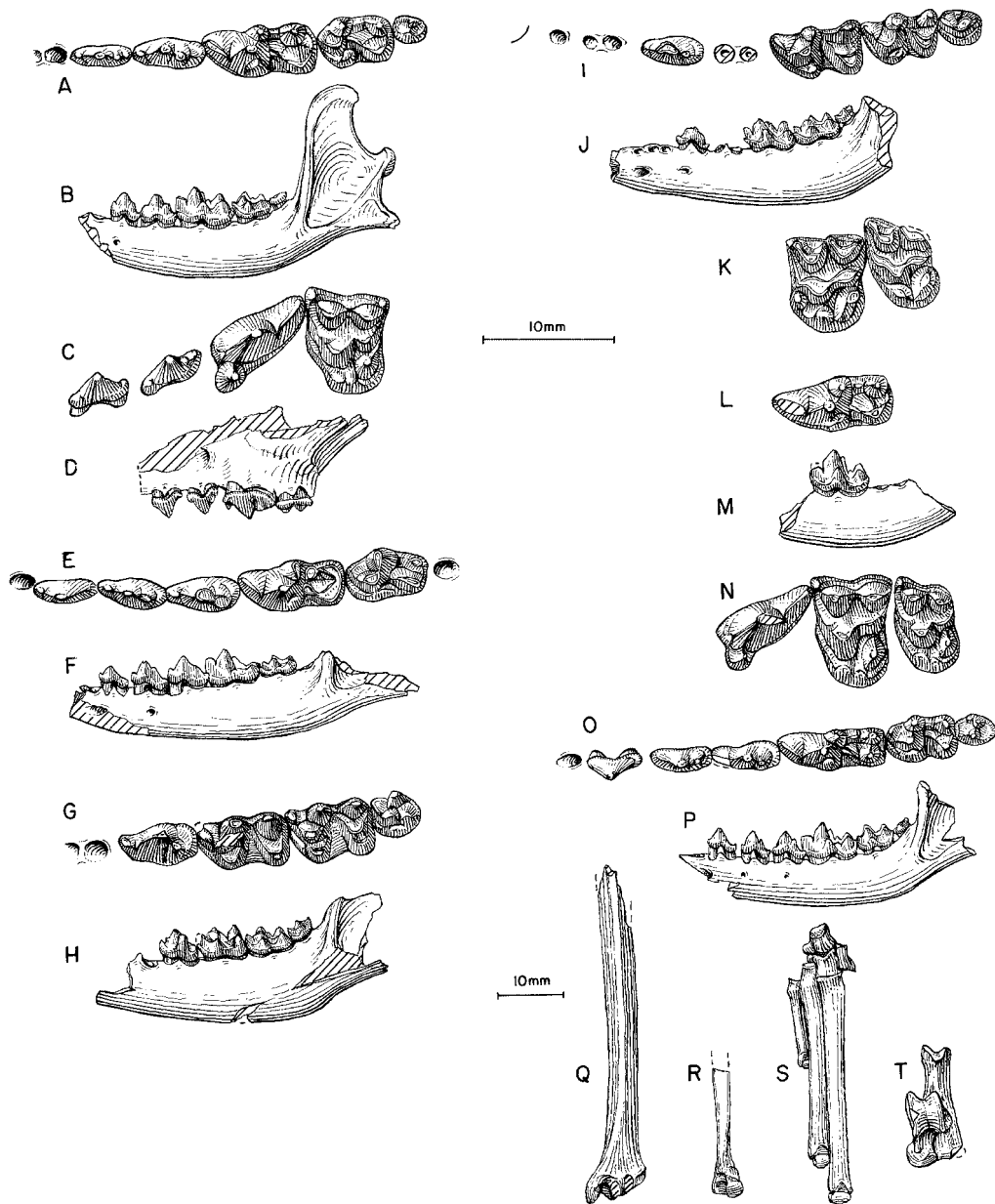


Fig. 24. **A**, Lower teeth and **B**, ramus (reversed from right side), *Cynarctoides acridens*, FMNH UC1547, east of Agate, Upper Harrison beds (late Arikareean), Sioux County, Nebraska. **C**, Upper teeth and **D**, lateral view of maxillary, *C. acridens*, FMNH UC1564, Agate area, Upper Harrison beds (late Arikareean), Sioux County, Nebraska. **E**, Lower teeth and **F**, ramus (reversed from right side), *C. acridens*, F:AM 49001, 18 mi southeast of Lusk, Upper Harrison beds (late Arikareean), Goshen County, Wyoming. **G**, Lower teeth and **H**, ramus (reversed from right side), *C. emryi*, UNSM 25455, holotype, Hemingford Quarry, Runningwater Formation (early Hemingfordian), Box Butte County, Nebraska. **I**, Lower teeth and **J**, ramus (reversed from right side), *C. emryi*, UNSM 25456, Hemingford Quarry. **K**, M1–M2, *C. emryi*, UNSM 25615, Hemingford Quarry. **L**, Crown view of m1, and **M**, ramus, *C. acridens*, AMNH 82558 (HC 144), holotype, 4 mi northeast of Agate, Upper Harrison beds (late Arikareean), Sioux County, Nebraska. **N**, Upper teeth, **O**, lower teeth, **P**, ramus, **Q**, distal tibia, **R**, distal fibula, **S**, partial foot, and **T**, astragalus-calcaneum, *C. acridens*, F:AM 99360, Runningwater Formation (early Hemingfordian), Dawes County, Nebraska. The longer (upper) scale is for **A**, **C**, **E**, **G**, **I**, **K**, **L**, **N**, and **O**, and the shorter (lower) scale is for the rest.

other hand, primitive relative to *C. acridens* in that its M1 hypocone is not surrounded by a narrow lingual cingulum, and in that it has a less complex and smaller M2 without a distinct paracone and an m1 without a metastylid and with a weaker protostylid.

**DESCRIPTION AND COMPARISON:** The holotype skull was severely flattened dorsoventrally, obscuring much of the original proportions. The dorsal skull roof, however, is relatively intact and reveals a smooth temporal area with separate (although rather weak) temporal crests as in *C. acridens* and *C. luskensis*. Both bullae are crushed but seem to show no enlargement over that seen in *C. luskensis*. As in *C. acridens*, the ectotympanic forms a fully closed ectotympanic ring (dorsal extension to the roof of the external auditory meatus) as opposed to the open, half ring in the primitive condition. In cranial proportion, *C. gawnae* is notable for its long and slender rostrum (length P1–M2 vs. palate width at P1 in fig. 21), characteristic of most advanced species of *Cynarctoides*.

The upper and lower teeth and the mandible are well preserved and clearly show intermediate characters between *C. luskensis* and *C. acridens*. Slight deepening of a transverse cleft on the lingual cingulum of M1 coupled with the rising of the posterior end of the cingulum creates a prominent hypocone, an advancement over that in *C. luskensis*. However, the hypocone still shows no sign of encirclement by a narrow cingulum on the lingual side, a derived condition that begins in *C. acridens*. The hypocone development on the M2 is also intermediate between *C. luskensis* (crestlike) and *C. acridens* (conate). The m1 protostylid remains small and fully attached to the protocone base. The m2 protostylid, on the other hand, is enlarged (in occlusal view) relative to that in *C. luskensis*. As in *C. luskensis*, the crista obliqua on m1 is still more or less sagittally oriented, instead of a more oblique orientation as in *C. acridens* and *C. emryi*.

**DISCUSSION:** In her unpublished dissertation on the geology and paleontology of the Zia Sand, Gawne (1973) described a new species of *Cynarctoides*, which was later re-

ferred to as “*Cynarctoides*, new species B” (Gawne, 1975), but never formally published. The content of her new species is the same as this study, and we take this opportunity to formally describe it.

*Cynarctoides gawnae* is an example of a transitional form that bridges the gap between *C. acridens*, which has many of the advanced characteristics of the genus, and *C. luskensis*, which has few. This combination of transitional features allows a sense of the actual steps shown by species of *Cynarctoides* in acquiring their peculiar morphology. The fact that the earliest records of *C. acridens* are from the late Arikareean of New Mexico and Nebraska suggests that *C. gawnae* must have had an equally long history, going back into the Arikareean (see further comments under *C. acridens*).

*Cynarctoides acridens* (Barbour and Cook, 1914)

Figures 23A–F, J–M, 24A–F, L–T

*Cynarctus acridens* Barbour and Cook, 1914: 226, pl. 1, figs. c, d. McGrew, 1937: 444, fig. 1.

*Nothocyon annectens* Peterson, 1907: Thorpe, 1922b: 429 (in part).

*Cynarctus mustelinus* Matthew, 1932: 2, figs. 2, 3.

“*Cynarctus*” *acridens* (Barbour and Cook): Matthew, 1932: 3.

*Cynarctoides acridens* (Barbour and Cook): McGrew, 1938a: 324, fig. 87 (in part). Galbreath, 1956: 373, fig. 1. Munthe, 1988: 98, figs. 23, 24; 1998: 134.

*Cynarctoides mustelinus* (Matthew): Galbreath, 1956: 373. Munthe, 1998: 134.

*Nothocyon* near *latidens* (Cope, 1881b): Macdonald, 1963: 209; 1970: 56.

*Nothocyon* aff. *minor* (Matthew, 1907): Gawne, 1975: 2.

*Cynarctoides*, new species A: Gawne, 1975: 2.

*Cynarctoides* cf. *C. acridens* (Barbour and Cook): Galusha, 1975b: 57.

**HOLOTYPE:** AMNH 82558 (HC 144), right partial ramus with m1 and m2 alveolus from 4 mi northeast of Agate, Upper Harrison Beds of Peterson (1907) (late Arikareean), Sioux County, Nebraska (fig. 24L, M).

**REFERRED SPECIMENS:** East of Porcupine Creek, lower part of Rosebud Formation (equivalent to Monroe Creek Formation or Harrison Formation of Macdonald, 1963:

157) (medial or late Arikareean), AMNH locality "Rosebud" 32, Shannon County, South Dakota: AMNH 12873, right ramal fragment with m1 (referred to *Nothocyon* near *latidens* by Macdonald, 1963: 209).

First hill south of *Syndyoceras* Hill, 0.5 mi west of Agate, Harrison Formation (late Arikareean), Sioux County, Nebraska: AMNH 81035 (HC 488), right ramus fragment with p4–m1.

Agate area, Upper Harrison beds (late Arikareean), Sioux County, Nebraska: F:AM 50229, partial left and right rami with c1–m3 (m1s broken), limb bone fragments, 9 mi southwest of Harrison, in high brown sand; F:AM 107600, isolated left M1; FMNH UC1547 (AMNH cast 88393), right ramus with p1–p2 alveoli and p3–m3, from east of Agate (fig. 24A, B); FMNH UC1564 (AMNH cast 88392), left maxillary and skull fragment with C1–P1 alveoli broken and P2–M1 (fig. 24C, D); and FMNH P26201, right partial ramus with p2–m3.

Eighteen mi southeast of Lusk, Upper Harrison beds (late Arikareean), Goshen County, Wyoming: F:AM 49001, right partial ramus with c1–p1 alveoli, p2–m2, and m3 alveolus (fig. 24E, F); and F:AM 49002, right isolated m1 from below high brown sand.

Runningwater Formation (early Hemingfordian), Box Butte County, Nebraska: F:AM 99364, right partial ramus with m2 and alveoli of c1–m1 and m3, Dry Creek, Prospect B; UNSM 25417, partial left ramus with c1, p2, p3–m2, and alveoli of p1, p3, and m3, UNSM loc. Bx-7; UNSM 25424, right partial ramus with p2–m2 and alveoli of c1–p1 and m3, UNSM loc. Bx-7; UNSM 25462, left partial ramus with c1–p3 alveoli and p4–m2, UNSM loc. Bx-22, 12 mi west and 4 mi north of Hemingford; UNSM 25463, left M1, Marsland Quarry, UNSM loc. Bx-22; UNSM 25464, right ramus fragment with m1–m2 and alveolus of m3, Marsland Quarry, UNSM loc. Bx-22; UNSM 25612, left partial ramus with c1–p3 alveoli and p4–m2, Hemingford area, UNSM loc. Bx-0; UNSM 25666, right ramus with c1–p1 alveoli, p2–m2, and m3 alveolus, Hemingford Quarry 7B, UNSM loc. Bx-7B; UNSM 25723, right partial ramus with p2–p3 and p4–m2 all broken, Hemingford Quarry 7B, UNSM loc. Bx-

7B; UNSM 25724, right partial ramus with m1–m2, and m3 alveolus, Hemingford Quarry 12B, UNSM loc. Bx-71; UNSM 25766, left M1, UNSM loc. Bx-7; UW 4141, left isolated broken M1, UW loc. V-34001, Marsland Quarry; UW 4142, left isolated m1, UW loc. V-34001, Marsland Quarry; UW 4143, left isolated broken m1, UW loc. V-34001, Marsland Quarry; and UW 4144, right ramus fragment with broken p4–m1, UW loc. V-34001, Marsland Quarry.

Runningwater Formation (early Hemingfordian), Cherry County, Nebraska: F:AM 49178, left partial ramus with p4–m2 and m3 alveolus, Antelope Creek; F:AM 107608, isolated left m1 (broken); YPM 12781, right partial ramus with p4 broken–m2 and m3 alveolus (referred to *Nothocyon annectens* by Thorpe [1922b: 429]), Antelope Creek.

Runningwater Formation (early Hemingfordian), Dawes County, Nebraska: AMNH 85956 (HC 1325), right ramus fragment with p4, Havorka Quarry; F:AM 25331, left ramus fragment with m1–m2 and alveolus of m3, from Belmont area; F:AM 25428, skull and ramus fragments with left P4–M1, right M1–M2, left p2–m1, and right p1–m3, Elder Ranch; F:AM 25429, partial right ramus with p2–p3, p4 broken, and m1–m2 broken, Marshall Ranch; F:AM 49098, left partial ramus with p3–m1, Woods Canyon Quarry; F:AM 49107, left partial ramus with p3–m1 and alveoli of p1–p2 and m2; F:AM 49108, left partial ramus with c1–m2 (broken); F:AM 49121, right partial ramus with p2, p4–m1, and alveoli of p1, p2, and m2–m3, Dunlap Camel Quarry; F:AM 49122, right ramus fragment with p4–m1, Dunlap Camel Quarry; F:AM 49123, left ramus fragment with m1 and alveolus of m2, "B" Quarry; F:AM 99360, skull fragments, isolated left and right P4–M2, right and left rami with p1 alveolus–m3, distal tibia and fibula, calcaneum, astragalus, tarsals, and metatarsals I, II, and III (fig. 24N–T); F:AM 99361, right partial ramus with p3–m1 and m2 broken, Pebble Creek; F:AM 99363, left ramus fragment with m2–m3, Woods Canyon; F:AM 99365, left partial ramus with p1–p2 both broken and p3–m3, Cottonwood Creek Quarry; F:AM 99366, right partial ramus with p1–p3 all broken, p4–m1, and m2 broken, Cottonwood Creek Quarry; F:AM 99367, right par-

tial ramus with m1 broken, Cottonwood Creek Quarry; F:AM 99368, isolated left m1, Cottonwood Creek Quarry; F:AM 99369, left ramus fragment with p4 root-m1, Cottonwood Creek Quarry; and F:AM 99371, left partial ramus with p3 alveolus-m2 and m3 alveolus, Cottonwood Creek Quarry.

Runningwater Formation (early Hemingfordian), Bridgeport Quarry (UNSM loc. Mo-115), Morrill County, Nebraska: UNSM 25434, right ramal fragment with m1 broken-m2 and m3 alveolus; UNSM 25435, left ramal fragment with p4-m1; UNSM 25437, right M1; UNSM 25444, left dp4; UNSM 25446, left M1; UNSM 25450, left M1; and UNSM 25460, right ramal fragment with m1-m3.

Schoolhouse Prospect No. 2, Box Butte Formation (late Hemingfordian), Dawes County, Nebraska: F:AM 99372, right partial ramus with p4-m3.

Dry Creek, Prospect A, Red Valley Member, Box Butte Formation (late Hemingfordian), Box Butte County, Nebraska: F:AM 95277, left partial ramus with p4 broken, m1, and m2 broken.

Ginn Quarry, in rocks temporally equivalent to the Sheep Creek Formation (late Hemingfordian), Dawes County, Nebraska: F:AM 49109, left partial maxillary with P3 broken-M1 and M2 broken (fig. 23D).

Split Rock Formation (late Hemingfordian), Granite Mountain, Fremont County, Wyoming (as listed in Munthe, 1988: 99): CMNH 14710, M2 fragment from UCMP V69190; CMNH 14371, M1 fragment from UCMP loc. 69190; CMNH 14172, c1 from UCMP loc. V69190; CMNH 14713, m1 from UCMP loc. V69190; CMNH 15844, mandible fragment with p3, broken p2, and root of p1, from UCMP loc. V69190-69192; CMNH 15845, M1 fragment from UCMP loc. V69190-69192; CMNH 15846, m1 from UCMP loc. V69190-69192; KUVF 20350, m2 fragment from UCMP loc. V69190-69192; KUVF 20358, m1 fragment, from UCMP loc. V69190-69192; MCZ 7317, maxillary fragment with P3-M2 and isolated P4, from UCMP loc. V69191; UCMP 21589, m2 from UCMP loc. V69191; UCMP 30084, m3 from UCMP loc. V77145; UCMP 121919, P4 fragment from UCMP loc. V69190; UCMP 121920, mandible frag-

ment with m1 from UCMP loc. V69190; UCMP 121921, m1 from UCMP loc. V69191; and UWBM 62576, left ramus with p3-m2.

Martin Canyon Local Fauna (early Hemingfordian), Logan County, Colorado: KUVF 9970, partial left and right basicranium, left maxillary with P3-M1 and M2 alveolus, left ramus fragment with m1-m2 and m3 alveolus, and right ramus fragment with m2-m3 (Galbreath, 1956: fig. 1).

Lemhi Valley, 40 mi south of Salmon, in talus about 15 ft below white zone, Geertson Formation (early Hemingfordian), Lemhi County, Idaho: F:AM 63270B, right ramal fragment with broken m1 and isolated M2.

Hidalgo Bluff, Oakville Formation (early Hemingfordian), Washington County, Texas: TMM-BEG 40067-180 (AMNH cast 99659), left isolated M1.

Sheep Creek Formation (late Hemingfordian), Sioux County, Nebraska: AMNH 20502, right partial ramus with m1-m2 (fig. 23E, F), holotype of *Cynarctus mustelinus* Matthew (1932: 2), Stonehouse Draw; AMNH 20503, right partial ramus with p2 alveolus, p3-p4, m1 alveolus, and m2-m3, paratype of *Cynarctus mustelinus* Matthew (1932: 2), Stonehouse Draw; AMNH 22399, right ramus with c1-p2 alveoli and p3-m3, Ashbrook Pasture near Sinclair Draw; AMNH 22399A, right partial edentulous ramus, Ashbrook Pasture near Sinclair Draw; AMNH 96677, partial left ramus with p4 and m1-m3 alveoli, Agate area; F:AM 49110, left partial ramus with c1-p1 alveoli and p2-m2 (m1 broken), Greenside Quarry; F:AM 49111, right partial ramus with p2-p3, p4 broken, and m1-m3 alveolus, Thomson Quarry; F:AM 49112, right partial ramus with p2-m3, Long Quarry (fig. 23J, K); and F:AM 49114, right partial ramus with p1 alveolus-m1 (p2, p4, and m2 all broken), Ravine Quarry.

Olcott Formation (early Barstovian), Sioux County, Nebraska: F:AM 49105, left ramus with i1-i3 broken alveoli and c1 broken-m3, *Synthetoceras* Quarry; F:AM 49126, right ramus with c1 alveolus-m3, Boulder Quarry (fig. 23L, M); F:AM 49127, left partial ramus with p1 alveolus-m2, Humbug Quarry; F:AM 49128, left ramus with c1-m3, Humbug Quarry; F:AM 49129,

left partial ramus with c1, p1–p4 alveoli, broken m1, m2, and m3 alveolus, Humbug Quarry; F:AM 49130, right ramus fragment with p1 alveolus, p2, and p3 alveolus–p4, Humbug Quarry; F:AM 49131, left partial ramus with m1–m2 and m3 alveolus, Humbug Quarry; F:AM 49136, right and left partial rami with c1–m1 and m2 broken, floor of Mill Quarry; F:AM 49137, left partial ramus with unerupted p2–p4, m1–m2 alveolus, and m3 unerupted, floor of Mill Quarry; F:AM 49138, right partial ramus with p4–m2 and m3 alveolus, Mill Quarry; and F:AM 49139, left ramus fragment p4 and m1 broken, Mill Quarry.

Observation Quarry, Sand Canyon Formation (early Barstovian), Dawes County, Nebraska: F:AM 25383, left isolated M1; F:AM 25384, left isolated M1; and F:AM 49120, right maxillary fragment with P4 broken.

Standing Rock Quarry, lower part of the Piedra Parada Member of the Zia Formation (late Arikareean), Sandoval County, New Mexico: F:AM 49203, crushed skull with I1–I3 all broken, C1, P1 alveolus–M2, and mandible with i3, c1 broken, and p1–m3 (p2 broken).

Blick Quarry, near the middle of the Chamisa Mesa Member of the Zia Formation (early Hemingfordian), Arroyo Pueblo drainage, Sandoval County, New Mexico: F:AM 49200, left ramus fragment with broken m1; F:AM 49202, left and right partial rami with i3 broken–m3 (p4–m1 both broken); F:AM 49211, left P4; F:AM 49212, partial mandible with c1–m3; F:AM 49234, left ramus fragment with m1 and isolated right m1; F:AM 49235, partial mandible with c1–m3, southwest corner of hill containing Blick Quarry, low; F:AM 49236, left partial ramus with c1–p1 alveoli and p2–m1 (p3 and m1 broken); F:AM 49237, right partial ramus with i1–c1 and p1 broken–m1 (p3 and m1 broken); F:AM 49242, left partial ramus with p3 root–m3; and F:AM 50161, right ramus fragment with m2 broken.

*Cynarctoides* Quarry, near the middle of the Chamisa Mesa Member of the Zia Formation and the same level as Blick Quarry (early Hemingfordian), Arroyo Pueblo drainage, Sandoval County, New Mexico: F:AM 49204, right and left ramus fragment with p2

and m2–m3 both broken; F:AM 49238, right and left partial rami with c1 broken–m2; F:AM 50160, left partial ramus with p4–m2 all broken; F:AM 63140, anterior part of skull with I1–I3 alveoli and C1–M2 and both partial rami with c1–m2 and m3 alveolus (fig. 23A–C); F:AM 63141, right partial ramus with p4–m1 both broken and m2; F:AM 63142, right and left partial maxillae with P4–M2; F:AM 63143, right isolated M1; F:AM 63150, anterior fragment of skull with I1–P1 alveoli and P2–M2; F:AM 63151, right partial ramus with c1–m2 (m1–m2 both broken) and m2 alveolus; F:AM 63152, right partial ramus with c1 broken, p1 alveolus, and p2–m3 (p4–m1 both broken); F:AM 63153A, two ramus fragment with p1–p3, p4, and m1 broken; F:AM 63153B, ramus fragment with broken c1 and broken base of teeth; and F:AM 63153C, ramus fragment and detached teeth including c1, p3, and broken p4.

South of Santa Cruz River, 50 ft below the Nambe White Ash Stratum, Nambe Member, Tesuque Formation (late Hemingfordian), Santa Fe County, New Mexico: F:AM 63144, right and left partial rami with c1 broken, p1–p3 alveoli, p4 broken, m1, and m2 broken.

Tesuque Grant, Skull Ridge Member of Tesuque Formation (early Barstovian), Santa Fe County, New Mexico: F:AM 49201, left ramal fragment with m1 broken and alveoli of m2–m3; and F:AM 63138, right partial ramus with c1 root, p1–p2 alveoli, p3 broken–m2, and m3 broken alveolus.

Barstow Formation (early Barstovian), San Bernardino County, California: F:AM 27497, left maxillary fragment with P4–M1, Yermo Quarry, 5 mi east of Yermo; and F:AM 27539, left partial maxillary with P4–M2, Sandstone Quarry, "Second Division."

DISTRIBUTION: Medial or late Arikareean of South Dakota; late Arikareean of Nebraska, Wyoming, and New Mexico; early Hemingfordian of Nebraska, Colorado, Idaho, Texas, and New Mexico; late Hemingfordian of Nebraska, Wyoming, and New Mexico; and early Barstovian of Nebraska, New Mexico, and California.

EMENDED DIAGNOSIS: Besides the larger size, derived characters that distinguish *Cynarctoides acridens* from *C. gawnae* are M1

hypocone surrounded by a narrow cingulum, M2 larger and more complex with a larger paraconule, broader p4, a metastylid on m1, and a stronger protostylid on m1. This species, however, lacks the extreme specializations in *C. emryi* such as the stylar cusps on the labial border of M1; M2 and m2 nearly equal in size to M1 and m1; robust p4 with laterally shifted posterior accessory cusp; selenodont-like lower molars with lingually directed crista obliqua; and talonid cusps nearly equal in height to those of the trigonids.

DESCRIPTION AND COMPARISON: Despite the large number of referred specimens listed above, the overall skull morphology of this species remains poorly known. Besides the basicranial fragments described by Galbreath (1956), a dorsoventrally flattened skull from the Zia Formation in New Mexico (F:AM 49203) supplies additional cranial morphology. As demonstrated by Galbreath (1956), the middle ear region of *C. acridens* is essentially that of a primitive canid. It has a moderately inflated bulla and a ventrally directed paroccipital process that is fully fused with the bulla. The ectotympanic extends dorsally to form a full tympanic ring. The mastoid process is not enlarged and there is no suprategmental fossa. The skull roof has paired temporal crests except for a small segment near the nuchal crest. The masseteric scar on the zygomatic arch is wide, making up two-fifths of its depth.

With the large sample of lower jaws available, a better appreciation of variation is possible. Although most of the horizontal rami remain slender (a derived character acquired since *C. luskensis*), some individuals of *C. acridens* show a stronger ramus, such as developed in *C. emryi*. These individuals also tend to broaden their p4 slightly, but not quite to the degree of robustness of the p4 in *C. emryi*.

The dentition of *Cynarctoides acridens* is highly derived. The M1 hypocone not only becomes higher but also is surrounded lingually by a narrow cingulum. The anterior end of the lingual cingulum is also enlarged, but not quite to the stage of an isolated cusp as in *C. emryi*. The m1 protostylid is enlarged at the expense of the protoconid. The protostylid is a distinct cusp fully detached from the base of the protoconid, in contrast

to being more closely appressed to the protoconid in *C. gawnae* and *C. luskensis*. A small metastylid is present on m1–m2 for the first time, and tends to be better developed in specimens from New Mexico than in those from the Great Plains. Cusps on m2 are higher-crowned and more conical than in *C. luskensis* and *C. gawnae*.

DISCUSSION: Despite the nearly identical size and shape of the holotypes of *Cynarctoides acridens* and *C. mustelinus*, Matthew (1932: 3) considered his *Cynarctus mustelinus* to differ generically from the former, which he thought to be nearer to “*Nothocyon*” *lemur* from John Day. Galbreath (1956) and Munthe (1988), on the other hand, failed to see any distinction even at the species level. As pointed out by Munthe (1988: 103), Matthew apparently allowed stratigraphic relationships to be a major factor in his taxonomic determination. At the time, *C. acridens* was known only from the Upper Harrison beds, whereas Matthew’s two specimens of *C. mustelinus* (AMNH 20502 and 20503) were from the Sheep Creek Formation. In light of the present records, it is clear that *C. acridens* had a nearly continuous range from the medial Arikarean through early Barstovian of the Great Plains and the southwestern United States. Furthermore, despite the multiple species of *Cynarctoides* newly described here, *C. acridens* remains the most persistent among all species of the genus both in terms of geologic range and geographic distribution. In fact, *C. acridens* coexisted with all advanced species of *Cynarctoides* (*C. luskensis* and above) in one area or at one time, and it was always more abundant and outlasted all other species when they did co-occur (fig. 141). It thus seems no coincidence that *C. acridens* was the first to be discovered and that it remained the only valid species recognized of the genus until this study.

#### *Cynarctoides emryi*, new species

Figure 24G–K

*Cynarctoides acridens* (Barbour and Cook, 1914): McGrew, 1938a: 328, fig. 88 (in part).

HOLOTYPE: UNSM 25455 (F:AM cast 96711), right partial ramus with p3 broken alveolus–m3 (m1 broken) (fig. 24G, H), from



Hemingford Quarry 7B (UNSM loc. Bx-7B), Runningwater Formation (early Hemingfordian), Box Butte County, Nebraska.

**ETYMOLOGY:** Named for Dr. Robert J. Emry of the National Museum of Natural History, the Smithsonian Institution, in recognition of his important fieldwork in Nebraska.

**REFERRED SPECIMENS:** From the type locality, Hemingford Quarry 7B (UNSM loc. Bx-7B), Runningwater Formation (early Hemingfordian), Box Butte County, Nebraska: UNSM 25456, right partial ramus with c1 broken, p1–p2 alveoli, p3, and p4 root–m3 (fig. 24I, J); UNSM 25615 (F:AM cast 96710), left partial maxillary with M1–M2 (fig. 24K); and UNSM 25722, right partial ramus with c1–m1 all broken.

Woods Canyon, Runningwater Formation (early Hemingfordian), Dawes County, Nebraska: F:AM 25432, right partial ramus with c1 broken, p1 alveolus, p2 broken–m1, and m2 alveolus; and F:AM 49106, right and left partial rami with p2–m1.

Stamen Ranch, Runningwater Formation (early Hemingfordian), Sioux County, Nebraska: F:AM 99362, right partial ramus with p4–m3.

Upper Harrison Beds (late Arikareean), Sioux County, Nebraska: FMNH P25548, right maxillary fragment with P4 alveolus and M1–M2 (McGrew, 1938a: fig. 88), from near Agate.

**DISTRIBUTION:** Late Arikareean to early Hemingfordian of Nebraska.

**DIAGNOSIS:** Derived characters that distinguish this species from *Cynarctoides acridens* and other more primitive species of the genus are: M1 with anterolabial stylar cusps and M2 with minute anterolabial stylar cusp; lack of connecting crest between paracone and metacone of M1–M2 (i.e., complete transverse division by a valley); p4 posterior accessory cusp laterally displaced; selenodont m1–m2; m1 trigonid shorter, protostylid larger relative to protoconid, entoconid extremely tall, much taller than hypoconid and about equal to height of metaconid; further enlargement of m2 to almost the same size as m1; m2 protostylid larger and entoconid extremely tall, much taller than hypoconid and approximating height of metaco-

nid; and m3 large with strong labial cingulum and protostylid.

**DESCRIPTION AND COMPARISON:** Teeth of *Cynarctoides emryi* reveal an animal with highly unique dental morphology. In almost every aspect of the dentition, *C. emryi* shows the extreme modifications of the *Cynarctoides* clade. The most obvious is the development of the almost selenodont-like upper and lower molars. Other species of *Cynarctoides* have upper molars whose cusps remained conical. In *C. emryi*, however, the paracone and metacone have developed an anterior and a posterior crista extending labially to form stylar cusps. The lingual cingulum in front of the hypocone has further differentiated into two additional cusps, one immediately lingual to the protocone (this cusp was probably independently acquired in certain population of *C. acridens*, e.g., F:AM 49109, fig. 23D) and one slightly more anterior and labial. Such enlargements of the cingular cusps contributed to the reduction of the protocone.

The M2 and m2 in *C. emryi* are almost identical in size and morphology to the M1 and m1 (fig. 24G, I, K), an obvious trend toward increasing the grinding surfaces that began in *C. acridens*. The m1–m2 also become relatively short and broad, and their talonid cusps have nearly the same height as the trigonid cusps. In correlation with the further enlarged protostylids in the m1–m2, the posterior accessory cusp of the p4 is also enlarged and laterally shifted to resemble a protostylid of the lower molars.

**DISCUSSION:** *Cynarctoides emryi* from the late Arikareean and early Hemingfordian of Nebraska coexists with *C. acridens*. It is interesting to note, however, that the more primitive *C. acridens* outlasted *C. emryi* and survived well into the early Barstovian. The former also had a much wider distribution (New Mexico and California, in addition to the states in the northern Great Plains).

As the phylogenetically terminal member of the *Cynarctoides* clade, *C. emryi* is the most hypocarnivorous of all species. In fact, the dental morphology of this small carnivoran has in many ways gone beyond the normal repertoire of a hypocarnivorous carnivoran and shows adaptations to insectivory or herbivory in its rather selenodont lower mo-

lars. Such a specialization is extremely rare among carnivorans, and is known only in lophocyonine viverrids in the Miocene of Europe (Fejfar and Schmidt-Kittler, 1984, 1987; Koufos et al., 1994).

*Phlaocyon* Matthew, 1899

*Bassariscops* Peterson, 1924.

*Aletocyon* Romer and Sutton, 1927.

TYPE SPECIES: *Phlaocyon leucosteus* Matthew, 1899.

INCLUDED SPECIES: *P. minor* (Matthew, 1907); *P. latidens* (Cope, 1881b); *P. annectens* (Peterson, 1907); *P. achoros* (Frailey, 1979); *P. multicuspus* (Romer and Sutton, 1927); *P. marslandensis* McGrew, 1941; *P. leucosteus* Matthew, 1899; *P. yatkolai*, new species; and *P. mariae*, new species.

DISTRIBUTION: Early Arikareean of Oregon and Wyoming; medial Arikareean of South Dakota and Florida; late Arikareean of South Dakota, Nebraska, Wyoming, Colorado, Florida and Texas; early Hemingfordian of Nebraska and Colorado; and late Hemingfordian of Nebraska.

EMENDED DIAGNOSIS: Synapomorphies that unite *Phlaocyon* are robust premolars, widened P4, quadrate (elongated) upper molars relative to P4, and wide m1 talonid. In cranial proportions, all *Phlaocyon* tend to have a deep jugal, a wide rostrum, and a wide zygomatic arch.

DISCUSSION: Because *Phlaocyon* and *Procyon* share convergent adaptations toward hypocarnivorous dentitions, earlier discussions on the phylogenetic relationships of *Phlaocyon* (mainly *P. leucosteus*) are mostly in the context of the evolution of procyonids. *Phlaocyon* was considered an intermediate form between the living raccoon (*Procyon*) and primitive canids (Wortman and Matthew, 1899; McGrew, 1938a, 1939, 1941). In her landmark study of the basicrania of fossil North American carnivorans, Hough (1948) first demonstrated the essentially canid middle ear region in *P. leucosteus*, a conclusion independently reached by Dahr (1949). Consistent with this conclusion, our present reference to *Phlaocyon* of several species, previously regarded as unrelated, fills much of the large gap between *P. leucosteus* and more primitive borophagines (such as *Ar-*

*chaeocyon*). Our descriptions of three new species below further demonstrate a hypocarnivorous clade that is considerably more diverse than previously thought, and our cladistic concept of *Phlaocyon* encompasses a morphological spectrum far beyond the traditional boundary of the genus (e.g., Peterson, 1928; Stevens, 1977: 34–35).

*Phlaocyon minor* (Matthew, 1907)

Figures 25, 26H–N

*Cynodesmus minor* Matthew, 1907: 189. Macdonald, 1963: 212.

*Tephrocyon* sp. Wood and Wood, 1937: 139, fig. 1 (13).

*Tomarctus minor* White, 1941b: 95.

*Nothocyon minor* Cook and Macdonald, 1962: 561. Macdonald, 1970: 57.

HOLOTYPE: AMNH 12877, right partial maxillary with P4–M2, left partial ramus with c1–p1 alveoli, p2–m1 (fig. 25C–F), and limb fragments, from 4 m. E. of Porcupine P.O. . . . E. of Porc[upine] Cr'k . . . upper Rosebud, AMNH "Rosebud" 22, Rosebud Formation (late Arikareean), Shannon County, South Dakota (Macdonald, 1963: 156).

REFERRED SPECIMENS: From the Wounded Knee-Rosebud fauna (late Arikareean), Shannon County, South Dakota: AMNH 12878, left partial ramus with p3 alveolus and p4–m3, from AMNH "Rosebud" 5, east of Porcupine Butte, upper Rosebud beds ("Rosebud Formation" of Macdonald [1963: 154]); and AMNH 13800, right and left rami with i1–m3, 2 mi west of American Horse Creek, Upper Rosebud Beds.

Little Muddy Creek, lower Arikaree Group (early Arikareean), Niobrara County, Wyoming: F:AM 49054 (fig. 25A, B), left partial ramus with p3 broken–m1 and m2 broken.

Turtle Butte Formation (medial Arikareean), Tripp County, South Dakota: SDSM 8540 (AMNH cast 98586), left partial ramus with p4–m2 and alveoli of p3 and m3.

*Syndyoceras* Hill, 0.5 mi west of Agate, Harrison Formation (late Arikareean), Sioux County, Nebraska: AMNH 81033 (HC 489), left ramus fragment with c1 broken–p1, p2–p4 alveoli, and m1 from first hill south in *Syndyoceras* layer.

Upper Harrison beds (late Arikareean),

south of Lusk, Wyoming: F:AM 27578, right and left partial rami with p1 alveolus–m2, Sand Gulch, Goshen County; F:AM 49073, right partial ramus with c1 broken, p1–p2 alveoli, and p4–m1, Royal Valley, Niobrara County; F:AM 49081, left partial ramus with p4 broken–m2 and m3 alveolus (fig. 25G, H), Silver Springs, Niobrara County; and F:AM 50223, right partial ramus with p3–m2, Jay Em Section, high, Goshen County.

Upper Harrison beds (late Arikareean), Van Tassel area, Niobrara County, Wyoming: F:AM 49004, skull with I3–M2 (P3 broken, fig. 26H–K), partial mandible with c1 broken–m3 (fig. 26L, M) and left humerus (fig. 26N) articulated with proximal end of ulna and radius, right distal end humerus, isolated vertebrae, and limb fragments, 1.5 mi southwest of Van Tassel, low.

Upper Harrison beds (late Arikareean), Guernsey area, Platte County, Wyoming: F:AM 50218, skull fragment with P4–M2 and partial mandible with c1–m3 (fig. 25I–K) from 3 mi southeast of Guernsey, 7 ft below the green-white layer.

Cedar Run Local Fauna, Cedar Creek, Oakville Formation (late Arikareean), Washington County, Texas: AMNH 30087, isolated right broken M1 (Wood and Wood, 1937: fig. 1 [13]).

DISTRIBUTION: Early Arikareean of Wyoming; medial to late Arikareean of South Dakota; late Arikareean of Nebraska, Wyoming, and Texas.

EMENDED DIAGNOSIS: As the most basal species of *Phlaocyon*, *P. minor* possesses all the synapomorphies (mostly in their initial stage of development) of the genus that can be used to distinguish it from primitive borophagines such as *Archaeocyon*, *Rhizocyon*, and *Cynarctoides*: robust and shortened premolars, quadrate M1, and widened m1 talonid. Additionally, *P. minor* has two autapomorphies, double temporal crests, and an elongated m2 relative to that of m1. On the other hand, *P. minor* lacks derived features in *P. latidens* and more derived species: widened P4 with a distinct lingual cingulum or hypocone, a cleft on lingual cingulum of M1 isolating the hypocone, and more distinct protostylid on m1.

DESCRIPTION AND COMPARISON: The present reference of F:AM 49004, a nearly complete

skull and mandible, furnishes morphologies previously unknown in *P. minor*. Although imperfectly preserved, especially in its fragmentary teeth, F:AM 49004 shows a cranium very close to that of *P. latidens*. The most prominent feature of the skull is the inflated braincase (braincase width in fig. 27). Such an expansion of the braincase seems to cause the temporal crests (very weak) to remain separate anterior to the inion. Other cranial proportions that suggest membership in the *Phlaocyon* clade include a deep jugal, a broad palate, and a wide zygomatic arch (see fig. 27). The temporal fossa is short (length M2 to bulla in fig. 27), which appears to be a feature in F:AM 49004 alone among *Phlaocyon* species. The paroccipital process is rodlike, ventrally oriented, and has almost no free tip (i.e., it is completely fused with the bulla). The mastoid process is not inflated. Both bullae are crushed inward, creating an appearance of much smaller bullae than is indicated by the position of their attachment to the surrounding bones. The anterior zygomatic arch still has a rather wide masseteric scar.

At the base of the *Phlaocyon* clade, *P. minor* shares only the initial development of the diagnostic features of the genus, and some of these dental characters are also variable. For example, the robustness of premolars, the widening of m1 talonid, and the enlarged m2 are only variably present in the known sample of *P. minor*. In contrast to the usually well-developed protostylids on m1 of *P. latidens*, this cusp occurs in *P. minor* only rarely (4 of 13 individuals) and is usually poorly developed or shows a rudimentary impression only when present. Such a stage of development of the protostylid is here postulated to be equivalent to that in *Cynarctoides lemur* (see further discussion under that species), although a larger sample is certainly desirable to improve statistical inference.

DISCUSSION: Cook and Macdonald (1962) commented on the close resemblance of *P. minor* to *P. latidens*, and this was their reason for including *minor* in *Nothocyon*. An editorial error in Macdonald (1963) left *minor* in *Cynodesmus*, but this was later corrected (Macdonald, 1970). White (1941b) noted the confusion about *Cynodesmus* created by Matthew's (1907) reference of *C. mi-*

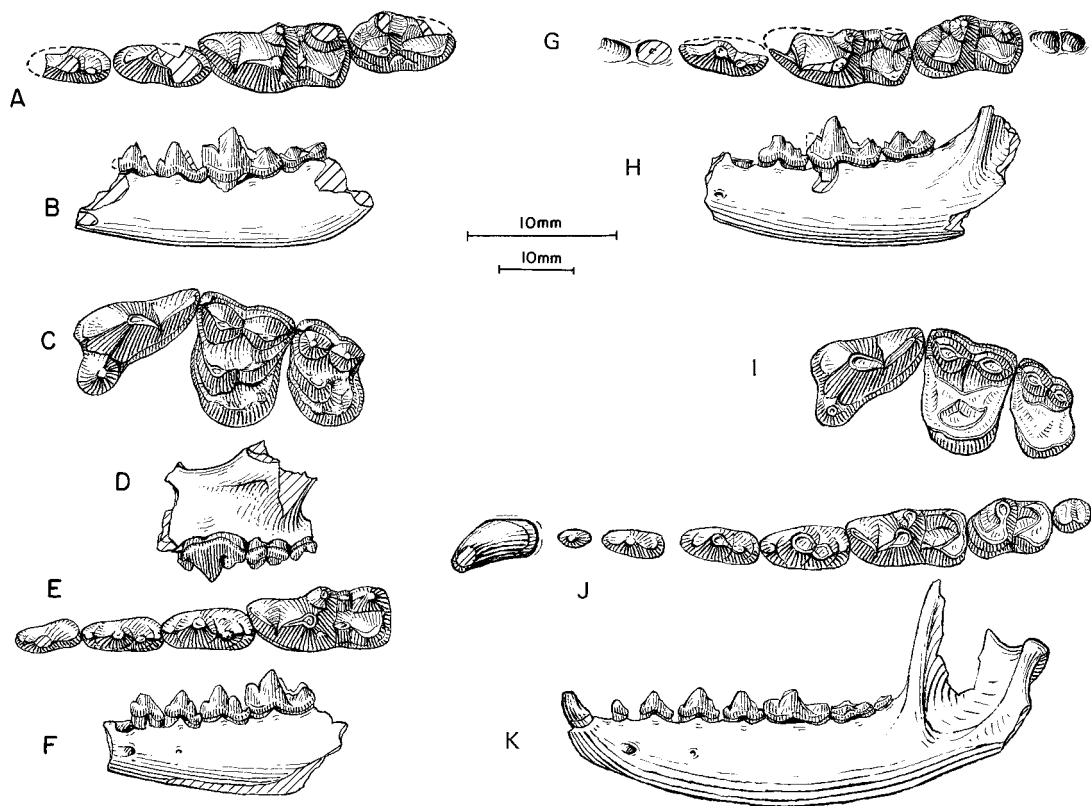


Fig. 25. *Phlaocyon minor*. **A**, Lower teeth and **B**, ramus, F:AM 49054, Little Muddy Creek, lower Arikaree Group (early Arikareean), Niobrara County, Wyoming. **C**, Upper teeth, **D**, lateral view of maxillary (reversed from right side), **E**, lower teeth, and **F**, ramus, AMNH 12877, holotype, Rosebud Formation (late Arikareean), Shannon County, South Dakota. **G**, Lower teeth and **H**, ramus, F:AM 49081, Upper Harrison beds (late Arikareean), Silver Springs, Niobrara County, Wyoming. **I**, Upper teeth, **J**, lower teeth, and **K**, ramus (M1–M2 and p1 reversed from right side), F:AM 50218, Upper Harrison beds (late Arikareean), Guernsey area, Platte County, Wyoming. The longer (upper) scale is for A, C, E, G, I, and J, and the shorter (lower) scale is for the rest.

*nor* and *C. thomsoni* to this genus. However, White's paper was overlooked by most subsequent authors, and the confusion continued until quite recently. *Cynodesmus* is now recognized as belonging to the Hesperocyoniinae (Wang, 1994: 61–62).

*Phlaocyon latidens* (Cope, 1881b)

Figure 26A–G

*Galecyon latidens* Cope, 1881b: 181. Cope, 1884: 915, pl. 70, figs. 4, 5.

*Cynodictis latidens* (Cope): Scott, 1898: 400.

*Nothocyon latidens* (Cope): Matthew, 1899: 62; 1932: 3. Wortman and Matthew, 1899: 127–130. Merriam, 1906: 15, pl. 2, figs. 6, 7. Peter-

son, 1907: 53. Thorpe, 1922a: 164. Hall and Martin, 1930: 283. Munthe, 1998: 138.

“*Cormocyon*” *latidens* (Cope): Fremd and Wang, 1995: 74.

**HOLOTYPE**: AMNH 6896, crushed partial skull with P3 alveolus, P4–M2, and left ramus with p1–p2 alveoli, p3–m2, and m3 alveolus (fig. 26A–E) from the John Day Basin, John Day Formation (?early Arikareean), Grant or Wheeler counties, Oregon.

**REFERRED SPECIMENS**: John Day Formation (early Arikareean), Grant or Wheeler counties, Oregon (biostratigraphic positions of some JODA specimens in the Turtle Cove Member are placed within a letter system by

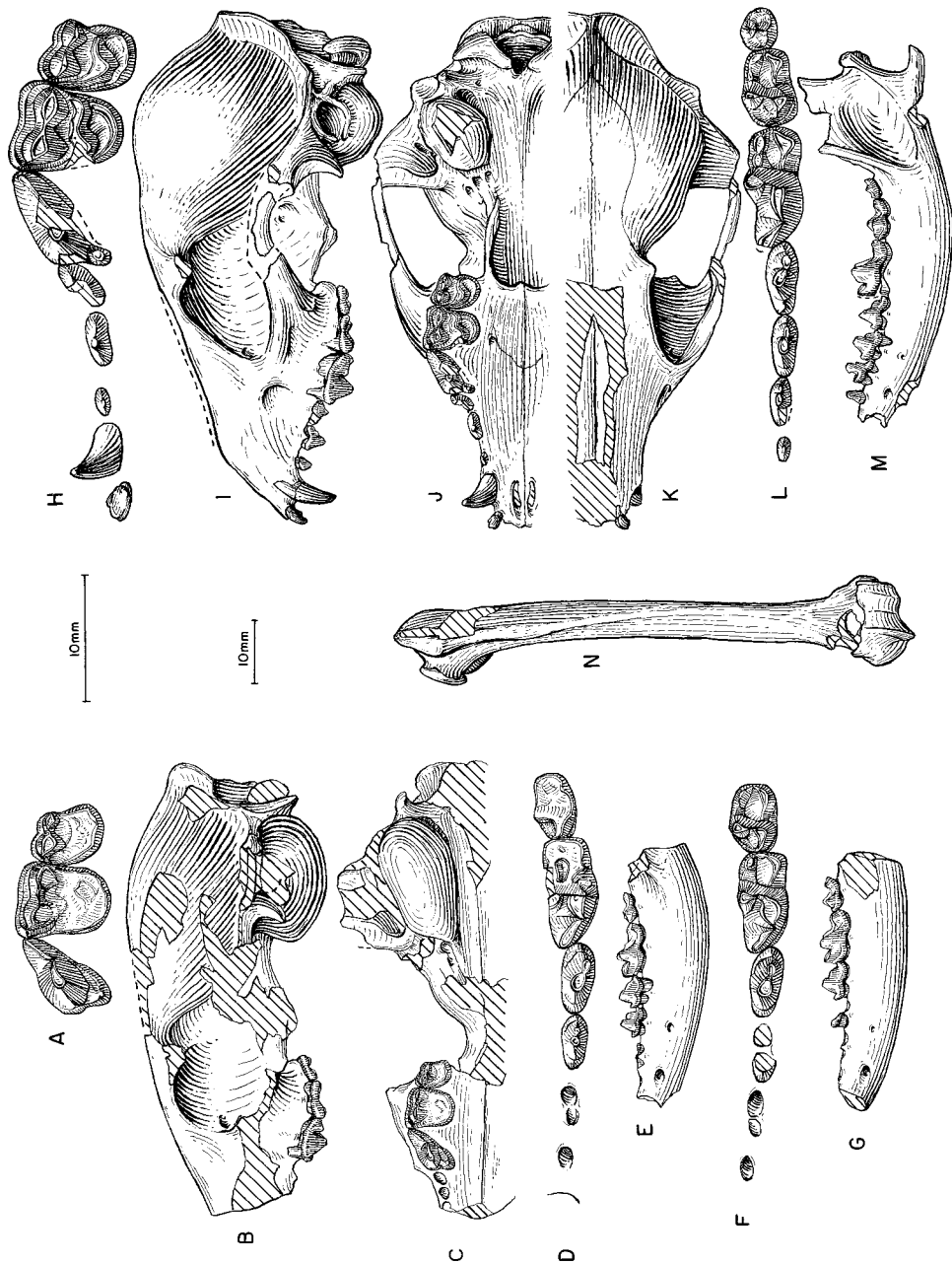


Fig. 26. A, Upper teeth, B, lateral view and C, ventral view of skull, D, lower teeth, E, ramus, *Phlaocyon latidens*, AMNH 6896, holotype, John Day Basin, John Day Formation (Early Arikarean), Oregon. F, Lower teeth and G, ramus (reversed from right side), *P. latidens*, AMNH 6897, John Day Basin. H, Upper teeth, I, lateral, J, ventral, and K, dorsal views of skull, L, lower teeth, M, ramus, and N, humerus, *Phlaocyon minor*, F:AM 49004 (zygomatic arch, P1, P2, P4, M1, and entire lower jaw reversed from right side), Upper Harrison beds (late Arikarean), Van Tassel area, Niobrara County, Wyoming. The longer (upper) scale is for A, D, F, H, and L, and the shorter (lower) scale is for the rest.

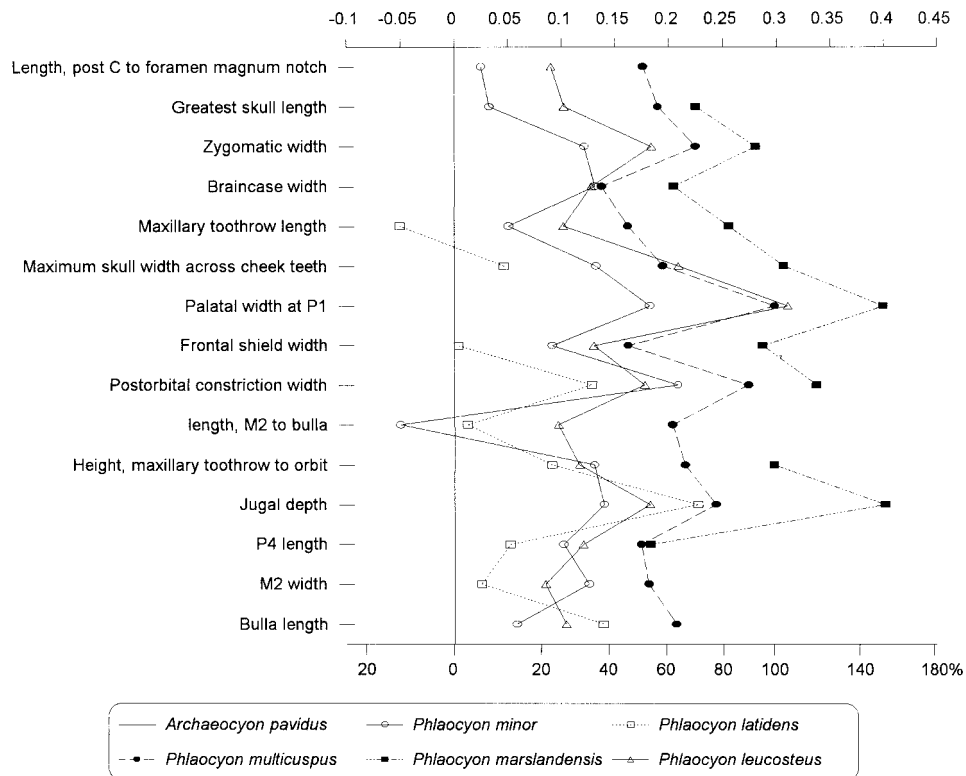


Fig. 27. Log-ratio diagram for cranial measurements of five species of *Phlaocyon* using *Archaeocyon pavidus* as a standard for comparison (straight line at zero). See text for explanations and appendix II for measurements and their definitions.

Fremd and Wang, 1995): AMNH 6836B, left ramus fragment with m1; AMNH 6897, right partial ramus with c1–p2 alveoli and p3 broken–m2 (fig. 26F, G); AMNH 6907, left ramus fragment with p4–m1; JODA 351, skull and mandible fragments with left C1, P3–M2, left c1–p1, and right c1 and p2–p4, unit F; JODA 363, right ramus fragment with p4–m1, unit E; JODA 711, right maxillary fragment with M1–M2; JODA 1251, broken left M1, unit E3; JODA 2753, left P4–M2, right p3–p4, unit E2; JODA 2809, left ramus fragment with m1–m2; JODA 2975 (AMNH cast 129657), right maxillary fragment with P4–M1, unit E2; JODA 3266, left ramus fragment with m1, unit E1; JODA 3384, left ramus fragment with p4–m2, unit E; JODA 3522, left M1, unit E1; JODA TF10921, right P4, unit A; JODA TF4924, right ramus fragment with m1, unit B; JODA TF4931, left ramus fragment with m1, unit D; UCMP

4094, right ramal fragment with p4–m1, UCMP loc. V76102; UCMP 760, right maxillary with P4–M2, and left and right rami with p1–m3 (p4 missing), UCMP loc. V76102; UCMP 10256, partial left ramus with p4–m1, Logan Butte loc. 898, Crook County; UCMP 76296, left ramus fragment with m1–m2, V-4849, Sheep Rock loc. 2; YPM 12699, skull fragment with P3 root and P4–M2; YPM 12794, right and left partial rami with p2, p3 broken–m1, and m2 alveolus; YPM 12795, right partial ramus with p4–m2; and YPM 12797, left ramal fragment with p4–m1.

DISTRIBUTION: Early Arikarean of Oregon.

EMENDED DIAGNOSIS: *P. latidens* possesses derived features distinct from *P. minor*: presence of a transverse cleft on the M1 lingual cingulum to delineate a conate hypocone, strong postprotoconal P4 lingual shelf, and more consistent presence of protostylid on

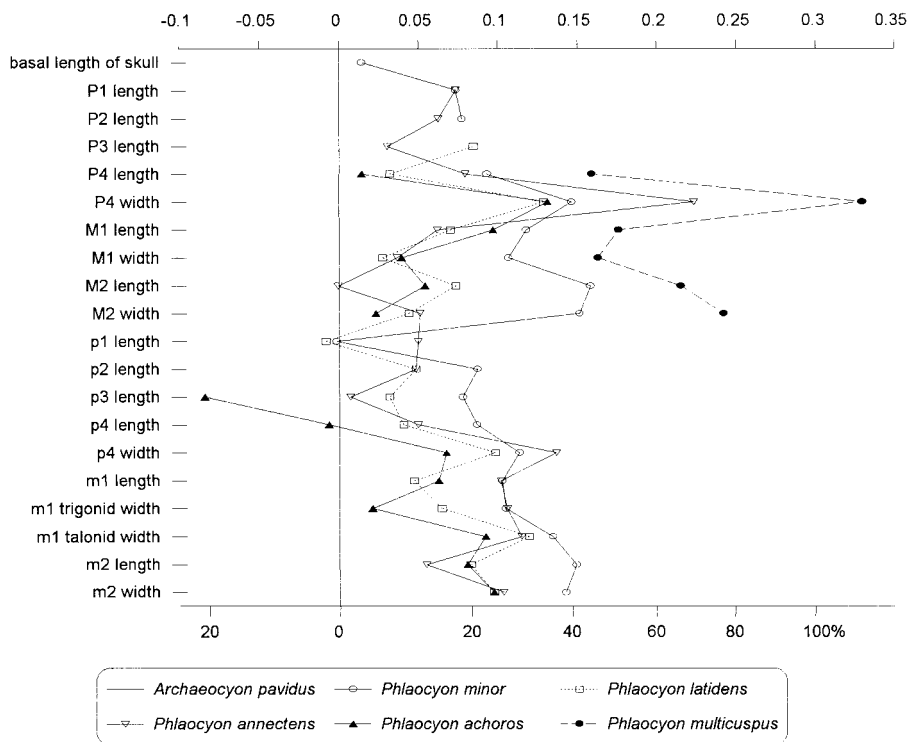


Fig. 28. Log-ratio diagram for dental measurements of five species of primitive *Phlaocyon* using *Archaeocyon pavidus* as a standard for comparison (straight line at zero). See text for explanations and appendix III for summary statistics of measurements and their definitions.

m1. Two autapomorphic characters that further distinguish *P. latidens* from *P. minor* and advanced *Phlaocyon* are an inflated tympanic bulla with a weak external auditory meatus lip and an enlarged m2. On the other hand, *P. latidens* still has a longer snout (as inferred from associated ramus), well-developed premolar cusplets, and crestlike talonid cusps on m1, in contrast to the shortened snout, simplified premolars, and conical talonid cusps in *P. annectens* and more derived species of *Phlaocyon*.

**DESCRIPTION AND COMPARISON:** The crushed holotype skull is still the main source of information about the cranial morphology of this species. Besides an enlarged bulla, ventrally oriented paroccipital process, and single temporal crest, little else can be learned about the general cranial morphology of AMNH 6896 because of the crushing and loss of the snout.

Dentally, *P. latidens* shows several derived characters of the *Phlaocyon* clade, al-

though most of them are still somewhat weak at this stage of development. The lingual cingulum of P4 is in an early stage of widening, especially toward the anterior end, in most specimens. The outlines of the upper molars are rather quadrate. There is a transverse cleft on the lingual cingulum of most of the M1s that helps to define an isolated hypocone, a feature not present in *P. minor*. The lower premolars show tendencies toward the robustness typical of the *Phlaocyon* clade, but still retain small cusplets on p2–p3. The frequency of occurrence of a protostylid on m1 (10 of 12 individuals; from AMNH, UCMP, and YPM collections only) is higher than in *P. minor* (4 of 13), and this cusp is also more distinct in *P. latidens*. Similar to *P. minor*, *P. latidens* also has an elongated m2, a shared derived feature not seen in other species of *Phlaocyon*.

**DISCUSSION:** For more than a century after their initial description by Cope (1879b, 1881b), *Cynarctoides lemur* and *Phlaocyon*

*latidens* have been considered as a pair of closely related species (mostly under the genus *Nothocyon*), co-occurring in the Turtle Cove Member of the John Day Formation. Indeed, their similar sizes and numerous shared primitive characters make differentiation of fragmentary dental materials difficult. In light of the phylogeny presented here, we recognize a number of derived features in *latidens* that individually may seem homoplastic or too weakly developed, but collectively point rather strongly to membership within the *Phlaocyon* clade.

*Phlaocyon annectens* (Peterson, 1907)

Figure 29

*Nothocyon (Galecyon) annectens* Peterson, 1907: 53, figs. 14, 15. Cook, 1909: 268.

*Phlaocyon willistoni* Peterson, 1924: 300, fig. 1. Untermann and Untermann, 1954: 186.

*Bassariscops willistoni* (Peterson): Peterson, 1928: 96, fig. 6 (in part). Frailey, 1979: 134. Munthe, 1998: 134.

*Nothocyon annectens* (Peterson): Hough, 1948: 106. Galbreath, 1956: 375.

?*Nothocyon* cf. *N. lemur* (Cope, 1879b): Stevens et al., 1969: 21, fig. 7A–C.

?*Nothocyon* cf. *N. annectens* (Peterson): Stevens, 1977: 30, fig. 9.

“*Nothocyon*” *annectens* (Peterson): Munthe, 1998: 134.

**HOLOTYPE:** CMNH 1602 (AMNH cast 89668), left and right partial maxillae with I1 broken–M2 and right and left partial rami with c1 broken–m3 (fig. 29F–I) from Carnegie Quarry 3, southeast of Carnegie Hill, Upper Harrison beds (late Arikareean), Sioux County, Nebraska.

**REFERRED SPECIMENS:** Upper Harrison beds (late Arikareean), Sioux County, Nebraska: AMNH 81030, left partial ramus with m1, 2 mi north of Agate Spring Quarry; and F:AM 49006, palate with I1–M1 and M2 broken and partial mandible with c1 and p1 alveolus–m3 (fig. 29C–E), 3 mi east and 2 mi south of Van Tassel.

Browns Park Formation (?medial or late Arikareean; exact stratigraphic position in relation to the better dated local faunas in Honey and Izett, 1988 is not clear), 1.5 mi southwest of Sunbeam, Moffat County, Colorado: CMNH 11332 (AMNH cast 89665) (holotype of *Phlaocyon willistoni* Peterson, 1924:

fig. 1), partial palate with I2–C1 broken, P1 root, P2 broken alveolus, and P3–M2 (M1 broken) (fig. 29A, B); and CMNH 11333 (AMNH cast 89667), right partial ramus with c1–m2 (all teeth broken or represented by alveoli).

Castolon Local Fauna, lower part of Delaho Formation (late Arikareean), Big Bend National Park, Brewster County, Texas: TMM 40635-66, right ramal fragment with p3 and m1 (Stevens et al., 1969: fig. 7A–C); TMM 40693-23, ramal fragment with m1; TMM 40849-10, right and left partial maxillary with P3–M2 (Stevens, 1977: fig. 9); TMM 40879-2, ramal fragment with m1; and TMM 40918-35, ramal fragment with alveoli for premolars.

**DISTRIBUTION:** Late Arikareean of Nebraska and Texas, and medial or late Arikareean of Colorado.

**EMENDED DIAGNOSIS:** *Phlaocyon annectens* is derived with respect to *P. latidens* and *P. minor* in its short snout; simplified, robust premolars; shorter P4 with enlarged protocone and an incipient hypocone or wide lingual shelf; and more conical talonid cusps of m1. *P. annectens* is primitive relative to more derived species of *Phlaocyon* in its unenlarged I3, incipient hypocone on P4, smaller P4 protocone, lack of a fully isolated hypocone on M1 lingual cingulum, lack of a cristid connection between entoconid and hypoconid of m1, and extremely weak protostylids on m1–m2.

**DESCRIPTION AND COMPARISON:** Beginning in *P. annectens*, the accessory and cingular cusplets on the premolars are reduced or lost in front or behind the main cusp, except on the p4; the P4 protocone is slightly enlarged; the P4 lingual cingulum is more widened or even begins to form a small hypocone as seen in CMNH 11332 (holotype of *Phlaocyon willistoni*); and the entoconid and hypoconid of m1 become more conical in contrast to the more crestlike cusps in *P. latidens* and *P. minor*. Other than the above derived characters, *P. annectens* remains primitive in all other aspects.

**DISCUSSION:** The overall size and shape of the holotype of *P. willistoni* is quite close to specimens of *P. annectens* from Nebraska. The Browns Park specimen, however, has a slightly more derived P4 with a larger,



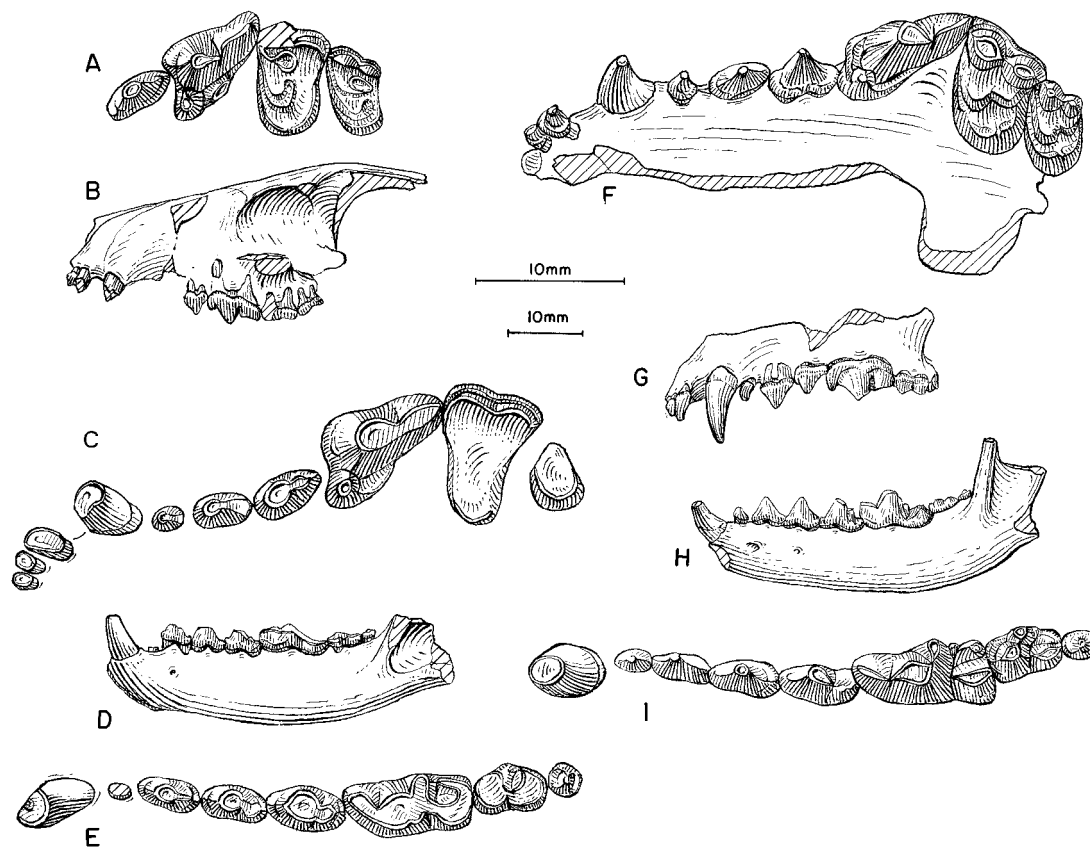


Fig. 29. *Phlaocyon annectens*. **A**, Upper teeth and **B**, lateral view of partial skull (reversed from right side), CMNH 11332 (holotype of *Phlaocyon willistoni*), Browns Park Formation (?medial or late Arikareean), 1.5 mi southwest of Sunbeam, Moffat County, Colorado. **C**, Upper teeth, **D**, ramus, and **E**, lower teeth, F:AM 49006, Upper Harrison beds (late Arikareean), 3 mi east and 2 mi south of Van Tassel, Sioux County, Nebraska. **F**, Upper teeth and **G**, lateral view of maxillary, **H**, ramus, and **I**, lower teeth, *P. annectens*, CMNH 1602, holotype, Carnegie Quarry 3, southeast of Carnegie Hill, Upper Harrison beds (late Arikareean), Sioux County, Nebraska. The longer (upper) scale is for A, C, E, F, and I, and the shorter (lower) scale is for the rest.

more distinct protocone, and a small hypocone. These features are within a normal range of species variation and represent intermediate stages in a trend toward more advanced taxa (e.g., *P. leucosteus* and *P. marlandensis*).

We follow Peterson (1924) in referring a second specimen from Brown's Park (CMNH 11333, an essentially edentulous ramus with a partial p3) to *Phlaocyon willistoni* (= *P. annectens*), based mainly on its size and robustness of the p3. If such a reference is correct, CMNH 11333 indicates a very shallow ramus in the type series. A third, smaller specimen, CMNH 11334 (a

partial ramus with m1–m2), was also described by Peterson, who acknowledged that it “undoubtedly represents an additional species” and called it “*?Phlaocyon*” (Peterson, 1924: 302–303, fig. 2). However, he was subsequently convinced that CMNH 11334 should belong to *P. willistoni* after all (Peterson, 1928: 98). We share with Peterson's earlier hesitation and place CMNH 11334 in *Cynarctoides roii* because of its primitive lower molar morphology that shows none of the signs of robustness characteristic of *Phlaocyon*.

The present reference of the materials from Castolon Local Fauna, Texas, is based

on the figures and descriptions by Stevens et al. (1969) and Stevens (1977). Although we follow Stevens (1977) in tentatively placing the Texas specimens in *P. annectens*, we note here that the Texas materials suggest a taxon of somewhat smaller size. For example, the lower carnassial in TMM 40635-66 is 8.2 mm long (Stevens et al., 1969: 21) as opposed to 9.7 mm for the holotype of *P. annectens*. That Stevens and her colleagues earlier (Stevens et al., 1969) equated the Castolon specimens with "*Nothocyon*" *lemur* is further evidence of the size problem. However, qualitatively, the Texas specimens have a widened P4 lingual cingulum and simplified premolars, derived characters that suggest the stage of development in *P. annectens*.

*Phlaocyon achoros* (Frailey, 1979)

Figure 30A-F

*Bassariscops achoros* Frailey, 1979 (in part): 134, figs. 3A, C-E, 4A, B, D. Munthe, 1998: 134.  
*Cynarctoides* sp. Frailey, 1979: 140, fig. 5A.

HOLOTYPE: UF 18389 (AMNH cast 105035), left P4 (fig. 30A), Buda Local Fauna (medial Arikareean), Alachua County, Florida (Frailey, 1979: figs. 3A, 4A, B).

REFERRED SPECIMENS: From type locality: UF 171365, left p4 (fig. 30D); UF 171366, left p4 (Frailey, 1979: fig. 3C); UF 171367, right p3; UF 16963, right M2 (fig. 30C); UF 171361, right M2; UF 171362, right M2; UF 16964, right m2; UF 16989 (AMNH cast 105036), isolated left m1 (Frailey, 1979: fig. 3D); UF 16991, right ramus with p2-m1 alveoli, m2 (fig. 30F), and m3 alveolus (Frailey, 1979: figs. 3E, 4D); UF 18390, talonid of left m1; UF 18415 (AMNH cast 105033), left isolated m1 (fig. 30E) (referred to *Cynarctoides* sp. by Frailey, 1979: fig. 5A); UF 18501, right maxillary fragment with M1 (fig. 30B); and UF 22778, right P4.

DISTRIBUTION: Medial Arikareean of Florida.

EMENDED DIAGNOSIS: *P. achoros* is more derived than *P. annectens* in its enlarged P4 protocone and initial development of a small hypocone on P4. *P. achoros* shares with its sister-species *P. multicuspus* several derived features: a distinct cingulum-like parastyle on P4, a well-developed paracone and

metacone on M1-M2, and a metacone split into two cusps. Besides its much smaller size, *P. achoros* is distinguishable from *P. multicuspus* in its lack of a conical hypocone on M2.

DESCRIPTION AND COMPARISON: Although individual teeth in Frailey's (1979: fig. 3) composite figure are within the approximate size ranges of each other, we identify two taxa in his hypodigm of *Bassariscops achoros*. One is represented by teeth with consistent hypocarnivorous features, such as extra cusps on upper molars, which we associate with the holotype. The other has more mesocarnivorous dentition, which we refer to *Cynarctoides lemur*. Under this new association, we redescribe *P. achoros* below.

In dental proportions, *P. achoros* is not much different from *P. annectens* (fig. 28). As noted by Frailey (1979), the P4 in the holotype of *P. achoros* is quite similar to that in *P. willistoni* (here synonymized with *P. annectens*). *P. achoros*, however, has a more elevated parastyle, which is even more developed in *P. multicuspus*. The M1-M2 are the most distinct with their cuspidate crown patterns. The paracone is enlarged to form a distinct cusp. The metacone is also enlarged and split into two smaller cusps. The P4-M2 thus assembled (fig. 30A-C) are far more consistent with the morphological pattern in *P. multicuspus*. The only major dental difference between *P. achoros* and *P. multicuspus* is the former's lack of a distinct hypocone on M2.

Allocation of the lower teeth is more difficult, partly due to the lack of comparable materials in *P. multicuspus* (known from a single skull). The lower premolars are referred to *P. achoros* with more confidence because of the ready differentiation of two morphotypes. Those referred to *P. achoros* have typically advanced *Phlaocyon* features of shorter, broader, and higher-crowned main cusps and more reduced posterior accessory cusps (fig. 30D), as contrasted to those referred to *Cynarctoides lemur*. Reference of the lower molars, however, is less certain. We chose UF 18415 and UF 16991 as representatives of the m1 and m2, respectively. Their enlarged talonids relative to trigonids and well-developed talonid cusps (especially en-

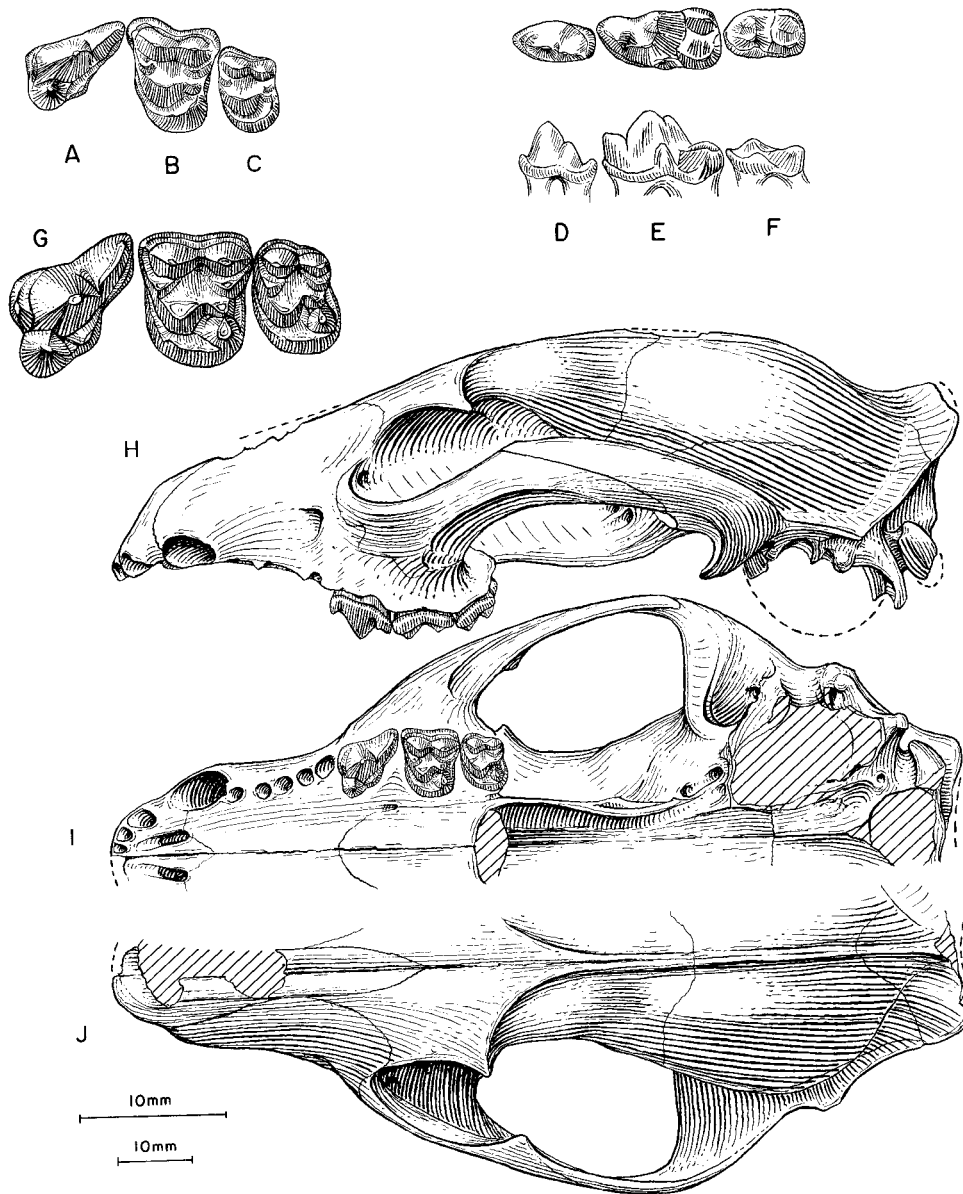


Fig. 30. **A–F**, *Phlaocyon achoros*, composite illustration of upper and lower teeth; **A**, P4, UF 18389, holotype; **B**, M1, UF 18501; **C**, M2, UF 16963; **D**, p4, UF 171365; **E**, m1, UF 18415; and **F**, m2, UF 16991 (M1, M2, and m2 reversed from right side), Buda Local Fauna (late Arikareean), Alachua County, Florida. **G**, Upper teeth, and **H**, lateral, **I**, ventral and **J**, dorsal views of skull, *Phlaocyon multicuspus*, FMNH UC1482, holotype, 3 mi southeast of Rawhide Buttes, ?Upper Harrison beds (late Arikareean), Goshen County, Wyoming. The longer (upper) scale is for A–G, and the shorter (lower) scale is for the rest. Illustrations for *P. achoros* by X. Wang.

toconid) and protostylids are commonly found in advanced *Phlaocyon*.

DISCUSSION: Reanalysis of the Buda materials, some of which were not included in Frailey's (1979) original descriptions, reveals at least three taxa among the small canids: *Cynarctoides lemur*, *Phlaocyon achoros*, and *Cormocyon* cf. *C. copei* (represented by a single M2). If our new hypodigm of *P. achoros* is correctly assembled, it becomes rather apparent that this Florida species, although still poorly known, is closely related to another rare taxon, *Aletocyon multicuspus* Romer and Sutton, 1927.

Small borophagines from the Buda Local Fauna seem to rather closely resemble those from the John Day Formation of Oregon, although it should be cautioned that the references to *Cynarctoides* and *Cormocyon* are based on very incomplete materials. This connection to the northwest is further suggested by a specimen from the Turtle Cove Member of John Day Formation, JODA 3051, a left maxillary fragment with P4–M2 (presently referred to *Cynarctoides lemur*). Incipient developments of features on JODA 3051 seem to suggest possible relationship to *P. achoros*: a raised P4 parastyle and incipient development of an extra cusp between metaconule and metacone on M1. While it may be tempting to trace the origin of the *achoros*–*multicuspus* clade to Oregon, we treat this specimen as a variation of *C. lemur* until additional material becomes available.

*Phlaocyon multicuspus* (Romer and Sutton, 1927)

Figure 30G–J

*Aletocyon multicuspus* Romer and Sutton, 1927: 460, figs. 1, 2. McGrew, 1938a: 331, fig. 91; 1941: 33. Hough, 1948: 104, fig. 11.

*Aletocyon multicuspidens* (Romer and Sutton): Dahr, 1949: 2.

*Aletocyon multicuspis* (Romer and Sutton): Munte, 1998: 134.

HOLOTYPE: FMNH UC1482 (AMNH cast 108069), partial skull with incisor alveoli, C1, P1–P3 alveoli, and P4–M2 (fig. 30G–J) from 3 mi southeast of Rawhide Buttes, "Lower Harrison," but more likely Upper Harrison beds (late Arikareean), Goshen County, Wyoming.

DISTRIBUTION: Late Arikareean of Wyoming.

EMENDED DIAGNOSIS: In addition to its much larger size, derived characters that distinguish *Phlaocyon multicuspus* from *P. annectens* and more primitive species include a further enlarged protocone and hypocone of P4. *P. multicuspus* shares with its sister-species *P. achoros* several derived characters: presence of a parastyle on P4, a paraconule on M1, a more distinct M1 metaconule, and an extra cusp between the metaconule and metacone of M1. *P. multicuspus* is unique among all species of *Phlaocyon* in its longer skull (a reversal) and a conate hypocone on M2. In addition, *P. multicuspus* lacks derived characters that are present in *P. leucosteus* and *P. marslandensis*: narrowed masseteric scar and enlarged I3. On the other hand, *P. multicuspus* is easily distinguished from *P. yatkolai* and *P. mariae* in its much smaller size and less massive premolars.

DESCRIPTION AND COMPARISON: *Phlaocyon multicuspus* is unique within the *Phlaocyon* clade in its mixture of a primitive-looking skull and a highly derived dentition. The proportional relationships of the skull of *P. multicuspus* are quite *Phlaocyon*-like, with a deep zygomatic arch of jugal, broad anterior palate, and narrow braincase (fig. 27). The posterior premaxillary process is widely separated from the frontal, as opposed to the near meeting of these two bones in *P. leucosteus*. Other primitive features include a wide masseteric scar on the lateral face of the zygomatic arch and a rodlike paroccipital process, in contrast to a much narrowed and ventrally facing masseteric scar and a plate-like paroccipital process in *P. leucosteus*. Also notable is a slightly domed forehead in *P. multicuspus*, indicating a small frontal sinus beneath the frontal bone.

Dental morphology of *P. multicuspus*, on the other hand, is very hypocarnivorous. In some ways, its teeth are the most advanced among species of the genus. This is mostly related to the cuspidate nature of its cheek-teeth. There are extra cusps that are not normally seen in other species of *Phlaocyon*: a small, but distinct parastyle on P4, a paraconule on M1–M2, a more distinct metaconule on M1–M2, an additional cusp between metaconule and metacone of M1–M2, and a

conical hypocone on M2. These derived features are also shared by *P. achoros*, indicating a sister-group relationship. Additionally, the M2 in *P. multicuspus* is enlarged to nearly the same size as the M1, in contrast to smaller M2s in other species of *Phlaocyon*.

DISCUSSION: McGrew (1941: 35) noted that "The similarity in general skull structure and basic tooth pattern between *Phlaocyon* and *Aletocyon* leaves no doubt that the two are closely related," a conclusion also reached by Dahr (1949). Nonetheless, McGrew agreed with Romer and Sutton (1927) that *Aletocyon* should be a distinct genus from *Phlaocyon*, apparently based on the perceived morphological distances. Although we do not recognize such distances as a criterion for taxonomy, the genus *Aletocyon* could be used to represent a small clade of its own consisting of *achoros* and *multicuspus*. Such a practice, however, would require the creation of additional generic names for pectinated species near the base of *Phlaocyon*, an option we chose not to use.

*Phlaocyon marslandensis* McGrew, 1941  
Figure 31C–I

*Phlaocyon marslandensis* McGrew, 1941: 33, figs. 12, 13. Dahr, 1949: 4. Frailey, 1978: 9.

HOLOTYPE: FMNH P26314 (AMNH cast 95585), left partial maxillary and premaxillary with I3–C1, P1–P3 alveoli, and P4–M1 (fig. 31G–I) from near Dunlap, Runningwater Formation ("Upper Marsland beds" of McGrew, 1941) (early Hemingfordian), Dawes County, Nebraska.

REFERRED SPECIMENS: Runningwater Formation (early Hemingfordian), Box Butte County, Nebraska: F:AM 99370 (fig. 31C–F), right fragment of skull with P1–M2, right partial ramus with i1 broken–m3 (p1 alveolus), right distal part of humerus, first phalanx, and fragments, below Dry Creek Prospect B; UNSM 25607, right partial maxillary with P4–M1, UNSM loc. Bx-7; UNSM 25641, right ramus with c1 broken, p1 alveolus, p2, p3–m1 alveoli, m2, and m3 alveolus, UNSM loc. Bx-27; UNSM 25659, left partial maxillary with P4–M1, M2 alveolus, UNSM loc. Bx-28; UNSM 26153 (AMNH cast 95577), partial palate with I1–

I3 alveoli, C1, P1 alveolus, P2–M1, and M2 alveolus, UNSM loc. Bx-7.

Runningwater Formation (early Hemingfordian), Sheridan County, Nebraska: Clinton Highway Locality, UNSM loc. Sh-101B: UNSM 5010-70, left ramus with c1 broken, p1–p2 alveoli, and p3–m3.

DISTRIBUTION: Early Hemingfordian of Nebraska.

EMENDED DIAGNOSIS: *Phlaocyon marslandensis* shares several derived characters with its sister-species *P. leucosteus* but differs from *P. multicuspus*, *P. annectens*, and more primitive species of the genus in having a relatively shorter rostrum such that the premolars are imbricated, a large I3, a lateral groove on the lower canine, tall crowned premolars, narrow and mostly ventrally oriented masseteric scar on the jugal, a cristid between the entoconid and hypoconid of m1, and a protostylid on m2. The premolar characteristics and the m2 protostylid can also be used to distinguish *P. marslandensis* from the *yatkolai-mariae* group. In addition to its larger size, *P. marslandensis* is distinguished from its sister-species *P. leucosteus* in its larger P4 protocone and less prominent protostylids on m1–m2.

DESCRIPTION AND COMPARISON: The partial skull of UNSM 26153 has much of the skull roof preserved, supplying cranial morphologies unknown in the holotype. In general, it has a heavier construction with deeper jugal, broader palate, broader snout, and stronger sagittal crest than that in *P. leucosteus* (fig. 27). The posterior premaxillary process does not meet the frontal. There is a modest inflation of the frontal area, indicating the presence of a frontal sinus beneath the frontal bone. The masseteric scar on the zygomatic arch is less than one-fourth of the total depth, being much more reduced than in *P. multicuspus*. Although the I3s in UNSM 26153 are missing, their alveoli clearly suggest an enlarged incisor. In F:AM 99370, a distal part of a humerus shows the presence of a small entepicondylar foramen.

DISCUSSION: McGrew (1941) suggested a close relationship between *Phlaocyon leucosteus* and his newly erected *P. marslandensis*, a conclusion consistent with the present phylogeny, even though characters in support of his conclusion (lack of a P4 par-

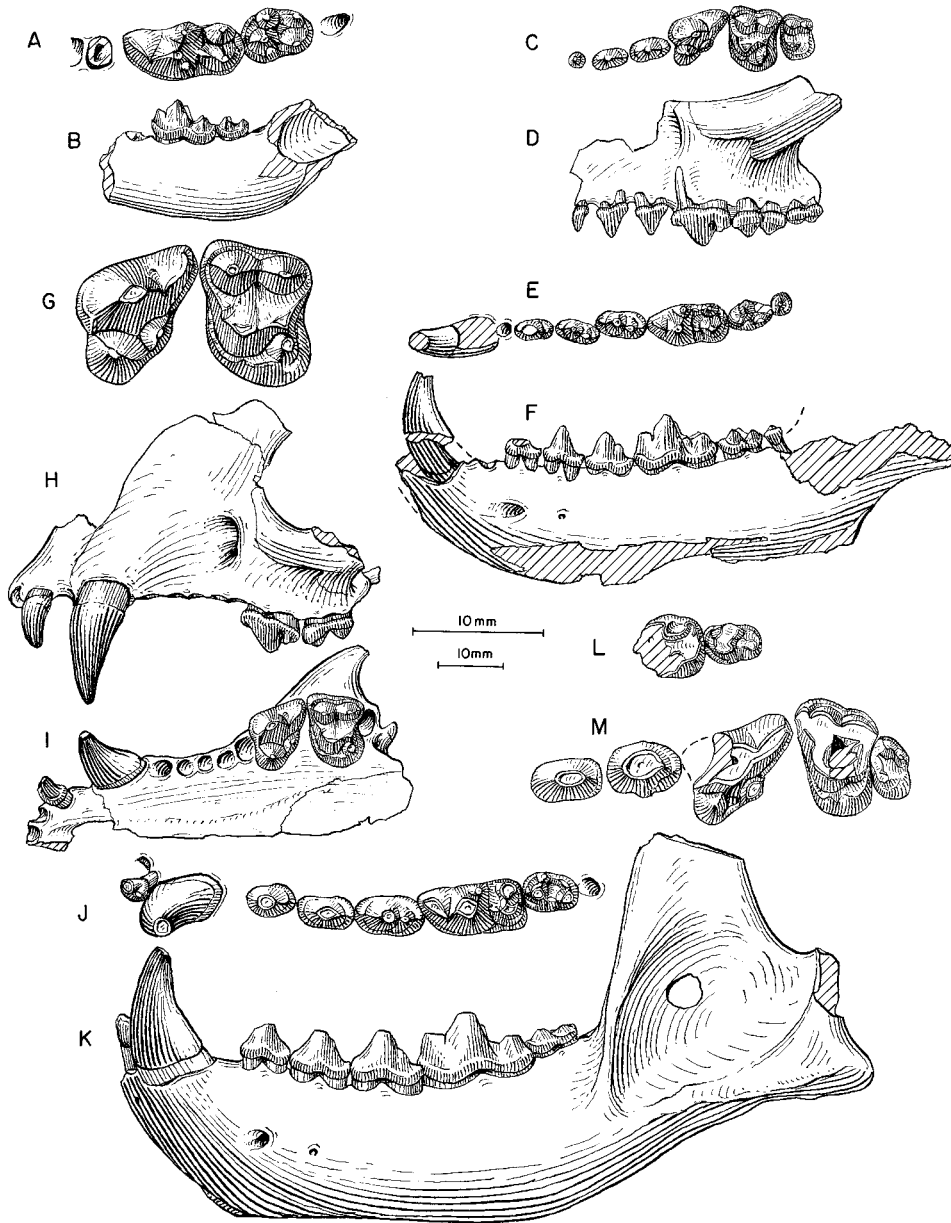


Fig. 31. **A**, Lower teeth and **B**, ramus (reversed from right side), *Phlaocyon leucosteus*, YPM 12801 (holotype of *Nothocyon latidens multicuspis*). **C**, Upper teeth, **D**, lateral view of maxillary, **E**, lower teeth, and **F**, ramus (all reversed from right side), *P. marslandensis*, F:AM 93370, Runningwater Formation (early Hemingfordian), Box Butte County, Nebraska. **G**, P4–M1, and **H**, lateral and **I**, ventral views of partial skull, *P. marslandensis*, FMNH P26314, holotype, from Dunlap, Runningwater Formation (early Hemingfordian), Dawes County, Nebraska. **J**, Lower teeth and **K**, ramus (reversed from right side), *P. yatkolai*, UNSM 62546, holotype, Runningwater Quarry, Runningwater Formation (early Hemingfordian), Box Butte County, Nebraska. **L**, Lower teeth and **M**, upper teeth, *P. mariae*, F:AM 25466, holotype, *Aletomeryx* Quarry, Runningwater Formation (early Hemingfordian), Cherry County, Nebraska. The longer (upper) scale is for **A** and **G**, and the shorter (lower) scale is for the rest.

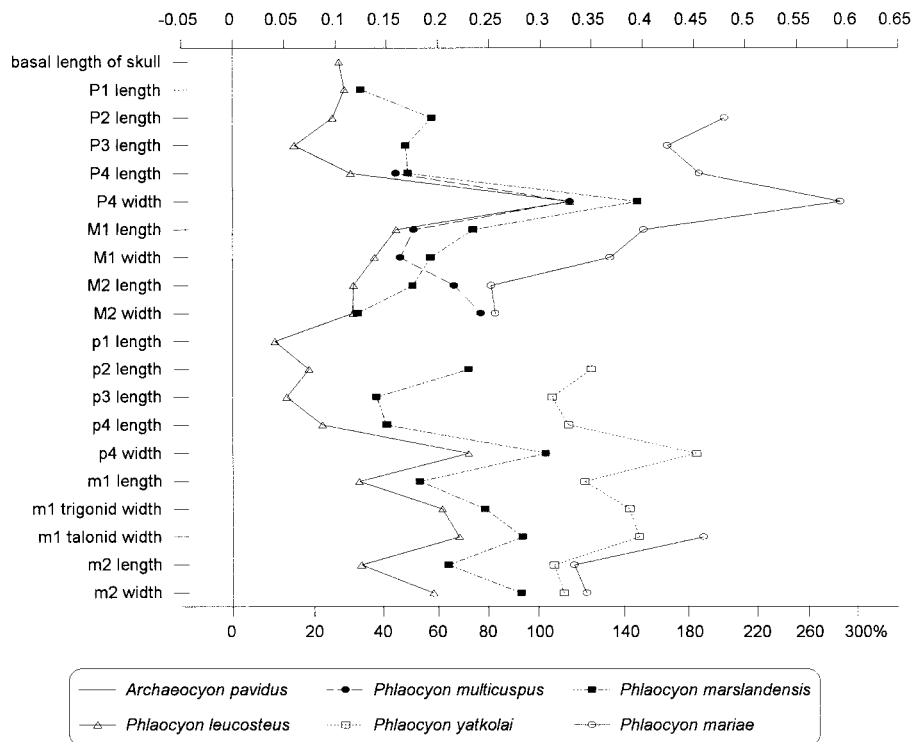


Fig. 32. Log-ratio diagram for dental measurements of five species of advanced *Phlaocyon* using *A. pavidus* as a standard for comparison (straight line at zero for y-axis). See text for explanations and appendix III for summary statistics of measurements and their definitions.

astyle and reduced anterolingual cingulum) turn out to be primitive in our analysis (see Phylogenetic Analysis below). McGrew further speculated that *P. marslandensis* was directly descendant from *P. leucosteus* partly because of a perceived age difference between the two species. Such a relationship, however, is presently contradicted by autapomorphies in *P. leucosteus*; that is, broadened p4 and better developed m2 protostylid.

*Phlaocyon leucosteus* Matthew, 1899

Figures 31A, B, 33–35

*Phlaocyon leucosteus* Matthew, 1899: 54. Wortman and Matthew, 1899: 131, pl. 6, fig. 10. McGrew, 1938a: 331; 1941: 33. Hough, 1948: 97. Dahr, 1949: 1. Frailey, 1978: 9. Munthe, 1998: 135.

*Nothocyon latidens multicuspis* Thorpe, 1922b: 430, fig. 3.

*Phlaocyon* sp.: Frailey, 1978: 8.

HOLOTYPE: AMNH 8768, skull with I1–

M2, mandible with i1–m3, and partial skeleton including scapula, right humerus, both radii, left ulna, right partial ulna, both front feet including carpals, metacarpals I–V and phalanges, both femora, both tibiae, both fibula, both rear feet including tarsals, metatarsals I–V with some phalanges, vertebrae, ribs, etc. (figs. 33, 35) from Martin Canyon, head of Dorby Creek, Martin Canyon beds (sensu Matthew, 1901; late Arikareean), Logan County, Colorado. Found with five partial skeletons of *Merycochoerus proprius magnus* thought to be part of “White River formation” and disconformably overlain by the Pawnee Creek beds of the Loup Fork Formation (Matthew, 1901: 401).

REFERRED SPECIMENS: South side of Dry Creek, Upper Harrison beds (late Arikareean), Box Butte County, Nebraska: F:AM 99349, anterior part of skull with C1–P3 alveoli and P4–M2.

Runningwater Formation (early Heming-

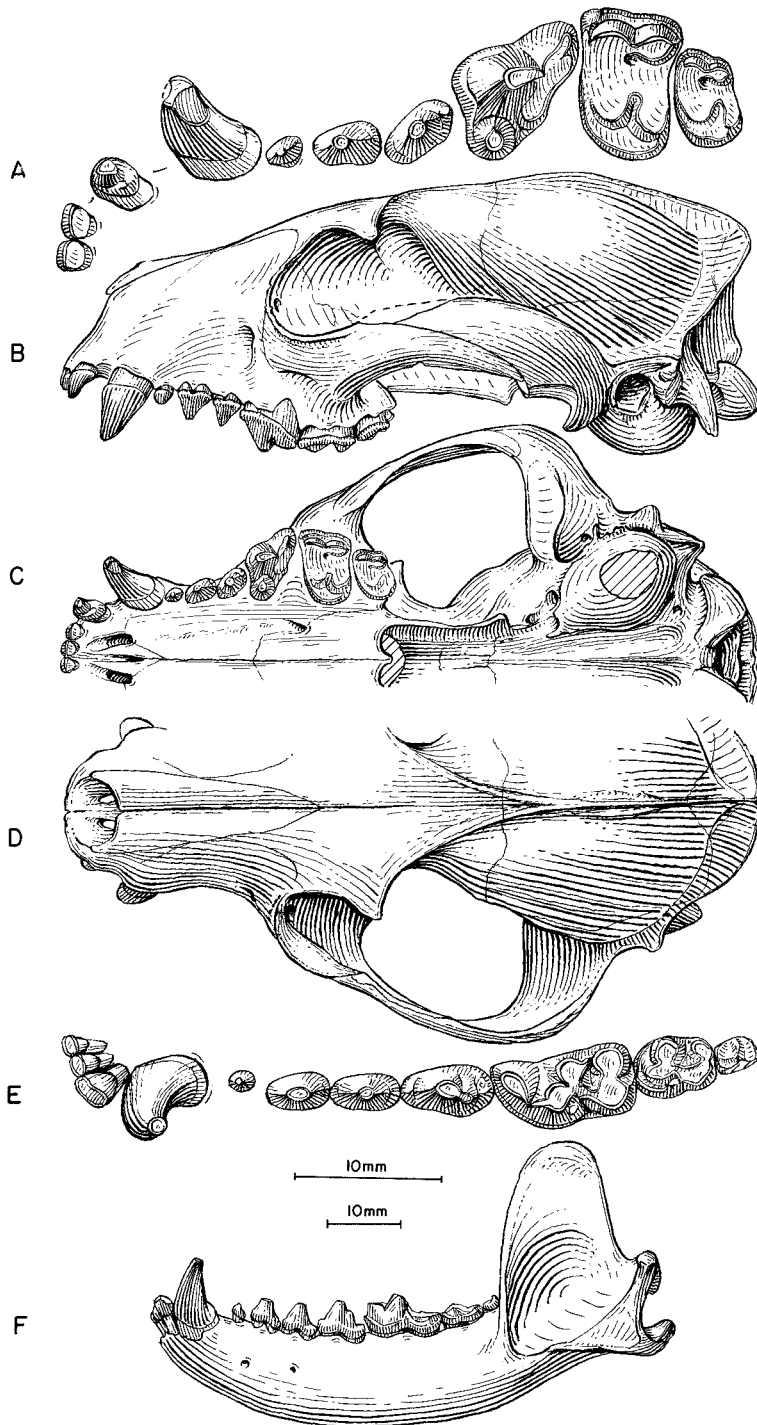


Fig. 33. *Phlaocyon leucosteus*. A, Upper teeth (C1 reversed from right side), B, lateral, C, ventral and D, dorsal views of skull, E, lower teeth, and F, ramus, AMNH 8768, holotype, Martin Canyon beds (early Hemingfordian), Logan County, Colorado. The longer (upper) scale is for A and E, and the shorter (lower) scale is for the rest.



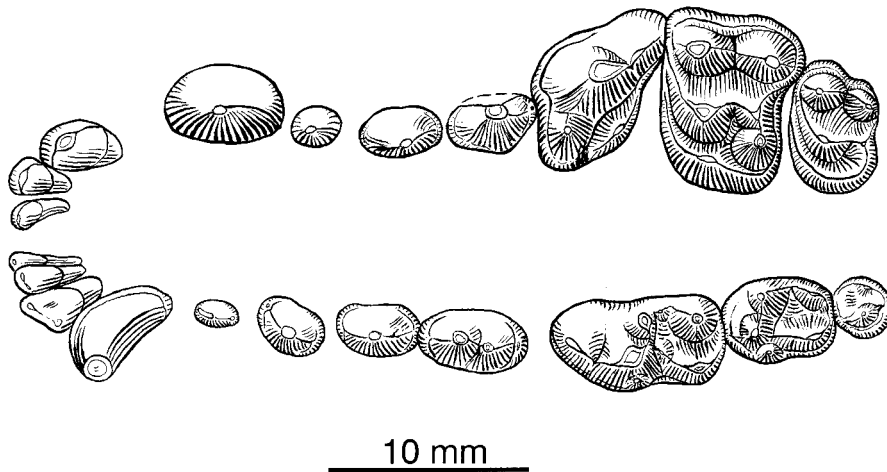


Fig. 34. *Phlaocyon leucosteus*, UNSM 26524, Runningwater Formation (early Hemingfordian), Cherry County, Nebraska. Illustration by X. Wang.

fordian), Cherry and Dawes counties, Nebraska: Antelope Creek: YPM 12801 (AMNH cast 88395), right partial ramus with p4 alveolus–m2 and m3 alveolus (fig. 31A, B) (holotype of *Nothocyon latidens multicuspis* Thorpe, 1922b. *Aletomeryx* Quarry: F:AM 49184, left ramus with i1–i3 alveoli, c1 broken, p1 alveolus, p2 broken–m1, and m2–m3 alveoli. Cottonwood Creek: F:AM 54467, right partial ramus with p4–m1 and m2 alveolus. Cottonwood Creek Quarry: F:AM 99348, right maxillary with P1–M2. UNSM loc. Cr-128: UNSM 26524, crushed skull with I1–M2, left and right rami with i1–m3 (fig. 34), five cervicals, partial left humerus, and other skeletal fragments.

Sand Canyon Region, Runningwater Formation (early Hemingfordian), Dawes County, Nebraska: F:AM 49118, right partial maxillary with P4–M1.

Sand Canyon Quarry, Red Valley Member, Box Butte Formation (late Hemingfordian), Dawes County, Nebraska: F:AM 99347, left ramus with c1–m1 alveoli, m2, and m3 alveolus (possibly reworked from the Runningwater Formation).

SB-1A Local Fauna (?late Arikarean), 1 mi north of Live Oak, Suwannee County, Florida: TRO 392, isolated right P4 (*Phlaocyon* sp. in Frailey, 1978: 8–9, fig. 2A, B).

DISTRIBUTION: Late Arikarean of Nebraska, ?late Arikarean of Florida, early Hem-

ingfordian of Colorado and Nebraska, and late Hemingfordian of Nebraska.

EMENDED DIAGNOSIS: Like its sister-species *Phlaocyon marslandensis*, *P. leucosteus* is derived with respect to *P. multicuspis* and other more primitive species of *Phlaocyon* in a relatively shorter rostrum with imbricated premolars, narrow masseteric scar, a large I3, a lateral groove on c1, tall premolars, and a cristid between entoconid and hypoconid of m1. Some of these characters can also be used to distinguish it from the *yatkolai-mariae* species group: relatively large I3, a lateral groove on c1, narrowed masseteric scar on the zygomatic arch, tall crowned premolars that are imbricated, and presence of a protostylid on m2. Within the *leucosteus-marslandensis* species group, *P. leucosteus* is distinguishable from *P. marslandensis* in its smaller size and slightly better developed m2 protostylid.

DESCRIPTION AND COMPARISON: After nearly 100 years since its initial description, the remarkable holotype of *Phlaocyon leucosteus* is still the best preserved and most complete specimen of all known species of the genus, and is also the only specimen of this species from the type locality. However, the holotype suffers from heavy wear on its teeth, obscuring much of the crown pattern on the molars. We are thus fortunate to have available a nearly complete skull and man-

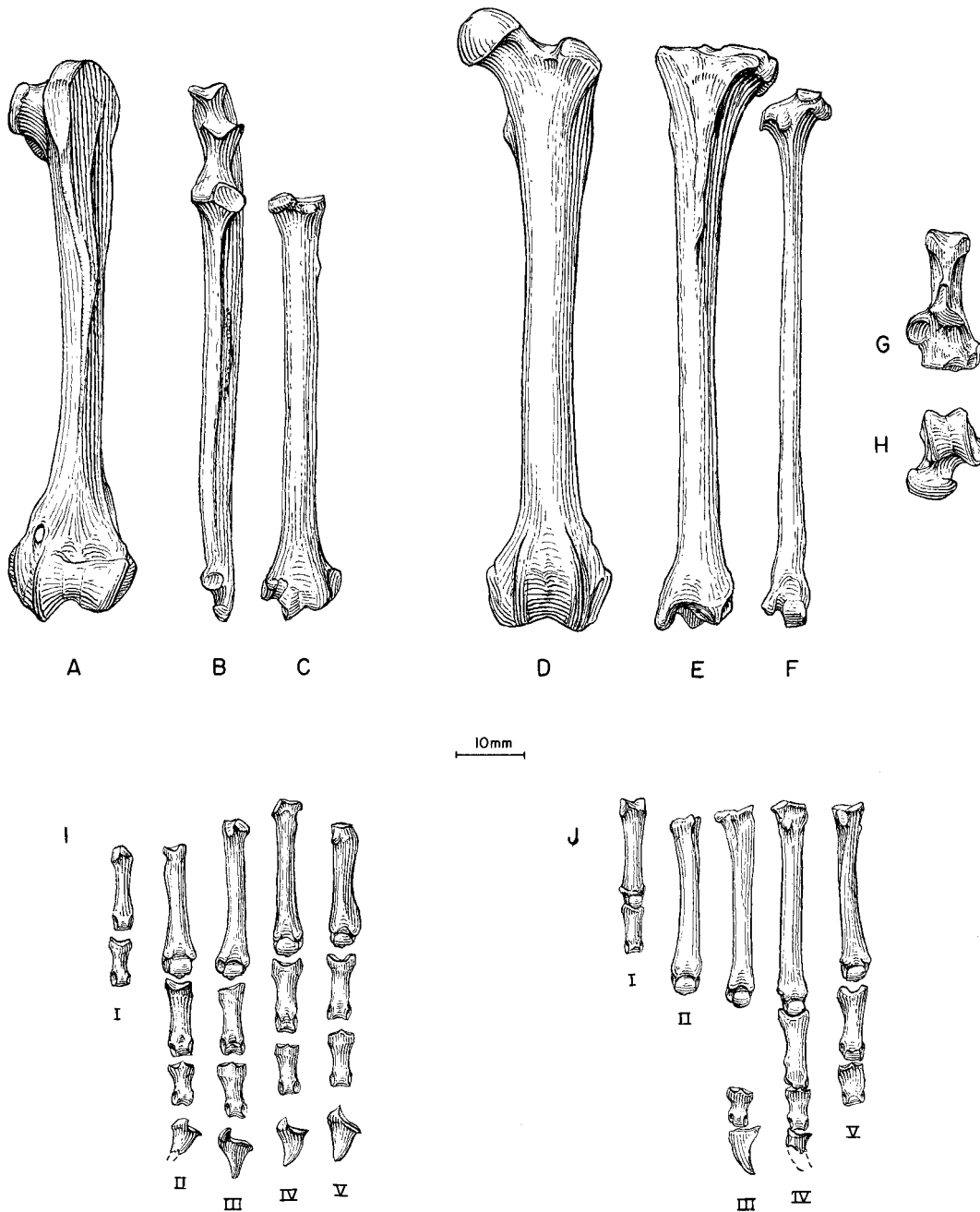


Fig. 35. *Phlaocyon leucosteus*. **A**, Humerus (reversed from right side), **B**, ulna (reversed from right side), **C**, radius, **D**, femur, **E**, tibia, **F**, fibula, **G**, calcaneum, **H**, astragalus, **I**, hand, and **J**, foot, AMNH 8768, holotype, Martin Canyon beds (early Hemingfordian), Logan County, Colorado.

dible of a younger individual from Nebraska with little wear on the teeth (UNSM 26524). With this additional specimen, plus other fragmentary materials, *P. leucosteus* is unquestionably the best known species of *Phlaocyon*.

Cranial morphologies peculiar to *P. leucosteus* (as compared to closely related species such as *P. multicuspus* and *P. marslandensis*) include a strong posterior process of premaxillary that nearly touches the frontal, large postorbital process of frontal, a laterally expanded paroccipital process to form a flat plate around the bulla, and slightly inflated mastoid process. Many of these features are probably related to the brachycephalic development of the skull. On the younger individual (UNSM 26524), however, these features are either less well-developed (premaxillary process and postorbital process) or not preserved (paroccipital process and mastoid process). Another cranial feature of *P. leucosteus* indicating its advanced status (shared with *P. marslandensis*) is a narrowed masseteric scar on the anterior portion of the zygomatic arch.

The angular process of the mandible is highly variable through age. Thus, the young individual (UNSM 26524) has a slender process similar to the condition of most primitive borophagines, whereas that in the much older AMNH 8768 consists of an extremely broadened internal ridge forming a large fossa on its dorsal face for the insertion of the medial pterygoid muscle. This latter condition is also in sharp contrast to that of another old individual, F:AM 49184, which has a posteriorly elongated angular process instead of the broadened one in AMNH 8768. In absence of other related cranial or dental differences, such differences in angular process construction are here regarded as variations within the species.

Dentally, *P. leucosteus* has the most hypocarnivorous teeth in the *Phlaocyon* clade. *P. leucosteus* shares with *P. marslandensis* such derived features as an enlarged I3, c1 with a lateral groove, high-crowned premolars, and a protostylid on m2. In contrast to *P. marslandensis*, the hypocone on M1 of *P. leucosteus* is partially connected to the metaconule but is more isolated from the lingual cingulum, due to a distinct cleft on the cin-

gulum. There is, however, no conate hypocone on the M2. A well-developed protostylid is present in m1–m2.

In *P. leucosteus*, the maximum length of the tibia is shorter than that of the femur. This shortened distal segment of the hindlimb is a derived condition relative to that in *Hesperocyon*, *Cormocyon copei*, *Archaeocyon leptodus*, and others. However, we do not know when this happened within the *Phlaocyonini* clade because of our lack of knowledge of the postcrania of other intermediate species.

DISCUSSION: See discussion under the genus *Phlaocyon* for a brief summary of past controversies on this species and the historical role it played in the debate of the origin of procyonids.

Frailey (1978: 9) commented that a single P4 from the SB-1A Fauna in Florida "could be within the limits of variation for *P. leucosteus*," but refrained from referring the specimen as such because of its somewhat smaller size. In view of the present expanded hypodigm of *P. leucosteus* from the Hemingfordian of western Nebraska, the Florida specimen does fall within its size range and thus is tentatively referred to this species.

### *Phlaocyon yatkolai*, new species

Figure 31J, K

HOLOTYPE: UNSM 62546, right ramus with i1–i2 alveoli, i3–c1, p2–m2, and m3 alveolus (fig. 31J, K) from Runningwater Quarry (UNSM loc. Bx-58), 19 mi east of Agate, base of the Runningwater Formation (early Hemingfordian), Box Butte County, Nebraska.

ETYMOLOGY: Named in honor of the late Daniel Yatkola who collected the type and made a landmark study of the stratigraphy of this area.

DISTRIBUTION: Early Hemingfordian of Nebraska.

DIAGNOSIS: In addition to its larger size, derived characters of this new species relative to the *leucosteus*–*marslandensis* species pair and other species of *Phlaocyon* are loss of p1, massive premolars, compression of m1 entoconid and hypoconid, and reduction of m1 metaconid. An unreduced m2 (relative to m1), presence of an m3, and lower and less

erect ascending ramus in *P. yatkolai* are the only observable differences (all primitive for *P. yatkolai*) between it and *P. mariae*.

DESCRIPTION AND COMPARISON: Lack of upper teeth in *Phlaocyon yatkolai* severely limits the scope of comparison. Membership of *yatkolai* within the *Phlaocyon* clade is indicated by only two observable characters: simplified and robust premolars and cristid connections between the entoconid and hypoconid of m1. The massiveness of its premolars seems not merely a proportional enlargement relative to its size, and, as shown in fig. 32, the premolars are larger relative to m1. *P. yatkolai* is also distinct from all other species of *Phlaocyon* in its reduced m1 metaconid and loss of p1, features commonly associated with hypercarnivory. The entoconid and hypoconid of m1 are closely compressed together instead of being separated by a deep valley as in all other species of *Phlaocyon*.

DISCUSSION: Despite the lack of comparable parts between the holotypes of *P. yatkolai* and *P. mariae* (mostly upper teeth), the basis of a sister relationship for these two species, as proposed in our phylogeny, is not limited to their massive premolars, which is the only codable character shown in the phylogeny, but also includes their common tendency toward hypercarnivorous dentition. Each, however, expresses this tendency by different parts (upper or lower) of the teeth that do not lend themselves to direct comparison. Our phylogeny predicts more dental synapomorphies when the question marks in the data matrix (table 2) left by the missing teeth are filled. Of the few common teeth that can be compared, those in *P. yatkolai* are more primitive, as indicated by its unreduced m2 and presence of m3.

*Phlaocyon mariae*, new species

Figure 31L, M

HOLOTYPE: F:AM 25466, upper and lower worn teeth and skull fragments including C1 broken, maxillary fragment with P2 broken—P3, detached broken P4s, maxillary fragment with M1 broken—M2, and left ramus fragment with m1 broken—m2 (fig. 31L, M) from *Aletomeryx* Quarry, near mouth of Antelope Creek, Runningwater Formation (early Hemingfordian), Cherry County, Nebraska.

ETYMOLOGY: Named in honor of S. Marie Skinner in recognition of her long career in assembling and documenting the collections from Nebraska.

DISTRIBUTION: Early Hemingfordian of Nebraska.

DIAGNOSIS: *Phlaocyon mariae* is the most apomorphic taxon with highly derived characters not seen in any other species of *Phlaocyon*: large size, high and erect ascending ramus, P4 elongate relative to length of molars with protocone relatively small, P4 hypocone larger than protocone, M1 transversely elongated, M1 parastyle enlarged, M1 hypocone reduced, M2 and m2 reduced relative to M1 and m1, and loss of m3. In addition, *P. mariae* shares with *P. yatkolai* the development of massive premolars.

DESCRIPTION AND COMPARISON: Besides being the largest *Phlaocyon* species, *P. mariae* is rather unusual in its curious mixture of hypo- and hypercarnivorous characters. On the one hand, it retains several hypocarnivorous characters acquired in more primitive species of *Phlaocyon* such as robust premolars and a P4 hypocone. On the other hand, it has a somewhat hypercarnivorous M1. Thus, the outline of the M1 is more transversely elongated than is usually the case in all species of *Phlaocyon* owing to an enlargement of its parastyle, a narrowing of the angle between labial and anterior borders of M1, and a shortening of its lingual cingulum, which nearly lost its anterior segment. Also, the conical hypocone on M1, a constant in all *Phlaocyon* except in *P. minor*, is almost lost—only a minor swelling is left on the lingual cingulum. Correlated with this hypercarnivorous trend is the reduction of the posterior molars: the upper and lower second molars are extremely small, compared to the larger M2s and m2s in most *Phlaocyon*, and the m3 is lost. In contrast to its anteroposteriorly shortened molars, the P4 is relatively elongated (fig. 32), and its protocone is reduced.

DISCUSSION: Breakage, wear, and poor preservation on the type and only specimen of this species hinder more complete assessment of its phylogenetic relationships. However, it is clear that this is an unusual taxon with a mixture of features as described above. The presence of hypercarnivorous

characters within a predominantly hypocarnivorous clade is puzzling and raises questions about its phylogenetic position. However, based on the limited codable characters, our cladistic analysis consistently places *P. mariae* in the terminal part of the *Phlaocyon* clade, and singles out the presence of massive premolars (more so than the already robust premolars in most *Phlaocyon*) as a derived feature to support a *P. yatkolai*-*P. mariae* sister relationship.

If our phylogeny is correct, *P. mariae* provides an example of a hypocarnivorous clade evolving to large body size and then reversing toward a more hypercarnivorous diet. *P. mariae* and *P. yatkolai* appear to be the first and earliest borophagine to attempt hypercarnivory.

#### **Borophagini**, new tribe

TYPE GENUS: *Borophagus* Cope, 1892.

INCLUDED GENERA: *Cormocyon* Wang and Tedford, 1992; *Desmocyon*, new genus; *Paracynarctus*, new genus; *Cynarctus* Matthew, 1902; *Metatomarctus*, new genus; *Euoplocyon* Matthew, 1924; *Psalidocyon*, new genus; *Microtomarctus*, new genus; *Protomarmarctus*, new genus; *Tephrocyon* Merriam, 1906; *Tomarctus* Cope, 1873; *Aelurodon* Leidy, 1858; *Paratomarctus*, new genus; *Carpocyon* Webb, 1969b; *Protepicyon*, new genus; *Epicyon* Leidy, 1858; and *Borophagus* Cope, 1892.

DISTRIBUTION: Arikareean through Blancan of North America.

DIAGNOSIS: In contrast to *Phlaocyonini* and other basal *Borophaginae*, *Borophagini* has a derived character of an elongated m1 trigonid. Most members of *Borophagini* also acquired synapomorphies, such as premaxillary contact with frontal, lack of laterally flared orbital rim of zygomatic arch, elaborate lateral accessory cusps on I3, and a cristid between the hypoconid and entoconid of m1.

DISCUSSION: Members of this clade embody the traditional sense of the subfamily *Borophaginae*. In contrast to its sister-clade *Phlaocyonini*, which primarily exploits the hypocarnivorous niches, the *Borophagini* clade is consisted of mostly meso- to hypercarnivorous taxa that often became progressively larger and terminated in durophagous taxa.

*Cormocyon* Wang and Tedford, 1992

TYPE SPECIES: *Cormocyon copei* Wang and Tedford, 1992.

INCLUDED SPECIES: *Cormocyon haydeni*, new species; and *Cormocyon copei* Wang and Tedford, 1992.

DISTRIBUTION: Early Arikareean of Oregon, early to late Arikareean of South Dakota, medial to late Arikareean of Wyoming, late Arikareean of Florida, and ?late Arikareean of Colorado.

EMENDED DIAGNOSIS: The paraphyletic *Cormocyon* differs from *Archaeocyon* and *Rhizocyon* in its derived characters, such as ventrally directed paroccipital process, enlarged M1 metaconule, and elongated m1 trigonid. Compared to the *phlaocyonines*, *Cormocyon* lacks the following hypocarnivorous characters of that clade: m1 protostylid and slender horizontal ramus for *Cynarctoides*, and shortened premolars, short upper carnassial, and widened m1 talonid for *Phlaocyon*. Primitive characters that distinguish *Cormocyon* from *Desmocyon* and more derived taxa are absence of a frontal sinus, lack of an encircling ectotympanic for the auditory meatus, and crestlike talonid cusps on m1.

DISCUSSION: In a short paper, Wang and Tedford (1992) attempted to clarify the concept of *Nothocyon*, which has become a taxonomic wastebasket for many small fossil canids ever since Matthew (1899) informally erected the genus [type species *N. geismarianus* (Cope, 1881b) by subsequent designation]. Much of the past confusion surrounding *Nothocyon* stems from the poorly preserved genoholotype (AMNH 6884, a single m1). A much better preserved specimen (AMNH 6885) was later referred to *geismarianus* by Cope (1883, 1884). Through the reference of YPM 12733 to *N. geismarianus*, we demonstrated that these two AMNH specimens represented quite different caniforms. *N. geismarianus* is a highly derived subparictine ursoid (Baskin and Tedford, 1996), whereas *Cormocyon copei* is a borophagine canid based on AMNH 6885. Wang and Tedford (1992), however, did not attempt to define the precise content of *Cormocyon*, pending results of this study, and it has served in similarly vague capacity as had *Nothocyon* (Wang, 1994; Wang and Tedford,

1996) as a basal borophagine. In the present study, *Cormocyon* is a paraphyletic genus at the base of the tribe Borophagini.

***Cormocyon haydeni*, new species**

Figures 36–38

*Nothocyon geismarianus* (Cope, 1878): Macdonald, 1963: 209.

**HOLOTYPE:** F:AM 49448, skull with I1–M2 (fig. 36A–D), both rami with I1–I2 alveoli and i3–m3 (fig. 36E, F), right humerus (fig. 37C) and partial left humerus, radius and ulna (fig. 37A, B), articulated lumbar, sacrum and pelvis, both femora (fig. 37E), left tibia (fig. 37G) and right partial tibia with articulated distal remnant of fibula and astragalus, left astragalus (fig. 37F), left partial pes including tarsals, metatarsals I–IV, and 4 first, 3 second, and 1 third phalanges (fig. 37D), Eagle Nest Butte, 260 ft above the base of the exposed section in rocks equivalent to the Harrison Formation (late Arikareean), Washabaugh County, South Dakota.

**ETYMOLOGY:** Named for Ferdinand Vanderveer Hayden, pioneer geologist of the Great Plains.

**REFERRED SPECIMENS:** Wounded Knee area, upper part of Sharps Formation (early Arikareean), 8 mi south of Porcupine, Shannon County, South Dakota: F:AM 49436, left maxillary with P3–M2.

Wounded Knee area, lower part of Rosebud Formation equivalent to the Monroe Creek Formation by Macdonald (1963) (medial Arikareean), Shannon County, South Dakota: AMNH 12872, right ramus with c1, p1–p2 alveoli, and p3–m2 (referred to *Nothocyon geismarianus* by Macdonald, 1963: 209), Porcupine Creek, “Rosebud 8” of Macdonald (1963: 154).

West of Spanish Diggings, upper part of the lower Arikaree Group (medial Arikareean), Niobrara County, Wyoming: F:AM 50228, left partial ramus with m1 broken–m2, and m3 alveolus.

Northwest and northeast of Lusk, in rocks referred to the Harrison Formation (late Arikareean), Niobrara County, Wyoming: F:AM 27575, left ramal fragment with m1–m2, north of Keeline; F:AM 49058 (in AMNH permanent exhibition), skull with I1–I3 alveoli and C1–M2 (fig. 38A–C) and right and

left partial rami with isolated c1, p1 alveolus–m2, and m3 alveolus (fig. 38D, E), north of Keeline; F:AM 49064, partial skull with I1–M2 (P1 root) (fig. 38F) and partial mandible with i3–m3 (c1 broken) (fig. 38G, H), from North Ridge; F:AM 54138, right partial ramus with p1–p3 alveolus, p4 broken–m1, and m2 alveolus, north of Keeline; and F:AM 105247, partial mandible with c1 broken–p2 and p3–p4 both broken. Ellicott Ranch, Steer Pasture: KUVF 32380, nearly complete skull with I1–P3 all broken and P4–M2.

**DISTRIBUTION:** Early to late Arikareean of South Dakota, and medial to late Arikareean of Wyoming.

**DIAGNOSIS:** *Cormocyon haydeni* is distinguished from the Phlaocytonini and more basal Borophaginae in its possession of an elongated m1. In contrast to *C. copei* and more derived forms, on the other hand, *C. haydeni* has a primitively flared dorsal rim of the anterior zygomatic arch. *C. haydeni* also has a relatively short temporal fossa as compared to *C. copei*.

**DESCRIPTION AND COMPARISON:** *Cormocyon haydeni* is larger than *Archaeocyon leptodus* and *A. falkenbachi*. Other than this size difference, the cranial proportions of *C. haydeni* are very similar to those of *A. leptodus*. *C. haydeni* has a slightly downturned paroccipital process that does not yet fully fuse with the bulla. The bulla is less anteriorly expanded as in *A. leptodus*. The M1–M2 are more quadrate in outline with a more symmetrical distribution of the internal cingulum.

Compared to the John Day *Cormocyon copei*, *C. haydeni* is smaller and has a relatively short temporal fossa. A direct measurement of the length of this fossa is the distance between the posterior margin of the M2 and the glenoid fossa (length of M2 to bulla in fig. 39). In this measurement, individuals of *C. copei* are consistent in having longer temporal fossae than in *C. haydeni*. As shown in the ratio diagram (fig. 40), dental measurements of *C. haydeni* are nearly indistinguishable from those of *C. copei*, except for somewhat smaller size of the lower cheekteeth of the former.

**DISCUSSION:** *Cormocyon haydeni* seems to be the most basal species of the Boro-

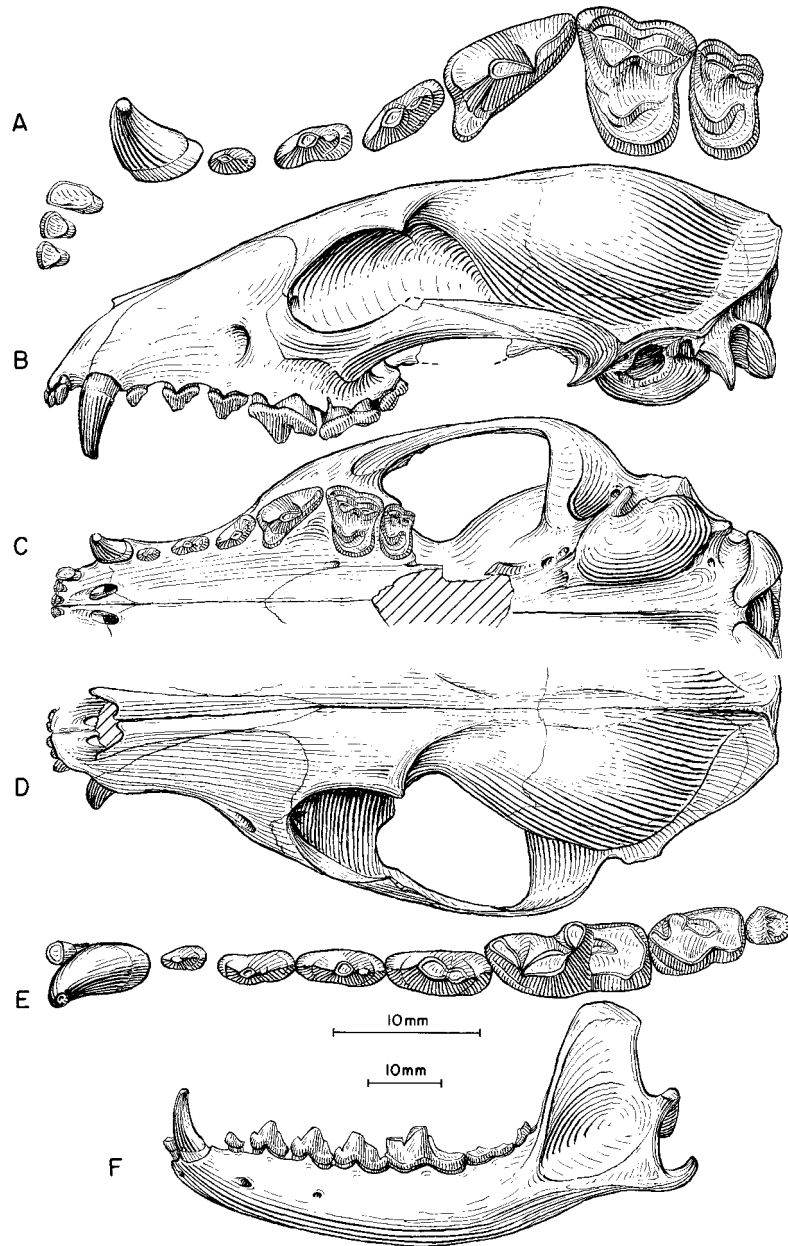


Fig. 36. *Cormocyon haydeni*. **A**, Upper teeth (M1–M2 reversed from right side), **B**, lateral, **C**, ventral, and **D**, dorsal views of skull, **E**, lower teeth, and **F**, ramus (reversed from right side), F:AM 49448, holotype, Eagle Nest Butte, in rocks equivalent to Harrison Formation (late Arikareean), Washabaugh County, South Dakota. The longer (upper) scale is for **A** and **E**, and the shorter (lower) scale is for the rest.

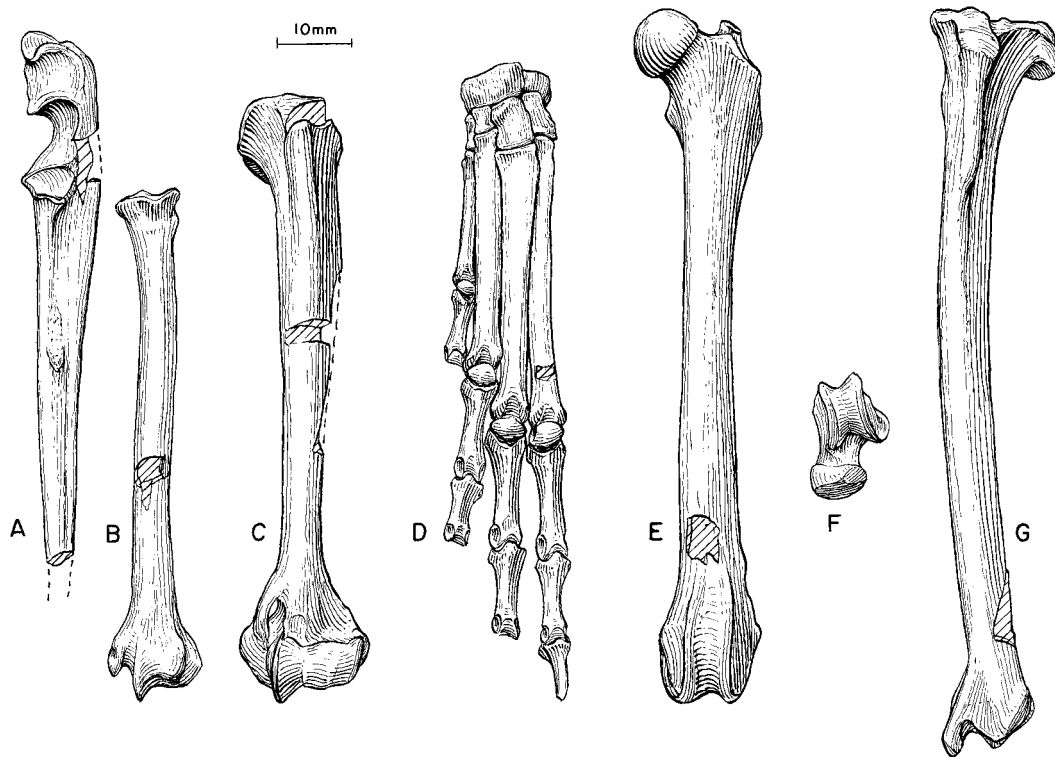


Fig. 37. *Cormocyon haydeni*. A, Partial ulna, B, radius, C, humerus (reversed from right side), D, partial foot, E, femur (reversed from right side), F, astragalus, and G, tibia, F:AM 49448, holotype, Eagle Nest Butte, in rocks equivalent to Harrison Formation (late Arikareean), Washabaugh County, South Dakota.

phagini clade that gave rise to most of the borophagines. This lineage of small, fox-like canids remains conservative throughout the Arikareean. Slight increase in size, downturned paroccipital process, and more cuspidate molars are a few characters that mark the difference of *C. haydeni* from such basal borophagines as *Archaeocyon* and *Rhizocyon*.

Reference of materials from the lower Rosebud Formation of South Dakota (AMNH 12872 and F:AM 49436) to *Cormocyon haydeni* is problematic. If correct, the early Arikareean occurrence of this species may be contemporaneous with the earliest occurrence of *C. copei*, as is predicted in our phylogeny. These two Rosebud specimens, however, have some peculiarities of their own (e.g., elongated carnassials) and may prove to be a different taxon given additional materials.

*Cormocyon copei* Wang and Tedford, 1992  
Figure 41

*Galecyon geismarianus* Cope, 1881b: 180 (in part); 1883: 240, figs. 5, 6 (in part); 1884: 915, 920.

*Cynodictis geismarianus* (Cope): Cope, 1889: 233, fig. 59 (in part).

*Nothocyon (Galecyon) geismarianus* (Cope): Matthew, 1899: 62 (faunal list).

*Nothocyon geismarianus* (Cope): Wortman and Matthew, 1899: 125 (in part). Matthew, 1909: 106 (faunal list). Thorpe, 1922a: 164. Hough, 1948: 100.

*Cormocyon copei* Wang and Tedford, 1992: 225. Fremd and Wang, 1995: 76. Munthe, 1998: 135.

*Leptocyon mollis* (Merriam, 1906): Fremd and Wang, 1995: 76 (in part).

HOLOTYPE: AMNH 6885, complete skull with I1–M2, mandible with i2–m3 (fig. 41), and articulated partial lumbar and sacral vertebrae and partial pelvis, from the John Day



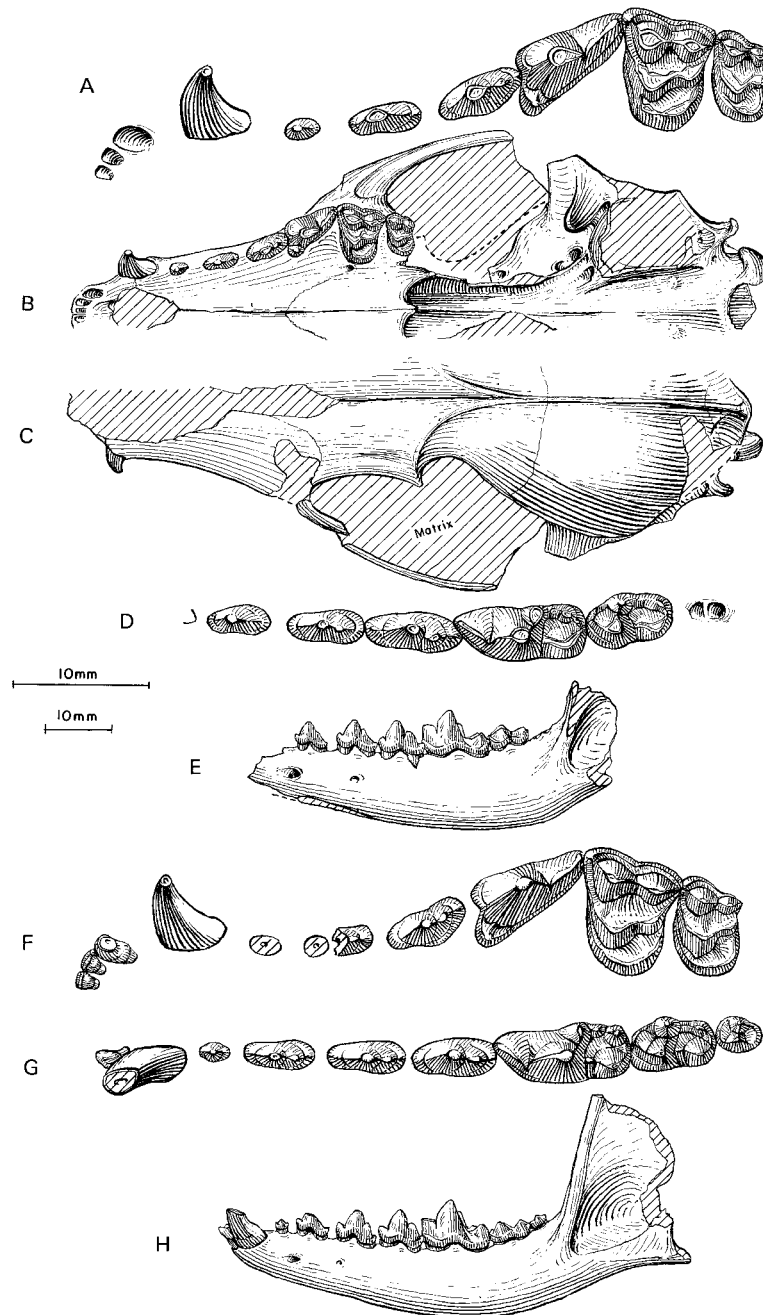


Fig. 38. *Cormocyon haydeni*. **A**, Upper teeth, **B**, ventral and **C**, dorsal views of skull, **D**, lower teeth, and **E**, ramus, F:AM 49058, north of Keeline, in rocks referred to Harrison Formation (late Arikareean), Niobrara County, Wyoming. **F**, Upper teeth, **G**, lower teeth, and **H**, ramus, F:AM 49064, North Ridge, in rocks referred to Harrison Formation. The longer (upper) scale is for A, D, F, and G, and the shorter (lower) scale is for the rest.

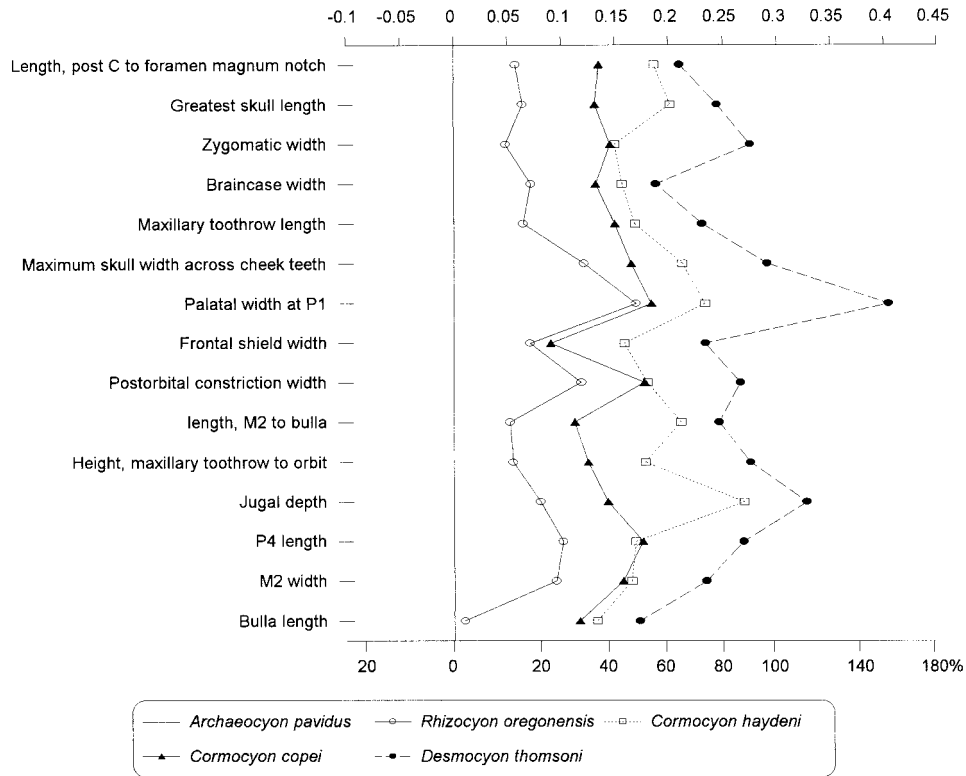


Fig. 39. Log-ratio diagram for cranial measurements of *Rhizocyon*, *Cormocyon*, and *Desmocyon* using *A. pavidus* as a standard for comparison (straight line at zero for y-axis). See text for explanations and appendix II for measurements and their definitions.

Basin, John Day Formation (?early Arikarean), Wheeler or Grant counties, Oregon.

REFERRED SPECIMENS: From the locality of the type (biostratigraphic positions of some JODA specimens in the Turtle Cove Member are placed within a letter system by Fremd et al., 1994): AMNH 6886, greater part of an articulated postcranial skeleton, including incomplete vertebral column, partial scapula, humerus, radius, ulna, metacarpals I, II, IV, and V, three first phalanges, partial pelvis, femur, and tibia (Cope, 1884: pl. LXXa, figs. 10–12); AMNH 6887, partial skull with P3–M2 all represented by roots; AMNH 6947, posterior half of skull; AMNH 6947A, rostral part of skull with alveoli for C1–P4; JODA 771, left ramal fragment with m1 and m2 alveolus; JODA 924, left P4, unit H; JODA 1630, right maxillary fragment with P4–M2, unit I; JODA 1750 (AMNH cast 129652), right partial ramus with p1–m1 and broken

c1 and m2, unit F; JODA 1755, left ramus with c1–m2, unit J; JODA 1809, right maxillary fragment with P4–M1, unit G; JODA 3004, left m2, unit K; UCMP 76608, right and left partial rami with p1 root–m3, Picture Gorge Locality 7, Zone 3, UCMP loc. V6681; UCMP 76748, partial skull with P2 broken–M2, right and left rami with c1 broken, p1–p2 alveoli, p3–m2, and m3 alveolus, and fragments of vertebrae, UCMP loc. V6505, Haystack loc. no.7; UCMP 76931, fragmentary palate with P3–M2 and both partial rami with c1–m2 (p2 broken), Picture Gorge loc. 22, UCMP loc. V66116; UCMP 77161, partial skull with P1 alveolus–M2, and right and left partial rami with p3–m3 (m1 broken), right and left distal part of humeri, and left distal part tibia, from UCMP loc. V6322, Haystack loc. no.8, level 2; UCMP 112181, rostral part of skull with C1 alveolus–M2, and right and left partial rami

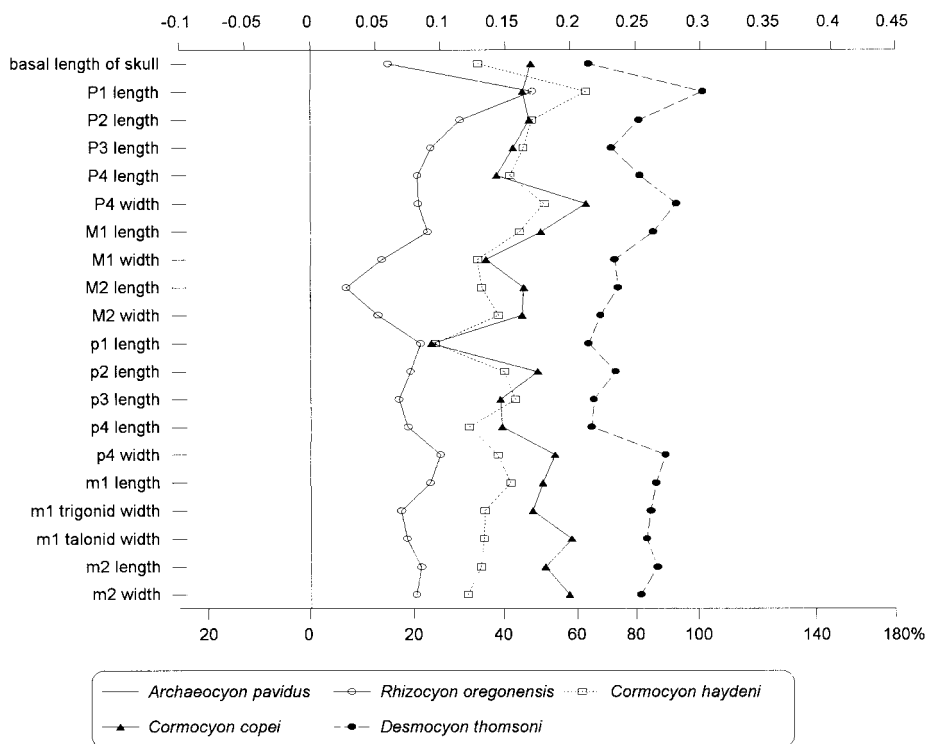


Fig. 40. Log-ratio diagram for dental measurements of *Rhizocyon*, *Cormocyon*, and *Desmocyon* using *A. pavidus* as a standard for comparison (straight line at zero for y-axis). See text for explanations and appendix III for summary statistics of measurements and their definitions.

with c1–m2, from UCMP loc. V6691, Haystack loc. no.12; YPM 12679, partial skull with C1 alveolus, P1–P4 roots, and M1–M2, Haystack Valley area; YPM 12679-1, anterior part of skull with I1–P1 alveoli, and P2–M2; and YPM 12700, skull fragment with P4–M2 and articulated right partial ramus with c1–p2 all alveoli, p3 (from left side), p4–m1, and m2–m3 alveoli, Camp Watson.

Buda Local Fauna (medial Arikareean), Alachua County, Florida: UF 16963c, left M2.

Troublesome Formation (?late Arikareean), Grand County, Colorado: UCMP 26770 (AMNH cast 129864), right maxillary fragment with P3–M2, Granby Locality, UCMP loc. 77027; UCMP 47873 (AMNH cast 129865), left partial ramus with p2 alveolus and p3–m1, Substation Locality, UCMP loc. 82045.

DISTRIBUTION: Early Arikareean of Oregon, medial Arikareean of Florida, and ?late Arikareean of Colorado.

EMENDED DIAGNOSIS: A synapomorphy that distinguishes *Cormocyon copei* and later borophagines from *C. haydeni* and more basal taxa is the lack of a laterally flared orbital rim of the zygomatic arch. Additionally, *C. copei* has a long temporal fossa, an autapomorphy that distinguishes it from *C. haydeni*.

DESCRIPTION AND COMPARISON: The holotype of *Cormocyon copei* is probably a female, judging from its small size and relatively gracile canines. It has the shortest P4 among all referred specimens (appendix III), and its P4 protocone is also very small. These proportional differences may reflect sexual dimorphism, but rigorous statistical testing is not possible with the small sample size.

Besides its larger size, *Cormocyon copei* is advanced over *C. haydeni* in its loss of a lateral flare on the orbital rim of the zygomatic arch and its deeper jugal contribution to the zygomatic arch (jugal depth in fig. 39). In some individuals (e.g., AMNH 6885 and

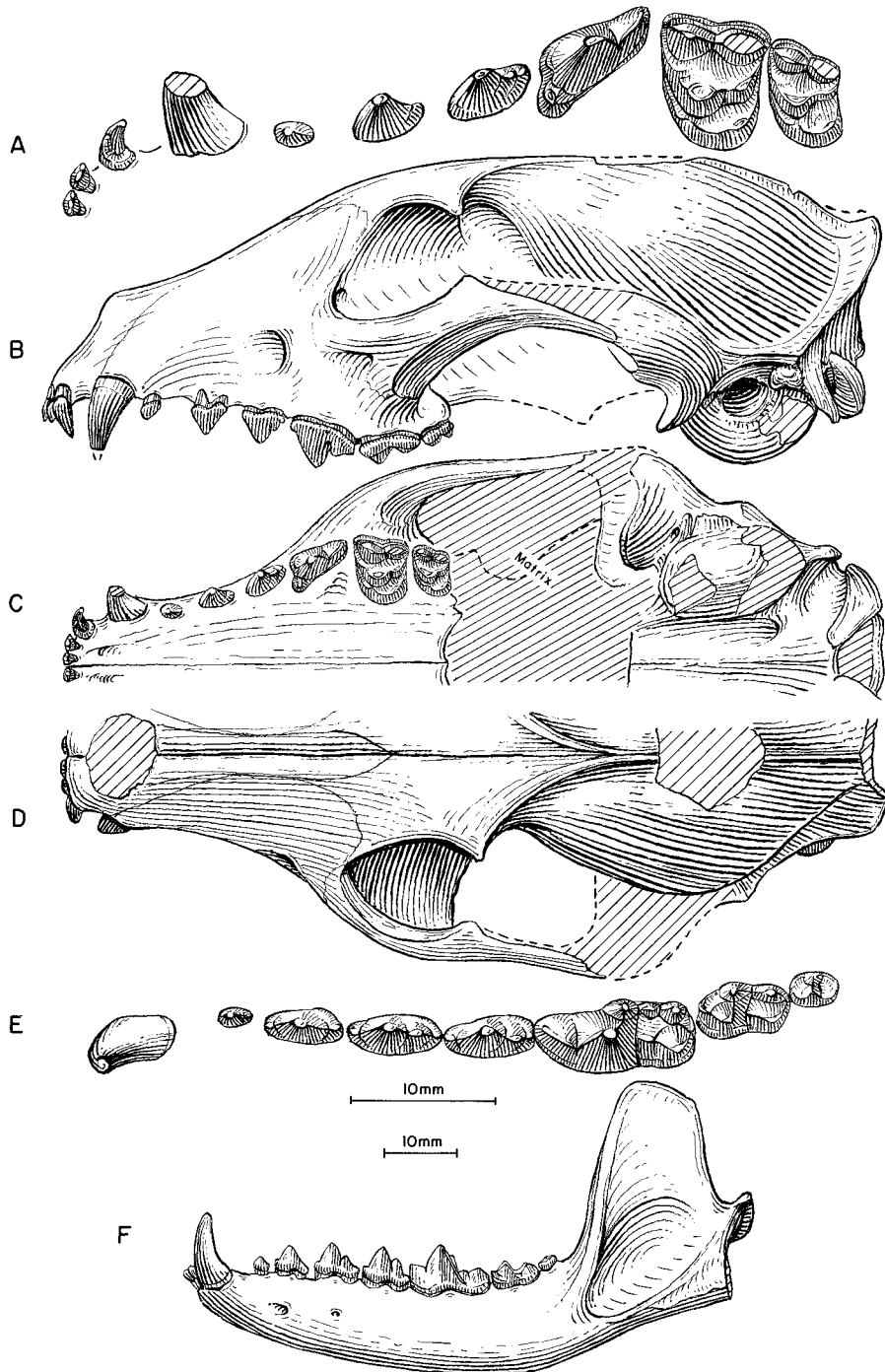


Fig. 41. *Cormocyon copei*. **A**, Upper teeth, **B**, lateral, **C**, ventral, and **D**, dorsal views of skull, **E**, lower teeth, and **F**, ramus, AMNH 6885, holotype, John Day Basin, John Day Formation (?early Arikareean), Oregon. The longer (upper) scale is for A and E, and the shorter (lower) scale is for the rest.

UCMP 77161) the anterior section of the jugal has a rounded dorsal border (rather than a flat and tilted surface in primitive forms), a character that is fully fixed in *Desmocyon thomsoni*. Additional John Day specimens referred to this species allow a better appreciation of variation and show incipient development of characters present in more derived taxa. Some individuals (AMNH 6885 and YPM 12700) display a gently domed forehead that suggests initial development of a frontal sinus shown in *D. thomsoni*. Although most individuals show a distinct metaconule on M1–M2, the lower molar talonids of some individuals still retain rather crestlike cusps. The holotype has the most conate talonid cusps.

Another consistent character that permitted us to distinguish the John Day *Cormocyon copei* from the Great Plains species *C. haydeni* is an elongated temporal fossa (length M2 to bulla in fig. 39). This long fossa and its associated long (anteroposteriorly) ascending ramus of the mandible is even more pronounced among the referred specimens (e.g., UCMP 76748 and 77161, YPM 12679). On the other hand, these referred specimens tend to have more primitive dental morphology in their crestlike talonid cusps of m1, in contrast to the conate cusps in the holotype.

**DISCUSSION:** Our present concept of *Cormocyon copei* is primarily based on specimens from the John Day Basin but includes some questionably referred specimens from Florida and Colorado. Two specimens from the Troublesome Formation of north-central Colorado are here referred to *C. copei* because of their size and dental morphology. The maxillary fragment (UCMP 26770) is undoubtedly a primitive borophagine with *copei*-like characteristics such as shortened P4, distinct metaconules of M1–M2, and a connection between the M2 metaconule and its lingual cingulum. The ramus fragment (UCMP 47873), however, has an m1 with a rather trenchant talonid that is quite hesperocyonine-like. Another peculiarity of the Colorado specimens is an elevated lingual cingulum on M2 and a transverse cleft on M1 that is similar to the initial development of a conate hypocone in *Phlaocyon*. On the other hand, its P4 completely lacks a hypo-

cone or a widened lingual cingulum that is characteristic of *Phlaocyon*. The above combination of peculiarities may suggest a distinct species for the Colorado materials, or even two species. We refrain from erecting a new taxon for lack of better materials and of larger series for evaluation of variation. As presently referred, the Colorado materials indicate the presence of a *C. copei*-like form outside the John Day Basin, but still to the west of the continental divide. A single M2 from the Buda Local Fauna of Florida is tentatively referred to *Cormocyon*.

*Cormocyon copei* is very close, in stage of evolution, to *C. haydeni* from the northern Great Plains. The *copei*–*haydeni* pair appears to mark an instance of sister-species on either side of the continental divide. As part of a nearly linear series of borophagines from *Cormocyon* to *Tomarctus*, this species pair occupies the starting point of a long evolutionary trend toward medium- to large-size predators. The possession of a derived condition on the zygomatic arch shows *C. copei* to be slightly more advanced than *C. haydeni*.

#### *Desmocyon*, new genus

**TYPE SPECIES:** *Cynodesmus thomsoni* Matthew, 1907.

**ETYMOLOGY:** Greek: *desmo*, bond, suggesting relationship; *cyon*, dog, an anagram of the genus *Cynodesmus*, to which the type species was originally referred.

**INCLUDED SPECIES:** *Desmocyon thomsoni* (Matthew, 1907), and *Desmocyon matthewi*, new species.

**DISTRIBUTION:** Late Arikareean of South Dakota, Wyoming, Nebraska, and Oregon; early Hemingfordian of Nebraska, New Mexico, and Florida.

**DIAGNOSIS:** Derived characters distinguishing *Desmocyon* and more derived taxa from *Cormocyon* are broad rostrum and palate, frontal sinus present but not penetrating post-orbital process, encircling ectotympanic forming an external auditory meatus ring, and deep zygoma. Compared to the Cynarcina, *Desmocyon* lacks the hypocarnivorous characters of that clade: a prominent subangular lobe, high mandibular condyle, short P4, m1 protostylid, wide m1 talonid, and

large m2. *Desmocyon* is primitive relative to *Metatomarctus* in that the I3 is not enlarged and lacks a well-developed lateral cusplet, and the P4 has only a weak anterior crest on the paracone.

*Desmocyon thomsoni* (Matthew, 1907)

Figures 42–44, 46E, F

*Cynodesmus thomsoni* Matthew, 1907: 186, figs. 4, 5; 1909: 112. Peterson, 1910: 267, fig. 62. Cook, 1912: 42. Hough, 1948: 103.

*Nothocyon* sp. Cook, 1909: 266; 1912: 42.

*Tomarctus thomsoni* (Matthew): White, 1941b: 95. Cook and Macdonald, 1962: 562. Macdonald, 1963: 209; 1970: 57.

*Nothocyon regulus* Cook and Macdonald, 1962: 560, fig. 1.

*Tomarctus thompsoni* [sic] (Matthew): Munthe, 1989: 13; 1998: 135.

HOLOTYPE: AMNH 12874, skull with I1–M2 (fig. 42A–C), mandible with i1–m3 (fig. 42D, E) and associated skeletal fragments including partial tibia, partial radius and ulna, carpals and incomplete metacarpals II–V, and phalanges. Matthew reported that the type was from the Upper Rosebud beds. Macdonald (1963: 209) listed the type locality as AMNH “Rosebud 24” and located the type locality by quoting from the 1906 field notes as “8 m. E. of Porcupine P.O. . . . N. of Porcupine Crk . . . upper Rosebud” (Macdonald, 1963: 156). He concluded that “Rosebud 24” is “probably Rosebud Formation” in the sense used by him (1963, 1970), late Arikarean.

REFERRED SPECIMENS: Wounded Knee area, Rosebud Formation (late Arikarean), Shannon County, South Dakota: AMNH 12874A, left ramal fragment with m1 broken; AMNH “Rosebud 17”; AMNH 12885, partial palate with C1, P1 alveolus, P2–P3, and P4–M1 broken, and left ramal fragment with m1; SDSM 5584 right isolated P4 from SDSM V5341; and SDSM 5585, right partial ramus with p3 alveolus and p4–m1 from SDSM V554.

*Syndyoceras* Hill, 0.5 mi west of Agate, Harrison Formation (late Arikarean), Sioux County, Nebraska: AMNH 81008 (HC 115, holotype of *Nothocyon regulus* Cook and Macdonald, 1962), right partial ramus with p4 alveolus, m1, and m2 alveolus.

Lusk area, Upper Harrison beds (late Ari-

kareean), Niobrara County, Wyoming: AMNH 13763, partial skull with P2–M2 and right and left partial rami with c1 broken–m3, 9 mi south of Lusk; F:AM 27566, right ramal fragment with m1 broken and m2; F:AM 27566A, partial right ramus with m1 broken and m2–m3 alveoli, north of Lusk; F:AM 49078, left ramal fragment with m2, Royal Valley; F:AM 49085, right partial ramus with p4 root–m1 broken, Royal Valley; F:AM 50207, partial mandible with c1, p1 alveolus, p2 broken–m2, and m3 alveolus, Royal Valley in white line; F:AM 50209, anterior part of skull with I3, C1 alveolus, and P1–M2 (P4 broken) and right ramus with c1 broken, p1–p3 alveoli, p4–m2, and m3 alveolus, Royal Valley; F:AM 50210, articulated fragment of skull with C1 and P4–M2 and partial mandible with c1, p2–p4 all broken, and m1–m2, Silver Springs; F:AM 50211, left ramus with c1, p1 alveolus, and p2 broken–m2, Freeman Ranch, south of Lusk; F:AM 50212, right partial ramus with c1 root and p1 broken–m1, Royal Valley; and F:AM 50213, fragmentary skull, right partial ramus with p3–m1, fragmentary limbs including an incomplete articulated pes with tarsals and proximal part of metatarsals II–IV, detached partial metatarsal V and isolated phalanges, and partial baculum, Silver Springs area.

Lusk area, Upper Harrison beds (late Arikareean), Goshen County, Wyoming: F:AM 27551, partial skull with C1–M2 and partial mandible with c1–m2 and m3 root, 16–20 mi southeast of Lusk; F:AM 27552, partial skull with P3–M2 (all broken) and articulated partial right ramus with m1 broken–m2; F:AM 27553, right partial ramus with c1 and p1 alveolus–m1, 18 mi southeast of Lusk; F:AM 27564, anterior part of skull with I1–I2 alveoli and I3–M1, 2 mi west of Jay-Em; F:AM 27569, anterior part of skull with I1–M1 and M2 broken, partial mandible with i1–m3, right partial humerus, right partial radius, right ulna, right incomplete manus with metacarpals II–V and phalanges, left metacarpal I, right femur, right tibia, partial pelvis, and vertebrae, 21 mi southeast of Lusk; F:AM 27570, left partial maxillary with C1–P2, isolated M1, both partial rami with c1 broken–p3 and m1–m2, 12–15 mi southeast of Lusk; F:AM 27571, partial skull with I3–

C1, P1–P2 roots, and P3–M2, 16–20 mi southeast of Lusk; F:AM 27572, partial palate with P2 root–M2 and both partial rami with p2–m2 and m3 alveolus, 12–15 mi southeast of Lusk; F:AM 27574, left ramal fragment with p4–m1 (broken), North Ridge on Highway 85; F:AM 49018; skull fragment, left metacarpals I, II, and V, incomplete left metacarpal III, left metatarsals III, IV, and V, and left calcaneum, 25 mi southeast of Lusk; F:AM 49065, left premaxillary-maxillary fragment with I3–C1 and partial maxillary with P3–M1, M2 broken, right and left partial rami with p2–m1 all broken and m2–m3, atlas, axis, distal fragment of humerus, proximal part of radius and ulna, articulated calcaneum and astragalus, and articulated tarsals and metatarsals II–IV, Jay-Em, high in section; F:AM 49066, right partial ramus with p2–m2, 20 mi southeast of Lusk, high Middle Brown Sand; F:AM 49067, partial skull with I1–M2, mandible with i1–m3, and associated limbs including partial humerus, radius, ulna, articulated manus with carpals, metacarpals I–V, some phalanges, partial femora, tibia, astragalus, and calcaneum, 18 southeast of Lusk, high in section; F:AM 49068, left partial maxillary with P4–M1 and M2 alveolus, right and left partial rami with c1 and p2–m1, partial radius and ulna, carpals, metacarpals III, IV, and V, calcaneum, astragalus, tarsals, incomplete metatarsals III, IV, and V, and vertebrae, Sand Gulch, high in section; F:AM 49082, right partial maxillary with P4–M2 (M1 broken) and right partial ramus with p2–p3 alveoli and m1–m3, 25 mi southeast of Lusk; F:AM 49083, right partial ramus with m1, 18 mi southeast of Lusk, middle brown sand; F:AM 49084, right partial ramus with p4 root and m1–m2, Jay-Em; F:AM 49087, left isolated p4, m1, and right m2, 18 mi southeast of Lusk; F:AM 49089, partial skull with C1 broken–M2 and partial mandible with c1–p1 both broken and p2–m3, 16 mi southeast of Lusk, high brown sand; F:AM 49090, left partial ramus with c1–p2 roots, p3, and p4–m1 both broken, 16 mi southeast of Lusk, middle brown sand; F:AM 49091, right ramus with p3 alveolus and p4–m2, 18 mi southeast of Lusk, high brown sand; F:AM 49092, left partial maxillary with P1, P2–P3 alveoli, P4, M1 broken, and M2 alveolus,

Jay-Em, high brown sand; F:AM 49094, partial skull with I3 broken, and C1–M2 (P1 alveolus) and left ramus with i1, i2–p2 alveoli, p3 broken, p4 alveolus–m2, and m3 alveolus, Jay-Em, high in section; F:AM 49095, partial left ramus with i2–m2 and m3 alveolus, 18 mi southeast of Lusk, high in section; F:AM 49097, skull with I1, I2 alveolus, I3–M2 (P1 alveolus), left ramus with c1–m3 (p4 alveolus), left humerus, right partial humerus, both radii and ulnae, carpals articulated with metacarpals II and III, detached metacarpal V, phalanges, both femora, right tibia, calcaneum, astragalus, tarsals articulated with proximal ends of metatarsals III–V, and partial baculum, Jay-Em, high in section; F:AM 50205, partial palate with P3–M2, 16 mi southeast of Lusk; F:AM 50206, partial right ramus with i2–m1 (all broken) and m2–m3, Sand Gulch, south end; F:AM 50208, right partial ramus with p2–p4 all broken, m1–m2, and m3 alveolus, 16 mi southeast of Lusk, light sand, west end; F:AM 54118, right partial ramus with c1, p1–p3 alveoli, p4, m1 broken, and m2 alveolus, Jay-Em, below white layer; and F:AM 105250, left partial ramus with c1, p1–p4 alveoli, m1, and m2–m3 alveoli, roadcut about 1 mi southeast of Podelack Ranch headquarters.

Spoon Buttes area, Upper Harrison beds (late Arikareean), Goshen County, Wyoming: F:AM 49086, right ramal fragment with m1, Spoon Buttes; and F:AM 54142, right and left partial maxillae with I1–M1, southwest of Spoon Buttes.

Lusk area, 18 Miles District, 18 mi southeast of Lusk, high brown sand, Upper Harrison beds (late Arikareean), Goshen County, Wyoming (The following four skulls and jaws, F:AM 49096A–D, were found associated with the limb elements in one field block. No direct association between limb elements and skulls was apparent; however, those limb elements marked F:AM 49096-1 [smaller] and F:AM 49096-2 [larger] are tentatively considered as representing two or more individuals. Additional limb elements are placed in F:AM 49096 that may represent one or more individuals.): F:AM 49096A, skull with I1–M2 and mandible i1–m3; F:AM 49096B, skull with I1–M2 (fig. 43A, B) and mandible i1–m3 (fig. 43C, D); F:AM



Fig. 42. *Desmocyon thomsoni*. **A**, Lateral, **B**, ventral, and **C**, dorsal views of skull (I1–I2 reversed from right side), **D**, lower teeth, and **E**, ramus (angular process reversed from right side), AMNH 12874, holotype, 8 mi east of Porcupine, Rosebud Formation (late Arikarean), Shannon County, South Dakota.



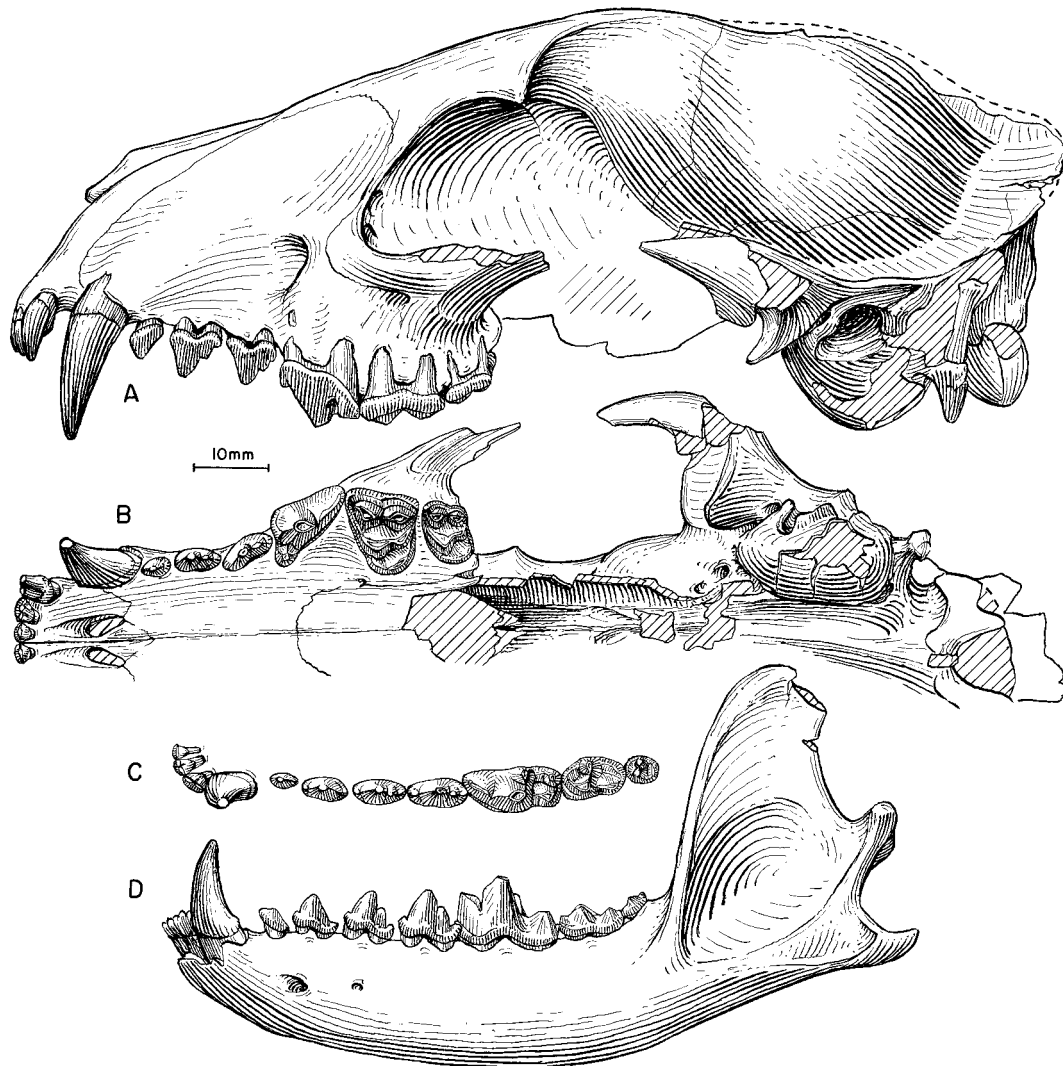


Fig. 43. *Desmocyon thomsoni*. **A**, Lateral and **B**, ventral views of skull (C1 reversed from the right side), **C**, lower teeth, and **D**, ramus (c1 and i1–i2 reversed from the right side), F:AM 49096B, 18 Miles District, Upper Harrison beds (late Arikareean), Goshen County, Wyoming.

49096C, skull with I1–M2 and mandible with i1–m3; F:AM 49096D, anterior half of skull with I1–M2 and partial mandible with i1–m3; F:AM 49096-1, right and left humeri, right partial radius, and two left femora; F:AM 49096-2, right and left humeri (fig. 44A) (?two individuals), left radius and ulna (fig. 44B, C), right femur (fig. 44D), right and left tibia both with fibula (fig. 44E, F); and F:AM 49096, following limbs associated with the above and may represent either the same

or other individuals included right proximal part of radius and ulna, left incomplete ulna, two right partial femora, right proximal part of tibia, right and left partial articulated pes with tarsals and metatarsals I–V (fig. 44G), and right partial articulated pes with calcaneum, astragalus, incomplete metatarsals III and IV, and complete metatarsal V.

Wheatland area, Upper Harrison beds (late Arikareean), Platte County, Wyoming: F:AM 27565, left partial ramus with p4–m3; F:AM

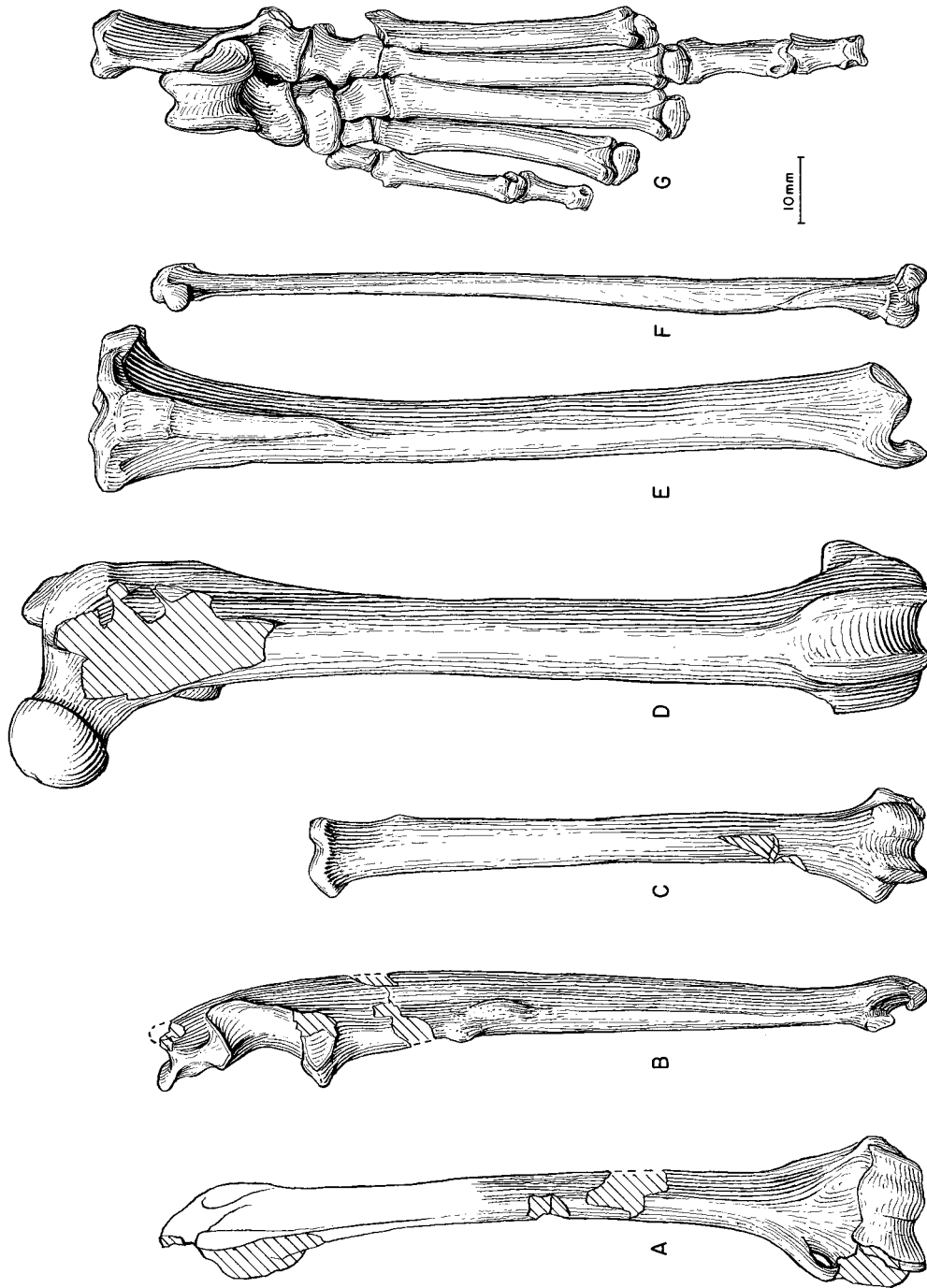


Fig. 44. *Desmocyon thomsoni*. A, Humerus, B, ulna, C, radius, D, femur (reversed from right side), E, tibia, F, fibula, and G, tarsi, metatarsi, and partial phalanges, F:AM 49096(2), 18 Miles District, Upper Harrison beds (late Arikarean), Goshen County, Wyoming.

49017 (referred to *Tomarctus thomsoni* by Munthe, 1989: 13), associated postcranial skeleton with partial axis, pelvis fragment, left humerus, right partial radius and ulna, right partial manus with carpals and metacarpals II, III, and IV, left femur, left tibia and fibula, left articulated pes with calcaneum, astragalus, tarsals, metatarsal I, incomplete metatarsals II, III, IV, and V, Uva Breaks, 10 ft above white layer; and F:AM 54119, partial skull with I1–I3 alveoli, C1–P4, partial mandible with c1 broken, p1–m2, and m3 alveolus and associated limb including distal end of both humeri, right and left radii, left ulna and right partial ulna, right metacarpal I, partial metacarpal III, left metacarpal IV and right partial metacarpal IV, left metacarpal V, and left calcaneum, Uva Breaks.

Guernsey area, Upper Harrison beds (late Arikareean), Platte County, Wyoming: F:AM 49088, posterior part of skull, both partial rami with p4–m3, axis, atlas, cervicals, and vertebrae, 6 mi west of Guernsey, high brown sand; and F:AM 49093, right and left rami with i1–m3, 2 mi southwest of Guernsey, 20 ft above white layer.

Upper Harrison beds (late Arikareean), Sioux County, Nebraska: AMNH 81026 (HC 485), right partial ramus with i1–i3 alveoli, c1–p1 broken, p2–m2, and m3 alveolus; AMNH 81027 (HC 240), left partial ramus with p3 root, p4–m1, and m2–m3 alveoli, 3 mi northeast of Agate, 15 ft above the contact with the lower Harrison; F:AM 49182, left partial ramus with p4–m1 both broken, m2, and m3 alveolus, 5–7 mi northeast of Agate, low in section; F:AM 49183, left ramus with i1–p3 alveoli, p4–m1, and m2–m3 alveoli, Morava Ranch; F:AM 49189, left ramal fragments with c1–p3 all broken and p4 broken–m2, south of Harrison, high brown sand; F:AM 49190, left maxillary with C1–M1, south of Harrison, high in section; F:AM 105251, left partial ramus with p2 alveolus, p3–m2, and m3 alveolus, northeast of Agate, surface below grayish low channel; KUVF 27672, partial skull and mandible with complete upper and lower teeth, partial postcranial skeleton with atlas, axis, two lumbar, distal left humerus, proximal left ulna, left radius, left and right femora, left and right tibiae, partial left foot with calcaneum, tar-

sals, metatarsals II–IV, and phalanges, from locality KU-NE-028, Dout Ranch, Sitting Hen and vicinity; and KUVF 27673, partial skull and mandible with most upper and lower teeth except for P1 and p1, and postcranial skeleton with partial atlas, axis, one cervical, three thoracics, four lumbar, left and right humeri, left and right ulna and radius, partial right manus with metacarpals II–V, and one medial phalanx, Dout Ranch.

Upper Harrison beds (late Arikareean), Cherry County, Nebraska: UNSM 26550, complete skull and mandible with entire upper and lower dentition and partial articulated skeleton, UNSM loc. Cr-127; UNSM 26664, complete skull with left and right I1–M2, partial left ramus with p4–m1, m2 broken, m3 alveolus, partial vertebral column with one cervical, one thoracic, five lumbar, sacrum, pelvis, partial right scapula, left radius, nearly complete left and right hindlimbs with femora, tibiae, fibulae, tarsals and metatarsals, and phalanges; and UNSM 6865–86, skull fragments with I3–M2 and left and right rami with i1–m3.

John Day Formation (?late Arikareean), Oregon: AMNH 7238, isolated right M1–M2 (No stratigraphic information is available on this specimen, which was collected by E. D. Cope parties. Based on the known range of this species, AMNH 7238 is probably from the Haystack Valley Member of the John Day Formation, i.e., late Arikareean).

Lower part of Runningwater Formation (early Hemingfordian), Dawes County, Nebraska: F:AM 49180, left partial ramus with p2–m3 (p4–m1 broken), 1.25 mi northwest of Marsland; F:AM 49188, left partial ramus with m1–m2, Cross Cut Prospect, Sand Canyon System; F:AM 54496, right partial ramus with p4–m1 and m2 broken, Hay Springs Creek; and F:AM 105096, right isolated P2 and two maxillary fragments with P3–P4, M1, and M2 alveolus, Hay Springs Creek.

Lower part of Runningwater Formation (early Hemingfordian), Box Butte County, Nebraska: F:AM 62890, partial skull with I1–I3 alveoli, C1–M2 (p1 alveolus) (fig. 46E, F), East Channel Prospect, type section of Runningwater Formation; and F:AM 99693, left partial ramus with p4 alveolus–m2 and m3 alveolus, Runningwater Quarry.

Lower part of Runningwater Formation (early Hemingfordian), Morrill County, Nebraska: Bridgeport Quarry 1 (UNSM loc. Mo-113): UNSM 25711, right ramal fragment with m1–m2; UNSM 25792, left partial maxillary, with P3 alveolus–M1; UNSM 25797 (F:AM cast 97147), left partial maxillary with P3–M1 and M2 alveolus; UNSM 25798, right partial maxillary with M1–M2; and UNSM 25799, left ramal fragment with m1–m2 and m3 alveolus.

Spiers Quarry, ?Runningwater Formation (early Hemingfordian), Dawes County, Nebraska: F:AM 49191, left partial ramus with m1 broken and m2–m3.

Jeep Quarry, Arroyo Pueblo drainage, upper part of Chamisa Mesa Member, Zia Formation (early Hemingfordian), Sandoval County, New Mexico: F:AM 50138, right ramal fragment with p4–m1; and F:AM 62775A, right edentulous ramus fragment with p1–m2 alveoli.

DISTRIBUTION: Late Arikareean of South Dakota, Wyoming, Nebraska, and Oregon; early Hemingfordian of Nebraska and New Mexico.

EMENDED DIAGNOSIS: Characters of *Desmocyon thomsoni* that are primitive with respect to *D. matthewi* are small frontal sinus that does not penetrate the postorbital process, frontal shield narrow relative to width of braincase, postorbital width of frontals narrow, and m1 talonid without transverse crest between entoconid and hypoconid and hypoconulid shelf absent.

DESCRIPTION AND COMPARISON: Besides its larger size, *Desmocyon thomsoni* has several cranial features that set itself apart from *Cormocyon* and more basal taxa. In cranial proportions, *D. thomsoni* has a relatively broader muzzle and wide palate, a deeper jugal contribution to the zygomatic arch, and a smaller bulla (fig. 39). An inflated frontal sinus first appears in *D. thomsoni*, as reflected by a slightly domed forehead and verified by dissected individuals (F:AM 49067, 49094, 49096A, 49097). In all of these individuals and others whose postorbital processes are broken, the sinus does not invade the postorbital process and generally ends before the postorbital constriction, rather than expanding behind the constriction. Also first appearing in *D. thomsoni* is a complete ecto-

tympanic ring, which bridges the top of external auditory meatus. Thus, the roof of the meatus is now formed by the dorsal extension of the ectotympanic instead of the squamosal. Fusion between the ectotympanic and squamosal sometimes obscure this relationship; however, a bony thickening in this part of the meatus is always visible in such cases to indicate the encircling ectotympanic.

On the other hand, isolated individuals of *Desmocyon thomsoni* begin to display the initial development of certain derived features seen in *D. matthewi*. For example, two specimens (the holotype and F:AM 49067) show an expanded posterior process of the premaxillary whose tip touches the nasal process of the frontal, a derived character fully established in *D. matthewi*. While such cases of advanced features suggest what is to come in phylogeny, they are judged to be interspecific variation since most specimens still show the primitive state.

The presence of *Desmocyon thomsoni* in the Runningwater Formation of Nebraska is established by excellent materials (under study by Bruce Bailey), which have none of the derived characters for *D. matthewi*. Such a recognition of *D. thomsoni* in the Runningwater Formation creates a problem of identification of more fragmentary materials. The nearly identical size of *D. thomsoni* and *D. matthewi* makes the differentiation difficult. We are forced to use more subtle dental criteria for species recognition, such as a slightly better developed anterior ridge of the paracone on P4 tending toward a parastyle and the presence of a transverse crest between the hypoconid and entoconid of m1, as indicative of *D. matthewi*. Stratigraphically, *D. thomsoni* generally occurs in the lower part of the Runningwater Formation whereas *D. matthewi* is mostly found in the upper part.

A much larger series of specimens is now referable to *Desmocyon thomsoni* than was available when the taxon was first described, mostly due to the contributions from the Frick Collection. Particularly noteworthy is the presence of a group of four individuals (F:AM 49096A–D) in a single block of matrix from southeast of Lusk, Wyoming, that affords a rare instance of observing individuals from a real population. All four individuals are adults with differing degree of wear

on their teeth. Although dental dimensions of the four individuals are very close, there are significant size differences in their limbs (we cannot, however, associate the skulls with particular sets of postcranial skeleton).

Two specimens, F:AM 49097 and 50213, can be positively sexed due to associations of a baculum. Two other individuals, UNSM 26550 and 26664 (under study by Bruce Bailey), lack a baculum, and they are here regarded as females. Our inference that the UNSM specimens truly lack a baculum is based on their excellent preservation. The postcranial skeleton in UNSM 26664 includes well-preserved, completely undistorted lumbar vertebrae and an intact sacrum-pelvis, in addition to articulated hindlimbs on both sides—the posterior half of the skeleton surrounding the baculum region is completely preserved. Both male individuals display markedly stronger canines, more robust lower jaws, and slightly broader (transversely) cheekteeth than do those of the female. Based on such criteria, we may infer the sex of other referred specimens.

DISCUSSION: Initial reference of *thomsoni* to *Cynodesmus* by Matthew (1907), along with “*C.*” *minor*, significantly expanded the concept of *Cynodesmus* and was followed by a series of other species later referred to this genus by other authors (e.g., Simpson, 1932; Macdonald, 1963). Such an expanded concept of *Cynodesmus* became an important feature of a phylogeny of canids proposed by Matthew (1924, 1930), in which *Cynodesmus* serves as a key link between *Hesperocyon* and *Tomarctus*, the latter being in turn postulated to be ancestral to almost all living canids. As a well-known taxon at the time, “*Cynodesmus*” *thomsoni* played an important role in past studies on canid phylogeny. Our own analysis suggests that *thomsoni* has no relevance in the initiation of the living canine clade, but is related to a long series of borophagines.

Certain individuals of *Desmocyon thomsoni* from the Upper Harrison beds of Nebraska (e.g., UNSM 26550 and 26664) are noticeably smaller than those from equivalent beds in Wyoming. Individuals from the late Arikareean of Wyoming can be up to 15% larger in total skull length than found in the Nebraska samples, and samples from

the Runningwater Formation tend to retain the small size. Such a size difference is generally beyond the sexual dimorphism encountered in living canids. Lacking any morphological characters to separate these samples, however, we must consider the possibility of size reduction within the species. It seems possible that the co-occurrence of *D. thomsoni* with the larger *Metatomarctus canavus* (and sometimes with *Paracynarctus kelloggi*) in some quarries in the Runningwater Formation may have caused size reduction in *D. thomsoni*.

### *Desmocyon matthewi*, new species

Figures 45, 46A–D

HOLOTYPE: F:AM 49177, articulated skull and mandible with all teeth represented (fig. 45), postcranial elements including the first four cervical vertebrae, partial humerus, partial radius and ulna, partial pelvis, and partial femur from Marshall Ranch, Cottonwood Creek, upper part of the Runningwater Formation (early Hemingfordian), Dawes County, Nebraska.

ETYMOLOGY: Named in honor of William Diller Matthew for his pioneering studies on canid phylogeny and his fundamental contributions to paleomammalogy.

REFERRED SPECIMENS: Upper part of the Runningwater Formation (early Hemingfordian), Dawes County, Nebraska: F:AM 49176, left maxillary fragment with isolated C1, P3 broken, isolated P4 broken, right and left partial rami with c1, p1–p2 alveoli, p3–m3 (m2 broken), partial humerus, radius (fig. 46A), partial ulna (fig. 46B), metacarpal I and partial metacarpal III, metatarsal II and incomplete metatarsals I and III, vertebrae, and phalanges, Elder Ranch, Cottonwood Creek; F:AM 49194, right ramus with c1–m2 and m3 alveolus, “B” Quarry; F:AM 61300, partial skull with I2–M2, “B” Quarry; F:AM 61301, left partial maxillary with P3–M1, D. C. Quarry; F:AM 104693, left partial ramus with p1–p3 alveoli, m1 broken–m2 and m3 alveolus, Cottonwood Creek Quarry; F:AM 104695, left partial ramus with p1 alveolus, p2–p3 broken, p4–m2, and m3 alveolus, Cottonwood Creek Quarry; F:AM 104699, right maxillary fragment with C1–P1 alveoli and P2–P3, “B” Quarry; F:

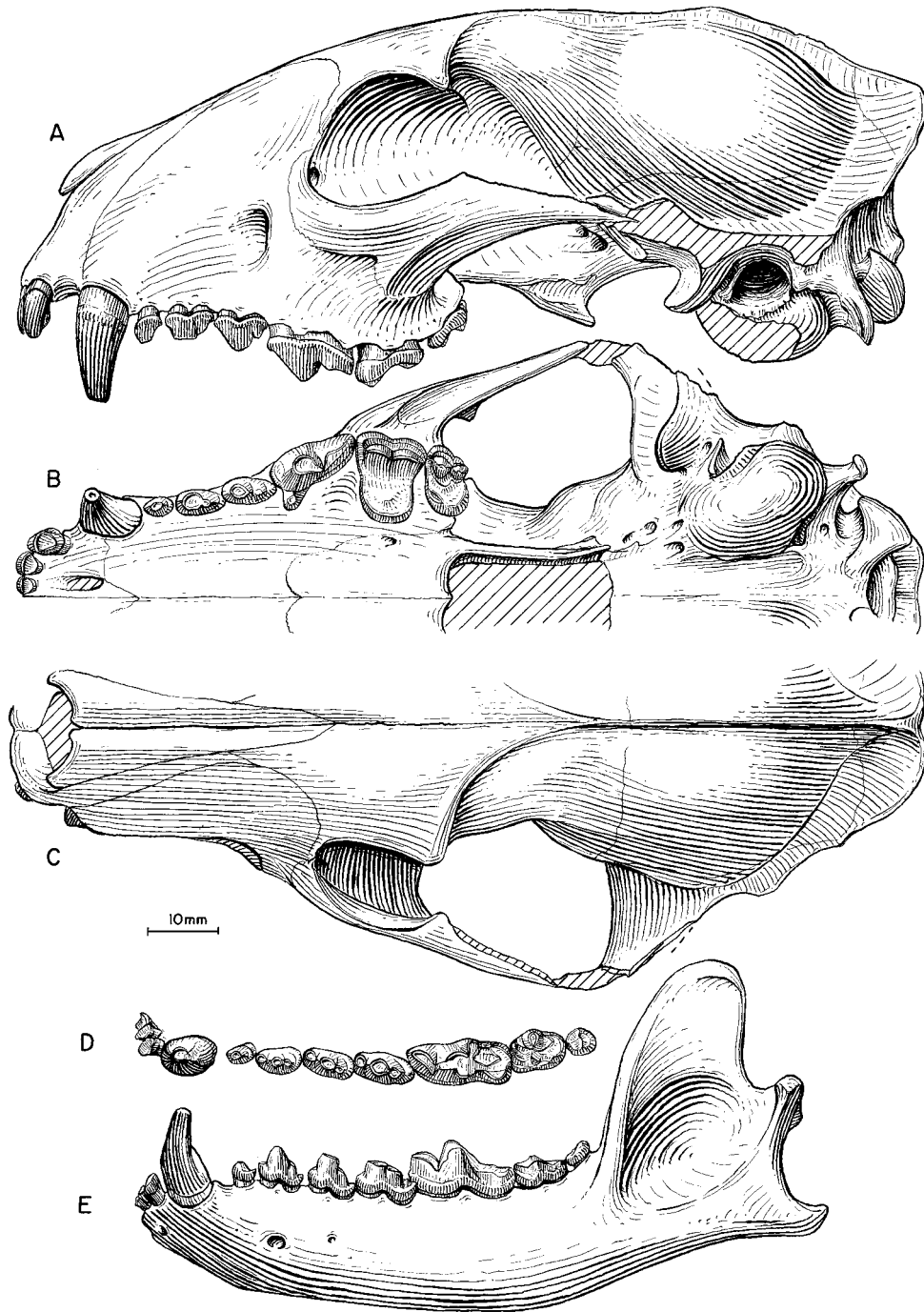


Fig. 45. *Desmocyon matthewi*. A, Lateral, B, ventral, and C, dorsal views of skull, D, lower teeth, and E, ramus, F:AM 49177, holotype, Marshall Ranch, Runningwater Formation (early Hemingfordian), Dawes County, Nebraska.

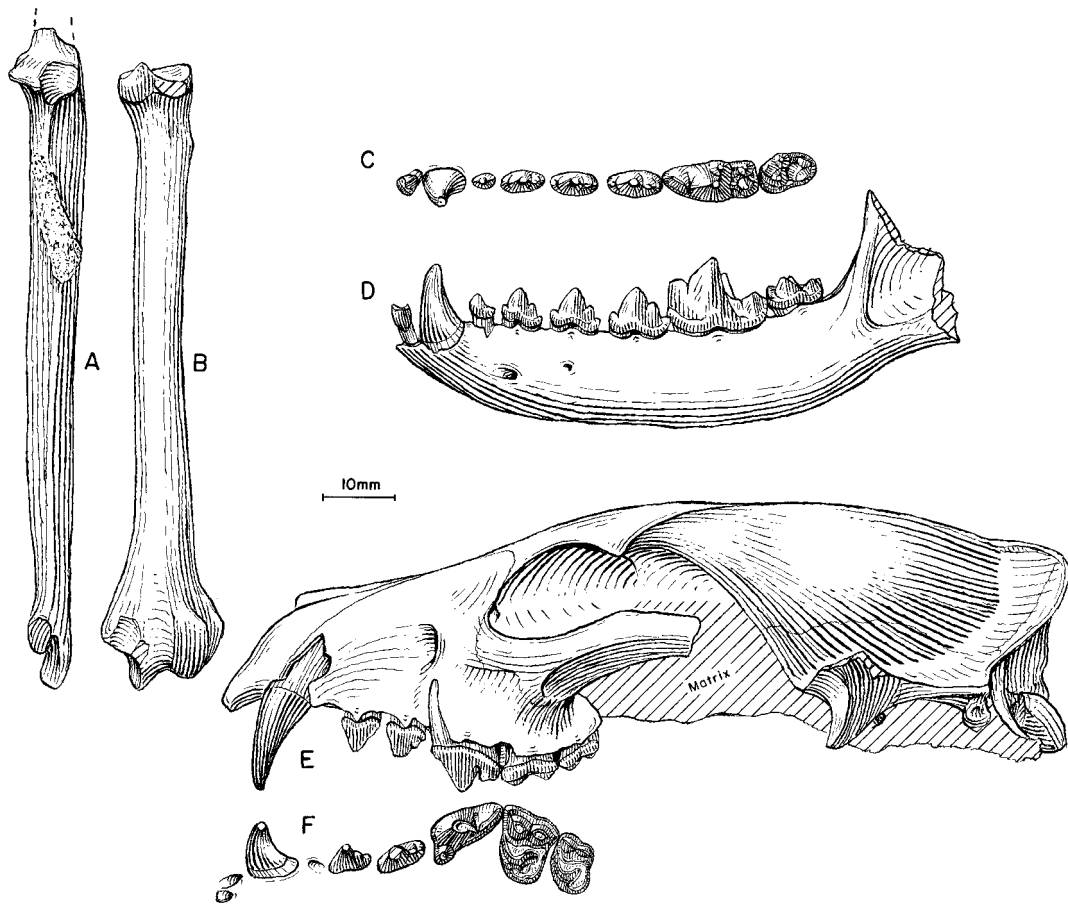


Fig. 46. **A**, Partial ulna and **B**, radius, *Desmocyon matthewi*, F:AM 49176, Elder Ranch, Runningwater Formation (early Hemingfordian), Dawes County, Nebraska. **C**, Lower teeth and **D**, ramus, *D. matthewi*, F:AM 49181, 4 ft above *Aletomeryx* Quarry, Runningwater Formation (early Hemingfordian), Cherry County, Nebraska. **E**, Lateral view of skull and **F**, upper teeth (M2 reversed from right side), *D. thomsoni*, F:AM 62890, East Channel Prospect, Runningwater Formation (early Hemingfordian), Box Butte County, Nebraska.

AM 104701, right ramal fragment with m1 broken, m2, and m3 alveolus, northwest of Marsland; F:AM 105335, left partial maxillary with P4–M1, Cottonwood Creek Quarry; and F:AM 105336, right ramus fragment with m1, Cottonwood Creek Quarry.

Upper part of the Runningwater Formation (early Hemingfordian), Cherry County, Nebraska: F:AM 25439, left partial ramus with i1–i3 alveoli and c1 broken–m2 (m1 broken and m3 alveolus), above *Aletomeryx* Quarry; F:AM 25467, right isolated M1, *Aletomeryx* Quarry, Antelope Creek; F:AM 49181, right and left rami with i3–m2 and m3 alveolus

(fig. 46C, D), 4 ft above *Aletomeryx* Quarry; F:AM 49185, left maxillary fragment with M1, right ramal fragment with m1–m2 and left isolated m2, upper *Aletomeryx* zone, 18 mi east of *Aletomeryx* Quarry; and F:AM 61299, right partial ramus with p1–p3 alveoli, p4–m1 both broken, m2, and m3 alveolus, 10 ft above *Aletomeryx* Quarry zone.

Upper part of Runningwater Formation (early Hemingfordian), Box Butte County, Nebraska: UNSM 25627 (F:AM cast 97146), right partial ramus with p4–m2 and m3 alveolus, Hemingford Quarry (UNSM loc. Bx-7).

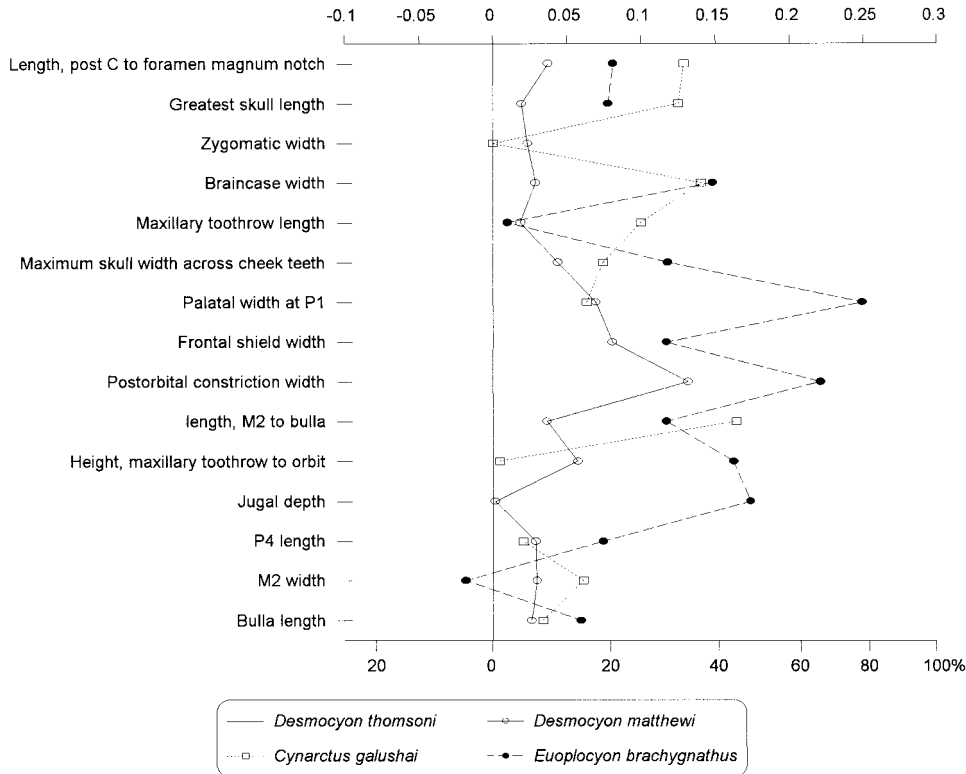


Fig. 47. Log-ratio diagram for cranial measurements of *Desmocyon*, *Cynarctus*, and *Euoplocyon* using *Desmocyon thomsoni* as a standard for comparison (straight line at zero). See text for explanations and appendix II for measurements and their definitions.

Runningwater Formation (early Hemingfordian), 2 mi west of Pole Creek, Cherry County, Nebraska: F:AM 61312, right ramus with c1 and p1 alveolus–m3; and F:AM 62880, isolated left m1.

Miller Locality (early Hemingfordian), Suwannee River, Dixie? County, Florida: KUVF 11453, right ramus with p1–p3 alveoli, p4–m1, and m2–m3 alveoli; KUVF 114454, right ramus with p2, p4, and alveoli of the rest of teeth; KUVF 114455, right ramus with p4–m1 and alveoli of the rest of cheekteeth; KUVF 114456, left ramal fragment with m1–m2; KUVF 114458, left ramus with c1–p2 alveoli and p3–m1; KUVF 114462, right ramal fragment with p1–p3 alveoli and p4; KUVF 114466, right ramus with p4–m1 and alveoli of the rest cheekteeth; KUVF 114467, left ramal fragment with c1–p3 alveoli and p4–m1 broken; KUVF 114472, left ramus with m1–m2, and

p4 and m3 alveoli; and KUVF 116621 (cast), left ramus with c1–p2 alveoli, p3–m2, and m3 alveolus.

DISTRIBUTION: Early Hemingfordian of Nebraska and Florida.

DIAGNOSIS: Synapomorphic features that distinguish *Desmocyon matthewi* and higher taxa from *D. thomsoni* are posterior process of premaxillary meeting nasal process of frontal; frontal sinus enlarged, penetrating postorbital process and extending posteriorly to near frontal-parietal suture; frontal shield wide relative to width of braincase; postorbital width of frontals greater; and m1 talonid usually with transverse cristid between entoconid and hypoconid.

DESCRIPTION AND COMPARISON: Although the tips of the premaxillary and frontal may begin to touch each other in some individuals of *Desmocyon thomsoni* and also in *Phlaocyon leucosteus* (probably due to its brachy-



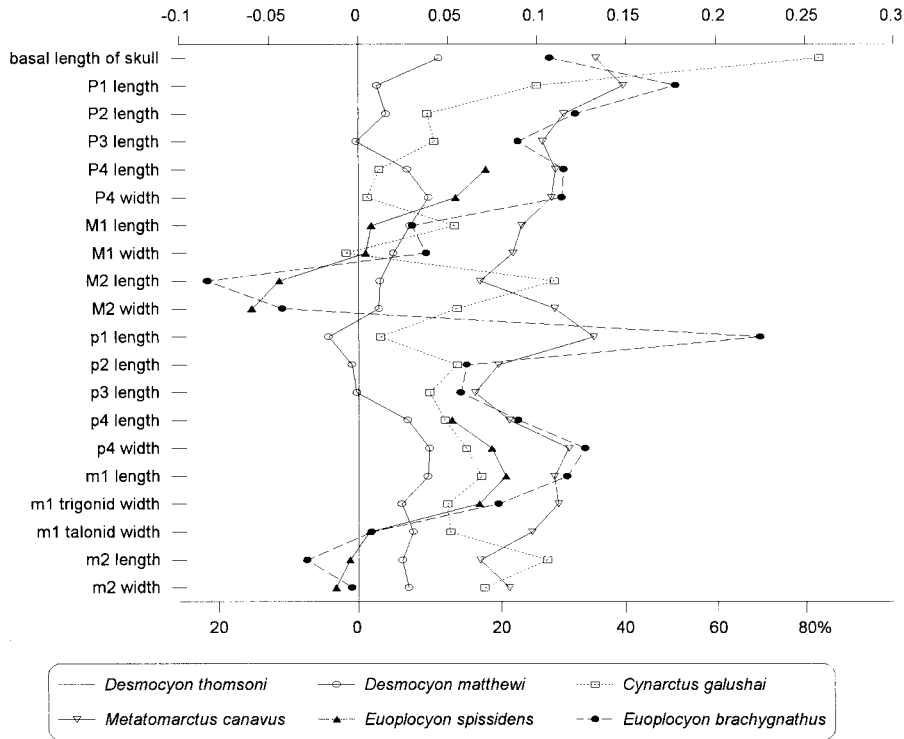


Fig. 48. Log-ratio diagram for dental measurements of *Desmocyon*, *Cynarctus*, *Metatomarctus*, and *Euoplocyon* using *Desmocyon thomsoni* as a standard for comparison (straight line at zero). See text for explanations and appendix III for summary statistics of measurements and their definitions.

cephalic skull), the contact of these two bones are firmly established only in *D. matthewi* and higher taxa—the transverse width of this zone of contact is 2 mm or more. The more extensive frontal sinus in *D. matthewi* can be inferred from its broader and more domed frontal shield in the holotype and can be observed in a dissected specimen, F:AM 61300. The sinus in the latter can be seen to invade the postorbital process extending back toward the frontal-parietal suture. Quantitatively, this sinus expansion is readily demonstrated in the ratio diagram of cranial measurements, which shows a conspicuously broadened postorbital constriction (fig. 47).

Dentally, *Desmocyon matthewi* is little different from *D. thomsoni* both in size and proportions (fig. 48), and as discussed under *D. thomsoni*, differentiation of fragmentary materials between *D. thomsoni* and *D. matthewi* is sometimes difficult. The only derived feature in *D. matthewi* is the usual possession of a transverse crest between the hypoconid

and entoconid in m1. Presence of this transverse crest delineates a small basin on the posterior end of the talonid—a hypoconulid shelf. Heavy wear on some specimens referred to *D. matthewi*, however, prevents direct observation of this feature.

The small sample, mostly fragmentary lower jaws, from the Miller Local Fauna of Florida is closely comparable with those from Nebraska. Nearly all (5 of 6 individuals) have acquired the transverse crest between the hypoconid and entoconid on m1s, a character of the species. The only noticeable variation is in the slightly longer m2s in the Florida sample.

**DISCUSSION:** Specimens of *Desmocyon matthewi* are rather rare and are confined to a few quarries in the upper part of the Runningwater Formation of Nebraska and the correlative Miller Local Fauna of Florida. This phylogenetically transitional species quickly gave rise to the more derived *Cynarctina* and *Metatomarctus*. Both *Metato-*

*marctus* and early members of the Cynarctina co-occur with *Desmocyon matthewi* in the early Hemingfordian of Nebraska.

SUBTRIBE CYNARCTINA MCGREW,  
1937, new rank

TYPE GENUS: *Cynarctus* Matthew, 1902.

INCLUDED GENERA: *Paracynarctus*, new genus; and *Cynarctus* Matthew, 1902.

DISTRIBUTION: Early Hemingfordian through early Clarendonian of North America.

EMENDED DIAGNOSIS: The Cynarctina shares with *Metatomarctus* a single derived character of a lateral accessory cusp on the I3 that distinguishes it from the more primitive *Desmocyon*. The cynarctine clade is distinguished from *Metatomarctus* and *Euoplocyon* in its hypocarnivorous characteristics: a small subangular lobe on mandible, high mandibular condyle, short P4 relative to upper molars, enlarged M2, m1 protostylid, elongated m2 with strong anterolabial cingulum, and m3 elongate with basined trigonid. In addition, the Cynarctina primitively lacks a distinct parastyle crest on the P4, as is present in *Metatomarctus* and more derived taxa.

*Paracynarctus*, new genus

TYPE SPECIES: *Paracynarctus sinclairi*, new species.

ETYMOLOGY: Greek: *para*, near; *Cynarctus*, indicating relationship to the genus *Cynarctus*.

INCLUDED SPECIES: *Paracynarctus kelloggi* (Merriam, 1911) and *Paracynarctus sinclairi*, new species.

DISTRIBUTION: Early Hemingfordian of Nebraska and Delaware; medial to late Hemingfordian of New Mexico; late Hemingfordian of Wyoming and Nevada; late Hemingfordian or early Barstovian of Colorado; Hemingfordian of California; early Barstovian of Nebraska, Nevada, California, and New Mexico; and late Barstovian of Nevada.

DIAGNOSIS: In addition to the derived characters shared by *Paracynarctus* and *Cynarctus* (see diagnosis of subtribe Cynarctina), three derived characters are possessed by all species of *Paracynarctus*: diastemata between premolars, P4 with strong lingual cingulum or hypocone, and cleft on lingual cingulum of M1 and M2 separating near cusplike devel-

opment of anterolingual cingulum from hypocone. In addition, most *Paracynarctus* lacks a transverse cristid on m1 talonid (a reversal). *Paracynarctus* is distinguishable from *Cynarctus* in its lack of synapomorphies of the latter clade: narrowed auditory opening, recurved c1, and elongated M1.

DISCUSSION: The presence of a small hypocone on the P4 and quadrate upper molars in *Paracynarctus* (especially in *P. sinclairi*), in contrast to the lack of these features in *Cynarctus*, suggests that *Paracynarctus* arrived at a moderate level of hypocarnivory in a way that differs from *Cynarctus*. Furthermore, *Paracynarctus* entirely lacks the numerous synapomorphies in the *Cynarctus* clade that are related to further reduction of premolars, enlargement of complex lower molars, narrowed auditory meatus, and other features. Despite such divergent approaches to hypocarnivory, there are several shared derived characters between *Paracynarctus* and *Cynarctus* that suggest a sister relationship (diagnosis of Cynarctina).

*Paracynarctus kelloggi* (Merriam, 1911)

Figures 49, 50, 51A–H

*Tephrocyon kelloggi* Merriam, 1911 (in part): 235, pl. 32, figs. 1, 2, 6, and 7; 1913: 367, fig. 9a, b. Green, 1948: 81.

*Tephrocyon* near *kelloggi* (Merriam): Merriam, 1911: 237, fig. 7; 1913: 368, fig. 13; 1916: 174, fig. 2a, b.

*Tomarctus kelloggi* (Merriam): Bode, 1935: 87. Munthe, 1988: 91, figs. 21, 22 (in part).

*Cynodesmus kelloggi* (Merriam): Stirton, 1939a: 628–629. Downs, 1956: 236.

*Cynodesmus casei* Wilson, 1939: 315, figs. 1, 2.

*Tomarctus casei* (Wilson): White, 1941b: 95.

*Tomarctus* ? *kelloggi* (Merriam): Henshaw, 1942: 108, figs. 1, 1a, 2, 2a. Munthe, 1998: 135.

*Tomarctus* cf. *T. thomsoni* (Matthew, 1907): Emry and Eshelman, 1998: 160, fig. 2M, L.

HOLOTYPE: UCMP 11562 (AMNH cast 27873), right and left partial rami with c1 broken—m2 (p3–p4 broken and m3 alveolus) (fig. 49G, H), from UCMP loc. 1065, Virgin Valley, Virgin Valley Formation (early Barstovian), Humboldt County, Nevada.

REFERRED SPECIMENS: From the type area, Virgin Valley, Virgin Valley Formation (early Barstovian), Humboldt County, Nevada: UCMP 11474 (Merriam, 1911: fig. 6), right

ramus with c1–m1 all broken and m2, UCMP loc. 1065; and UCMP 15546 (IT 114), right maxillary fragment with P4–M1.

From Split Rock Formation (late Hemingfordian), Fremont County, Wyoming (listed by Munthe, 1988, in part): ACM 11391 (AMNH cast 89734) (Munthe, 1988: figs. 21, 22), partial skull with P4–M2 (fig. 49A, B), basicranium, occiput, right and left rami with c1–m3 (fig. 49C, D), scapholunar, trapezium, trapezoid and metacarpal I, from UCMP loc. V69191, 15 ft above *Brachycrus* Quarry of Falkenbach (1936–1938); CMNH 14708, m3, from UCMP loc. V69190; KUVF 20356, m2, from V69190–69192; MCZ 7321, P4, and two p4s, from V69190–V69192; UCMP 121912 and F:AM 95409 (one individual), P4 fragment, lingual halves of both M1s, both M2s, c1, both p2s, p4, fragments of both m1s, and m2 from UCMP loc. V77149; UCMP 121913, ramal fragment with m1–m2, from V77149; UCMP 121914, ramal fragment with m1, from V77149; UCMP 121915, ramal fragment with p1–p2 from V69190; UCMP 121916 and 121917, M2s, from V69192; UCMP 121918, p4, from V69192; and KUVF 20355, M1, from V69190–69192.

Upper part of the Runningwater Formation (early Hemingfordian), Dawes County, Nebraska: F:AM 99351, left partial ramus with p2–p3, p4 alveolus, and m1 broken, Warren Barnum Ranch.

Canyada Pilares, northern Ceja del Rio Puerco area, local green zone, in Canyada Pilares Member, Zia Formation (early Hemingfordian), New Mexico: F:AM 27352, left premaxillary-maxillary with I1–I2, I3 broken, and C1–M2 (fig. 49E, F).

Pollack Farm Site (Delaware Geological Survey locality Id11-a), lower shell bed of Cheswold sands, lower Calvert Formation (late early Hemingfordian), near Cheswold, Delaware: USNM 475812, isolated right P4 (referred to *Tomarctus* cf. *T. thomsoni* by Emry and Eshelman, 1998: fig. 2M, L).

Kiva Quarry near the divide between Canyada de Zia and Canyada Piedra Parada, Zia Formation (late Hemingfordian), Jemez Creek Area, Sandoval County, New Mexico: F:AM 50142, left ramus with i1–i3 broken and c1–m3 (p1 broken); and F:AM 50144, right ramus with c1–m3 (fig. 49I, J).

Massacre Lake Local Fauna (late Hemingfordian), Washoe County, Nevada: UCMP loc. V6161: UCMP 75844, left maxillary with P1–P3 alveoli and P4–M1. Big Basin: USGS M1094, left maxillary fragment with M1–M2.

White Operation Wash, “Double Purple” layer of the Nambe Member, Tesuque Formation (late Hemingfordian), Santa Fe County, New Mexico: F:AM 50140, right partial ramus with p4 broken, m1, m2 alveolus, and m3 unerupted.

Spruce Gulch, 5 mi south of State Bridge, in a volcanic tuff in North Park Formation, late Hemingfordian or early Barstovian (presence of *Brachycrus* and *Mylagaulus* in this locality [Robinson, 1968] suggests a late Hemingfordian or early Barstovian age instead of the late Arikarean estimated by Wilson, 1939), Eagle County, Colorado: UM 18955 (holotype of *Cynodesmus casei* Wilson, 1939), premaxillary-maxillary with C1–P1 broken and P2–M2.

Santa Fe Area, Skull Ridge Member and correlatives, Tesuque Formation (early Barstovian), Santa Fe County, New Mexico: F:AM 27394, right partial ramus with c1–p3 alveoli, p4–m1, and m2 broken; F:AM 27396, anterior part of skull with I1–C1 all broken, P1–P3, and P4–M2 all broken, 3 mi from Cuyamunque; F:AM 27399, left partial ramus with c1 and p2–m2, Tesuque; F:AM 27487, palate with I1–C1 all broken and P1–M2, and mandible with i1–i3 all broken and c1–m3, west of Tesuque (fig. 51A–D); F:AM 27488, left partial ramus with p2–p3 alveoli, p4, and m1 broken–m2, Cuyamunque; F:AM 50135, right premaxillary-maxillary with I2–P4 broken and M1–M2, lower part of light band, east of Tesuque Fault; F:AM 50136, right partial ramus with p4 root and m1–m3 all broken, west of Tesuque, Tesuque Boundary wash, light band east of Tesuque Fault; F:AM 50137, anterior part of skull with I1–M1 and M2 broken (fig. 51E, F), 1 mi east of Cuyamunque; F:AM 50187, right partial ramus with c1 alveolus and p1–m3 all broken, partial left ulna, Tesuque; and F:AM 105097, right partial ramus with p3–m2 (broken) and alveoli of i1–p2, 5 ft below Ash A in block no. 3 south of Arroyo Seco, Skull Ridge.

Phillips Ranch, UCMP loc. 2577, Bopesta

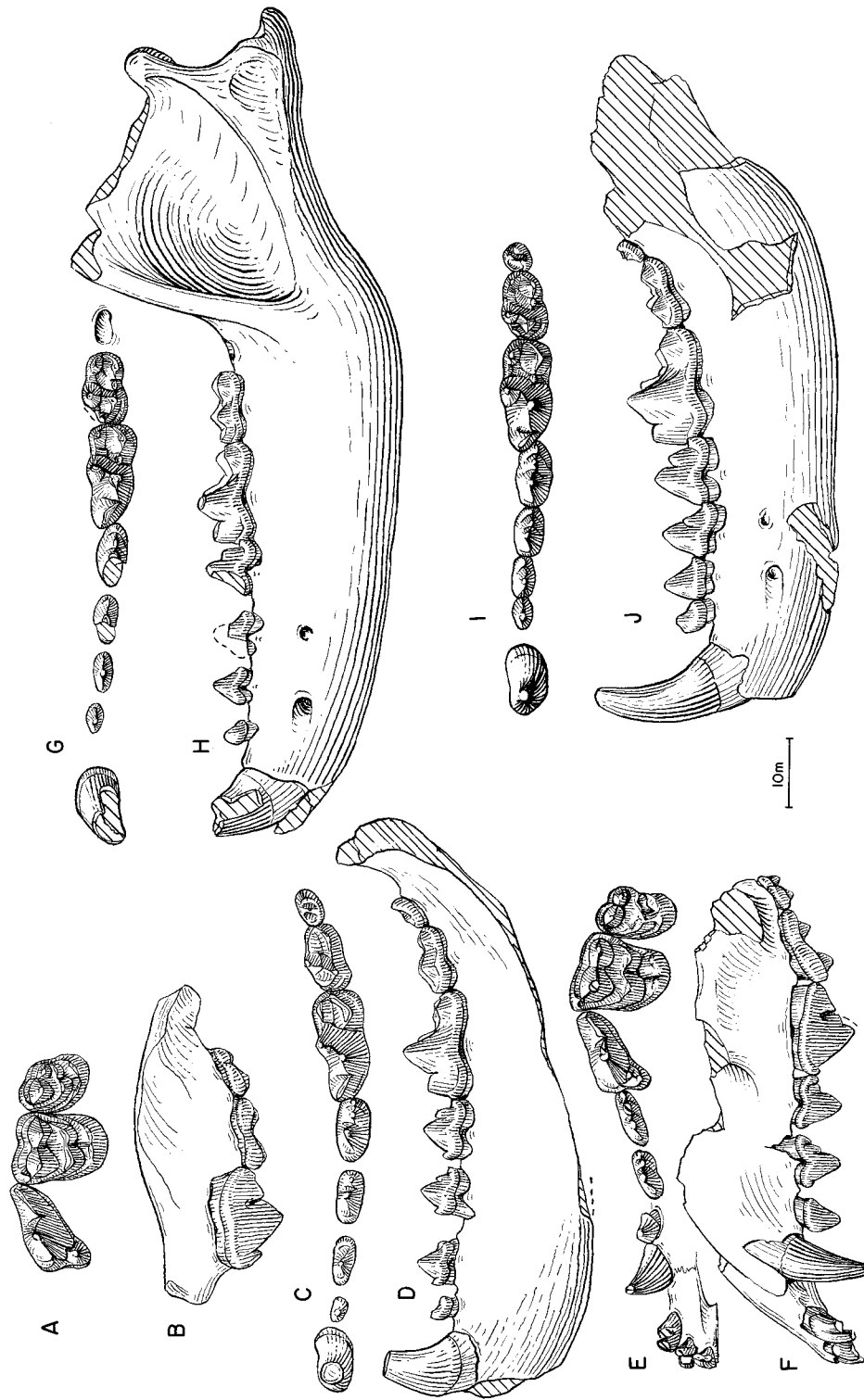


Fig. 49. *Paracynarctus kelloggi*. A, Upper teeth, B, lateral view of maxillary, C, lower teeth, and D, ramus, ACM 11391 (all reversed from right side), 15 ft above *Brachycrus* Quarry, Split Rock Formation (late Hemingfordian), Fremont County, Wyoming. E, Upper teeth and F, lateral view of partial skull, F:AM 27352, Canyonada Pilares Member, Zia Formation (medial Hemingfordian), New Mexico. G, Lower teeth and H, ramus, UCMP 11562, holotype, Virgin Valley, Virgin Valley Formation (early Barstovian), Humboldt County, Nevada. I, Lower teeth and J, ramus, F:AM 50144 (all reversed from right side), Kiva Quarry, Zia Formation (late Hemingfordian), Sandoval County, New Mexico.

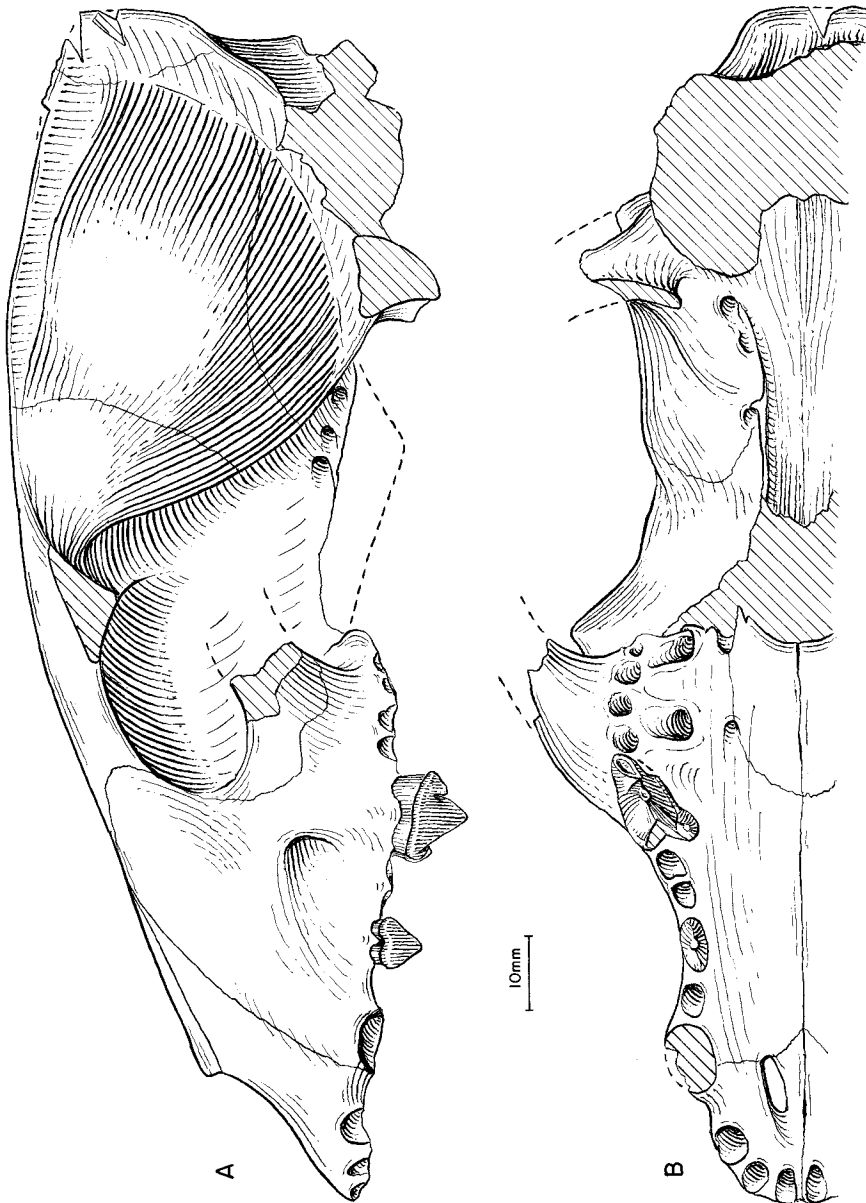


Fig. 50. *Paracynarctus kelloggi*. **A**, Lateral and **B**, ventral views of skull (crushing of skull partially restored), F:AM 61001, Steepside Quarry, Barstow Formation (early Barstovian), San Bernardino County, California.

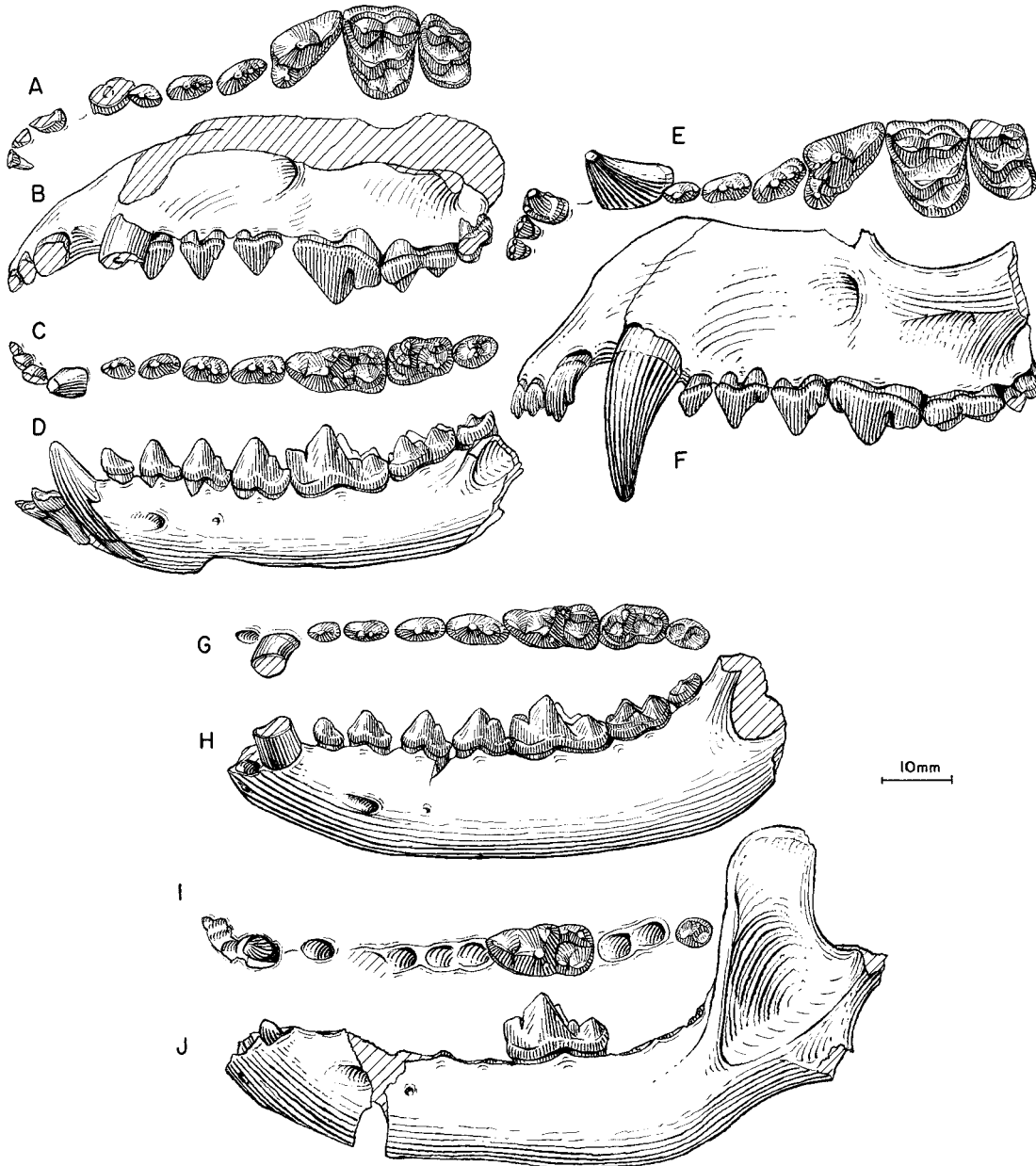


Fig. 51. **A**, Upper teeth (M2 reversed from right side), **B**, lateral view of partial skull, **C**, lower teeth, and **D**, ramus (reversed from right side), *Paracynarctus kelloggi*, F:AM 27487, Santa Fe area, Skull Ridge Member, Tesuque Formation (early Barstovian), Santa Fe County, New Mexico. **E**, Upper teeth (reversed from right side) and **F**, lateral view of partial skull, *P. kelloggi*, F:AM 50137, 1 mi east of Cuyamunque, Skull Ridge Member, Tesuque Formation. **G**, Lower teeth and **H**, ramus, *P. kelloggi*, F:AM 61000 (all reversed from right side), Steepside Quarry, Barstow Formation (early Barstovian), San Bernardino County, California. **I**, Lower teeth and **J**, ramus, *Paracynarctus sinclairi*, F:AM 61007, Humbug Quarry, Olcott Formation (early Barstovian), Dawes County, Nebraska.

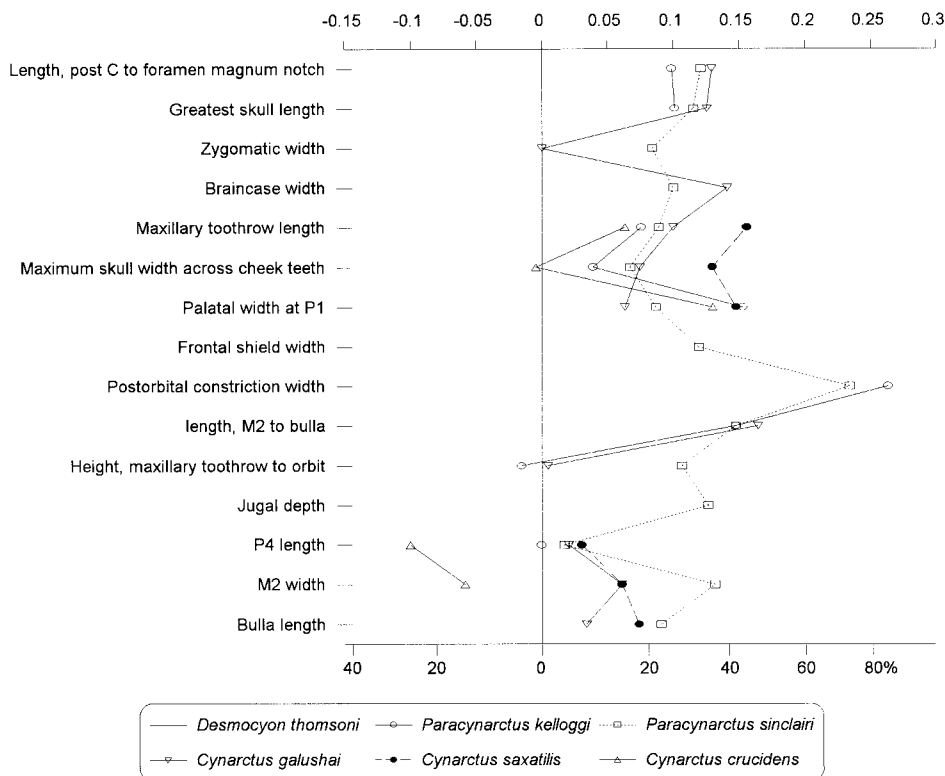


Fig. 52. Log-ratio diagram for cranial measurements of *Paracynarctus* and *Cynarctus* using *Desmocyon thomsoni* as a standard for comparison (straight line at zero). See text for explanations and appendix II for measurements and their definitions.

Formation (late Hemingfordian), Kern County, California: UCMP 45119, left ramal fragment with p4–m1.

Steepside Quarry, Barstow area, Barstow Formation (early Barstovian), San Bernardino County, California: F:AM 61000, left and right partial rami with i3–m3 (fig. 51G, H); F:AM 61001, crushed skull with P2, P4, and alveoli of the rest of teeth (fig. 50); F:AM 61002, right partial ramus with c1, p2–p3 broken, p4–m2, and m3 alveolus; F:AM 61003, left partial ramus with c1–p1 alveoli and p2–m3 (m1–m2 broken); F:AM 61004, right partial ramus with i2 root–c1, p1–p4 broken, m1, and m2 broken; and F:AM 61005, left partial ramus with c1 and p1 root–m3 (m1 broken).

Siebert Formation, Tonopah Local Fauna (LACM loc. 172) (late early Barstovian), San Antonio Mountains, near Tonopah, Nye County, Nevada: LACM-CIT 789 (Henshaw,

1942: pl. 3, figs. 2, 2a), left ramal fragment with m1–m2; LACM-CIT 1235 (Henshaw, 1942: pl. 3, figs. 1, 1a), left partial ramus with p1–m1 and m2 alveolus; UCMP 15972, right and left ramal fragments with m1 and m2; and UCMP 15975, left maxillary fragment with P4–M1 and M2 broken and an isolated M1.

Home Station Pass, unnamed formation (late Barstovian), Pershing County, Nevada: F:AM 49299, right isolated M2; and F:AM 49299A, left isolated M2.

DISTRIBUTION: Early Hemingfordian of Nebraska and Delaware; early to late Hemingfordian of New Mexico; late Hemingfordian of Wyoming, Nevada, and California; late Hemingfordian or early Barstovian of Colorado; early Barstovian of Nevada, California, and New Mexico; and late Barstovian of Nevada.

EMENDED DIAGNOSIS: Synapomorphies

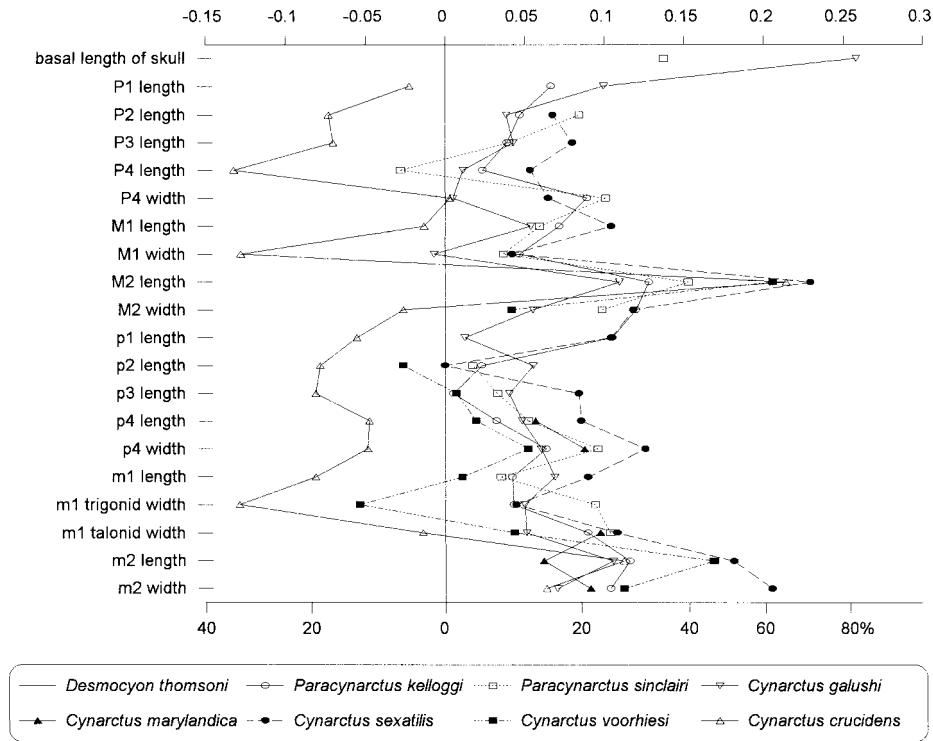


Fig. 53. Log-ratio diagram for dental measurements of *Paracynarctus* and *Cynarctus* using *Desmocyon thomsoni* as a standard for comparison (straight line at zero). See text for explanations and appendix III for summary statistics of measurements and their definitions.

uniting *P. kelloggi* and *P. sinclairi* are a small diastemata between premolars, P4 with strong lingual cingulum or hypocone, and enlarged M1 lingual cingulum which has a transverse cleft. Characters of *P. kelloggi* that are primitive with respect to *P. sinclairi* are horizontal ramus not narrowed, P4 lacking a conical hypocone, and smaller and less quadrate M1 and M2.

**DESCRIPTION AND COMPARISON:** Despite the numerous referred specimens above, our knowledge of the cranial morphology of this species is still incomplete. The best cranial material available is a crushed skull from the Barstow Formation of California (F:AM 61001). Supplemented by other cranial fragments (e.g., F:AM 50137 and descriptions of ACM 11391 in Munthe, 1988), we may observe the following cranial and dental features. The premaxillary is in full contact with the nasal process of frontal. The frontal sinus reaches the frontal-parietal suture. The nuchal crest is broadly fan-shaped in posterior

view, and the lambdoidal crest above the mastoid area is not reduced as in *Microtomarctus* and *Tomarctus*. The opening for the external auditory meatus is large, in contrast to markedly reduced opening in *Cynarctus*.

Upper incisors of *P. kelloggi* are complex. The I3 has small lateral and lingual accessory cusps in addition to the two cusps on the tip. In some individuals, the P1–P3 are slightly reduced in size and are simple in morphology as compared to those in *Desmocyon matthewi* and *Metatomarctus*. The P4 is short and wide (except F:AM 27352), and has a strong lingual cingulum. Such cingulum is particularly well-developed in all Barstovian specimens. All M1s consistently have an elongated lingual cingulum, which is divided by a transverse cleft to delineate a conical hypocone (at this stage, it is still a slight enlargement on the posterolingual corner of the cingulum). The M2 is slightly enlarged relative to the M1 (fig. 53).

The lower canine lacks the sharply re-



curved condition in *Cynarctus*. Lower premolars are small, and some are separated by short diastemata, although individuals from California and New Mexico tend to have more closely spaced premolars, as seen in *Desmocyon matthewi* and more basal taxa. The talonid of m1 is relatively wide. A transverse crest between the entoconid and hypoconid is either lacking or only vaguely developed, and as a result, the talonid basin is wider and deeper than those in *Cynarctus*. The m2 is markedly elongated, often with a well-developed anterolabial cingulum. The m3 is also long.

**DISCUSSION:** Previous studies of *Paracynarctus kelloggi* placed it in *Tomarctus*, *Tephrocyon*, or *Cynodesmus* (see synonym list above). As summarized by Munthe (1988: 96–98), the low-crowned premolars in *P. kelloggi* seemed at odds with other species of *Tomarctus* in the traditional sense (*Desmocyon* through *Tomarctus* in this study), which tend to have strong, high-crowned, multicuspid premolars. In the broader view afforded by this study, *P. kelloggi* has a combination of meso- and hypocarnivorous characters (including the low-crowned premolars) to be a cynarctine, and, more specifically, its development of a strong P4 lingual cingulum and a cleft on the M1 lingual cingulum further ally itself to *P. sinclairi*.

The early Hemingfordian presence of *P. kelloggi* is indicated by a jaw fragment from the upper part of the Runningwater Formation of Nebraska (F:AM 99351). This individual agrees in some aspects of the dental morphology of *P. kelloggi* (reduction of premolars, widening of the m1 talonid, presence of a protostylid on m1, and a deep talonid basin). Pending additional materials from this locality, it may be viewed as an early representative of this species.

Wilson's (1939) *Cynodesmus casei* from Spruce Gulch, Colorado, is here synonymized with *Cynarctus galushai*. Based on his descriptions and illustrations (Wilson, 1939: 315–317, figs. 1, 2), the holotype of *casei* possesses all the diagnostic characters of *Paracynarctus kelloggi*, although it is slightly smaller in dental dimensions.

Emry and Eshelman (1998: 160, fig. 2M, L) recently referred a single P4 from the Pollock Farm Site, Delaware, to *Tomarctus cf.*

*T. thomsoni*. Their published figure shows that this upper carnassial has a strong cingulum on both anterior and lingual sides, and a narrower cingulum on the labial side. Furthermore, the P4 has a large protocone and a small parastyle. All of these features suggest a cynarctine affinity, although the limited material available prevents from a secure identification. If our reference of the Delaware specimen to *Paracynarctus kelloggi* is correct, it is only the second record of cynarctine in the east coast of United States (the other is *Cynarctus marylandica*; see below).

### *Paracynarctus sinclairi*, new species

Figures 51I, J, 54

**HOLOTYPE:** F:AM 61009, skull with I1–I3 alveoli and C1–M2 (P1 alveolus) (fig. 54), from Quarry 2, Olcott Formation (early Barstovian), Sioux County, Nebraska.

**ETYMOLOGY:** Named for the eminent vertebrate paleontologist W. J. Sinclair of Princeton University who directed collecting in the Sioux County area early in the twentieth century.

**REFERRED SPECIMENS:** Olcott Formation (early Barstovian), Dawes County, Nebraska: F:AM 49135, right partial maxillary with P4–M2, New Surface Quarry; F:AM 61007, left partial ramus with c1 erupting, m1, m3 unerupted, and alveoli of i1–i3, p1–p4, and m2 (fig. 51I, J), Humbug Quarry; F:AM 61008, left partial ramus with p2 and p4 and alveoli for p1, p3, and m1–m3, Quarry 2; F:AM 61008A, left ramus with i1–p1 alveoli, p2, p3–p4 alveoli, m1 broken, and m2–m3 alveoli, Boulder Quarry; and F:AM 61040, partial right ramus with c1–p1 alveoli and p2–m3 (m2 broken), West Sinclair Draw.

Observation Quarry, Sand Canyon Formation (early Barstovian), Dawes County, Nebraska: F:AM 54480, right isolated M2; F:AM 61006, right isolated P4; and F:AM 105095, left broken isolated M1.

**DISTRIBUTION:** Early Barstovian of Nebraska.

**DIAGNOSIS:** Derived characters that distinguish *P. sinclairi* from *P. kelloggi* are the presence of a P4 hypocone and larger and subquadrate M1–M2.

**DESCRIPTION AND COMPARISON:** The excel-

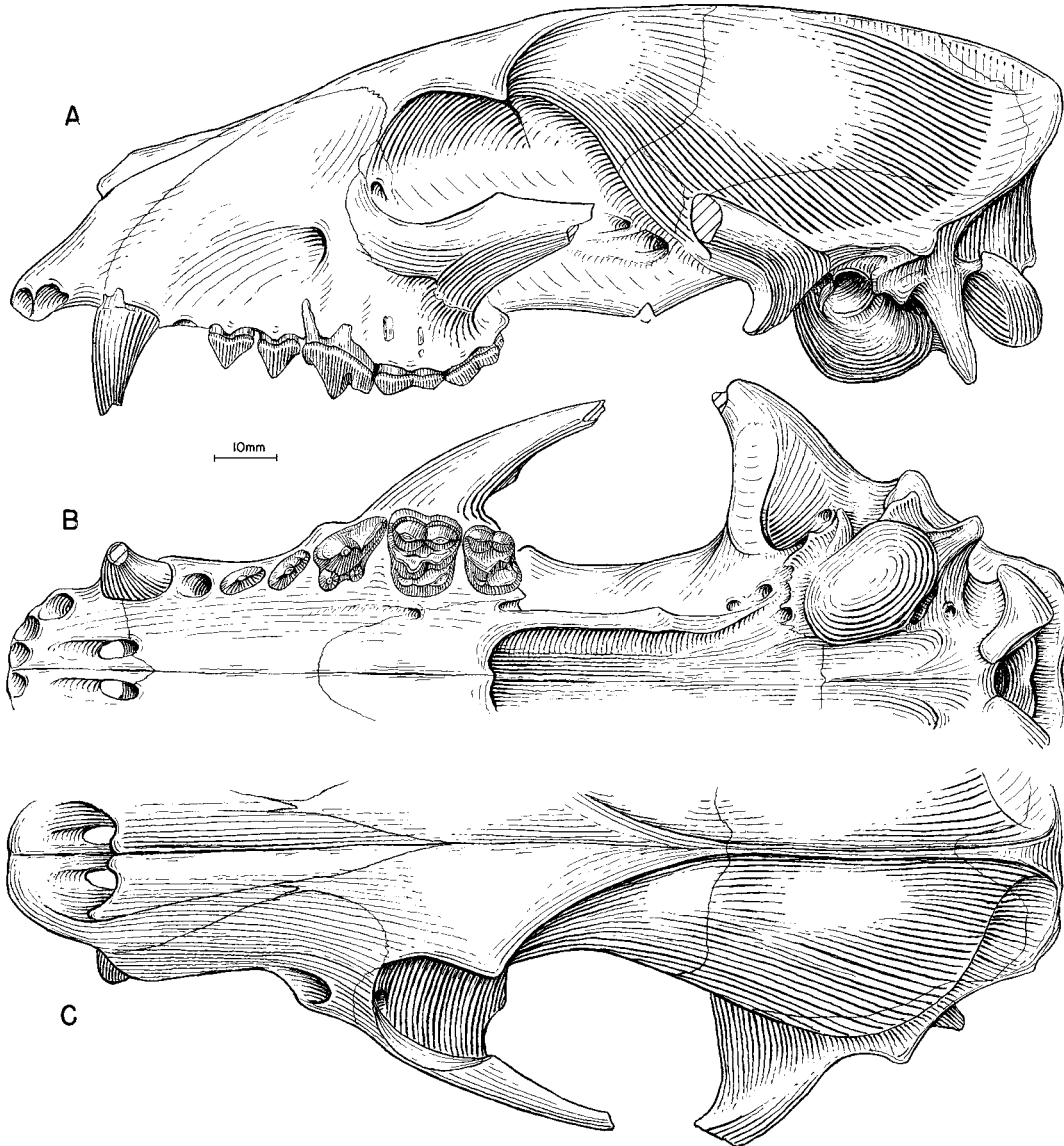


Fig. 54. *Paracynarctus sinclairi*. A, Lateral, B, ventral, and C, dorsal views of skull, F:AM 61009, holotype, Quarry 2, Olcott Formation (early Barstovian), Sioux County, Nebraska.

lently preserved skull of the holotype affords a suitable basis of comparison of the cranial morphology of this species. The premaxillary process is in full contact with the nasal process of the frontal, and the contact region is 2.5 mm in the narrowest section. The frontal sinus is well developed and extends to the frontal-parietal suture. The nuchal crest is not expanded posteriorly as it is in *Microto-*

*marctus* and *Tomarctus*, and its outline forms a broad fan as in *Cynarctus*, *Psalidocyon*, and more primitive forms. The bulla is moderately inflated but not as bulbous as in *Cynarctus*. The opening for the external auditory meatus is relatively large and still has a V-shape notch toward the postglenoid process, in contrast to narrowed, rounded external openings in *Cynarctus*.

The upper premolars are slightly reduced, both in size and accessory cusplets, relative to those in *Metatomarctus*. The P4 is short relative to the M1, and has a distinct hypocone (F:AM 61009) or a prominent enlargement of the anterior segment of the lingual cingulum just behind the protocone (F:AM 49135, 61006). The M1 in the holotype is nearly quadrate because of the widening of the lingual cingulum, especially toward the anterolingual corner. This expansion of the lingual border, however, is not as prominent in F:AM 49135 and 105095. F:AM 49135 and 61006 are also significantly smaller in size than the holotype (averaging 21% smaller in all dental measurements), and may represent a distinct species when more complete materials are known. The M2 is large, as in *P. kelloggi*.

No associated lower jaw exists for *P. sinclairi*, and the present reference to this species of four partial rami is necessarily provisional. A weak subangular lobe is present in F:AM 61008A but is less developed in F:AM 61007 because of the younger age of the latter. The m1 in F:AM 61007 is somewhat peculiar in its prominent development of a conical cristid obliqua anterior to the hypoconid behind the protoconid. This cusp is not present in F:AM 61008A or is weakly developed in most other *Cynarctina*. There is a protostylid in F:AM 61007, but it is so weak that no more than a slight impression is visible. The m1 in F:AM 61007 is also highly crenulated. As in *P. kelloggi*, the m2 is enlarged.

DISCUSSION: The moderately hypocarnivorous dentition in *P. sinclairi* has a distinctly different configuration from those of *Cynarctus*. In *P. sinclairi* the form of the P4 hypocone and the quadrate M1 with its strong lingual cingulum, but not a distinct, conical hypocone, is opposite to the case in *Cynarctus*. Both forms of hypocarnivory in *Paracynarctus* and *Cynarctus* are evidently derived features with respect to primitive conditions in *Metatomarctus* and *Desmocyon matthewi*, and that in *P. kelloggi* and *P. sinclairi* thus helps to define a clade distinct from *Cynarctus*.

*Cynarctus* Matthew, 1902

TYPE SPECIES: *Cynarctus saxatilis* Matthew, 1902.

INCLUDED SPECIES: *Cynarctus galushai*, new species; ?*Cynarctus marylandica* (Berry, 1938); *Cynarctus saxatilis* Matthew, 1902; *Cynarctus voorhiesi*, new species; and *Cynarctus crucidens* Barbour and Cook, 1914.

DISTRIBUTION: Early Barstovian of Maryland and California; late Barstovian of Nebraska, Colorado, and California; early Clarendonian of Nebraska, South Dakota, and Texas; late Clarendonian of Nebraska; and Clarendonian of Texas.

EMENDED DIAGNOSIS: Derived characters that distinguish *Cynarctus* from *Paracynarctus* are an auditory meatus of small diameter with a small lip, M1 transversely narrow and subquadrate, c1 strongly recurved, and p4 posterolingual shelf with weak "metastylid" sometimes present. In addition, *Cynarctus* and *Paracynarctus* share several derived dental features distinguishable from those of *Metatomarctus* and more primitive taxa: a weak subangular lobe, a high mandibular condyle, short P4 relative to M1, enlarged M2, presence of a m1 protostylid, widened m1 talonid, and elongated m2 and m3.

DISCUSSION: Of the several independent attempts by the borophagines to develop hypocarnivorous dentitions, *Cynarctus* has gone the farthest. As the name implies, *Cynarctus* is rather ursidlike in many features, such as in the reduction of its premolars, posterior expansion of M2, shortening of m1 trigonid, and enlargement of the m1 talonid. Matthew (1902) initially thought *Cynarctus* was an amphicyonid, and did not mention this genus in his subsequent treatment of the canid phylogeny (Matthew, 1924, 1930). McGrew (1937, 1938a), on the other hand, was impressed by its hypocarnivorous dentition and placed *Cynarctus*, along with *Cynarctoides* and *Phlaocyon*, in the Procyonidae.

Basiscranial morphology of *Cynarctus*, available for *C. galushai* and *C. crucidens* from the F:AM collection, shows a typical canid middle ear (i.e., inflated entotympanic bulla, presence of an alisphenoid canal, absence of a deep suprameatal fossa). Coupled with typical borophagine cranial and dental features, more clearly seen in *C. galushai*, these morphologies firmly place *Cynarctus* within the borophagine clade.

*Cynarctus galushai*, new species

Figure 55

HOLOTYPE: F:AM 27543, crushed skull with I1–I3 alveoli, C1, and P1 alveolus–M2 and right and left partial rami with i1–m2 (fig. 55A, B), Valley View Quarry, “Second Division,” Barstow Formation (late early Barstovian), San Bernardino County, California.

ETYMOLOGY: Named in honor of Ted Galusha, Frick Curator Emeritus, American Museum of Natural History, who collected many of the specimens cited in this paper.

REFERRED SPECIMENS: “Second Division,” Barstow Formation (late early Barstovian), San Bernardino County, California: F:AM 27542, left ramus with i3 root–m3 (p1 alveolus and p3 broken) (fig. 55E, F), Valley View Quarry.

“First Division,” Barstow Formation (early late Barstovian), San Bernardino County, California: F:AM 27268, right and left partial rami with i1–p1 alveoli, p2–m2, and m3 alveolus, no data but preservation suggests *Hemicyon* Quarry; F:AM 27283, left partial maxillary with P4 broken–M1 and M2 alveolus, no locality data; F:AM 27312, right partial ramus with p4–m2 and alveolus of p3; F:AM 27545, left partial ramus with c1, p1 and p3 alveoli, p2 broken, and p4–m2, Skyline Quarry; F:AM 27546, left partial ramus with p2–p4, m1 broken, m2 root, and m3 alveolus, Skyline Quarry; F:AM 27547A, right partial ramus with c1 broken, p2, m1, and alveoli of p1, p3, p4, and m2, Skyline Quarry; F:AM 27547B, right partial ramus with p4–m1 and roots of p1–p3 and m2, Skyline Quarry; F:AM 27550, palate with I1–C1 alveoli, P1–M2, and isolated left I3 (fig. 55C, D), Skyline Quarry; F:AM 61011, left partial ramus with c1–p2 alveoli, p3–m1 broken, and m2, Skyline Quarry; F:AM 61015, partial mandible with c1 and p1 alveolus–m3 (p3 broken), Skyline Quarry; F:AM 67130, left ramal fragment with p4–m1, Skyline Quarry; and F:AM 67367, left partial ramus with c1 broken, p3–m1, associated isolated m2 (p2, m2, and m3 alveoli), Sunnyside Quarry.

DISTRIBUTION: Early to late Barstovian of California.

DIAGNOSIS: *Cynarctus galushai*, the basal-

most species of the genus, shares with *C. saxatilis* through *C. crucidens* derived characters for the genus: small external auditory meatus, M1 transversely narrow, received c1, and presence of a weak cusp on p4 posterolingual shelf. *C. galushai* can be further distinguished from *Paracynarctus* in its primitive state of the following characters: absence of a widened P4 lingual cingulum and lack of anteriorly expanded M1 lingual cingulum. No autapomorphic characters are recognized for *C. galushai*. Characters of *C. galushai* that are primitive with respect to *C. saxatilis* through *C. crucidens* are premolars more closely spaced; P4 protocone of moderate size and lingual cingulum weak; M1 and M2 labial cingulum strong; m1 protostylid and metastylid weak, metaconid of moderate size and low relative to height of protoconid; and m2 metaconid moderately high, anterolabial cingulum weak, protostylid weak, and metastylid weak or absent.

DESCRIPTION AND COMPARISON: The holotype, although severely crushed dorsoventrally, represents the best cranial material available. Much of the skull roof is collapsed onto the basicranium. Despite this damage, the frontal sinus can still be seen to extend to the frontal-parietal suture. The nuchal crest is fan-shaped in outline, as is in *Psalidocyon*, and the lambdoidal crest is complete. The bullae are not crushed (better preserved on the left side) and show a narrow opening for the external auditory meatus, as is characteristic of *Cynarctus*. The mandible in the holotype is less distorted than is the cranium. It has a rather elevated ventral border of the masseteric fossa (nearly to the level of the upper border of the horizontal ramus). However, some referred specimens of this species (e.g., F:AM 27542, 27546, 61015) have lower masseteric fossae. There is a weak subangular lobe.

Dental morphology of *C. galushai* is only slightly modified toward the hypocarnivorous dentition that characterizes the advanced species from *C. saxatilis* and above. Premolars are generally short and lower crowned, although not as markedly so as in more derived species such as *C. voorhiesi* and *C. crucidens*. The M1 begins to show a slightly transversely narrowed appearance, but this proportional trait is still subtle at this stage

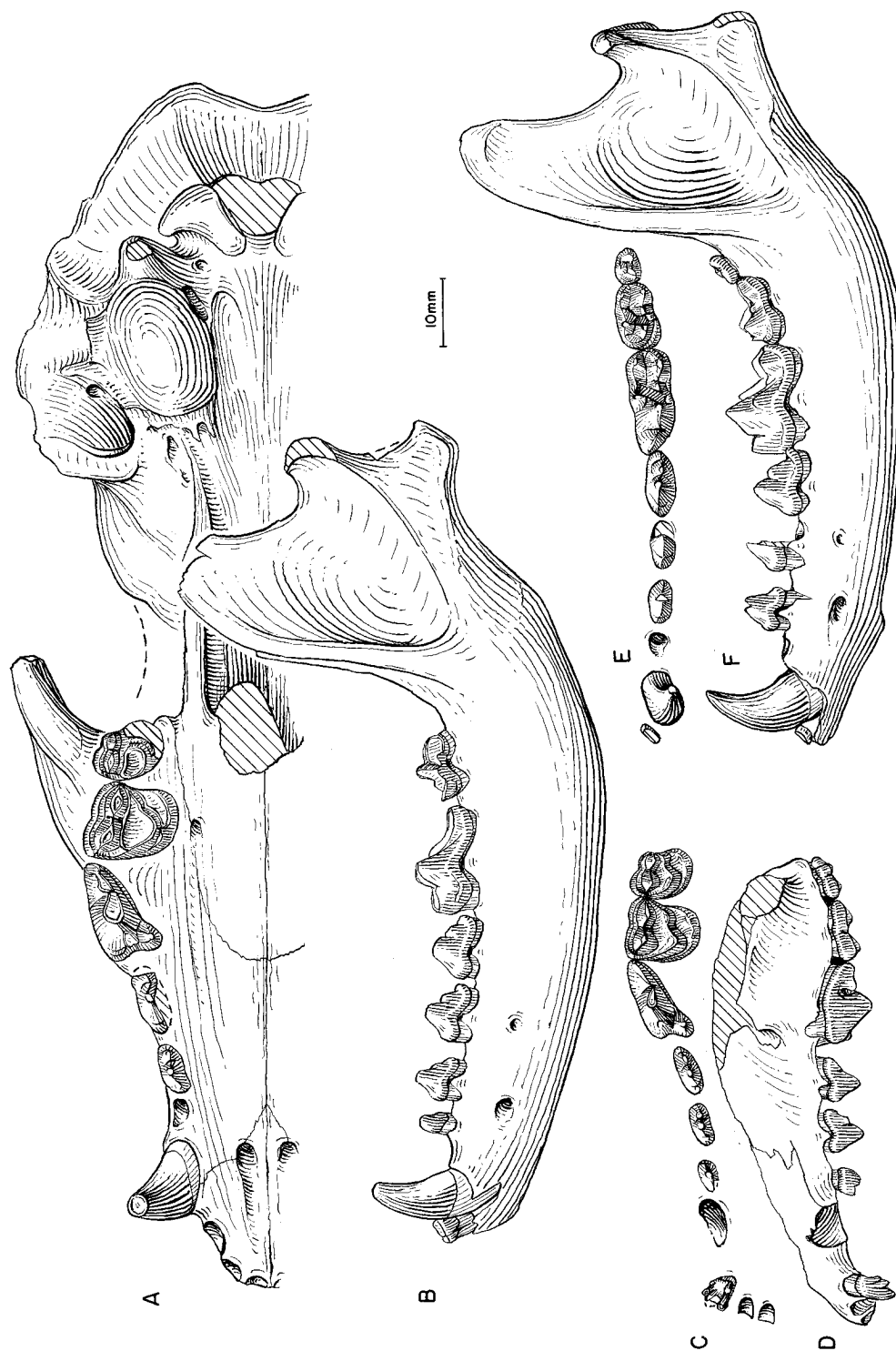


Fig. 55. *Cynarctus galushai*. **A**, Ventral view of skull and **B**, ramus, F:AM 27543, holotype, "Second Division," Barstow Formation (late early Barstovian), San Bernardino County, California. **C**, Upper teeth and **D**, lateral view of partial skull, F:AM 27550, Skyline Quarry, "First Division," Barstow Formation (early late Barstovian), San Bernardino County, California. **E**, Lower teeth and **F**, ramus, F:AM 27542, Valley View Quarry, "Second Division," Barstow Formation (late early Barstovian), San Bernardino County, California.

(see fig. 53). Similarly, the enlargement of the M2 is only in the beginning stage, which is more readily observable in the ratio diagram (fig. 53). The metaconule of M1–M2 is slightly enlarged relative to those in *Desmocyon matthewi*, and the lingual cingulum of M1–M2 is thickened to suggest an initiation of a conate hypocone.

Besides the slight decrease in size, the lower premolars remain largely unmodified from those in *Desmocyon matthewi*. In some individuals there is a tiny cusp on the lingual base of the principal cusp of the p4. The lower molars begin to show the proportions of the genus, but only in the most rudimentary way: slight widening of m1 talonid and elongation of m2–m3. An additional hypocarnivorous character is a small protostylid present on the m1s of all individuals.

DISCUSSION: *C. galushai* represents an early stage of hypocarnivorous specializations in the *Cynarctus* clade. Characters indicative of membership in this clade include the presence of a narrow external meatus, a transversely narrowed M1, a recurved c1, as well as less well-defined features such as the occasional occurrence of a small cusp on the posteromedial side of the p4 main cusp. While these characters in *C. galushai* permit recognition of a cladogenetic event branching off a mesocarnivorous lineage close to *Metatomarctus*, there remains a rather large morphological gap between *C. galushai* and the extremely derived morphology in *C. saxatilis* through *C. crucidens* (see further discussion under *C. saxatilis*).

?*Cynarctus marylandica* (Berry, 1938)

Figure 56A, B

*Tomarctus marylandica* Berry, 1938: 159, fig. 68a–d. Downs, 1956: 236. Munthe, 1998: 135.  
*Cynarctus marylandica* (Berry): Tedford and Hunter, 1984: 137.  
*Tomarctus kelloggi* (Merriam, 1911): Munthe, 1988: 97.

HOLOTYPE: USNM 15561 (AMNH cast 48836), left m2 and m1 lacking paraconid (fig. 56A, B) from 1.25 mi south of Plum Point Wharf, Calvert Formation (early Barstovian), Calvert County, Maryland.

REFERRED SPECIMEN: 1.5–2 mi north of Parker Creek, Calvert Formation (early Bar-

stovian), Calvert County, Maryland: USNM 299471 (AMNH cast 127312), left ramal fragment with p4 and alveoli of p3 and m1.

DISTRIBUTION: Early Barstovian of Maryland.

EMENDED DIAGNOSIS: Two autapomorphic features that separate this species from other *Cynarctus* are a strong crest on the posterior face of protoconid on m1 and a strong transverse crest between the entoconid and hypoconid of m2. Primitive characters in common with *C. galushai* are unreduced p4, m1 protostylid very weak and metastylid lacking, and m2 metaconid not enlarged and approximating protoconid in size, with anterolabial cingulum weak, protostylid weak, and metastylid absent.

DESCRIPTION AND COMPARISON: The only feature of this species that is indicative of *Cynarctus* is a protostylid on the m1. However, this protostylid is less developed than those in *C. galushai*, and at such initial stage of development it can be found in isolated individuals of other medium-size, mesocarnivorous borophagines such as *Metatomarctus canavus* (e.g., F:AM 49197, 99358, 99359).

DISCUSSION: Tedford and Hunter (1984: 137) suggested that the Maryland materials may be a primitive member of *Cynarctus*, comparable with early Barstovian species elsewhere. The meager materials available shroud the true identity of this taxon, which is one of only three known borophagine dogs from the Miocene of the northeast coast (the other two are *Paracynarctus kelloggi* and *Metatomarctus canavus*). The available materials do not even permit confident assignment of its generic position, although its placement within the medium-size Borophaginae seems likely. The distinct crest on the posterior face of the m1 trigonid, however, is not seen in other borophagines. Such peculiarity suggests the distinctness of this species, which may prove different in other aspects as well when more is known about it.

*Cynarctus saxatilis* Matthew, 1902

Figures 56G, H, 57A–D

*Cynarctus saxatilis* Matthew, 1902: 281, fig. 1; 1932: 2. Barbour and Cook, 1914: 225. Evan-

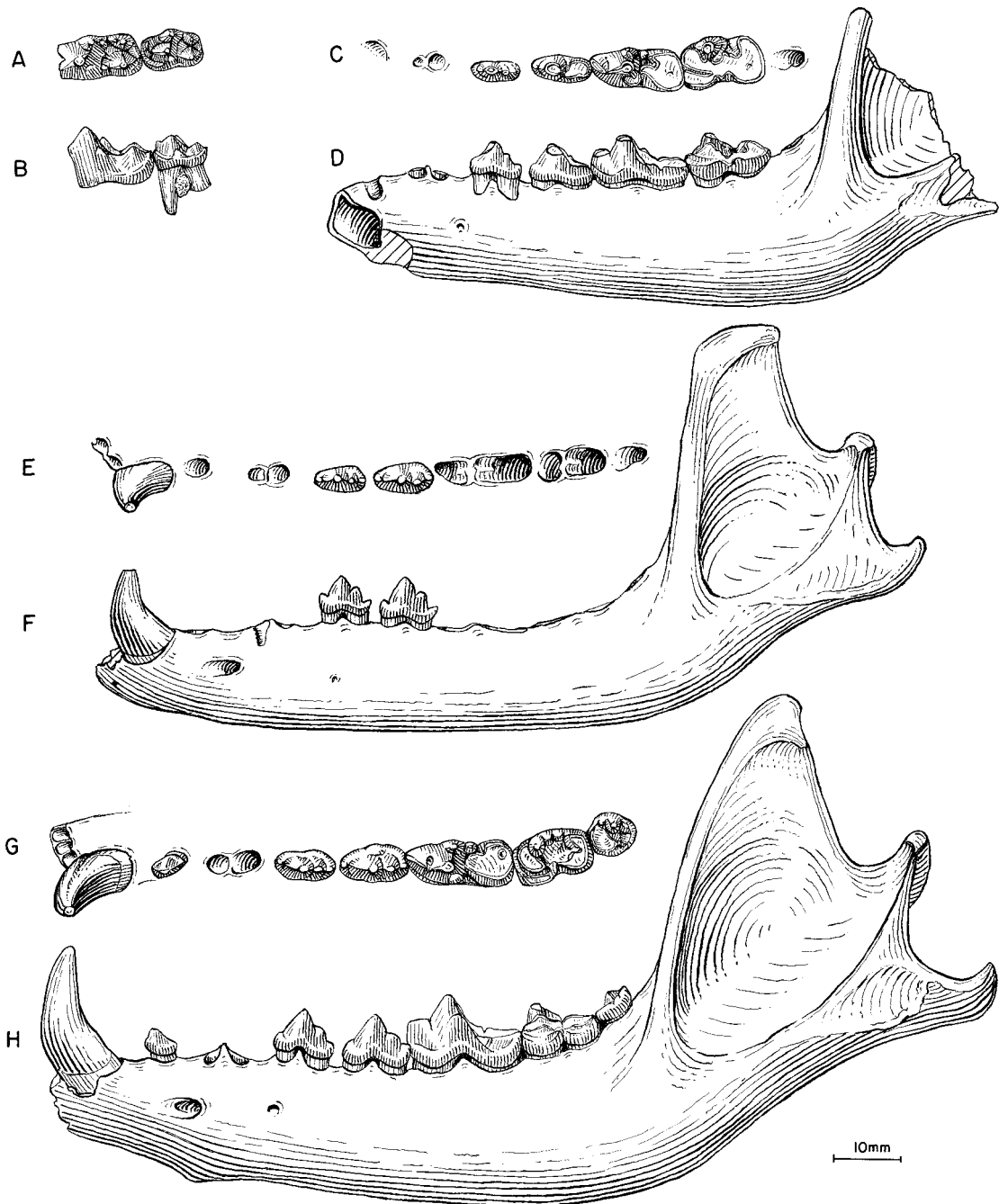


Fig. 56. **A**, Occlusal and **B**, buccal views of m1–m2, *?Cynarctus marylandica*, USNM 15561, holotype, 1.25 mi south of Plum Point Wharf, Calvert Formation (early Barstovian), Calvert County, Maryland. **C**, Lower teeth and **D**, ramus (reversed from right side), *Cynarctus voorhiesi*, F:AM 105094, holotype, Lucht Quarry, Burge Member, Valentine Formation (late Barstovian), Brown County, Nebraska. **E**, Lower teeth and **F**, ramus (reversed from right side), *C. voorhiesi*, F:AM 49144, Lucht Quarry. **G**, Lower teeth and **H**, ramus, *C. saxatilis*, AMNH 9453 (part of the ascending ramus and p1 reversed from right side), holotype, Cedar Creek, Ogallala Group (late Barstovian), Logan County, Colorado.

der, 1986: 28, fig. 4. Voorhies, 1990a: A134; 1990b: 122. Munthe, 1998: 135.  
*Cynarctus crucidens* Barbour and Cook, 1914: McGrew, 1938a: 329.  
*Carpocyon cuspidatus* (Thorpe, 1922b): Evander, 1986: 27, fig. 8C (in part).

HOLOTYPE: AMNH 9453, right and left rami with i1–i3 alveoli and c1–m3 (p2 alveolus) (fig. 56G, H), Cedar Creek, 40 mi north of Sterling, Ogallala Group (late Barstovian), Logan County, Colorado.

REFERRED SPECIMENS: Pawnee Creek area, Ogallala Group (late Barstovian), Weld or Logan County, Colorado: AMNH 6836, left isolated m1.

Norden Bridge Quarry, Niobrara River, Cornell Dam Member, Valentine Formation (early late Barstovian), Brown County, Nebraska (listed by Voorhies, 1990a: A134): USNM 352392, right ramus with p4–m1 and partial m2 alveolus.

Crookston Bridge Member, Valentine Formation (early late Barstovian), Cherry and Knox counties, Nebraska: Railway Quarry A (UNSM loc. Cr-12): UCMP 29891 (Evander, 1986: fig. 4), left ramus with i1–i3 alveoli, and c1–m3 (fig. 57A, B); and UNSM 25834, right partial maxillary with P3–M2 (referred to *Carpocyon cuspidatus* by Evander, 1986: fig. 8C). Stewart Quarry (UNSM loc. Cr-150): UNSM 1061-96, left maxillary fragment with M1–M2. Sand Lizard Quarry (UNSM loc. Kx-120): left ramus with p2–m2 and m3 alveolus. West Valentine Quarry (UNSM loc. Cr-114): UNSM 2685-87, right maxillary with P3 broken–M2.

Devil's Gulch, upper part of Devil's Gulch Member, 10 ft below the Burge Member, Valentine Formation (late Barstovian), Brown County, Nebraska: FMNH P25537 (AMNH cast 97782), rostral part of skull with I1 alveolus–M2 (fig. 57C, D) (referred to *Cynarctus crucidens* by McGrew, 1938a: 329, fig. 89) and crushed posterior half of skull. (The latter is an uncataloged F:AM specimen with field data of "Box 152, Elliot Quarry, Neb. 1935." According to the recollection of M. F. Skinner [personal commun.], a complete skull was discovered by the F:AM field party in the Devil's Gulch and left uncollected for some time. The Field Museum field party later collected the front half, i.e., FMNH P25537, and the F:AM

crews got what remained of the skull. The morphology, bone preservation and breakage, and enclosing rock matrix are generally consistent with the assumption that the two halves belong to a single individual, although the field label, "Elliot Quarry," is not [the possibility of mislabeling is likely]. The F:AM half skull is now deposited in the FMNH.)

Valentine Formation (late Barstovian), Webster County, Nebraska: Myers Farm (UNSM loc. Wt-15A): UNSM 21669, right m2.

DISTRIBUTION: Late Barstovian of Colorado and Nebraska.

EMENDED DIAGNOSIS: Characters of *C. saxatilis* shared with *C. voorhiesi* and *C. crucidens* that are derived with respect to *C. galushai* are premolars anteroposteriorly short and more widely spaced, with p2 isolated by diastemata; P4 protocone strong; M1 and M2 labial cingulum weak to absent lateral to metacone; M1 hypocone large and well delineated; M2 large with length approximating that of M1; m1 with distinct protostylid and strong metastylid; m2 protoconid small, extremely strong metaconid, strong metastylid, extremely large anterolabial cingulum, and strong protostylid; and m3 with well-developed metaconid. Primitive characters of *C. saxatilis* relative to those in *C. voorhiesi* and *C. crucidens* are premolars large and transversely wide; P4 lacking parastyle and lingual cingulum weak; M1 metastyle weak with a cingulum surrounding protocone; M2 not exceeding M1 in length, metacone relatively small and not expanded posteriorly; p4 posterior cusplet moderate in size; m1 trigonid moderately long relative to length of talonid; m2 relatively short; and coronoid process of mandible tall and depth of mandible below masseteric line shallow.

DESCRIPTION AND COMPARISON: Nearly a century after its first description, specimens of *C. saxatilis* remain rare in museum collections. The holotype is still the best mandible available, and the present reference of FMNH P25537 to this species permits observation of the skull and upper teeth. Consistent with cranial characteristics of other species of *Cynarctus* (e.g., *galushai* and *crucidens*), the skull of *C. saxatilis* has a well-developed frontal sinus extending to the frontal-parietal suture and invading the post-



orbital processes. The bulla is bulbous and has a narrow opening of the external auditory meatus. The palate is not narrowed, and the infraorbital foramen is not compressed into a vertical slit as is in *C. crucidens*.

Dentally, *C. saxatilis* has begun to acquire the highly hypocarnivorous characters typical of later species of the genus. The following features first appear in the upper cheek-teeth of this species: enlargement of P4 protocone, a distinct hypocone on M1–M2, elongation of M2, and reduction of labial cingulum of M1–M2. Modifications in the lower molars are even more dramatic, leading to an increased grinding area. A distinct anterolabial cingulum is formed on the m1, and this cingulum similarly becomes a broad shelf on the m2 that displaces the trigonid far to the lingual side. The trigonid of m1 is low and short in contrast to a much enlarged talonid. Accessory cusps, such as the protostylid and metastylid, are well developed on both m1 and m2. The m2 has a high, lingually positioned metaconid that dominates the trigonid, and its protoconid and paraconid form a low ridge curving anteriorly around the metaconid. The m3 has a broad, semicircular basin in front of a transverse ridge formed by the protoconid and metaconid.

On the other hand, the dental morphology of *C. saxatilis* still shows a certain primitiveness relative to *C. voorhiesi* and *C. crucidens*. The premolars are not as extremely reduced as in the latter two species. The M1–M2 still have a lingual and labial cingulum. The M2 hypocone is not posteriorly expanded, and thus the length of the M2 does not exceed that of the M1. The m1 trigonid is not as greatly reduced as in the more advanced species, and the m1 protostylid is not detached from the protocone to form a discrete cusp.

**DISCUSSION:** In his study of FMNH P25537, McGrew (1938a: 323) stated that the agreement in size and proportion between his Field Museum specimen and the holotype of *C. crucidens* is so close that the assignment of this specimen to *C. crucidens* is “practically certain.” Our own observations, however, suggest that FMNH P25537 is significantly larger than all other specimens assigned to *C. crucidens*, and its dentition oc-

cludes more precisely with the holotype of *C. saxatilis*, which although mentioned by McGrew (1938a), was not critically compared. The generally more primitive dental morphology of FMNH P25537 lends further support to its reference to *C. saxatilis*.

Such reference, however, is not without problems. Besides the larger size and stronger premolars, the lower molar morphology of the holotype of *C. saxatilis* is very close to that of *C. crucidens*. This is, however, in contrast to the more primitive upper molars in FMNH P25537, which lacks the extreme hypocarnivorous features shown in *C. crucidens*, such as reduction of upper molar cingulum, elongation of M2, and posterior expansion of M2 hypocone. Therefore, the possibility exists that FMNH P25537 may represent yet another species more primitive than *C. saxatilis*. Until associated upper and lower jaws become available, FMNH P25537 is best referred to *C. saxatilis*.

In *C. saxatilis*, most of the dental characteristics of advanced species of *Cynarctus* are established. Toward the more primitive side of the *Cynarctus* clade, however, there exists a large morphological gap between *saxatilis* and *galushai*, as reflected by the numerous apomorphic characters separating the two species (fig. 140).

#### *Cynarctus voorhiesi*, new species

Figure 56C–F

**HOLOTYPE:** F:AM 105094, right partial ramus with c1–p2 alveoli, p3–m2, and m3 alveolus (fig. 56C, D), Lucht Quarry, Burge Member, Valentine Formation (late late Barstovian), Brown County, Nebraska.

**ETYMOLOGY:** Named for Michael R. Voorhies in recognition of his studies of late Cenozoic faunas and stratigraphy of Nebraska.

**REFERRED SPECIMENS:** Burge Member, Valentine Formation (late late Barstovian), Brown and Cherry counties, Nebraska: F:AM 49143, left isolated M2, Lucht Quarry, Brown County; F:AM 49144, right ramus with i1–i3 alveoli, c1, p1–p2 alveoli, p3–p4, and m1–m3 all alveoli (fig. 56E, F), Lucht Quarry, Brown County; F:AM 49151, right partial ramus with i1–i3 alveoli, c1 broken, p1 root–m1, and m2–m3 alveoli, June Quarry, Brown County; F:AM 49152, left partial

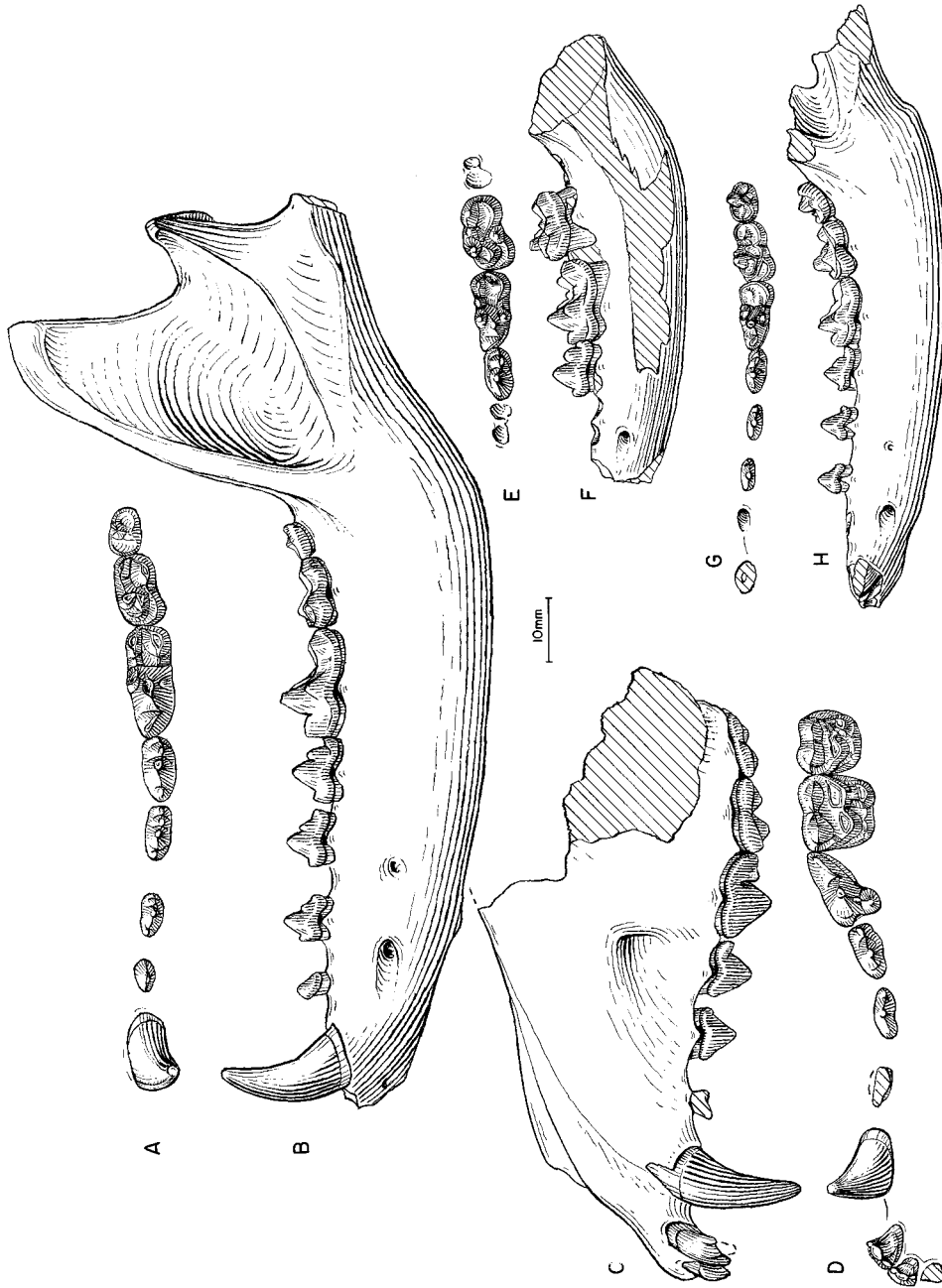


Fig. 57. **A**, Lower teeth and **B**, ramus, *Cynarctus saxatilis*, UCMP 29891, Railway Quarry A, Crookston Bridge Member, Valentine Formation (early late Barstovian), Cherry County, Nebraska. **C**, Lateral view of partial skull and **D**, upper teeth, *C. saxatilis*, FMNH P25537, Devil's Gulch, Devil's Gulch Member, Valentine Formation (late Barstovian), Brown County, Nebraska. **E**, Lower teeth and **F**, ramus (reversed from right side), *C. cruidens*, F:AM 49307, MacAdams Quarry, Clarendon Beds (early Clarendonian), Donley County, Texas. **G**, Lower teeth and **H**, ramus (reversed from right side), *C. cruidens*, UNSM 25465, holotype, Williams Canyon, Cap Rock Member, Ash Hollow Formation (early Clarendonian), Brown County, Nebraska.

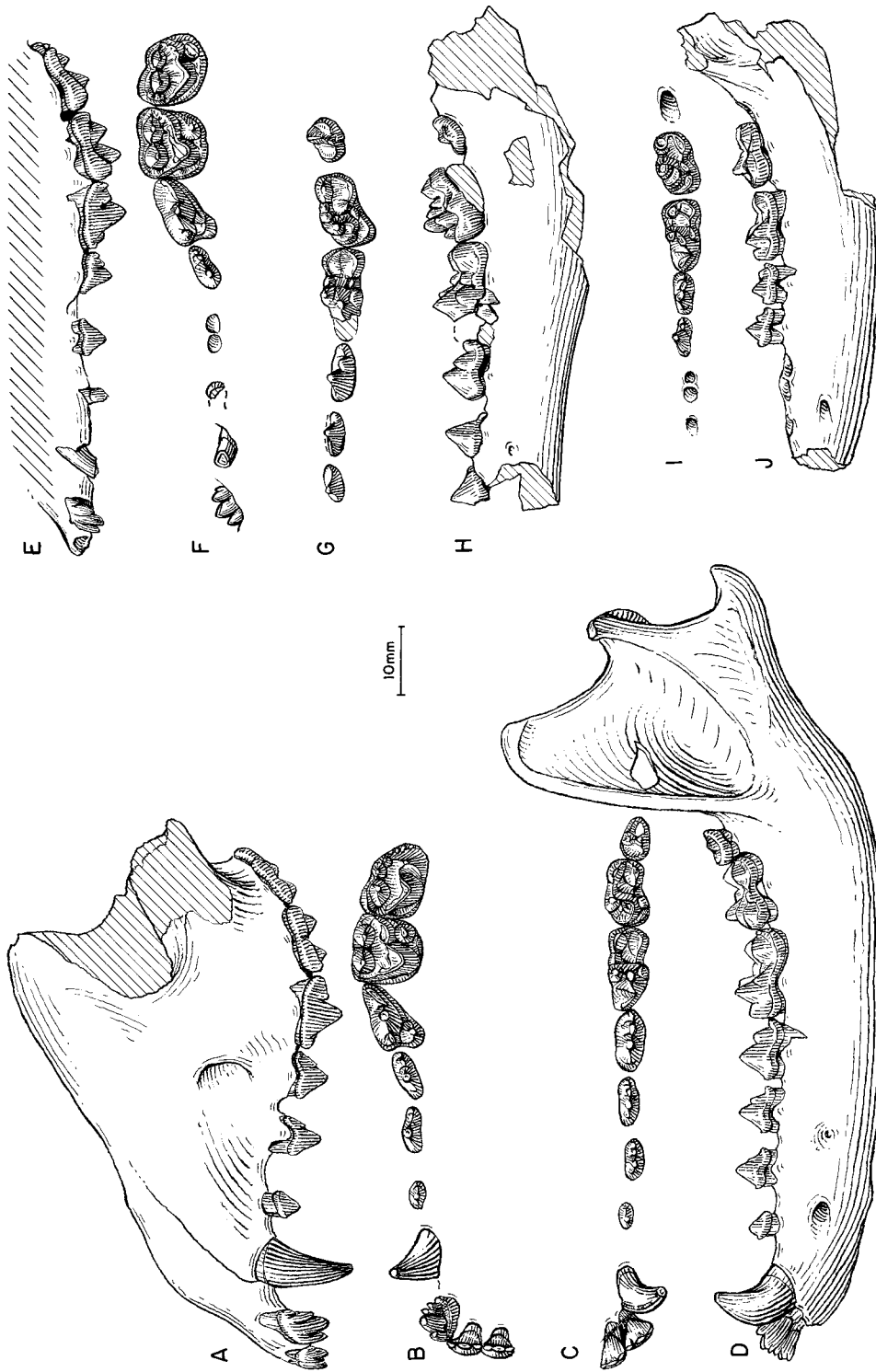


Fig. 58. *Cynarctus crucidens*. **A**, Lateral view of partial skull, **B**, upper teeth, **C**, lower teeth, and **D**, ramus, F:AM 49172 (**C** and **D** reversed from right side), Medicine Creek, Cap Rock Member, Ash Hollow Formation (early Clarendonian), Cherry County, Nebraska. **E**, Lateral and **F**, occlusal views of upper teeth, **G**, lower teeth, and **H**, ramus, F:AM 49312, Quarry 6, Clarendon Beds (early Clarendonian), Donley County, Texas. **I**, Lower teeth and **J**, ramus, F:AM 49146, Bear Creek Quarry, Merritt Dam Member, Ash Hollow Formation (late Clarendonian), Cherry County, Nebraska.

ramus with p1 alveolus, p2 broken–m2, and m3 alveolus, June Quarry, Brown County; F:AM 49153, right partial ramus with i1–p2 alveoli and p3–m2 all broken, 300 yd south of Lucht Quarry; and F:AM 105093, right ramal fragment with c1–p2 alveoli, p3–p4, and m1 alveolus, Midway Quarry, Cherry County.

DISTRIBUTION: Late late Barstovian of Nebraska.

DIAGNOSIS: *C. voorhiesi* is derived with respect to *C. saxatilis* in having a smaller size; premolars more widely spaced, smaller, and transversely narrower; p3–p4 posterior accessory cusplets weaker; m1 trigonid, especially the paraconid, shorter relative to length of talonid; and m2 more elongate relative to m1. The above derived characters of *C. voorhiesi* are shared with *C. crucidens*. Primitive characters in contrast to *C. crucidens* are coronoid process tall, more robust horizontal ramus, less posteriorly expanded M2 hypocone, and broader and larger premolars.

DESCRIPTION AND COMPARISON: Specimens of *C. voorhiesi* are limited to a few ramal fragments and an isolated M2. This new species from the latest Barstovian is transitional between the late Barstovian *C. saxatilis* and Clarendonian *C. crucidens* in its intermediate status in size, reductions of premolars, and enlargement of molars. Thus, *C. voorhiesi* still has a rather robust horizontal ramus instead of the slender ramus in *C. crucidens*. On average, dental measurements are 13% larger than those of *C. crucidens* but 13% smaller than those of *C. saxatilis* (appendix III). The premolars are more reduced and narrower than in *C. saxatilis* but are still larger than in *C. crucidens*. The M2 is close to the stage of evolution in *C. crucidens* except for the slightly less posteriorly expanded hypocone. Lower molars of all specimens are heavily worn. The proportions of different parts, however, are still readily observable. Most m1s are larger than those of *C. crucidens* and have relatively longer trigonids.

DISCUSSION: Although poorly represented by fragmentary materials, *C. voorhiesi* fills a morphological gap between *C. saxatilis* and *C. crucidens*. It is almost exactly intermediate, both in size and shape, between the latter two species. Stratigraphically, *C. voorhiesi* (Burge Member of Valentine Formation) is

also intermediate between the occurrences of *C. saxatilis* (Devil's Gulch and Crookston Bridge members of Valentine Formation) and *C. crucidens* (mostly Ash Hollow Formation or equivalent strata), and there is no known overlap in their occurrences in Nebraska (fossil records in other states are too poor to see any pattern). These morphological and stratigraphic intermediacies, coupled with the lack of any apparent autapomorphies in *C. voorhiesi*, suggest an anagenetic lineage in the advanced *Cynarctus*.

*Cynarctus crucidens*  
Barbour and Cook, 1914

Figures 57E–H, 58

*Cynarctus crucidens* Barbour and Cook, 1914: 225, pl. 1, figs. a, b. Matthew, 1932: 2. Munthe, 1998: 135.

*Cynarctus fortidens* Hall and Dalquest, 1962: 137, figs. 1, 2. Munthe, 1998: 135.

HOLOTYPE: UNSM 25465 (AMNH cast 14307), right partial ramus with i1–i3 alveoli, c1 broken, and p1 alveolus–m3 (fig. 57G, H) from Williams Canyon (or Quinn Canyon), tributary of Plum Creek, level equivalent to Clayton Quarry, Cap Rock Member, Ash Hollow Formation (early Clarendonian), Brown County, Nebraska (M. F. Skinner, personal commun.).

REFERRED SPECIMENS: Cap Rock Member, Ash Hollow Formation (early Clarendonian), Antelope, Cherry, and Brown counties, Nebraska: Clayton Quarry: F:AM 49148, right isolated m1. East Clayton Quarry: F:AM 49150, right and left m1s; F:AM 49170, right ramal fragment with i1–i3 alveoli, c1 root, and p1–p4 all alveoli; and F:AM 49174, right isolated M2. Medicine Creek, south side of Niobrara River: F:AM 49172, anterior part of skull with I1–M2 (fig. 58A–D), basicranium with bulla, right ramus with i2–m3, first five cervical vertebrae, both partial scapulae, right partial humerus, both radii and ulnae with distal epiphyses missing, and both partial tibiae. Poison Ivy Quarry (UNSM loc. Ap-116): UNSM 2000-78, anterior partial skull with I1–M2; and UNSM PI1597, left ramal fragment with i1–p3.

Merritt Dam Member, Ash Hollow Formation (late Clarendonian), Cherry County, Nebraska: F:AM 25142, right partial ramus

with m1 and alveoli for p3–p4 and m2–m3, Kat Quarry; F:AM 49145, left premaxillary maxillary with I1–I3 alveoli, C1, and P1 alveolus–M2, Bear Creek Quarry; F:AM 49146, left partial ramus with p1–p2 alveoli, p3–m2, and m3 alveolus (fig. 58I, J), Bear Creek Quarry; F:AM 49147, right partial ramus with c1, p1–p2 alveoli, p3–m1, and m2–m3 alveoli, Bear Creek Quarry; and F:AM 105092, left isolated m1, Gallup Gulch Quarry.

Hollow Horn Bear Quarry, undifferentiated beds of the Ogallala Group, temporally equivalent to the Cap Rock Member of the Ash Hollow Formation (early Clarendonian), Todd County, South Dakota: F:AM 49401, right partial maxillary with M1–M2; F:AM 49402, right partial maxillary with P4–M1 alveoli and M2; F:AM 49403A, left isolated M1; F:AM 49403B, left isolated M1; F:AM 49403C, left isolated M1; F:AM 49403D, left isolated M1; F:AM 49403E, left isolated M1; F:AM 49404, right ramus with i1–i3 alveoli and c1–m3; F:AM 49405, left ramus with i1–i3 alveoli and c1–m3; F:AM 49406, left partial ramus with i1–i3 alveoli, c1 broken, p1 alveolus, p2–p3, p4 alveolus, m1–m2, and alveolus of m3; F:AM 49407, left isolated M2; F:AM 49408, right isolated M1; F:AM 49409, left isolated m1; F:AM 49419, left isolated m1; F:AM 49419A, left isolated M2; F:AM 49419B, left isolated P4; F:AM 49420, right broken isolated m1; F:AM 105091, left isolated m1; and F:AM 105091A, right isolated m1.

Kilpatrick Quarry (= Quarry 7), Laucomer Member, Snake Creek Formation (early Clarendonian), Sioux County, Nebraska: AMNH 22405, left isolated m1.

Clarendon Beds (early Clarendonian), Donley County, Texas: F:AM 49302, left immature maxillary fragment with dP3 broken–dP4, MacAdams Quarry; F:AM 49303, left premaxillary fragment with I1 alveolus–I3, detached teeth including canines and right M1–M2, Quarry 2, Lewis Place, Spade Flats; F:AM 49304, right isolated M1, MacAdams Quarry; F:AM 49305, right maxillary fragment with M1–M2, MacAdams Quarry; F:AM 49306, right and left rami with i1 alveolus–m2 and m3 alveolus, MacAdams Quarry; F:AM 49307, right partial ramus with p3 alveolus–m2 and m3 alveolus (fig. 57E, F),

MacAdams Quarry; F:AM 49308, left partial ramus with i1–p3 alveoli, p4–m2, and m3 alveolus, MacAdams Quarry; F:AM 49309, left partial ramus with p2–p4 alveoli, m1 broken–m2, and m3 alveolus, MacAdams Quarry; F:AM 49310, left partial ramus with p1–p3 all broken, p4–m2 (m1 broken), MacAdams Quarry; F:AM 49311, right isolated M1, Quarry 1 of Gidley; F:AM 49312, articulated crushed partial skull with I3 erupting, C1–P1 both broken, P3–M2, lower jaws with c1 broken–m3 (fig. 58E–H), partial left and right humeri articulated with incomplete radius and ulna, and partial pelvis articulated with femur and partial tibia, White Fish Creek, Quarry 6; F:AM 49313, left ramal fragment with c1, p1–p3 alveoli, p4, and m1 alveolus–m2, MacAdams Quarry; F:AM 70768, crushed immature skull with dC1, P1 alveolus, and dP2–dP4, MacAdams Quarry; F:AM 105089, right ramal fragments with p3 broken–p4 and detached broken m1 and m2, MacAdams Quarry, 10 mi north of Clarendon; F:AM 105090, left partial ramus with c1 broken and p1 alveolus–m3 (p4 broken), MacAdams Quarry; KUVF 11353 (holotype, *Cynarctus fortidens* Hall and Dalquest, 1962: fig. 1), right maxillary fragment with P3–M1, in “bluff on west side of Turkey Creek, approximately 75 ft above stream, Raymond Farr Ranch” (Hall and Dalquest, 1962: 137); and KUVF 11354 (Hall and Dalquest, 1962: fig. 2), right ramal fragment with m2, same locality as above.

Highway Pit, 0.75 mi north of Lipscomb, Ogallala Group (Clarendonian), Lipscomb County, Texas: F:AM 105088, left ramal fragment with m2.

DISTRIBUTION: Early Clarendonian of Nebraska, South Dakota, and Texas; late Clarendonian of Nebraska; and Clarendonian of Texas.

EMENDED DIAGNOSIS: Unique or further development of derived characters that distinguish *Cynarctus crucidens* from all other species are P1–P2 and p1–p2 small and narrow and isolated by longer diastemata; P4 parastyle; M1 strong metastyle, labial cingulum at metacone lacking; M2 anteroposteriorly elongate and exceeding M1 length, hypocone large and posteriorly situated, metastyle well developed, and strong posterior cingulum; p4 with large, low posterior ac-

cessory cusplet; m1 trigonid extremely short and narrow relative to length and width of talonid; m2 entoconid and hypoconid strong, conical cusps; coronoid process of mandible low; and horizontal ramus slender and depth of mandible below masseteric line deep (elevated lower border of the masseteric fossa).

**DESCRIPTION AND COMPARISON:** The cranial morphology of *C. crucidens* is still incompletely known. Skull fragments of F:AM 49172 show that the maxillary region of the palate is narrowed compared to *C. saxatilis*, whereas the anterior tip of the palate is not. This narrowing of the cheek region also causes a compression of the infraorbital canal, which becomes slitlike in cross-section rather than more open as in *C. saxatilis* and more primitive taxa. The basicranial fragment in F:AM 49172 has a well-preserved bulla, which is very bulbous and has a very narrow opening for the external auditory meatus. In the mandible the lower border of masseteric fossa is elevated to the level of the base of lower molars, and the coronoid crest is relatively low.

As the terminal species of the *Cynarctus* clade, *C. crucidens* possesses the most hypocarnivorous dental features of all species. The upper and lower incisors are highly cuspidate, together forming a comblike structure. In addition to more prominent developments of individual cusps, the I3 has added another small accessory cusp on the lateral ridge, totaling two lateral accessory cusps instead of one, as in *C. saxatilis*. Correspondingly, the i3 has an additional cusplet between the lateral and central cusps. These multicuspid incisors form a longer transverse blade and together they occupy a broader anterior tip of the snout. The upper and lower premolars (except P4) are widely spaced from each other and are considerably reduced compared to those of *C. saxatilis*, *C. voorhiesi*, and other cynarctines. Advanced features of the P4 include a distinct parastyle and a wider lingual cingulum (especially prominent in F:AM 49145). Advancement of the M1, relative to that in *C. saxatilis*, is mainly in the reduction of the cingula: both the lingual cingulum surrounding the protocone and the labial cingulum are lost or extremely reduced. The M2 is greatly expanded posteriorly due to enlargement of the hypo-

cone, slightly more so than in *C. voorhiesi*, such that its outline is anteroposteriorly elongated, compared to the more or less quadrate M2 in *C. saxatilis*. Besides the much smaller size and more reduced premolars, the lower cheekteeth of *C. crucidens* are quite similar to those of *C. saxatilis* and *C. voorhiesi* in both proportions and cusp morphologies.

**DISCUSSION:** Hall and Dalquest's (1962) contrast of their *C. fortidens* with *C. crucidens* was apparently based on FMNH P25537 (a partial skull), which was referred to *C. crucidens* by McGrew (1938a: 330) but is presently assigned to *C. saxatilis* (see further comments under that species). Therefore, the few diagnostic characters cited by Hall and Dalquest are differences between their *C. fortidens* and *C. saxatilis* (contrary to Hall and Dalquest [1962: 138], however, the holotype of *C. fortidens* is smaller, not larger, than FMNH P25537). A larger sample of the Clarendon materials is now available in the Frick Collection, and they show unambiguously the characteristics of *C. crucidens*, which has seniority over *C. fortidens*.

There is a tendency toward decreasing size from earlier species of *Cynarctus* (such as *saxatilis* and *galushai*) to the terminal species *crucidens*. Superposed on this overall size reduction is the reduction of the premolars, which may help explain the rather large coefficients of variance in most measurements of the premolars in *C. crucidens* (appendix III), especially for the upper premolars.

#### *Metatomarctus*, new genus

**TYPE SPECIES:** *Cynodesmus canavus* Simpson, 1932.

**ETYMOLOGY:** Greek: *meta*, between; in allusion to the intermediate position of this genus between *Tomarctus* and the more primitive borophagines.

**INCLUDED SPECIES:** *Metatomarctus canavus* (Simpson, 1932), *Metatomarctus* sp. A, and *Metatomarctus* sp. B.

**DISTRIBUTION:** Early Hemingfordian of Nebraska, New Mexico, Florida, and Delaware; late Hemingfordian of Wyoming and California; and early Barstovian of Nevada.

**DIAGNOSIS:** Derived characters that distinguish *Metatomarctus* and higher taxa from

*Desmocyon matthewi* are I3 with one lateral accessory cusplet (shared with the Cynarctina) and initial development of an anterior crest on the P4. *Metatomarctus* is primitive with respect to *Euoplocyon*, *Psalidocyon*, and higher taxa in its less elaborate I3 with a single accessory cusp. In contrast to the Cynarctina clade, *Metatomarctus* lacks such derived characters as subangular lobe of the mandible, high mandibular condyle, reduced premolars, shortened P4, small protostylid of m1, wide m1 talonid, and elongated m2.

*Metatomarctus canavus* (Simpson, 1932)

Figure 59

- Cynodesmus canavus* Simpson, 1932: 19, fig. 4. White, 1941b: 91.  
*Tomarctus thomasi* White, 1941b: 94, pl. 14, fig. 3; 1942: 8, pl. 7, fig. 1. Downs, 1956: 236.  
*Tomarctus canavus* (Simpson): White, 1942: 8, pl. 2, fig. 2, pl. 6, figs. 1–3; 1947: 502. Olsen, 1956a: 2, figs. 1, 4. Downs, 1956: 236. Wang, 1994: 125. Munthe, 1998: 135.  
*Nothocyon insularis* White, 1942: 7, pl. 1, fig. 3; 1947: 502, fig. 2.  
*Tomarctus kelloggi* (Merriam, 1911): Munthe, 1988: 91 (in part).  
*Tomarctus* sp. Reynolds et al., 1995: 108.  
*Tomarctus* cf. *T. canavus* (Simpson): Emry and Eshelman, 1998: 160, fig. 2N–P.

HOLOTYPE: UF V-5260, right partial ramus with p2, p3 alveolus, p4–m2, m3 alveolus (fig. 59A, B), from Thomas Farm Local Fauna, Hawthorn Formation (late early Hemingfordian), Gilchrist County, Florida.

REFERRED SPECIMENS: Thomas Farm Local Fauna, Hawthorn Formation (late early Hemingfordian), Gilchrist County, Florida: AMNH 27674, partial left ramus with p2–p3 alveoli, p4–m1, and m2 alveolus; AMNH 27674A, isolated right m1; MCZ 3628 (AMNH cast 129643), partial skull with P4–M1, partial right ramus with c1–p1 alveoli, p2 broken, p3–m2, and m3 alveolus (White, 1942: pl. 6; Olsen, 1956a: fig. 1); MCZ 3641, M1; MCZ 3673, maxillary with P4–M1; MCZ 3674, maxillary with P4–M1; MCZ 3682 (AMNH cast 129681) (holotype of *Tomarctus thomasi* White, 1941b), partial left maxillary with P4–M2; MCZ 3712 (White, 1942: pl. 7), partial right ramus with c1–p1 alveoli, p2–m2, and m3 alveolus; MCZ 3713, ramus with p2 and p4–m2; MCZ 3728,

maxillary with P2–M2; MCZ 3812 (AMNH cast 129682) (holotype of *Nothocyon insularis* White, 1942), partial right maxillary with P4 broken–M2; MCZ 3813 (White, 1942: pl. 2, fig. 2), left maxillary with P2, P3 alveolus, P4–M1, and M2 alveolus; MCZ 3924, ramus with p4–m1; MCZ 4242 (White, 1947: fig. 2D, E), partial right ramus with c1–p1 alveoli, p2–m1, and m2–m3 alveoli; MCZ 4334, ramus with p2–m2; MCZ 4507, ramus with m1; MCZ 5814, ramus with m1; MCZ 7146, maxillary with P4–M1; MCZ 7147, ramus with p4–m1; MCZ 7148, ramus with m1–m2; MCZ 7307, ramus with p2–m1; MCZ 7308, ramus with p4–m2; SDSM 525 (formerly MCZ 3967), right partial ramus with p2, p3 alveolus, and p4–m2; UF 926, right M1; UF 927, left broken M1; UF 3532, right ramus with c1–m2 alveoli; UF 17652, left M1; UF 17654, left m1; UF 17655, left P4; UF 19781, right ramus with c1–m3 alveoli; UF 19788, right immature ramus with c1 erupting, dp4 broken, and m1–m2 erupting; UF 19795, right ramus with p2–p4 alveoli, m1–m2, and m3 alveolus; UF 19952, right ramus with p2–p3 alveoli, p4–m1, and m2 alveolus; UF 58957, left maxillary fragment with P4–M2; UF 59089, left and right maxillary fragments with P4 broken–M2; UF 60527, left ramus fragment with p2–p4 (p3 broken); UF 66925, right ramal fragment with p1–p3 alveoli and p4; UF 94786, right m1; UF 94854, right ramal fragment with m2; UF 94855, left maxillary with P1–P3 alveoli and P4–M2; UF 94856, right m1; UF 94857, left ramus with c1–p3 alveoli, p4, m1 alveolus, m2, and m3 alveolus; UF 94858, left M1; UF 94859, left P2; UF 94860, left M2; UF 94861, right P3; UF 94862, talonid of right m1; UF 94866, right ramus with p3 alveolus, and p4–m2; UF 94868, right ramus with c1–p3 alveoli, p4–m2, and m3 alveolus; UF 94869, left immature ramus with c1 and p2–p4 erupting and dp3; UF 94870, left M2; UF 94873, left m2; UF 94875, right ramal fragment with p4; UF 94886, left P4; UF 94887, left broken M1; UF 94888, right M1; UF 94889, right p4; UF 94891, right ramal fragment with p2, p3 alveolus, and p4 broken; UF 94899, left M1; UF 95001, broken left m1; UF 95002, talonid of left m1; UF 95003, talonid of left m1; UF 154100, right ramus with c1–p1 al-

veoli, p2, p3 alveolus, and p4–m1; UF 165879, left ramus with p1–p2, p3 alveolus, p4–m1, and m2–m3 alveoli; UF V-5653, left and right maxillae with P1 alveolus, P2, P3 alveolus, and P4–M2; UF V-5658 (AMNH cast 48841), isolated right m1; UF V-5668, right M1; UF V-5669, right M2; UF V-5670, right P4; UF V-5707, partial crushed skull with C1–P3 alveoli and P4–M2; UF V-5766 (AMNH cast 48837), partial right maxillary with P4–M2; UF V-5767 (AMNH cast 48832), partial right ramus with p1–m2 and m3 alveolus; UF V-6266, partial right ramus with p1–p2 alveoli and p3 broken–p4; UF V-6267, right ramal fragment with i1–p3 alveoli and p4; UF V-6282, partial right ramus with p4–m1 all broken and m2 alveolus; UF V-6283, right ramal fragment with m2; UF V-6284, left ramal fragment with p1–p2 alveoli and p3; UF V-6288, left ramal fragment with m2 and m3 alveolus; UF V-6331, right ramus with p1–m1 alveoli, m2, and m3 alveolus; UF V-8946, right M1; UF V-9162, left ramal fragment with p4; UF V-9173, broken left M1; UF V-9174, left M1.

Pollack Farm Site (Delaware Geological Survey locality Id11-a), lower shell bed of Cheswold sands, lower Calvert Formation (late early Hemingfordian), near Cheswold, Delaware: USNM 475817, isolated right m1 (referred to *Tomarctus* cf. *T. canavus* by Emry and Eshelman, 1998: fig. 2O, P); and USNM 475930, isolated left m2 (referred to *Tomarctus* cf. *T. canavus* by Emry and Eshelman, 1998: fig. 2N).

Jeep Quarry or Jeep Quarry horizon, Arroyo Pueblo drainage, upper part of Chamisa Mesa Member, Zia Formation (early Hemingfordian), Sandoval County, New Mexico: F:AM 50139A, left ramal fragment with broken c1, p1 alveolus, and broken p2; and F:AM 50141, right ramal fragment with c1–m1 all broken, and isolated m3.

Hemingford Area, upper part of the Runningwater Formation (late early Hemingfordian), Box Butte, Cherry, and Dawes counties, Nebraska: UNSM 25597, left partial ramus with p1–p2 alveoli and p3–m1, UNSM loc. Bx-7; UNSM 25600, partial right ramus with p1 alveolus–m2 and m3 alveolus, UNSM loc. Bx-7B; UNSM 25601, right ramus with c1, p1–p3 alveoli, p4–m1, and m1–m2 alveoli, UNSM loc. Bx-7; UNSM 25602,

right ramus with c1 alveolus–m2 and m3 alveolus, UNSM loc. Bx-7B; UNSM 25605, right partial maxillary with P4–M1 and M2 alveolus, UNSM loc. Bx-9; UNSM 25609, left partial ramus with p1 alveolus–m1 and m2–m3 alveoli (fig. 59S, T), UNSM loc. Bx-7; UNSM 25613, right partial ramus with p3 alveolus, p4–m1 both broken, and m2, UNSM loc. Bx-7; UNSM 25614, left partial ramus with m1, Bx-12; UNSM 25616 (F:AM cast 97102), right partial ramus with p1 alveolus–m2, UNSM loc. Bx-7; UNSM 25620, right partial maxillary with P4 broken–M2, UNSM loc. Bx-7; UNSM 25621, partial left ramus with c1 broken–m2 and m3 alveolus, UNSM loc. Bx-7B; UNSM 25623, right ramal fragment with m1 broken and m2–m3, Hemingford Quarry 11A (UNSM loc. Bx-11); UNSM 25626, partial right ramus with p1 alveolus–m2, UNSM loc. Bx-22; UNSM 25635, left ramus with i1–i3 alveoli, c1, p1 alveolus, p2–p4, and m1–m3 alveoli, UNSM loc. Bx-7; UNSM 25640, partial left maxillary with P3 alveolus–M2, UNSM loc. Bx-12; UNSM 25653, right maxillary with P2 broken–M2, UNSM loc. Bx-7; UNSM 25654, right partial ramus with p4–m1 and m2 root, UNSM loc. Bx-7; UNSM 25655, right and left partial maxillary with P1 alveolus–M2, UNSM loc. Bx-12; UNSM 25658 (AMNH cast 107922), left ramus with c1–p1 alveoli, p2–m1, and m2 broken–m3 alveolus (fig. 59Q, R), UNSM loc. Bx-7; UNSM 25660, partial ramus with p1–m3 alveolus, UNSM loc. Bx-7; UNSM 25662 (AMNH cast 107923), partial skull with C1 root–M2 (P1 alveolus) (fig. 59P), UNSM loc. Bx-51; UNSM 25669, left partial ramus with p3–m1, UNSM loc. Bx-27; UNSM 25813, left partial maxillary with P3 broken–M2 and left partial ramus with p2–m3 (p4 broken), near Nonpareil Sand Pit; UNSM 25814, right partial ramus with p3–m2, UNSM loc. Bx-7B; UNSM 25815, left partial ramus with c1–p1 broken, p2–p4, and m1 broken, UNSM loc. Bx-7B; UNSM 25816, partial right ramus with i1 alveolus–m1, UNSM loc. Bx-7B; UNSM 25817, right partial ramus with p4–m2, UNSM loc. Bx-12D; UNSM 25818, left partial ramus with c1, p1 alveolus–m1 broken, and m2 alveolus, no locality data; UNSM 25827 (AMNH cast 124024), right partial ramus with p4 root–m2 and m3



alveolus, UNSM loc. Cr-101; and UNSM 26159, right partial ramus with c1, p1–p3 alveoli, p4, m1–m2 both broken, and m3 alveolus, no data, Dawes County.

Clinton Highway Locality (UNSM loc. Sh-101B), Runningwater Formation (early Hemingfordian), Sheridan County, Nebraska: UNSM 5008-70, partial left and right maxillary with I2–M2.

Dry Creek Prospect B, Runningwater Formation (early Hemingfordian), Box Butte County, Nebraska: F:AM 99353, left isolated m2; F:AM 99354, right isolated p4; F:AM 99355, left isolated p4; F:AM 99356, right ramal fragment with p4; F:AM 99357, left partial ramus with p1 alveolus–p4 and m1 broken; F:AM 99358, left ramus with i1–i3 alveoli, c1, p1 alveolus–m2, and m3 alveolus; and F:AM 99359, left ramus with i1–i3 alveoli, c1, p1 alveolus–m2, and m3 alveolus.

Other localities in the Runningwater Formation (early Hemingfordian), Dawes County, Nebraska: F:AM 25419, right partial ramus with p2 alveolus, p3–p2, and m3 alveolus, Ahren Prospect, Cottonwood Creek; F:AM 49197, partial adolescent skull with I2–P3 all erupting, dP4, P4 erupting, both partial rami with p3–p4 erupting, m1–m2, and m3 erupting (fig. 59C–F) and postcranial fragments, Elder Ranch, Cottonwood Creek; F:AM 49198, premaxillary and partial maxillary with I1 alveolus, I2–P1, p2 alveolus, and P4–M2, Pepper Creek; F:AM 49199, left ramus with c1–m3 (fig. 59G, H), both partial humeri (fig. 59K), right radius (fig. 59J), both ulnae (fig. 59I), metacarpal III (fig. 59M), partial pelvis, partial right femur, distal ends of both tibiae (fig. 59N, O), calcaneum (fig. 59L), broken astragalus, and vertebrae, Pebble Creek; F:AM 104694, right partial ramus with c1 broken, p1 alveolus, p2–p3, m1, and m2–m3 alveoli, NW $\frac{1}{4}$ , sect. 36, T30N, R49W; and F:AM 104700, right and left partial rami with c1 broken, p1 alveolus, and p2–p4, Sand Canyon Region.

Two mi west of Pole Creek, Runningwater Formation (early Hemingfordian), Cherry County, Nebraska: F:AM 61313, right partial ramus with i1–p1 alveoli, p2–m2 (m1 broken), and m3 alveolus; and F:AM 61314, right partial ramus with p4–m1.

Bridgeport Quarries, Runningwater For-

mation (early Hemingfordian), Morrill County, Nebraska: UNSM loc. Mo-113: UNSM 25713, left ramal fragment with m1–m2 and m3 alveolus; UNSM 25800, right maxillary with P3 alveolus–M1 and M2 alveolus; UNSM 25802, left maxillary with C1–P3 alveoli and P4 broken–M2; UNSM 25803, right maxillary with P4–M1; UNSM 25804, left ramus with c1, p1 alveolus, p2–m1 all broken, and m2–m3 alveoli; UNSM 25805, right ramus with p2–m2 and m3 alveolus; UNSM 25835, right ramal fragment with m1 broken and m2–m3 alveoli; UNSM 25-6-7-34-SP, right maxillary with P3 broken–M2; UNSM 37-6-7-34-SP, right M1; and UNSM 24-6-7-34-SP, left maxillary fragment with M1–M2. UNSM loc. Mo-114: UNSM 25735, left ramus with p1–m1 all broken and m2. UNSM loc. Mo-116: UNSM 25734, right ramus with c1–p3 alveoli, p4–m1 broken, and m2 alveolus.

Split Rock Formation (late Hemingfordian), Fremont County, Wyoming: UW 926, partial skull and mandible with complete dentition (referred to *Tomarctus kelloggi* by Munthe, 1988), Rattlesnake Hills, UW loc. 50001.

Hackberry Local Fauna (late Hemingfordian), Lanfair Valley, eastern Mohave, California: AMNH 129879 (cast of San Bernardino County Museum collection), left ramus with i2–c1 and p2–m2 (referred to *Tomarctus* sp. by Reynolds et al., 1995).

DISTRIBUTION: Early Hemingfordian of Nebraska, New Mexico, Florida, and Delaware; and late Hemingfordian of Wyoming and California.

EMENDED DIAGNOSIS: Only known species and its characters are those listed for the genus.

DESCRIPTION AND COMPARISON: Despite the large number of referred specimens, our knowledge of *Metatomarctus canavus* is still mostly limited to teeth and jaws. *M. canavus* is significantly larger than the contemporaneous *Desmocyon matthewi*, with dental measurements on average 23% larger. In *M. canavus*, a lateral cusplet is present on the I3. Another derived character first appearing in *M. canavus* is a more distinct anterior crest on the paracone on P4 than those seen in most *D. matthewi*, initiating a trend toward a distinct parastyle in later taxa. This initial

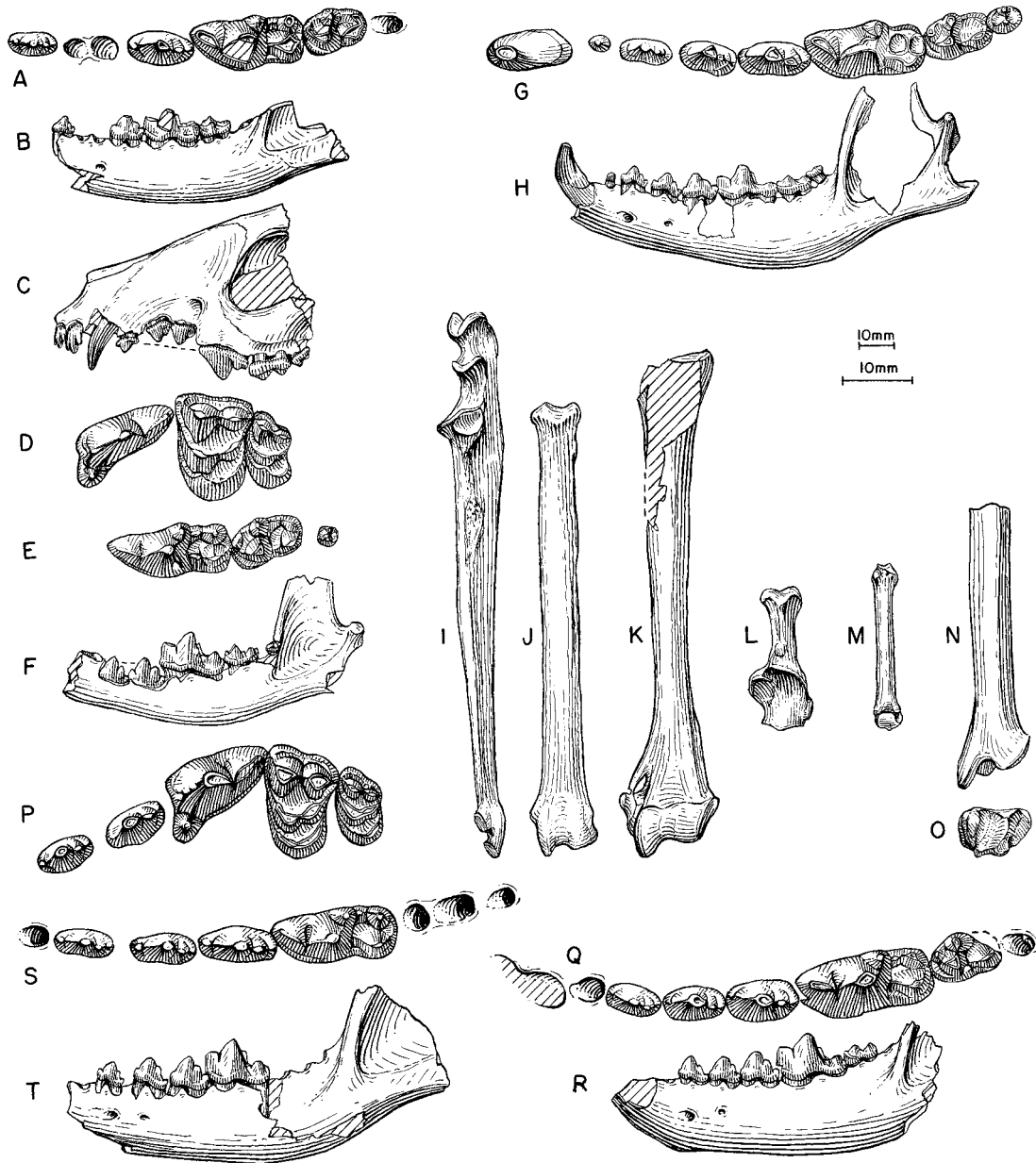


Fig. 59. *Metatomarctus canavus*. **A**, Lower teeth and **B**, ramus (reversed from right side), UF V-5260, holotype, Thomas Farm Local Fauna, Hawthorn Formation (early Hemingfordian), Gilchrist County, Florida. **C**, Lateral view of partial skull, **D**, upper teeth, **E**, lower teeth, and **F**, ramus, F:AM 49197, Elder Ranch, Runningwater Formation (early Hemingfordian), Dawes County, Nebraska. **G**, Lower teeth, **H**, ramus, **I**, ulna, **J**, radius, **K**, partial humerus, **L**, calcaneum, **M**, metacarpal III, and **N**, anterior and **O**, distal views of distal tibia, F:AM 49199 (J, K, L, N and O reversed from right side), Pebble Creek, Runningwater Formation. **P**, Upper teeth, UNSM 25662, Hemingford Area, Runningwater Formation. **Q**, Lower teeth and **R**, ramus, UNSM 25658, Hemingford Quarry, Runningwater Formation. **S**, Lower teeth and **T**, ramus, UNSM 25609, Hemingford Quarry, Runningwater Formation. The longer (lower) scale is for A, D, E, G, P, Q, and S, and the shorter (upper) scale is for the rest.

development of a parastyle varies from a rather distinct parastyle in UNSM 25662 (fig. 59P) to a weak anterior crest in F:AM 49198. The crest leading to the protocone and lingual to the anterior crest is also distinct.

Compared to *Euoplocyon* and later taxa, *Metatomarctus canavus* is primitive in its less elaborate I3 lateral accessory cusplet (i.e., one cusplet vs. two or more in *Euoplocyon* and others). Compared to the cynarctine clade, on the other hand, *M. canavus* has a primitively undeveloped subangular lobe, low mandibular condyle, unshortened P4, no protostylid on m1, and a normally proportioned m2 that is not elongated.

Specimens from the early Hemingfordian of New Mexico are too poorly preserved to be certain about their identity. The size and morphology of F:AM 50141 is in general agreement with the type series from Florida.

DISCUSSION: Six nominal species had been proposed for the median-size canids from the Thomas Farm local fauna, not counting other carnivorans such as amphicyonids. The last synthesis of Thomas Farm canids was by Olsen (1956a), who recognized only two species: "*Cynodesmus*" *iamonensis* Sellards (see Wang, 1994: 120) and "*Tomarctus*" *canavus*. We agree with Olsen's assessment, and the contrasting characters listed by him underline some of the fundamental differences between hesperocyonine and borophagine canids, such as the presence in *M. canavus* of a distinct metaconule and a broader lingual cingulum on M1, as well as a transverse crest between the hypoconid and entoconid of m1. Furthermore, the premolars of *M. canavus* have more distinct anterior accessory cusplets. These characters are lacking in all hesperocyonines, including "*Cynodesmus*" *iamonensis*, which was referred to the genus *Osbornodon* by Wang (1994). *Osbornodon iamonsensis* is known to occur both in the Thomas Farm Local Fauna and in the Runningwater Formation of Nebraska (Wang, 1994). It is thus of interest that *Metatomarctus canavus* is also recognizable in both locations. The coexistence of both species in the early Hemingfordian of Florida and Nebraska is further evidence of the broad zoogeographic distribution of these medium-size canids.

#### *Metatomarctus* sp. A

*Tomarctus* cf. *T. optatus* (Matthew, 1924): Stirton, 1939a: 633.

REFERRED SPECIMENS: High Rock Canyon 2 (UCMP loc. 1107) (early Barstovian), Humboldt County, Nevada: UCMP 38290, left ramal fragment with crushed m1–m2; and UCMP 38301, right ramal fragment with m1 and broken m2.

DISTRIBUTION: Early Barstovian of Nevada.

DESCRIPTION AND COMPARISON: The most conspicuous features of this species and *Metatomarctus* sp. B are their slender cheek-teeth with narrow premolars and nearly longitudinally oriented shearing blade of m1. The two species are probably closely related and form a small clade of their own. Their relationships to other borophagines, however, are difficult to determine, owing to the paucity of materials. Although the longitudinally oriented shearing blades resemble those of *Psalidocyon*, we chose to view this as a parallel development because of other morphological differences. For example, this species pair lacks the anteriorly canted p3 main cusp (seen only in *Metatomarctus* sp. B) and m1 paraconid, features that are unique to *Psalidocyon*. Besides the extremely trenchant m1 trigonids, these two species seem to fall within the stage of evolution of *Metatomarctus*. It is likely that they form a small clade derivable from the base of *Metatomarctus*, and when more is known about their morphology, they may deserve a generic status of their own.

Only the m1–m2 are available from the two referred specimens of *Metatomarctus* sp. A. Although mediolateral compression of UCMP 38290 has certainly contributed to its slender appearance, the m1 on UCMP 38301 is essentially not deformed. The shearing blade (trigonid) on both specimens is even more longitudinally oriented than in *Psalidocyon*. Our scant knowledge of this form makes it inappropriate to erect a new species.

#### *Metatomarctus* sp. B

*Tephrocyon*? compare *rurestris* (Condon, 1896): Merriam, 1911: 239, fig. 8a, b; 1913: 370, fig. 15a, b.

*Tephrocyon*? sp: Merriam, 1911: 241, fig. 9a, b; 1913: 370, fig. 16a, b.

*Tomarctus* large species: Downs, 1956: 236.

REFERRED SPECIMENS: High Rock Canyon 2 (UCMP loc. 1107) (early Barstovian), Humboldt County, Nevada: UCMP 12503, left ramal fragment with p4–m1 (Merriam, 1911: fig. 8; 1913: fig. 15a, b); and UCMP 12504, left ramal fragment with p4–m1 (Merriam, 1911: fig. 9; 1913: fig. 16a, b).

DISTRIBUTION: Early Barstovian of Nevada.

DESCRIPTION AND COMPARISON: Preservation of the above referred specimens is slightly better than for *Metatomarctus* sp. A. With the presence of the p3, the trenchant morphology of the lower cheekteeth is even more evident than in *Metatomarctus* sp. A. The sharp-edged p3 and m1 trigonid once again remind one of the conditions in *Psalidocyon*, but other details are inconsistent with the latter genus. As noted for *Metatomarctus* sp. A above, we consider the trenchant cheekteeth in this species an independent character from *Psalidocyon*, an assertion to be verified by future discoveries.

As noted by Stirton (1939a: 633), there is a large size difference among the High Rock Canyon dogs. There are clearly two size groups (e.g., m1 length of UCMP 38290 is 19.3 mm as compared to 24.5 mm in UCMP 10254), indicating the coexistence of two sister-species of this peculiar clade. Close examination also reveals that there may be more than one taxon among the large-size group (*Metatomarctus* sp. B). UCMP 10253 has a relatively wider m1 talonid than in UCMP 10254, a feature seen in hypocarnivorous clades such as *Cynarctus*. As is the case in *Metatomarctus* sp. A, we refrain from formally erecting a new species for *Metatomarctus* sp. B because of insufficient materials.

#### *Euoplocyon* Matthew, 1924

TYPE SPECIES: *Aelurocyon?* *brachygnathus* Douglass, 1903.

INCLUDED SPECIES: *Euoplocyon spissidens* (White, 1947) and *Euoplocyon brachygnathus* (Douglass, 1903).

DISTRIBUTION: Early Hemingfordian of Florida; and early Barstovian of Montana, Nebraska, California, and Oregon.

EMENDED DIAGNOSIS: A single derived character that distinguishes *Euoplocyon* from

*Metatomarctus* and more primitive taxa is the presence of two lateral cusplets on I3. *Euoplocyon* lacks the enlarged parastyle on P4 that is present in *Psalidocyon* and others. It does not have a posteriorly extended nuchal crest, as found in *Microtomarctus* and later clades. On the other hand, it has a primitively large opening for the external auditory meatus, in contrast to the narrow openings in *Cynarctus* and *Metatomarctus* and more derived taxa. Autapomorphies of *Euoplocyon* include an elongated paroccipital process with a long free tip (seen only in *E. brachygnathus*) and a hypercarnivorous dentition with reduced M1 metaconule, m1 protoconid tall and trenchant, m1 metaconid usually absent but occasionally present as a weak crest (but never a distinct cusp), m1 talonid trenchant with a dominant and centrally located hypoconid, m1 entoconid reduced to a weak cingulum, and m2 metaconid reduced or absent.

DISCUSSION: Among medium-size borophagines, *Euoplocyon* is the most hypercarnivorous in terms of its trenchant lower carnassial. The development of a trenchant talonid of carnassial in *Euoplocyon* and other extinct and living taxa such as *Enhydrocyon*, *Cuon*, *Speothos*, and one species of *Aelurodon* (e.g., *A. taxoides magnus* Thorpe, synonymized with *A. ferox* in this study) inspired Matthew (1924, 1930) to place them all in a group to be distinct from the "typical" canids with basined talonids. Recent studies by us on the extinct hesperocyonines (Wang, 1994) and living canines (Tedford et al., 1995) demonstrate that hypercarnivorous dentitions, as in hypocarnivorous and mesocarnivorous ones, are equally subject to parallelisms. A completely trenchant talonid developed at least five times in the two other major clades of canids: three times among the living canines (in *Speothos*, the *Cuon-Lyaon* clade, and the extinct South American *Protocyon* [Berta, 1988]), and twice among the hesperocyonines (in *Enhydrocyon* and *Ectopocynus*), although the hesperocyonines initially had a rather trenchant talonid. The borophagines independently developed trenchant heels at least twice: in *Euoplocyon* and in advanced *Aelurodon*.

Tedford and Frailey (1976) first pointed out a possible relationship of *Euoplocyon*

with advanced borophagines such as *Tomarctus* and *Aelurodon*, based mostly on dental similarities. We now have cranial materials that show a generalized skull without the advanced cranial features in advanced borophagines such as *Aelurodon*. Such cranial structures suggest a relatively basal position in the phylogeny, near *Psalidocyon* and *Microtomarctus*.

Dentally, the hypercarnivorous morphology in *Euoplocyon* appears rather suddenly without intermediate forms, given the phylogenetic position postulated in this study. When the relatively more primitive *E. spissidens* first appears in the late early Hemingfordian Thomas Farm Local Fauna, its lower carnassial is already that of a highly advanced form. None of the other Hemingfordian or earlier borophagines display any tendency toward a trenchant talonid on m1 (most are in the opposite direction toward a more basined talonid). This may suggest that *Euoplocyon* originated in the southern part of North America, where vertebrate fossils earlier than the Thomas Farm Local Fauna are poorly represented. The fact that similar-size canids, such as *Osbornodon iammonensis* and *Metatomarctus canavus*, occur in both the Hawthorn Formation in Florida and the Runningwater Formation in Nebraska, whereas *E. spissidens* is restricted to Florida, further suggests that *E. spissidens* could have dispersed to the northern Great Plains but did not.

*Euoplocyon spissidens* (White, 1947)

Figure 60N–Q

*Aelurocyon spissidens* White, 1947: 497, fig. 1A, B.

*Parictis bathygenus* White, 1947 (in part): 500, fig. 2A.

*Enhydrocyon spissidens* (White): Olsen, 1958: 597, fig. 3A–C.

*Euoplocyon spissidens* (White): Tedford and Frailey, 1976: 5, fig. 2C, D. Munthe, 1998: 136.

*Osbornodon iammonensis* (Sellards, 1916): Wang, 1994 (in part): 120 (MCZ 3930 only).

**HOLOTYPE:** MCZ 4246, (AMNH cast 56015), left partial ramus with p2–p3 alveoli, p4–m1, and m2 alveolus (fig. 60N, O) from the Thomas Farm Local Fauna, Hawthorn Formation (late early Hemingfordian), Gilchrist County, Florida.

**REFERRED SPECIMENS:** From the type local-

ity: MCZ 3930 (AMNH cast 129639), left partial maxillary with P4–M2 (referred to *Parictis bathygenus* White, 1947: fig. 2A); and MCZ 7310 (AMNH cast 56017) (Tedford and Frailey, 1976: fig. 2C, D), left partial ramus with p4–m2 (fig. 60P, Q).

**DISTRIBUTION:** Late early Hemingfordian of Florida.

**EMENDED DIAGNOSIS:** Primitive characters that distinguish *E. spissidens* from *E. brachygnathus* are p4 less robust, m1 and m2 talonids longer and wider, m2 metaconid distinct but smaller than protoconid, and lower tooththrow and anterodorsal part of horizontal ramus less deflected laterally.

**DESCRIPTION AND COMPARISON:** Almost no additional material is available except the present reference of a maxillary fragment (MCZ 3930) previously referred to *Parictis bathygenus* by White (1947: 500) and to *Osbornodon iammonensis* by Wang (1994: 120). This maxillary has canidlike upper molars and cannot belong to the same species represented by the holotype lower jaw of the ursoid *Parictis* (?*Cynelos*) *bathygenus*. The size of the upper carnassial is significantly smaller than the type of *O. iammonensis*, and its relatively small M2 is in sharp contrast to the enlarged M2 in *O. iammonensis*. The upper teeth of MCZ 3930 compare favorably, both in size and shape, to those of *E. brachygnathus*. The only subtle difference is a more posteriorly positioned P4 protocone than is the case in *E. brachygnathus*. If the present reference is correct, reduction of the metaconule of M1 in *E. spissidens* is already as advanced as that in *E. brachygnathus*, as would be expected for the highly trenchant m1 of *E. spissidens*.

The anterior horizontal ramus of *Euoplocyon spissidens* is not laterally deflected as in *E. brachygnathus*. Of the few known lower teeth, *E. spissidens* is little different from *E. brachygnathus* in dental dimensions (appendix III)—the two species are almost indistinguishable on the ratio diagram (fig. 48). Qualitatively, however, the early Hemingfordian *E. spissidens* possesses a few primitive features relative to the early Barstovian *E. brachygnathus*: the m1 entoconid shelf, although considerably reduced, is slightly wider than in *E. brachygnathus*; and the m2 metaconid is not yet completely lost.

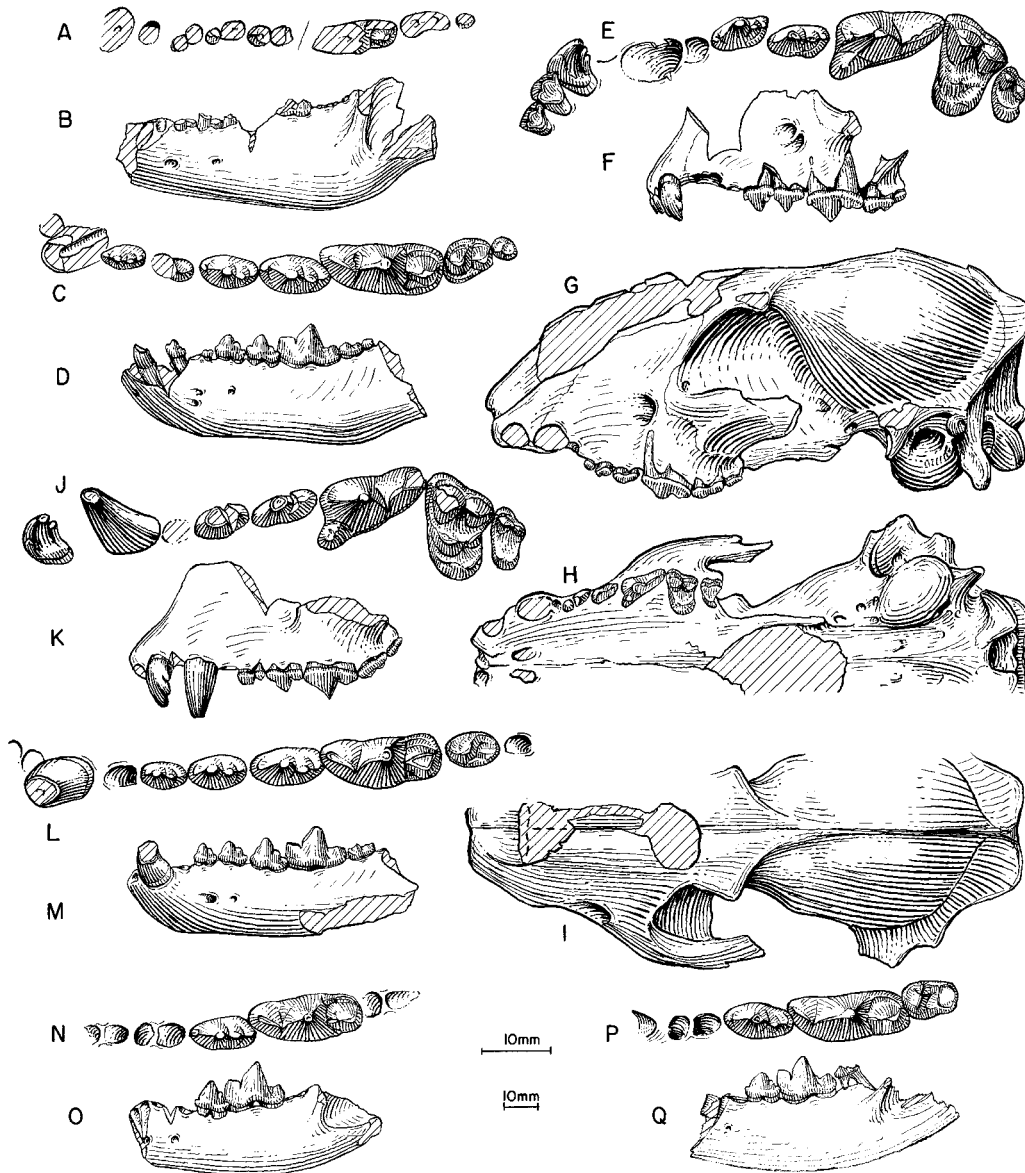


Fig. 60. **A**, Occlusal and **B**, lateral views of ramus, *Euoplocyon brachygnathus*, CMNH 752, holotype, near New Chicago, Flint Creek beds (early Barstovian), Granite County, Montana. **C**, Lower teeth and **D**, ramus, *E. brachygnathus*, AMNH 18261 (holotype of *E. praedator*), Sheep Creek Quarry, Olcott Formation (early Barstovian), Sioux County, Nebraska. **E**, Upper teeth and **F**, lateral view of maxillary, *E. brachygnathus*, F:AM 25489, Trojan Quarry, Olcott Formation, Sioux County, Nebraska. **G**, Lateral, **H**, ventral, and **I**, dorsal views of skull (reversed from right side), *E. brachygnathus*, F:AM 50120, Steep Side Quarry, Green Hills Fauna, Barstow Formation (early Barstovian), San Bernardino County, California. **J**, Upper teeth and **K**, lateral view of maxillary, *E. brachygnathus*, F:AM 50123, Steep Side Quarry. **L**, Lower teeth and **M**, ramus (m2 reversed from right side), *E. brachygnathus*, F:AM 27314, Barstow Formation. **N**, Lower teeth and **O**, ramus, *E. spissidens*, MCZ 4246, holotype, Thomas Farm Local Fauna, Hawthorn Formation (early Hemingfordian), Gilchrist County, Florida. **P**, Lower teeth and **Q**, ramus, *E. spissidens*, MCZ 7310, Thomas Farm Local Fauna. The longer (upper) scale is for **A**, **C**, **E**, **J**, **L**, **N**, and **P**, and the shorter (lower) scale is for the rest.

DISCUSSION: With the fragmentary materials available, we have little more information than when this species was last examined by Tedford and Frailey (1976). Consequently, the various arguments proposed in that paper for assignment of this Thomas Farm species to *Euoplocyon* are still valid, and little can be added except the larger phylogenetic perspective afforded in this study.

If *spissidens* is correctly referred to *Euoplocyon* as a primitive species of that genus, it follows that the broadened palate and the associated lateral deflection on the lower jaw of *E. brachygnathus* must have been derived within the *Euoplocyon* clade, independent from those in advanced borophagines such as *Aelurodon* and *Epicyon*. As commented under the genus *Euoplocyon*, these features, as commonly associated with hypercarnivorous dentitions, have been developed several times during the history of the Canidae.

*Euoplocyon brachygnathus* (Douglass,  
1903)

Figure 60A–M

*Aelurocyon? brachygnathus* Douglass, 1903: 173, fig. 16.

*Euoplocyon praedator* Matthew, 1924: 103. Tedford and Frailey, 1976: 6, fig. 2A, B. Munthe, 1998: 136.

*Euoplocyon?* sp. Gazin, 1932: 50, fig. 3.

?*Aelurodon brachygnathus* (Douglass): Vanderhoof and Gregory, 1940: 152.

*Aelurodon brachygnathus* (Douglass): McGrew, 1944b: 79.

HOLOTYPE: CMNH 752 (AMNH cast 101208), left partial ramus with i1–i3 broken alveoli and c1–m3 all represented by roots or broken teeth (fig. 60A, B), near New Chicago, Flint Creek beds (early Barstovian), Granite County, Montana.

REFERRED SPECIMENS: From the Olcott Formation (early Barstovian), Sioux County, Nebraska: AMNH 18261, left ramus with i1–i3 alveoli, c1 broken, and p1–m3 (p2 broken) (fig. 60C, D), Sheep Creek Quarry (holotype of *Euoplocyon praedator* Matthew, 1924); F:AM 25488, left partial ramus with i1–p1 alveoli and p2–m1 (p4 alveolus), Humbug Quarry; F:AM 25489, left premaxillary and maxillary with I1–M2 (C1–P1 alveoli) (fig. 60E, F), Trojan Quarry (Sinclair Quarry No. 4, horizon A); F:AM 25442, left ramus with

i1–i3 alveoli, c1–m2, and m3 alveolus, Echo Quarry; F:AM 25443, left ramus with i1–m3 (p1 and p3 alveoli), Echo Quarry; F:AM 105333, left partial ramus with i1–p1 alveoli, p2, and p3–m1 all broken, Echo Quarry; and F:AM 129867, left ramus with i1–i3 alveoli, broken c1, p1 alveolus, and broken p2–m3, Quarry 2.

Green Hills Fauna, Barstow Formation (early Barstovian), San Bernardino County, California: F:AM 27225, left ramus with c1 broken–m2 and m3 alveolus, Green Hills; F:AM 27314, partial mandible with c1–m2 (p1 and m3 alveoli) (fig. 60L, M), ?Second Division; F:AM 27315, right and left partial rami with unerupted p4–m3, Green Hills; F:AM 27315A, left immature partial ramus with c1 erupting, unerupted p3 and p4, and m2–m3; F:AM 27315B, right and left rami with i3–m1 and m2–m3 alveoli, Green Hills; F:AM 27532, left premaxillary and left and right partial maxillae with I1–I2 roots and I3–M2, Green Hills; F:AM 50120, crushed skull with I3–P1 alveoli and P2 broken–M2 (fig. 60G–I), Steep Side Quarry; F:AM 50122, left partial maxillary with I3 broken–P3 and P4 broken, Steep Side Quarry; F:AM 50123, left premaxillary–maxillary with I1–I2 alveoli and I3–M2 (P1 alveolus and P2 broken) (fig. 60J, K), Steep Side Quarry; F:AM 67325, right partial ramus with p2–p3 alveoli and p4 broken–m1, Steep Side Quarry, upper level; and F:AM 67326, left partial ramus with p1 alveolus, p2–p3 both broken, p4–m1, and m2 alveolus (F:AM 67325 and 67326 being possibly one individual), Steep Side Quarry; and F:AM 67327, right partial premaxillary–maxillary with I1–P2, Steep Side Quarry.

Skull Spring Local Fauna (LACM-CIT loc. 57), Butte Creek Formation (early Barstovian), Malheur County, Oregon: LACM-CIT 392, left isolated m1 (Gazin, 1932: fig. 3).

DISTRIBUTION: Early Barstovian of Montana, Nebraska, California, and Oregon.

EMENDED DIAGNOSIS: Derived characters that separate *Euoplocyon brachygnathus* from *E. spissidens* are p4 more robust; m1–m2 talonids shorter and narrower, metaconid absent; and lower tooththrow and anterodorsal part of the horizontal ramus strongly deflected laterally. Autapomorphies for *E. brach-*

*ynathus* (although their status in *E. spissidens* is unknown) include mastoid large and knoblike, long free tip of paroccipital process, and partitioned infraorbital canal.

**DESCRIPTION AND COMPARISON:** Cranial morphology of this species is known only from a crushed skull from the Barstow Formation (F:AM 50120). Reference of this skull is based on its short snout and broad palate, which correspond to similarly shortened mandible and lateral deflected lower premolars, and secondarily on the entirely shearing mode of wear on its premolars, as would be expected for a highly hypercarnivorous lower dentition. Furthermore, its narrowed heel of M1 that lacks a metaconule is what would be expected for a trenchant talonid of m1. F:AM 50120 suffers from heavy crushing on top of the skull. This distortion and the advanced age of this individual (as indicated by heavy wear) make many bony sutures difficult to recognize. Thus, it is not clear whether the premaxillary is in contact with the frontal, although this is likely because of well-developed lateral cusplets on I3, which seem related to a stronger, more securely anchored premaxillary process. A moderate frontal sinus is probably present on F:AM 50120, judging from the slightly enlarged supraorbital region. However, the sinus does not seem to extend behind the post-orbital constriction because of a lack of inflation in this area typically associated with a large sinus. The nuchal crest is low and lacks the posterior extension seen in *Microtomarctus* and more advanced taxa. The most unambiguous hypercarnivorous feature of the skull is its broadened palate and shortened rostrum (palate width at P1 and length of P1–M2 in fig. 47), apparently in parallel with similar features in *Aelurodon* and the *Epi-cyon–Borophagus* clade. The opening for the external auditory meatus is large with a V-shape notch on the anterior edge of the opening, and lacks a bony lip for the meatus. The mastoid process of *E. brachygnathus* is inflated, as in *Enhydrocyon*, but in contrast to the latter, the paroccipital process is prominently elongated so that it has a free tip 9 mm long. These peculiarities in the mastoid and paroccipital processes are apparently autapomorphies, since taxa above and below *Euoplo-cyon* lack these features. Another aut-

apomorphic feature is a tendency for the infraorbital canal to be partitioned into two foramina by a septum—a complete septum is present in F:AM 25489, and a partial septum is seen on the right side of F:AM 50120 (the left canal is undivided).

Except for the highly hypercarnivorous lower carnassial, teeth of *Euoplo-cyon brachygnathus* exhibit typical medium-size borophagine characteristics, with well-developed cusplets on incisors and premolars. Two distinct lateral cusplets are present on I3 (seen on F:AM 25489, 50123, and 67327), and the premolars are similarly cuspidate with distinct cingular and accessory cusplets, even on P1 and p1, features that are not seen in *Enhydrocyon*. A parastyle on P4 is almost entirely lacking in the Barstow sample, and it is weakly developed in only one individual (F:AM 25489) from the Snake Creek sample. The wear on the upper premolars in F:AM 50120 (fig. 60H) represents mostly a shearing mode (a longitudinal, nearly vertical facet on the lingual face of all premolars that are self-sharpening), in contrast to a predominantly crushing mode of wear in most mesocarnivorous borophagines (flattening of the principal cusps of the premolars). The M1 is slender and its metaconule is conspicuously absent among closely related borophagines that always have a distinct metaconule. Reduction of the metaconule is consistently correlated with a trenchant m1 talonid, as seen in hypercarnivorous canines (e.g., *Speothos*) and hesperocyonines (e.g., *Enhydrocyon*). The M2 is reduced relative to the M1.

Evidence for hypercarnivory is more clearly seen on the lower teeth, especially the m1. As in *Euoplo-cyon spissidens*, the metaconid is lost in all individuals. In general, the talonid of m1 is more reduced (narrowed) than in *E. spissidens*. The entoconid either is completely lacking or is represented by a narrow and low cingulum on the lingual edge of the talonid. In all individuals, the metaconid on m2 is lost except for a transverse crest leading down the apex of the protoconid, in contrast to the small metaconid in *E. spissidens*.

**DISCUSSION:** No additional material of *Euoplo-cyon brachygnathus* is known from the type locality. Although the only tooth fragment remaining on the holotype is a partial



talonid of m1, as well as the roots of the cheekteeth, the horizontal ramus (fig. 60A, B) displays the characteristic shape of this species, which is much better represented in material from the Olcott Formation of Nebraska and the Barstow Formation of California. The combination of a short and deep horizontal ramus with a laterally deflected anterodorsal region is not seen in other contemporaneous canids. Its narrow and trenchant m1 talonid and its close spacing of the cheekteeth provide additional evidence that *E. brachygnathus* is conspecific with *E. praedator* from the Lower Snake Creek Fauna. As such, *E. brachygnathus*, a fitting name but based on a poorly preserved holotype, has priority over Matthew's *E. praedator*.

As the terminal member of a small, precociously hypercarnivorous clade, *Euoplocyon brachygnathus* displays several traits convergent with those in the *Aelurodon* clade. For example, a broadened palate and the associated lateral eversion of the anterior mandible are typical features of the latter clade. Dentally, *E. brachygnathus* also shares with the *Aelurodon* clade a reduced M2 and m2, as well as a general trend of a reduced M1 metaconule and narrowed m1 talonid. However, the generally primitive cranial configuration of *E. brachygnathus* (e.g., relatively small frontal sinus, nuchal crest not expanded, and large opening for auditory meatus) indicates a phylogenetic position close to *Metatomarctus*, not to *Aelurodon*.

### *Psalidocyon*, new genus

TYPE SPECIES: *Psalidocyon marianae*, new species.

ETYMOLOGY: Greek: *psalido*, scissors; *cyon*, dog.

INCLUDED SPECIES: Type species only.

DISTRIBUTION: Early Barstovian of New Mexico and Nebraska.

DIAGNOSIS: A synapomorphic feature shared with *Microtomarctus* and higher taxa is a pronounced P4 parastyle, which is absent in *Euoplocyon* and more primitive taxa. Derived characters unique to this genus are incisors tall-crowned and complex; canine large with lingual surface compressed and concave, anterolingual crest and posterolingual crest present; P1–P3 and p1–p4 tall-

crowned and complex with sharp anterior and posterior blades; m1 trigonid very open with sectorial paraconid-protoconid blade and metaconid very large; m2 metaconid large, much taller than protoconid; and deep horizontal ramus. Characters of *Psalidocyon* that are primitive relative to *Microtomarctus* are nuchal crest not posteriorly expanded and lambdoidal crests unreduced.

### *Psalidocyon marianae*, new species

Figure 61

HOLOTYPE: F:AM 27397, skull with I1–M2, mandible with i1–m3 (fig. 61A–F) and associated limbs, including partial scapula, humerus, femur, tibia, and questionably associated partial manus and nearly complete pes, from southeast of White Operation, Skull Ridge Member, Tesuque Formation (early Barstovian), Santa Fe County, New Mexico.

ETYMOLOGY: Named in honor of Marian Galusha for her contributions in the field and office during and following the work of the Frick Laboratory in the southwestern United States.

REFERRED SPECIMENS: From Olcott Formation (early Barstovian), Sioux County, Nebraska: F:AM 25490, right partial ramus with c1–p4 and m1 broken, Trojan Quarry (= Quarry 4 of Horizon A); F:AM 61295, left partial ramus with i1–p1 alveoli and p2–m1, Humbug Quarry; F:AM 61296, right partial ramus m1–m2 and m3 alveolus (fig. 61G, H), Echo Quarry; F:AM 61297, left partial ramus i2–m1 (p1–p2 broken), Echo Quarry; and F:AM 61298, right partial ramus with m1–m2 and m3 alveolus, Quarry 2.

DISTRIBUTION: Early Barstovian of New Mexico and Nebraska.

EMENDED DIAGNOSIS: As for genus.

DESCRIPTION AND COMPARISON: The holotype skull and mandible are only slightly crushed laterally. In overall cranial proportions, *Psalidocyon* closely resembles *Desmocyon matthewi* (fig. 62). The premaxillary process appears to be in contact with the nasal process of the frontal, although breakage in this area makes the observation less certain. The dorsal profile of the skull indicates a well-developed frontal sinus extending posteriorly to the frontal-parietal suture. The nu-

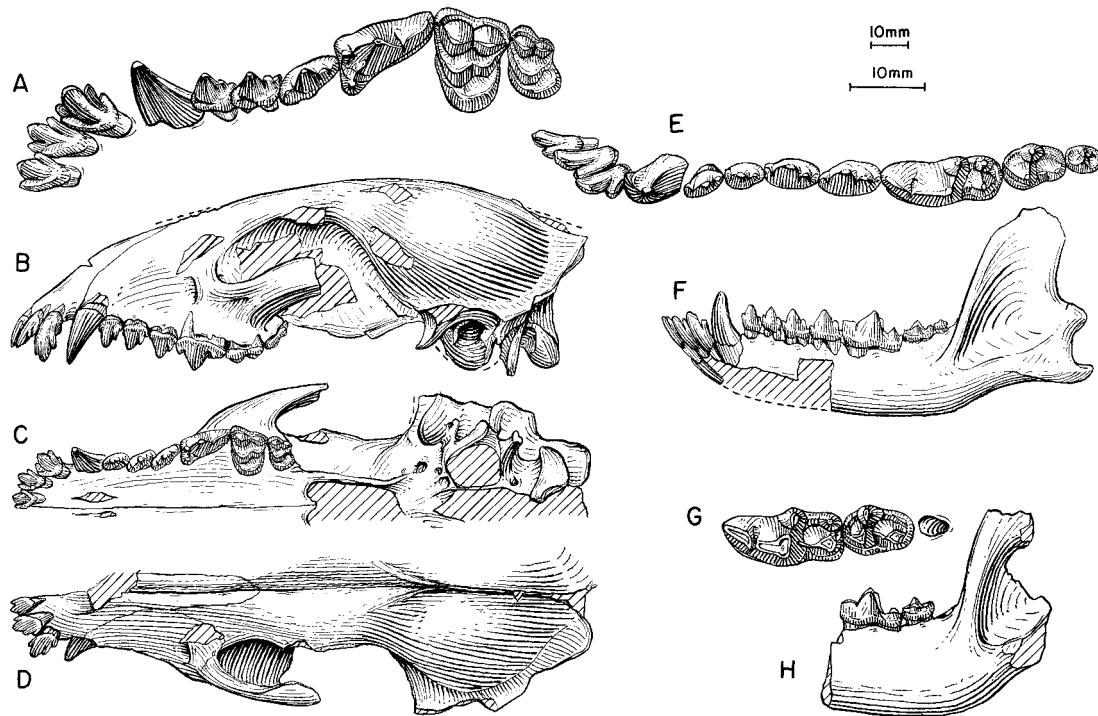


Fig. 61. *Psalidocyon marianae*. **A**, Upper teeth (I1–I2 reversed from right side), **B**, lateral, **C**, ventral, and **D**, dorsal views of skull, **E**, lower teeth, and **F**, ramus (p2, m2, and ascending ramus reversed from right side), F:AM 27397, holotype, southeast of White Operation, Skull Ridge Member, Tesuque Formation (early Barstovian), Santa Fe County, New Mexico. **G**, Lower teeth and **H**, ramus (reversed from right side), F:AM 61296, Echo Quarry, Olcott Formation (early Barstovian), Sioux County, Nebraska. The shorter (upper) scale is for B, C, D, E, and H, and the longer (lower) scale is for the rest.

chal crest is fan-shaped in the posterior view. The lambdoidal crest is sharp and unreduced. Both bullae are broken, especially the caudal entotympanic part. The opening for the external auditory meatus is large and lacks an external lip. The paroccipital process is laterally expanded and forms a deep pocket between it and the bulla. The mastoid process is small and recedes beneath a prominent horizontal shelf. The horizontal ramus has a weak subangular lobe.

The entire dentition of the holotype is nearly perfectly preserved. Although all permanent teeth are fully erupted, there is little trace of wear on any tooth. Dental morphology of this species is quite unusual in its development of sharp blades along the entire dental battery from incisors through premolars. These sharp blades are formed on the lateral edges of the incisors and on the an-

terior and posterior edges of the main cusps of canines and premolars. The cutting edges are further enhanced by the high crowns of these teeth. Despite the sharp blades on the premolars, the tips of these teeth usually indicate apical rather than shearing wear, as is common in most borophagines of similar size. The upper incisors are procumbent and have a prominent main cusp with one or two accessory cusps on either side. The C1 is short and straight with a strong anterolingual ridge that bends lingually to form a lingual groove on the canine. The large upper and lower premolars are imbricated within the jaws in young individuals. Premolar accessory and cingular cusps are distinct, and the right P2 in the holotype even has two posterior accessory cusplets that create a serrated posterior cutting edge. The premolars also have a narrow lingual cingula. The P4 has a

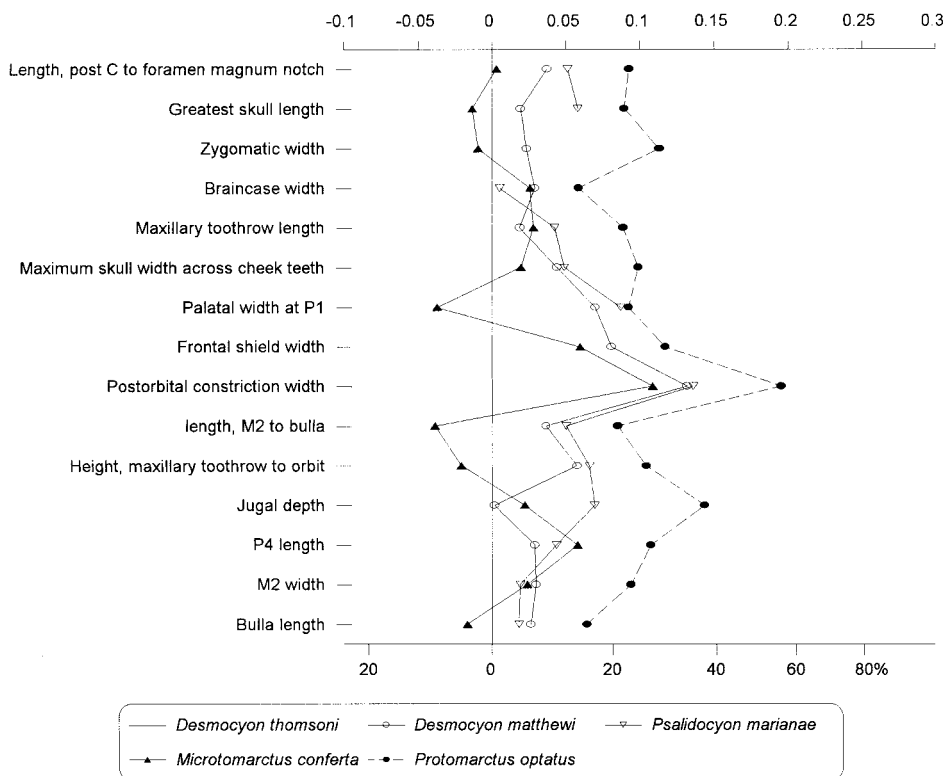


Fig. 62. Log-ratio diagram for cranial measurements of *Desmocyon*, *Psalidocyon*, *Microtomarctus*, and *Protomarctus* using *Desmocyon thomsoni* as a standard for comparison (straight line at zero). See text for explanations and appendix II for measurements and their definitions.

distinct parastyle, and its protocone is reduced. Like other premolars, the anterior and posterior blades of the P4 paracone are sharp-edged. The upper molars remain primitive and are indistinguishable from those of *Metatomarctus*.

The lower incisors have a large medial cusp and smaller, but distinct lateral cusps. Like the upper canines, the anterolingual ridge of the lower canine bends lingually to form a prominent groove. The outline of the m1 is more slender than for taxa of similar size. The cutting blade on m1 is more longitudinally oriented than in *Metatomarctus*, and the talonid cusps are more cuspidate with a strong transverse crest. The m2 has a dominant metaconid, exceeded only by advanced species of *Cynarctus*.

DISCUSSION: Although represented by a few ramal fragments only, *Psalidocyon marianae* is positively identified in the Olcott

Formation of Nebraska because of the highly characteristic dental morphology. Besides the autapomorphies mostly related to the blade-like incisors and premolars, the skull and upper molars of *Psalidocyon* are rather typical of medium-size, mesocarnivorous borophagines, not unlike those of *Desmocyon matthewi* and *Metatomarctus*. This combination of primitive and derived characters best places it above *Metatomarctus* and below *Microtomarctus*.

Rudimentary development of the bladelike premolars and canines can be found in a partial mandible (F:AM 49181; fig. 46C, D) from the early Hemingfordian of Nebraska, presently referred to *Desmocyon matthewi*. This individual shows sharp anterior crests on the premolars, a distinct anterolingual crest on the c1, and a thin-bladed lower carnassial. In the absence of upper dentitions, which are critical in evaluating relationships

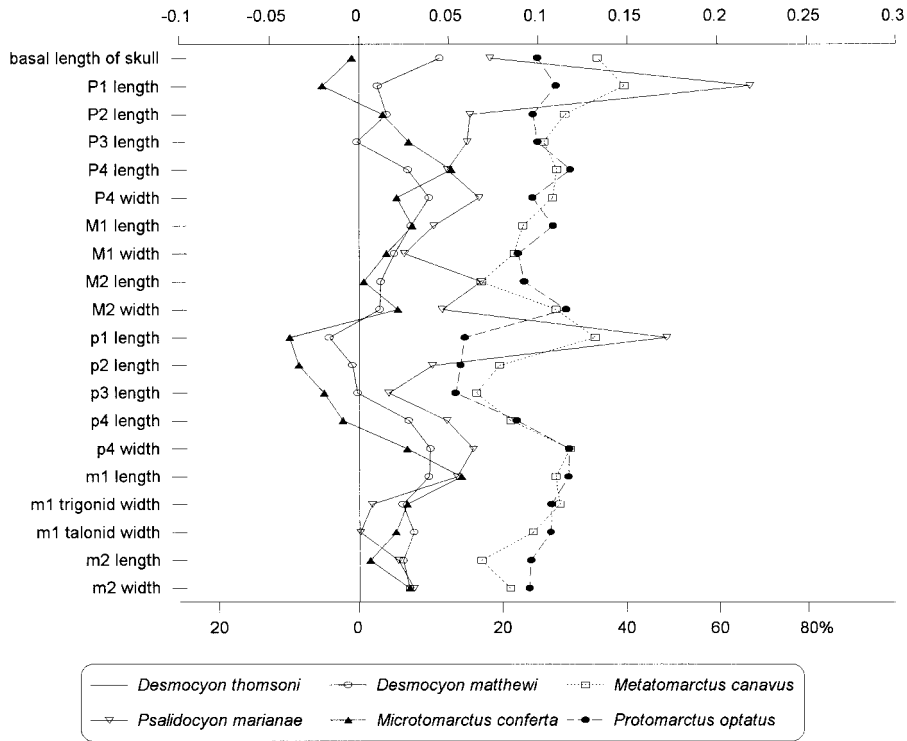


Fig. 63. Log-ratio diagram for dental measurements of *Desmocyon*, *Metatomarctus*, *Psalidocyon*, *Microtomarctus*, and *Protomarctus* using *Desmocyon thomsoni* as a standard for comparison (straight line at zero). See text for explanations and appendix III for summary statistics of measurements and their definitions.

of closely related species, we chose to explain these features on F:AM 49181 as an individual variation of *D. matthewi*, rather than as an early occurrence or a primitive species of *Psalidocyon*. Such an earlier appearance of *Psalidocyon*-like features in a more primitive taxon of *D. matthewi* is roughly consistent with our phylogenetic conclusions, which place these two genera not far apart.

#### *Microtomarctus*, new genus

TYPE SPECIES: *Tephrocyon conferta* Matthew, 1918.

ETYMOLOGY: Greek: *micro*, small, plus *tomarctus*.

INCLUDED SPECIES: Type species only.

DISTRIBUTION: Late Hemingfordian of New Mexico; early Barstovian of Nevada, California, New Mexico, Nebraska, and Colora-

do; late Barstovian of Texas, California, Colorado, and New Mexico.

DIAGNOSIS: Synapomorphic features shared with *Metatomarctus* and higher taxa are posterior expansion of the nuchal crest that overhangs the occipital condyle, and lambdoidal crests suppressed. Characters unique to this genus are small size, brachycephalic skull, and small, short canines. Characters of *Microtomarctus* that are primitive relative to *Protomarctus* are frontal sinus relatively smaller and less complex, auditory meatus of large diameter with V-shaped opening, and a single lateral accessory cusplet on I3 (here interpreted as a reversal).

#### *Microtomarctus conferta* (Matthew, 1918)

Figures 64–66

?*Tephrocyon* cf. *temerarius* (Leidy, 1858): Matthew and Cook, 1909: 376 (AMNH 13859).

*Tephrocyon confertus* Matthew, 1918: 189, fig. 1.  
*Nothocyon vulpinus coloradoensis* Thorpe, 1922b: 430, fig. 2.  
*Tomarctus confertus* (Matthew): Matthew, 1924: 96, fig. 17. Hough, 1948: 107. Downs, 1956: 237.  
*Tomarctus paulus* Henshaw, 1942: 105, pl. 2, figs. 3, 4a. Downs, 1956: 237. Munthe, 1998: 135.  
*Nothocyon vulpinus* (Matthew, 1907): Galbreath, 1953: 100.  
*Tomarctus* cf. *T. paula* (Henshaw): Honey and Izett, 1988: 20, fig. 8.  
*Tomarctus?* *confertus* (Matthew): Munthe, 1998: 135.

HOLOTYPE: AMNH 17203, right ramus with i1–i3 alveoli, c1–m2 (p1 and p3 alveoli) (fig. 64A, B), 23 mi south of Agate, Lower Snake Creek Fauna, Olcott Formation (early Barstovian), Sioux County, Nebraska.

REFERRED SPECIMENS: Lower Snake Creek Fauna, Olcott Formation (early Barstovian), Sioux County, Nebraska: AMNH 13859, left ramal fragment with c1–p4 alveoli, m1 broken, and m2–m3, 23 mi south of Agate (referred to *?Tephrocyon* cf. *temerarius* by Matthew and Cook, 1909: 376); AMNH 17204, left partial ramus with p3–m2, 23 mi south of Agate; AMNH 17205, left ramus with c1 and p1 alveolus–m2, 23 mi south of Agate; AMNH 17206, left partial ramus with m1–m2 and m3 alveolus, 23 mi south of Agate; AMNH 18253, partial skull, premaxillary missing, C1–P2 alveoli, and P3–M2, Quarry B, figured by Matthew (1924, fig. 17); AMNH 18254, left partial ramus with p3–p4 and all alveoli, Quarry A; AMNH 20056, 3 isolated teeth of two or more individuals, right M1 and two right m1s, 23 mi south of Agate; AMNH 20064, right ramal fragment with p4–m1, West Sinclair Draw; F:AM 61024, left partial ramus with c1, p1–p2 alveoli, p3–m1, and m2–m3 alveoli, Version Quarry; F:AM 61025, right partial ramus with i1–i3 alveoli, c1, p1 alveolus, p2–m2, and m3 alveolus, Humbug Quarry; F:AM 61026, right partial ramus with c1–p4, m1 broken–m2, and m3 alveolus, Echo Quarry; F:AM 61027, left partial ramus with c1 and p1 alveolus–m1, Quarry 2; F:AM 61028, right partial ramus with m1–m2 and m3 alveolus, New Surface Quarry; F:AM 61029, left partial ramus with c1–p3 alveoli, p4–m2, and m3 alveolus, Echo Quarry; F:AM 61030,

right ramal fragment with c1 alveolus and p2–p3, New Surface Quarry; F:AM 61031, partial skull with C1–P3 alveoli, P4, and M1–M2 alveoli, Echo Quarry; F:AM 61032, left partial maxillary with P2–P4, Echo Quarry; F:AM 61033, right ramus with i1–p1 all alveoli, p2–m2, and m3 alveolus, Echo Quarry; F:AM 61034, left partial ramus with p1–p2 alveoli, p3 broken–m2, and m3 alveolus, Quarry 2; F:AM 61035, left partial ramus with p2–p3 alveoli, p4–m1, and m2–m3 alveoli, Echo Quarry; F:AM 61036, right partial ramus with i3–c1 broken, p1 alveolus–m2 (p2 broken), Echo Quarry; F:AM 61037, left ramus with i1–i3 alveoli, c1, p1 alveolus–m2, and m3 alveolus, Echo Quarry; F:AM 61038, partial skull with P2–M2, Echo Quarry; F:AM 61039, partial skull with P2–M2 (fig. 64C–E), Echo Quarry; F:AM 67776, partial humerus, Echo Quarry; F:AM 67776B, partial humerus, Quarry 2; F:AM 67777A, partial radius, West Sand Quarry; F:AM 67778 and 67778A, partial ulna; F:AM 67787, femur, Echo Quarry; F:AM 67787A, partial femur, Echo Quarry; F:AM 67788, tibia, Echo Quarry; F:AM 67789, partial femur, New Surface Quarry; and AMNH 97232, detached teeth including P4, M2, and m1, Quarry A.

Green Hills Fauna, Barstow Formation (early Barstovian), San Bernardino County, California: F:AM 27272A, left and right maxillary fragments with P4–M2, second layer above Rak Division; F:AM 27284, right broken isolated P4, ?Second Division lower layer; F:AM 27297, left partial ramus with i3 broken–c1, p1 alveolus–m1, and m2 broken–m3 alveolus; F:AM 27297A, right and left rami with c1–m2, lower Green Hills Quarry; F:AM 27299, crushed skull with I1 broken–M2 and mandible with i1–m2, Deep Quarry; F:AM 27299A, crushed anterior part of skull with I3–P3 alveoli, P4–M1, and M2 alveolus, second layer above Third Division; F:AM 27299B, mandible with i1–m2 and m3 alveolus, Deep Quarry; F:AM 27299C, right crushed partial ramus with c1 broken, p2–p4, and m1–m2 both broken, Deep Quarry; F:AM 27530, crushed anterior part of skull with C1–P2 alveoli and P3–M2, lower Green Hills Quarry; F:AM 50121, fragmentary skull with P4 broken–M2, upper level of Steepside Quarry; F:AM 61019, right ramal

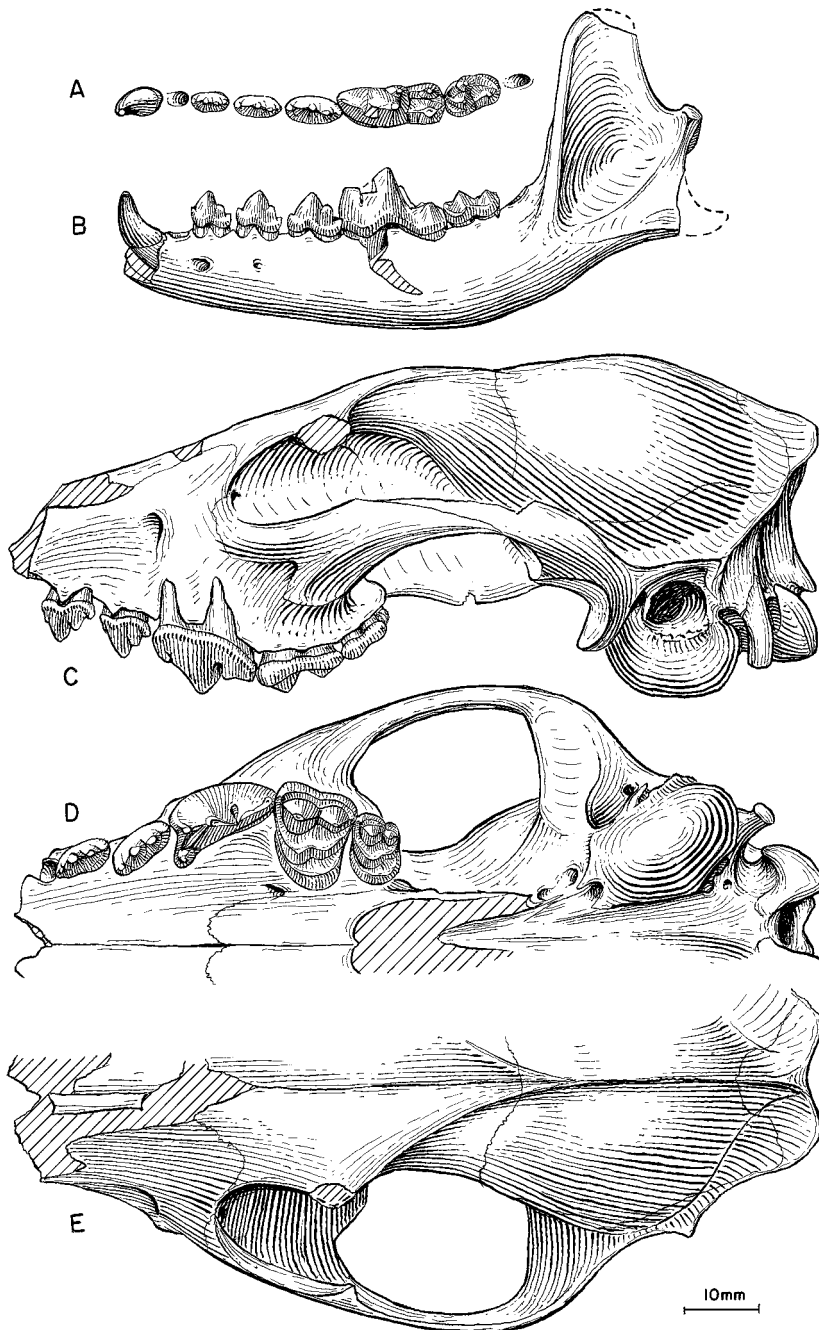


Fig. 64. *Microtomarctus conferta*. **A**, Lower teeth and **B**, ramus (reversed from right side), AMNH 17203, holotype, 23 mi south of Agate, Olcott Formation (early Barstovian), Sioux County, Nebraska. **C**, Lateral, **D**, ventral, and **E**, dorsal views of skull (bulla and P2 reversed from right side), F:AM 61039, Echo Quarry, Olcott Formation.

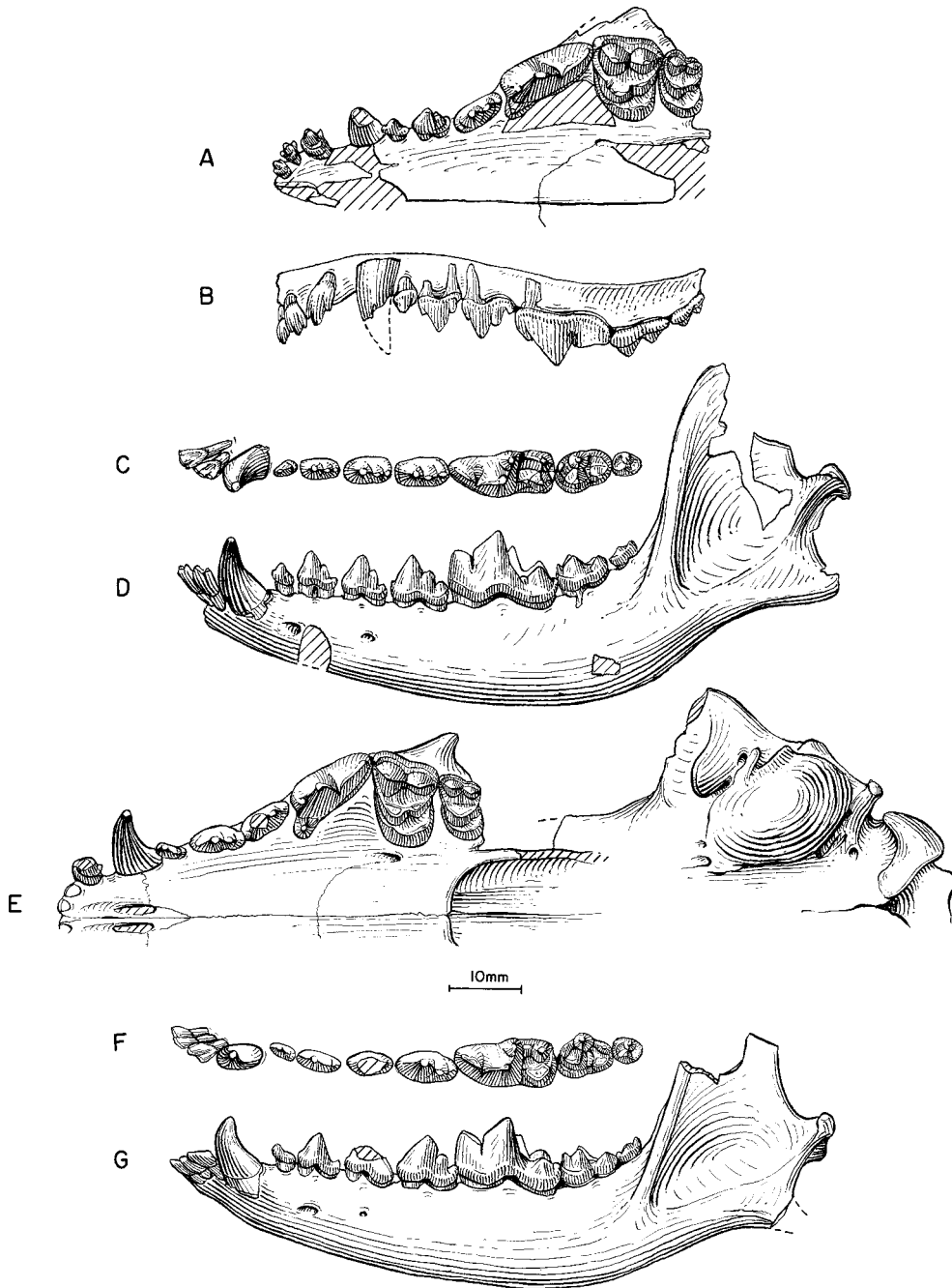


Fig. 65. *Microtomarctus conferta*. A, Ventral and B, lateral views of maxillary and upper teeth, C, lower teeth, and D, ramus, LACM-CIT 1229 (holotype of *Tomarctus paulus*), Siebert Formation, Tonopah Local Fauna (late early Barstovian), San Antonio Mountains, Nye County, Nevada. E, Ventral view of skull, F, lower teeth, and G, ramus, F:AM 27548, Skyline Quarry, "First Division," Barstow Formation (early late Barstovian), San Bernardino County, California.

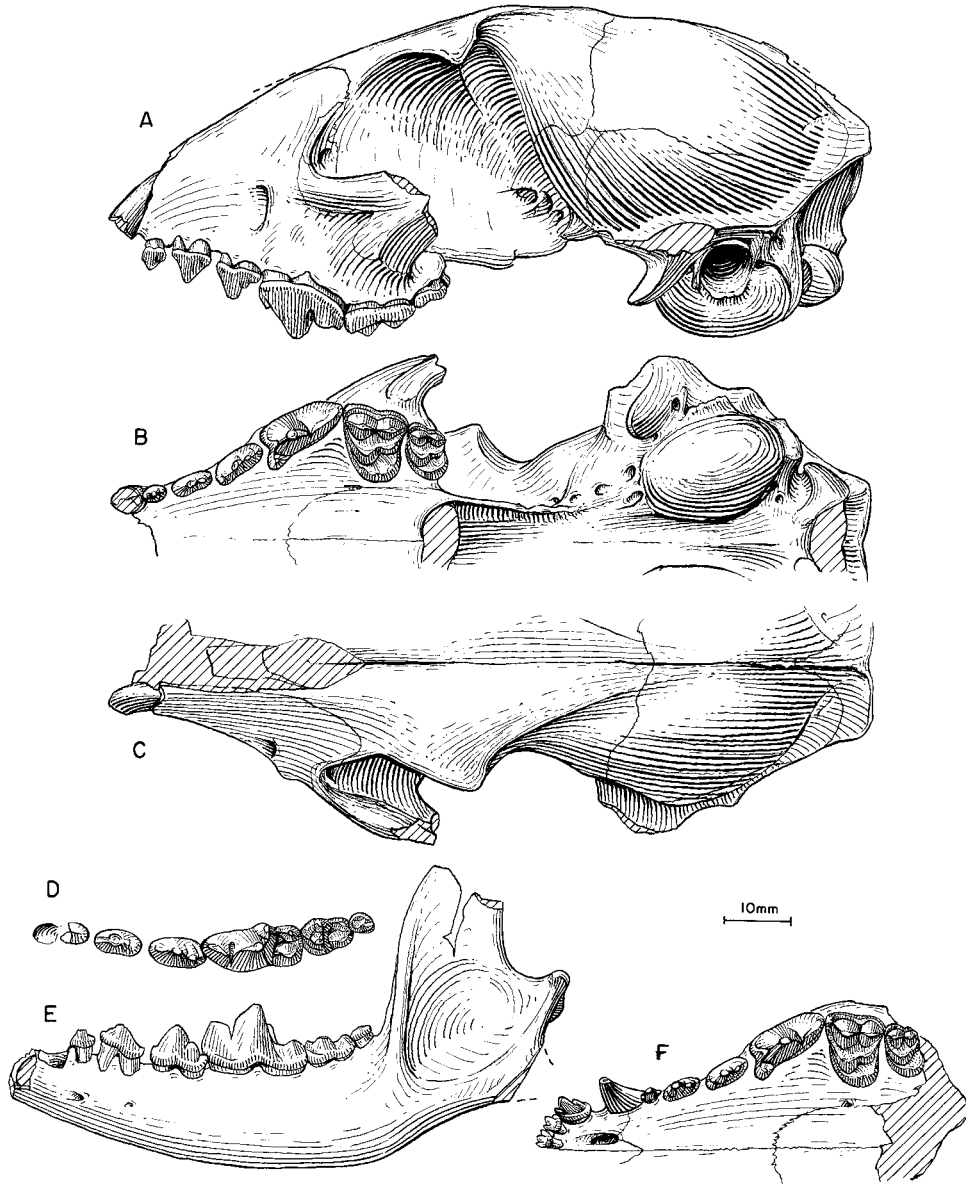


Fig. 66. *Microtomarctus conferta*. A, Lateral, B, ventral, and C, dorsal views of skull, D, lower teeth, and E, ramus (anterior part of ramus and p2–p3 reversed from right side), F:AM 27398X, Pojoaque Bluffs, Pojoaque Member, Tesuque Formation (early late Barstovian), Santa Fe County, New Mexico. F, Ventral view of partial skull (reversed from right side), F:AM 27398, Santa Cruz, Pojoaque Member, Tesuque Formation.

fragments with c1, p1 alveolus, p2, broken p3, and m1–m2, upper level of Steepside Quarry; F:AM 61019A, left ramal fragment with c1–m1 broken, upper level of Steepside Quarry; F:AM 61020, anterior half of skull with I1–P1 alveoli, P2, and P3 alveolus–M2

(M1–M2 broken), Steepside Quarry upper level; F:AM 61021, right partial maxillary with P4 broken–M2, Steepside Quarry upper level; F:AM 61022, left partial maxillary with P3–M2, Steepside Quarry upper level; and F:AM 61023, right partial ramus with c1



broken, p1 alveolus–m2, and m3 alveolus, Steepside Quarry upper level.

Yermo Local Fauna, 5 mi east of Yermo, Barstow Formation (early Barstovian), San Bernardino County, California: F:AM 27522, crushed anterior part skull with I1–P3 alveoli and P4–M2; F:AM 27527, right partial ramus with p3 broken–m3; F:AM 27527A, left partial ramus with c1, and p1 alveolus–m1; F:AM 27527B, left partial ramus with p2, p4 broken, and m1; F:AM 27527C, right partial ramus with c1–p1 alveoli, p2–m1 (p4 broken), and m2–m3 alveoli; 27527D, left partial ramus with p3 broken–m2 and m3 alveolus; F:AM 61063, right partial ramus with p2–p3 alveoli, p4–m1 both broken, and m2–m3 alveoli; F:AM 61063A, right partial ramus with m1 broken–m2 and m3 alveolus; F:AM 61063B, right partial maxillary with P4–M2; and F:AM 61063C, left partial maxillary with P4 broken–M2.

Kiva Quarry, 2 mi southwest of Zia Pueblo, Jemez Creek area, Zia Formation (late Hemingfordian), Sandoval County, New Mexico: F:AM 50143, right and left partial rami with c1–m2 and m3 alveolus.

Nambe Member, Tesuque Formation (late Hemingfordian), Santa Fe County, New Mexico: F:AM 67373, right partial ramus with i1–p2 all broken, p3, p4–m1 both broken, and m2–m3, north side of fault block south of Santa Cruz River drainage, 35 ft below No. 1 White Ash; and F:AM 105257, right partial ramus with m1–m2 both broken, East Cuyamunque, Nambe Pueblo Grant.

Skull Ridge area, Skull Ridge Member, Tesuque Formation (early Barstovian), Santa Fe County, New Mexico: F:AM 27383B, right partial ramus with p1–p2 alveoli, p3, p4 broken, and m1–m3 alveoli, Santa Cruz; F:AM 27391, right partial ramus with c1–m2 all broken; 27391A, left partial ramus with c1–p1 alveoli, and p2–m2 all broken; F:AM 27396A, left partial ramus with p3 broken–m3 (m1 broken); F:AM 27396B, right partial ramus with c1–p1 alveoli, and p2–m2 all broken, South Skull Ridge; F:AM 27396C, left partial ramus with p4–m2, 3 mi from Cuyamunque, left side of road; F:AM 27396D, anterior part of skull with I1–P3 alveoli and P4–M2 all broken; F:AM 27398Z, right partial maxillary with P4–M2 and right partial ramus with c1 broken–m3, south

Skull Ridge; F:AM 27473, skull with C1, P1–P3 alveoli, and P4–M2; F:AM 27478, right and left partial rami with p2 root and p3–m3, Upper Skull Ridge; F:AM 50164, anterior part of mandible with i1–c1 all broken, p1–p4, and m1 broken, west Cuyamunque, Tesuque Pueblo just south of north boundary; F:AM 50165, associated partial rami with p4–m3, Cuyamunque; F:AM 50166, right partial ramus with c1–p1 alveoli, p2, p3 alveolus, p4–m1 both broken, and m2 alveolus, base of channel above Ash “F”; F:AM 50167, partial mandible with i1–c1 all broken, p1 alveolus–p4, and m1–m2 both broken, Joe Rack Wash; F:AM 50168, left partial ramus with c1 broken, p1–p2 alveoli, and p3–m2 all broken, Skull Ridge, Nambe Creek side of Divide, 12 ft above Ash “B”; F:AM 50169, left partial ramus with p1–p2 alveoli, p3–m2, and m3 alveolus, 8 ft below Ash “B”; F:AM 50170, partial mandible with c1–m3 alveoli; F:AM 50171, left partial ramus with i3–c1 both broken, p1–p2 alveoli, p3 broken, P4, and m1 broken; F:AM 50172, partial skull with I3–M2, White Operation District above white layer; F:AM 50173, right partial ramus with c1–p3 all broken, p4, and m1–m3 all broken; F:AM 50174, right partial ramus with p4 broken–m2 and m3 alveolus; F:AM 50175, right partial ramus with c1–m2 all broken or roots, Skull Ridge area; F:AM 50176, right partial ramus with p4 and m1 broken; F:AM 50177Y, right m1, White Operation District; F:AM 50178, partial palate with left and right P4 broken and M1–M2, west Cuyamunque, white ash east of central fault; F:AM 50179, anterior part of skull with P3 broken–M2, North Skull Ridge, 40 ft above white layer; F:AM 50180, right and left partial maxillary with C1 and P2–M2, no locality data; F:AM 50182, left ramus with i1–m3, below white layer; F:AM 50188, crushed anterior part of skull with I1–M2 and both partial rami with c1 broken–m3 (m1 broken), Tesuque Grant between Arroyo Ancho and Rio Tesuque; F:AM 67336, left partial ramus with i1–p3 alveoli and p4–m3 all broken, north of Tesuque Grant, north boundary Tesuque East, Cuyamunque; F:AM 67337, right partial ramus with p4–m1 roots and m2 broken–m3, Joe Rack Wash, channel above

Ash "F"; and F:AM 67338, left ramus fragment with p4–m1 all broken.

Cold Spring Fauna, Fleming Formation (early late Barstovian), 8 mi south of Livingston, Polk County, Texas: F:AM 63292, right and left partial rami with p1, p2–p3 both broken, p4, m1 broken, m2, and m3 alveolus.

UCMP loc. V5433, Raine Ranch Formation (late early Barstovian), 3.5 mi south of Carlin, Elko County, Nevada: UCMP uncataloged (AMNH cast 80131), right ramus with c1–m2 and m3 alveolus.

Siebert Formation, LACM-CIT loc. 172, Tonopah Local Fauna (late early Barstovian), San Antonio Mountains, near Tonopah, Nye County, Nevada: LACM-CIT 1229 (AMNH cast 116109) (holotype of *Tomarctus paulus* Henshaw, 1942), anterior part of skull with I1–M2 with fragments and mandible with i2–m3 (fig. 65A–D); LACM-CIT 1232, right and left rami with c1, p1 alveolus, and p2–m3; LACM 15973, right ramus with c1–p4 alveoli and m1 broken; LACM 15975, left maxillary fragment with P4–M2 broken; and LACM 15976, left partial ramus with p3 broken–m1 and m2 root.

Valley View Quarry, "Second Division," Barstow Formation (late early Barstovian), San Bernardino County, California: F:AM 27533, skull with I1–C1 alveoli and P1–M2 and partial mandible with i2–c1 broken and p1–m3 (p3–m1 all broken); F:AM 27549, left ramus with c1 broken, p1 alveolus–m1, and m2 broken–m3 alveolus; F:AM 61042, crushed anterior part of skull with I3–P3 alveoli and P4–M2; F:AM 61043, left premaxillary-maxillary and right partial maxillary with I1–M2 (P1 alveolus); and F:AM 61056, left partial ramus with p1–p4 alveoli, m1 broken, and m2–m3 alveoli.

"First Division," Barstow Formation (early late Barstovian), San Bernardino County, California: F:AM 18012, right and left partial rami with c1 broken–p3 and p4 broken–m2, Mayday Quarry; F:AM 27253A, left ramus with i1–i3 alveoli, c1 broken, p1 alveolus–m2, and m3 alveolus, North End lower layer; F:AM 27270, right partial ramus with c1–p3 roots, p4, and m1 broken–m2 alveolus, Barstow area; F:AM 27291, right partial ramus with i3–c1 alveoli, p1, p2 alveolus–m1, and m2 alveolus, North End lower layer; F:AM 27294, crushed partial skull with P1 alveo-

lus–M2 (P2 broken), North End; F:AM 27296, left partial ramus with p2–m1, *Hemicyon* Stratum; F:AM 27298, right partial ramus with i1–p1 alveoli, p2–m2, and m3 alveolus, North End lower layer; F:AM 27298A, right partial ramus with i1–i3 alveoli and c1–m1 (p1 alveolus and p2 broken), *Hemicyon* Stratum; F:AM 27298B, left ramus fragment with p4–m1, *Hemicyon* Stratum; F:AM 27524, right maxillary fragment with P3 broken, P4–M2, North End; F:AM 27525, right ramus fragment with i1–i3 roots, c1 root, p1–p3, p4–m1 roots, and m2–m3, North End; F:AM 27526, right maxillary fragment with P4–M2 (M1 broken); F:AM 27528, right and left partial rami c1, p2–m2, and m3 alveolus; F:AM 27534, partial skull with I1–I3, C1 broken, and P1–M2, Mayday Quarry; F:AM 27541, right partial ramus with i1–p1 alveoli, p2–m2, and m3 alveolus, Skyline Quarry; F:AM 27547, left partial ramus with p1 alveolus, p2–m1, and m2–m3 alveoli, Skyline Quarry; F:AM 27548, crushed skull with I1–I2 alveoli and I3–M2 and mandible with i1–m3 (fig. 65E–G), Skyline Quarry; F:AM 61010, right partial maxillary P4–M1 all broken, New Year Quarry; F:AM 61044, left partial ramus with c1, p1–p2 alveoli, p3 broken–m1, and m2 broken, North End; F:AM 61045, right partial ramus with c1 and p1 alveolus–m1, Skyline Quarry; F:AM 61046, right partial maxillary with P4–M2, Hidden Hollow Quarry; F:AM 61047, left partial maxillary with P4–M2 (M1 alveolus), Leader Quarry; F:AM 61048, left partial maxillary with P4 broken–M2, Mayday Quarry; F:AM 61049, right and left rami with i2–i3 alveoli and c1–m3 (p1 alveolus), Skyline Quarry; F:AM 61050, left partial ramus with p3 alveolus, p4 broken–m2, and m3 alveolus, Skyline Quarry; F:AM 61051, right partial ramus c1–p4 alveoli, m1 broken, and m2–m3 alveoli, North End; F:AM 61052, left partial ramus c1 broken, p1–p2 alveoli, p3–m1, and m2–m3 alveoli, Skyline Quarry; F:AM 61053, right partial ramus with p2–m1 all broken, and m2 alveolus, Yule Tide Quarry; F:AM 61054, right partial ramus c1 broken–p1 alveolus and p2–m2, New Hope Quarry; F:AM 61055, left partial ramus with p3–m2 all erupting, Leader Quarry; F:AM 61057, crushed skull with I1–P3 alveoli and P4 broken–M2, Hidden Hollow

Quarry; F:AM 61058, crushed partial skull with P3–M2 all broken, Skyline Quarry; F:AM 61058A, crushed partial skull with C1–P1 alveolus and P2–M2, Skyline Quarry; F:AM 61058B, left partial ramus with c1–p3 alveoli, p4–m2, and m3 alveolus, Skyline Quarry; F:AM 61058C, right partial ramus with p4 broken–m1, Skyline Quarry; F:AM 61059, anterior part of skull with I1–I2, I3–C1 both broken, and P1–M2 and both partial rami with c1 broken–m3, Leader Quarry; F:AM 61060, left partial maxillary P3–M2, Leader Quarry; F:AM 61061, left partial maxillary with P3 alveolus–M2, Leader Quarry; F:AM 61062, right partial ramus with i3–p4 and m1 broken, Leader Quarry; F:AM 67129, right partial ramus c1 broken–m2 (p3, p4, and m1 all broken), 2 ft above Skyline Quarry; F:AM 67131, right ramus fragment with p2–p3 alveoli and p4–m1 both broken, Skyline Quarry; and F:AM 67146, left partial ramus with p1–p3 alveoli and p4–m1, Leader Quarry.

Pawnee Creek Formation (late early Barstovian), near Grover, Weld County, Colorado: F:AM 28322, left isolated M1, Pawnee Creek area; F:AM 28346, left partial maxillary with P4 broken–M2, north of 3 Points Pit and 40 ft above East and West Pits; F:AM 67877, distal part humerus, Pawnee Quarry; F:AM 67878, left radius, Pawnee Quarry; and F:AM 105258, left partial ramus with c1 alveolus, p2–p4 all broken, m1–m2, and m3 alveolus, R. Day Ranch, 3 Points, west side.

“Gerrys Ranch” (see Galbreath, 1953: 100), Ogallala Group (?early Barstovian), Weld County, Colorado: YPM 12812, left ramal fragment with p3–m1 (holotype of *Nothocyon vulpinus coloradoensis* Thorpe, 1922b: 430, fig. 2).

Horse Quarry, Pawnee Creek Formation (early late Barstovian), near Grover, Weld County, Colorado: F:AM 28320A, left partial ramus with p1–p2 alveoli, p3 broken–p4, and m1 broken; F:AM 28321, right and left edentulous rami with p2–m3 alveoli; F:AM 28353, left ramus with c1, p1–p2 alveoli, p3–m2, and m3 alveolus; and F:AM 61041, right partial ramus with p3 broken, p4, m1 broken, and m2 alveolus.

Martin Canyon, Ogallala Group (early late Barstovian), Cedar Creek, horizon E, Weld

County, Colorado: AMNH 9041, right partial ramus with p2–m1 (p3 broken) and m2 alveolus.

Pojoaque Member of the Tesuque Formation (early late Barstovian), Santa Fe and Rio Arriba counties, New Mexico: F:AM 27376, right partial ramus with c1 root and p1–m1 all broken; F:AM 27377, right partial ramus with c1 broken, and p2–m1 all broken, Camel Area; F:AM 27378, right and left partial rami with c1 and p2–m3, Third Division; F:AM 27392, right partial ramus with m2–m3, lower Pojoaque Bluffs; F:AM 27393, right partial ramus with p2–m2 all broken and m3, Santa Fe general area; F:AM 27398, palate with I1–M2 (fig. 66F), Santa Cruz; F:AM 27398X, partial skull with C1 broken–M2 and both rami with c1–p1 alveoli and p2 broken–m3 (fig. 66A–E), Pojoaque Bluffs; F:AM 27398Y, partial skull with I3 alveolus, C1 broken, P1–P2 alveoli, and P3 broken–M2, Pojoaque; F:AM 50184, partial mandible with i1–p2 roots and p2–m3 all broken, Santa Cruz, east of Tesuque fault, top of light band; F:AM 50185, partial left ramus with c1 broken, p1–p2 alveoli, and p3–m1, Tesuque area; F:AM 50186, right partial ramus with p3 alveolus, p4–m1 both broken, and m2–m3 alveoli, Tesuque area; F:AM 50203, anterior part of skull with I1–M2 all broken and eroded and associated (but possibly not from the same individual) right and left partial rami with c1 broken–m3 (m2 broken), south Santa Cruz; F:AM 62770, partial skull with I1–I3 alveoli, C1 broken, P1–P3 alveoli, and P4–M2, West Cuyamunque; F:AM 62772, right ramal fragment with p4 alveolus–m1 and m2 root, West Cuyamunque; and F:AM 67339, right and left partial rami with i1–m2 all broken, seventh wash, Santa Cruz area.

South fork of Three Sands Hills Wash, Rio del Oso–Abiquiu locality, Chama El Rito Member, Tesuque Formation (late Barstovian), Rio Arriba County, New Mexico: F:AM 50181, left partial maxillary with P1–P4 alveoli and M1 broken–M2.

Jemez Creek Area, tributary of Canyada De Zia, Zia Formation (unnamed beds above the Zia Sand of Galusha, 1966) (late early Barstovian), Sandoval County, New Mexico: F:AM 50191, crushed partial skull with P2–M2, greenish sand; and F:AM 50193, right

partial ramus with i1–p4 and m1–m3 alveoli, greenish sand.

Jemez Creek Area, tributary of Canyada De Zia, Zia Formation (unnamed beds above the Zia Sand of Galusha, 1966) (early late Barstovian), Sandoval County, New Mexico: F:AM 50190, skull fragment, incomplete atlas and axis, left maxillary fragment with P4–M2 and right isolated P4–M1, and right and left partial rami with p2 alveolus–m2 (m1 broken) and m3 alveolus, channel above the cliff-forming sands.

Cedar Springs Draw Local Fauna (early late Barstovian), Browns Park Formation, Moffat County, Colorado (list following Honey and Izett, 1988: 20): USGS D856-1, anterior part of skull with M1 broken and M2, right ramus with c1–p2 alveoli, and p3 broken–m3; and USGS D856-2, right premaxillary and maxillary with I3–P1.

DISTRIBUTION: Late Hemingfordian of New Mexico; early Barstovian of Nevada, California, New Mexico, Nebraska, and Colorado; late Barstovian of Texas, California, Colorado, and New Mexico.

EMENDED DIAGNOSIS: As for genus.

DESCRIPTION AND COMPARISON: Although earlier descriptions of this species by Matthew (1918, 1924) were based on fairly complete skull and lower jaws, a much larger sample of *Microtomarctus conferta* is now available that covers a much larger geographic region than was originally known. The most conspicuous feature about *M. conferta* is its small size as compared to most other *Tomarctus*-like taxa, both more primitive and derived than *M. conferta*. This reduction in size is also accompanied by a slightly brachycephalic skull with a short temporal fossa (length of M2 to bulla in fig. 62). Thus, the rostrum is relatively short and the premolars tend to imbricate slightly. Besides this small size, the only other derived cranial character of *M. conferta* that distinguishes it from the more primitive *Psalidocyon*, cynarctines, and *Metatomarctus* is a posteriorly expanded nuchal crest, which overhangs the occipital condyle. In posterior view, the nuchal crest is more quadrate instead of the fan-shape crest in *Psalidocyon*, *Paracynarctus*, *Cynarctus*, and other genera. Accompanying this expansion of the nuchal crest is a reduction of the lambdoidal crest

above the mastoid process. The lambdoidal crest becomes indistinct and does not project to form a thin crest as in more primitive taxa. A dissected frontal area (F:AM 61038) shows that the frontal sinus lacks an elaborate system of septa first seen in *Protomarctus*, but is relatively more expanded in the postorbital constriction than in *Psalidocyon* and more primitive taxa (fig. 62). Also primitive is a relatively large opening of external auditory meatus in *M. conferta*, in contrast to the reduced openings in *Protomarctus*.

Dentally, *Microtomarctus conferta* shares with *Psalidocyon* a distinct P4 parastyle that is formed from the raised anterior cingulum. This parastyle is sharp-edged and distinctly triangular in anterior view. The I3 has a small lateral cusplet only, in contrast to the larger and more numerous cusplets in *Tomarctus*. Corresponding to the smaller body size, the sizes of the teeth are more or less proportionally reduced as compared with those of *Metatomarctus*.

DISCUSSION: Henshaw (1942: 105) contrasted his *Tomarctus paula* (emended by Honey and Izett, 1988: 23; see also etymology under *T. breviostris*) from *conferta* in the following manner: “P4 elongate with protocone set very far forward. Upper molars very wide transversely. Lower dentition differs from *T. conferta* type in narrower premolars with only moderately high cusps. m1 short, not compressed. m2 moderately long and narrow.” Such differences are quite subtle between the Lower Snake Creek and Tonopah samples, and are readily subsumed within the normal range of variation of a species given the large sample from the wide geologic and geographic distribution determined in this study. Therefore, on morphological ground, *T. paulus* is considered synonymous with *Microtomarctus conferta*.

A few individuals presently referred to *Protomarctus optatus* from the Sheep Creek Formation (e.g., AMNH 20498, F:AM 61281) have nearly identical dental dimensions as some of the large individuals of *Microtomarctus conferta*. These individuals, however, have a narrowed external auditory meatus, and thus belong to *P. optatus* rather than *M. conferta*.

The small size of *Microtomarctus conferta* is here interpreted to be a result of size re-

duction, as is implied in our phylogeny. The successively more primitive outgroups (*Psalidocyon*, primitive species of cynarctines, and *Metatomarctus*) are all larger than *Microtomarctus*, as are *Protomarctus* and more derived taxa. Size reduction is rare in canids, and occurs only within *Cynarctus* (see further discussion under *C. crucidens*) up to this point of phylogeny of the borophagines (later, *Aelurodon stirtoni* and *Borophagus orc* also underwent size reduction). The presence of large samples of *M. conferta* suggests the prevalence of a species in the early Barstovian that successfully occupied a mesocarnivorous niche previously held by mostly hserocyonine canids and amphicyonids.

This size reduction is especially pronounced in the New Mexico sample. Thus, the late Hemingfordian individuals (e.g., F:AM 50143, 67373) are among the largest *Microtomarctus conferta* (m1 length of 17 mm), whereas a few individuals from the late Barstovian of Santa Cruz area (F:AM 50203, 62770, 62772, 67339) are among the smallest (m1 length of 13.0–14.5 mm). These individuals are, on average, 12% smaller than the rest of specimens referred to *M. conferta*. Although such size difference may be more than that between some closely related species recognized in this study, we failed to find any other morphological features to indicate divergence within *conferta*. We thus regard the small size of these individuals as intraspecific variation, or due to anagenetic processes near the end of the *M. conferta* lineage.

### *Protomarctus*, new genus

TYPE SPECIES: *Tomarctus optatus* Matthew, 1924.

ETYMOLOGY: Greek: *pro*, before; in allusion to its ancestral status to *Tomarctus*.

INCLUDED SPECIES: Type species only.

DISTRIBUTION: Early Hemingfordian of Colorado and New Mexico; and late Hemingfordian of Nebraska, Wyoming, and California.

DIAGNOSIS: *Protomarctus* is derived with respect to *Microtomarctus* and more primitive taxa in its multichambered frontal sinus that reaches to, or slightly passes, the frontal-parietal suture and its narrowed opening for

external auditory meatus. On the other hand, *Protomarctus* is primitive with respect to *Tephrocyon*, *Aelurodontina*, and *Borophagina* in its less enlarged postorbital process of frontal. *Protomarctus* can be further distinguished from *Aelurodontina* in its primitive features such as less broadened forehead, palate not widened, nuchal crest not laterally compressed, premolars not enlarged, M1 paracone not high-crowned and with a distinct metaconule, m1 metaconid and entoconid unreduced, and m2 metaconid unreduced. *Protomarctus* is distinct from primitive members of *Borophagina*, such as *Paratomarctus* and *Carpocyon*, in its absence of the following derived characters: prominently domed forehead, a short tube for auditory meatus, reduced premolars with weakened cusplets, p4 enlarged relative to p2–p3, and reduced P4 protocone.

### *Protomarctus optatus* (Matthew, 1924)

Figure 67

*Tomarctus optatus* Matthew, 1924: 98, figs. 18, 19. Skinner et al., 1977: 342. Munthe, 1988: 87; 1998: 135.

*Tephrocyon (Canis) temerarius* (Leidy, 1858): Peterson, 1910: 268, fig. 63 (CMNH 2404).

*Tephrocyon temerarius* (Leidy): Merriam, 1913: 366, fig. 7 (CMNH 2404).

*Tomarctus brevirostris* (Cope, 1873): Downs, 1956: 233.

*Tomarctus* cf. *T. optatus* (Matthew): Galusha, 1975b: 56.

HOLOTYPE: AMNH 18916, mandible with i1–c1, p1 alveolus, and p2–m3 (fig. 67A, B) from Thomson Quarry (Skinner et al., 1977: 342), east side of Stonehouse Draw, Sheep Creek Formation (late Hemingfordian), Sioux County, Nebraska.

REFERRED SPECIMENS: Martin Canyon Quarry A (KUVF loc. CO-48), Martin Canyon beds (early Hemingfordian), Logan County, Colorado: KUVF 45128, left maxillary with P4–M2.

Sheep Creek Formation (late Hemingfordian), Sioux County, Nebraska: Stonehouse Draw: AMNH 14175, right partial ramus with p4–m1 and p3 and m2 alveoli; AMNH 14176, right partial maxillary with P4–M1 and M2 alveolus (Matthew, 1924: fig. 19); AMNH 18236, right immature partial ramus with c1 erupting, dp3 broken–dp4, and m1

unerupted, Ashbrook Pasture, Sinclair Draw; AMNH 18669, right partial maxillary with P4–M2 and left partial maxillary with P4 root and M1–M2 (another individual), Ashbrook Pasture; AMNH 18915, right ramus with c1–m3; AMNH 18917, right partial ramus with m1–m2 and m3 alveolus; AMNH 18918, right partial ramus with p4–m2 (m1 broken) and m3 alveolus; AMNH 20494, left partial maxillary with M1–M2; AMNH 20498, partial skull with I1–P1 alveoli, P2, P3 alveolus, and P4–M1; AMNH 20499, right maxillary with P4–M2; AMNH 20500, right partial ramus with p3 alveolus–m2; AMNH 21445, right partial ramus with c1, p1–p2 alveoli, p3–m2, and m3 alveolus; AMNH 26904, left partial ramus with m1 (c1–p4 and m2 all alveoli); AMNH 26905, left partial ramus with c1–p2 alveoli and m1. Thomson Quarry: F:AM 61244, left partial ramus with p2–p4 alveoli and m1–m3; F:AM 61245, right partial ramus with p1–p3 alveoli, p4–m2, and m3 alveolus; F:AM 61246, left partial ramus with c1, p1 alveolus–m1 (p4 broken), and m2 alveolus; F:AM 61247, right partial ramus with i1–p3 alveoli, p4–m1, and m2 broken–m3 alveolus; F:AM 61254, right partial ramus with i1–p1 alveoli, p2–m2, and m3 alveolus; F:AM 61255, right partial ramus with i1 alveolus–m2 (p3 broken) and m3 alveolus; F:AM 61257, left partial ramus with c1–p2, p3 alveolus–m2, and m3 alveolus; F:AM 61266, right partial ramus with i1–p1 alveoli, p2 broken–m2, and m3 alveolus; F:AM 61271, left partial ramus with c1 broken, p2, p3–m2, p1, and p3 and m3 alveoli; F:AM 61272, right ramus with c1–p1 alveoli, p2–m2, and m3 alveolus (fig. 67C, D); F:AM 61273H, left partial ramus with m1–m2; F:AM 61273I, right partial ramus with p2–m1 all broken, m2, and m3 alveolus; F:AM 61279, posterior part of skull, premaxillary-maxillary fragment with I1 alveolus, I2–I3, and broken C1 alveolus, right and left detached maxillary fragments with P3 broken–M1 and associated limbs (61279A–D) of two or more individuals including F:AM 61279A, humerus and partial femur; F:AM 61279B, immature right partial femur; F:AM 61279C, immature left tibia; F:AM 61279D, left tibia and right partial tibia, patella, left calcaneum and astragalus, tarsals, metatarsal I, right and left metatarsals IV

(two individuals), and two first phalanges; F:AM 61281, partial skull with I1–I3 alveoli, C1–P4 (P1 alveolus), and M1–M2 alveoli; F:AM 61287, right partial maxillary with P3 broken–M2; F:AM 61291, left partial maxillary with P4–M1; and F:AM 61294, right partial maxillary with P2–P4. Greenside Quarry: F:AM 61249, left ramus with c1–m2 (p1 and m3 alveoli); F:AM 61250, right partial ramus with i1–p1 alveoli, p2, p3 alveolus, p4–m1, and m2–m3 alveoli; F:AM 61251, left ramus with c1–m3 (p1 alveolus); F:AM 61252, left partial ramus with i3–p1 alveoli, p2–m2, and m3 alveolus; F:AM 61253, left partial ramus with i1–p2 alveoli, p3, p4 alveolus, m1, and m2–m3 alveoli; F:AM 61260, left partial ramus with c1–m1 (p1 alveolus); F:AM 61262, right ramus with i1–i3 alveoli, c1–m2, and m3 alveolus; F:AM 61267, left ramus with i1–i3 alveoli, c1–p2 broken, and p3–m3; F:AM 61269, left ramus with c1–p1 alveoli, p2–m2, and m3 alveolus; F:AM 61273G, left partial ramus with p4–m2 and m3 unerupted; F:AM 61273J, right ramal fragments with c1–m1 broken (p1 alveolus), and m2 broken–m3; F:AM 61273K, right partial ramus with m2 and m3 alveolus; F:AM 61273L, left ramal fragment with p3–p4 and m1–m3 alveoli; F:AM 61273N, left ramal fragment with m2–m3; F:AM 61274, skull with I1 alveolus–M2; F:AM 61275, right partial maxillary with C1–P1 alveoli and P2–M2; F:AM 61277, right partial maxillary with C1–P3 alveoli, P4–M1, and M2 alveolus; F:AM 61278, skull with I1–I2 alveoli and I3–M2 (P1 alveolus) (fig. 67E–G); F:AM 61280, partial skull with I1–I3 alveoli and C1–M2 (P3 alveolus); F:AM 61285, right partial maxillary with P4–M2; and F:AM 61289, right partial maxillary with P4–M2. Long Quarry: F:AM 25288, left partial ramus with c1 and p1 alveolus–m1; F:AM 61018, left partial ramus with p1 alveolus–m2 (p3 root and m1 broken); F:AM 61258, left partial ramus with c1 broken, p1 alveolus–m1, and m2 broken–m3 alveolus; F:AM 61261, right partial ramus with c1 broken–p1 alveolus and p2–m1; F:AM 61263, left ramus with c1–p2 alveoli, p3–m2, and m3 alveolus; F:AM 61264, right ramus with c1, p1–p3 alveoli, p4–m2, and m3 alveolus; F:AM 61268, right partial ramus with c1–m3 (p1 alveolus); F:AM 61273B, left partial ra-

mus with p1–p3 alveoli and p4–m1; F:AM 61273D, right partial ramus with m1; F:AM 61282, left maxillary with C1–P1 alveoli, P2 broken–M1, and M2 broken; F:AM 61284, left premaxillary maxillary with I1–I2 alveoli, I3 broken–C1, P1 alveolus–P3, and P4 broken; F:AM 61288, skull fragments and left partial maxillary with P4–M2; and F:AM 61293, left partial maxillary with P4 broken–M2. Hilltop Quarry: F:AM 61248, right ramus with i1–i3 alveoli, c1, p1–p2 alveoli, and p3–m3; F:AM 61256, right partial ramus with c1, p1–p2 alveoli, and p3–m2; F:AM 61265, right ramus with i3–c1 all broken, p1–m2, and m3 alveolus; F:AM 61273, left partial ramus with p3–m1, and m2 alveolus; F:AM 61273E, right partial ramus with p3–p4 alveoli, m1–m2, and m3 alveolus; F:AM 61273F, right partial ramus with m1 and m2–m3 alveoli; F:AM 61286, left isolated P4; and F:AM 61290, left partial maxillary with P4–M1. Ashbrook Quarry: F:AM 61270, right ramus with c1–m2 and m3 alveolus; F:AM 61273C, right ramal fragment with detached p4 and m1–m2; F:AM 61273M, left partial ramus with c1–p3 all broken or alveoli and p4; and F:AM 61276, left maxillary with C1–P3 alveoli, P4–M1 both broken, and M2. Watson Ranch: F:AM 61292, right partial maxillary with P4–M2. Thistle Quarry: F:AM 61273A, right ramal fragment with m1 and m2 alveolus; and F:AM 61283, left maxillary with C1–M2 (P1–P2 alveoli). Vista Quarry: F:AM 61259, right ramus with c1–m1 (p1 alveolus) and m2–m3 alveoli. Ravine Quarry: F:AM 61135, left partial ramus with i3–p1 alveoli, p2, p3 alveolus–m1, m2 broken, and m3 alveolus. Conference Quarry: F:AM 105255, right partial ramus with p4–m1 both broken, m2, and m3 alveolus. Northwest of Snake Den Hill, 55 ft above base of Sheep Creek Formation: F:AM 105256, right ramal fragment with p4 broken and m1–m2.

Whistle Creek, Runningwater or Sheep Creek Formation (Hemingfordian), Sioux County, Nebraska: CMNH 2404, left partial ramus with p4–m2 and m3 alveolus (referred to *Tephrocyon* (*Canis*) *temerarius* by Peterson, 1910: 268, fig. 63 and Merriam, 1913: 366, fig. 7).

Rocks temporally equivalent to the Sheep Creek Formation (late Hemingfordian),

Dawes County, Nebraska: Ginn Quarry: F:AM 54493, right maxillary with C1–M2 (P1 alveolus); F:AM 54494, right partial maxillary with P4–M1 and M2 alveolus; F:AM 54495, left ramus with c1 broken, p1–p3 alveoli, p4–m2, and m3 alveolus; F:AM 61183, anterior part of skull with I1–P1 alveoli, P2, and P3 alveolus–M2; and F:AM 61184, left partial maxillary with M1–M2. “G” Quarry: F:AM 49195, right ramus with c1–p4, m1 alveolus, m2, and m3 alveolus.

Sand Canyon Region, Red Valley Member, Box Butte Formation (late Hemingfordian), Box Butte County, Nebraska: F:AM 95279, crushed palate with I1–M2 and mandible with i1–m1, and m2 broken (referred to *Tomarctus* cf. *T. optatus* by Galusha, 1975b: 56).

Box Butte Formation (late Hemingfordian), Box Butte County, Nebraska: UNSM 25652 (AMNH cast 97101), left partial maxillary with P4–M1 and M2 alveolus, UNSM loc. Bx-0.

Split Rock Formation (late Hemingfordian), Granite Mountain, Fremont County, Wyoming (as listed in Munthe, 1988: 87): CMNH 14709, M2, from UCMP loc. V69192; UCMP 121910, partial skull with I3–M2 (P1 alveolus), UCMP loc. V77155; and UCMP 121911, M1, from UCMP loc. V69190.

Arroyo Pueblo drainage, near middle of Chamisa Mesa Member, Zia Formation (early Hemingfordian), Sandoval County, New Mexico: Blick Quarry: F:AM 50198, immature partial skull with dC1, P1, dP2–dP4, P2–P3 unerupted, and P4–M2 erupting, and mandible with di1–di2, i3 broken, dc1, p1, dp2 broken–dp4, p2–p4 unerupted, and m1–m2 erupting. *Cynarctoides* Prospect: F:AM 62777, palate with C1–P2 alveoli, and P3 broken–M2.

Barstow area, Barstow Formation (late late Hemingfordian), San Bernardino County, California: Rak Division: F:AM 27149, crushed skull with I3 alveolus–C1 broken, P1–P3 broken, and P4–M2. Third Division: F:AM 27288, right and left partial rami with c1, p1–p2 alveoli, and p3–m2.

DISTRIBUTION: Early Hemingfordian of Colorado and New Mexico; and late Hemingfordian of Nebraska, Wyoming, and California.

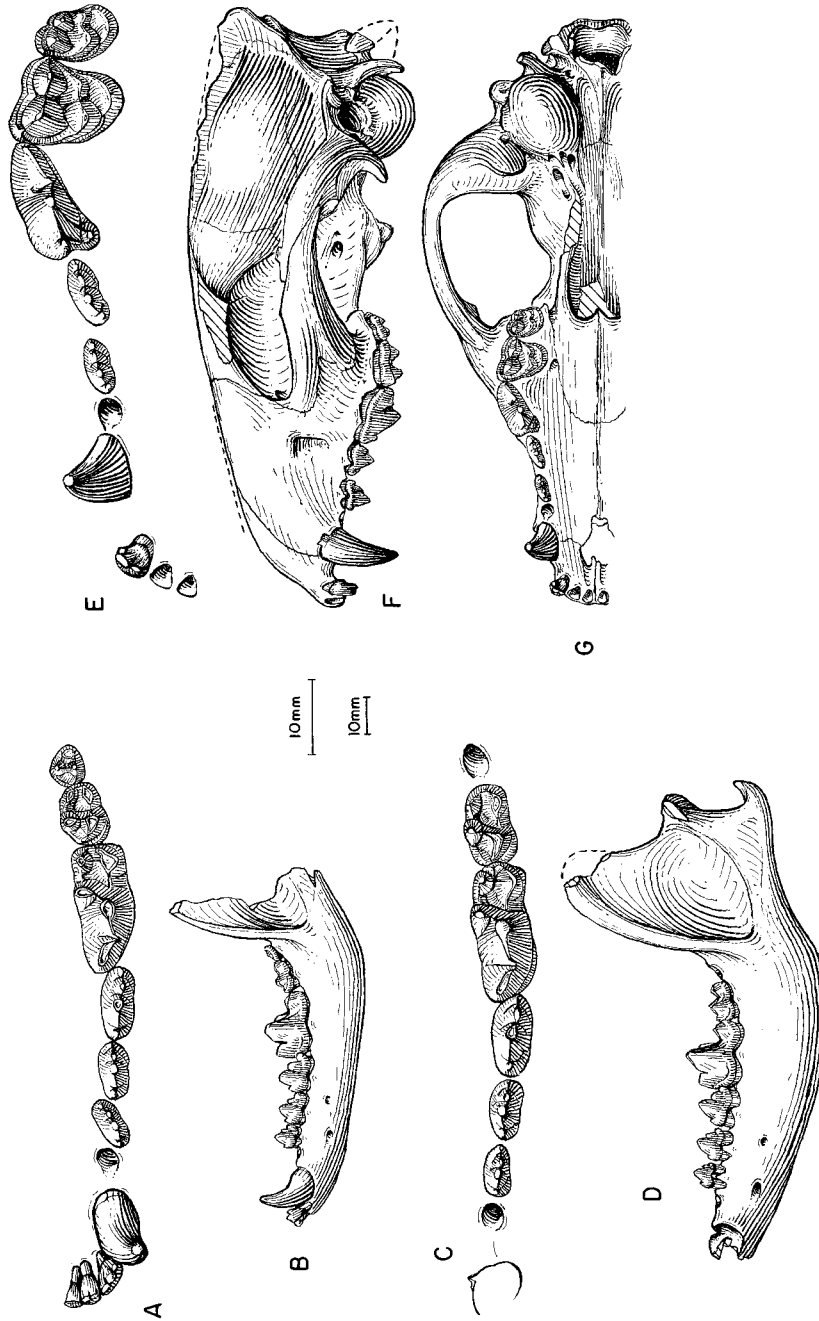


Fig. 67. *Protomarctus optatus*. A, Lower teeth and B, ramus (i3 reversed from right side), AMNH 18916, holotype, Thomson Quarry, Sheep Creek Formation (late Hemingfordian), Sioux County, Nebraska. C, Lower teeth and D, ramus (reversed from right side), F:AM 61272, Thomson Quarry. E, Upper teeth and F, lateral and G, ventral views of skull, F:AM 61278, Greenstone Quarry, Sheep Creek Formation (late Hemingfordian), Sioux County, Nebraska. The longer (upper) scale is for A, C, and E, and the shorter (lower) scale is for the rest.



EMENDED DIAGNOSIS: As for genus.

DESCRIPTION AND COMPARISON: Numerous upper and lower jaws as well as several skulls permit good knowledge of the cranial and dental morphology of *Protomarctus optatus* and its variation. Most of the specimens are represented by materials from the Sheep Creek Formation or equivalent strata in the northern Great Plains. Specimens from the various quarries in the Sheep Creek Formation constitute a fairly uniform sample, except for a few individuals (e.g., AMNH 20498, F:AM 54493, 61184, 61281) that approach the upper range of *Microtomarctus conferta*.

*Protomarctus optatus* is on average 27% (basal length of skull) larger than *Microtomarctus conferta* and is approximately the same size as *Desmocyon*, whereas it is about 12% (basal length of skull; 11% for m1 length) smaller than *Tomarctus hippophaga*. The frontal sinus is noticeably more inflated than in *Desmocyon* and *Microtomarctus*. Externally, the forehead is more domed than the latter genera, and this inflation can be seen to pass behind the frontal-parietal suture. A dissected specimen of *P. optatus* (F:AM 61278) reveals that the sinus extends beyond the frontal-parietal suture by more than 5 mm. The frontal bone in this skull also bears partial septa (at least two) that partition the sinus into chambers. The diagonally oriented septa form either a vertical partitioning of the sinus or they bend horizontally to enclose a partial chamber. Skulls from Thomson Quarry (F:AM 61279 and 61281) generally show less inflation than those from Greenside Quarry (F:AM 61274, 61278, 61280), despite the higher stratigraphic position of the former.

The premaxillary process is in full contact with the nasal process of the frontal. As in *Microtomarctus conferta*, the nuchal crest of *Protomarctus optatus* is posteriorly expanded to overhang the occipital condyle. The bulla is inflated ventrally and in the posterolateral corner in front of the paroccipital process. The external auditory meatus has a smaller opening than in *M. conferta*, and the ectotympanic forms a short lip surrounding the meatus.

Dentally, *Protomarctus optatus* is little more derived than *Desmocyon matthewi* and

*Microtomarctus* except for its two additional lateral cusplets on I3. On the other hand, premolars of *P. optatus* are primitive with respect to both Aelurodontina and Borophagina clades: they are not as uniformly enlarged as in the Aelurodontina (first developed in *Tomarctus hippophaga*), nor as uniformly reduced as in *Paratomarctus* in the Borophagina clade.

Two specimens from the early Hemingfordian Chamisa Mesa Member of the Zia Formation, New Mexico, are referred to this species (Munthe [1988: 89] listed "Zia Sand" under the geographic distribution of *Tomarctus optatus*, probably based on the same F:AM specimens, but did not elaborate). The New Mexico individuals are slightly larger than those from the northern Great Plains, but their P4 parastyles are less distinctly formed. Other than these variations, the New Mexico specimens are a close match with the topotype series from Nebraska.

DISCUSSION: Matthew (1924) compared his newly erected *Tomarctus optatus* with "*T. brevirostris*" (now *T. hippophaga*) and *T. temerarius* (*Paratomarctus*) and found it to be somewhat intermediate in size and morphology. He (1924: 100) noted that the "smaller size and somewhat more slender proportions" were the only distinctions of *T. optatus* when compared to *T. hippophaga*. In fact, he suggested that *T. optatus* may be a "primitive mutant" of *T. hippophaga*, but preferred to hold the names distinct pending further evidence. Even with the complete cranial materials available to this study, Matthew's observation is essentially correct; that is, differences between these two species are small (as also are between *Protomarctus optatus* and *Paratomarctus temerarius*). Besides the small size and slender teeth noted by Matthew, the only cranial features we can add are the primitively narrow frontal shield and the less enlarged postorbital process of the frontal in *optatus*. As indicated by the primitive states of these features in *optatus*, we recognize it as a critically positioned taxon on the verge of giving rise to two great Borophagini clades: Aelurodontina and Borophagina. *Protomarctus optatus* possesses the right combination of morphology and is in the right stratigraphic level to be ancestral to both clades.

Galusha (1975b: 56) noted the transitional nature of an anterior skull fragment and its associated mandible (F:AM 95279) from the Red Valley Member of Box Butte Formation. Its dental morphology is intermediate between that of *Desmocyon matthewi* of the Runningwater Formation and that of *Protomarctus optatus* from the Sheep Creek Formation. The teeth of F:AM 95279 are very close to the average dental dimensions of both *Metatomarctus canavus* and *P. optatus*. Its I3 has two lateral accessory cusplets, in contrast to one cusplet in *Protomarctus* and *Microtomarctus*, and its P4 bears a distinct parastyle, although the latter still does not assume the prominence shown by most individuals of *P. optatus* from the Sheep Creek Formation. We agree with Galusha (1975b) that despite its intermediate morphology and stratigraphic relationship, F:AM 95279 has essentially reached the general stage of development of *P. optatus*.

*Tephrocyon* Merriam, 1906

TYPE SPECIES: *Canis rurestris* Condon, 1896.

INCLUDED SPECIES: Type species only.

DISTRIBUTION: Early Barstovian of Oregon and Texas.

EMENDED DIAGNOSIS: *Tephrocyon* is derived with respect to *Protomarctus* and more primitive taxa in its larger size, more pronounced postorbital process of frontal (a character also shared with Aelurodontina and Borophagina), slightly more broadened palate, and an elongated m2 (an autapomorphy). *Tephrocyon* is distinguishable from Aelurodontina in its primitive characters such as nuchal crest not laterally compressed, premolars not enlarged, M1 paracone not high-crowned and with a distinct metaconule, m1 metaconid and entoconid unreduced, and m2 metaconid unreduced. On the other hand, *Tephrocyon* differs from members of Borophagina in its lack of the following derived characters: domed forehead, short tube for auditory meatus, small premolars with reduced cusplets, p4 enlarged relative to p2–p3, and reduced P4 protocone.

DISCUSSION: Shortly after Merriam's (1906) establishment of *Tephrocyon*, a number of medium-size taxa were referred to it

by him (Merriam, 1913) and *Tephrocyon* quickly became a taxonomic wastebasket for many *Canis*-like taxa. The popularity of the genus, however, was diminished soon after Matthew's (1924, 1930) influential studies of canid evolution. Matthew's resurrection of Cope's (1873) *Tomarctus*, which has priority over *Tephrocyon*, proved to be more enduring. *Tephrocyon* had since been rarely mentioned in the literature, except in connection with its type species *T. rurestris*.

*Tephrocyon rurestris* (Condon, 1896)

Figure 68

*Canis rurestris* Condon, 1896: 11, pl. 1.

*Tephrocyon rurestris* (Condon): Merriam, 1906: 6, pl. 1, figs. 1–3; 1913: 362, figs. 1–5. Thorpe, 1922a: 175. Matthew, 1924: 89.

*Tomarctus rurestris* (Condon): Downs, 1956: 231, figs. 10, 11. Munthe, 1998: 135.

*Tomarctus* cf. *rurestris* (Condon): Shotwell, 1968: 37, fig. 14A.

*Tomarctus* cf. *T. kelloggi* (Merriam): Shotwell, 1968: 37, fig. 17E, F.

HOLOTYPE: UO 23077 (AMNH cast 97225), skull with C1 broken, P1 alveolus–M2 (P3 broken), and mandible with c1–p1 alveoli and p2–m3 (fig. 68) from near Cottonwood Creek, Mascall Formation (early Barstovian), Grant County, Oregon.

REFERRED SPECIMENS: From the Mascall type area, Oregon (referred by Downs, 1956; Shotwell, 1968): UCMP 39297, partial left m1 (Downs, 1956: fig. 12c), UCMP loc. V4834; UO 24191, partial ramus with p4–m1; UO 24192, maxillary fragment with P4; YPM 12713, left P4, M1–M2, right P4, and left m2 and m3 (Downs, 1956: fig. 12a), Cottonwood Creek; YPM 12720, right m1 (Downs, 1956: fig. 12b), Crooked Creek; and YPM 14312, left M1 (Downs, 1956: fig. 12d).

Red Basin Local Fauna, Butte Creek Volcanic Sandstone (early Barstovian), Malheur County, Oregon: UO 20552, left ramal fragment with m1 and m2–m3 alveoli; UO 21499, isolated left m2; UO 21559 (Shotwell, 1968: fig. 17E, F), right ramal fragment with m1–m2; UO 22837, crushed right maxillary fragment with P4–M1; UO 23132, isolated right M1; UO 23386, isolated right P3; UO 23496, isolated left m1; and UO 23497, isolated left m2.

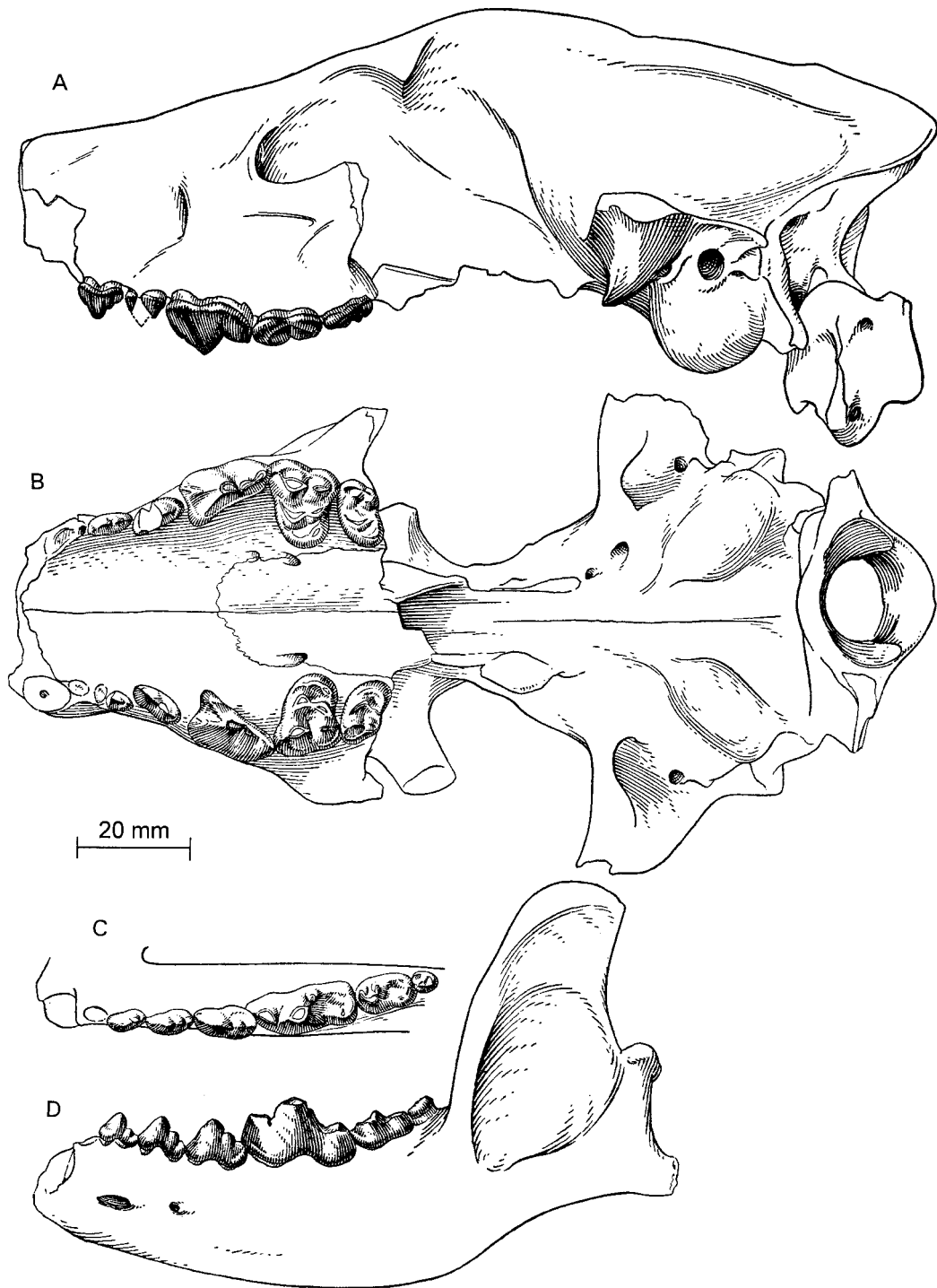


Fig. 68. *Tephrocyon rurestris*. A, Lateral and B, ventral views of skull, C, lower teeth, and D, ramus, UO 23077, holotype, near Cottonwood Creek, Mascall Formation (early Barstovian), Grant County, Oregon. Modified from Downs (1956: fig. 10).

DISTRIBUTION: Early Barstovian of Oregon.  
EMENDED DIAGNOSIS: As for genus.

DESCRIPTION AND COMPARISON: The well-preserved holotype, UO 23077, is still the best material for this species. The geologically younger *Tephrocyon rurestris* (early Barstovian) is larger than the older (Hemingfordian) *Protomarctus optatus* (14% larger in m1 length, but a much smaller percentage in premolar length). The skull seems slightly more derived toward the Aelurodontina clade. There is a moderate frontal sinus, probably reaching to the frontal-parietal suture as suggested by its external profile. The forehead is quite flat, as is commonly the case in Aelurodontina but is in contrast to the domed profile in the Borophagina clade. The postorbital process of frontal is laterally expanded in contrast to a narrowed postorbital constriction, also a common occurrence of the aelurodontine clade (fig. 71). The sagittal crest is higher than in *P. optatus* and slightly overhangs the occipital condyle. The opening for the external auditory meatus is narrow. The palate shows an initial stage in the broadening seen in the aelurodontine clade.

Dentally, *Tephrocyon rurestris* and *Protomarctus optatus* are quite similar. Cheek-teeth for *T. rurestris* are proportionally slender (see fig. 72). The m1–m2 are also more elongated than in *P. optatus*. The premolars of *T. rurestris* are neither enlarged, as in the aelurodontines, nor reduced, as in *Paratomarctus*.

DISCUSSION: As the genoholotype of *Tephrocyon* (Merriam, 1906), *T. rurestris* played an important role in shaping the early concept of a centrally positioned genus in the canid phylogeny, mostly because Merriam (1913) referred a number of mesocarnivorous taxa to it. Matthew's (1924, 1930) authoritative study on canid phylogeny, however, resurrected Cope's earlier (1873) genus *Tomarctus* as having priority. The Mascal *T. rurestris* has since been mostly regarded as just another species of *Tomarctus* (Downs, 1956; Shotwell, 1968). Although our present phylogeny places *T. rurestris* in a trichotomy with the Aelurodontina and Borophagina clades, subtle features, such as flat forehead, broadened palate, and heightened sagittal crest, indicate that *T. rurestris* may be closer to the Aelurodontina side. However, *T. ru-*

*restris* does not have the widened premolars that are a derived character for the aelurodontine clade. Lacking better samples of *T. rurestris*, it is not clear if the above-cited aelurodontine features are independent developments or simply individual variation. In any case, the presence of an autapomorphy (i.e., an elongated m2) in *T. rurestris* and its entirely Columbia Plateau distribution suggest that it was not an anagenetic lineage leading directly to *Tomarctus*.

Fragmentary specimens from the Red Basin Local Fauna (Shotwell, 1968) are slightly smaller than the holotype of *Tephrocyon rurestris*, but are otherwise consistent with most aspects of dental morphology of *T. rurestris*, especially the slender, elongated m2. On the other hand, two rami from Trail Creek Quarry, Wyoming, referred to *Tomarctus rurestris* by Voorhies (1965), are presently placed in *Paratomarctus temerarius*.

#### Aelurodontina, new subtribe

TYPE GENUS: *Aelurodon* Leidy, 1858.

INCLUDED GENERA: *Tomarctus* Cope, 1873 and *Aelurodon* Leidy, 1858.

DISTRIBUTION: Early Barstovian through late Clarendonian of North America.

DIAGNOSIS: A single synapomorphy unites all members of Aelurodontina: uniformly robust lower premolars with distinct accessory cusplets. Advanced members of this clade further acquire derived characters, such as broadened palate, paroccipital process elongated with long free tip, anteromedial part of ramus strongly deflected laterally, high sagittal crest, nuchal crest laterally compressed and overhanging occipital condyle, I3 with three lateral accessory cusplets, M1 paracone high crowned, M1 metaconule small to absent, m1 metaconid reduced to absent, m1 talonid short and narrow, m1 entoconid small to absent, and m2 metaconid small to absent. Members of Aelurodontina generally lack the derived characters for the Borophagina clade: prominently domed forehead, shortened rostrum, reduced I3 lateral cusplets, reduced anterior premolars, reduced premolar cusplets, p4 enlarged relative to p2–p3, and reduced P4 protocone.

*Tomarctus* Cope, 1873

TYPE SPECIES: *Tomarctus brevirostris* Cope, 1873.

INCLUDED SPECIES: *Tomarctus hippophaga* (Matthew and Cook, 1909) and *Tomarctus brevirostris* Cope, 1873.

ETYMOLOGY: Simpson (in Honey and Izett, 1988) has pointed out that *Tomarctus* is feminine in gender and the International Commission on Zoological Nomenclature (1985: article 31) states that adjectival species names must conform in gender with that of their genus. Although *Tomarctus* was assembled by Cope from Greek roots, he placed the Latin neuter *brevirostris* as its adjective. In this work we have tried to abide by ICZN article 31 and its directive article 34 to provide justified emendation of species names associated with *Tomarctus* or its derivatives.

DISTRIBUTION: Early Barstovian of Colorado, Nebraska, New Mexico, and California; and late Barstovian of Colorado and Texas.

EMENDED DIAGNOSIS: The single derived character that unites *Tomarctus* and the *Aelurodon* clade is the enlarged premolars. *Tomarctus* is also distinguishable from *Protomarctus* by its larger size, wider forehead, and more complex septa within the frontal sinus. Primitive characters that distinguish *Tomarctus* from *Aelurodon* are sagittal crest lower, bulla not hypertrophied, mastoid process small, P4 protocone less reduced, P4 parastyle smaller, upper molars not reduced relative to P4, M1 lingual cingulum not restricted to the posterolingual border, m1 talonid not narrowed, m2 less reduced, and m2 metaconid approximately equal to protoconid in height.

DISCUSSION: *Tomarctus* is one of the most confused taxa in the studies of Tertiary canids, both because of the many species that had been erected under this genus and because of its purported central position in the line of descent to the living wolves (*Canis*) and foxes (*Vulpes*). This confusion originated from Matthew's (1924, 1930) early syntheses of the phylogeny of the Canidae, which followed a scheme that recognized two dichotomous lines of canids, i.e., taxa with basined vs. trenchant m1 talonids—a structure highly homoplastic throughout the

history of canid evolution. *Tomarctus*, with a fully basined talonid, was thus postulated to be ancestral to not only all large borophagines, but also to all living canids with a basined talonid. Matthew's scheme proved to be profoundly influential, and *Tomarctus* played an important role in nearly all past interpretations of the geological history of dogs. It is clear from our phylogenetic analysis that, even allowing a horizontal (or gradational) classification, the various species referred to *Tomarctus* (sensu lato) occupy primitive positions in various clades of advanced borophagines and are far removed from any living canid. Cladistically, *Tomarctus* is still a paraphyletic genus in the present classification and pertains to the Aelurodontina clade only.

*Tomarctus hippophaga*  
(Matthew and Cook, 1909)

Figures 69, 70

*Tephrocyon hippophagus* Matthew and Cook, 1909: 373, fig. 4. Cook, 1912: 44. Merriam, 1913: 364, fig. 6. Sinclair, 1915: 76. Matthew, 1918: 185. Munthe, 1998: 135.

*Tomarctus brevirostris* (Cope, 1873): Matthew, 1924: 91, figs. 11–16 (in part). Colbert, 1939: 65. Hough, 1948: 107 (AMNH 18243, mislabeled by Hough as AMNH 18234).

*Tomarctus hippophagus* (Matthew and Cook): VanderHoof, 1931: 19.

HOLOTYPE: AMNH 13836, right ramus with i2–i3 alveoli and c1–m2 (p1 and m3 alveoli) (fig. 69G, H), Quarry 2, East Sinclair Draw, Lower Snake Creek Fauna, Olcott Formation (early Barstovian), Sioux County, Nebraska.

REFERRED SPECIMENS: Lower Snake Creek Fauna, Olcott Formation (early Barstovian), Sioux County, Nebraska: Quarry A: AMNH 18249, partial left ramus with c1–p1 alveoli, p2–m2, and m3 alveolus; AMNH 18250, left partial maxillary with P4–M1; and AMNH 18251A, right ramus fragment with m1. Quarry B: AMNH 18242, skull with I1–P1 alveoli and P2–M2 (Matthew, 1924: figs. 12, 13); AMNH 18247, right partial maxillary with P4 broken–M2; and AMNH 18248, left partial ramus with c1, p1–p3 alveoli, p4–m2, and m3 alveolus. Sheep Creek Quarry: AMNH 18243, skull with C1–M2 (P1 alveolus) (Matthew, 1924: figs. 14, 15); and

AMNH 18244, skull with I1, I2–P1 alveoli, and P2–M2, and right partial ramus with c1–p1 alveoli, p2–m2, and m3 alveolus (Matthew, 1924: figs. 11, 16; fig. 70E–J). Echo Quarry: F:AM 61114, right partial ramus with i1–p4 alveoli, m1–m2, and m3 alveolus; F:AM 61116, left partial ramus with c1–p4 alveoli, m1, and m2–m3 alveoli; F:AM 61131, left partial ramus with i1–i3 alveoli, c1, p1–p3 alveoli, p4, m1 broken, and m2–m3 alveoli; F:AM 61132, left ramus with i1–p4 alveoli, m1, and m2 broken–m3 alveolus; F:AM 61133, right partial ramus with p4–m2 and m3 alveolus; F:AM 61134, left partial ramus with i3–p4, m1–m2 roots, and m3 alveolus; F:AM 61137, right ramus with c1–p3 alveoli, p4–m1, and m2–m3 alveoli; F:AM 61138, left partial ramus with i3–p3 alveoli, p4–m1, and m2–m3 alveoli; F:AM 61149, right partial ramus with c1–m1; F:AM 61154, left ramus with i1–p1 alveoli, and p2–m1 (p3 alveolus, p4 broken, and m2–m3 alveoli); F:AM 61155, left ramus with c1–m1 and m2–m3 alveoli; F:AM 61156, skull with I1 alveolus, I2, I3 alveolus, C1 root, P1 alveolus, and P2–M2 (fig. 70A–D); F:AM 61174, left ramus with c1, p1 alveolus, p2–m2, and m3 alveolus (fig. 69C, D); F:AM 61174A, partial right premaxillary-maxillary with I3–P1 alveoli and P2–M2 (fig. 69E, F); F:AM 61176, right partial ramus with i1–i3 alveoli and c1 broken–m1 (p1 alveolus and p2 broken); F:AM 61177B, right ramal fragment with m1 and m2 alveolus; F:AM 61177H, left partial ramus with p3 broken–m2; F:AM 61177K, left partial ramus with m1–m2; and F:AM 61181, posterior part of skull. Mill Quarry: F:AM 61145, right partial ramus with i2 alveolus, i3–m1, and m2–m3 alveoli; F:AM 61152, right ramus with c1–m2 (p1 and p3 alveoli, m1 broken, and m3 alveolus); F:AM 61177D, left partial ramus with m1–m2 and m3 alveolus; and F:AM 61180, posterior part of skull. Sinclair Draw: F:AM 61177G, left ramal fragment with m1 and m2–m3 alveoli. East Sinclair Draw: AMNH 81526 (HC 1168), left isolated m1; AMNH 83440 (HC 616), right partial ramus with c1–p1 alveoli and p2–m2; F:AM 25486, right ramus with i1–i3 alveoli, c1 broken, p1 alveolus–m1, and m2–m3 alveoli; F:AM 61173, right partial maxillary with P4–M1; and F:AM

61177E, right partial ramus with m1 and m2 alveolus. Quarry 2, East Sinclair Draw: AMNH 13837, right partial ramus with c1–p1 alveoli, p2, p3 alveolus–m1, and m2–m3 alveoli; AMNH 13838, right partial ramus with m1–m2 and m3 alveolus; AMNH 13839, right partial ramus with c1–p2 alveoli, p3–p4, and m1–m3 alveoli; AMNH 13840, right partial ramus with c1–p4 alveoli, m1, and m2–m3 alveoli; AMNH 83420 (HC 336), right ramal fragment with c1–m1 (all broken); F:AM 25495, left partial ramus with p2 broken–m3; F:AM 25497, right partial ramus with i1–i3 alveoli, c1, p2–m1, and m2 broken; F:AM 61115, right partial ramus with i1–i3 alveoli, c1, p1–p3 alveoli, p4–m1, and m2–m3 alveoli; F:AM 61118, left partial ramus with i1–c1 alveoli, p2–m1, and m2–m3 alveoli; F:AM 61119, left partial ramus with c1–m1 (p1 and m2–m3 alveoli); F:AM 61120, right partial ramus with c1–m2 (p1 and m3 alveoli); F:AM 61144, right ramus with i1–p1 alveoli and p2–m3 (m1 broken); F:AM 61150, right partial ramus with c1 alveolus–m1 and m2–m3 alveoli; F:AM 61161, right partial maxillary with P1 alveolus–P4 and M1 alveolus; F:AM 61164, right partial maxillary with P4–M1 and M2 alveolus; F:AM 61170, right maxillary fragment with P3–P4 both broken; F:AM 61177, left partial ramus with p4 broken–m2 and m3 alveolus; F:AM 61177M, left partial ramus with m1 and m2–m3 alveoli; F:AM 61177O, right partial ramus with p1–p3 alveoli, p4 broken–m1, and m2 broken; F:AM 61178A, right partial ramus with i1–i3 alveoli and c1 broken–p4; and F:AM 61179H, posterior cranial fragment. West Sinclair Draw: F:AM 25496, right ramus fragment with m1. Humbug Quarry: F:AM 61136, right partial ramus with c1–p1 alveoli and p2 broken–m1; F:AM 61139, right ramus with c1–m2 (p1 and m3 alveoli); F:AM 61140, left partial ramus with c1 alveolus and p2–m1 (p3 alveolus); F:AM 61141, right ramus with c1 broken–m2 (p1 and m3 alveoli); F:AM 61142, right ramus with i1–p1 alveoli, and p2–m2 (m1 broken and m3 alveolus); F:AM 61143, left partial ramus with i2–p1 alveoli and p2–m2 (m1 broken); F:AM 61146, right ramus with i1–i3 alveoli, c1, p1 alveolus, and p2–m3 (fig. 69A, B); F:AM 61147, right partial ramus with p1 alveolus–m1 (p3 alveolus); F:AM

61148, left partial ramus with i3–c1 alveoli, p3 broken–m2, and m3 alveolus; F:AM 61160, posterior part of skull and separate premaxillary-maxillary with I1–P1 alveoli and P2–M2; F:AM 61162, right maxillary fragment with P3–P4; F:AM 61165, left partial maxillary with P4–M2; F:AM 61166, left partial maxillary with P3–M1 (both P4 and M1 broken); F:AM 61177A, left partial ramus with p2 broken–m2 (p4 broken and m3 alveolus); F:AM 61177F, right partial ramus with m1–m3; F:AM 61177I, right partial ramus with p2 broken–m1; F:AM 61177J, right partial ramus with p3–m1; F:AM 61177U, left partial ramus with i1–p1 alveoli, p2–p4, m1 alveolus, m2 broken, and m3 alveolus; F:AM 61177W, right partial ramus with p1 alveolus, p2–p3 both broken, p4, m1 alveolus, m2, and m3 alveolus; F:AM 61177X, left partial ramus with p1 alveolus, p2 broken–p4, and m1 alveolus; F:AM 61178D, left immature partial ramus with c1–p1 alveoli, dp2–dp4, and m1 unerupted; F:AM 61179, posterior part of skull; F:AM 61179A, posterior part of skull; F:AM 61179B, posterior part of skull; F:AM 61179E, cranial fragment; F:AM 61179D, posterior part of skull; and F:AM 61179I, cranial fragment. Quarry 3: F:AM 61153, left partial ramus with p2–m2 and m3 alveolus. Quarry 6: AMNH 22370, right partial ramus with c1–p3 alveoli, p4, and m1–m3 alveoli. Quarry 7, Kilpatrick Pasture: AMNH 21477A, isolated left M1, left M2, and m2. Grass Root Quarry: F:AM 21448C, left and right maxillary fragments with P2–P3, P4 root, and M1–M2. Jenkins Quarry: F:AM 61157, right and left partial maxillary with C1–P1 alveoli, P2 broken–M2, and skull fragments. Boulder Quarry: F:AM 61113, left partial ramus with i1 alveolus, and c1 broken–m2 (p3, p4, and m3 alveoli); F:AM 61163, right partial maxillary with P3–M1; F:AM 61167, left partial maxillary with P4–M2; F:AM 61177Y, right partial ramus with c1–p4 alveoli, m1 broken, and m2–m3 alveoli; and F:AM 61177Z, left partial ramus with c1–p4 (p1 alveolus). Surface Quarry: F:AM 61177C, right ramus fragment with m1–m2. East Sand Quarry: F:AM 61168, right partial maxillary with P4–M1; F:AM 61177L, right partial ramus m1–m2 and m3 alveolus; F:AM 61179J, posterior part of

skull; and F:AM 104806, right ramal fragment with p4–m1 alveoli and m2–m3, below East Sand Quarry. West Sand Quarry: F:AM 61117, right ramus with c1 broken–m2 (p1 and m3 alveoli).

Lower Snake Creek Fauna, Olcott Formation (early Barstovian), unallocated, Sioux County, Nebraska: AMNH 13841, right partial ramus with p1 alveolus, p2–p3, and roots of p4–m1; AMNH 13850, right isolated upper M1, left isolated lower m1, two left ramal fragments with p2–p4; AMNH 20058, three isolated lower m1s; AMNH 20059, left and right ramal fragments with m1–m2; AMNH 20069, left isolated P4; AMNH 22377, left partial maxillary with P3–M1, “Ashbrook Pasture, Olcott Hill” (although label as from the Upper Snake Creek, this specimen was probably mislabeled); AMNH 83417, isolated left P4, left p3, and left m2; AMNH 83434, right partial ramus with p2 alveolus–m2 and m3 alveolus; AMNH 96682A, left ramal fragment with m1–m2; AMNH 96682B, right ramal fragment with m1–m2 and m3 alveolus; and AMNH 96682C, left isolated lower m1.

Observation Quarry, Sand Canyon Formation (early Barstovian), Dawes County, Nebraska: F:AM 54485, left isolated P4; F:AM 61187, right maxillary fragment with P3 alveolus–P4; F:AM 61188, right partial ramus with c1 broken, p2–p4, m1–m2 both broken, and m3 alveolus; F:AM 61189, left partial ramus with c1, p1–p3 alveoli, p4–m2, and m3 alveolus; F:AM 67987, left incomplete humerus; F:AM 67988, metacarpal I; F:AM 67988A, metacarpal II; F:AM 67988B, incomplete metacarpal III; F:AM 67988D, metacarpal V; F:AM 67988E, metacarpal V; F:AM 67988G, calcaneum; F:AM 67988H, broken astragalus; and F:AM 104805, right partial ramus with c1 broken, p1 alveolus–p4, and m1–m2 both broken.

Sand Canyon Formation (early Barstovian), Dawes County, Nebraska: Expectation Prospect: F:AM 61185, right premaxillary-maxillary with I1–I3 alveoli, and C1–M2 (P1 alveolus, P2 and P4 both broken). Survey Quarry: F:AM 61186, right isolated M1; F:AM 67988C, partial metacarpal II; and F:AM 67988I, first phalanx. School House Prospect, Pepper Creek: F:AM 61315, right ramus with c1–m2 and m3 alveolus; F:AM

61316, left ramus with i1–c1 all broken and p1–m3; F:AM 61317, left partial maxillary with P4–M2; F:AM 61318, left maxillary fragment with P4–M1 alveoli and M2; and F:AM 67990, incomplete radius.

Mud Hills Area, Green Hills and Second Division faunas, Barstow Formation (early Barstovian), San Bernardino County, California: Steepside Quarry: F:AM 61190, left ramus with c1 broken–m2 (m1 broken); F:AM 61191, right partial ramus with c1 broken, p1–p2 alveoli, p3 broken–m2, and m3 alveolus; F:AM 61192, right and left partial rami with i3–m3 (p1 alveolus); F:AM 61193, left partial maxillary with P4–M2 (M1 broken), left ramus with c1–m2 (p1 and p3 alveoli and p4–m1 both broken), m3 alveolus, and associated cervical vertebrae (F:AM 61193A); F:AM 61194, right partial ramus with c1–m1; F:AM 61195, right partial ramus with c1–p3 alveoli, p4 broken–m1, and m2–m3 both broken; F:AM 61196, crushed mandible with i2–m3 (i2–c1 and m1–m2 all broken); F:AM 61197, left ramus with c1–m3; F:AM 61198, right partial ramus with p2 alveolus–m2 (p3 and m1 broken); F:AM 61199, left partial ramus with i3–p3 roots and p4 broken–m1; F:AM 61200, left ramus with c1 broken–m2 (m1–m2 both broken) and m3 alveolus; F:AM 61201, right ramus fragment with m1 broken and m2–m3; F:AM 61201A, left ramal fragments with c1–m2 all broken; F:AM 61202, right ramus with c1–p1 alveoli, p2–m2 (m1 broken), and m3 alveolus; F:AM 61203, right and left partial rami with c1–m2 (p3–m1 all broken); F:AM 61204, right ramus with premolar alveoli and m1–m2 both broken; F:AM 61205, left partial ramus with i2–m2 (p1 alveolus and m1–m2 broken); F:AM 61206, right and left partial rami with c1 broken–m3 (p1 broken); F:AM 61207, maxillary fragment with C1 and both rami with i3–c1 broken and p1 alveolus–m2; F:AM 61208, left partial ramus with p1–p3 alveoli, p4–m2, and m3 alveolus; F:AM 61209, right partial ramus with c1–p3 alveoli, p4–m1, and m2 alveolus; F:AM 61210, right partial ramus with p2 broken–m1; F:AM 61211, right partial ramus with p4 broken–m2; F:AM 61212, right partial ramus with i3–p4 and m1 broken; F:AM 61215, skull with I1–P1 alveoli, P2–P4 all broken, M1, and M2 broken; F:AM 61216,

partial skull with P3 broken–M2; F:AM 61217, crushed partial skull with P2–M2; F:AM 61218, crushed partial skull with P4–M1 both broken and M2; F:AM 61219, anterior part of skull with I1–P1 alveoli and P2 broken–M2; F:AM 61220, crushed skull with I1–P3 alveoli and P4–M2; F:AM 61221, left partial maxillary with P4–M2 (M1 broken); F:AM 61222, right partial maxillary with P3 alveolus–M2; F:AM 61223, right partial maxillary with P4, M1 broken, and M2 root; F:AM 61225, left partial maxillary with P3 broken–M2 (M1 broken); F:AM 61226, right and left partial maxillae with P3 broken–M2 and detached C1; F:AM 61227, right partial maxillary with P3 broken–M2; F:AM 61228, left partial maxillary with P4 broken–M2; F:AM 61229, right and left broken and incomplete maxillae and left partial premaxillary–maxillary with I1–I2 roots, and C1–M2; F:AM 61230, left partial maxillary with I1–P1 alveoli, P2 broken–P3, and a separate maxillary fragment with P4–M1; F:AM 61231, two associated left maxillary fragments with C1–P2 and M1–M2 and teeth fragments; F:AM 61231A, left premaxillary fragment with C1; F:AM 61232, right partial maxillary with P4 broken–M2; F:AM 61233, crushed fragment of skull with P2–P3 alveoli and P4–M2 all broken; F:AM 61234, crushed partial skull with C1–P3 alveoli and P4–M2 all broken; F:AM 61235, skull fragment with C1 broken, P1 and P3 alveoli, and P4–M2 all broken; F:AM 61236, posterior part of skull; and F:AM 105302, posterior part of skull. Green Hills: F:AM 27150, palate with P2 broken–M2 and mandible with i3–m3; F:AM 27505, left partial ramus with c1 broken–m2 (p1 and p2 broken); F:AM 27510, crushed partial skull with P3–M2 and both rami with c1 broken–m3 (p1 alveolus and m1 broken); F:AM 27512, left partial maxillary with P4–M2; F:AM 27513, left maxillary fragment with P3–P4; F:AM 27514, right ramus with i3 alveolus–m1 and m2 root; F:AM 27515, right partial ramus with p1 alveolus–m2 (m1 broken); F:AM 27516, left partial ramus with p1–p3 alveoli, p4–m2, and m3 alveolus; F:AM 27517, left partial ramus with c1–p4 and m1 broken; F:AM 27518, right partial ramus with i3 broken–m2 (p1 alveolus and p2 broken); F:AM 27519, right and left rami with c1–m2 and m3 alveolus; F:AM 27520, left



partial ramus with c1–p2 alveoli, p3–m2, and m3 alveolus; F:AM 27521, right partial ramus with p4–m3; F:AM 27531, right and left partial maxillae with P4 broken–M2; and F:AM 67335, left partial ramus with c1–p4 alveoli and m1–m2. First layer above Third Division: F:AM 27272, partial palate with P3 broken–M2; and F:AM 27285, immature left and right partial rami with dp2 broken, dp3, and m1 unerupted. Second layer above Third Division: F:AM 27263, right and left partial rami with i2–m3 (c1 broken). Lower Second Division: F:AM 27511, crushed partial palate with P2–M2 (P3 broken). Sunder Ridge Quarry: F:AM 61213, right and left partial rami with c1–m2 (p1 broken). Turbin Quarry: F:AM 61214, right ramal fragment with m1 broken–m2. No locality data: F:AM 27262, right partial ramus with p3–m2; F:AM 27262A, right partial ramus with c1–p4 and m1–m2 both broken; F:AM 27264, right partial ramus with P4–M2; F:AM 27265, right maxillary fragment with M1; F:AM 27271, left ramus with i1–c1 broken, p1 broken, p2–m1 all broken, and m2; and F:AM 27271A, isolated left m1.

Yermo Quarry, Barstow Formation (early Barstovian), San Bernardino County, California: F:AM 27507, right partial maxillary with P4–M2; F:AM 27509, right partial ramus with p4 root–m2; F:AM 27529, right and left partial rami with c1–m3 (p1 and p4 alveoli); F:AM 61237, anterior part of skull with I1–M2; F:AM 61238, partial skull with P1–P3 alveoli and P4–M2 all broken; F:AM 61239, left partial maxillary with P4–M1 and M2 broken; F:AM 61240, right and left partial maxillae with P4–M2; F:AM 61242, left partial ramus with p2–m2 all broken; and F:AM 61243, left isolated m1.

Skull Ridge Member, Tesuque Formation (early Barstovian), Santa Fe County, New Mexico: Southeast of White Operation Wash: F:AM 27379, partial skull with P1–P3 alveoli, P4 broken, and M1–M2; F:AM 27381, right partial ramus with p3–m2 (p4 broken) and m3 alveolus; F:AM 27382, left and right ramal fragments with broken p2–m3 (p2–m2 all broken); F:AM 27383, right partial ramus with p4–m1 both broken, m2, and m3 unerupted; and F:AM 27384, edentulous left partial ramus with c1–m3 alveoli. Skull Ridge: F:AM 27383A, right partial maxillary

with P4–M2. Cuyamunque: F:AM 27470, skull with I1–M2 (most teeth broken or heavily worn). One mi north of White Operation: F:AM 50154, left and right partial rami with c1 broken–m2 (p1–p2 and m3 alveoli).

Kent Quarry (UCMP loc. V5666), Dry Canyon West Side 2, Cuyama Valley, Caliente Formation (early Barstovian), Ventura County, California: UCMP 50670, partial anterior skull with I1–M2 (I3 broken) and mandible with i3–m2 and m3 alveolus; and UCMP 51104, skull fragments with P3–M1 and partial left and right bullae.

DISTRIBUTION: Early Barstovian of Nebraska, New Mexico, and California.

EMENDED DIAGNOSIS: Compared to *Tomarctus brevirostris*, *T. hippophaga* is primitive in having palate not widened, nuchal crest not laterally narrowed, and M1 paracone less high-crowned.

DESCRIPTION AND COMPARISON: The numerous previously undescribed materials from the Olcott Formation represent a marked improvement in quantity and quality of specimens over that available to Matthew (1924, his *Tomarctus brevirostris*). This is especially true for the exquisitely preserved materials from the Echo Quarry. In addition, large samples from the lower part of the Barstow Formation are referred to this species for the first time. These and a small sample from the Tesuque Formation, New Mexico, suggest that *Tomarctus hippophaga* was widespread in the early Barstovian.

A nearly perfect skull (F:AM 61156; fig. 70A–D) from the Echo Quarry permits an undistorted view of this species, as opposed to the crushed skulls from other quarries described by Matthew (1924). With the increased fidelity of cranial structures, it is possible to ascertain that *Tomarctus hippophaga* has a relatively narrower palate than does *T. brevirostris* (as exemplified by a similarly undistorted skull, F:AM 61158) (see Description and Comparison under *T. brevirostris*). Apparently a young adult, because of the lack of wear on teeth, F:AM 61156 has relatively narrow forehead (distance between the supraorbital rim) in contrast to older individuals (AMNH 18242–44) that have broader foreheads (fig. 70E–H). On a dissected partial skull (F:AM 61181), the large

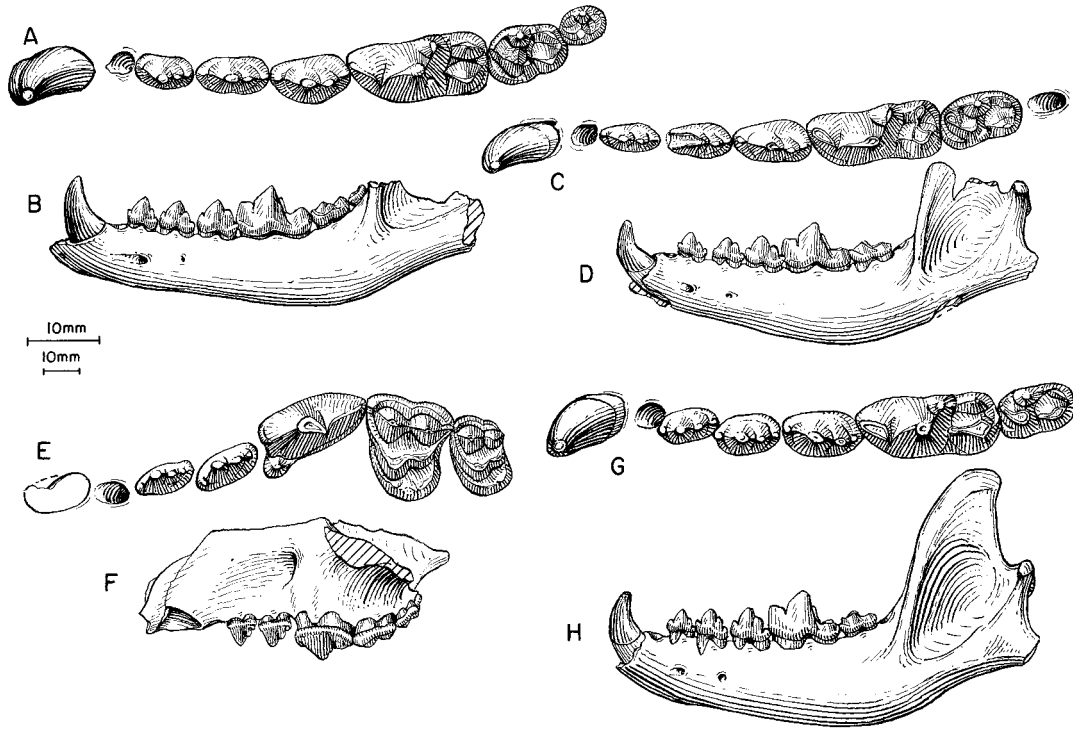


Fig. 69. *Tomarctus hippophaga*. **A**, Lower teeth and **B**, ramus (reversed from right side), F:AM 61146, Humbug Quarry, Olcott Formation (early Barstovian), Sioux County, Nebraska. **C**, Lower teeth and **D**, ramus, F:AM 61174, Echo Quarry, Olcott Formation (early Barstovian), Sioux County, Nebraska. **E**, Upper teeth and **F**, lateral view of maxillary (reversed from right side), F:AM 61174A, Echo Quarry. **G**, Lower teeth and **H**, ramus (reversed from right side), AMNH 13836, holotype, Quarry 2, East Sinclair Draw, Olcott Formation (early Barstovian), Sioux County, Nebraska. The longer (upper) scale is for A, C, E, and G, and the shorter (lower) scale is for the rest.

frontal sinus can be seen to be partitioned by a horizontal septum into anterodorsal and posteroventral chambers including a sinus in the postorbital process that communicates through a restricted passage with the posteroventral chamber. Other than the above-noted features, *T. hippophaga* is quite similar in cranial proportions to *Protomarctus optatus* and *Tomarctus brevirostris* (fig. 71).

*Tomarctus hippophaga* is larger than *Protomarctus optatus* (13% in basal skull length and 11% in m1 length, all pooled averages). Signaling its affinity with the Aelurodontina, *T. hippophaga* has enlarged lower premolars and this enlargement is rather uniform on all premolars instead of differential enlargement of p4 over p2–p3 as in the Borophagina. The massiveness of the premolars is mainly reflected in the width of the tooth and is in

clear contrast to the immediate primitive state in *P. optatus*. Other than the robust premolars, teeth of *T. hippophaga* are little different from those of *P. optatus*.

Specimens from the Barstow Formation are on the whole 5% (pooled average of all dental measurements) smaller than their counterparts in the Lower Snake Creek Fauna in Nebraska. The California individuals also tend to be more primitive in their narrower foreheads and less massive premolars. Such minor differences aside, the California sample is closest, both in size and overall morphology, to the toptotypical materials of *Tomarctus hippophaga* in Nebraska. We interpret these variations from the California sample as representing a primitive population of the lineage.

Referred individuals from the Tesuque

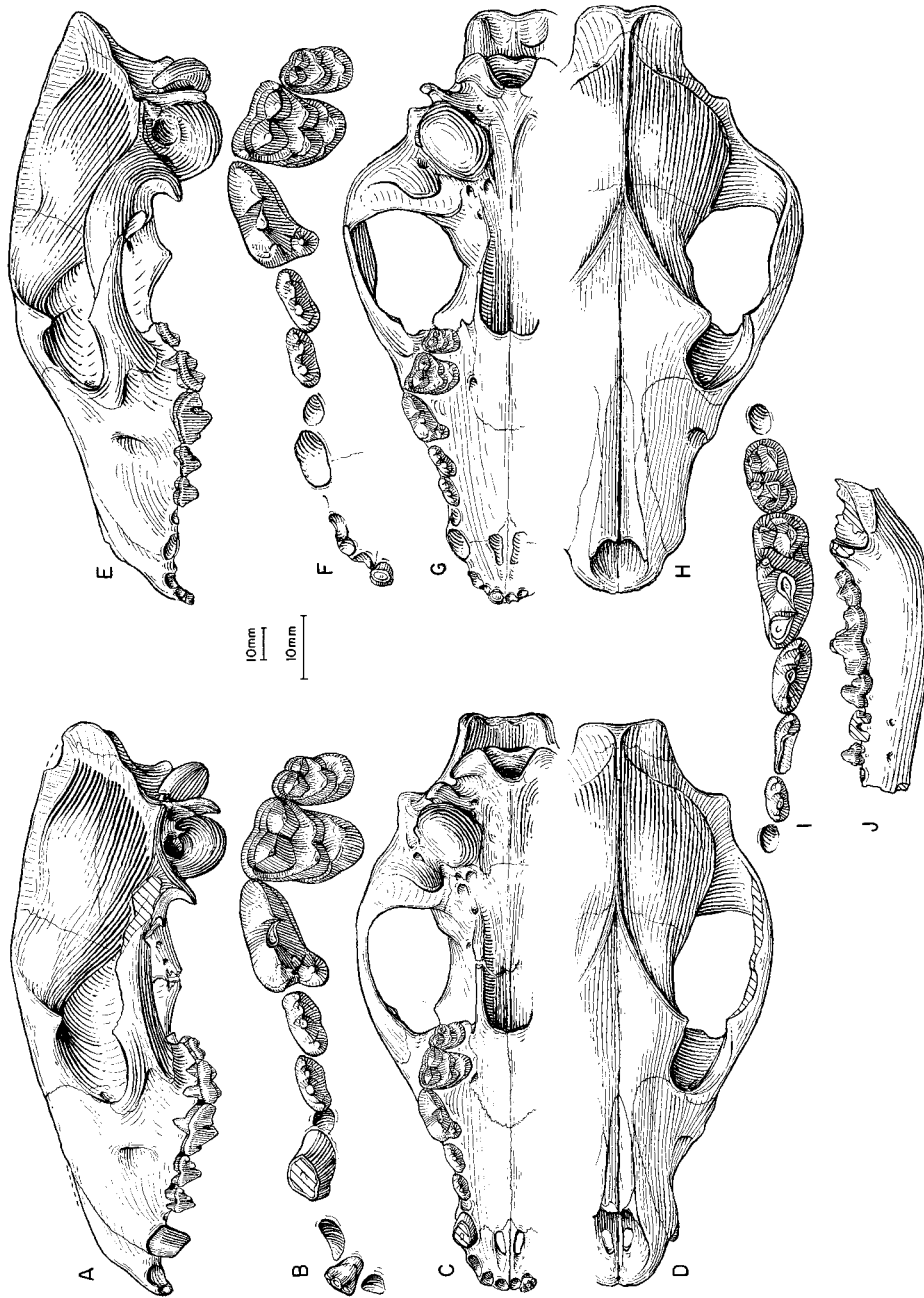


Fig. 70. *Tomarctus hippophaga*. A, Lateral, B, enlarged occlusal, C, ventral and D, dorsal views of skull and upper teeth, F:AM 61156, Echo Quarry, Olcott Formation (early Barstovian), Sioux County, Nebraska. E, Lateral, F, enlarged occlusal, G, ventral, and H, dorsal views of skull and upper teeth (I1 and P2-P3 reversed from right side). I, lower teeth, and J, ramus (reversed from right side), AMNH 18244, Sheep Creek Quarry, Olcott Formation (early Barstovian), Sioux County, Nebraska. The shorter (upper) scale is for A, C, D, E, G, H, and J, and the longer (lower) scale is for the rest.

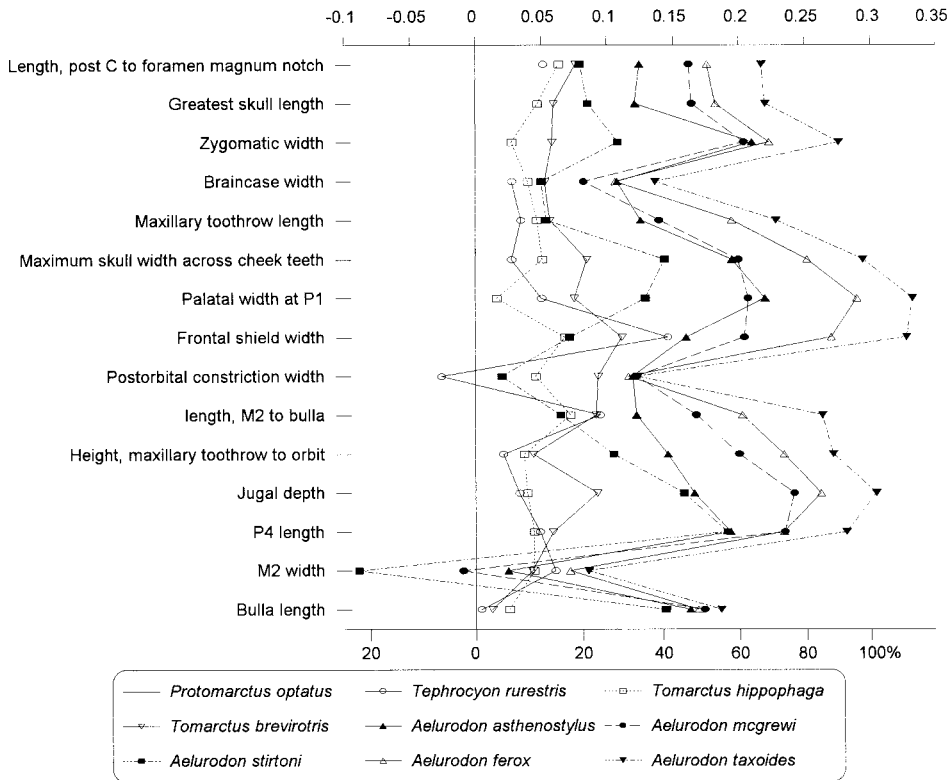


Fig. 71. Log-ratio diagram for cranial measurements of *Tephrocyon*, *Tomarctus* and *Aelurodon* using *Protomarctus optatus* as a standard for comparison (straight line at zero). See text for explanations and appendix II for measurements and their definitions.

Formation are less well represented both in quantity and quality of materials. Most of the specimens match very well, in size and shape, with the topotype series from Nebraska. One skull (F:AM 27470), however, is substantially larger and is in the same size category as *Tomarctus brevirostris*. Teeth of F:AM 27470 are severely worn and badly broken. This large individual has an unbroadened palate and its nuchal crest is not narrowed laterally, features that suggest its assignment to *T. hippophaga*.

DISCUSSION: *Tomarctus hippophaga* was initially compared with *Tephrocyon rurestris* from the Mascall Formation of Oregon by Matthew and Cook (1909), who made no reference to *Tomarctus brevirostris*. Shortly afterward, Matthew began to suspect that *brevirostris* from the Pawnee Creek area of Colorado might be conspecific with *hippophaga*. However, he did not act on this suspicion un-

til the publication of his influential treatise on the Snake Creek faunas, when he was finally convinced that the faunas from the Pawnee Creek and Snake Creek were very close in age, and *T. hippophaga* was thus synonymized under *T. brevirostris* (Matthew, 1924). Matthew's authoritative treatment on the relationships of canids in the 1924 volume proved to be very influential, and except for one brief mention of *Tomarctus hippophaga* by VanderHoof (1931: 19), his taxonomic decision was followed by all subsequent students. Thus, *T. hippophaga* has all but disappeared from the literature.

Matthew himself, however, still harbored some lingering doubts about this decision. Indeed, there is a substantial size difference between the holotypes of *Tomarctus brevirostris* and *T. hippophaga*—the lower carnassial of the former is 16% longer than that of the latter. Furthermore, there are individ-

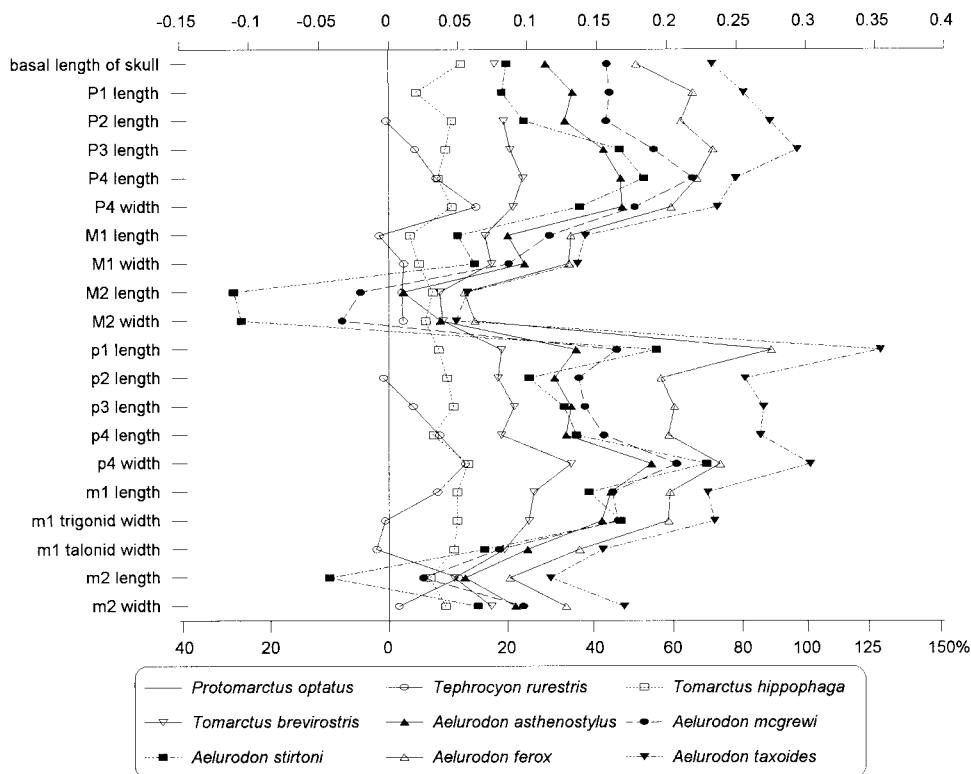


Fig. 72. Log-ratio diagram for dental measurements of *Tephrocyon*, *Tomarctus*, and *Aelurodon* using *Protomarctus optatus* as a standard for comparison (straight line at zero). See text for explanations and appendix III for summary statistics of measurements and their definitions.

uals in the Lower Snake Creek Fauna that possess even smaller carnassials than that of the holotype of *T. hippophaga*, making the variation in size even greater. Associated with the size differences are some cranial characters in certain large individuals from the Olcott Formation that suggest more than one species is present in the Snake Creek Fauna. Our resurrection of *T. hippophaga* is thus an attempt to account for these quantitative and qualitative differences (see further discussion under *Tomarctus brevirostris*).

Without explicit reference to specimens, Barbour and Cook (1917: 180) listed *Tephrocyon* cf. *hippophaga* to occur in the Valentine beds in Nebraska. We could find no such occurrence in these younger strata.

*Tomarctus brevirostris* Cope, 1873

Figure 73

*Tomarctus brevirostris* Cope, 1873: 2. Matthew, 1899: 68; 1901: 359; 1924: 91 (in part). Hay,

1902: 775. Cope and Matthew, 1915: pl. CXIXc, fig. 4. Munthe, 1998: 135.  
*Aelurodon francisi* Hay, 1924: 2, pl. 3, figs. 1, 2.  
 Wilson, 1960: 991 (in part). Munthe, 1998: 136.  
*Aelurodon simulans* Hay, 1924: 2, fig. on p. 3.  
 ?*Aelurodon francisi* (Hay): Vanderhoof and Gregory, 1940: 153.  
*Tomarctus* sp.: Repenning and Vedder, 1961: table 235.1.

HOLOTYPE: AMNH 8302, right ramal fragment with p4 alveolus–m1 (fig. 73O, P) from Court House Butte, Pawnee Creek Formation (probably early Barstovian), Weld County, Colorado.

REFERRED SPECIMENS: Pawnee Creek Formation (late early Barstovian), Weld County, Colorado: Middle Horizon near Hereford: F: AM 28302, left partial ramus with p4–m1 (fig. 73M, N). Question Mark Pit, southwest side: F:AM 67319, right ramus with c1–m3 (fig. 73E, F); F:AM 67320, right partial ramus with i1–i3 alveoli, c1 broken, p1–p3 al-

veoli, p4 broken-m1, and m2-m3 alveoli; and F:AM 67322, left partial ramus with c1 broken, m1 broken, and alveoli of the remaining teeth. Three Point, East Side Pit: F:AM 67321, left partial ramus with c1-p1 alveoli, and p2 broken-m2 (p3 alveolus, p4-m1 broken, and m3 alveolus). Pawnee Quarry: F:AM 105304, left partial maxillary with P4-M2 all broken. Big Spring Quarry: F:AM 105305, right isolated M1. No locality data: F:AM 28314, left and right partial maxillary with C1-M2 (molars extremely worn); and F:AM 28319, immature right ramal fragment with dp4 and m1.

Pawnee Creek Formation (early late Barstovian), Logan and Weld counties, Colorado: Cedar Creek: AMNH 9455, immature left ramus with di1, dc1, dp2, dp4, and m1 unerupted. Horse Quarry: F:AM 28315, right partial maxillary with P4 and M1-M2 alveoli; and F:AM 28317, left partial ramus with i1-p2 alveoli, p3-m1, and m2 alveolus.

Olcott Formation (early Barstovian), Sioux County, Nebraska: Humbug Quarry: F:AM 61158, partial skull with C1, P4-M2, and alveoli of all other teeth (fig. 73A-D); F:AM 61169, left partial maxillary with P2-P4 (P3 alveolus and M1 broken); F:AM 61177Q, left partial ramus with p2-p3 alveoli, p4-m1, and m2 alveolus; F:AM 61177V, right partial ramus with i1-p1 alveoli and p2-p4. Boulder Quarry: F:AM 61123, left ramus with i1-i3 alveoli, c1, p1 alveolus-m1, and m2 alveolus. Echo Quarry: F:AM 61121, left ramus with i1-i3 alveoli, and c1-m1 (p1 alveolus and m2-m3 alveoli); F:AM 61122, right ramus with i1-i3 alveoli, and c1-m2 (p1 and m3 alveoli). Ashbrook Pasture: AMNH 13834, left partial maxillary with M1-M2; AMNH 20057, right isolated M1; AMNH 22400, left maxillary with P4 broken-M2, right ramus with i1-p1 alveoli, p2-m2, and m3 alveolus; and AMNH 81031 (HC 273), right partial maxillary with C1-P1 alveoli and P2-P4. East Sinclair Draw: F:AM 25487, partial left ramus with p2-p3 alveoli, p4-m1, and m2 alveolus, Horizon C. East Sand Quarry: F:AM 61151, right ramus with i3-p1 alveoli, p2, p3 alveolus-m1, and m2-m3 alveoli. Jenkins Quarry: F:AM 61177R, left isolated m1. West Sand Quarry: F:AM 61129, right ramus with i2-m2 (p1 and m3 alveoli). Quarry A: AMNH 18251,

left partial ramus with p3-m2 and right partial ramus with m1 and m2-m3 alveoli. Quarry B: AMNH 18246, left partial maxillary with P1-P3 alveoli and P4-M2 (fig. 73G, H). Quarry 2: F:AM 61125, left ramus with i1-p1 alveoli, and p2-m2 (m1 broken and m3 alveolus); F:AM 61130, left ramus with c1-p1 alveoli, p2-m2, and m3 alveolus (fig. 73I, J); F:AM 61171, right maxillary fragment with M1 broken-M2; F:AM 61177P, left partial ramus with m1-m2; F:AM 61178, left partial ramus with i1-i3 alveoli, c1, and p1 alveolus-p4; and F:AM 61179C, posterior part of skull. Quarry 8: F:AM 61127, right partial ramus with i1-i3 alveoli, c1, p1-p2 alveoli, and p3-m2. New Surface Quarry: F:AM 61124, right partial ramus with c1-p3 alveoli, p4-m1, and m2 roots; F:AM 61126, left partial ramus with c1-p1 alveoli, p2-m2, and m3 alveolus; F:AM 61128, left partial ramus with c1-p1 alveoli, p2-m1, and m2-m3 alveoli; F:AM 61175, partial left maxillary with P2 alveolus and P3 broken-M2; F:AM 61177N, left ramal fragment with m1; F:AM 61177S, left ramal fragment with m1-m2 and m3 alveolus; F:AM 61178B, right ramal fragment with p2 alveolus-p4; F:AM 61179F, skull fragments, posterior part; and F:AM 61179G, posterior part of skull. Version Quarry: F:AM 61159, right maxillary with P1 alveolus-M2; and F:AM 61177T, right partial ramus with p4 broken-m2 and m3 alveolus, ?Version Quarry or Pocket 34. Seventeen mi south of Agate (from Upper Snake Creek beds, but probably reworked): AMNH 81096 (HC 515), isolated right m1.

Second Division Fauna, Barstow Formation (late early Barstovian), San Bernardino County, California: Valley View Quarry: F:AM 27502, right ramus with c1-m2 (p1 alveolus) and m3 alveolus; F:AM 27538, right and left rami with i1-c1 all broken and p1-m3; F:AM 27544, right partial ramus with i1-p1 roots and p2-m2 (p3 and m3 alveoli); F:AM 27544A, left partial ramus with p4 broken-m3; and F:AM 31100, right ramus with i2-i3 roots and c1-m2. No locality data: F:AM 27260, left maxillary with P4-M2; and F:AM 27261, right partial ramus with p2-p4 all broken and m1-m3.

East Caliente Range, Caliente Formation (early Barstovian), San Luis Obispo County,

California: USGS M1005, isolated P4 and M1 (referred to *Tomarctus* sp. by Repenning and Vedder, 1961: table 235.1), 4 ft below middle Triple Basalt.

Skull Ridge Member, Tesuque Formation (early Barstovian), Santa Fe County, New Mexico: Skull Ridge: F:AM 61182, crushed anterior part skull with I3–M2, partial left and right rami with p3–m2, and limb fragments including metapodial fragments and 9 phalanges. Third District: F:AM 27368, left maxillary fragment with P3–M1.

J. Niscavit Farm, from a well at a depth of 22 ft, Grimes Prairie, 12 mi east of Navasota and 3 mi north of Stoneham, possibly equivalent to the Cold Spring fauna (Wilson, 1960: 991) of Fleming Formation (late Barstovian), Grimes County, Texas: TMM-TAMU 2379 (AMNH cast 97240) (holotype of *Aelurodon francisi* Hay, 1924), left partial ramus with p3–m3 (fig. 73K, L).

Noble Farm fauna (late Barstovian) (stratigraphically equivalent to Grimes Prairie, the type locality of *A. francisi*, according to VanderHoof and Gregory, 1940: 153), Moore County, Texas: TMM-TAMU 2186 (AMNH cast 97772) (holotype of *Aelurodon simulans* Hay, 1924), right partial ramus with p3–m2 (m1 broken) and m3 alveolus.

DISTRIBUTION: Early Barstovian of Colorado, Nebraska, New Mexico, and California; and early late Barstovian of Colorado; late Barstovian of Texas.

EMENDED DIAGNOSIS: Synapomorphies shared by *Tomarctus brevirostris* and *Aelurodon* but distinguishing it from *T. hippophaga* are broadened palate, posterodorsally produced nuchal crest that is laterally compressed, reduction of lambdoidal crest, and high-crowned M1 paracone relative to metacone. Primitive characters that distinguish *T. brevirostris* from *Aelurodon* are sagittal crest lower, bulla not hypertrophied, mastoid process small, P4 protocone less reduced, P4 parastyle smaller, upper molars not reduced relative to P4, M1 lingual cingulum not restricted to the posterolingual border, m1 talonid not narrowed, m2 less reduced, and m2 metaconid approximately equal to protoconid in height.

DESCRIPTION AND COMPARISON: Our re-shuffling of the hypodigm of *Tomarctus* admits, in addition to the toptype materials

from Colorado, only a small portion of the total Lower Snake Creek samples and excludes all of the specimens described by Matthew (1924, see Discussion below). The newly referred skull from Humbug Quarry (F:AM 61158, fig. 73A–D) is entirely undistorted, unlike the crushed skulls figured in Matthew (1924), and affords secure knowledge about its cranial morphology. In overall cranial proportions, *T. brevirostris* is slightly more advanced than *T. hippophaga* toward the *Aelurodon* clade. In the ratio diagram figure 71, the pattern for *T. brevirostris* begins to assume the shape for various species of *Aelurodon*, although still in its initial stage. The most obvious difference is a broader palate. This broadening of the palate is not merely due to its overall larger size; there is a 17% increase in palate breadth across widest points of cheekteeth (P4–M1 juncture) vs. a 7% increase in basal length of skulls (only the undistorted skulls are measured: F:AM 61158 for *T. brevirostris* and F:AM 61156 for *T. hippophaga*). The broadened palate is also indicated by the laterally deflected horizontal rami of the lower jaws. The frontal sinus has about the same degree of inflation as in *T. hippophaga*, and the postorbital process is similarly well developed. The nuchal crest is slightly more produced posteriorly and narrower laterally than that in *T. hippophaga*. The external auditory meatus has a slightly longer lip, and the paroccipital process is more posteriorly expanded, increasing the area of the lateral scar.

Dental differences between *Tomarctus brevirostris* and *T. hippophaga* are subtle and often involve proportional relationships. *T. brevirostris* is on average 10% larger (pooled average of all dental measurements) than *T. hippophaga*. Signaling the further advancement toward the *Aelurodon* clade, the premolars of *T. brevirostris* are stronger than those of *T. hippophaga*; its M2 and m2 are slightly reduced relative to M1 and m1, and the M1 shows an appreciable crown height difference between paracone (higher) and metacone. Other than these subtle proportional differences, the cusp morphology of upper and lower molars is quite similar to those of *T. hippophaga*.

Compared with *Aelurodon*, on the other hand, *T. brevirostris* is more easily distin-

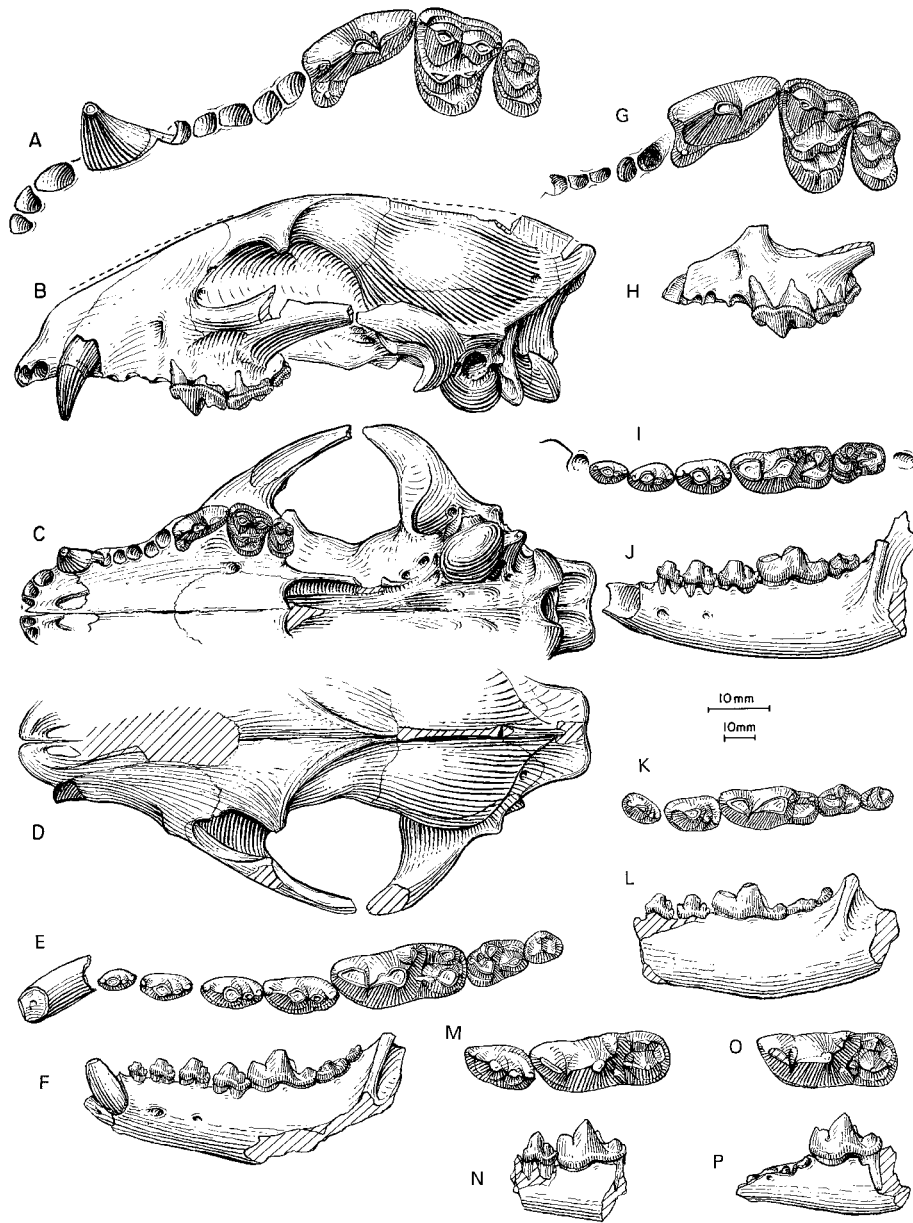


Fig. 73. *Tomarctus brevirostris*. **A**, Upper teeth and **B**, lateral, **C**, ventral, and **D**, dorsal views of skull, F:AM 61158, Humbug Quarry, Olcott Formation (early Barstovian), Sioux County, Nebraska. **E**, Lower teeth and **F**, ramus (reversed from right side), F:AM 67319, Question Mark Pit, Pawnee Creek Formation (late early Barstovian), Weld County, Colorado. **G**, Upper teeth and **H**, lateral view of maxillary, AMNH 18246, Quarry B, Olcott Formation. **I**, Lower teeth and **J**, ramus, F:AM 61130, Quarry 2, Olcott Formation. **K**, Lower teeth and **L**, ramus, TMM 2379 (holotype of *Aelurodon francisi*), J. Niscavit Farm, beds possibly equivalent to the Cold Spring Fauna of Fleming Formation (late Barstovian), Grimes County, Texas. **M**, Lower teeth and **N**, ramus, F:AM 28302, middle Horizon near Hereford, Pawnee Creek Formation (late early Barstovian), Weld County, Colorado. **O**, Occlusal and **P**, lateral views of ramus and m1 (reversed from right side), AMNH 8302, holotype, Court House Butte, Pawnee Creek Formation (probably early Barstovian), Weld County, Colorado. The longer (upper) scale is for A, E, G, I, K, M, and O, and the shorter (lower) scale is for the rest.



guished by its primitive cranial and dental morphology. The sagittal crest in *T. brevirostris* is still low, the bulla is not prominently inflated, and the paroccipital process is not quite as elongated as in *Aelurodon*. The P4 parastyle is not strong. The m1 talonid remains broad, and the m2 metaconid is still large.

DISCUSSION: Established on a ramal fragment with a single m1 from the Pawnee Creek Formation in Colorado, *Tomarctus brevirostris* was largely ignored by subsequent students until Matthew's (1924) reference of complete cranial and dental materials from the Lower Snake Creek Fauna of Nebraska. These referred materials played an important role in establishing *T. brevirostris* as a primitive ancestor to nearly all later canids (see further discussion under the genus).

After many years of hesitation following the establishment of *Tephrocyon hippophaga* (Matthew and Cook, 1909), Matthew (1924) finally concluded that *Tomarctus brevirostris* and *T. hippophaga* were probably conspecific, mainly because of his increasing confidence that the Pawnee Creek beds (now Formation), where the type of *T. brevirostris* was recovered, and the Lower Snake Creek beds (now Olcott Formation) were roughly coeval. However, he did have some lingering doubts about this conclusion: "it is quite probable that the species [*T. brevirostris* and *T. hippophaga*] are identical, but adequate proof of this is lacking, and they may yet prove to be distinct" (Matthew, 1924: 89). Although Matthew's observation was based on quite good materials (three lightly crushed skulls) from the Lower Snake Creek Fauna, considerably more materials from both the Olcott Formation and the Pawnee Creek Formation have been accumulated since his last review. With the additional materials, we now recognize the validity of both *T. brevirostris* and *T. hippophaga* and the presence of both within the Lower Snake Creek Fauna.

Our reestablishment of these two species comes from two lines of evidence. First, there is a wide range of variation in size among the Lower Snake Creek samples, and it exceeds the normal variation of a species, even if one takes into account the temporal dimension of the fauna (see appendices II

and III). Second, a well-preserved skull from the Humbug Quarry (F:AM 61185) demonstrates that *Tomarctus brevirostris* possesses the initial development of several derived characters normally found only in *Aelurodon*, such as broadened palate, narrowed nuchal crest, and elongated paroccipital process, that contrast with the absence of these features in other skulls from the Lower Snake Creek quarries (including those described by Matthew, 1924). This advanced-looking skull is near the higher end of the size range among the Lower Snake Creek materials and is about the same size as the topotype series from Colorado. We thus hypothesize that among the Lower Snake Creek samples there is a small proportion of large-size individuals referable to *T. brevirostris* that are distinct from most individuals typified by the holotype of *T. hippophaga*. Such a hypothesis engenders a problem in the allocation of hypodigms—fragmentary specimens of intermediate size are difficult to allocate to one species or another—but is preferable to the alternative that does not discriminate the morphological differences within the samples, i.e., lumping everything into a single species, as proposed by Matthew (1924).

At a size almost identical to that of *Tomarctus brevirostris*, *Aelurodon francisi* (Hay, 1924) is almost indistinguishable from the former except in a few subtle features: a reduced metaconid, a slightly narrowed talonid, and a relatively reduced lingual side of the talonid that restricts the entoconid to a more anterior position. Although these features may suggest a taxon in the initial stage of development toward the *Aelurodon* clade, we tentatively place the Texas material in *Tomarctus* because of its lack of robust premolars so typical of *Aelurodon*.

Hay (1924: 2) also proposed *Aelurodon simulans* as a species distinct from *A. francisi*, even though he admitted that "at first this specimen [holotype of *A. simulans*] was taken to belong to *Ae. francisi*." Subsequent authors (VanderHoof and Gregory, 1940; Wilson, 1960) had all failed to see any distinction between the two species, a conclusion with which we agree. The only observable difference between the poorly preserved holotypes of these two Texas species is a rela-

tively more slender p3–p4 in *A. simulans*, a distinction easily encompassed by variation within species of similar size.

The referred specimens of *A. francisi* (Wilson, 1960) from the Cold Spring Fauna, however, clearly represent a large, more derived form (see *A. ferox*). The Cold Spring specimens agree well in size with *A. ferox*, and their advanced dental features, such as three lateral accessory cusplets on I3 (Wilson, 1960: fig. 4h), high-crowned M1 paracone, and prominent P4 parastyle, indicate the presence of this widespread species of *Aelurodon* in the late Barstovian of Texas.

Henshaw (1942) referred one upper canine and one m1 (LACM-CIT 774) to *Tomarctus brevirostris* from late early Barstovian sites near Tonopah in the San Antonio Mountains, Nevada. According to his figure (Henshaw, 1942: fig. 3), the upper canine is too long to be a canid. The m1, on the other hand, is too worn to be sure of its identity, and its size and proportions are slightly smaller than *T. brevirostris* as defined in this study (its size is closer to *Tomarctus hippophaga*). Its occurrence in the early Barstovian of Nevada is thus questionable.

#### *Aelurodon* Leidy, 1858

*Prohyaena* Schlosser, 1890: 25.

*Strobodon* Webb, 1969a: 43.

TYPE SPECIES: *Aelurodon ferox* Leidy, 1858.

INCLUDED SPECIES: *A. asthenostylus* (Henshaw, 1942); *A. mcgrewi*, new species; *A. stirtoni* (Webb, 1969a); *A. ferox* Leidy, 1858; and *A. taxoides* Hatcher, 1893.

DISTRIBUTION: Early Barstovian of Nebraska, Colorado, Nevada, and California; late Barstovian of Colorado, Nebraska, South Dakota, New Mexico, Texas, and California; early Clarendonian of South Dakota, Nebraska, New Mexico, Oklahoma, Texas, Florida, and Nevada; late Clarendonian of Nebraska, New Mexico, and California; and Clarendonian of Kansas.

EMENDED DIAGNOSIS: Species of *Aelurodon* share many derived features that differ from *Tomarctus*: high sagittal crest, enlarged bulla, enlarged mastoid process, P4 parastyle strong, P4 protocone reduced, reduced M1–M2 and m2, M1 lingual cingulum reduced

anteriorly, m1 talonid narrowed, shortened m2, and m2 metaconid reduced. Besides the *A. mcgrewi*–*stirtoni* clade, advanced species of *Aelurodon* acquire further derived characters, such as extremely broadened palate, transversely straight upper incisor row, massive premolars with very strong cusplets, extremely high sagittal crest, and more posterodorsally produced nuchal crest.

DISCUSSION: The strikingly robust skull and teeth of *Aelurodon*, mirroring in many ways the cranial and dental construction of bone-crushing hyaenids, attracted the attention of early vertebrate paleontologists (see Baskin, 1980, for a recent summary). Such attention quickly resulted in a proliferation of names during the pioneering era of North American vertebrate paleontology. In the first comprehensive review, VanderHoof and Gregory (1940) listed more than a dozen nominal species of “*Aelurodon*” (including *Epicyon*) but went little beyond reiteration of many of the previous “species,” essentially following the phylogenetic scheme advanced by Matthew (1924, 1930). Shortly afterward, McGrew (1944b) offered the insight that the multiple species of *Aelurodon* may be divided into two groups—the *A. taxoides* species group and the “*A.*” *saevus* species group—an idea further elaborated by Mawby (1964, 1965). In attempting to determine to which of these two groups the type species *A. ferox* belongs, Richey (1979: 108) took note of a crest between the P4 protocone and paracone in the *taxoides* group and concluded that the holotype of *A. ferox*, lacking this crest, probably belonged to the *saevus* group. Baskin (1980), however, investigated the P4 morphology in greater depth and determined that the genus *Aelurodon* should be restricted to the *A. taxoides* group, and *Epicyon* should be resurrected for the “*A.*” *saevus* group. Baskin’s phylogenetic outline is basically consistent with our own analysis, although his P4 protocone synapomorphy is not completely unique within *Epicyon* and is also shared by *Borophagus*.

#### *Aelurodon asthenostylus* (Henshaw, 1942), new rank

Figures 74–76

*Aelurodon wheelerianus asthenostylus* Henshaw, 1942: 111, pl. 4, figs. 1, 2.

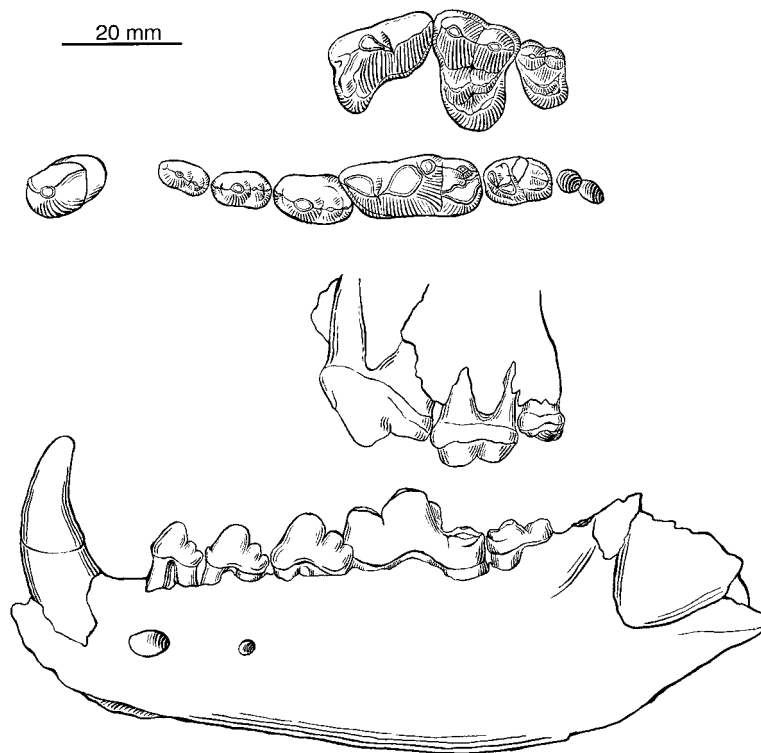


Fig. 74. *Aelurodon asthenostylus*. LACM-CIT 781, holotype, Siebert Formation (late early Barstovian), San Antonio Mountains, near Tonopah, Nye County, Nevada. Ramus and lower teeth reversed from right side. Illustration by X. Wang.

**HOLOTYPE:** LACM-CIT 781 (formerly LACM-CIT 2816), partial palate with left and right P4–M2 and partial mandible with left and right c1–m2 (fig. 74), from Tonopah Local Fauna, LACM-CIT loc. 172-C, Siebert Formation (late early Barstovian), San Antonio Mountains, near Tonopah, Nye County, Nevada.

**REFERRED SPECIMENS:** From the type locality: LACM-CIT 775, left maxillary with P4 broken–M1; and LACM-CIT 776, partial mandible with p3–m2.

Second Division Fauna, Mud Hills, Barstow Formation (late early Barstovian), San Bernardino County, California: F:AM 27161, partial skull with C1–P1 alveoli, P2–M2, and partial mandible with c1–p1 alveoli and p2–m3 (fig. 75A–F); F:AM 27221, left maxillary with I1 broken–M2 (P1–P2 broken); F:AM 27223, left partial ramus with i2–p1 all broken and p2–m2 (p3, m1, and m2 all broken); and F:AM 27162 and 27162A, fragmentary

posterior partial skull with P4 broken–M2, mandible with i2–c1 all broken, p1–m2, and m3 alveolus, radius, partial ulna, metacarpals III, IV, and V, calcaneum, astragalus, and proximal part of metatarsals IV and V.

Barstow Fauna, Barstow Formation (early late Barstovian), San Bernardino County, California: North End: F:AM 27154, palate with I1–I2 alveoli, I3–M2, and mandible with i2–m3; F:AM 27158, left partial maxillary with P4–M2 and right partial ramus with p1 alveolus–m2 (p4 alveolus) (upper and lower jaws probably do not belong to the same individual); F:AM 27174, left ramus with c1 broken and p2 broken–m3; F:AM 67070, right partial ramus with p3–m2 all broken. Skyline Quarry: F:AM 31106, left partial ramus with c1–m2. Four ft below New Year Quarry: F:AM 61709, right and left maxillary with I1 alveolus, I2, I3–P2 alveoli, P3 broken–M2, and both rami with c1–m2 (p1 alveolus, m1–m2 both broken).

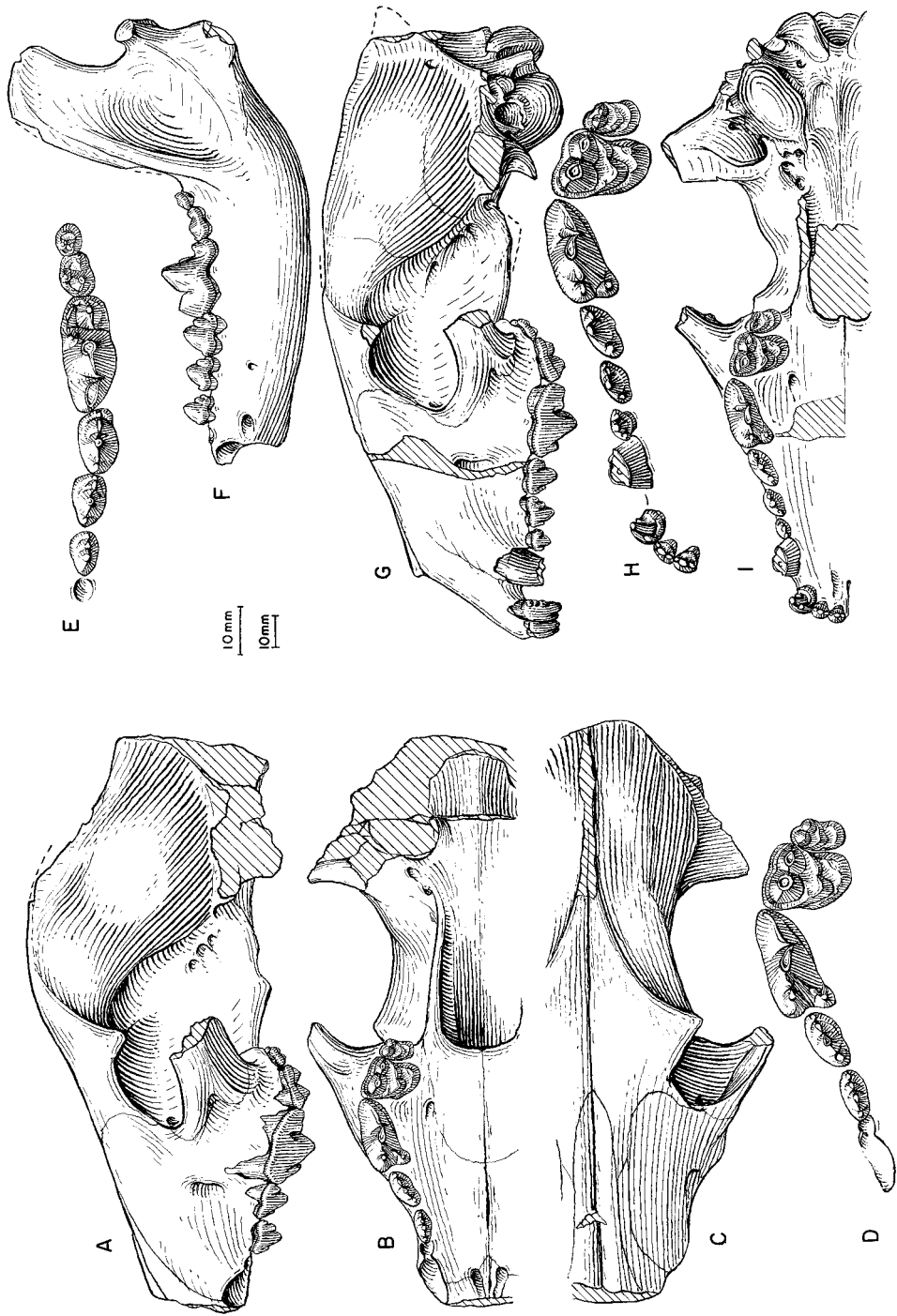


Fig. 75. *Aelurodon asthenostylus*. A, Lateral, B, ventral, and C, dorsal views of skull, D, upper teeth, E, lower teeth, and F, ramus, F:AM 27161, Second Division Barstow Bluffs, Barstow Formation (late early Barstovian), San Bernardino County, California. G, Lateral view of skull, H, upper teeth, and I, ventral view of skull, F:AM 27159, *Hemicyon* Stratium, Barstow Formation (early late Barstovian), San Bernardino County, California. The longer (upper) scale is for D, E, and H, and the shorter (lower) scale is for the rest.

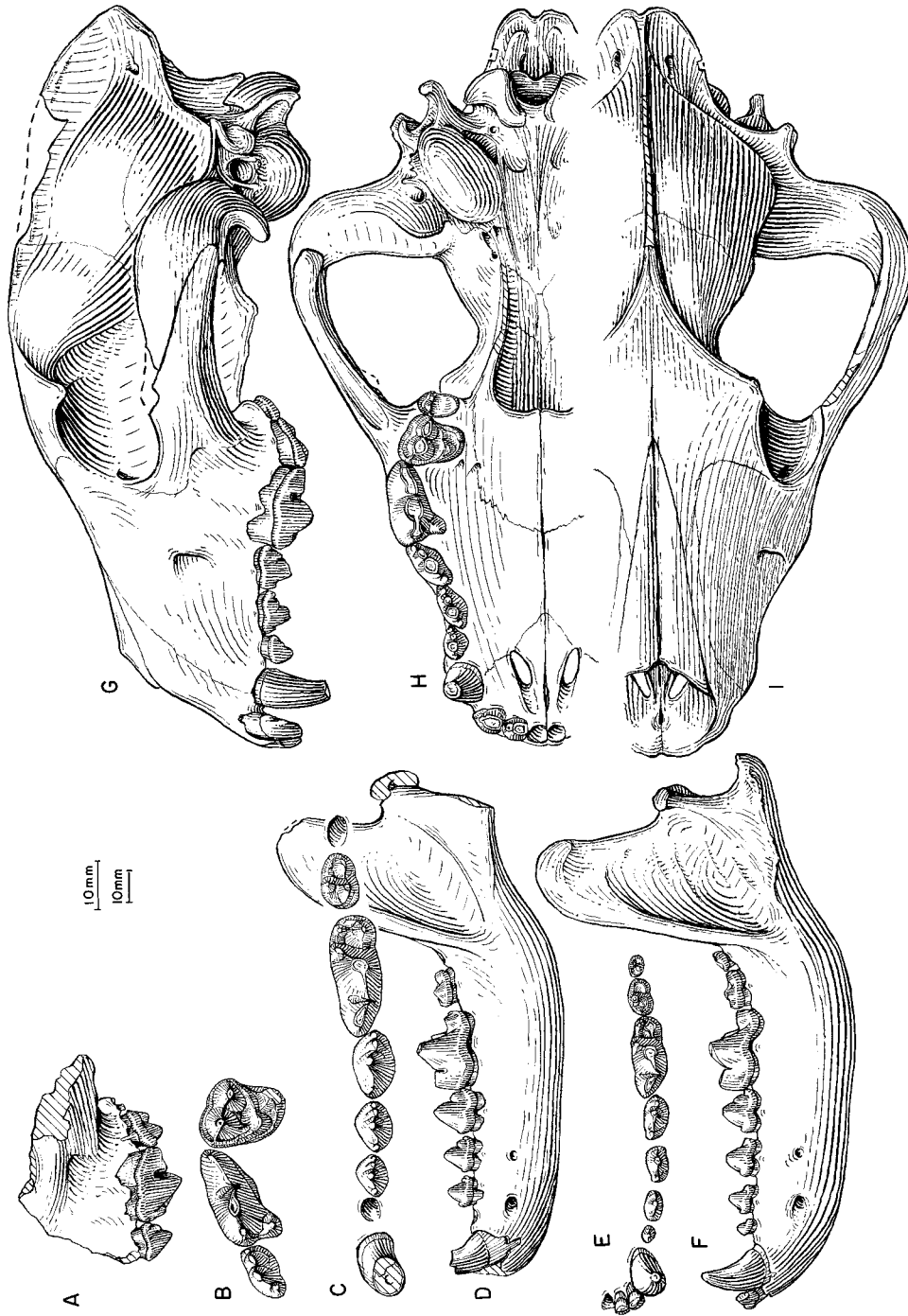


Fig. 76. *Aelurodon asthenostylus*. A, Lateral and B, enlarged occlusal views of maxillary and upper teeth, C, lower teeth, and D, ramus, F: AM 27170A, *Hemicyon* Stratum, Barstow Formation (early late Barstovian), San Bernardino County, California. E, Lower teeth and F, ramus, F: AM 28356, Horse Quarry, Pawnee Creek Formation (early late Barstovian), Weld County, Colorado. G, Lateral, H, ventral, and I, dorsal views of skull (crushed frontal area restored), F: AM 28351, Pawnee Buttes, Pawnee Creek Formation (late early Barstovian), Weld County, Colorado. The longer (upper) scale is for B and C, and the shorter (lower) scale is for the rest.

New Year Quarry: F:AM 67072, right partial ramus with c1–m2 (p1 alveolus). Prospect near Chert Ridge: F:AM 67063, left partial maxillary with P4–M2; F:AM 67065, right partial ramus with i1–p1 roots and p2–m2 (m2 broken and m3 alveolus). New Hope Quarry: F:AM 67068, left partial ramus with c1 broken and p2–m2; F:AM 67077, left partial ramus with i3–c1 both broken and p1 alveolus–m2 (p2, p4, and m1 all broken). Hidden Hollow Quarry: F:AM 67062, partial skull with C1–M2 (P1 and P4 both broken); F:AM 67071, right and left rami with i1–c1 (i3 broken), p1 alveolus, and p2–m3; F:AM 67074, right and left rami with c1–m3; F:AM 67075, right ramus with c1 and p4–m3; F:AM 67079, left partial ramus with i1–m1 (p1 alveolus); and F:AM 67080, palate with I2–I3, C1–P2 alveoli, and P3–M2. Leader Quarry: F:AM 67064, right and left partial maxillae with C1–M2 (P1 alveoli) and skull fragments; and F:AM 67076, right ramus with i1–i3 alveoli, c1 broken, p1 alveolus, p2 broken–m2, and m3 alveolus. First Division: F:AM 67067, right maxillary fragment with P4–M1 both broken, detached broken premolars and incisors, and left partial ramus with p3 broken–m3 (m1 broken). *Hemicyon* Stratum (some specimens are questionably referred to this quarry): F:AM 27155, anterior part of skull with I1–P1 alveoli and P2–M2; F:AM 27155A, left partial maxillary with P3–M2; F:AM 27157, anterior part of skull with I1–P1 alveoli and P2–M2; F:AM 27157A, right partial maxillary with P4–M2 (M1 broken); F:AM 27158A, left partial maxillary with P4–M1; F:AM 27159, skull with I1–M2 (fig. 75G–I); F:AM 27160, crushed partial skull with I1–P2 alveoli and P3–M2; F:AM 27163, anterior part of skull with I2 broken–M2; F:AM 27164, partial skull with C1–P2 alveoli, P3–M1 both broken, and M2 alveolus; F:AM 27165, partial skull with P1–P3 alveoli and P4–M2 (M1 broken); F:AM 27166, anterior part of skull with C1–P1 alveoli and P2 broken–M2; F:AM 27166A, crushed partial skull with P4 broken–M2; F:AM 27168, left partial maxillary with P2 broken–M2; F:AM 27169, right partial maxillary with P3–M2; F:AM 27170, left maxillary fragment with P3–M1; F:AM 27170A, left partial maxillary with P3–M1, right and left rami with c1–m2 (p1

and m3 alveoli) (fig. 76A–D); F:AM 27171, crushed partial skull with P3 alveolus and P4 broken–M2; F:AM 27172, partial skull with P2 broken, P3 alveolus, and P4–M2; F:AM 27173, right and left partial rami with c1 broken–m3; F:AM 27178, left partial ramus with m1–m3; F:AM 27181, right partial ramus with c1 broken–m2 (p2 broken) and m3 alveolus; F:AM 27182, right ramus with c1–p3, p4–m2 all broken, and m3; F:AM 27186, left partial ramus with m1–m3; F:AM 27187, left partial ramus with m1 broken–m3; F:AM 27188, left ramus with c1–m3 (p1 alveolus); F:AM 27190, right partial ramus with p1 alveolus–m3; F:AM 27191, right partial ramus with c1 broken–p1 alveolus, p2–m2, and m3 alveolus; F:AM 27192, left partial ramus with c1–m2 (p1 and m3 alveoli); F:AM 27193, left partial ramus with p1 alveolus–m2; F:AM 27194, left partial ramus with p4–m3; F:AM 27195, left partial ramus with c1–m1 (p2 alveolus); F:AM 27196, left partial maxillary with P4–M2; F:AM 27198, right partial ramus with c1 broken–m2 (p1 alveolus and p2–p3 both broken); F:AM 27199, left partial ramus with c1–m2 (p1 alveolus and p4 broken); F:AM 27200, left partial ramus with p3–m2 (m1 broken) and m3 alveolus; F:AM 27201, left partial ramus with c1–m2 (p1 and m3 alveoli); F:AM 27203, left partial ramus with c1 broken–m2 (p1 alveolus and p4–m1 both broken); F:AM 27204, right partial ramus with p2–p3 and p4–m1 both broken; F:AM 27206, left partial ramus with p3–m2; F:AM 27207, right ramal fragment with m1–m2 both erupting; F:AM 27208, left ramal fragment with p3–m2 (p4–m1 both broken); F:AM 27209, right partial ramus with c1 broken–m3 (p1 and p3 alveoli and p2 broken); F:AM 27215, left partial immature ramus with dp4 broken and c1–m1 all unerupted; F:AM 31101, partial mandible with i1–m2 (p1 alveolus) and m3 alveolus; F:AM 67069, left partial ramus with c1 alveolus and p2 broken–m3; and F:AM 67084, posterior part of skull. Horizon below Split Ridge: F:AM 67073, right and left rami with c1–m3 (p3 and p4 both broken).

Pawnee Creek Formation (late early Barstovian), Weld County, Colorado: Pawnee Buttes: AMNH 9359, immature anterior part of skull with dI3, dC1, dP3–dP4, erupting

I1–I2, P1, and erupting P4. Two mi west of Quarry: F:AM 28351, skull with I1 alveolus–M2 (fig. 76G–I). Davis Ranch, first canyon east of the Kiota Road: F:AM 67323, right partial ramus with c1, p1–p3 alveoli, p4–m2 and m3 alveolus. Hereford, middle horizon: F:AM 28301, right and left rami with c1 broken, p1, p2 broken, p4–m2, and m3 alveolus. No locality data: F:AM 28310, right partial maxillary with P3 broken–M2; F:AM 28312, left maxillary fragment with broken M1; F:AM 28312A, right partial maxillary with P4–M2; and F:AM 70800, right isolated M1.

Pawnee Creek Formation (early late Barstovian), Weld County, Colorado: Horse Quarry: F:AM 28309, left maxillary with I1–I2 alveoli, I3 broken, and C1 alveolus–M1 (P2–P3 broken and M2 alveolus); F:AM 28311, right ramus with i1–i3 alveoli, c1, p2–m1, and m2–m3 alveoli; F:AM 28313 and 28313A, left partial maxillary with P2–P3 alveoli, P4, and M1–M2 both broken, and right metacarpal II; F:AM 28329, right broken m1; F:AM 28354, left partial ramus with c1 and p2–m1; F:AM 28355, right isolated M2, mandible with i1–m2 and m3 alveolus, both femora, left tibia and fibula, both calcanea and astragali, left metatarsals II, IV, and V, and right metatarsals III and IV, vertebrae, and ribs; F:AM 28356, mandible with i1 alveolus–m3 (fig. 76E, F) and associated limb elements of more than one individual including, left humerus, two left radii, left ulna with distal end missing, and left metacarpals III, IV, and V; F:AM 28357, left partial maxillary with M1–M2; and F:AM 107720, posterior part of skull.

Surprise Quarry, Hay Springs Creek Drainage, Sand Canyon Formation (early Barstovian), Dawes County, Nebraska: F:AM 25417, left partial maxillary with P4–M2.

Driftwood Creek, Ogallala Group (early late Barstovian), Hitchcock County, Nebraska: AMNH 96687, left partial ramus with i2–p1 alveoli, p3–p4 both broken, m1 alveolus, m2, and m3 alveolus.

DISTRIBUTION: Early Barstovian of Nebraska, Colorado, Nevada, and California; and early late Barstovian of Nebraska, Colorado, and California.

EMENDED DIAGNOSIS: As distinguished

from *Tomarctus*, derived characters of *Aelurodon asthenostylus* that are shared with advanced species of *Aelurodon* include sagittal crest high, bulla enlarged, mastoid process enlarged, P4 protocone reduced, P4 parastyle strong, M1 and M2 smaller relative to carnassial, M1 lingual cingulum reduced anteriorly, m1 talonid narrowed, m2 reduced, and m2 metaconid low relative to protoconid. *A. asthenostylus*, on the other hand, is primitive relative to the derived species of *Aelurodon* in its smaller size (except *A. stirtoni*), paroccipital process less elongated, I3 less enlarged, premolars less massive and lacking distinct anterior cingular cusps, and M1 with large metaconule. In addition, *A. asthenostylus* lacks the synapomorphy for the *A. mcgrewi–stirtoni* clade, that is, extremely reduced M2 and m2. Compared to the *A. ferox–taxoides* clade, *A. asthenostylus* is primitive in its less broadened contact of premaxillary and frontal, lower sagittal crest, nuchal crest less posterodorsally produced, and I3 with two lateral accessory cusplets only. An autapomorphy for *A. asthenostylus* is its prominently broadened palate.

DESCRIPTION AND COMPARISON: Large samples of skulls and jaws from the Barstovian of California and Colorado greatly increase our knowledge of this species, originally named from Tonopah, Nevada. Unlike *Tomarctus*, which shows only the initial developments of aelurodontine cranial proportions, the skull of *Aelurodon asthenostylus* displays many derived characteristics of the clade. The pattern of cranial proportions of *A. asthenostylus* in the ratio diagram (fig. 71) is consistent with other species of *Aelurodon*, with a relatively deep and wide zygomatic arch, broad rostrum, and reduced M2. The palate is noticeably broadened relative to that in *Tomarctus* and the *A. mcgrewi–stirtoni* clade. Contact between the premaxillary and frontal is strong, but less than that in the *A. ferox–taxoides* clade. The frontal sinus is at a stage of development similar to *Tomarctus*, in which the sinus is extended posteriorly slightly beyond the frontal-parietal suture. The sagittal crest can be as low as in *Tomarctus*, but some individuals (F:AM 67062, F:AM 28351, and probably F:AM 27161) have acquired a crest as high as those in *A.*

*mcgrewi*. The nuchal crest is narrow in posterior view, but not as posteriorly expanded as in the *A. ferox-taxoides* clade. The mastoid process is enlarged. The paroccipital process is strongly built, sometimes with a long free tip.

*Aelurodon asthenostylus* has the dental proportions of later aelurodontines with its strong premolars, large P4 parastyle, high-crowned M1 paracone, reduced M1 metaconule, and reduced size of M1–M2 and m2, characters that readily distinguish themselves from those in *Tomarctus*. The premolars, however, generally lack the strong development of accessory cusps, especially the anterior cusplets, that are better developed in more derived species of *Aelurodon*. The P4 has a more reduced protocone than in *Tomarctus*. Other tendencies toward hypercarnivory include long shearing blades for upper and lower carnassials, reduced m1 metaconid, reduced m1 entoconid relatively to the hypoconid, reduced m1 talonid, reduced m2 metaconid, and smaller m2–m3—all evolved to enhance the shearing part of dentition at the expense of the grinding part.

DISCUSSION: Most of the derived features possessed by *Aelurodon asthenostylus* are those of the traditional concept of *Aelurodon*. It appears to have gradually evolved to *A. ferox* and, if so, our division of these two forms is more out of convenience of reflecting an anagenetic rather than a cladogenetic event. On the other hand, there is a larger morphological gap between *Tomarctus brevirostris* and *A. asthenostylus*. This gap is of interest since we can observe a rapid replacement of *Tomarctus* by *Aelurodon* with a brief coexistence of these two in the Barstow and Pawnee Creek formations. Although still poorly known, several partial lower jaws from the Valley View Quarry of the Second Division Fauna are tentatively identified as *Tomarctus brevirostris* (see referred specimens under the species). Most specimens of *A. asthenostylus*, on the other hand, are from the Barstow Fauna, suggesting a replacement of *Tomarctus* by *A. asthenostylus* in the late early Barstovian of southern California. In the Pawnee Creek Formation of Colorado, however, these two taxa apparently coexisted (at least found together in Horse and Mastodon quarries, see also Discussion under

*Protepicyon raki* for its distinctions from *A. asthenostylus*).

Individuals from the Pawnee Creek Formation in Colorado are in general slightly larger and more derived than those from the Barstow Formation, and they bridge the gap between the typical members of *A. asthenostylus* and *A. ferox*. The link provided by the Colorado form suggests a rather continuous transformation from *A. asthenostylus* to *A. ferox*, with the implication that the division between these taxa is somewhat arbitrary.

### *Aelurodon mcgrewi*, new species

Figure 77C–G

*Aelurodon wheelerianus* (Cope, 1877): Cope, 1881a: 388 (in part); 1883: 245, fig. 11a, b (in part). Matthew and Gidley, 1904: 250, fig. 3 (in part). Cope and Matthew, 1915: pl. CXIXa, figs. 1–3 (in part). Barbour and Cook, 1917: 179, fig. 6 (in part). Colbert, 1939: 65 (in part). *Prohyaena wheelerianus* (Cope): Schlosser, 1890: 25 (in part). *Strobodon stirtoni* (Webb, 1969a): Evander, 1986: 28, figs. 5, 7E, 8E (in part). *Aelurodon* cf. *A. wheelerianus* (Cope): Voorhies, 1990a: A118 (in part).

HOLOTYPE: AMNH 22410, partial skull with I1–I2 alveoli and I3–M2, right ramus and left partial ramus with i1–i2 alveoli and i3–m3 (p1 broken) (fig. 77E–G), complete cervical vertebrae, partial right scapula, left humerus, and postcranial fragments, south of Norden, Devil's Gulch Member, Valentine Formation (late Barstovian), Brown County, Nebraska.

ETYMOLOGY: Named for Paul O. McGrew in recognition of his many contributions to knowledge of the Neogene rocks and faunas of the Great Plains and for his study, with R. A. Stirton, of the Borophaginae.

REFERRED SPECIMENS: Crookston Bridge Member, Valentine Formation (late Barstovian), Cherry and Keyapaha counties, Nebraska (following list by Evander, 1986): Railway Quarry A (UNSM loc. Cr-12): UNSM 76620, right immature ramus with c1 erupting, p1–p4 alveoli, m1 broken, m2 alveolus, and m3 erupting (Evander, 1986: figs. 5, 7E). Railway Quarry B (UNSM loc. Cr-13): UCMP 63657, right partial maxillary with P2–M2 (Evander, 1986: fig. 8E) (fig.



77C, D). Stewart Quarry (UNSM loc. Cr-150): UNSM 1481-95: right ramus with i1-m2 (p1 alveolus) and m3 alveolus. Devil's Jump Off: F:AM 25174, left partial ramus with i3-p2 alveoli, p3-m1, m2 broken, and m3 alveolus. Ripple Quarry: F:AM 70600, left partial ramus with c1-p1 alveoli, p2-p4 all broken, and m1-m2. Schoettger Quarry: F:AM 61744, left partial ramus with p3 alveolus, and p4-m2.

Devil's Gulch Member, Valentine Formation (late Barstovian), Brown and Cherry counties, Nebraska: Three mi above the Garner Bridge on the north side of the Niobrara River: F:AM 61778, skull with I1-M2 and associated right incomplete m1 and left humerus. Fairfield Creek, North Fork: F:AM 35131, left partial ramus with p1-m1, m2 root, and m3 alveolus.

Republican River beds (late Barstovian), Ogallala Group, Red Willow County, Nebraska: AMNH 8307 (referred to *Aelurodon wheelerianus* by Cope, 1883: fig. 11a, b), anterior part of skull with I3 broken-M2, mandible with i1-m3, skull fragments, partial radius and ulnae, carpus, and cervical vertebrae.

DISTRIBUTION: Late Barstovian of Nebraska.

DIAGNOSIS: *Aelurodon mcgrewi* shares with most species of *Aelurodon* derived features that are distinct from the more primitive *A. asthenostylus*: long free tip on the paroccipital process, enlarged I3, P1-P3 and p1-p4 massive and with more distinct anterior cingular cusplets, and M1 metaconule reduced or absent. In addition, *A. mcgrewi* shares a derived character with *A. stirtoni* that is distinct from the *A. ferox-taxoides* clade: M2 metacone reduced or absent. *A. mcgrewi* is distinguishable from *A. stirtoni* in its primitive status of the following characters: larger size, higher sagittal crest, nuchal crest more posteriorly expanded, posterior border of M1 not prominently recurved, m2 not extremely shortened, and m2 metaconid present. In contrast to the *A. ferox-taxoides* clade, *A. mcgrewi* lacks derived characters of that clade: broad contact between premaxillary and frontal, extremely high sagittal crest, extremely broad palate, transversely straight upper incisor row, and I3 with three lateral accessory cusplets.

DESCRIPTION AND COMPARISON: *Aelurodon mcgrewi* is overall quite similar to *A. ferox*, especially to its earlier representatives. *A. mcgrewi* is close to *A. ferox* not only in size, but in cranial proportions, as shown in the ratio diagrams (fig. 71). However, derived features such as a reduced M2 and m2 and a broadened p4 show *A. mcgrewi* to be a member a small clade with *A. stirtoni*. The increasingly stronger premolars at the expense of the grinding part the dentition (M1-M2 and m1 talonid-m3) is a general trend within the aelurodontine clade, but in *A. mcgrewi* this is manifested in a slightly different way. Thus, its p4 is relatively more broadened (fig. 72) and its M2 has a more reduced metacone. *A. mcgrewi* has only a moderately broadened palate, a primitive character relative to *A. asthenostylus*, suggesting that the narrower palate in *A. stirtoni* may have been a character reversal.

DISCUSSION: Cope (1881a, 1883) referred a partial rostrum and mandible, AMNH 8307, from the Republican River of Nebraska to his earlier erected species *Canis wheelerianus* Cope, 1877, and changed the generic assignment of this species to *Aelurodon*. *A. wheelerianus* was based on a partial ramus lacking all the teeth from Santa Fe, New Mexico, and the poor status of preservation of the holotype became the source of considerable uncertainty surrounding its identity (see also discussion under *A. ferox*). Cope's referred specimen from Nebraska has since been illustrated repeatedly (Cope, 1883: fig. 11a, b; Matthew and Gidley, 1904: fig. 3; Cope and Matthew, 1915: pl. CXIXa, figs. 1-3; Barbour and Cook, 1917: fig. 6), and with its well-preserved teeth became the focus of attention of this species instead of its poorly preserved holotype. In this sense *A. wheelerianus* thus symbolized a small-size *Aelurodon*, in contrast to the larger *A. taxoides*, and even became the basis of a new genus *Prohyaena* proposed by Schlosser (1890: 25). Although lacking much of the posterior and dorsal parts of the skull, AMNH 8307 preserves such derived dental features as reduced M2 with a vestigial metacone, relatively widened p4, and shortened m2. These subtle features signal its position in *A. mcgrewi*, despite its general similarity to *A.*

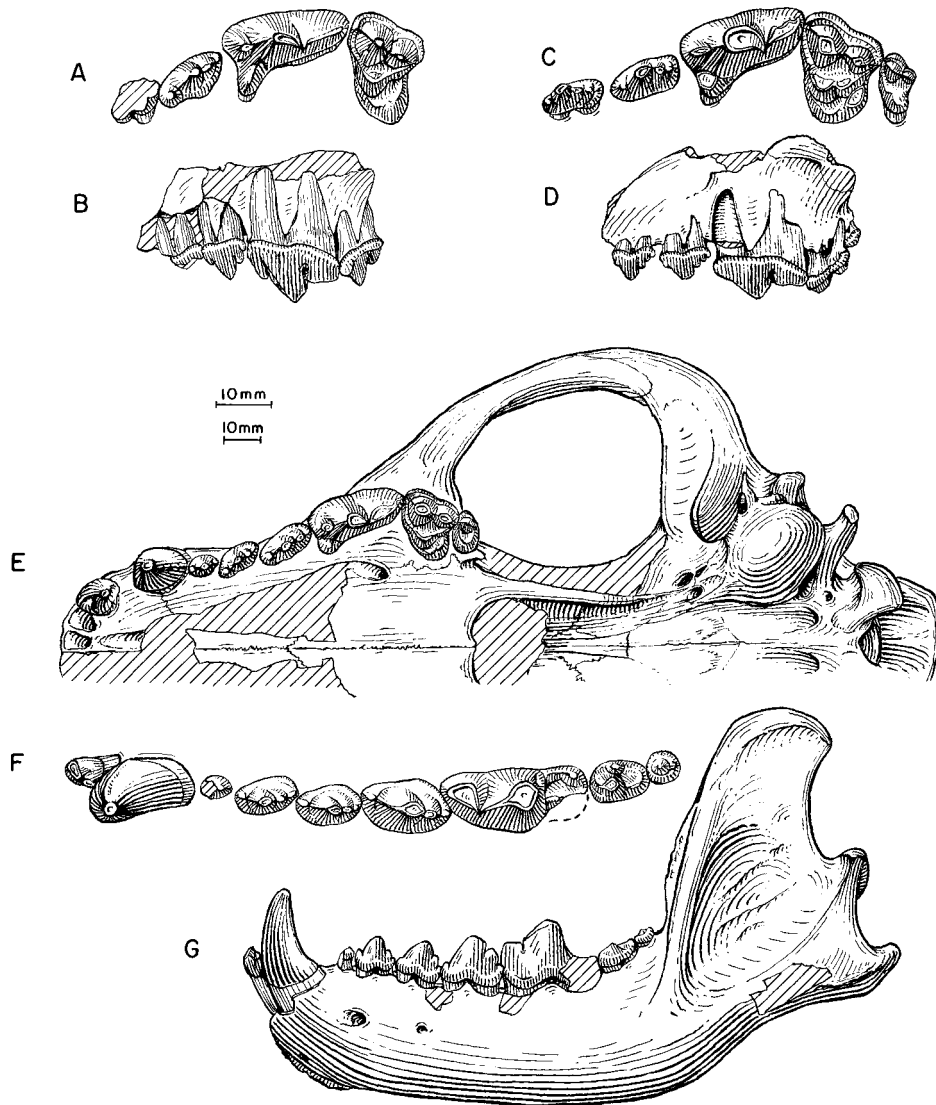


Fig. 77. **A**, Enlarged occlusal and **B**, lateral views of maxillary and upper teeth, *Aelurodon stirtoni*, UCMP 33473, holotype, Fence Line Locality, Burge Member, Valentine Formation (late late Barstovian), Cherry County, Nebraska. **C**, Enlarged occlusal and **D**, lateral views of maxillary and upper teeth, *A. mcgrewi*, UCMP 63657, Railway Quarry B, Crookston Bridge Member, Valentine Formation (late Barstovian), Cherry County, Nebraska. **E**, Ventral view of skull, **F**, lower teeth, and **G**, ramus (reversed from right side), *A. mcgrewi*, F:AM 22410, holotype, south of Norden, Devil's Gulch Member, Valentine Formation (late Barstovian), Brown County, Nebraska. The longer (upper) scale is for **A**, **C**, and **F**, and the shorter (lower) scale is for the rest.

*ferox* (*A. wheelerianus* of most past references).

Evander (1986: 28, figs. 5, 7E, 8E) referred two specimens from the Railway quarries, Crookston Bridge Member of Valentine Formation, to *Strobodon stirtoni*. His refer-

ence was mainly based on UCMP 63657, a maxillary fragment with P2–M2 (another figured specimen is UNSM 76220, a partial ramus with a broken m1). Evander's figure of this specimen (fig. 8E), however, shows a M1 with a rather unreduced metaconule and un-

shortened internal cingulum. The only dental features that suggest *A. stirtoni* appear to be its overall small size (compared to *A. ferox* from the same Railway quarries; see Evander, 1986: table 2) and its relatively small M2, which still has a distinct metacone in contrast to the loss of this cusp in *A. stirtoni*. It seems possible that the two specimens from the Railway quarries represent a primitive form of *A. mcgrewi*.

Our identification of *Aelurodon mcgrewi*, from the Devil's Gulch Member of the Valentine Formation, that gave rise to *A. stirtoni*, from the Burge Member of the Valentine Formation, helps to bridge the morphological gap between *A. stirtoni* and other species of *Aelurodon*. It also provides evidence for character reversals, such as smaller size, lower sagittal crest, and narrow palate, in *A. stirtoni*.

*Aelurodon stirtoni* (Webb, 1969)

Figures 77A, B, 78, 79

*Strobodon stirtoni* Webb, 1969a: 43, fig. 8a, b.  
Voorhies, 1990a: 40. Munthe, 1998: 136.

**HOLOTYPE:** UCMP 33473, left partial maxillary with P2 broken—M1 and M2 alveolus (fig. 77A, B) from Fence Line Locality (UCMP loc. V3331), Burge Member, Valentine Formation (late late Barstovian), Cherry County, Nebraska.

**REFERRED SPECIMENS:** Burge Member, Valentine Formation (late late Barstovian), Cherry County, Nebraska: Swallow Quarry (UNSM loc. Cr-16): UNSM 25789 (AMNH cast 97286), skull with I1–M2 (P1 alveolus) and left and right rami with c1–m3 (p1 alveolus) (fig. 78); F:AM 25171, right ramus with i3 alveolus–m2 (p1 alveolus) and m3 alveolus; and F:AM 25175, skull with I2 broken–M2 (P1 alveolus and P2–P3 both broken), and left ramus with c1 broken–m2 (p1–p3 alveoli and p4–m1 both broken). Burge Quarry: F:AM 25177, right partial ramus with c1, p1–p2 alveoli, p3–m2 (m1 broken), and m3 alveolus; F:AM 25178, right ramus with i1–i3 alveoli, c1, p1 alveolus–m2, and m3 alveolus (fig. 79A, B); F:AM 25179, left ramus with i1–i3 alveoli, c1 broken–p1 alveolus, p2–m2, and m3 alveolus; and F:AM 25181, partial left ramus with c1 broken, p1 alveolus, and p2–m1. Gordon Creek: F:AM

25182, left ramus with i1–i3 alveoli, c1, p1 alveolus–m1, and m2–m3 alveoli. Deep Creek: F:AM 25110, left ramus with i1 alveolus–c1, p1–p2 alveoli, p3–m2, and m3 alveolus. June Quarry: USNM 215320 (AMNH cast 129868), partial skull with I1–M2 and mandible with i1–m3, and incomplete skeleton with baculum (Munthe, 1989: figs. 5D, 6C, 7C, 9C, 11D, 12D–F, 13, 14B, 15C, 17D, 18A). Spring Canyon, 1 mi from mouth of Snake River: UNSM 25694, anterior half skull with I2–I3, C1–P1 alveoli, and P2–M2.

Pojoaque and Chama El Rito members of Tesuque Formation (late Barstovian), Santa Fe and Rio Arriba counties, New Mexico: West Santa Cruz: F:AM 27492, partial skull with I1–I2 alveoli and I3–M2 (P1 alveolus and P3 broken) and both rami with i3–c1 both broken, and p1 alveolus–m3 (m1 broken) (fig. 79C–G). Santa Cruz, Second Wash: F:AM 27367, left maxillary fragment with erupting P4; and F:AM 27474, immature palate with dC1, dP3–dP4 both broken, I2 erupting, C1 erupting, and P2–M1 all erupting. Santa Clara: F:AM 27481, crushed articulated fragments of skull with I1 root–M2 (I3, C1, and P2–M2 all broken). *Aelurodon* Wash, Rio del Oso, Abiquiu: F:AM 70501, left partial ramus with p1 (detached), p2–m2, and premaxillary fragment with C1.

**DISTRIBUTION:** Late late Barstovian of Nebraska and late Barstovian of New Mexico.

**EMENDED DIAGNOSIS:** *Aelurodon stirtoni* is distinguished from the more primitive *A. mcgrewi* in its autapomorphous features: smaller size, sagittal crest low (a reversal), nuchal crest not posteriorly expanded (reversal), extremely recurved posterior border of M1, further shortened m2, and m2 metaconid absent.

**DESCRIPTION AND COMPARISON:** Through collections at the AMNH, UNSM, and USNM, *Aelurodon stirtoni* is now much better known than when it was first described more than 25 years ago. Three nearly complete skulls and several well-preserved rami are available. All northern Great Plains specimens are from the Burge Member of the Valentine Formation and, consistent with this short interval, the sample is rather uniform in size and morphology.

The overall size of *Aelurodon stirtoni* is

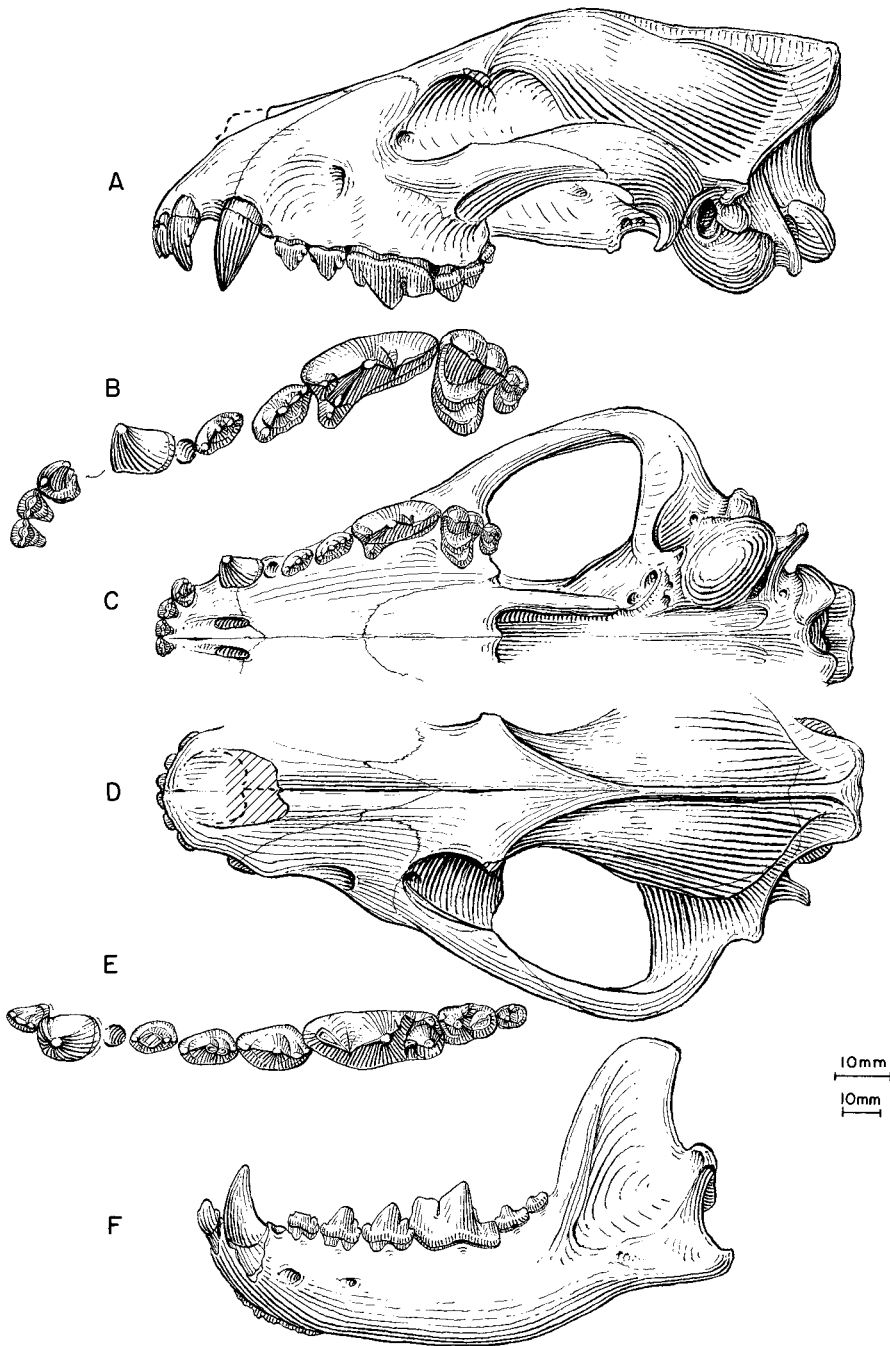


Fig. 78. *Aelurodon stirtoni*. **A**, Lateral, **B**, enlarged occlusal, **C**, ventral, and **D**, dorsal views of skull (zygomatic arch reversed from right side) and upper teeth (M2 reversed from right side), **E**, lower teeth and **F**, ramus (m3 reversed from right side), UNSM 25789, Swallow Quarry, Burge Member, Valentine Formation (late late Barstovian), Cherry County, Nebraska. The longer (upper) scale is for B and E, and the shorter (lower) scale is for the rest.

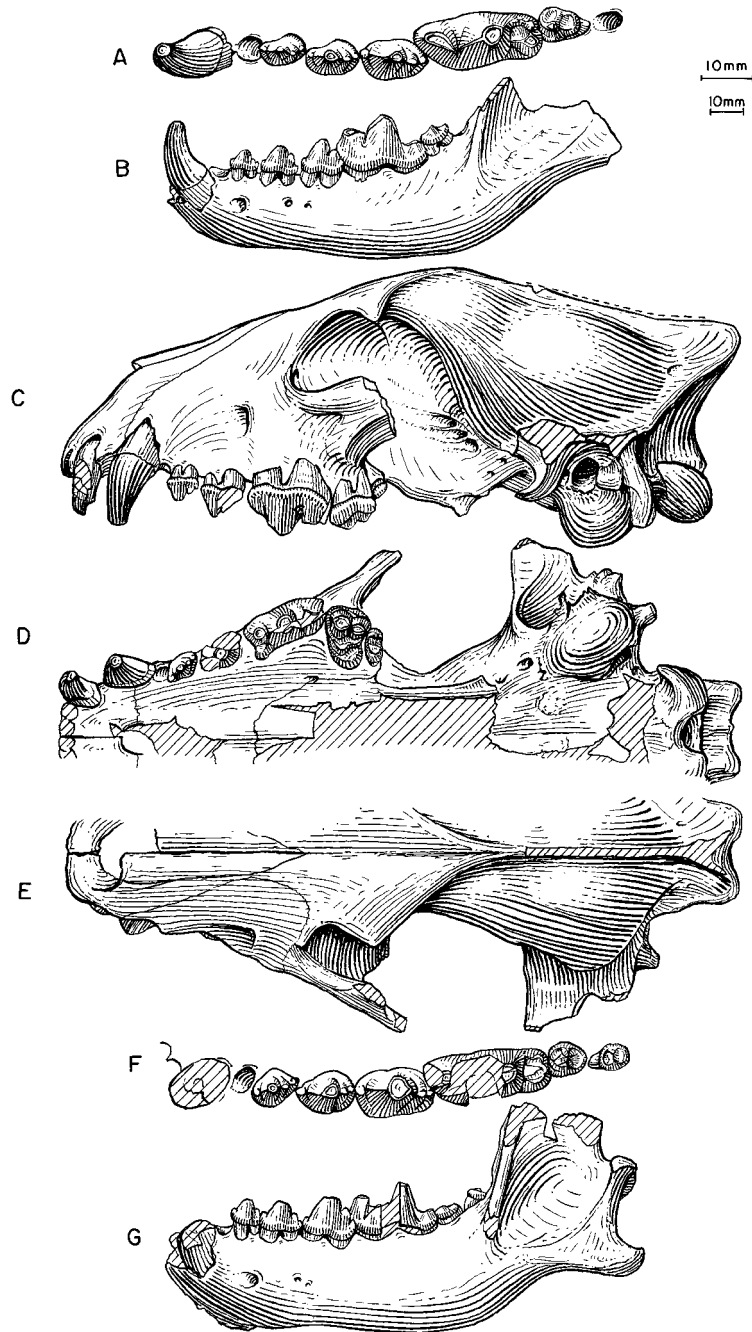


Fig. 79. *Aelurodon stirtoni*. **A**, Lower teeth and **B**, ramus (reversed from right side), F:AM 25178, Burge Quarry, Burge Member, Valentine Formation (late late Barstovian), Cherry County, Nebraska. **C**, Lateral, **D**, ventral, and **E**, dorsal views of skull (reversed from right side), **F**, lower teeth, and **G**, ramus (reversed from right side), F:AM 27492, West Santa Cruz, Pojoaque Member, Tesuque Formation (late Barstovian), Santa Fe County, New Mexico. The longer (upper) scale is for A and F, and the shorter (lower) scale is for the rest.

significantly smaller than that of *A. mcgrewi* (which is 18% larger than the former in average basal length of skull, although dental dimensions average only 9% larger). The general skull proportions of *A. stirtoni* are not very different from *Tomarctus*: the palate is only slightly broadened, the sagittal crest is low (probably a reversal), and the nuchal crest only slightly overhangs the occipital condyle. On the other hand, the proportional patterns of the ratio diagram of the skull of *A. stirtoni* (fig. 71) are unmistakably *Aelurodon*-like, with a broad muzzle, wide and deep zygomatic arch, narrow postorbital constriction, narrow braincase, enlarged bulla, and large mastoid process.

Dentally, this species is not difficult to recognize because of the distinctive shape of M1 and very reduced M2 and m2. The P4 is relatively longer than either of the more anterior premolars (P1–P3) or the molars, as compared to those in *Aelurodon asthenostylus* and more derived *A. ferox-taxoides* clade (fig. 72). The P4 parastyle has a distinct lateral ridge from its apex leading up to the crown base in contrast to the lack of such a ridge in the latter clade. The uniquely “twisted” appearance of M1, i.e., a sharp curve on the posterior border, is largely due to the combination of a shortened talon, a reduced metaconule (practically lost), and a more posterolingually restricted lingual cingulum (hypocone). The M2 is extremely reduced (but still double-rooted) and simple in cusp morphology. It is dominated by a paracone, and the metacone is absent. As in *A. mcgrewi*, the p4 is broadened, mostly due to a small lingual “lip” at the posterolingual corner of the tooth. Hypercarnivorous tendencies on the m1 are mainly manifested in the reduced talonid relative to a long shearing blade of the trigonid. In all except two individuals (F:AM 25182 and UNSM 25789), the m1 metaconid is reduced to a mere vertical ridge, and, correspondingly, the m2 metaconid is lost except in F:AM 25179. In most individuals, the m1 entoconid is reduced to a low longitudinal ridge to allow more space for a prominent hypoconid.

Specimens from the Pojoaque Member of the Tesuque Formation, New Mexico, are almost identical to the Burge sample both in size and dental morphology. F:AM 27474

and 27481 have the characteristically twisted M1s (as for their northern Plains counterparts), whereas F:AM 27492 has a slightly more primitive looking M1 (less sharply recurved posterior border), as in *A. mcgrewi*. The latter has otherwise the typical cranial and dental morphology of the species.

DISCUSSION: The distinctly “twisted” M1 of a maxillary fragment from the Burge Member of the Valentine Formation led Webb (1969a) to erect a new genus *Strobodon*. The M1 is so uniquely shaped among Borophagini that, even with the fragmentary holotype, a new genus seemed warranted. We now recognize an *A. mcgrewi-stirtoni* clade that is linked to the *A. ferox-taxoides* clade. Among the limited sample of the *Aelurodon mcgrewi-stirtoni* clade, we can observe a rather distinct morphological transformation from *A. mcgrewi* in the Devil’s Gulch Member to *A. stirtoni* in the Burge Member of the Valentine Formation. The geologically older *A. mcgrewi* is closer in morphology to *A. asthenostylus* and the presumed primitive ancestor of *A. ferox*. *A. mcgrewi* seems to have the right combination of primitive and derived morphology and to be the right geological age to be an ancestor of *A. stirtoni*. If this scenario is correct, we are also witnessing a size reduction in *A. stirtoni*, probably in response to the dominant, large-size *A. ferox-taxoides* clade.

The relatively brief span represented by the Devil’s Gulch and Burge members implies that morphological transformation from *Aelurodon mcgrewi* to *A. stirtoni* must have happened quickly, in less than 500,000 m.y. Such a high rate of evolution is in contrast to that in the much longer lasting species pair *A. ferox* and *A. taxoides* for more than 5 million years from the early late Barstovian through the Clarendonian. Such a rapid emergence of *A. stirtoni*, in the face of what must have been formidable competition from *A. ferox*, is achieved by size reduction and exploiting more hypercarnivorous niches.

#### *Aelurodon ferox* Leidy, 1858

Figures 80, 81, 82D, E

*Aelurodon ferox* Leidy, 1858: 22; 1869: 68, pl. 1, figs. 13, 14. VanderHoof and Gregory, 1940: 148, fig. 4a–c. McGrew, 1944b: 79. Baskin,

- 1980: 1349, fig. 1A. Evander, 1986: 29, figs. 6, 7F, 8F. Munthe, 1998: 136.
- Canis wheelerianus* Cope, 1877: 302, pl. 69, figs. 2, 2b.
- Aelurodon wheelerianus* (Cope): Cope, 1881a: 388. Scott, 1890: 67. VanderHoof and Gregory, 1940: 148. Gregory, 1942: 347. McGrew, 1944b: 79. Voorhies, 1990a: A118, figs. A25–A30 (in part).
- Prohyaena wheelerianus* (Cope): Schlosser, 1890: 25 (in part).
- Aelurodon platyrhinus* Barbour and Cook, 1917: 173, figs. 1–4.
- Aelurodon* near *wheelerianus* (Cope): Thorpe, 1922b: 439.
- Aelurodon taxoides magnus* Thorpe, 1922b: 440, figs. 9–11.
- Tephrocyon marshi* Thorpe, 1922b: 436, fig. 6.
- Euoplocyon taxoides magnus* (Thorpe): Matthew, 1924: 104.
- Aelurodon marshi* (Thorpe): VanderHoof and Gregory, 1940: 153. Evander, 1986: 30. Munthe, 1998: 136.
- Aelurodon taxoides* (Hatcher, 1893): VanderHoof and Gregory, 1940: 149 (in part). Webb, 1969a: 41 (in part). Baskin, 1980: 1349 (in part).
- Aelurodon francisi* (Hay, 1924): Wilson, 1960: 991, fig. 4b–k (in part).
- Aelurodon haydeni* (Leidy, 1858): Messenger and Messenger, 1977: 98, fig. 1g–i.
- Aelurodon* cf. *A. ferox* (Leidy): Voorhies et al., 1987: 62.
- HOLOTYPE:** USNM 523 (AMNH cast 9960), right isolated P4 (fig. 80F, G), “in the valley of the Niobrara River” (Leidy, 1858: 22), Nebraska. VanderHoof and Gregory (1940: 143) suggested that the type locality “is probably the exposure about 1 mi east of Fort Niobrara, near Valentine, Nebraska.” Skinner and Johnson (1984: 244), however, found no evidence that the Hayden Expedition had collected in the vicinity of Fort Niobrara, which was not founded until April of 1880.
- REFERRED SPECIMENS:** Hottell Ranch Quarry (UNSM loc. Bn-10), undifferentiated bed in Ogallala Group temporally equivalent to the Cornell Dam Member of the Valentine Formation (early late Barstovian), Banner County, Nebraska: UNSM 3029-47, left ramus with i2–c1, p1 alveolus, p2–m2, and m3 alveolus.
- Cornell Dam Member, Valentine Formation (early late Barstovian), Brown County, Nebraska: Norden Bridge Quarry (UNSM loc. Bw-106): F:AM 107754, left isolated incomplete m1; F:AM 107755, left maxillary fragment with C1–P1 alveoli and P2–P3; UNSM 2091-77, right maxillary with P4–M2; UNSM 2519-76, left maxillary fragment with M1–M2; UNSM 83891, partial skull with I1–M2 (Voorhies, 1990a: fig. A29); UNSM 83892, right maxillary with P4–M2; UNSM 83898, right ramus with c1–m3; UNSM 83899, right ramus with p3–m2 and m3 alveolus; UNSM 83900, right ramus with i1–i3 alveoli, c1, p1 alveolus, p2–m2, and m3 alveolus; UNSM 83901, right ramus with c1, p1 root, p2–m2; UNSM 83902, right ramus with i2–c1, p1–p2 alveoli, and p3–m1; UNSM 83903, left ramus with i1–i3 alveoli, c1, p1 alveolus, p2–m2, and m3 alveolus; UNSM 83904, right ramal fragment with m1–m2; UNSM 83905, left ramal fragment with c1–p2, p3 alveolus, and p4–m1 broken; UNSM 83906 immature left ramus with erupting c1 and p2–m2 (Voorhies, 1990a: fig. A31C, D); USNM 352360, skull with I1–M2 (Voorhies, 1990a: figs. A25–27); USNM 352361, partial left rostrum with I1–M2 (P1 alveolus) (Voorhies, 1990a: fig. A28); and USNM 352364, right ramus with i2, i3 alveolus, c1, p1 alveolus–m2, and m3 alveolus (Voorhies, 1990a: fig. A30).
- Crookston Bridge Member, Valentine Formation (late Barstovian), Boyd, Cherry, and Knox counties, Nebraska: Railway Quarry A (UNSM loc. Cr-12; list following Evander, 1986): F:AM 61742, left ramus with i1–i3 alveoli, c1, p1 alveolus, p2–m2, and m3 alveolus (fig. 80D, E); F:AM 61743, left partial ramus with c1–p3 alveoli, p4–m2, and m3 alveolus; F:AM 61745, left partial maxillary with P3–M2; F:AM 67476, right metacarpal IV; UCMP 33188, left maxillary fragment with P3 and P4 broken; UNSM 1093, skull with complete dentition (holotype of *A. platyrhinus* Barbour and Cook, 1917) (fig. 80A–C); UNSM 25931, right premaxillary fragment with I3 and right isolated M1; UNSM 26020, right ramus with c1, p1 alveolus–m1, and m2–m3 alveoli (Evander, 1986: figs. 6, 7F); UNSM 76621, anterior part of skull with I1–I2 alveoli and I3–M2 (P1 and P3 alveoli) (Evander, 1986: fig. 8F); UNSM 76622, left partial ramus with c1 broken–p3; UNSM 76623, right P4 broken; UNSM 76624, left humerus; UNSM 76625,

left ulna; UNSM 76626, right ulna, distal end missing; UNSM 76627, left distal part of humerus; UNSM 76628, left proximal end of femur; UNSM 76629, left distal part of tibia; UNSM 76630, right calcaneum; UNSM 76631, right calcaneum; UNSM 76632, right metatarsal III; UNSM 76633, left metacarpal III; UNSM 76634, left metacarpal IV; UNSM 76635, right metacarpal III; and UNSM 76636, left metatarsal II. Crookston Bridge Quarry (UNSM loc. Cr-15): F:AM 107719, left isolated m2. Jamber Quarry (UNSM loc. Bd-6): UNSM 9401, left ramus with c1-m2 and m3 alveolus (referred to *Aelurodon haydeni* by Messenger and Messenger, 1977: fig. 1g-i). Four Gate Quarry (UNSM loc. Kx-148): UNSM 2126-90, nearly complete skull with I1-I2, I3-P1 alveoli, and P2-M2. Sand Lizard Quarry (UNSM loc. Kx-120): UNSM 2137-75, left ramus with i1-i3 alveoli and c1-m3 (p1 alveolus); and UNSM 2155-95, right ramus with p3-m1 and m2 alveolus. West Valentine Quarry (UNSM loc. Cr-114): UNSM 2330-87, nearly complete skull with entire upper dentition; UNSM 2556-87, left ramus with p4-m1, m2 alveolus, and erupting m3; UNSM 2569-87, left ramus with p2-m2; and UNSM 3700-86, right ramal fragment with i1-p1 alveoli and p2-p4.

Devil's Gulch Member, Valentine Formation (late Barstovian), Brown, Cherry, and Keyapaha counties, Nebraska: Devil's Gulch below Horse Quarry: F:AM 25230, skull with I1-M2 and mandible with i1-m3, partial axis, and atlas. Devil's Gulch upper zone: F:AM 25127, left partial ramus with i2-c1 broken, p1-p4, and m1-m2 both broken. Devil's Gulch Horse Quarry: F:AM 25226, partial skull with I3-P1 alveoli and P2-M1; F:AM 25227, left partial ramus with p2-m2; F:AM 25228, left ramus with i3 broken-m3; F:AM 25229, left partial ramus with c1 and p1 alveolus-m2; F:AM 61747, left partial ramus with p2 alveolus, p3-m2, and m3 alveolus; F:AM 61748, left ramal fragment with m1 erupting and detached p4 unerupted; F:AM 67002, posterior part of skull; F:AM 67003, posterior part of skull; F:AM 67343, right maxillary fragment with P4; and F:AM 107718, right detached P4. West fork of Deep Creek: F:AM 61746, skull with I1 alveolus-M2, left ramus with c1 broken, p2

broken-m2, and m3 alveolus, and partial skeleton including the entire cervical vertebrae, five broken thoracics, most lumbar, partial left and right scapulae, left humerus, left radius, left ulna, right pelvis, metacarpal III, both metacarpals V, carpals, tarsals, calcaneum, metatarsals II, IV, and V, and phalanges, 25 ft below the Burge Member; and F:AM 70624, anterior part of skull with I1-I2, I3-C1 alveoli, and P1-M2, left ramus with i2-m2 and m3 alveolus, axis, third-fourth cervicals, broken thoracics and lumbar, left humerus, right radius, partial left radius, partial right ulna, metacarpals II and V, metatarsals III and incomplete IV, scapholunar, and two proximal phalanges, 20 ft below the Burge Member. First canyon of Snake River: F:AM 67346, immature partial skeleton including skull with dI2, dC1, dP2-dP4, and P4-M1 unerupted, left and right rami with di2-c1, dp2-dp4, and m1 unerupted, atlas through fifth cervical vertebrae, partial manus, partial tibia, and partial pes. Steer Creek: F:AM 67344, posterior part of skull, 40 ft below Burge Member. White Cliffs on Plum Creek: F:AM 70610, left partial ramus with p3-m2. Nenzel Quarry: F:AM 70609, right partial ramus with m1-m2 and m3 alveolus. Sawyer Quarry: F:AM 54203, right ramus with c1-p1 alveoli, p2-m2 (p4 broken), and m3 alveolus; and F:AM 54204, right partial ramus with p3-m2. Meisner Quarry: F:AM 25247, crushed skull with I1-I2 alveoli and I3-M2 (P4 broken) and left ramus with c1-p3 alveoli, p4-m1, m2 broken, and m3 alveolus. First canyon west of Bailing Springs, south side of Niobrara River, South of Cody: F:AM 61749, right partial ramus with c1-p2 alveoli, p3-m2, and m3 broken. Southeast of Springview in Keyapaha County: UNSM 1222-91, left ramus with c1-p4 all broken and m1-m2.

Burge Member, Valentine Formation (late late Barstovian), Cherry and Knox counties, Nebraska: Burge Quarry: F:AM 61753, skull with I2-M2 (fig. 81); F:AM 61754, partial skull with I1-M2; F:AM 61755, partial skull with I1-I2 alveoli, I3, C1-P1 alveoli, and P2-M2; F:AM 61756, right maxillary with P1-M2; F:AM 61757, skull with I1-M2 (P1 root); F:AM 61759, left isolated M1; F:AM 61762, left ramus with c1 broken, p1 alveo-



lus-m2 (p3 broken and m3 alveolus); F:AM 61763, right ramus with i2 broken, i3-p1 alveoli, p2-m2, and m3 alveolus; F:AM 61766, left ramus with m1 and alveoli of all other teeth; F:AM 61767, left ramus with c1 broken, p1 alveolus-m2, and m3 alveolus; F:AM 61770, right ramus with i1-p1 alveoli, p2-m1, and m2-m3 alveoli; F:AM 61771, left ramus with i1-i3 alveoli and c1-m3 alveolus (fig. 82D, E); F:AM 67004, immature right maxillary fragment with P1 alveolus, dP2-dP4, and P4-M1 unerupted; F:AM 67005, immature right maxillary fragment with dP3-dP4, and M1 unerupted (this may be the same individual as F:AM 67004); UCMP 32241 (referred to *Aelurodon taxoides* by Webb, 1969a: 41), nearly complete right ramus with i1-i3 alveoli, c1-m2, and m3 alveolus; and UCMP 32558, left ramus with c1 alveolus, p2-m1 all broken, and m2-m3 alveoli. June Quarry: F:AM 61758, right partial maxillary with P2-M2; F:AM 61775, right isolated m1; and F:AM 107717, right partial ramus with i1-i3 alveoli, c1 broken, p1 alveolus-p4, and m1 broken. East fork of Deep Creek: F:AM 61772, left ramus with i2-m1, m2 broken, and m3 alveolus. White Point Quarry: F:AM 61776, left partial ramus with i1-i3 alveoli, c1, and p1 alveolus-p4. Lucht Quarry: F:AM 61774, left partial ramus with m1 broken-m2 and m3 alveolus. Midway Quarry: F:AM 61768, right partial ramus with c1-p1 alveolus, p2-m2, and m3 alveolus; F:AM 61765, right and left rami with i1-i3 alveoli and c1-m3 alveolus; and F:AM 61773, left ramus with c1-p1 alveoli, p2-m1, m2 broken, and m3 alveolus. East fork of Fairfield Creek: F:AM 61761, right and left rami with i1-m2 and m3 alveolus, broken atlas, partial fibula, and phalanges; and F:AM 107716, right ramal fragment with m2 and m3 alveolus. Gordon Creek Quarry (UNSM loc. Cr-14): F:AM 61764, right partial ramus with i1 and p2 unerupted, dp3-dp4 both broken, and m1-m2 both erupting; and UNSM 25932, left ramus with c1, p1-p2 alveoli, p3 broken-m1, and m2-m3 alveoli. Meisner Slide: F:AM 61777, left partial ramus with i1-i3 alveoli, c1 broken, p1 alveolus-p4, and m1 broken. Talus in connection with Moore Creek Quarry No. 1: F:AM 25128, right partial ramus with m1 broken-m2. Bug Prospect (UNSM loc. Kx-119):

UNSM 46815, partial skull and complete mandible with I1-M2 and i1-m2.

Valentine Formation, Nebraska: Tihen Locality (UCMP loc. 6259), Keyapaha County: UCMP 64726, isolated right P1-M2 (P4 broken), left and right rami with c1, p1 alveolus-m2, and m3 alveolus. A few mi east of mouth of Antelope Creek, Cherry County: YPM 10057 (holotype for *Aelurodon taxoides magnus* Thorpe, 1922b: 440, figs. 9-11), partial right maxillary-premaxillary with I1-C1 alveoli and P1 broken-M1, both rami with c1-m3. West of mouth of Minnechaduzza Creek, Cherry County: YPM 12787 (holotype of *Tephrocyon marshi* Thorpe, 1922b: 436, fig. 6), left ramus with p2-p3, p4 alveolus, and m1-m2. "Niobrara River": YPM 10060 (referred to *Aelurodon* near *wheelerianus* by Thorpe, 1922b: 439), partial maxillary with P4-M1, left ramus with c1, p1 alveolus, p2-p3, and part of m1-m2.

Hardin Bridge, Niobrara River, Ogallala Group, temporally equivalent to the Burge Member of the Valentine Formation (late Barstovian), Sheridan County, Nebraska: F:AM 70604, right ramus with i3 alveolus, c1, p1 alveolus-m2, and m3 alveolus.

From 2.9 mi east of White Clay, along the Nebraska-South Dakota state line, Ogallala Group, temporally equivalent to the upper part of the Valentine Formation (late Barstovian), Nebraska and South Dakota: F:AM 61750, crushed fragmentary skull with both partial maxillae with P4-M2 and broken detached teeth, and both rami with c1 broken-m3 (p1-p3 broken), 14 mi north of Nebraska-South Dakota state line; F:AM 61751, right and left partial rami with c1-m3 (p1 alveolus), south side of the Nebraska-South Dakota state line; and F:AM 61752, left partial maxillary with P4-M2.

Hazard Homestead Locality (UNSM Hk-104), Driftwood Creek, Republic River, Ogallala Formation (late Barstovian, temporally equivalent to Crookston Bridge Member of Valentine Formation), Hitchcock County, Nebraska: UNSM 8539, right maxillary fragment with P3-p4 broken; UNSM 91072, left premaxillary-maxillary with I1-P1 alveoli, P2, P3 alveolus, and P4-M2; UNSM 91073, fragmentary skull with P3-M2; UNSM 91074, right maxillary with P3-M2 (P3-M1 all broken); UNSM 91076, par-

tial anterior skull with I1–P1 alveoli and P3–M2; UNSM 91077, left ramus with i1–i3 alveoli, c1, p1 alveolus, and p2–m2 broken; UNSM 2015-90, left m1; UNSM 1000-89, right ramus with p2–m1; and UNSM 1255-91, partial mandible with i2, c1–m1, and m2–m3 alveoli.

Ogallala Group (late Barstovian), Knox County, Nebraska: Spatz Quarry (UNSM Kx-103): UNSM 26126, partial left and right rami with p2–m2. 1.1 mi west of Miller Creek on Devil's Nest Road (UNSM loc. Kx-116): UNSM 8538, left ramus with c1–m2 and m3 alveolus.

Niobrara River, NE¼ of SE of sect. 20, T29N, R45W, ?Valentine Formation (?late Barstovian), Sheridan County, Nebraska: F:AM 61779, isolated right I2, broken right P4, and isolated left p4–m2.

Cold Spring Fauna, Fleming Formation (early late Barstovian), San Jacinto and Polk counties, Texas (referred to *Aelurodon francisi* by Wilson, 1960: 991): TMM-BEG 31191-9 (AMNH cast 89630), left ramal fragment with c1–p1 broken and p2–p3 (Wilson, 1960: fig. 4b, c); TMM-TAMU 2634B (AMNH cast 89630), partial left ramus with p4–m2 (m1 broken); TMM-BEG 31191-23 (AMNH cast 89624), right partial maxillary with P4–M1 (Wilson, 1960: fig. 4d, e), Site 2; TMM-BEG 31191-30 (AMNH cast 89617), left isolated P4 (Wilson, 1960: fig. 4f, g) and left isolated P3, Site 2; and TMM-BEG 31183-72 (AMNH cast 89620), isolated I1, I2, and I3 (Wilson, 1960: fig. 4h–k), and right maxillary fragment with P4 alveolus and M1, Site 2.

Santa Cruz area, Pojoaque Member of Tesuque Formation (late Barstovian), Rio Arriba and Santa Fe counties, New Mexico: F:AM 27340A, right and left rami with i3–m3, partial right scapula, both humeri (crushed), partial left and right ulnae, both radii, partial left hand with carpals, metacarpals I, IV, and V, proximal through distal phalanges, partial left and right femuri, partial left and right tibia, partial left and right feet with calcaneum, astragalus, tarsals, metatarsals I–V, and proximal through distal phalanges, between Second and Third washes; F:AM 27341, fragmentary skull with I1–P3 alveoli and P4–M2 all broken, Red Sand; F:AM 27343, left ramus with i1–p1 alveoli and

roots, p2–m1 all broken, and m2–m3, Second District; F:AM 27345, partial crushed skull with C1 broken–M2 (P1 alveolus and P3 broken); F:AM 27346, skull with I1–I3 alveoli and C1–M2 (P3 and M2 broken), and mandible with c1–m3 (p1 alveolus), Red Sand; F:AM 27347, crushed posterior part of skull with M1–M2 and detached maxillary fragments with C1 alveolus and P1 broken–P4, Red Layer, ?Second Wash; F:AM 27349, right and left rami with i1–i2 alveoli, i3–m2, and m3 alveolus, Third Wash; F:AM 27350, immature right and left maxillary fragments with dP4 and P3–M1 unerupted, both rami with di3, dp3–dp4, p1, and unerupted p4–m2; F:AM 27351A, edentulous left ramus with all alveoli; F:AM 27351B, left partial ramus with p3–m1 all broken; F:AM 27356, immature skull with di2 broken–dP4 and unerupted P4–M1, and mandible with di3–dp4 and unerupted p4–m1; F:AM 27357, crushed partial skull with I1–P1 alveoli, P2, and P4 broken–M2, and left partial ramus with i1–p1 alveoli, p2–p4, and m1–m3 alveoli, Rio Grande Slope; F:AM 27358, partial mandible with c1–m2 and m3 unerupted, between First and Second washes; F:AM 27360, partial palate with I1–M1 (M2 broken); F:AM 27479, mandible with i1–m2 and m3 alveolus, isolated upper canine, atlas, caudal vertebrae, both scapulae, left and partial right humeri, both ulnae, both radii, carpals, metacarpals I–V, pelvis, both femora, both tibiae, both calcaneum, astragalus, tarsals, metatarsals I, incomplete II, III–V, phalanges, and fragments, Rio Grande Slope; F:AM 27491, broken maxillary fragments and teeth including I3–C1 and P2–M2 all broken, “green,” east of Red Layer; F:AM 61722, left partial maxillary with P4–M1 both broken and M2, Second Wash; F:AM 61723, right ramus with i1 alveolus–m2 (p2–p4 broken) and m3 alveolus, two partial thoracics, two lumbar, seven caudals, partial left and right scapulae, left and partial right humeri, pelvis, partial baculum, right femur, patella, right tibia, nearly complete right foot with calcaneum, astragalus, tarsals, metatarsals I–V, and proximal, middle, and distal phalanges, Santa Cruz Grant, 100 yd west of survey stake; F:AM 61733, left partial ramus with p2 broken–m2 and m3 alveolus, First Wash; F:AM 61734, left ramal fragment with p4 broken–

m1, head of First Wash; and F:AM 107708, left partial maxillary with P4 broken—M2, Third Wash.

Pojoaque Bluffs area, Pojoaque Member of Tesuque Formation (late Barstovian), Rio Arriba and Santa Fe counties, New Mexico: AMNH 8309, left partial maxillary with P2 alveolus and P3—M2 all broken; F:AM 27351, right partial ramus with m1—m2 both broken, Pojoaque, right side of Santa Fe Road, 2 mi from Tesuque; F:AM 27351C, right and left partial rami with c1 broken and p3—m2 all broken, lower Pojoaque Bluffs; F:AM 27490, skull with I1—I3 alveoli and C1—M2 (P4 broken), south Pojoaque Bluffs; F:AM 61721, right and left partial maxillae with P3—M2 and detached broken C1, southwest Pojoaque Bluffs; F:AM 61724, right ramus with i2—m3 (m1 broken), southwest Pojoaque Bluffs; F:AM 61725, left partial ramus with p2—m2 all broken, central Pojoaque Bluffs; F:AM 61729, left ramus with all teeth represented by alveoli or broken, south Pojoaque Bluffs; F:AM 61730, partial skull with I1—P1 alveoli and P2—M2, West Pojoaque; F:AM 61736, fragmentary skull with I1—I2, I3 alveolus, and C1—M1 (P1 alveolus), southeast of Pojoaque Bluffs; F:AM 107705, right partial ramus with c1—p4 and m1 alveolus, head of the tributary of first large wash; F:AM 107706, left ramus with c1 broken, p1 alveolus, p2—m2 (p3 and m1 broken), and m3 alveolus, south Pojoaque Bluffs; and F:AM 107707, crushed partial skull with C1 and P2—M1, both partial rami with c1 and p2—m2, partial humerus, incomplete right radius and ulna, right calcaneum, metacarpals II, III, and IV, and phalanges, middle of Jacona Grant, west of Jacona Fault.

Rio del Oso—Abiquiu area, Chama el Rito Member of Tesuque Formation (late Barstovian), Rio Arriba County, New Mexico: F:AM 61719, crushed skull with I3—M2 and both rami with c1 broken—m3 (p1 alveolus), near the head of Three Sands Hills Wash; F:AM 61720, anterior part of skull with I1 alveolus, I2—C1 all broken, P1 alveolus—M1, and M2 alveolus, south fork of Three Sands Hills Wash; F:AM 61731, right immature ramal fragment with c1 and p2—p4 unerupted and m1 broken, South Ojo Caliente; F:AM 61732, right maxillary fragment with M1 broken, mandible with i1—m3, both partial

humeri, left radius, and right partial femur, Chama el Rito area; F:AM 61735, left ramal fragment with m1 broken, middle Ojo Caliente; F:AM 61737, two left maxillary fragments with left P4 and M1—M2, Ojo Caliente; F:AM 67362, left immature partial ramus with dc1 broken, dp2—dp4 all broken, and p4—m1 unerupted, Ojo Caliente; and F:AM 107736, left partial ramus with m1 broken and m2—m3, Chama el Rito area.

Lower part of the Ojo Caliente Member, Tesuque Formation (late Barstovian), Rio Arriba County, New Mexico: Conical Hill Quarry: F:AM 67370, crushed partial skull with I1 alveolus, I2 broken—C1, P1 alveolus—P4, and M1—M2 both broken; F:AM 67371, right ramus with c1 broken, p1 alveolus, p2—p3 both broken, p4—m2, and m3 alveolus; and F:AM 67372, left ramus with i1—i3 alveoli, c1, p1 alveolus—m1, m2 broken, and m3 alveolus.

Jemez Creek area, undifferentiated beds in the Zia Formation (late Barstovian), Sandoval County, New Mexico: Rincon Quarry: F:AM 61726, immature skull with C1 and P2—P3 all erupting, dP4, P4 unerupted, and M1; F:AM 61727, right partial maxillary with P4 alveolus and M1—M2; and F:AM 61728, right and left rami with c1—p1 alveoli and p2—m3 (p3 broken). East fork of the Canyada de las Milpas: F:AM 107704, right ramal fragment with p2—m2 (p3 broken) and partial left ulna.

Upper part of the Pojoaque Member of the Tesuque Formation and possibly Chamita Formation (Clarendonian), Rio Arriba and Santa Fe counties, New Mexico: F:AM 27340, crushed skull with I2—I3 alveoli and C1—M2 (P1 and P3 alveoli), no locality data; F:AM 27344, right ramus with c1 broken, p1—p2 alveoli, p3 broken—m2 (m1 broken), and m3 alveolus, 1 mi upriver from San Juan Bridge; F:AM 27348, partial skull with I1—M2 and mandible with i1—m3, Chimayo; F:AM 27351D, left ramal fragment with m1—m2 both broken, Battleship Mountain; F:AM 50159, right premaxillary fragment with I1—I2 alveoli and I3, and right maxillary fragment with P4—M1 both broken, Battleship Mountain District; F:AM 67057, left ramus with c1—m3 all broken or alveoli, red layer, north Santa Clara River; and F:AM 67059,

right and left partial maxillae with P2–M2, near springs, west of San Ildefonso.

DISTRIBUTION: Late Barstovian of Nebraska, South Dakota, Texas, and New Mexico; and Clarendonian of New Mexico.

EMENDED DIAGNOSIS: *Aelurodon ferox* shares with *A. taxoides* derived characters that distinguish it from other species of *Aelurodon*: larger size; broad contact of premaxillary and frontal; strong, laterally expanded postorbital process of frontal; extremely high and thin-bladed sagittal crest and more posterodorsally produced nuchal crest; more broadened palate; incise battery aligned in straight transverse line; I3 larger with three lateral accessory cusplets; and premolars larger and more massive. *A. ferox* lacks the following advanced features that are present in *A. taxoides*: a weak symphyseal flange on the horizontal ramus, a more reduced P4 protocone, and an m2 metaconid extremely reduced or absent.

DESCRIPTION AND COMPARISON: Abundant materials from the Frick Collection, together with those in the UNSM and USNM collections, constitute an adequate sample for evaluation of the temporal and spatial variations of this species. Except for its smaller size, the proportional patterns of the cranium of *A. ferox* are almost identical to those of *A. taxoides* (fig. 71). Particularly noteworthy in the ratio diagram are the high contrasts between a wide frontal shield and a narrow postorbital constriction and between a wide zygomatic arch and a narrow braincase. As in *A. asthenostylus*, the skull takes a front-heavy appearance with a very broad palate, robust rostrum, and wide open external and internal nares, in contrast to the relatively slender construction of its posterior half of the skull. The forehead in *A. ferox* is also broadened, partly due to the laterally expanded postorbital process of frontal. Specimens with dissected frontals (F:AM 25230 and 61746) reveal essentially the same degree of complexity in frontal sinus as those in *Tomarctus brevirostris*. The multichambered sinus extends into the postorbital process but does not expand much beyond the frontal-parietal suture posteriorly, in contrast to the more elaborate sinus in the *Epicyon–Borophagus* clade. This enlargement of the supraorbital area, coupled with a deep zygomatic arch, results in a rel-

atively small orbit. Beginning in *A. ferox*, the sagittal crest is extremely high and forms a thin blade with a relatively straight dorsal edge. The posterior expansion of the nuchal crest overhangs the occipital condyle by more than 20 mm. Basicranially, *A. ferox* has an enlarged mastoid process and an elongated paroccipital process with a long free tip, characteristic of the aelurodontine clade.

Dentally, *A. ferox* continues the tendency toward a larger and more complex I3—three lateral accessory cusps are common in this species, in contrast to two or fewer in more primitive taxa. The premolars are strong relative to the molars, a tendency that began in *A. asthenostylus*, and there is a slight tendency for the anterior premolars to become disproportionately larger than in *A. asthenostylus* (fig. 72). These robust premolars also have more distinct accessory and cingular cusplets. More noticeable is the addition of a small anterior cingular cusp in all premolars, which is shared by the *A. mcgrewi–stirtoni* clade but is generally absent in *A. asthenostylus*. As in the more primitive species of *Aelurodon*, the P4 protocone is rather reduced. However, most individuals still retain a small cuspidate protocone rather than the almost complete absence of a protocone as in *A. taxoides*. The M1 continues the trend toward increased crown height of the paracone relative to the talon, as well as a reduced metaconule and internal cingulum. The M2 is small, as in *A. asthenostylus*, but not as strongly reduced as in *A. stirtoni*.

Although still retaining the fundamentally bicuspid talonid, the lower carnassial is increasingly hypercarnivorous in its long trigonid blade vs. reduced metaconid, short and narrowed talonid, and lower, anteriorly restricted entoconid (as contrasted to a higher and larger hypoconid). All these features vary to a greater or lesser extent within the presently defined hypodigm, which encompasses a span of approximately 3 m.y. in the late Barstovian. However, the apparent general tendency is that geologically younger individuals have a greater degree of development of these features. The m2 still has a distinct metaconid, in contrast to its near loss in *A. taxoides*.

DISCUSSION: The single isolated P4 of USNM 523, the genoholotype of *Aelurodon*

*ferox*, has been the source of frustration for generations of paleontologists, with the question of the identity of *Aelurodon* being generally at issue (see Baskin, 1980, for a recent review). Such uncertainty about the holotype may have been responsible for the general reluctance of most authors to refer additional materials to this species (except Evander, 1986). On the other hand, the status of Cope's (1877) *Aelurodon wheelerianus* is equally uncertain. The holotype from the "Santa Fe marls" is a partial ramus with all cheekteeth broken near the base and may properly belong to the category of nomen vanum (sensu Chorn and Whetstone, 1978; Mones, 1989). However, the subsequent reference (Cope, 1883: 245, fig. 11a, b) to *A. wheelerianus* of a partial palate and nearly complete mandible (AMNH 8307, presently referred to *A. mcgrewi*; see further discussion under this species) from Red Willow County, Nebraska, helped to perpetuate the application of this name for the small-size *Aelurodon* in the Valentine Formation (e.g., Voorhies, 1990a, 1990b).

Despite the lack of a clear concept of the type species, the name *Aelurodon* has been in such wide usage that even authors who regarded the genoholotype as specifically indeterminate (VanderHoof and Gregory, 1940; McGrew, 1944b) were unwilling to discard *A. ferox*, just to be able to continue the use of the generic name. Recently, Baskin (1980) demonstrated that even the meager USNM 523 preserves the highly diagnostic feature in which the P4 protocone lacks a connection to the parastyle, and is thus distinct from *Epicyon* (McGrew's "A." *saevus* species group), contrary to Richey's (1979) interpretation of USNM 523. In light of our phylogenetic framework, Baskin's diagnosis remains a valid characterization of these large hyenalike borophagines. Thus, even though the lack of a protocone to parastyle connection on P4 is a primitive condition in *Aelurodon*, this feature, coupled with its large size and the bulbous shape of the parastyle (in contrast to the often triangular parastyle in *Epicyon*), is sufficient to permit a reasonable conclusion that the genoholotype is very close to, if not synonymous with, *A. platyrhinus* (Evander, 1986) or *A. taxoides* (Voorhies, 1990a).

Questions still remain, however, with regard to its specific identity. Within the present hypodigm, based on large series of well-preserved materials, the size of USNM 523 falls within the two most derived species of *Aelurodon*: "*platyrhinus*" and *taxoides*. The size of P4 in both of these species overlap extensively, and USNM 523 falls in the middle of the range of overlap (fig. 83). Our specific assignments of individual specimens are largely based on stratigraphic relationships (see below). Therefore, our decision to retain *A. ferox* as distinct from *A. taxoides* continues to be somewhat arbitrary, and is motivated by the desire to maintain generic stability. In this, we are in partial agreement with VanderHoof and Gregory (1940), who voiced the suspicion that *A. ferox*, *A. platyrhinus*, and *A. taxoides* are synonymous, but they nevertheless decided to retain *A. ferox* as a distinct species.

As we cannot recognize any autapomorphic features for *A. ferox*, and we can observe that larger size and other derived features for *A. taxoides* are acquired through geologically successively younger individuals in the northern Great Plains, it seems possible that the latter gradually evolved from *A. ferox* anagenetically. Such a succession can also be observed in parallel in other parts of North America. In fact, there seems to be no natural break in the morphology to mark the boundary of the *ferox*-*taxoides* species pair (fig. 84), and fragmentary specimens were assigned to one species or another based mainly on the association of fauna (i.e., Mammal Age) rather than morphology. As such, our presentation of the hypodigm assumes a sense of chronospecies for these two taxa. If this was indeed the case, our division of these two species, mostly along the Barstovian-Clarendonian boundary (sensu Tedford et al., 1987), would be somewhat arbitrary and affected by the controversy of the placement of the boundary in Nebraska (see Voorhies, 1990a, 1990b). An exception to this theme involves a few specimens from Battleship Mountain and San Ildefonso sites (Clarendonian) of New Mexico. These specimens come from high in the Pojoaque Member of the Tesuque Formation or possibly from the Chamita Formation. These localities and levels produce taxa of Clarendonian age,

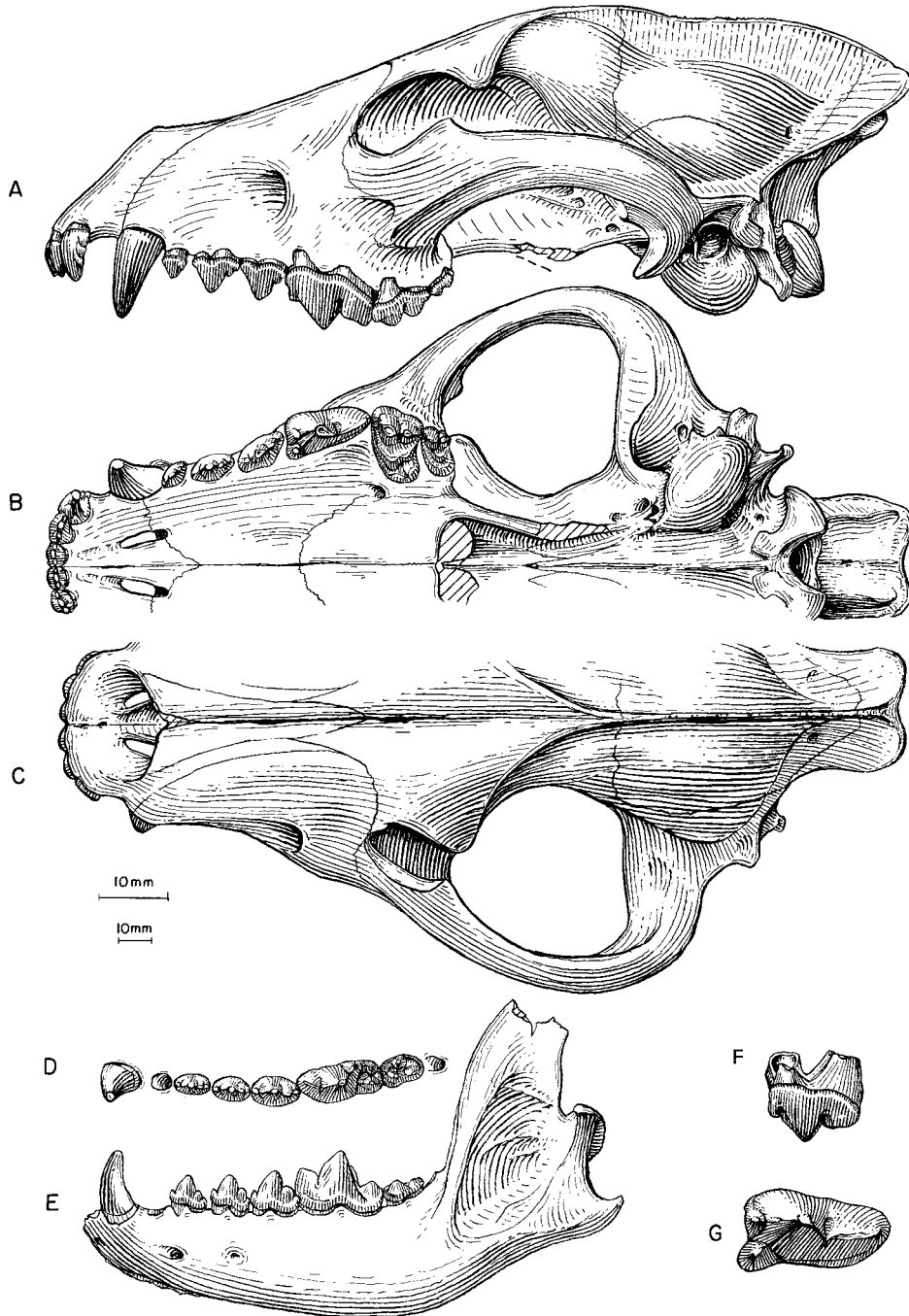


Fig. 80. *Aelurodon ferox*. **A**, Lateral, **B**, ventral, and **C**, dorsal views of skull, UNSM 1093 (holotype of *A. platyrhinus*), Railway Quarry A, Crookston Bridge Member, Valentine Formation (late Barstovian), Cherry County, Nebraska. **D**, Lower teeth and **E**, ramus, F:AM 61742, Railway Quarry A. **F**, Lateral and **G**, enlarged occlusal views of P4 (reversed from right side), USNM 523, holotype, "valley of the Niobrara River," Nebraska. The longer (upper) scale is for G, and the shorter (lower) scale is for the rest.

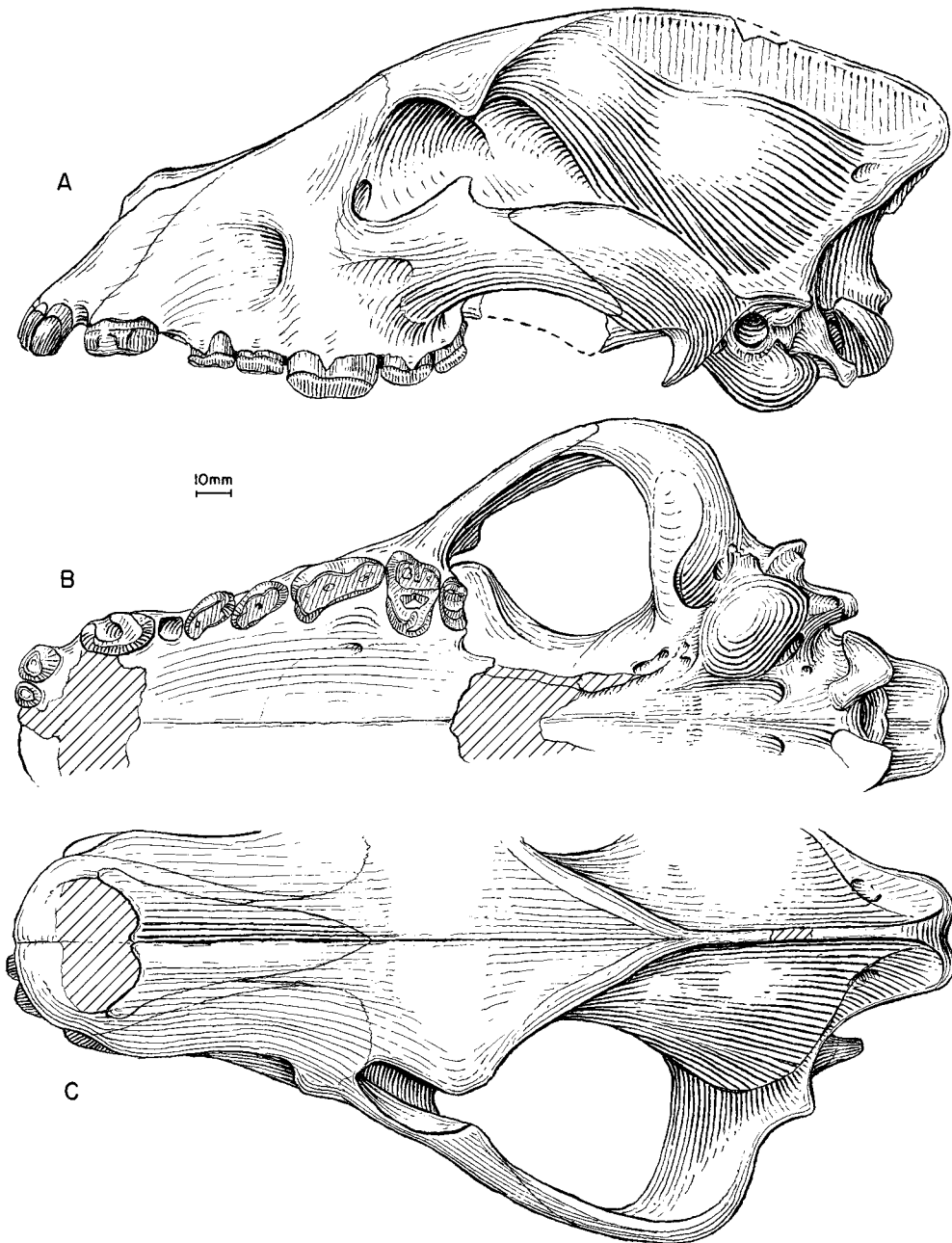


Fig. 81. *Aelurodon ferox*. **A**, Lateral, **B**, ventral, and **C**, dorsal views of skull, F:AM 61753, Burge Quarry, Burge Member, Valentine Formation (late late Barstovian), Cherry County, Nebraska.

but lack of precise biostratigraphy lends some uncertainty to the age of individual specimens. Individuals from these localities are comparable in size to *A. ferox* and are

markedly smaller than *A. taxoides* from other Clarendonian localities.

The resulting division of the two morphospecies represents approximately the

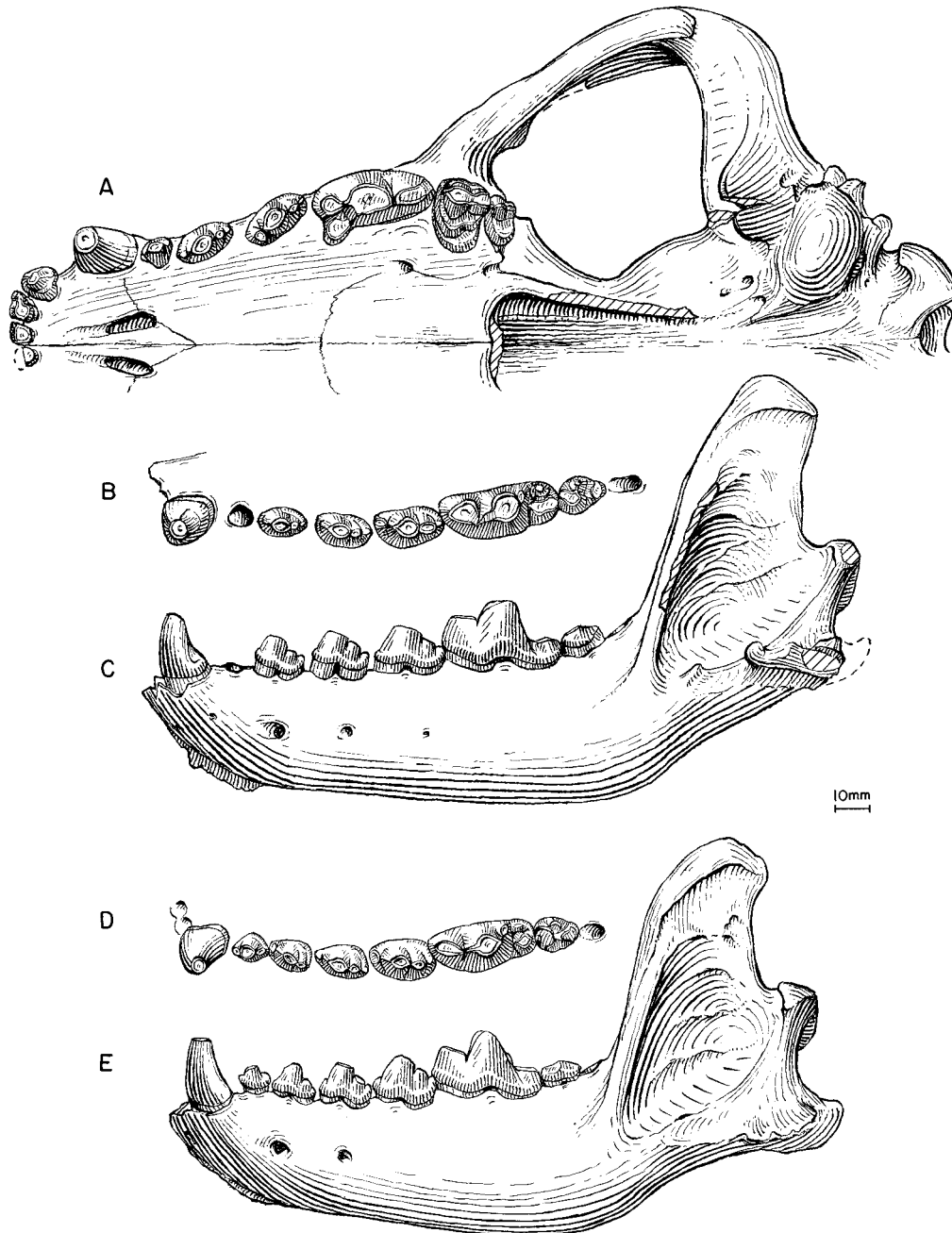


Fig. 82. **A**, Ventral view of skull, *Aelurodon taxoides*, F:AM 67047, 1 mi west of Dixon, Dixon Member, Tesuque Formation (late Barstovian–Clarendonian), Rio Arriba County, New Mexico. **B**, Lower teeth and **C**, ramus, *A. taxoides*, YPM-PU 10635, holotype, “Loup Fork,” Ash Hollow Formation (Clarendonian), Sheridan County, Nebraska. **D**, Lower teeth and **E**, ramus, *A. ferox*, F:AM 61771, Burge Quarry, Burge Member, Valentine Formation (late late Barstovian), Cherry County, Nebraska.



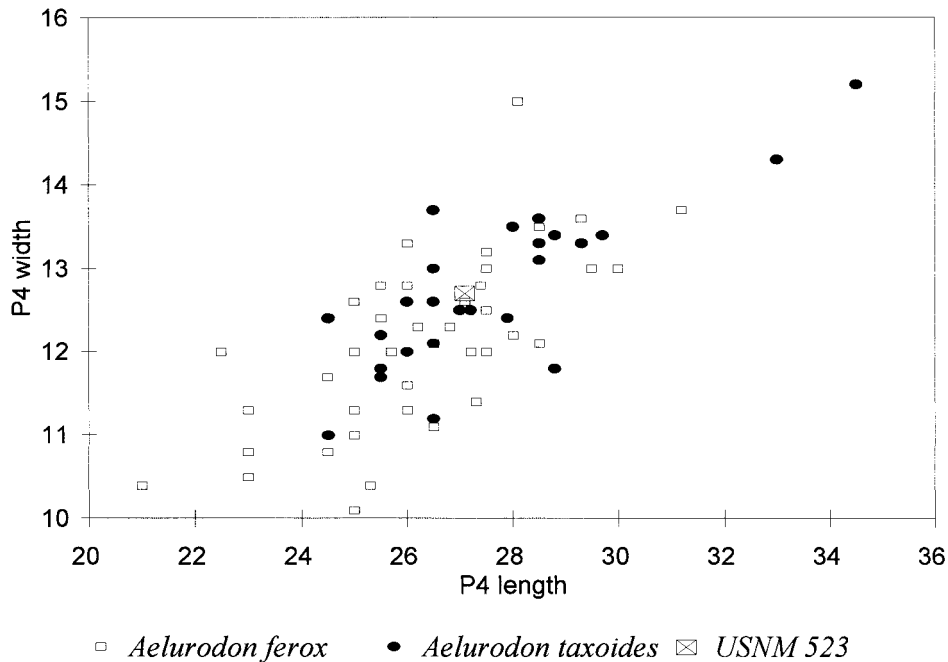


Fig. 83. Scatter diagram of P4 length vs. P4 width for *Aelurodon ferox* and *A. taxoides* showing the position of the holotype of *A. ferox* (USNM 523).

same amount of variation in size (e.g., coefficient of variation for m1 length is 5.5 in *ferox* and 6.9 in *taxoides*; see other CVs in appendix III) shown by most other borophagines in this study. In the present hypodigm, there is a significant size difference from the oldest individuals in the Cornell Dam Member of the Valentine Formation to the youngest individuals in the Burge Member of the Valentine Formation. At the extreme ends, the size difference can be as large as 23% (in basal lengths of skull, see appendix II), an amount of variation we attribute to the approximately 3 m.y. span of steady evolution of this species in the late Barstovian (fig. 84).

Similarly, at the lower end of the stratigraphic range of *A. ferox*, individuals from the Cornell Dam and Crookston Bridge members of the Valentine Formation are transitional between *A. asthenostylus* (especially the Pawnee Creek sample in Colorado) and individuals from the upper part of the Valentine Formation. Besides a slightly larger size, the specimens from the lower members of the Valentine Formation are only

slightly more advanced toward hypercarnivory than is *A. asthenostylus*, and distinctions between *A. asthenostylus* and the more "typical" members of *A. ferox* in the upper Valentine Formation are blurred by these intermediate forms.

#### *Aelurodon taxoides* Hatcher, 1893

Figures 82A–C, 85, 86

*Aelurodon taxoides* Hatcher, 1893: 236, pl. 1, figs. 2, 2a. Matthew and Gidley, 1904: 250. VanderHoof and Gregory, 1940: 149 (in part). Gregory, 1942: 345, figs. 8, 9. McGrew, 1944b: 79. Macdonald, 1960: 967, fig. 4. Wilson, 1960: 993, fig. 5c, d. Webb, 1969a: 41. Baskin, 1980: 1349 (in part). Munthe, 1998: 136.

?*Tephrocyon* sp. Matthew and Cook, 1909: 376, fig. 5.

?*Cuon* sp. Matthew and Cook, 1909: 376.

*Aelurodon* cf. *A. aphobus* (Merriam): Macdonald, 1948: 57, figs. 3, 4.

*Tomarctus propter* Cook and Macdonald, 1962: 562, fig. 2. Skinner et al., 1977: 356.

*Aelurodon* cf. *taxoides* (Hatcher): Dalquest and Hughes, 1966: 80, fig. 2. Dalquest et al., 1996: 131.

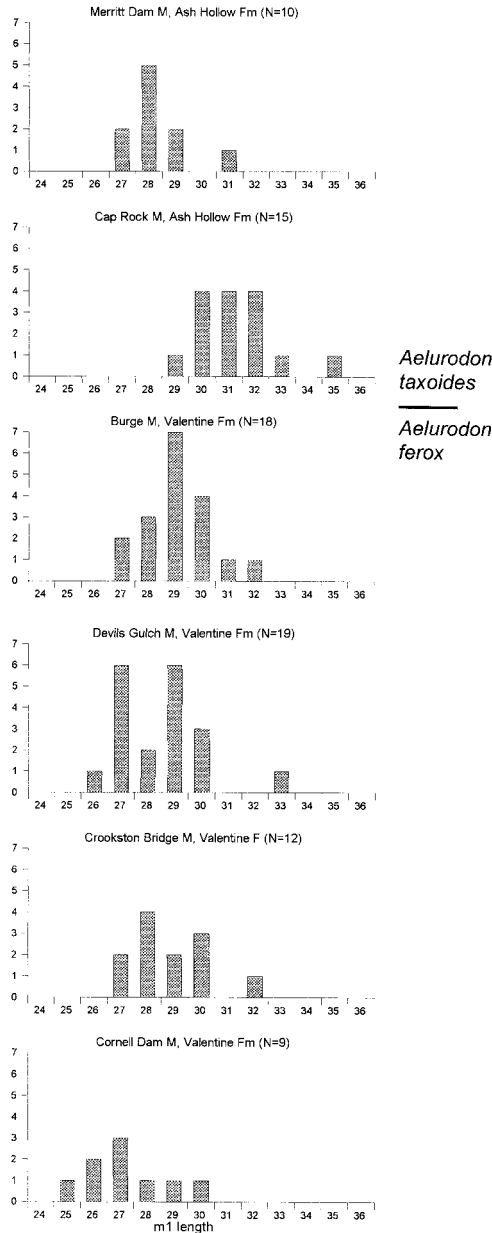


Fig. 84. Histograms of the length of m1 in *Aelurodon ferox* and *A. taxoides* in different stratigraphic positions (members of the Valentine and Ash Hollow formations) in the late Barstovian through Clarendonian of Nebraska. Note the general increase in size through time except in the end member (Merritt Dam Member), where this tendency is reversed.

*Aelurodon* cf. *A. taxoides* Hatcher, 1893: Skinner and Johnson, 1984: 299.

**HOLOTYPE:** YPM-PU 10635 (AMNH cast 97777), left ramus with i1–i3 alveoli, c1, p1 alveolus–m2, and m3 alveolus (fig. 82B, C), and atlas from the “Loup Fork” (Ash Hollow Formation, Clarendonian), south side of the Niobrara River, midway between the mouths of Pine and Box Butte creeks, Sheridan County, Nebraska.

**REFERRED SPECIMENS:** Undifferentiated beds of the Ogallala Group temporarily equivalent to the Ash Hollow Formation (early Clarendonian), Thomas Fox Ranch, Mission Local Fauna, Mellette County, South Dakota (list follows Macdonald, 1960): SDSM 553, left ramus with i1–i3 alveoli, c1–m2, and m3 alveolus (Macdonald, 1960: fig. 4); SDSM 572, left ramal fragment with m2–m3; SDSM 573, left ramal fragment with c1 and p4; SDSM 5652, partial skull with P3–M2; SDSM 53277, right ramus with c1, roots of p1–p4, and m1; SDSM 53278, right ramal fragment with p1 alveolus and p2–p3; SDSM 53279, right ramal fragment with p1 alveolus, p2, p3 alveolus, and p4; and SDSM 55185, isolated left P4. George Thin Elk Gravel Pits (same locality as above): F:AM 67328, crushed partial skull with I1–P2 alveoli and P3–M2; and F:AM 107715, right partial maxillary with P4–M2 all broken.

Undifferentiated beds of the Ogallala Group temporarily equivalent to Ash Hollow Formation (early Clarendonian), South Dakota: AMNH 10813, left maxillary fragment with P1 and P2 broken. Canyon of the Little White River: AMNH 97737, left isolated P4. Spring Creek: F:AM 67029, skull fragments with I1–P1 alveoli, P2 broken, and P3 alveolus, talus of slide on Little White River; F:AM 67439, left distal tibia; and F:AM 67440, left metacarpal II. Rosebud Agency Quarry: F:AM 67483, right femur.

Undifferentiated beds of the Ogallala Group temporarily equivalent to Ash Hollow Formation (early Clarendonian), Big Springs Canyon, Bennett County, South Dakota: AMNH 10891A, partial tibia; F:AM 67481, left humerus; F:AM 67482, right tibia; and UCMP 32588, complete mandible with left and right i1–i3 alveoli, c1–m2, and m3 al-

veolus (referred to *Aelurodon taxoides* by Gregory, 1942: figs. 8, 9), UCMP loc. V3322.

Undifferentiated beds (early Clarendonian) of the Ogallala Group, temporally equivalent to the Cap Rock Member of the Ash Hollow Formation, Hollow Horn Bear Quarry, Todd County, South Dakota: F:AM 67006, right and left maxillae with I1–I3 alveoli and C1–M2 (P1 alveolus) (fig. 85A, B); F:AM 67007, left maxillary fragment with P4; F:AM 67008, right and left rami with i2–m3 (fig. 85C, D); F:AM 67009, left partial ramus with c1, p1 alveolus, p2–p4, m1 alveolus, m2, and m3 alveolus; F:AM 67010, right maxillary fragment with P3; F:AM 67010A–C, detached right P1, detached right P3, and detached left p4; F:AM 67427, left partial humerus; F:AM 67427A, left partial humerus; F:AM 67428, left radius; F:AM 67429 and 67429A, B, three partial ulnae; F:AM 67430, right partial femur; F:AM 67484, right tibia; F:AM 67431, proximal part of metatarsal V; and 67431A, left calcaneum.

Undifferentiated beds (early Clarendonian) of the Ogallala Group, temporally equivalent to the Cap Rock Member of the Ash Hollow Formation, 0.25 mi west of Wounded Knee Creek, 0.5 mi south of South Dakota state line, Cherry County, Nebraska: UNSM 50792, left maxillary with P4–M1 and mandible with i3–m3 (p1 alveolus).

Cap Rock Member, Ash Hollow Formation (early Clarendonian), Brown County, Nebraska: Clayton Quarry: F:AM 67012, right partial maxillary with P3–M1; F:AM 67019, right ramal fragment with m2 and m3 alveolus; F:AM 67434, right radius; and F:AM 107714, left isolated p4. East Clayton Quarry: F:AM 67011, left partial maxillary with P3–P4 both broken and M1–M2; and F:AM 67018, right ramus with c1 broken, p1 alveolus–m2, and m3 alveolus. Fairfield Creek No. 3: F:AM 25100, left ramus with i2 and c1–m3, both radii, partial right ulna, partial metacarpals II and V, partial left tibia, partial pes with metatarsal II and incomplete III and IV, tarsals, and phalanges (referred to *Aelurodon* cf. *A. taxoides* by Skinner and Johnson, 1984: 299).

Cap Rock Member, Ash Hollow Formation (early Clarendonian), Cherry, Keyapaha, and Knox counties, Nebraska: West fork of

Deep Creek: F:AM 67042, right partial ramus with i1–p1 alveoli, p2–p3, p4–m1 both broken, and m2–m3 alveoli; and F:AM 67455H, left calcaneum. Between Garner and Crane bridges: F:AM 67028, right partial ramus with p3–m1 (p4 broken) and m2–m3 alveoli. Spring Canyon: F:AM 67026, left partial ramus with p2–m1; and F:AM 67027, left ramal fragment with p3 broken–p4. Mensinger Quarry: F:AM 70615, left detached M1; and F:AM 107713, left ramal fragment with m1 broken–m2. Garner Quarry: F:AM 67330, right partial ramus with c1, p1 alveolus, p2–m1 (p3 alveolus), and m2–m3 alveoli; and F:AM 107712, right isolated m2. Northeast of Springview: F:AM 67030, left partial maxillary with P4 broken–M2, and isolated left P1. West of Boiling Spring flat: F:AM 67345, right and left partial rami with i2, i1 and i3 alveoli, c1–m2 (p1–p2 alveoli), and m3 alveolus, canyon on south side of Niobrara River about due west of Boiling Spring flat. Jonas Wilson Ranch: F:AM 107711, right partial ramus with m1 broken–m2 and m3 alveolus, talus near June Quarry, base of Cap Rock. Above Bug Prospect (UNSM loc. Kx-119B): UNSM 2061–84, right ramus with i1, c1 broken, p1 alveolus, and p2–m2. No locality data: F:AM 25101, left partial ramus with p4–m1; and F:AM 25129, right partial ramus with p4–m2.

Merritt Dam Member, Ash Hollow Formation (late Clarendonian), Sheridan, Brown, Cherry, and Hitchcock counties, Nebraska: Rhino Horizon No. 3 Quarry: F:AM 25111, right ramus with i2–p1 alveoli, p2–m2, and m3 alveolus (fig. 85E, F); F:AM 67022, right partial ramus with i2–p2 alveoli, p3–m1, and m2 alveolus; F:AM 67023, right broken m1; F:AM 67522, left partial humerus; and F:AM 67523, right partial ulna. Bear Creek Quarry: F:AM 67013, crushed skull with I1–M2; F:AM 67014, right and left partial maxillae with P3–M1; F:AM 67015, partial posterior skull; F:AM 67016, right ramus with i1–i3 alveoli and c1–m2 (p1–p2 broken and m3 alveolus); F:AM 67017, right and left rami with c1–m2 (p1 alveolus) and m3 alveolus; F:AM 67020, left ramus with c1–m2 and m3 alveolus; F:AM 67021, right and left rami with c1–m1 (p1 alveolus) and m2–m3 alveoli; F:AM 67024, right isolated P3; F:AM 67432, left humerus; F:AM 67432A,